

UNCLASSIFIED

AD NUMBER

ADB006505

NEW LIMITATION CHANGE

TO

Approved for public release, distribution
unlimited

FROM

Distribution authorized to U.S. Gov't.
agencies only; Test and evaluation; Jan
1975. Other requests shall be referred to
the Commander, Frankford Aersenal, Attn:
SARFA-MDS-D, Philadelphia, PA, 19137.

AUTHORITY

DA ltr, 17 Aug 1976.

THIS PAGE IS UNCLASSIFIED

AD B006505

AD

FA-TT-75005

ON THE ACCURACY OF FLECHETTES BY DYNAMIC
WIND TUNNEL TESTS, BY THEORY AND
ANALYSIS, AND BY ACTUAL FIRINGS

January 1975

Distribution limited to U.S. Government agencies only - Test and Evaluation - January 1975. Other requests for this document must be referred to Commander, Frankford Arsenal, ATTN: SARFA-MDS-D, Philadelphia, PA 19137.

D D C
RECORDED
SEP 17 1975
RECORDED
E

Munitions Development & Engineering Directorate



U.S. ARMY ARMAMENT COMMAND
FRANKFORD ARSENAL
PHILADELPHIA, PENNSYLVANIA 19137

DISPOSITION INSTRUCTIONS

Destroy this report when it is no longer needed. Do not return it to the originator.

The findings in this report are not to be construed as an official Department of the Army position unless so designated by other authorized documents.

UNCLASSIFIED

SECURITY CLASSIFICATION OF THIS PAGE (When Data Entered)

REPORT DOCUMENTATION PAGE		READ INSTRUCTIONS BEFORE COMPLETING FORM
1. REPORT NUMBER FA-TT-75005	2. GOVT ACCESSION NO.	3. RECIPIENT'S CATALOG NUMBER
4. TITLE (and Subtitle) ON THE ACCURACY OF FLECHETTES BY DYNAMIC WIND TUNNEL TESTS, BY THEORY AND ANALYSIS, AND BY ACTUAL FIRINGS		5. TYPE OF REPORT & PERIOD COVERED Technical Engineering Report 6. PERFORMING ORG. REPORT NUMBER
7. AUTHOR(s) J.D. Nicolaides L.E. Lijewski (University of C.W. Ingram M.J. Garsik Notre Dame)		8. CONTRACT OR GRANT NUMBER(s) DAAA25-71-C0447, Mod.P00002
9. PERFORMING ORGANIZATION NAME AND ADDRESS Frankford Arsenal Attn: SARFA-MDS-D Philadelphia, PA 19137		10. PROGRAM ELEMENT, PROJECT, TASK AREA & WORK UNIT NUMBERS AMCMS: 662603.11.H7800 DA: 1W662603AH78
11. CONTROLLING OFFICE NAME AND ADDRESS ARMCOM		12. REPORT DATE January 1975 13. NUMBER OF PAGES 358
14. MONITORING AGENCY NAME & ADDRESS (if different from Controlling Office)		15. SECURITY CLASS. (of this report) UNCLASSIFIED 16a. DECLASSIFICATION/DOWNGRADING SCHEDULE N/A
16. DISTRIBUTION STATEMENT (of this Report) Distribution limited to U.S. Government agencies only - Test and Evaluation January 1975. Other requests for this document must be referred to the Commander, Frankford Arsenal, Attn: SARFA-MDS-D, Philadelphia, PA 19137.		
17. DISTRIBUTION STATEMENT (of the abstract entered in Block 20, if different from Report)		
18. SUPPLEMENTARY NOTES Coordinator - Walter J. Schupp, SARFA-MDS-D.		
19. KEY WORDS (Continue on reverse side if necessary and identify by block number) Flechette Flash x-ray Dispersion Transitional ballistics Trajectory Supersonic wind tunnel Jump angle Flechette dispersion theory		
20. ABSTRACT (Continue on reverse side if necessary and identify by block number) The accuracy and dispersion of flechettes are investigated 1) by an exploratory firing program, 2) by a supersonic dynamic testing wind tunnel program, 3) by development of a theory for jump and dispersion for computer computation and analysis and 4) by precision range firings at Frankford Arsenal. The exploratory firing program reveals the importance of fin and body damage, the blast region, and saboting. The dynamic wind tunnel program		

UNCLASSIFIED

SECURITY CLASSIFICATION OF THIS PAGE(When Data Entered)

20. ABSTRACT (Cont'd)

yields the static and dynamic aeroballistic stability coefficients on various flechette designs. The theory and analysis program has presented the effects of the initial launching conditions, the various stability coefficients and asymmetries and has provided accuracy criteria. Lastly, the flechette firing range program provided a correlation between theory and experiment which clearly suggests that high accuracy and low dispersion in flechettes is possible when optimum aerodynamic design is coupled with good saboting and minimization of blast.

UNCLASSIFIED

SECURITY CLASSIFICATION OF THIS PAGE(When Data Entered)

TABLE OF CONTENTS

	page
INTRODUCTION	2
DISCUSSION	4
SUMMARY	10
APPENDIX A	
Exploratory Flechette Firing Program	11
APPENDIX B	
Dynamic Supersonic Wind Tunnel Tests of Four-Flechette Configurations	17
APPENDIX C	
Dispersion Theory of High Fineness Ratio, Cruciform Fin Bodies	111
APPENDIX D	
Frankford Arsenal Experimental Ballistics Firing Program of Flechettes	339

INTRODUCTION

The backbone of ballistics has been the spin stabilized projectile. Virtually, all ordnance from small arms to artillery has almost exclusively utilized the spin stabilized projectile over the last century. Its predecessor was the cannonball and spherical shot. Just as the elongated spin stabilized projectile yielded a marked improvement over the less efficient cannonball, so also fin stabilized ammunition offers great aeroballistic improvements over the spin stabilized projectile. It has only been in recent years that the fin stabilized projectile has come under serious consideration. Some success was achieved by the Germans during World War II with Naval projectile artillery. During the Korean War fin stabilized anti-tank ammunition was introduced which improved the effectiveness of the shape change because of its low spin. In recent years the accuracy of fin stabilized projectiles has improved due to the application of the Tricyclic Theory, the use of dynamic supersonic wind tunnel tests, and improved launching techniques. Because of their small size and the desire for very inexpensive manufacture, the flechette has not received the careful attention that it requires to achieve high accuracy. It is essential that manufacturing techniques, saboting techniques, launching techniques, blast suppression techniques, optimized aeroballistic design procedures, dynamic wind tunnel tests, accuracy theory studies, computer analysis, and precision firings all be undertaken and optimized to achieve good flechette accuracy and low dispersion.

The purpose of this study is to explore flechette design and performance with a view towards achieving high accuracy and low dispersion. Specifically, exploratory firing programs were carried out by Frankford Arsenal, by the Ballistics Laboratories and by the University of Notre Dame. The results of the Notre Dame Flechette Firing Program are summarized in Appendix A.

A dynamic wind tunnel testing program was also carried out by the university on various flechette designs so as to determine the essential static and dynamic aeroballistic stability coefficients. The results of this dynamic wind tunnel program are summarized in Appendix B.

Of particular importance is the development of a computer theory for flechette flight performance, accuracy and dispersion. This theory together with an extensive computer analysis is given in Appendix C. Finally, flechette firings were carried out in the precision range at Frankford Arsenal and a correlation of theory and experiment is also provided in Appendix C. along with a physical evaluation of dispersion.

Based on the theory, sabot design and launcher changes were made in order to reduce the values of those parameters which affect dispersion. A second series of firings were conducted and the analysis of the results is provided in Appendix D.

DISCUSSION

Exploratory Flechette Firing Program

The exploratory flechette firing program both at Frankford Arsenal and at the university have provided an opportunity to measure flechette spin, to measure flechette accuracy and dispersion, to identify fin damage and body damage due to stripper, to provide an approximate measure of dynamic stability at long range, to provide a first hand appreciation of the strong blast region and to concentrate on sabot design, separation, and transition all as affecting flechette flight performance and accuracy.

In addition a transition ballistic range was set up and optimized at Frankford Arsenal to obtain initial condition data using flash x-ray photography. A complete description of the set-up is provided in Appendix C.

BRL conducted free flight tests in their transonic Spark Range to obtain aerodynamic data on the various flechettes under consideration. These data were used in the preliminary development of the dispersion theory and are compared with the wind tunnel results in Appendix B.

Dynamic Supersonic Wind Tunnel Tests of Four Flechette Configurations

In order to obtain both static and dynamic wind tunnel data on flechette configurations, special tests were carried out at the University of Notre Dame which utilizes its unique vertical down flow supersonic wind tunnel and utilizes its one-degree-of-freedom pitching dynamic support instrumentation. Four flechette configurations were constructed and tested. The data from these dynamic tests was measured on a photo-comparator and reduced and fitted by using the Wobble program. The Notre Dame data on $C_{M\alpha}$ and $C_{Mq} + C_{M\dot{\alpha}}$ is in good agreement with the data obtained by the Ballistic Research Laboratory at small angles of attack and small mach numbers. At the larger angles of attack, the Notre Dame data is as much as four times larger as the BRL data in damping and as much as two times larger than the $C_{M\alpha}$ data. Thus, the nonlinearities which have been uncovered in the dynamic wind tunnel tests are of considerable importance in evaluating flechette flight performance and in evaluating flechette accuracy and dispersion. No wind tunnel data was obtained on the important Magnus moment. This omission is considered extremely serious and it is recommended that future studies be carried out in

this area. It is also recommended that the aerodynamic characteristics of the different flechette designs be evaluated with a view towards improvement in performance and accuracy.

Preliminary tests were carried out in obtaining the rolling motion of flechettes at the various angles of attack and in obtaining three-degrees-of-freedom wind tunnel tests where models were able to freely pitch, yaw, and roll. The exploratory rolling tests were carried out in the supersonic wind tunnel at Picatinny Arsenal. Good success was obtained on the basic configuration at small angles of attack. At the large angles of attack the sting support mechanism bent and thus had to be redesigned. These rolling tests have demonstrated that it will be quite possible to obtain excellent free rolling motion performance of flechettes at small and large angles of attack using instrumentation at Picatinny Arsenal.

Three-degree-of-freedom dynamic wind tunnel tests were explored in a preliminary way in the Notre Dame vertical down supersonic wind tunnel. In these tests the model was able to freely pitch and yaw and the afterbody with fins was able to roll freely. The forebody however did not roll. The tests were of marginal success but suggested that complete success could be achieved with more effort. It is specifically suggested that the new 3-D testing procedures originally explored at Notre Dame be continued in the Picatinny Arsenal and/or the BRL wind tunnels.

It should be emphasized that the nonlinear aeroballistic dynamic stability coefficients obtained in the Notre Dame program represent a major finding which was extensively utilized in the performance analysis and accuracy computations. It is considered essential that all future flechette designs undergo complete dynamic wind tunnel testing and range firings in order to permit accurate computations of the true dynamic flight performance, accuracy and dispersion of flechettes.

Dispersion Theory of High Fineness Ratio, Cruciform Fin Bodies

A complete jump and dispersion theory is setforth for the free flight performance of flechettes. The six-degree-of-freedom equations of motion are coded for various computer computations which indicated that the flechette accuracy theory accurately predicts the jump and dispersion of flechettes.

In order to determine realistic values for the initial conditions of flight and for the actual dispersion of flechettes, test firings are carried out in order to obtain special experimental data. The raw experimental data is fitted by the least squares method and thereby placed into the form of initial flight conditions. These initial conditions are then applied to the theory. Six-degree-of-freedom numerical computations are used to evaluate the dispersion of eight test rounds. The good agreement between the theory and test firing results indicate that the methods of data analysis and the flechette accuracy theory together provide a precise means of predicting the dispersion of flechettes.

The analysis of the firing data indicates that the large initial conditions of flechette flight result from a strong impulse imparted to the flechette in the muzzle blast regime. It is found that if the transverse impulse imparted to the flechette is equal to an opposite angular impulse then the dispersion will be zero. Since these two impulses rarely balance and always exist, flechette dispersion is generally large. However, by controlling sabot design and muzzle blast, the transverse and angular momentums can be reduced and partially balanced thereby yielding excellent accuracy and low dispersion.

Of particular importance is the invalidation of the classical maximum yaw theory long used in exterior ballistics.

More specifically the complete jump and dispersion theory for flechettes has been reduced to three governing equations which represent flechettes having high, low and very low roll rates. These three theories were found to be accurate by evaluation against six-degree-of-freedom, numerical computations of the equations of motion. It was found therefore that they accurately predict the jump and dispersion of flechettes.

The computer program undertaken to evaluate the flechette accuracy theory includes 201 special case runs carried out in four parts. The first part validates the theory with respect to the aerodynamic restoring and damping moments. The effect of these moments on dispersion was found to depend on the initial conditions.

The second part validated the theory with respect to the aerodynamic Magnus force and moment. The effects on dispersion were found to be

very small and of no consequence unless the total dispersion of a particular round was of the same order of magnitude as a Magnus effect.

The third part validated the theory with respect to aerodynamic asymmetries (mass asymmetry, inertia asymmetry, etc.) and roll rate. All three theories were found to be validated in this phase and found to be quite accurate. Aerodynamic asymmetries causing a trim of 1° have little effect on the dispersion of fast rolling flechettes.

Slower rolling flechettes were found to have in general increasingly large dispersion values as the roll rate decreased. It can be concluded that for flights which are prone to aerodynamic asymmetry and fin damage, a high roll rate is essential to low dispersion and increased accuracy.

The fourth part validates the theory with respect to gravity. The theory indicates a lateral contribution to dispersion from gravity in addition to the vertical contribution. However, for the flechette this lateral contribution was found to be minimum.

In general, the agreement between the flechette accuracy theory and the computer computations were excellent and account for the effect of the initial launching conditions as well as the static and dynamic stability coefficients and asymmetries. Further, simple equations are given in order to achieve the desired accuracy and optimization.

SUMMARY

By an exploratory firing program, by a supersonic dynamic wind tunnel testing program, by the development of an accuracy theory for jump and dispersion, by computer computations and analysis, and by precision range firings at Frankford Arsenal, flechette accuracy and dispersion is explained, evaluated and improved.

The firing program revealed the importance of fin and body damage, the blast region and sabotaging. The dynamic wind tunnel program yielded values for the important static and dynamic stability coefficients. The flechette accuracy theory was confirmed by numerical integration of the 6-D equations on the high speed computer where the effects of initial conditions, stability coefficients and asymmetries was revealed and evaluated. Finally, by a flechette firing program in the new Frankford Arsenal Ballistics Range, excellent correlation between theory and experiment for flechette accuracy was obtained.

APPENDIX A

EXPLORATORY FLECHETTE FIRING PROGRAM

Two flechette firing programs were carried out at the University of Notre Dame. The first program was carried out in the Army Firing Range located under the football stands in the Rockne Stadium. In these first firing tests the actual flechette and its sabot were fired at full hypersonic velocity using a man barrel with sabot stripper. The firings were carried out with the assistance of technical personnel from Frankford Arsenal and under the direct supervision of Army ROTC personnel stationed on the campus and responsible for the Firing Range. These firings revealed two very important discoveries. By firing through light drawing paper yaw cards and by examining the impression left by the passage of the flechette, it was possible to obtain a positive confirmation that the fins were being seriously damaged and/or bent by the stripper. This finding was transmitted to the cognizant Frankford Arsenal personnel where suitable corrective changes were initiated and finalized thereby eliminating the problem of fin damage.

The second major finding of the first flechette firing program, insofar as university investigators were concerned, was the recognition of the tremendously intensive and long muzzle blast regime. While a standard .22 projectile is fired in the range with little noise and little blast, the flechette system of basically the same weight but fired at large velocity yields a

tremendous concussion and a tongue of fire, blast and flame stretching some 3-4 feet. The importance of the recognition of the strong blast region lies in its effect in disturbing the flechette at launch and thereby contributing to inaccuracy.

The first firing program therefore revealed fin damage due to sabot strippers and a large blast region which contributed to jump and inaccuracy.

The second flechette firing program carried out at the university utilized an air gun in simple subsonic launchings. The range setup is shown in Figure 1. The purpose of this special firing setup was to explore various sabotaging techniques. In this program sabots of both pusher design and puller designs were investigated. Also body inset sabot designs were studied, see Figure 2. Representative target data is illustrated in Figure 3 where effects of sabot designs are clearly evident. Various flechette and sabot designs are shown in Figures 4 and 5.

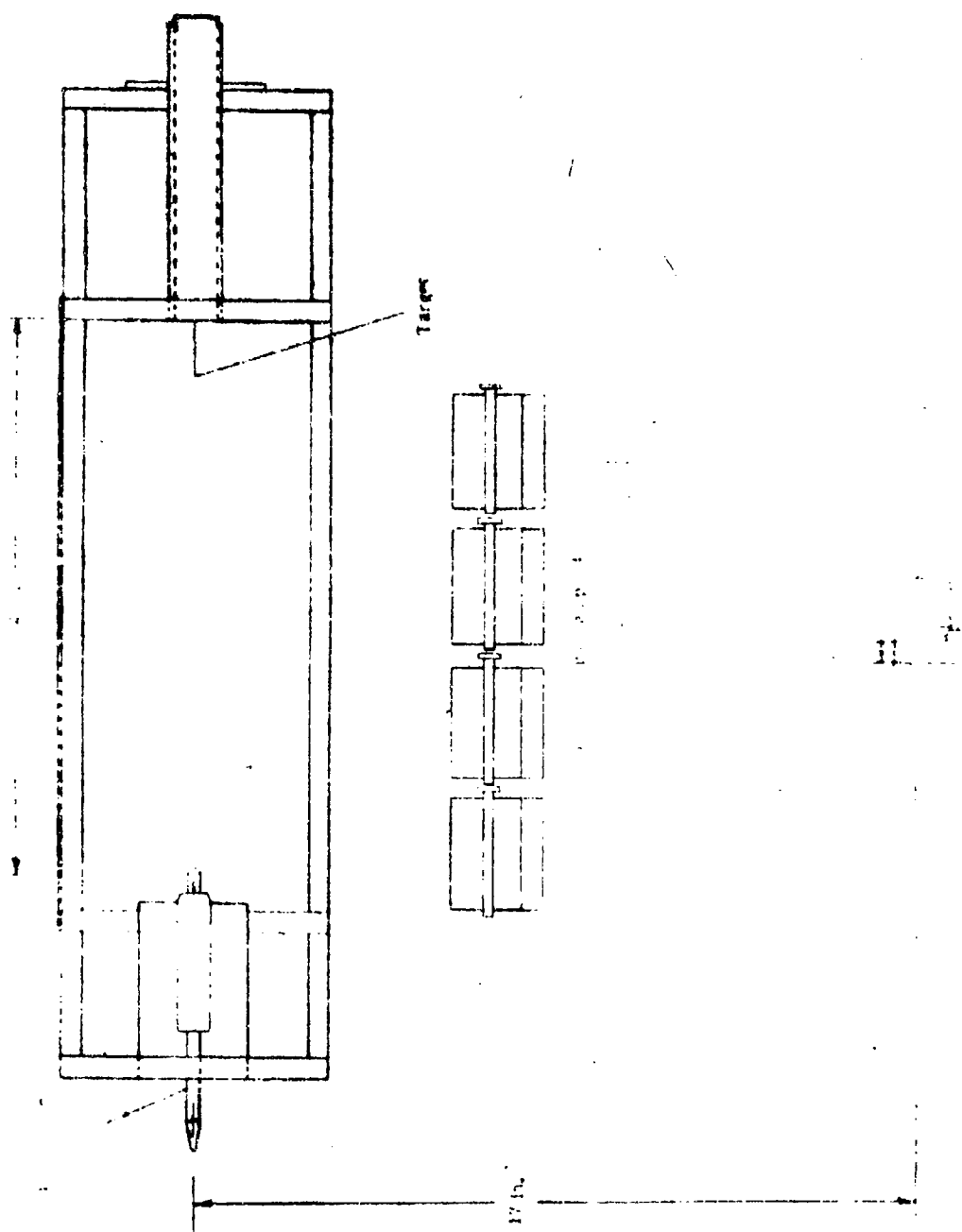


Figure 1. Subsonic Firing Range

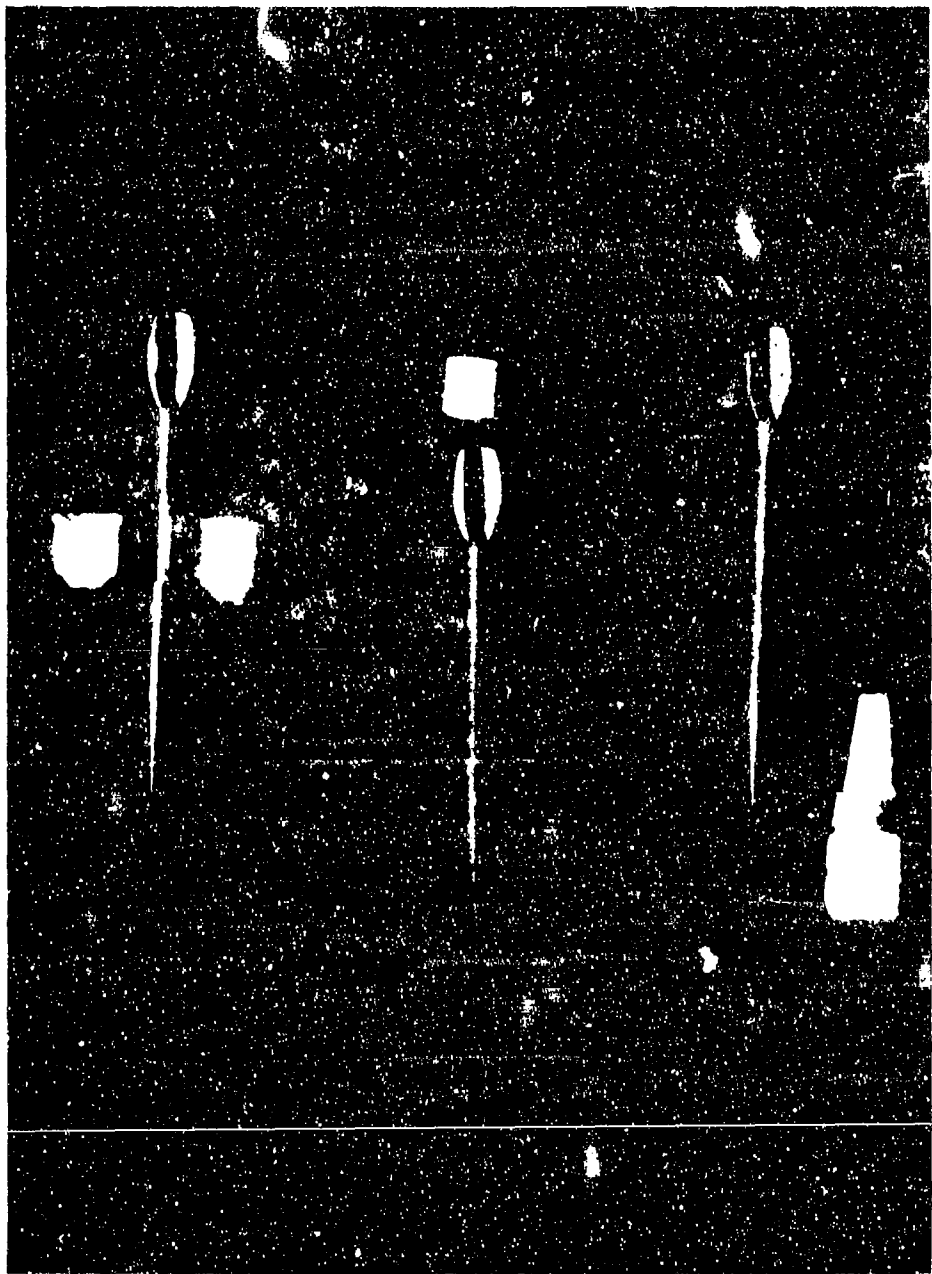


Figure 2. Flechette Sabot Designs

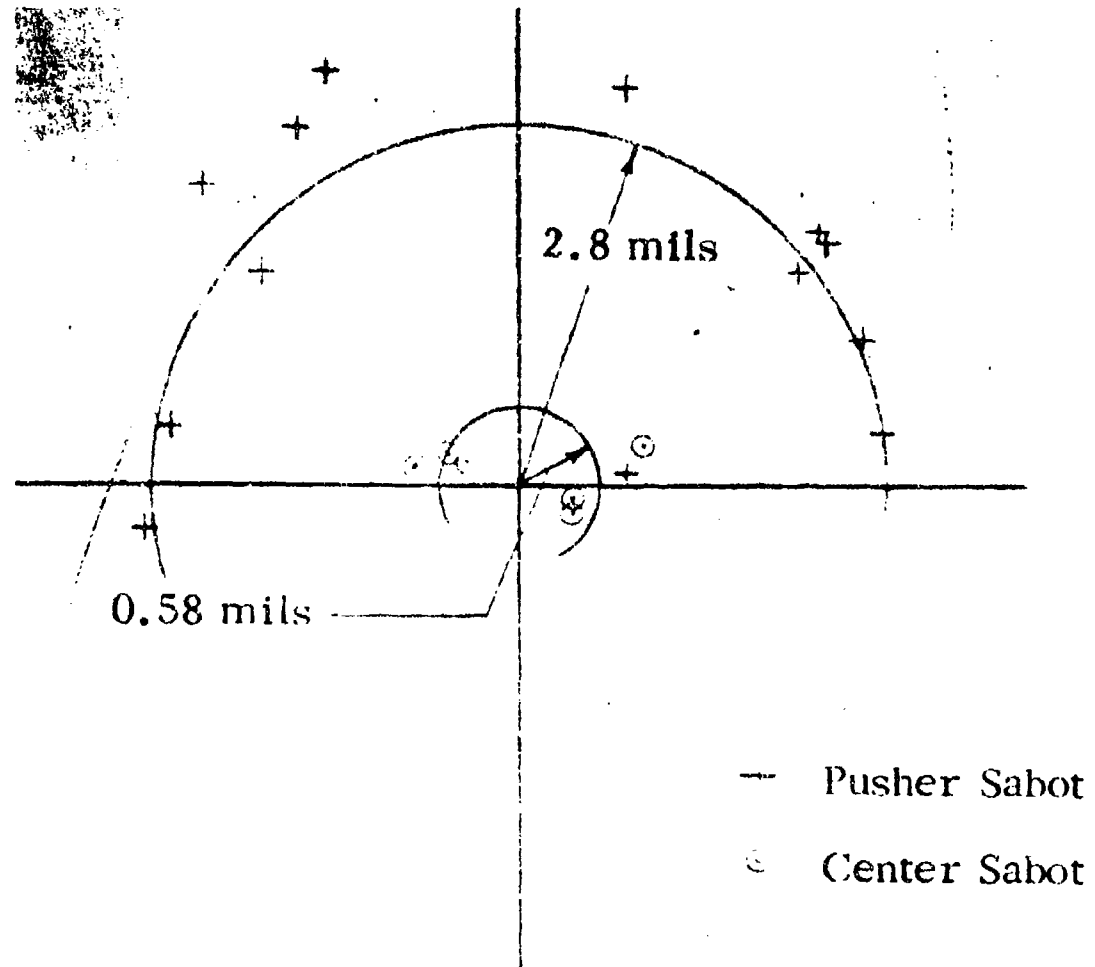


Figure 3. Comparison of Pusher and Center Sabot Results Flechette Testing

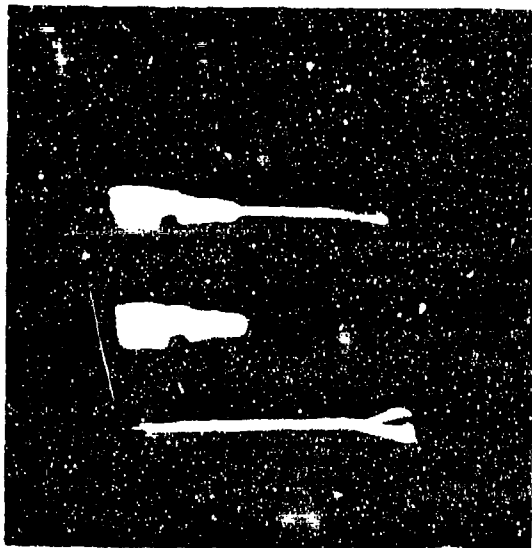
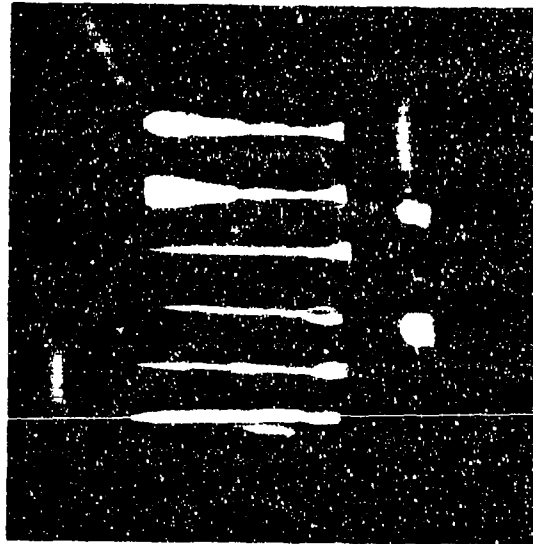


Figure 4. Producibility Sabot - R & D Flechette



5. Various Puller and Pusher Sabots and Flechette Configurations

APPENDIX B

DYNAMIC SUPERSONIC WIND TUNNEL TESTS OF FOUR-FLECHETTE CONFIGURATIONS

DYNAMIC SUPERSONIC WIND TUNNEL TESTING*

ABSTRACT

The linear values of the static pitching moment stability coefficient, $C_{M\alpha}$, and the damping moment stability coefficient, $C_{Mq} + C_{M\dot{\alpha}}$, are determined versus angle of attack for four flechette designs. The program is carried out in a vertical supersonic wind tunnel using a one-degree-of-freedom dynamic testing technique. This method allows the model to go through free one-degree-of-freedom angular oscillations. Stability parameters are extracted from a film record of this motion and the stability coefficients are computed using the WOBBLE computer program. Good repeatability of the results is shown for low angle of attack.

*Prepared by Michael Garsik.

TABLE OF CONTENTS

	Page
TABLE OF CONTENTS	18
LIST OF FIGURES	20
LIST OF SYMBOLS	23
INTRODUCTION	25
AEROBALLISTIC THEORY	29
Axis Systems	29
Linear Theory	29
Computation of Aerodynamic Stability Parameters	37
Computation of Linear Stability Coefficients	37
EXPERIMENTAL TECHNIQUE	39
One-Degree-of-Freedom Wind Tunnel Test Procedure	39
One-Degree-of-Freedom Data Reduction Procedure	53
Tunnel Velocity Measuring Technique	53
ONE DEGREE-OF-FREEDOM TEST RESULTS	59
One-Degree-of-Freedom Data Reduction	59
One-Degree-of-Freedom Stability Coefficients	59
CONCLUSION	94
APPENDIX A	95

TABLE OF CONTENTS (concluded)

	Page
APPENDIX B	96
APPENDIX C	98

LIST OF FIGURES

Number	Title	Page
1	Space Fixed Axis System	30
2	Aeroballistic Axis System	31
3	Static and Dynamic Fluid Forces	33
4	Single-Degree-of-Freedom Motion	38
5	Schematic of Ground Point	40
6	Schematic of Olin	41
7	Schematic of Swaged Point	42
8	Schematic of Tracer	43
9	Supersonic Wind Tunnel	44
10	Flechette Mounted in Supersonic Wind Tunnel	45
11	Exterior Support System	46
12	Exterior Support System (Exploded View) . .	47
13	Retaining Mechanism	51
14	Camera Set-Up	52
15	Optical Comparator	54
16	Reduction Coordinates	55
17	Velocity Measurement Set-Up	56
18	Representative Plot P.E. vs Time	61
19	λ_1 vs Time (Ground Point)	62
20	ω_1 vs Time (Ground Point)	63
21	K_1 vs Time (Ground Point)	64

LIST OF FIGURES (continued)

Number	Title	Page
22	K_T vs Time (Ground Point)	65
23	λ_1 vs Time (Olin)	66
24	ω_1 vs Time (Olin)	67
25	K_1 vs Time (Olin)	68
26	K_T vs Time (Olin)	69
27	λ_1 vs Time (Swaged Point)	70
28	ω_1 vs Time (Swaged Point)	71
29	K_1 vs Time (Swaged Point)	72
30	K_T vs Time (Swaged Point)	73
31	λ_1 vs Time (Tracer)	74
32	ω_1 vs Time (Tracer)	75
33	K_1 vs Time (Tracer)	76
34	K_T vs Time (Tracer)	77
35	C_{M_α} vs α (Ground Point)	78
36	$(C_{M_q} + C_{M_\alpha})$ vs α (Ground Point)	79
37	C_{M_α} vs α (Olin)	80
38	$(C_{M_q} + C_{M_\alpha})$ vs α (Olin)	81
39	C_{M_α} vs α (Swaged Point)	82
40	$(C_{M_q} + C_{M_\alpha})$ vs α (Swaged Point)	83
41	C_{M_α} vs α (Tracer)	84
42	$(C_{M_q} + C_{M_\alpha})$ vs α (Tracer)	85

LIST OF FIGURES (continued)

Number	Title	Page
43	C_{M_α} vs Mach Number (Ground Point)	86
44	$(C_{M_q} + C_{M_{\dot{\alpha}}})$ vs Mach Number (Ground Point)	87
45	C_{M_α} vs Mach Number (Olin)	88
46	$(C_{M_q} + C_{M_{\dot{\alpha}}})$ vs Mach Number (Olin)	89
47	C_{M_α} vs Mach Number (Swaged Point)	90
48	$(C_{M_q} + C_{M_{\dot{\alpha}}})$ vs Mach Number (Swaged Point)	91
49	C_{M_α} vs Mach Number (Tracer)	92
50	$(C_{M_q} + C_{M_{\dot{\alpha}}})$ vs Mach Number (Tracer) . . .	93

LIST OF SYMBOLS

a	Local speed of sound (feet/second)
a_T	Total speed of sound (feet/second)
C_{M_α}	Static pitching moment stability coefficient (rad^{-1})
	$C_{M_\alpha} = \frac{M_\alpha \alpha}{Q S d}$
C_{M_q}	Damping moment stability coefficient (rad^{-1})
	$C_{M_q} = \frac{M_q q}{Q S d \frac{q d}{2V}}$
$C_{M_{\dot{\alpha}}}$	Damping moment stability coefficient due to aerodynamic lag (rad^{-1})
	$C_{M_{\dot{\alpha}}} = \frac{M_{\dot{\alpha}} \dot{\alpha}}{Q S d \frac{\dot{\alpha} d}{2V}}$
$C_{M_{\delta_\epsilon}}$	Aerodynamic asymmetry moment stability coefficient (rad^{-1})
	$C_{M_{\delta_\epsilon}} = \frac{M_{\delta_\epsilon} \delta_\epsilon}{\delta_\epsilon Q S d}$
d	Reference length, missile diameter (ft.)
$I = I_y = I_z$	Pitching moment of inertia (slugs/feet 2)
$K_{1,2}$	Amplitude of nutation and precession arms (rad)
K_3	Trim mode (rad)
L, M, N	Moments about X, Y, Z aeroballistic axes (ft-lb)
M_α	Pitching moment derivatives (ft-lbs/rad)
$M_{\dot{\alpha}}$	Damping moment derivative due to aerodynamic lag (ft-lbs sec/rad)

LIST OF SYMBOLS (continued)

M_q	Damping moment derivative (ft-lbs sec/rad ²)
M_{δ_e}	Asymmetry moment derivative (ft-lbs/rad)
p, q, r	Angular rates about aeroballistic axes (rad/sec)
Q	Dynamic pressure $Q = \frac{1}{2} \rho U^2$ (lb/ft ²)
R	Gas constant
S	Reference area, $S = \frac{\pi d^2}{4}$ (ft ²)
t	Time (sec)
T_t	Total temperature °R
U	Total velocity (ft/sec)
X, Y, Z	Aeroballistic axes
x, y, z	Space-fixed axes
α	Angle of attack (rad)
β	Angle of sideslip (rad)
θ, ψ, ϕ	Euler angles (rad or deg)
ρ	Air density (slugs/ft ³)
$\lambda_{1,2}$	Damping rate (rad/sec)
$\omega_{1,2}$	Nutation and precession frequency (rad/sec)
γ	Ratio of specific heats, $\frac{c_p}{c_v}$
δ	Phase angle (rad)

INTRODUCTION

With the advent of more advanced analysis techniques¹ today's aerodynamicist has the power to achieve a better understanding of the free flight performance of a flight vehicle. Data such as angular motion, jump angle and dispersion can now be extracted from free flight data and studied² so that previously undetected instabilities and design failures can be corrected. Obviously from this there arises a clear need for development of free flight simulations.^{3,4} The random method used in trying to solve the problems of stability and flight performance would prove dangerous and costly if full scale flight tests were conducted. It would be much cheaper and safer to experiment with new designs on models of the actual configuration. This presents the problems of simulating free flight motions so that data can be extracted and the new designs evaluated just as if the test were conducted on a full scale model in free flight.

Ballistic range firings was one of the initial attempts at a flight simulation technique. It involved taking photographs at various stations along a firing range of a model that had been launched from a gun. Because of the limitations on the types of motion that could be observed, the lack of control of initial conditions, and other limiting factors, it soon became apparent that a more sophisticated method of simulation was necessary. Attention was turned to the wind tunnel.

Attempts to study the angular motions of flight vehicles in the wind

tunnel began by mechanically reproducing them. This technique ran into several problems, in particular separating the driving mechanism response from the aerodynamic response and the fact that the technique is limited in that a mechanical response, rather than a free one, to the flow field is used. In recent years the most successful wind tunnel simulation technique, dynamic wind tunnel testing, has been developed. Actually there are several types of dynamic wind tunnel testing. The free flight angular oscillation method exhibits complete six-degree-of-freedom motion and needs no external support system, however certain limitations to this technique do exist. The duration of the simulation is restrictive hence length of the "flight" is very short. Also, a lack of control of initial conditions prohibits the study of particular flight modes. Another method, that of constrained angular oscillations, eliminates these disadvantages at the expense of introducing new ones. The most predominate disadvantage is the interference effects of the support system on the response of the model to the flow field. This assumes that the problem of building an adequate support system can be solved. It is important to have control over the initial conditions and the length of the simulation run in order to simulate the free flight angular motions in the wind tunnel. Of course, the choice of which method to use depends on the careful consideration of the problem at hand and the experimental limitations which could be allowed and not interfere with the test being carried out.

With regard to the constrained angular oscillation technique and its use in the supersonic wind tunnel, several methods have been

developed. The gas bearing system is one that is ideally suited to the study of low fineness ratio, non-finned bodies such as projectiles. It does not lend itself to the study of high fineness ratio finned bodies quite as well. One of the drawbacks of this technique is the high cost of construction and maintenance of the system. The jewel bearing support system has been utilized in supersonic wind tunnel testing to observe the rolling motion of various models of flight vehicles. Such a system has been successfully employed in determining the roll damping moment and induced roll moment stability coefficients for different flight configurations.

This investigation is intended to determine the linear pitching moment and damping moment stability coefficients of four flechette configurations in a supersonic regime. The study was conducted under a contract awarded to the Department of Aerospace and Mechanical Engineering at the University of Notre Dame by Frankford Arsenal, Philadelphia, Pa. The contract deals with a study of the jump angle and dispersion of the flechette configurations. An underlying intent will be to document the constrained angular oscillation technique used in the supersonic wind tunnel tests.

In order to study the performance of the flechette configurations and to be able to predict their flight path, a basic understanding of the stability of the rounds must be obtained. Adequate stability prediction requires that techniques of flight simulation be used which will produce continuous results for supersonic conditions.

The actual steps taken in developing such a program of dynamic wind tunnel tests were: 1) adapting the one-degree-of-freedom free oscillation technique to the supersonic wind tunnel; 2) recording the one degree of freedom angular oscillations of the models in the supersonic wind tunnel by high speed photography techniques; 3) reducing the motion of the models to numerical values of angle of attack; 4) fitting the Aero-ballistic Theory to the angular data obtained to determine the stability parameters $K_{N,P}$, $\lambda_{N,P}$, $\omega_{N,P}$ ^{5,6}; 5) computing the aerodynamic stability coefficients from Linear Theory using the stability parameters, model parameters, wind tunnel Mach number and density; 6) analyzing the interference of the support system by checking the repeatability of results.

To accomplish the goals set down a unique method of supporting the pure pitch flechette models are utilized.⁷ It involved suspending the model in the test section of the University of Notre Dame's vertical supersonic wind tunnel and allowing it to go through free one-degree-of-freedom oscillations. The low friction in the system allowed continuous motions to be obtained and recorded and the stability coefficients to be extracted from the angular data.

AEROBALLISTIC THEORY

Axis Systems

Two basic axis systems are used. The space fixed axis system (Figure 1) is the system in which the data is recorded. The aeroballistic axis system (Figure 2) is the system in which the equations of motion are expressed. By choosing the x -axis of the space fixed system to coincide with the velocity vector the data is made directly compatible to the equations of motion. From Figures 1 and 2 it is seen that $\theta = \alpha$ and $q = \dot{\theta}$. Care must be taken in extending this comparison beyond this point.

The linear theory for a missile constrained at its center of gravity for one-degree-of-freedom pure pitching is as follows.

Linear Theory

In the development of the Linear Theory several assumptions are made:

1. Aerodynamic coefficients are constant
2. Velocity and density are constant
3. All angular motions except roll are small enough that the small angle approximations may be used:

$$\sin x = \tan x = x$$

$$\cos x = 1$$

4. The missile has mirror symmetry and trigonal or greater rotational symmetry.

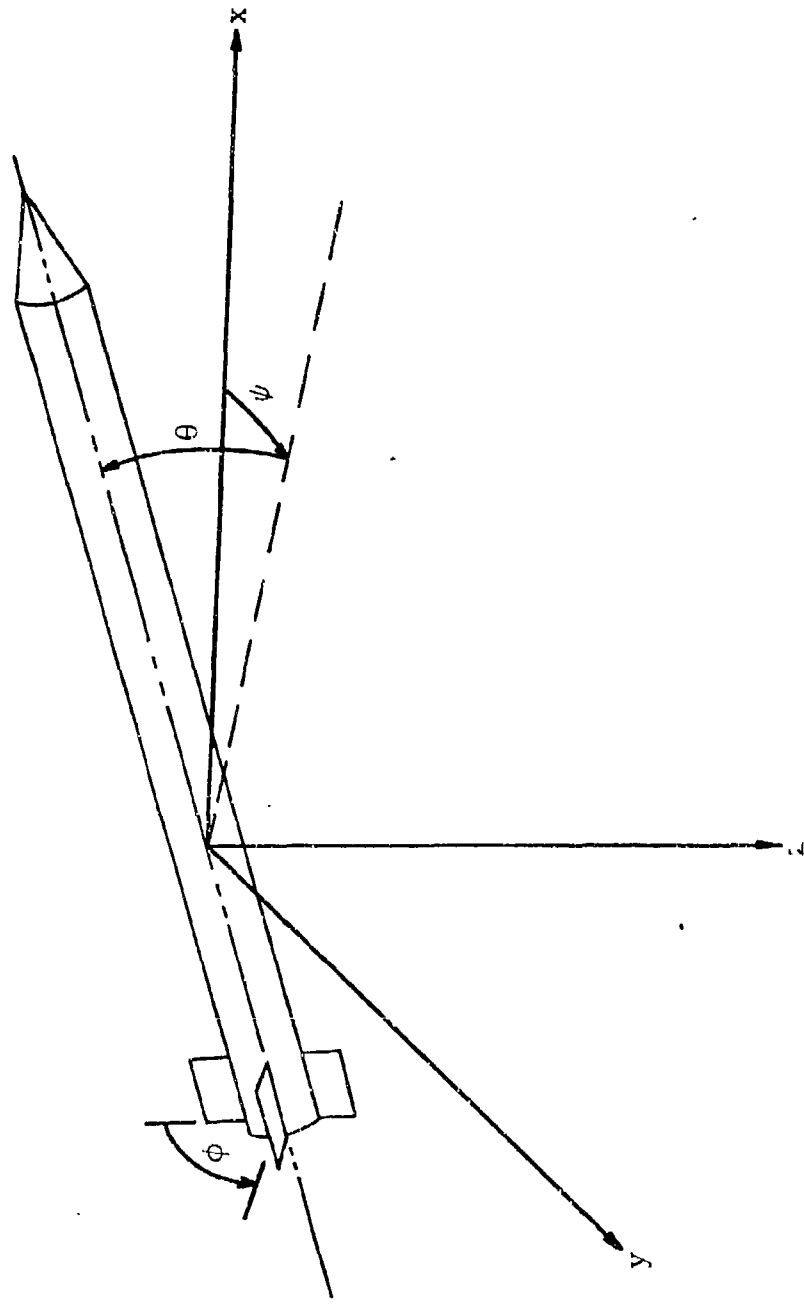


Figure 1. Space Fixed Axis System

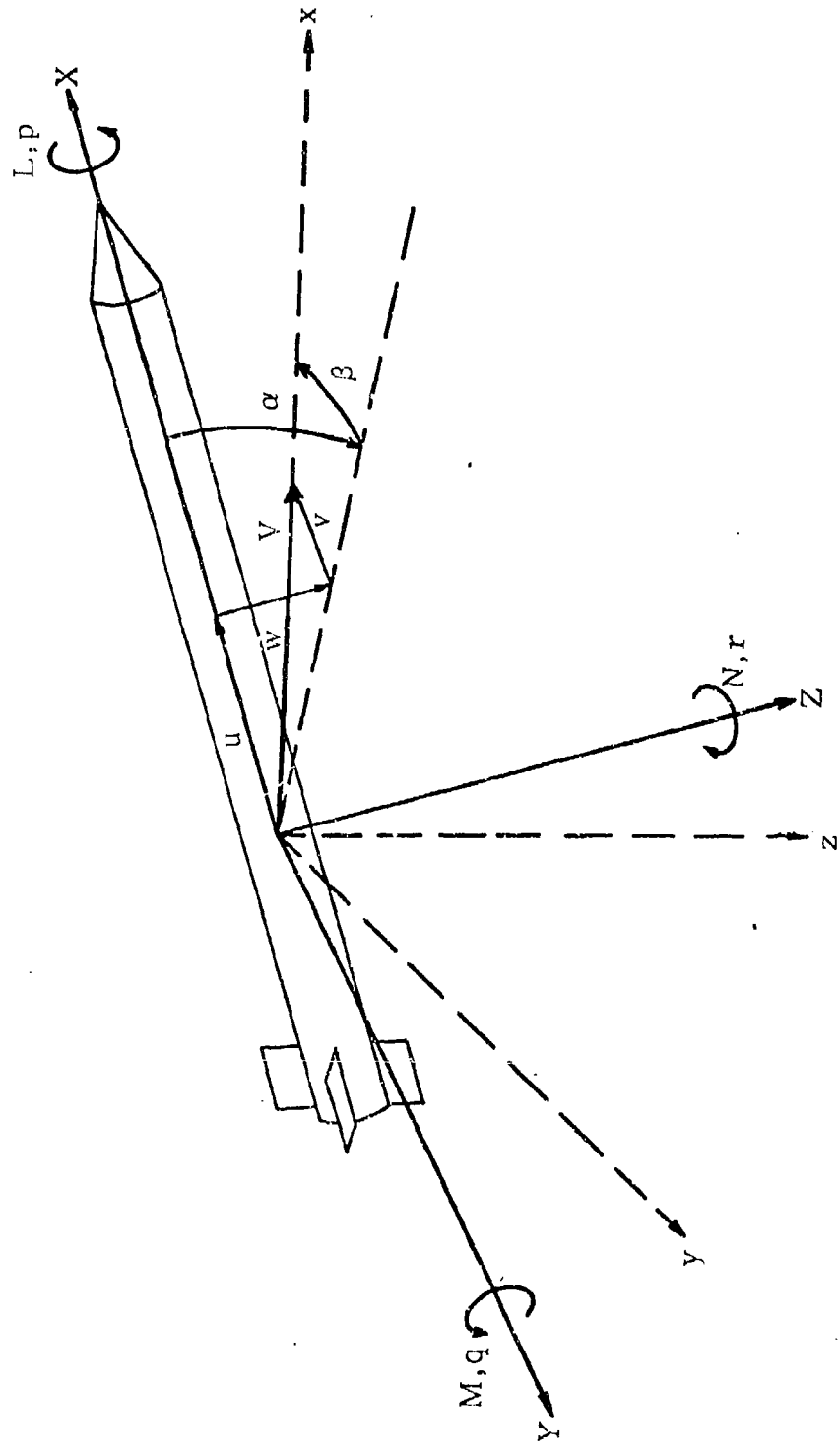


Figure 2. Aeroballistic Axis System

The fundamental differential equation of motion for the rotational motion is

$$M = I \ddot{\theta} \quad (1)$$

The sum of the acting aerodynamic moments, shown in Figure 3, which are assumed to vary linearly with angle of attack is

$$M = M_{\alpha} \alpha + M_q q + M_{\dot{\alpha}} \dot{\alpha} + M_{\delta_e} \delta_e \quad (2)$$

where

$$\begin{aligned} M_{\alpha} &= C_{M_{\alpha}} \frac{1}{2} \rho U^2 S d \\ M_q &= C_{M_q} \left[\frac{d}{2u} \right] \frac{1}{2} \rho U^2 S d \\ M_{\dot{\alpha}} &= C_{M_{\dot{\alpha}}} \left[\frac{d}{2u} \right] \frac{1}{2} \rho U^2 S d \\ M_{\delta_e} &= C_{M_{\delta_e}} \frac{1}{2} \rho U^2 S d \end{aligned} \quad (3)$$

Because of the selection of the particular axis systems and their orientation, Equation 1 can be rewritten as

$$M = I \ddot{\alpha} \quad (4)$$

Equation 2 can be rewritten as

$$M = M_{\alpha} \alpha + M_q q + M_{\dot{\alpha}} \dot{\alpha} + M_{\delta_e} \delta_e \quad (5)$$

Combining Equations 4 and 5 and rearranging

$$\ddot{\alpha} - \left[\frac{M_q + M_{\dot{\alpha}}}{I} \right] \dot{\alpha} - \left[\frac{M_{\alpha}}{I} \right] \alpha = M_{\delta_e} \delta_e \quad (6)$$

and

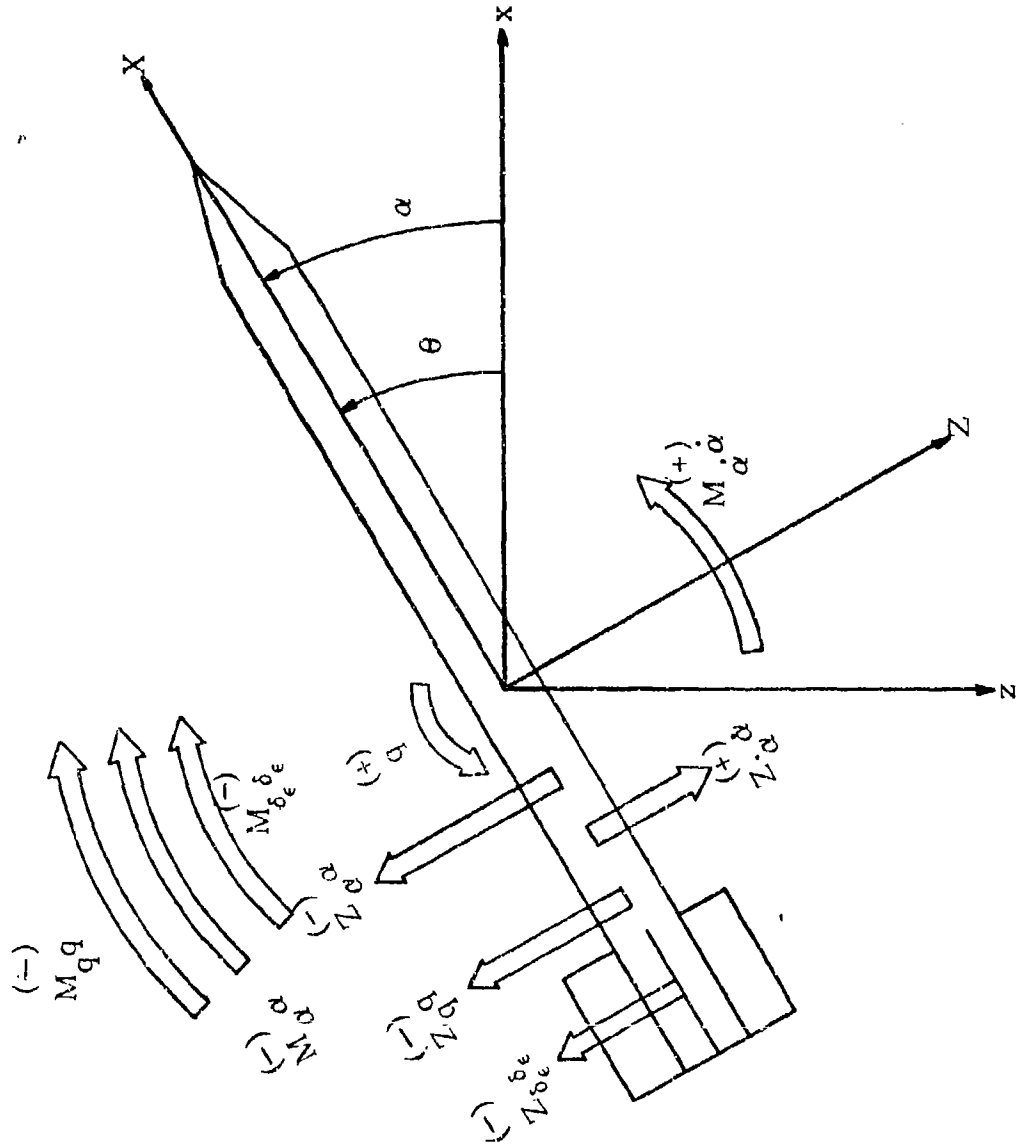


Figure 3. Static and Dynamic Fluid Forces

$$\alpha + N_1 \dot{\alpha} + N_2 \alpha = N_3 \quad (7)$$

where

$$\begin{aligned} N_1 &= - \left[\frac{M_q + M_\delta}{I} \right] \\ N_2 &= - \left[\frac{M_\alpha}{I} \right] \\ N_3 &= \left[\frac{M_\delta \delta_e}{I} \right] \end{aligned} \quad (8)$$

Solving for the homogeneous solution to Equation 7 assume a solution of the form

$$\alpha = K e^{\phi t} \quad (9)$$

Differentiation of this yields

$$\dot{\alpha} = \phi K e^{\phi t} \quad \ddot{\alpha} = \phi^2 K e^{\phi t} \quad (10)$$

Substitute Equation 9 and 10 into the homogeneous form of Equation 7

$$\phi^2 K e^{\phi t} + N_1 \phi K e^{\phi t} + N_2 K e^{\phi t} = 0$$

$$\phi^2 + N_1 \phi + N_2 = 0$$

which has a solution of the form

$$\phi_{1,2} = - \frac{N_1}{2} \pm \frac{1}{2} \sqrt{N_1^2 - 4N_2} \quad (11)$$

For missiles in air the assumption that the products of stability derivatives are negligible when compared to themselves (i.e. $N_1^2 \ll N_2$)

can be made. This is generally a good assumption and will be made here. Hence Equation 11 can be written

$$\begin{aligned}\phi_{1,2} &= -\frac{N_1}{2} \pm i\sqrt{N_2} \\ &= \lambda_{1,2} + i\omega_{1,2}\end{aligned}\tag{12}$$

The homogeneous solution has the form

$$\alpha = K_1 e^{(\lambda_1 + i\omega_1)t} + K_2 e^{(\lambda_2 - i\omega_2)t}\tag{13}$$

where

$$\lambda_1 = \lambda_2 = \left[\frac{d}{2u} \right] \frac{1}{2} \rho U^2 S d - \frac{C_M q + C_M \dot{\alpha}}{2I}\tag{14}$$

$$\omega_1 = \left[\frac{C_M \dot{\alpha} + \frac{1}{2} \rho U^2 S d}{I} \right]^{1/2}\tag{15}$$

$$\omega_2 = \left[\frac{C_M \dot{\alpha} + \frac{1}{2} \rho U^2 S d}{I} \right]^{1/2}\tag{16}$$

and

$$C_M \dot{\alpha} = -\frac{2I\omega^2}{\rho U^2 S d}\tag{17}$$

$$(C_M q + C_M \dot{\alpha}) = \frac{8I\lambda}{\rho U S d}\tag{18}$$

Solving for the particular part of the solution of Equation 7 consider the steady state case of no pitching, Equation 7 would be

$$N_2 \alpha = N_3$$

$$\alpha = \frac{N_3}{N_2} = -\frac{M_{\delta_e} \delta_e}{M_\alpha} = K_3 \quad (19)$$

This is the particular part of the solution of Equation 7. The complete solution is

$$\alpha = K_1 e^{(\lambda_1 + i\omega_1)t} + K_2 e^{(\lambda_2 + i\omega_2)t} + K_3 \quad (20)$$

where K_1 and K_2 are found from initial conditions and are

$$K_{1,2} = \frac{\dot{\alpha}_0 - \phi_{2,1} \alpha_0}{\phi_{1,2} - \phi_{2,1}} + \frac{\phi_{2,1} K_3}{(\phi_{1,2} - \phi_{2,1})} \quad (21)$$

Since the magnitudes of ϕ_1 and ϕ_2 are always equal and K_3 is constant

$$K_1 = K_2 = K$$

Since

$$e^{i\omega t} = \cos \omega t + i \sin \omega t$$

Equation 19 can be written as

$$\alpha = 2K e^{\lambda t} \cos \omega t + K_3$$

or in a more general form

$$\alpha = K_0 e^{\lambda t} \cos(\omega t + \delta) + K_3 \quad (22)$$

where

$$K_0 = 2K$$

Equation 22 is the basic modal which will be used to fit the one-degree-of-freedom data. A physical representation of what Equation 22 means and how it reduces the Tricyclic Theory to a pure pitching motion case is shown in Figure 4. The two arms K_1 and K_2 have been replaced by a single arm of length K where $K = K_1 + K_2$. This arm is rotating at a rate $\omega = \omega_1$ and has an initial orientation of $\delta = \delta_1$. The cosine function projects this arm onto the vertical axis of the aeroballistic axis system to give values of θ . This "projection" follows the pure pitching of the model as if it would look when observed from the rear.

Computation of Aerodynamic Stability Coefficients

To fit Equation 22 to the angular oscillation data the WOBBLE computer program was used. This program fits the theory to short segments of the data in overlapping pieces so that the stability parameters λ_1 , ω_1 and K_1 are determined as functions of time.

Computation of Linear Coefficients

Using the velocity and model parameters (Appendix A) along with λ_1 , ω_1 and K_1 the pitching moment stability coefficient, $C_{M\alpha}$, and the damping moment stability coefficient, ($C_{Mq} + C_{M\dot{\alpha}}$), were computed. Equations 17 and 18 were used to compute these coefficients as functions of time.

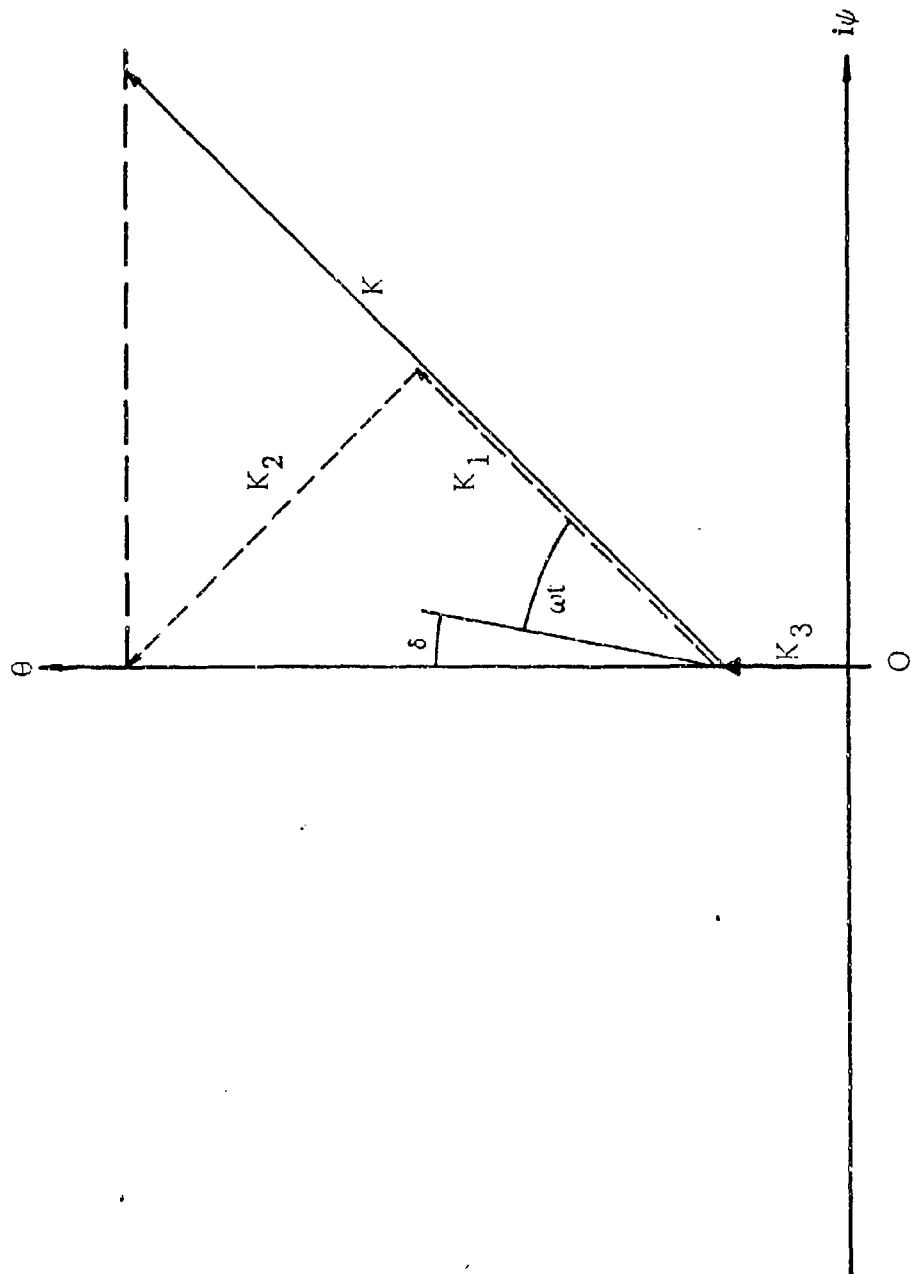


Figure 4. Single-Degree-of-Freedom Motion

Experimental Technique

Four different configurations were tested, the Ground Point, Olin, Swaged Point, and Tracer. Schematic representations of the model configurations are given in Figures 5, 6, 7, and 8 respectively.

One-Degree-of-Freedom Wind Tunnel Test Procedures

All of the tests were carried out in the University of Notre Dame's vertical supersonic wind tunnel shown in Figure 9. This wind tunnel features a vertical test section fitted with interchangeable steel and glass walls. A steel wall was used on one side to give maximum support to the model support system and a glass wall was used on the other side to allow observation of the models. The basic idea behind the support system is shown in Figures 10, 11, 12 and 12a.

To mount the model in the tunnel the following system was used. A length of piano wire 0.030" in diameter was inserted through the hole in the glass wall and into a syringe tube. The purpose of the two syringe tubes, one on each side of the model, was to insure that the model would remain in the center of the wind tunnel test section after it was released and allowed to oscillate. After running the wire through the first syringe tube, it was pushed through a small hole 0.040" in diameter drilled perpendicular to the longitudinal axis at the center of gravity of the model. The wire was then pushed through the second syringe tube and guided out of the test section through a hole in the steel wall. The wire was secured outside the wind tunnel test section by a system shown in Figure 11. On

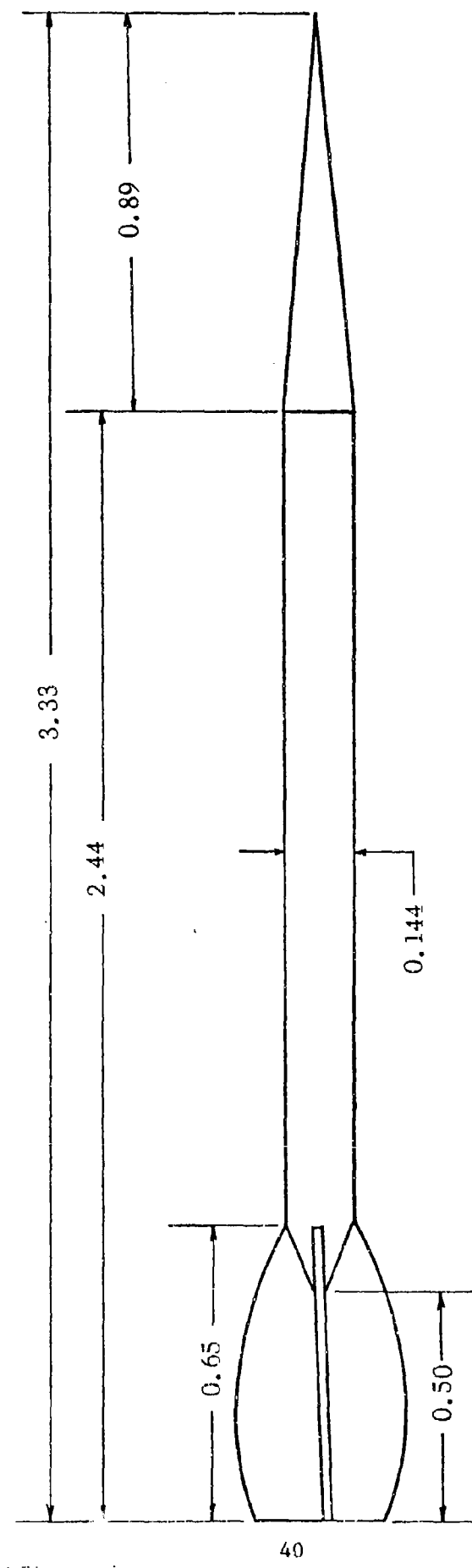


Figure 5. Ground Point Wind Tunnel Model

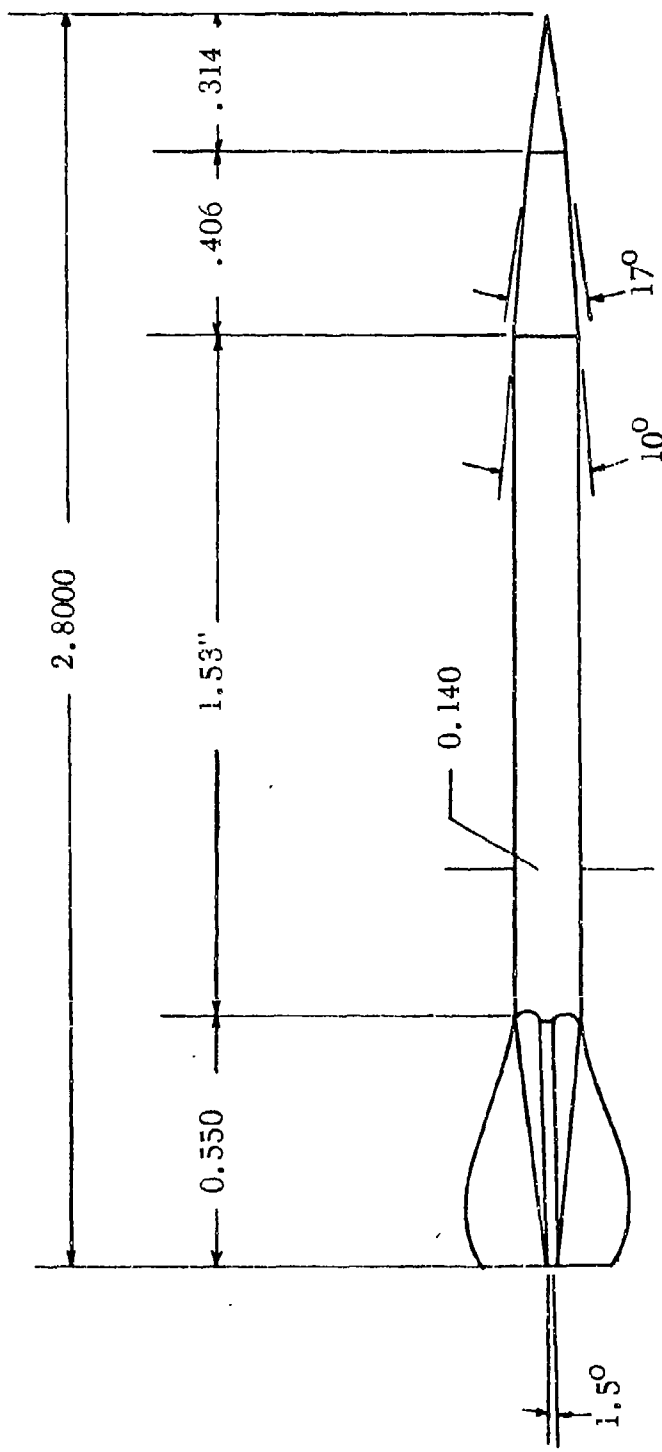


Figure 6. Olin Wind Tunnel Model

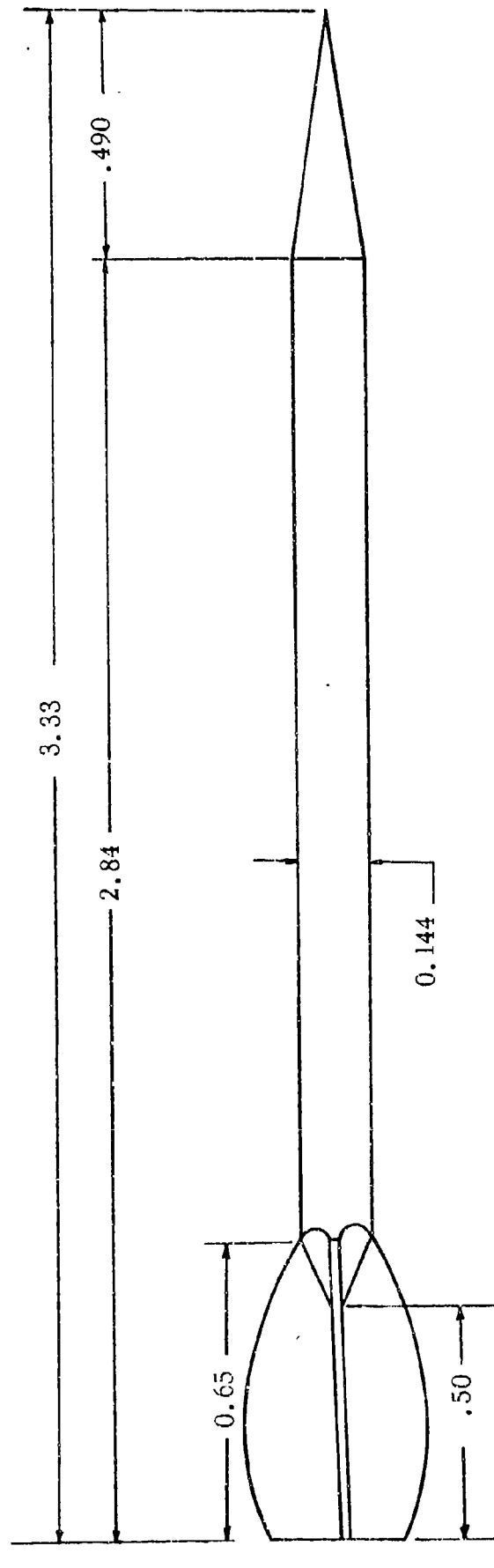


Figure 7. Swaged Point Wind Tunnel Model

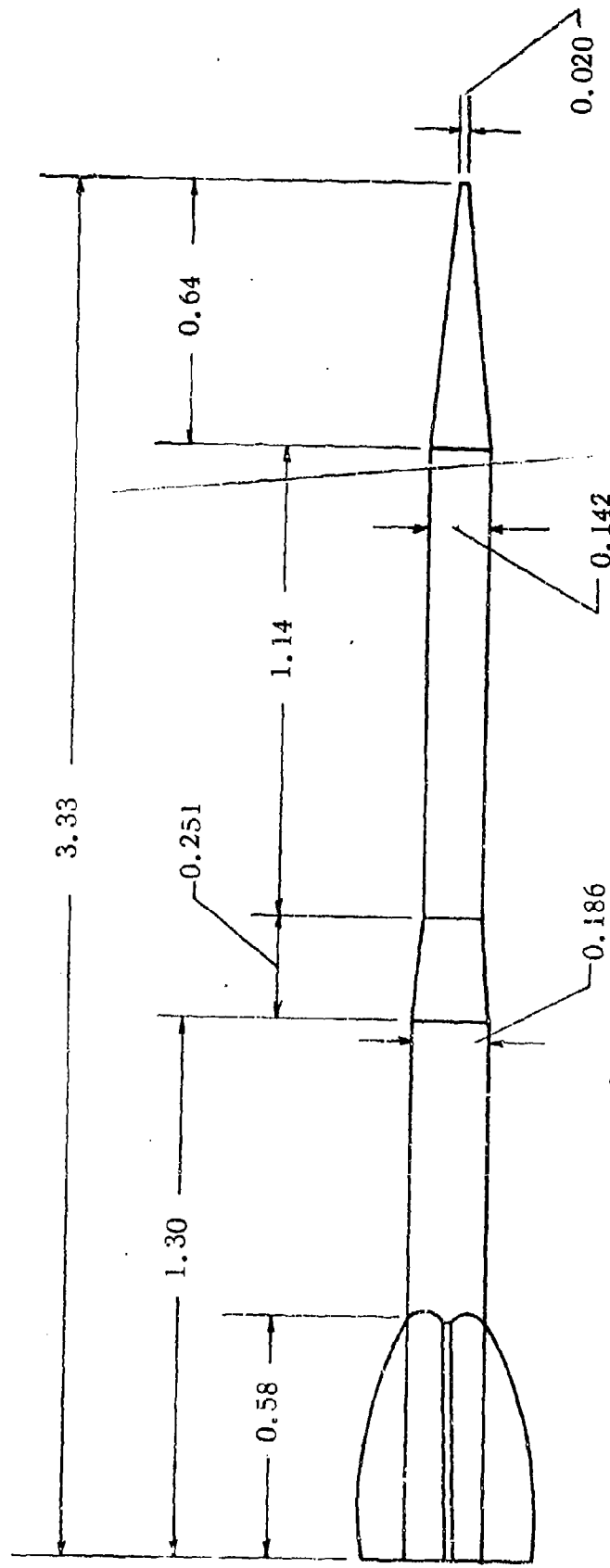


Figure 8. Tracer Wind Tunnel Model

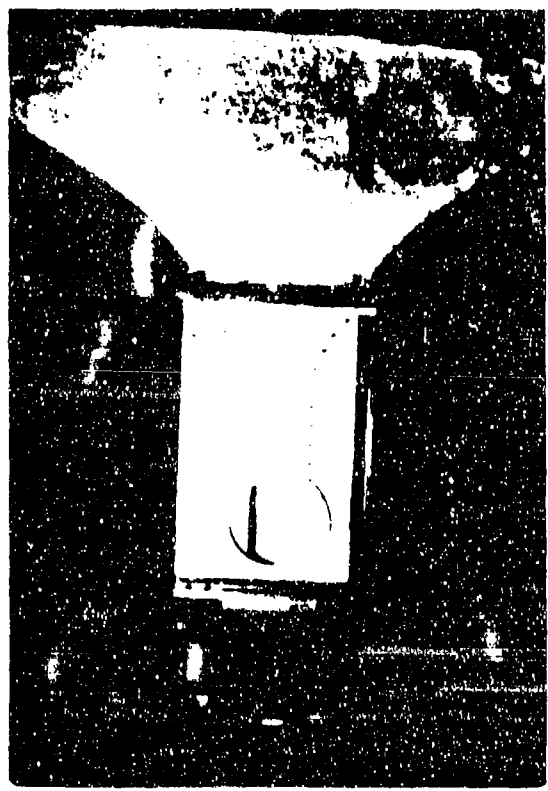


Figure 9. Vertical Supersonic Wind Tunnel

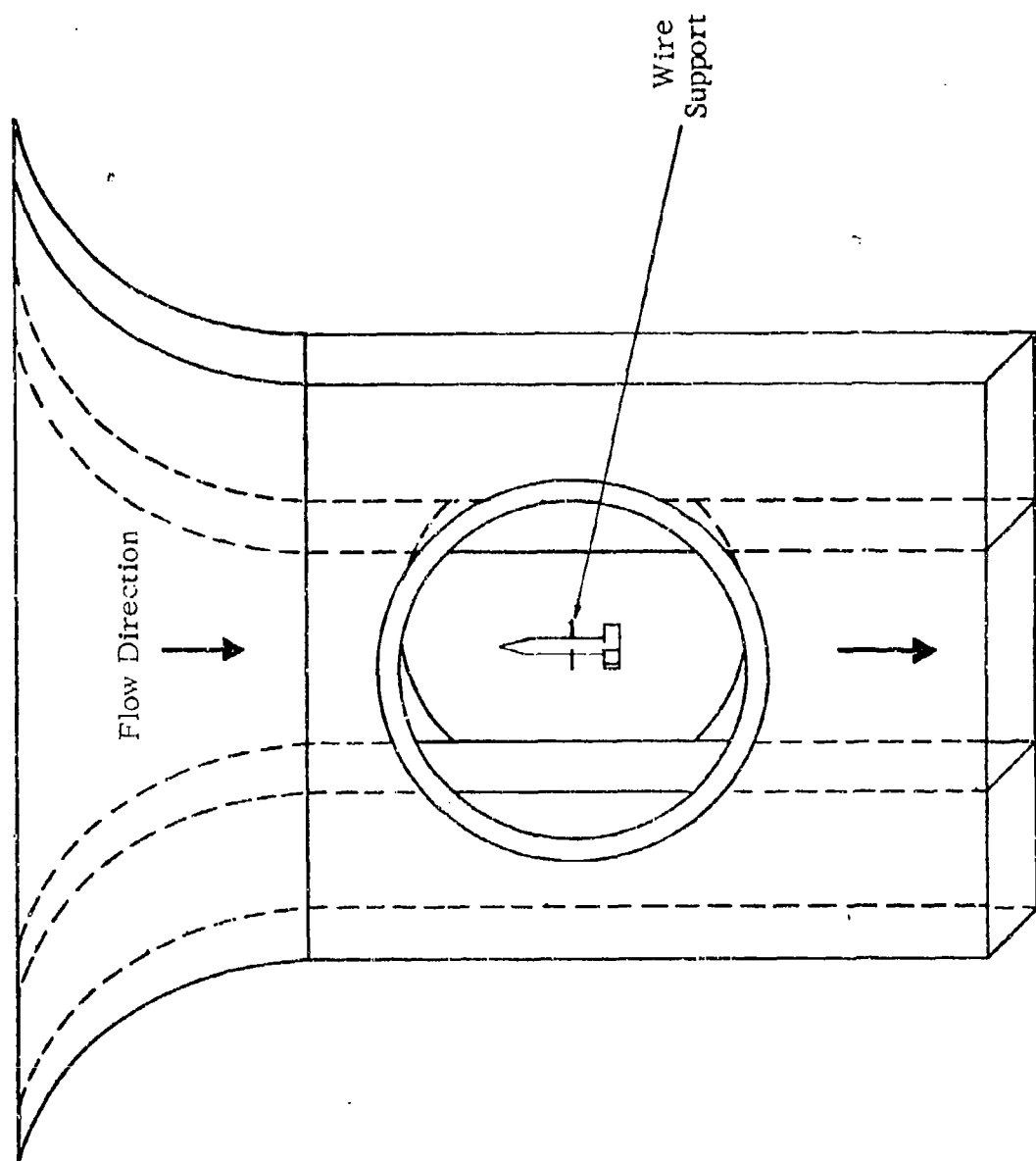


Figure 10. Flechette Mounted in Supersonic Wind Tunnel

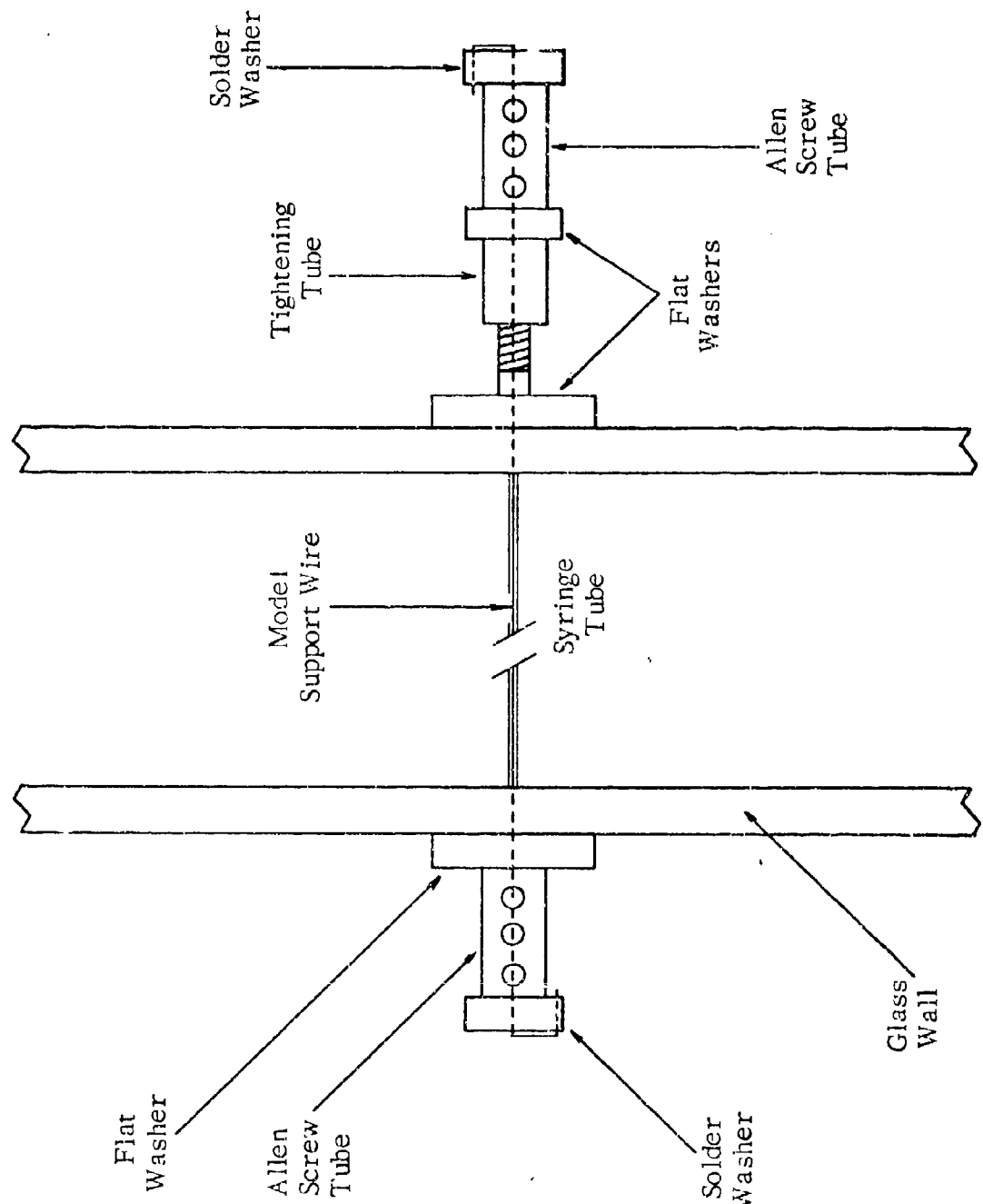


Figure 11. Exterior Support System

Figure 12. Exterior Support System (Exploded View)

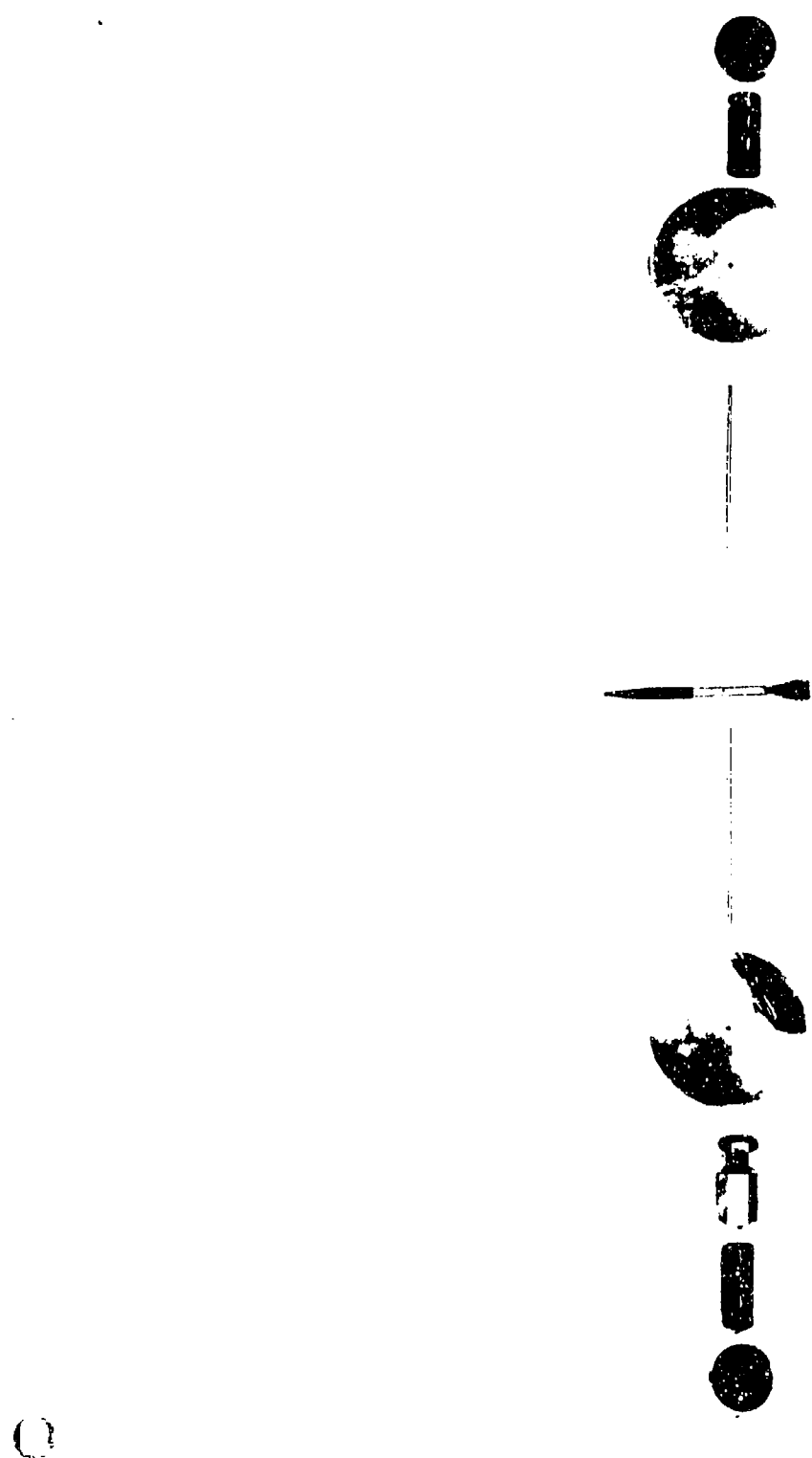
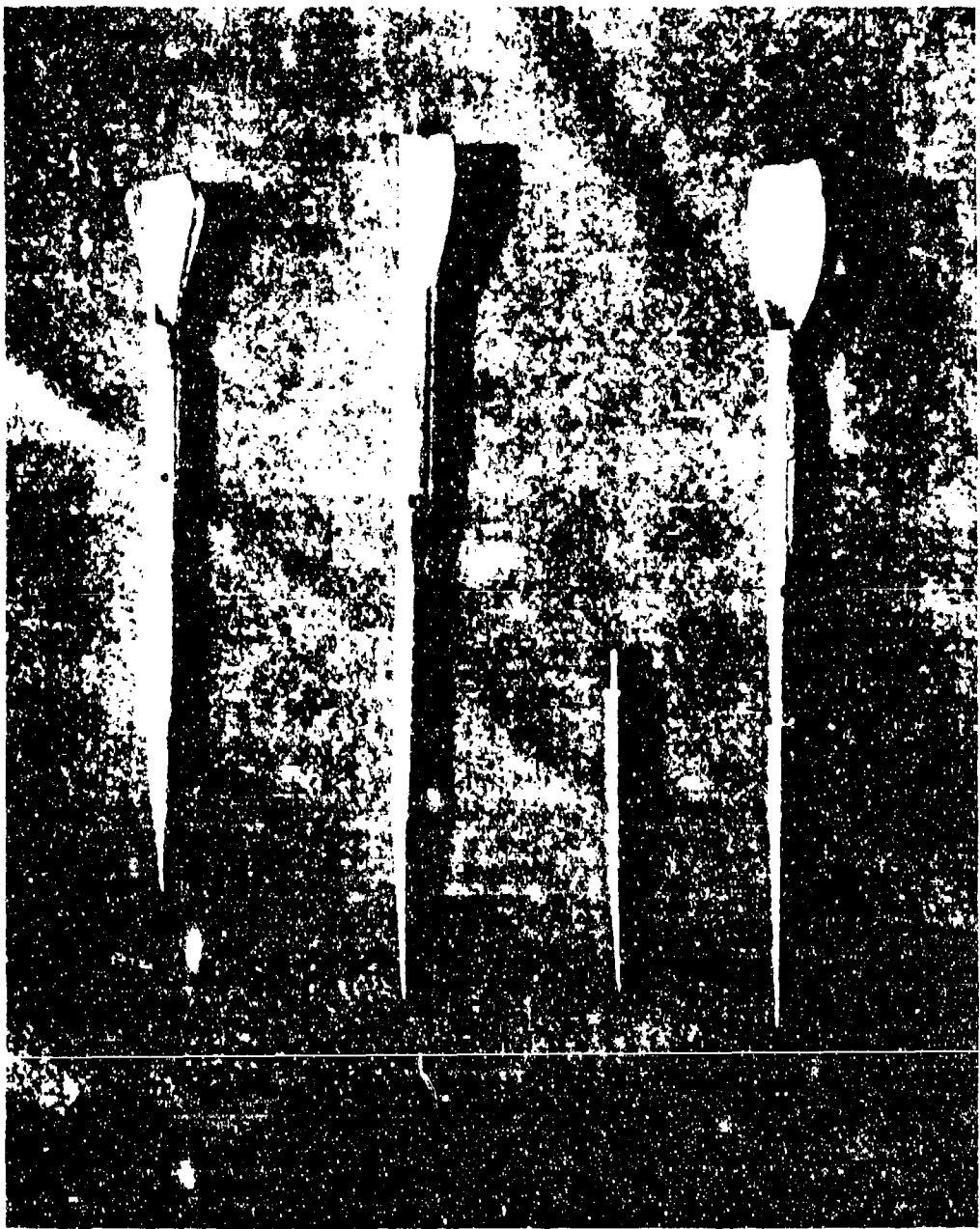


Figure 6. Supersonic Wind Tunnel Models



the glass wall side the wire was put through a hole in a flat washer placed flush against the glass wall. The hole in the washer had a diameter closer in size to the diameter of the wire than the hole in the glass wall. This cut down on the disturbance of the flow caused by the presence of the hole in the wall of the test section. Next, the wire was secured by placing it through an Allen screw tube and a solder washer. An Allen screw tube is a long cylinder with a small diameter hole drilled along its longitudinal axis and three small holes drilled perpendicular to the axis. These holes have been tapped to accommodate Allen screws which can be tightened to clamp down on the piano wire and hold it in place. A solder washer is a short cylinder containing two small diameter holes, one at the center and one near the outer edge. After running the wire through the center hole it can be bent around into the second hole at the outer edge. This hole also has a small hole drilled perpendicular to it and tapped to hold an Allen screw. As in the Allen screw tube, this Allen screw can be tightened down on the support wire to secure it. This system holds the support wire on the glass wall side of the test section.

After running the wire through the steel wall side it was pushed through a flat washer identical to the one on the glass wall side. A tightening tube was placed next in position and the wire was guided through it. A tightening tube is two concentric cylinders which are matched by threading. The length of the tube can be adjusted to the desired size by rotating the outer tube about the inner one. Finally, the

piano wire was secured using an Allen screw tube and a soldier washer. This completed the setting up of the support system. One advantage not already mentioned comes to light at this point. The models could be easily removed and inserted into the test section of the wind tunnel.

After the support system was in place the tension in the wire was adjusted by changing the length of the tightening tube. The tension was set so that the model would not change its vertical position after the tunnel was turned on. The model was then rotated 180° and held in place by a retaining mechanism shown in Figure 13. This system consisted of an extendable retainer which was placed around the nose of the model to secure it at its initial angle of attack. The retainer was connected to a release wire which could be manually operated from outside the tunnel. When the release wire was pulled the retainer would slip off the nose of the model and the model would be free to oscillate.

To record the oscillations of the model a Wollensak Fastex high speed motion picture camera was used. The camera was set-up as shown in Figure 14 on the glass wall side of the test section. Two floodlights, one just above the camera position and one above the inlet of the wind tunnel, were used to provide maximum lighting of the model in the test section. The camera was operated at a speed of 3000 frames per second for three seconds with a lens opening of f5.6.

Upon completing all preparations the tunnel was started following the procedure in Appendix B. The retainer was pulled back and the subsequent angular motion of the model was recorded.

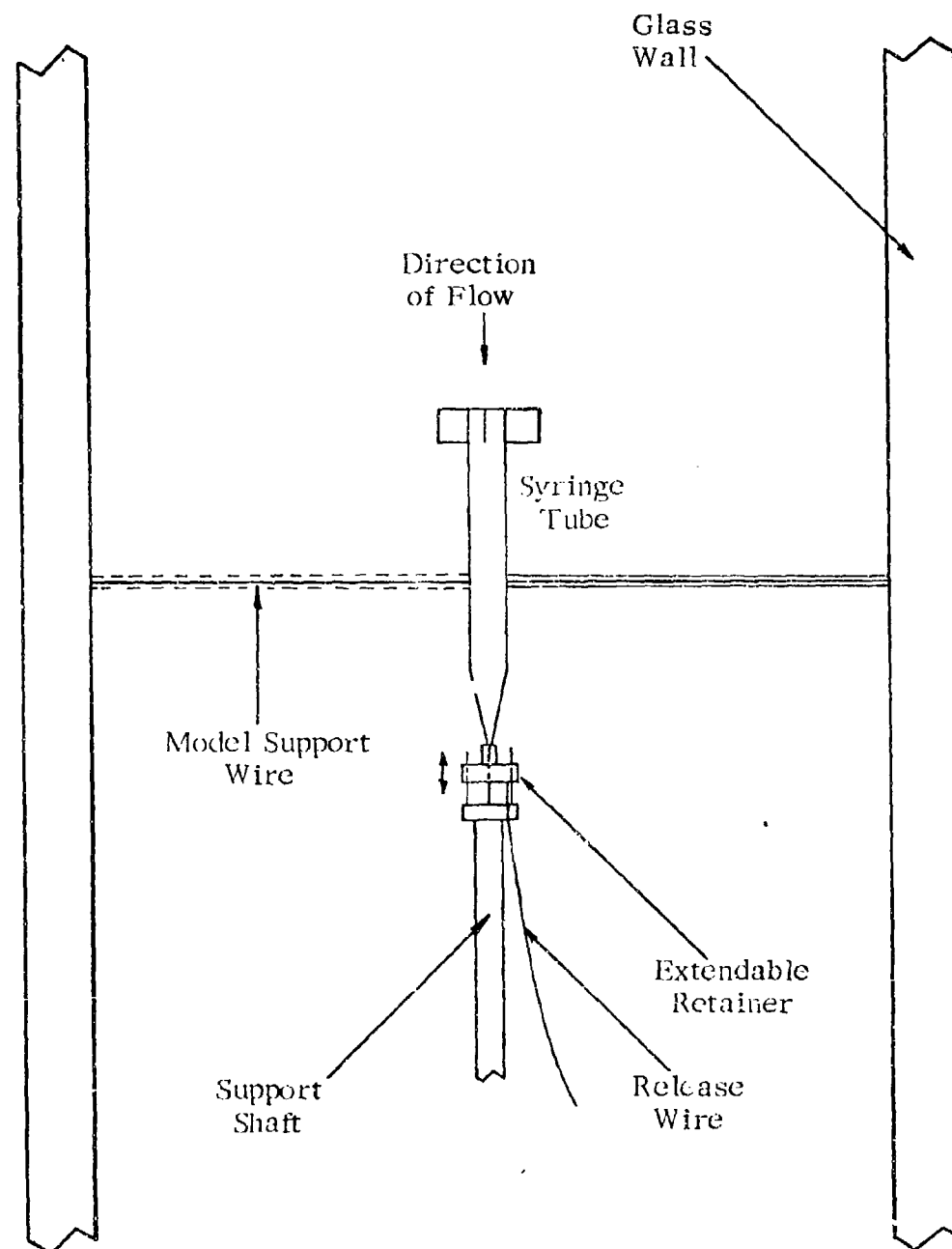


Figure 13. Retaining Mechanism

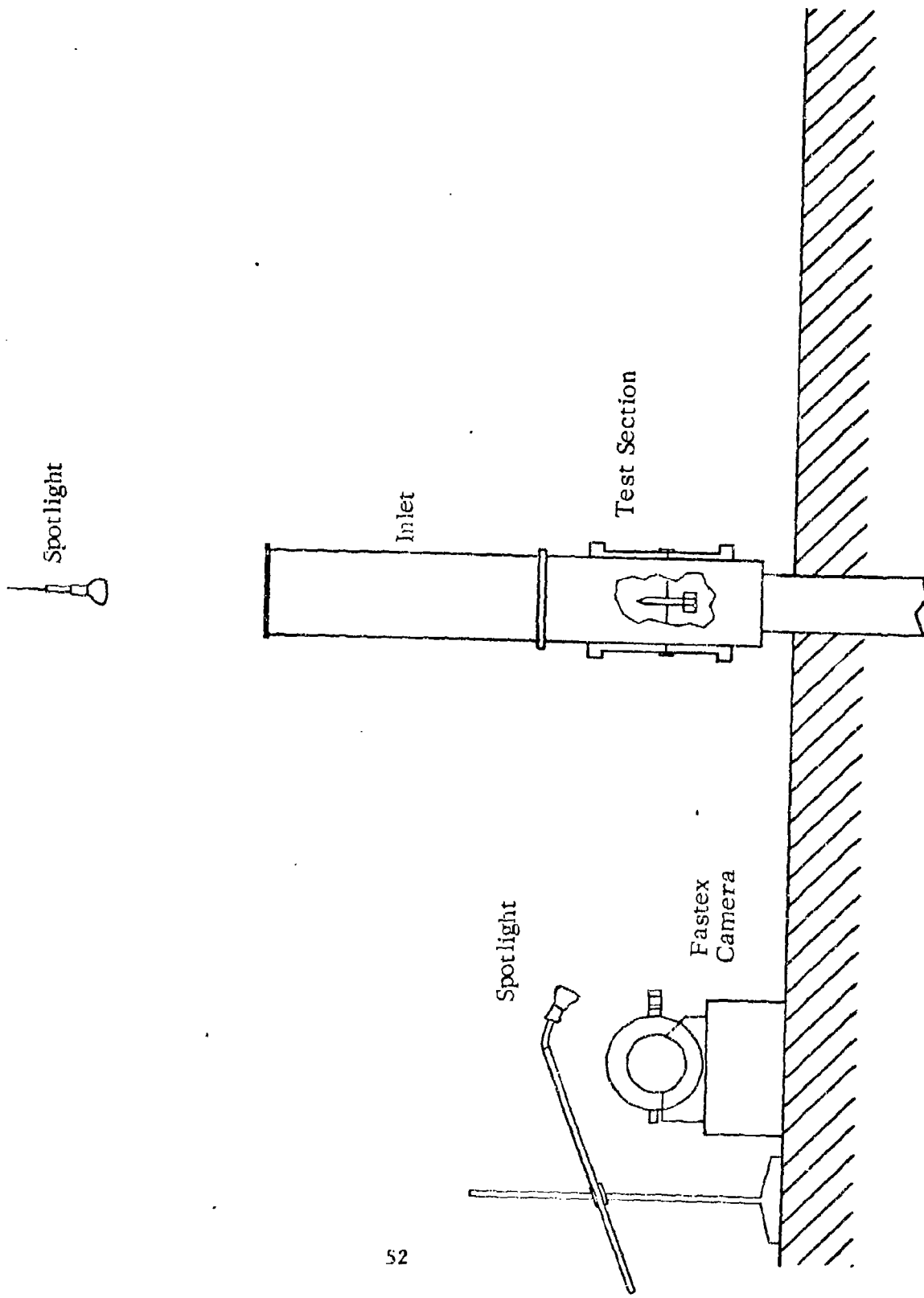


Figure 14. Camera Setup

One-Degree-of-Freedom Data Reduction Procedure

The one-degree-of-freedom oscillations were converted to numerical values of angle of attack in the following manner. Two reference dots at a known distance apart had been placed on the steel wall in the test section behind the model. These dots were included in each frame of the film record of the angular motions of the model. The dots were placed such that a horizontal line running between them was above the highest point that the model with the largest radius would reach. For each configuration the radius of oscillation, the distance from the pivot point to the nose of the model, was also known. The relative coordinates of the reference dots and the nose of the model were determined from the data film using an optical comparator shown in Figure 15. A computer program called REDUCE, presented in Appendix C, using these coordinates and the known conversion distance between the reference dots was then employed to produce a time history of the angular oscillations of the model. A schematic of the reduction coordinates is presented in Figure 16.

Velocity Determination Technique

Since all the tests were not conducted on the same day it was necessary to determine the velocity in the wind tunnel on the particular day the test was conducted. A method of measuring the static pressure in the test section was necessary to do this. A system like the one in Figure 17 was used to do this

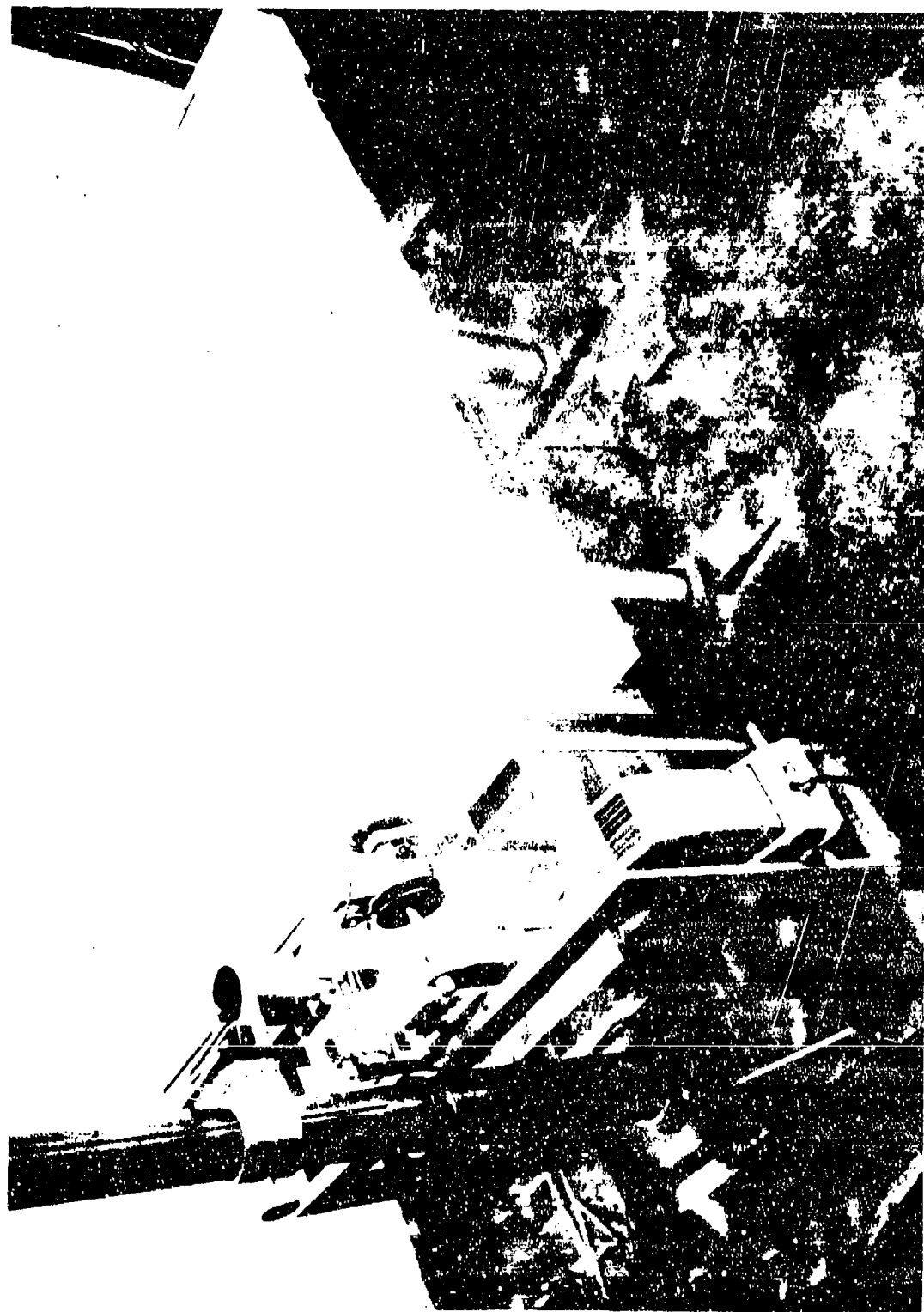
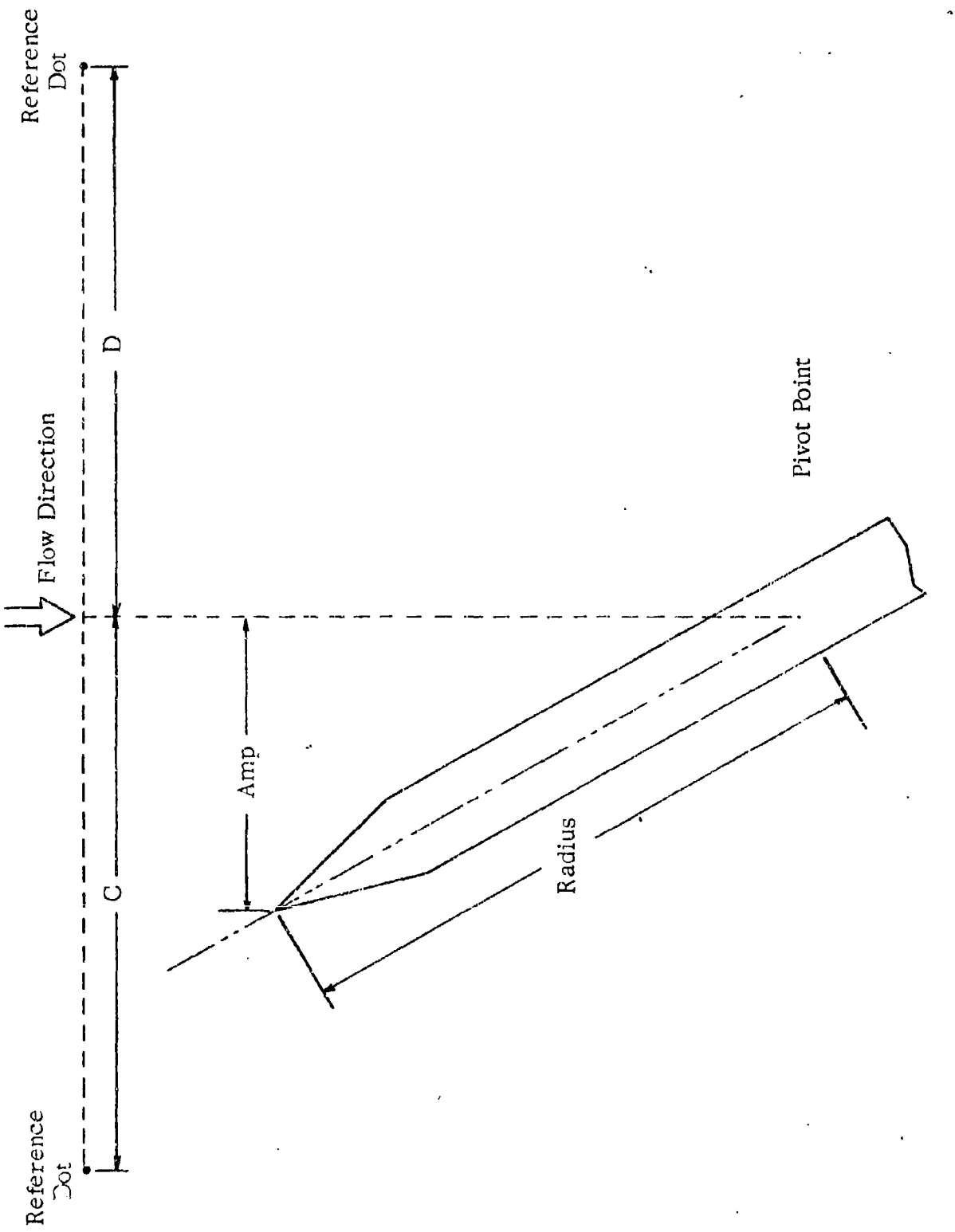


Figure 15. Optical Comparator



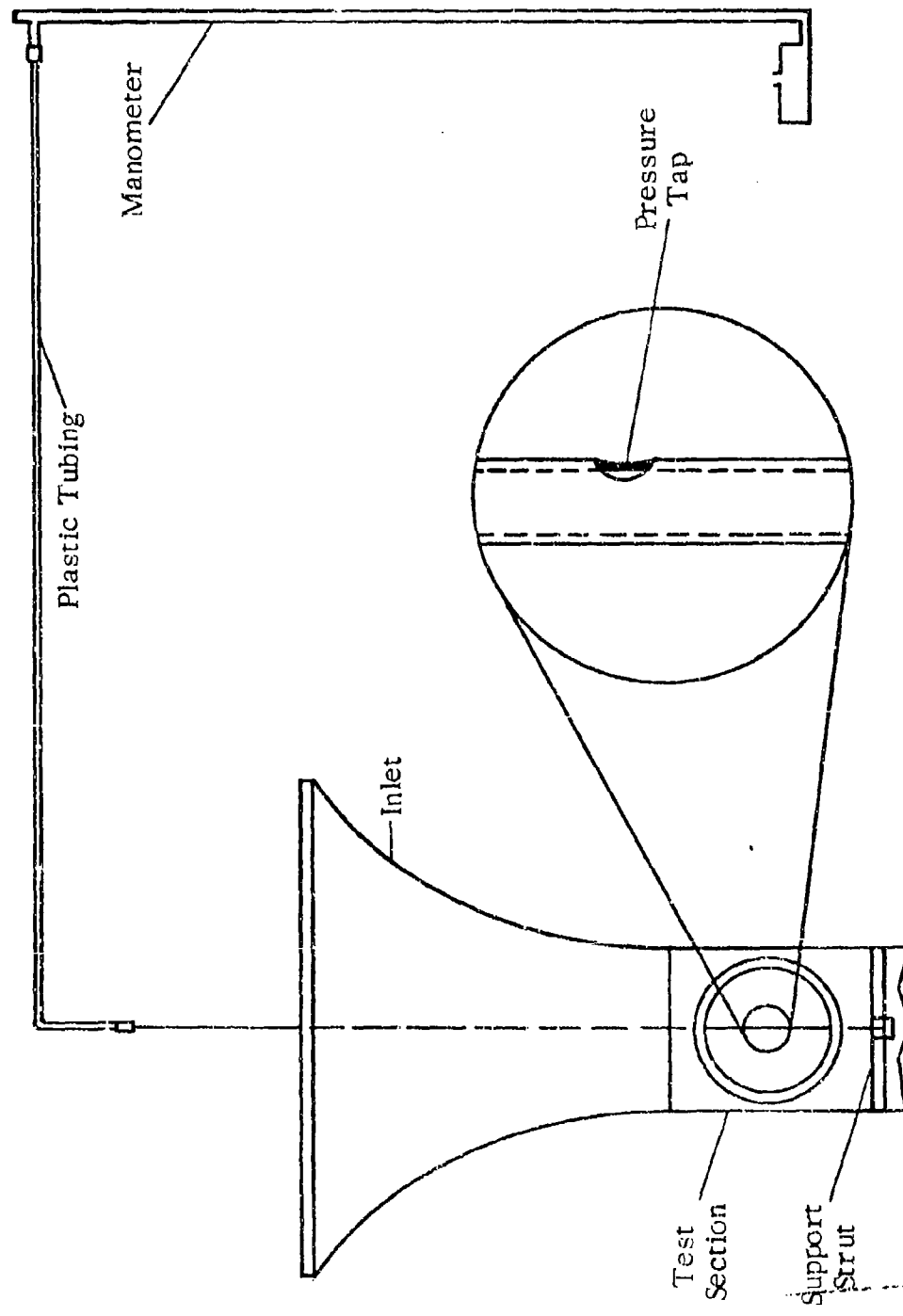


Figure 17. Velocity Measurement Setup

A long thin tube was placed in the inlet of the wind tunnel and lowered until the end reached the support strut just below the test section. This end of the tube was secured to the strut to help maintain the position of the tube near the center of the wind tunnel test section. A small hole had been drilled in the side of the tube to coincide with the position of the model when the tube was in place. The end of the tube in the tunnel was sealed and the open end was connected to a manometer by a length of plastic tubing. This upper end was fastened so as to put tension on the tube and prevent it from moving about in the test section when the pressure measurement was being taken. Any movement of the tube would affect the pressure reading and produce an incorrect value of the velocity.

Before starting the tunnel a tare reading was made on the manometer and the stagnation or total pressure was taken from a barometer. Since the manometer scale did not coincide with that of the barometer the tare reading and barometer reading, which should have been equal had their scales coincided, were different. This difference was a correction factor which would have to be added to the pressure reading taken when the tunnel was on to give the actual static pressure. The tunnel was turned on and the pressure was recorded. Having all of these pressure readings the ratio of static to total pressure could be solved for using the following formula:

$$\frac{p}{P_t} = \frac{p_{\text{read}} + (P_t - P_{\text{tare}})}{P_t}$$

where

$$(P_t - P_{tare}) = \text{correction factor}$$

Once this ratio was known the Mach number could be found in the Isentropic Flow Tables of Reference 8. For the REDUCE computer program it was necessary to put the velocity in units of feet per second from the Mach number. A sample calculation of this is shown in Appendix D.

ONE-DEGREE-OF-FREEDOM TEST RESULTS

One-Degree-of-Freedom Data Reduction

The WOBBLE computer program was used to fit the Aeroballistic Theory to the one-degree-of-freedom angular data obtained from the REDUCE program. The data was fitted in segments of 1.8 cycles and the stability parameters K_1 , K_T , λ_1 , and ω_1 were determined by WOBBLE at a time interval of 0.03 seconds. The stability parameter K_T , the trim arm, is analogous to the K_3 in the Linear Theory and is due to aerodynamic asymmetries in the configurations. The average percent error of the fitting of the theory to the data for all the tests carried was less than 3%. A representative plot of probable error (P.E.) versus time is given in Figure 18. The stability parameters were obtained from the fits as functions of time. Plots of the stability parameters versus time for all the configurations are presented in Figures 19 through 34.

One-Degree-of-Freedom Stability Coefficients

The pitching moment and damping moment stability coefficients, $C_{M\alpha}$ and $(C_{Mq} + C_{M\dot{\alpha}})$, were obtained versus time from the WOBBLE fits. Plots of the mean values of the coefficients per fit versus mean angle of attack per fit are presented in Figures 35 through 42 for all the configurations. These plots give an approximation of how the coefficients vary with angle of attack. Included on these graphs are Ballistic Range Laboratory (BRL) results for the respective configurations and

coefficients. The BRL data was plotted at an angle of attack of 2° .

Figures 43 through 50 are plots of BRL results for the stability coefficients versus Mach number for all the configurations. Mean values of the Notre Dame results for the coefficients at low angles of attack are included on these graphs. The Notre Dame data was plotted at a Mach number of 1.3 which was an average value of all the tests carried out.

An important point which should be brought up at this point is the discrepancy in the definition of the damping moment stability coefficient between the two sets of results. The computations in this investigation were carried out using a factor of $(\frac{d}{2u})$ in the definition of the damping moment stability coefficient (see Equation 3). The BRL definition used a factor of $(\frac{d}{u})$ causing the respective computed values of $(C_{Mq} + C_{M\dot{\alpha}})$ to be off by a factor of two. To account for this and allow the results to be directly compared, the BRL values of $(C_{Mq} + C_{M\dot{\alpha}})$ were increased by a factor 2 before plotting. This essentially gave all the values presented a uniform definition and allowed the comparisons of the results to be made.

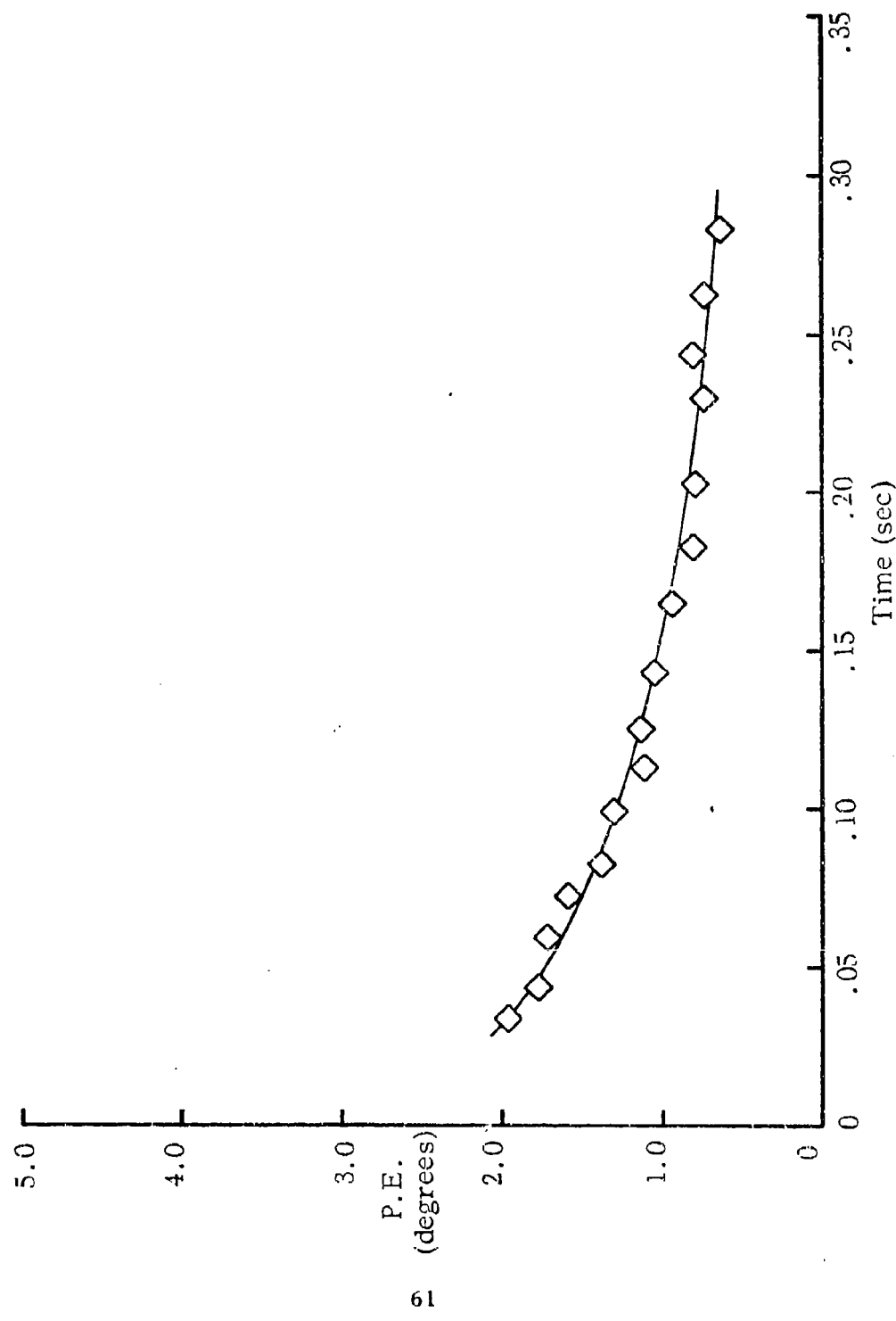


Figure 18. Probable Error versus Time

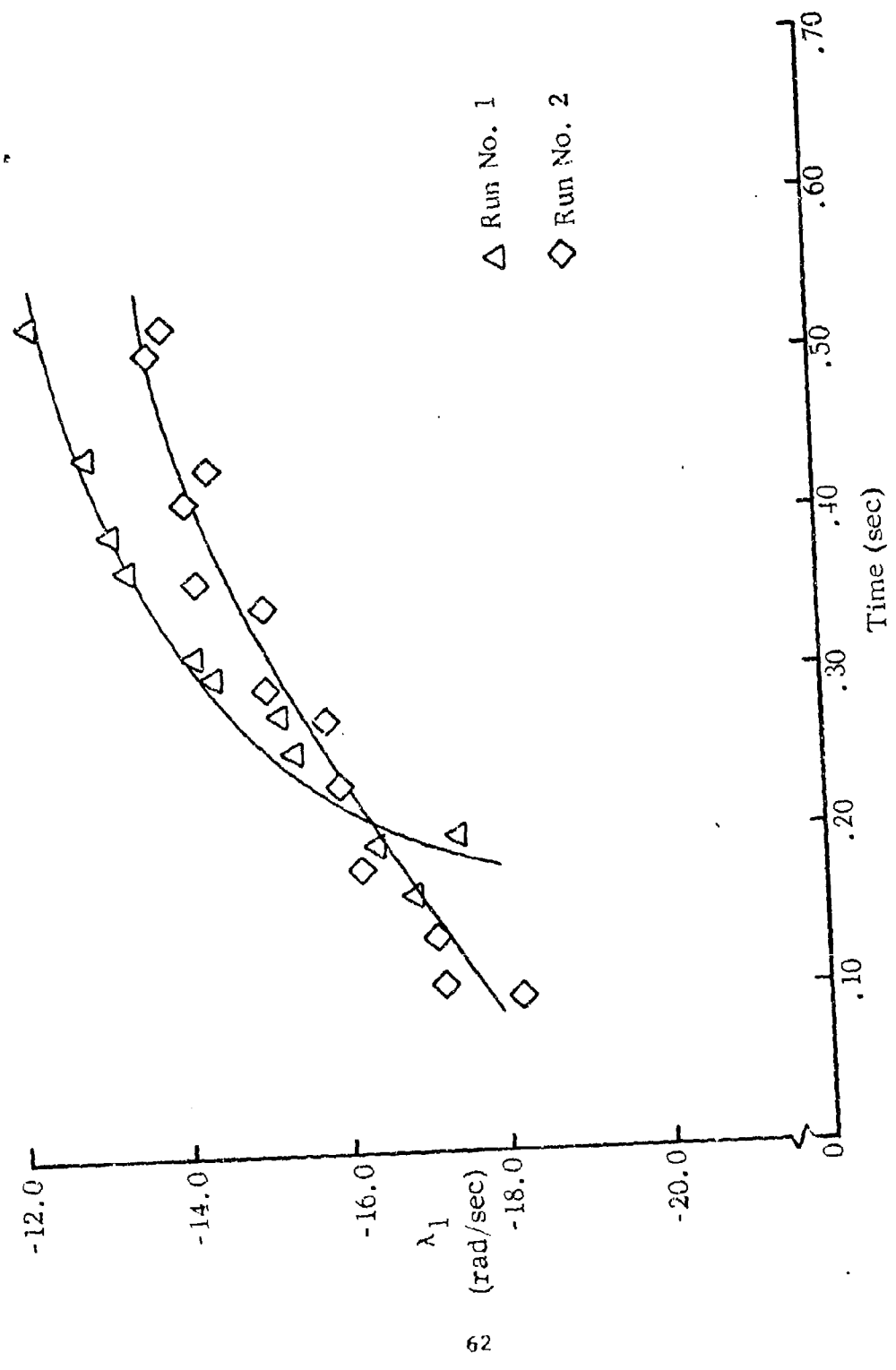


Figure 19. λ_1 versus Time (Ground Point)

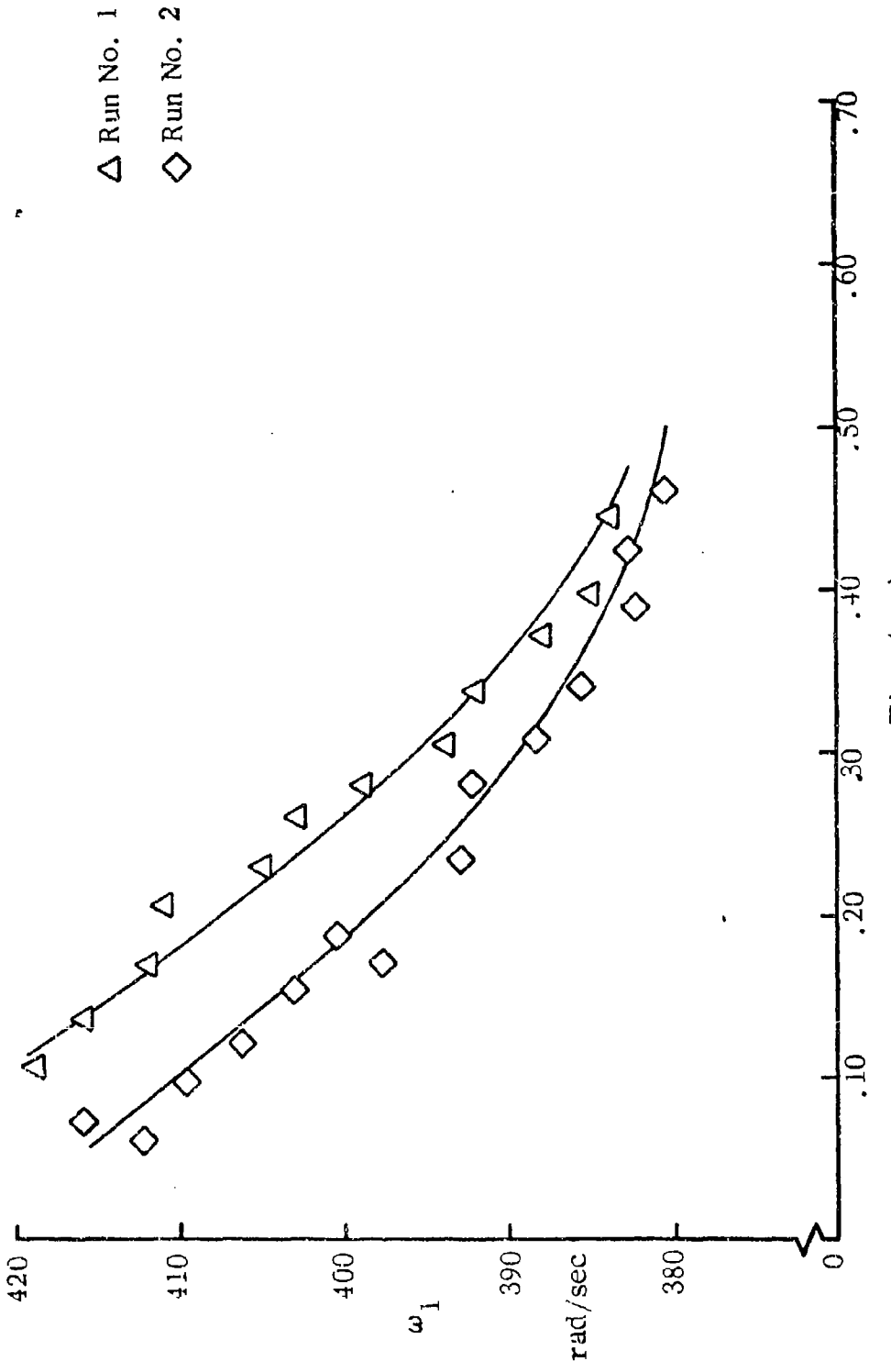


Figure 20. ω_1 versus Time (Ground Point)

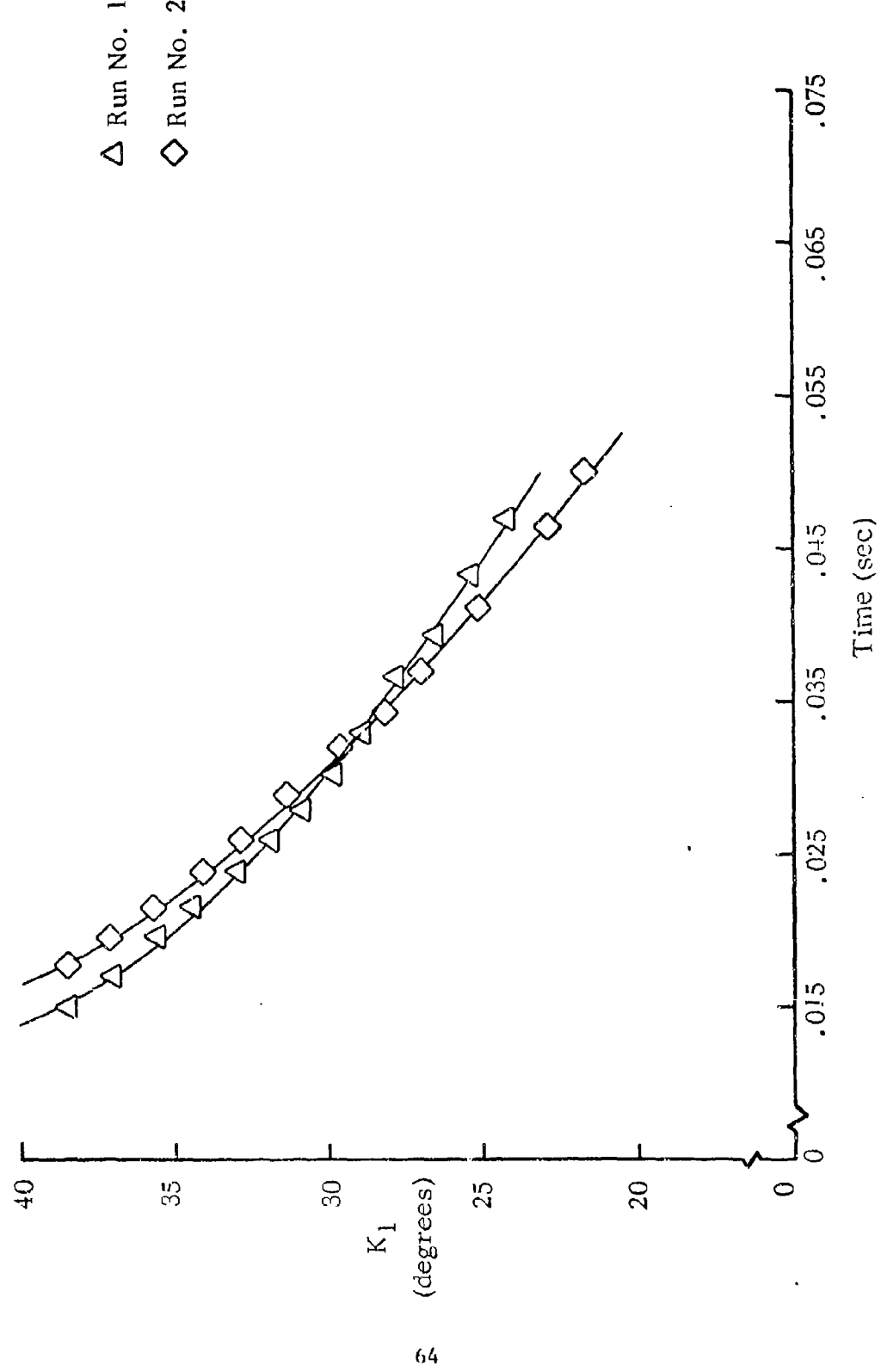


Figure 21. K_1 versus Time (Ground Point)

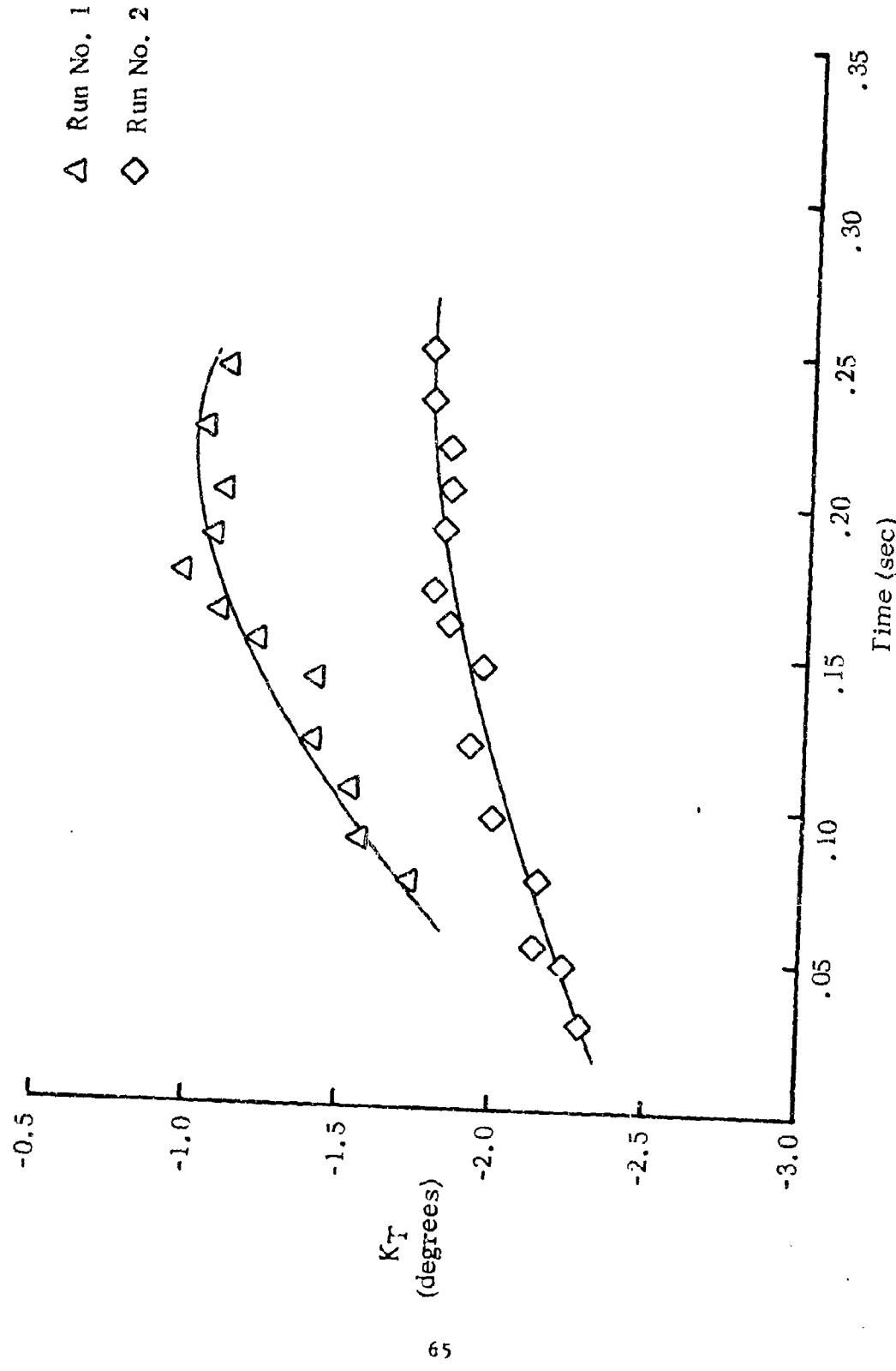


Figure 22. K_T versus Time (Ground Point)

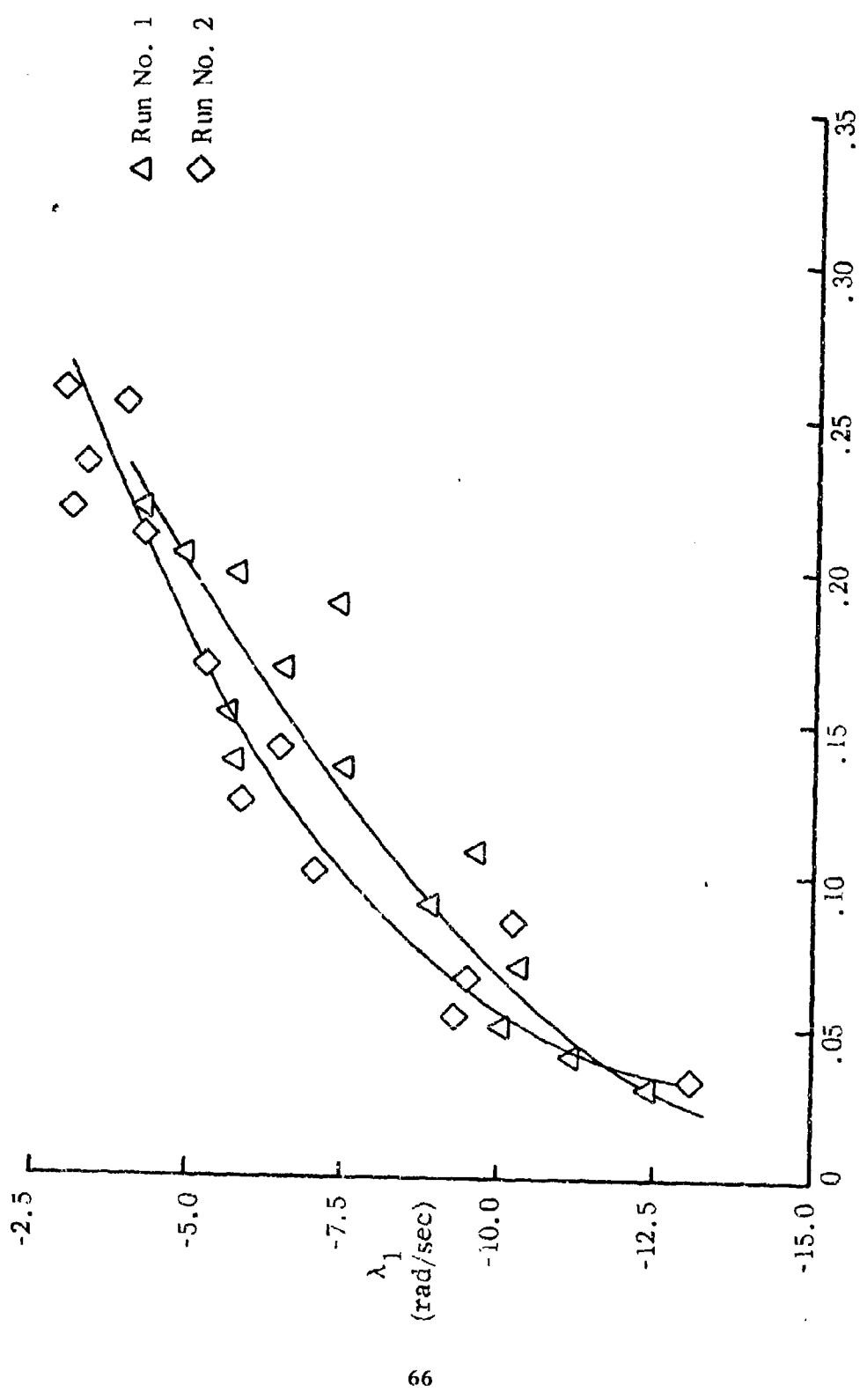


Figure 23. λ_1 versus Time (0.1n)

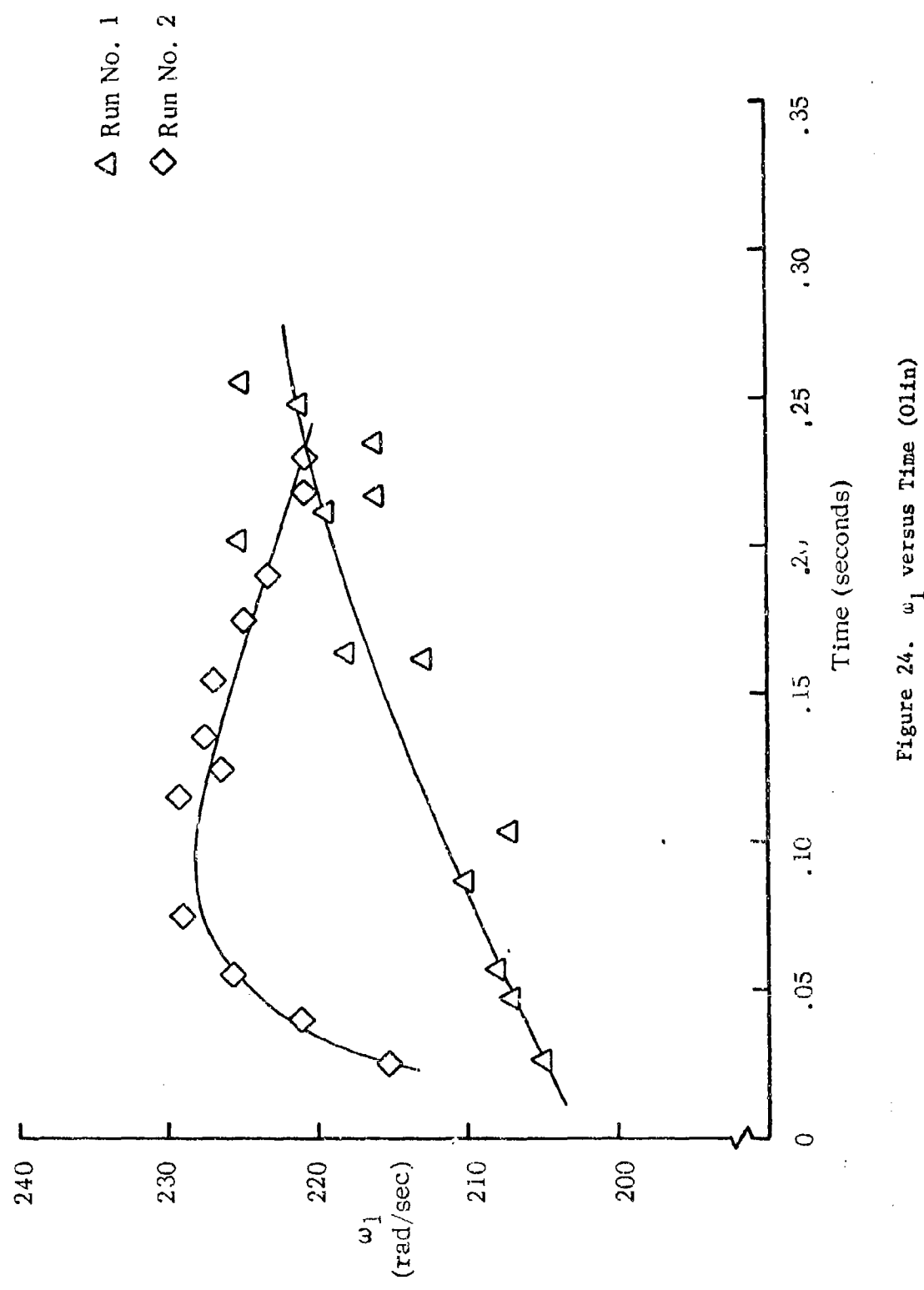


Figure 24. ω_1 versus Time (Olin)

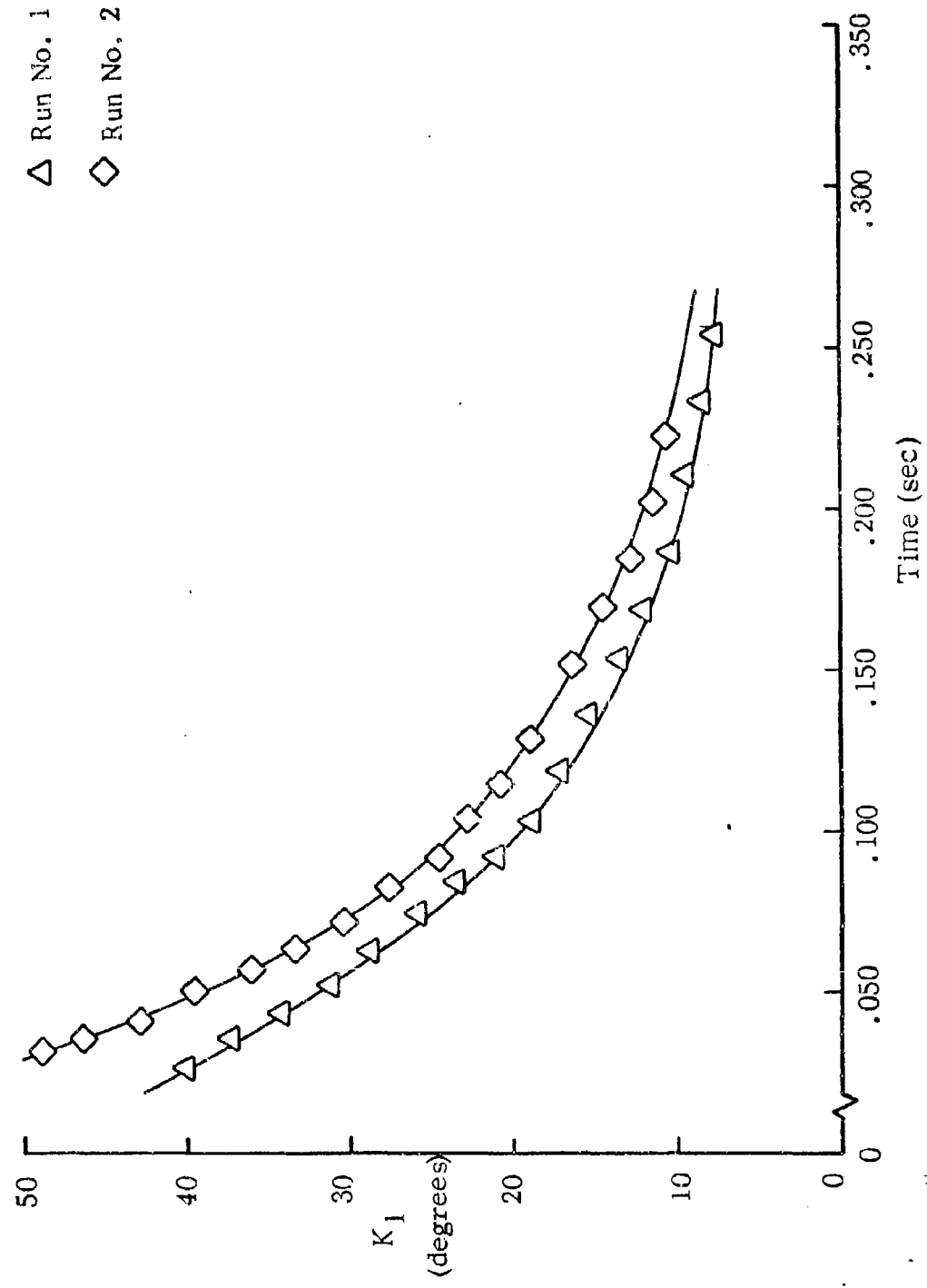


Figure 25. K_1 versus Time (0fin)

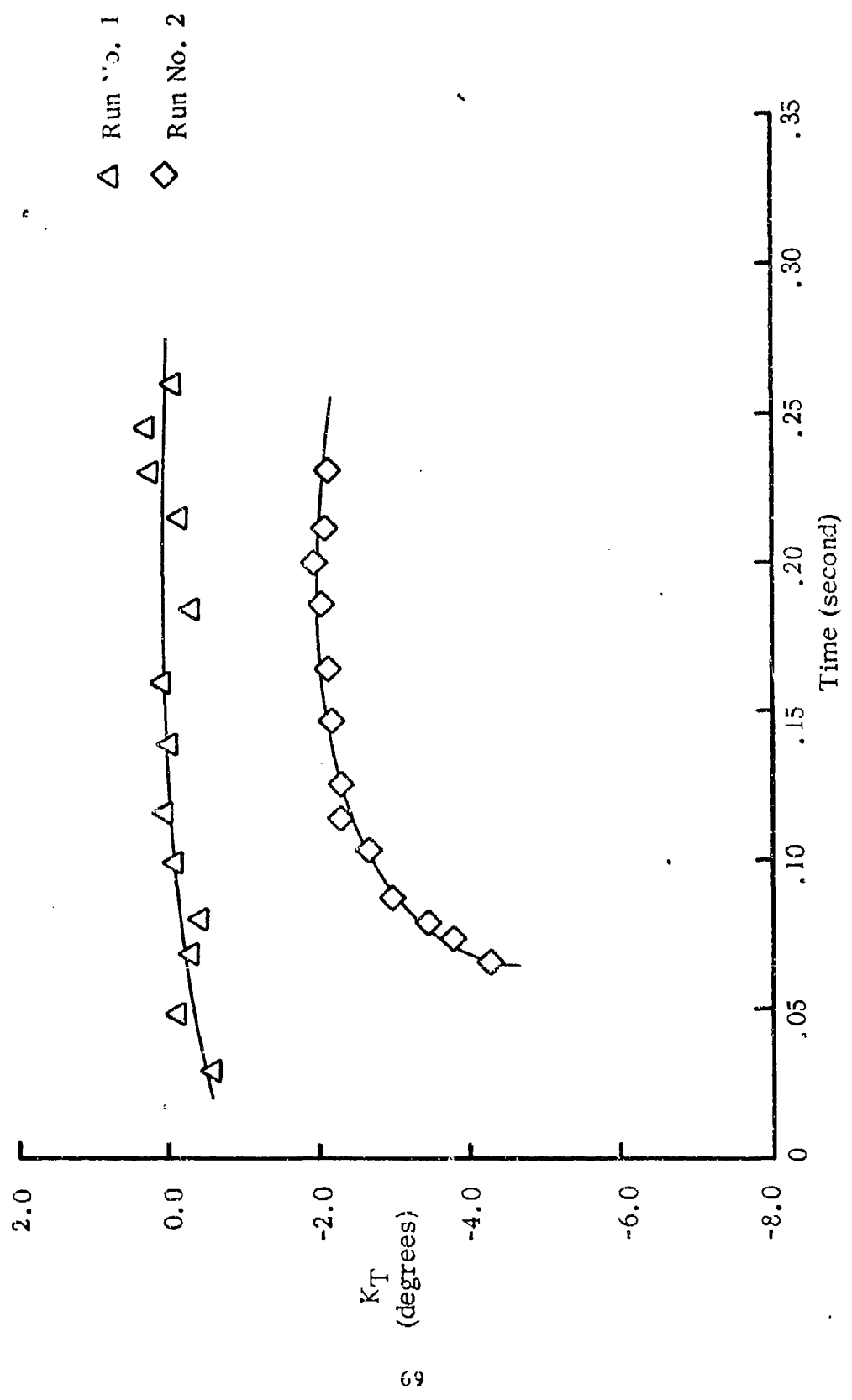


Figure 26. K_T versus Time (0lin)

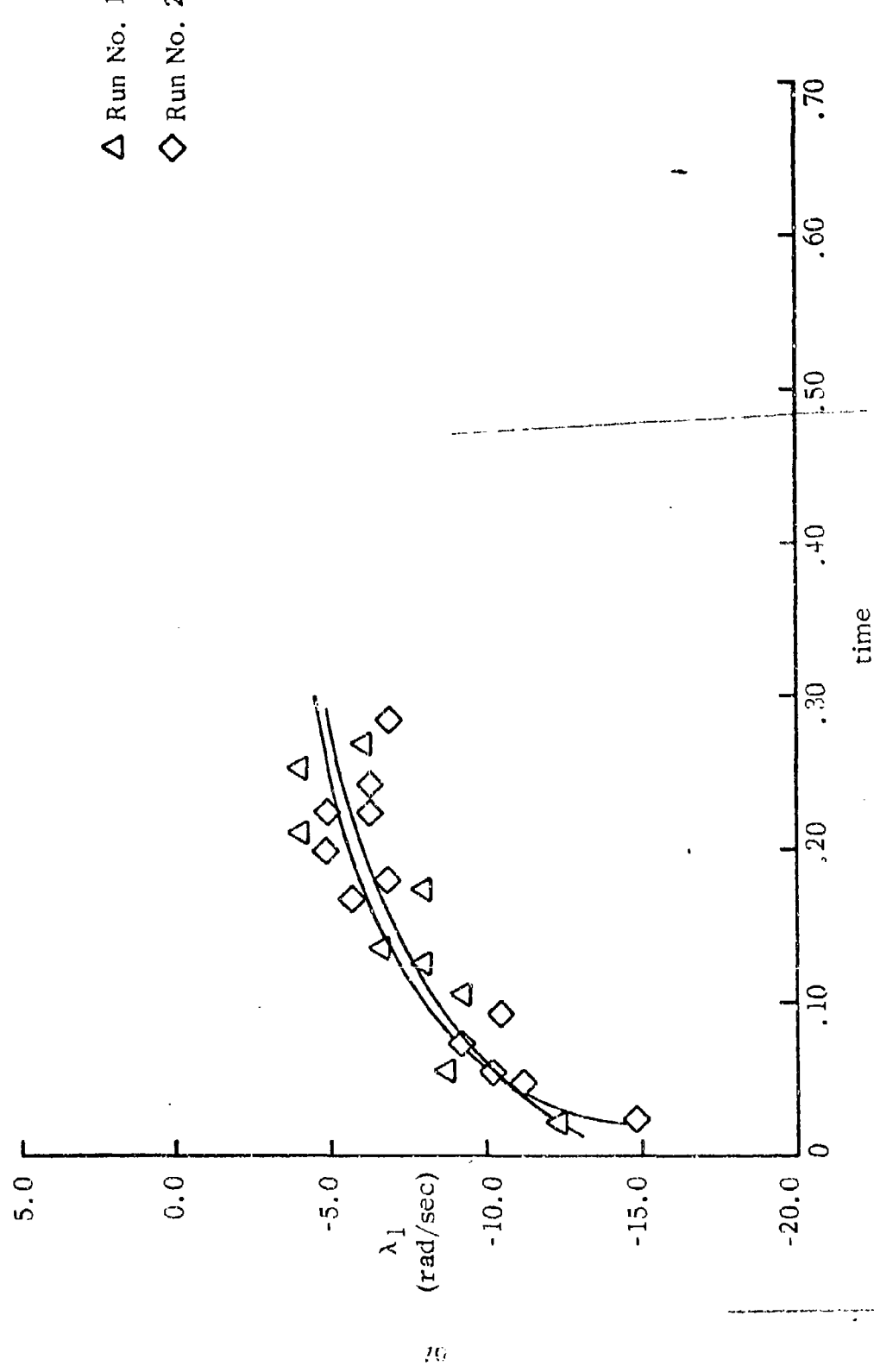


Figure 27. λ_1 versus Time (Swaged Point)

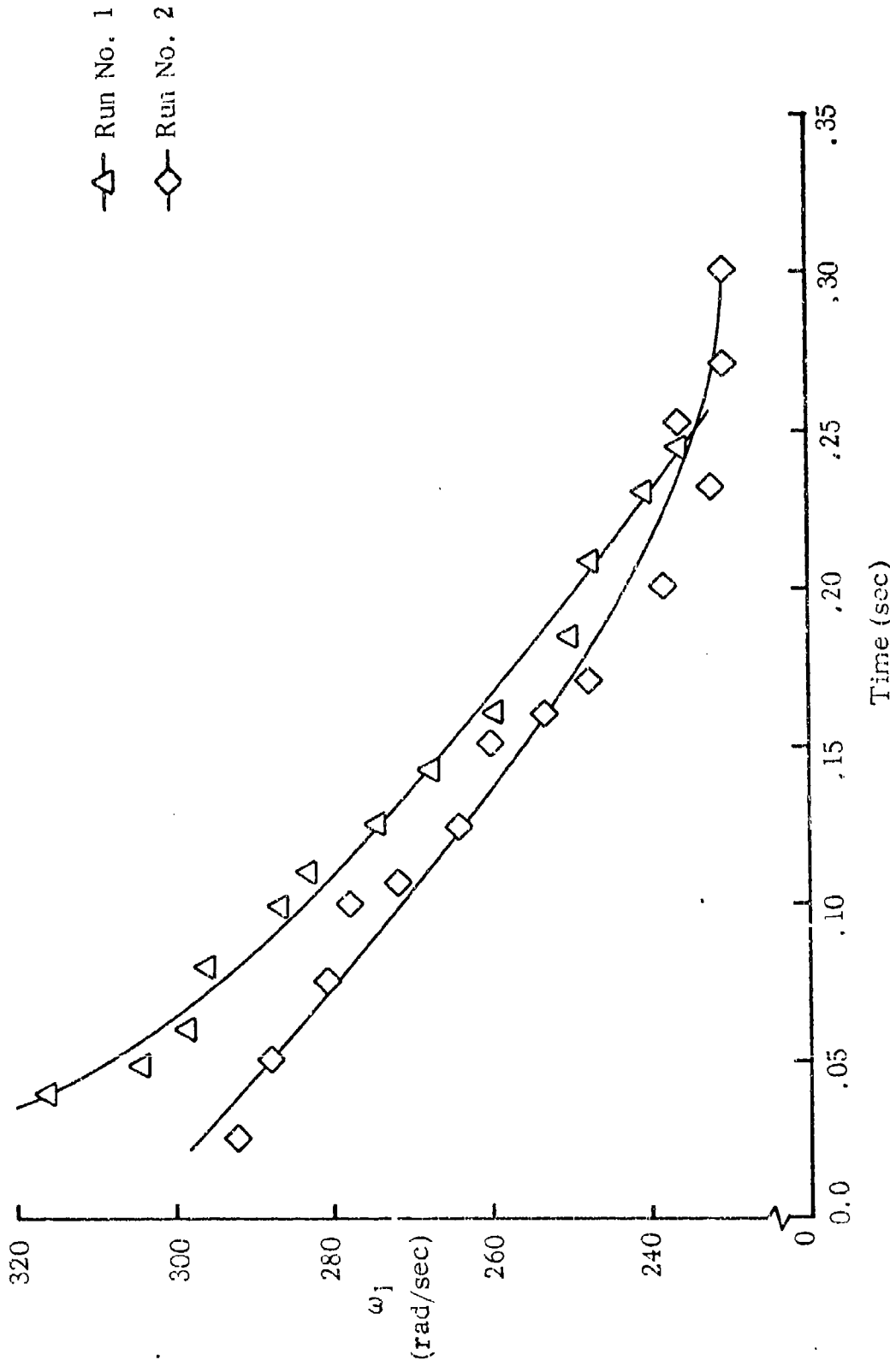


Figure 28. ω_1 versus Time (Swaged Point)

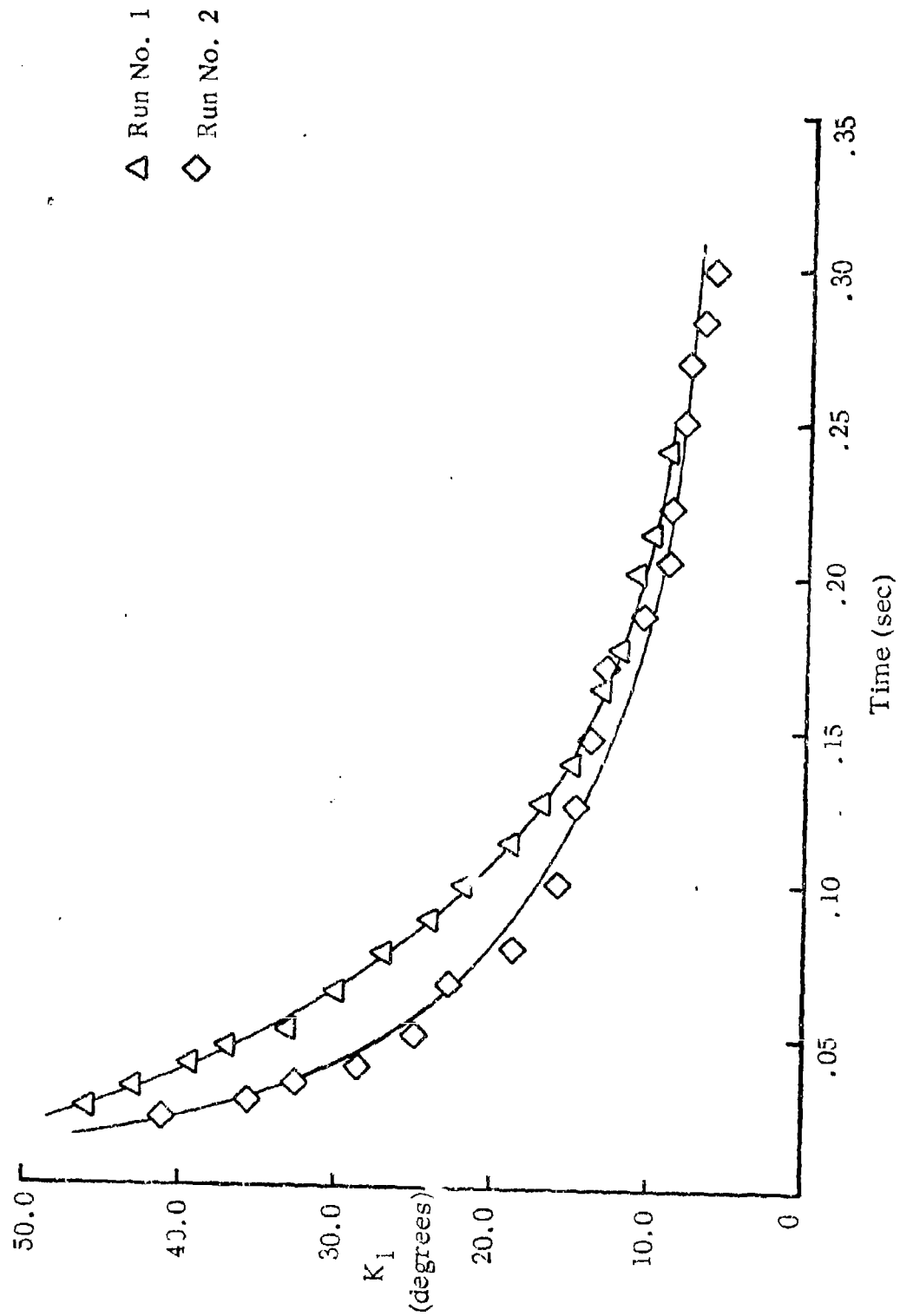


Figure 29. K_1 versus Time (Swaged Point)

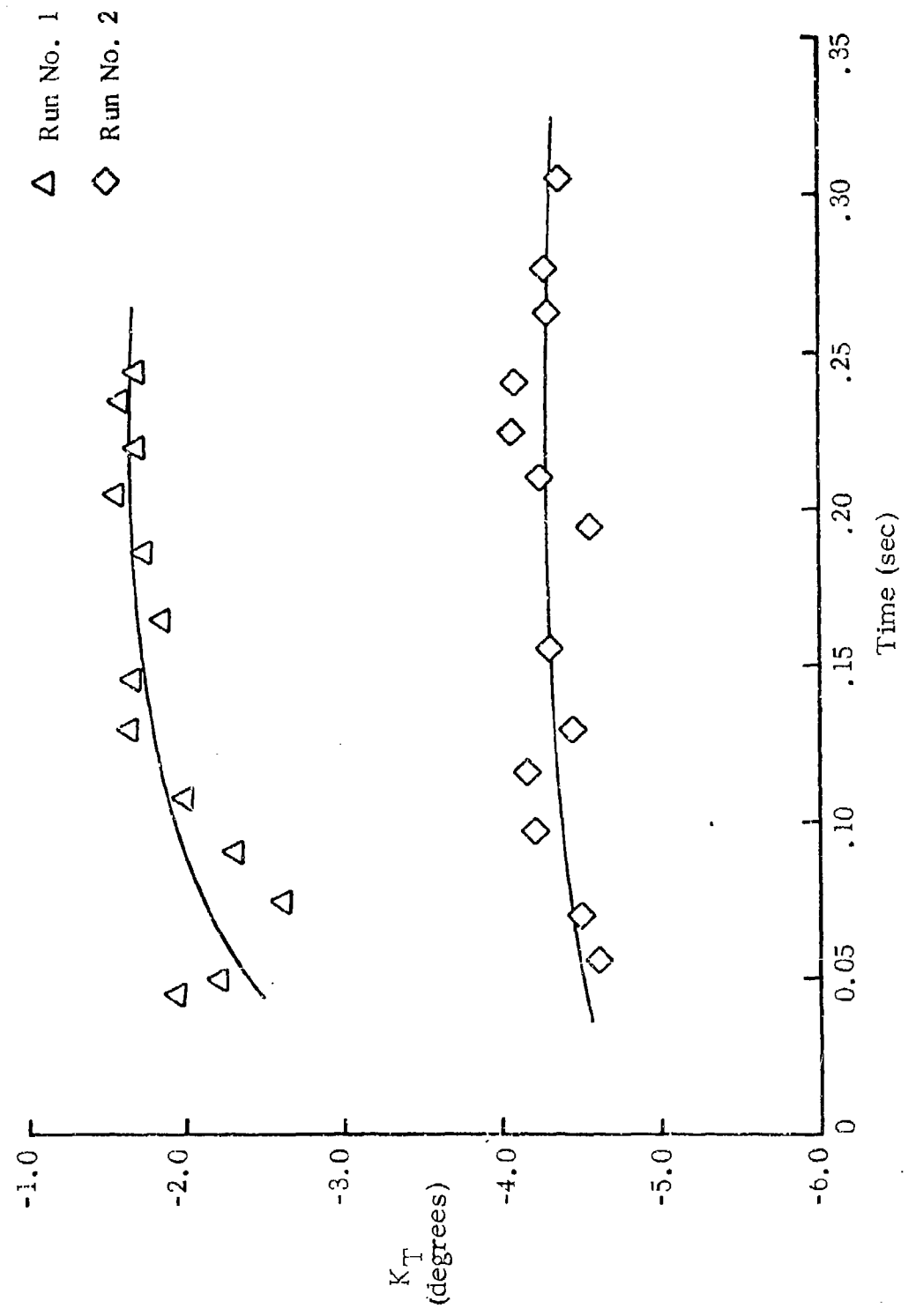


Figure 30. K_T versus Time (Swaged Point)

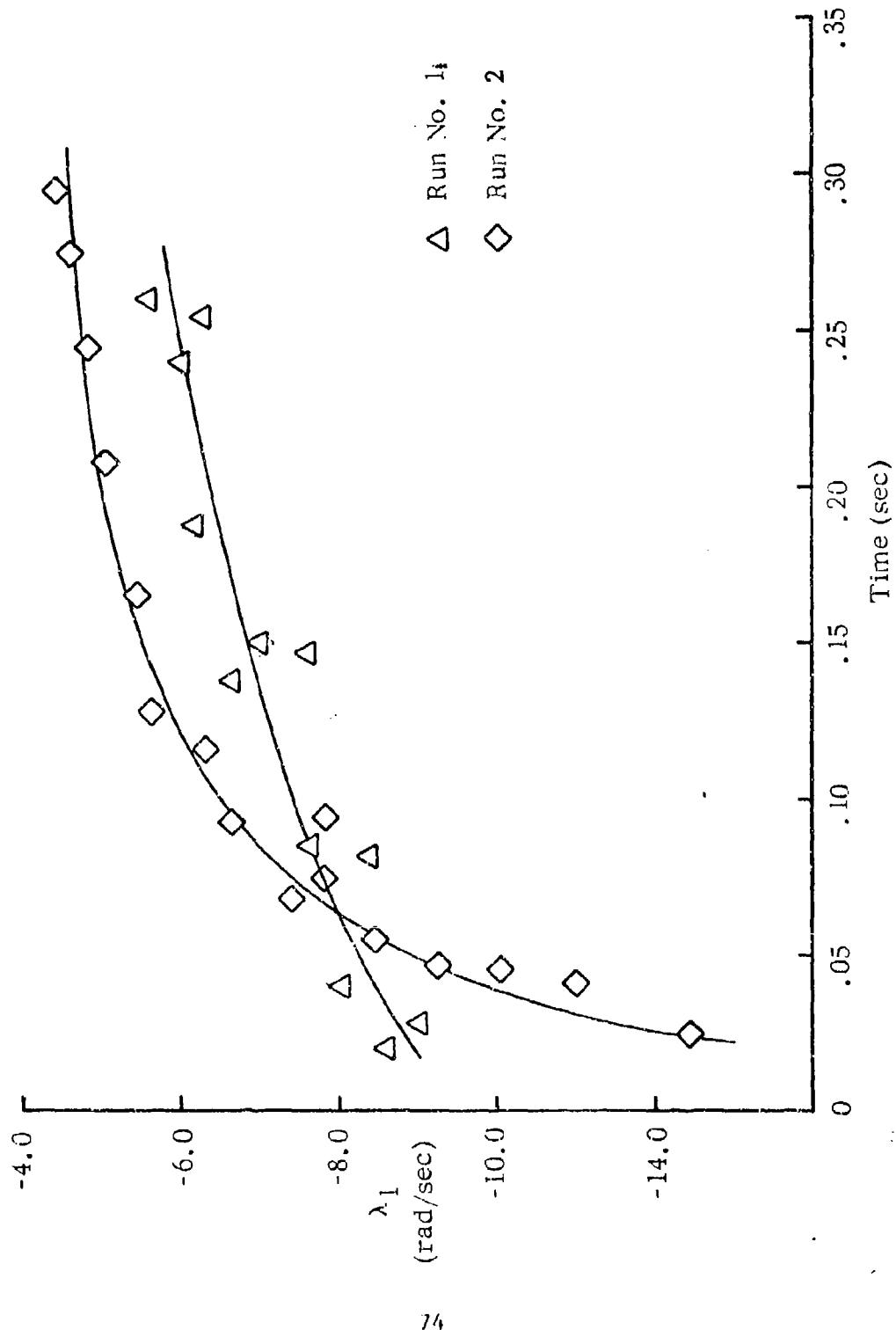


Figure 31. λ_1 versus Time (Tracer)

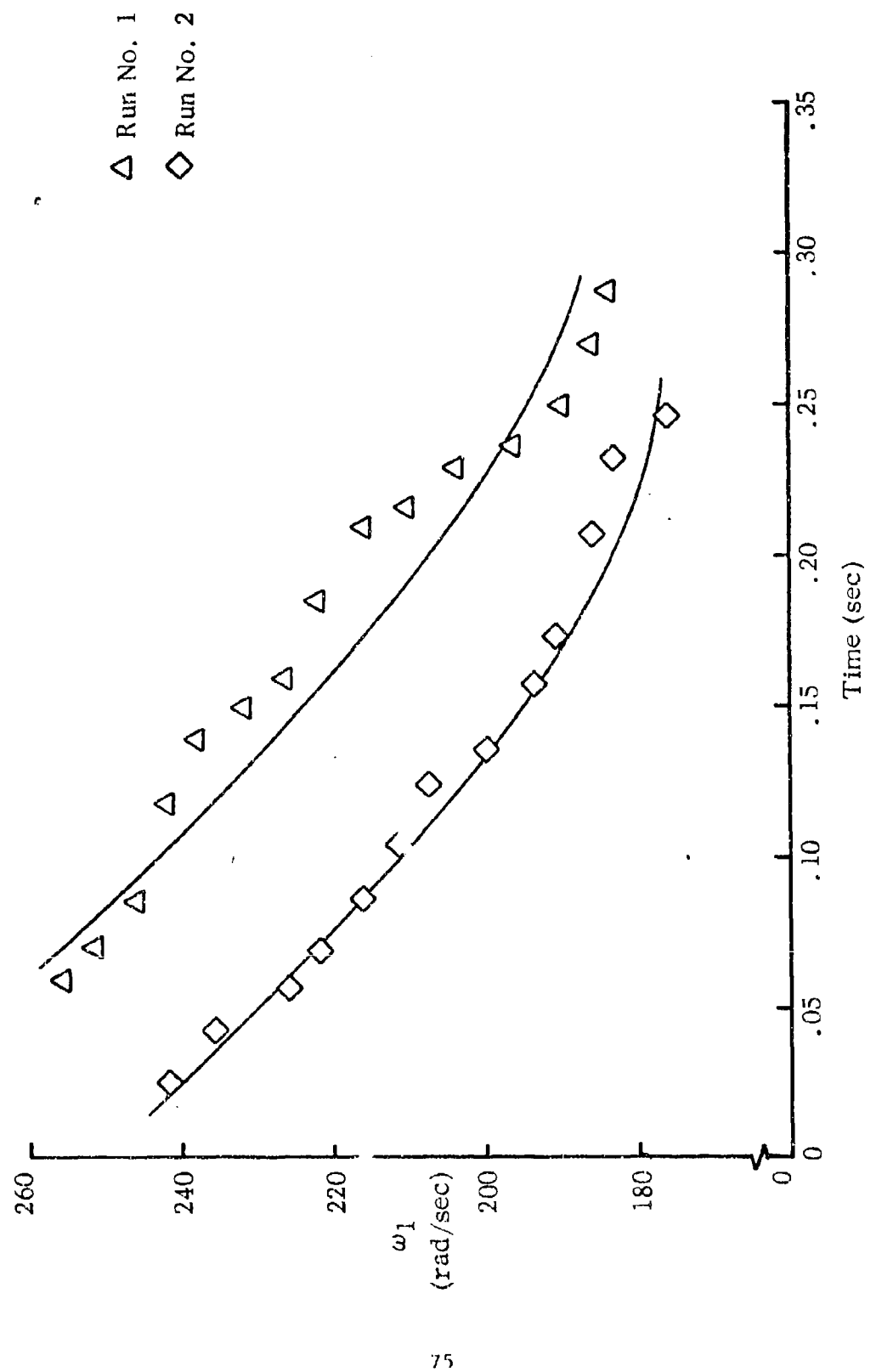


Figure 32. ω_1 versus Time (Tracer)

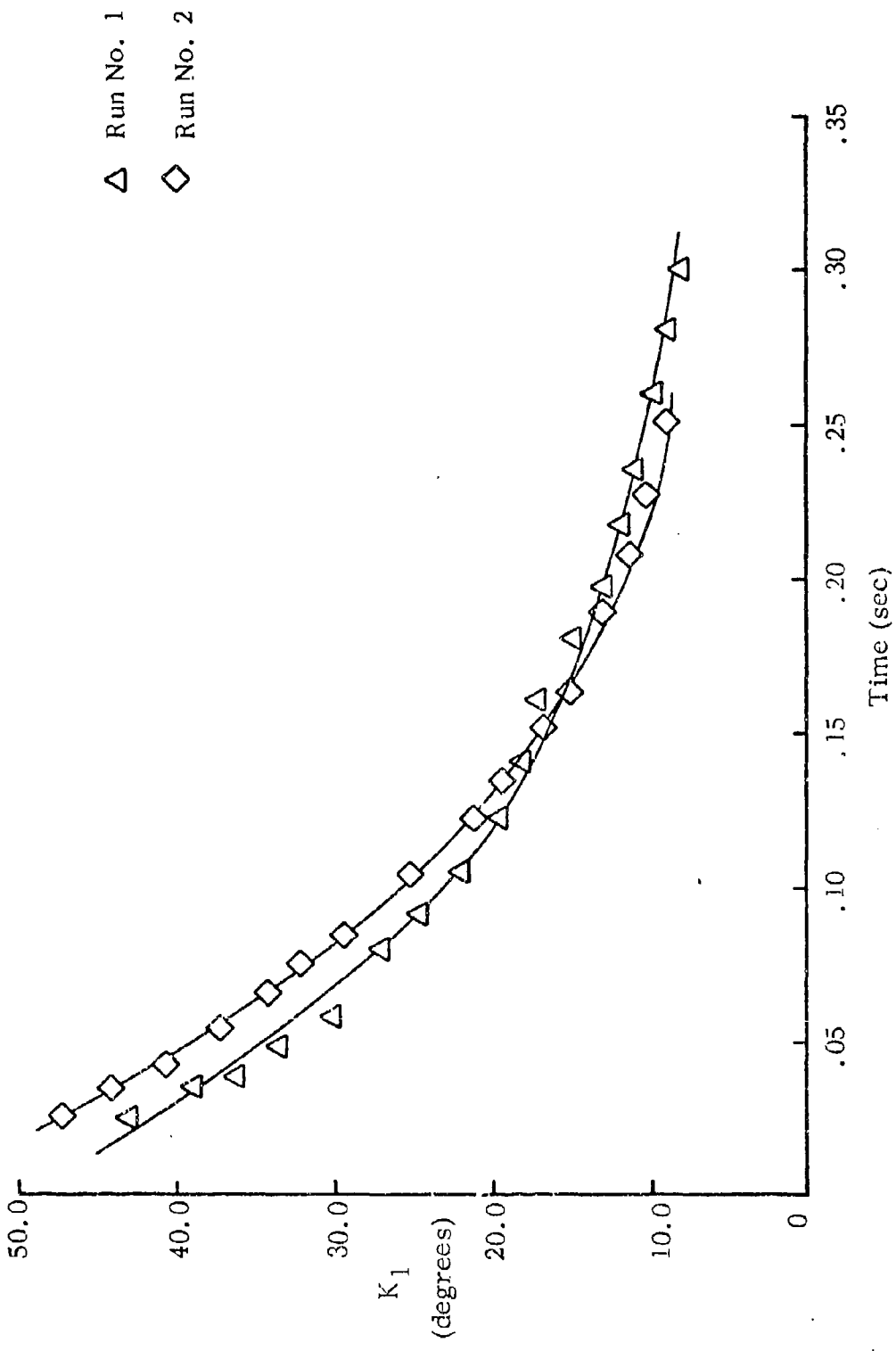


Figure 33. K_1 versus Time (Tracer)

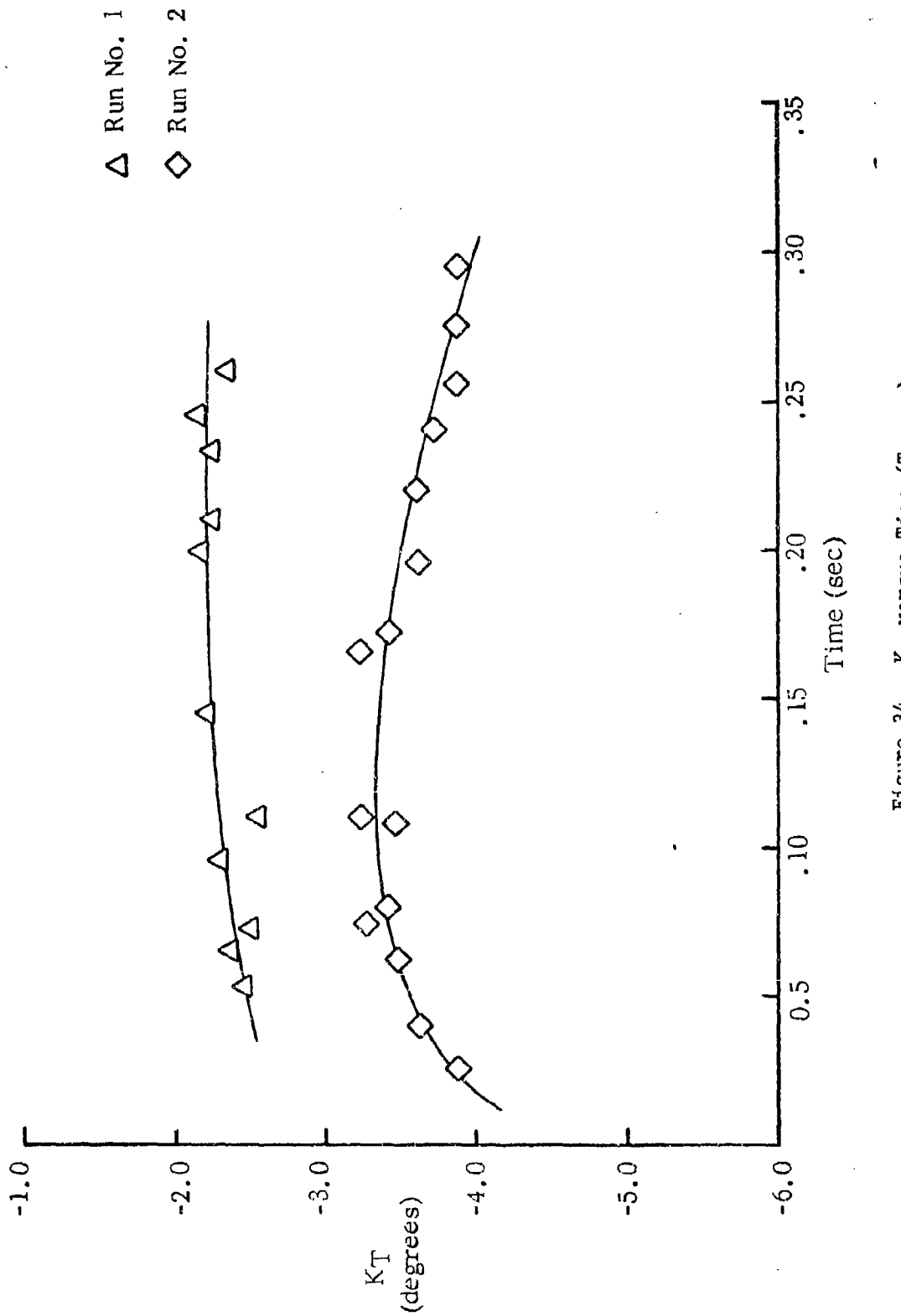


Figure 34. K_T versus Time (Tracer)

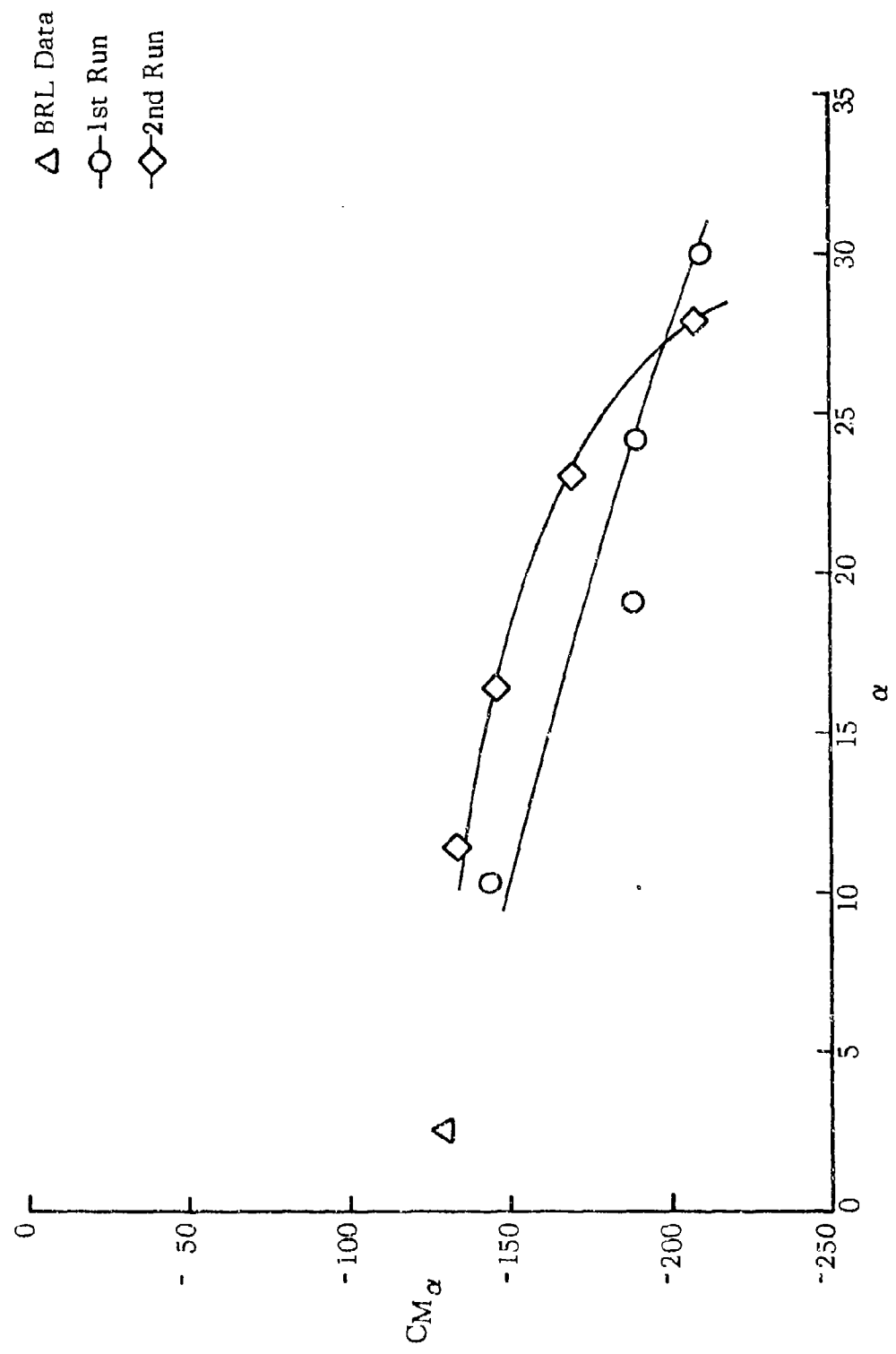


Figure 35. $C_{M\alpha}$ vs α (Ground Point)

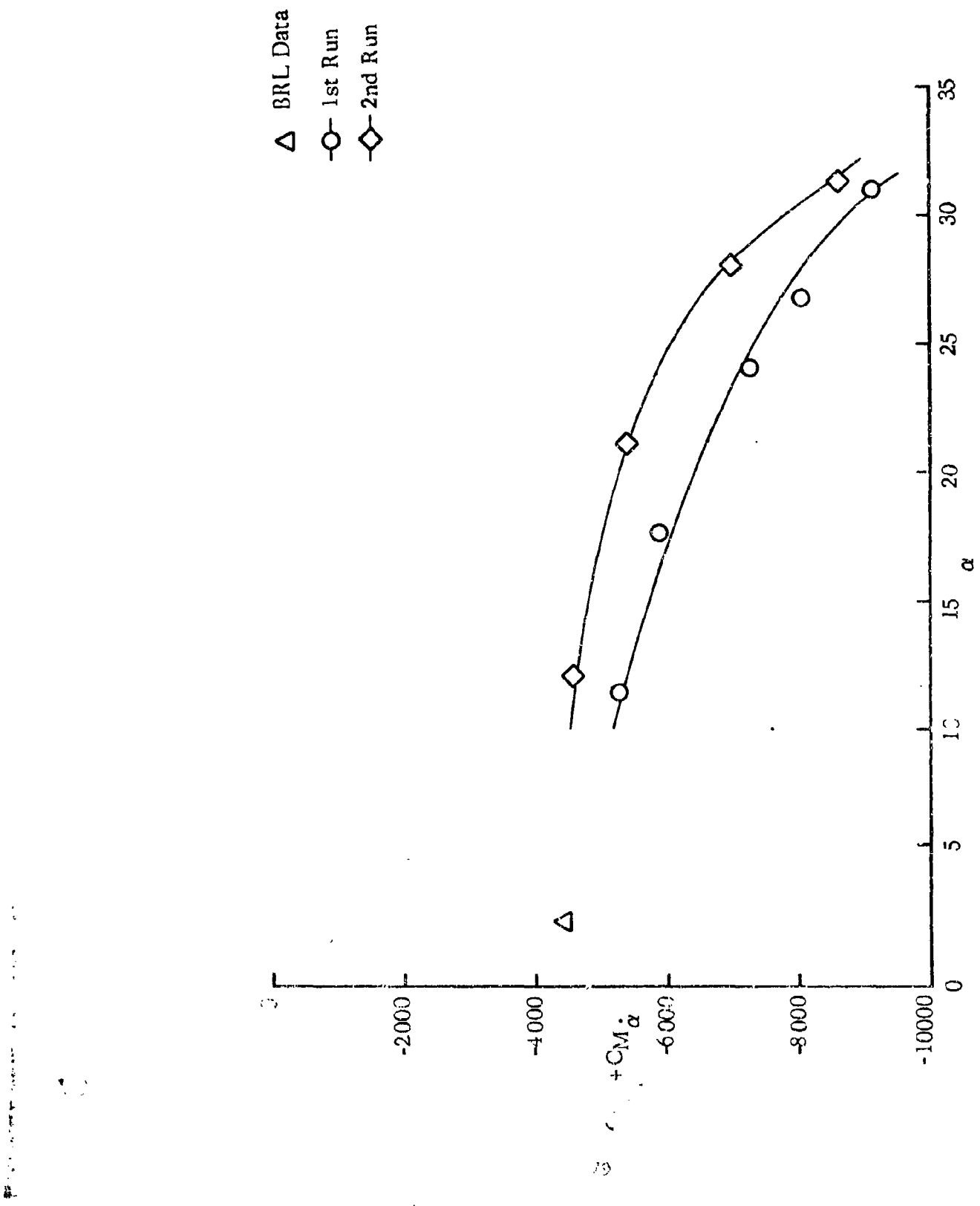


Figure 36. $C_M + C_L$ vs α (G.P.)

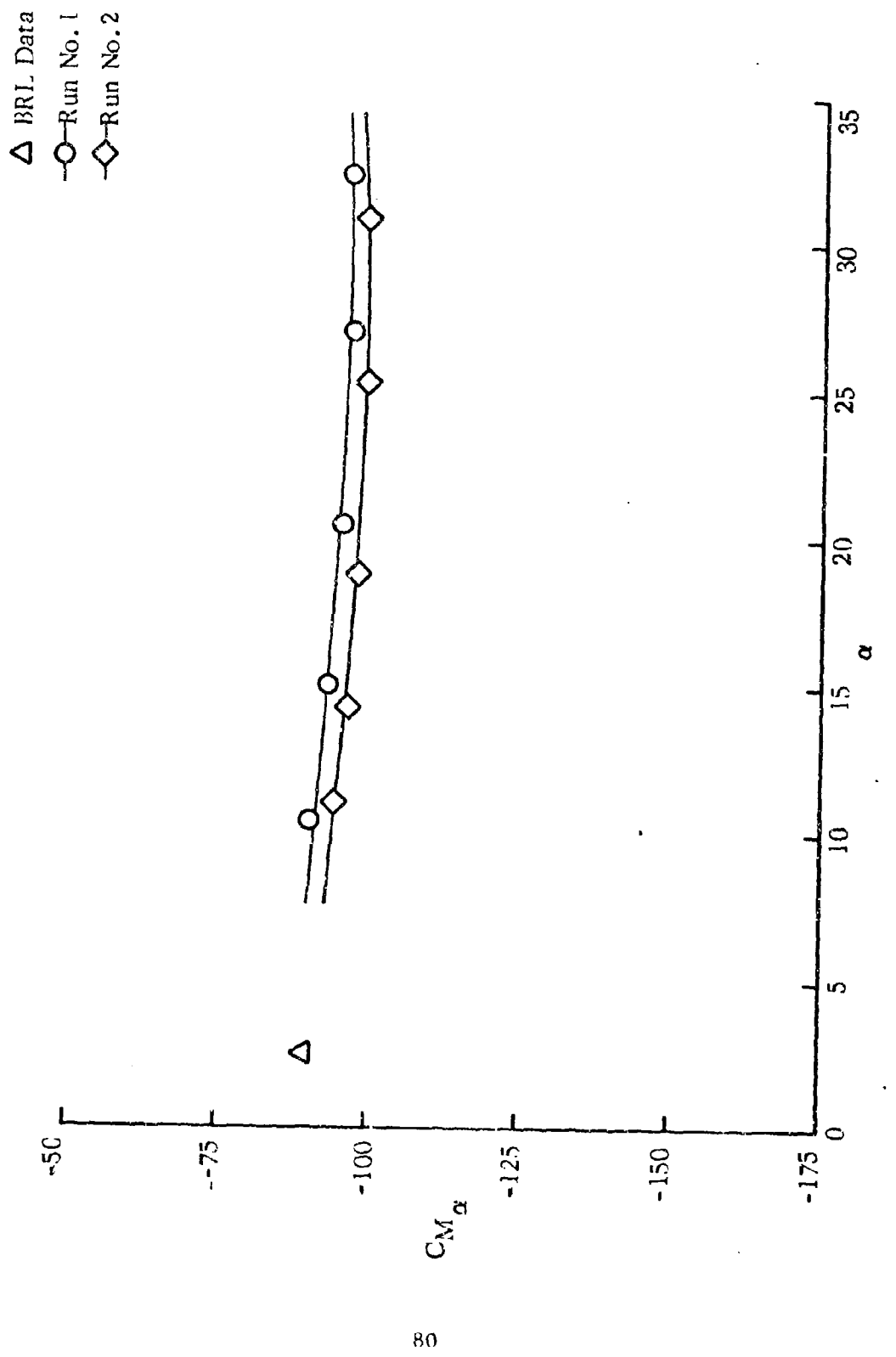


Figure 37. C_{M_α} vs α (Olin)

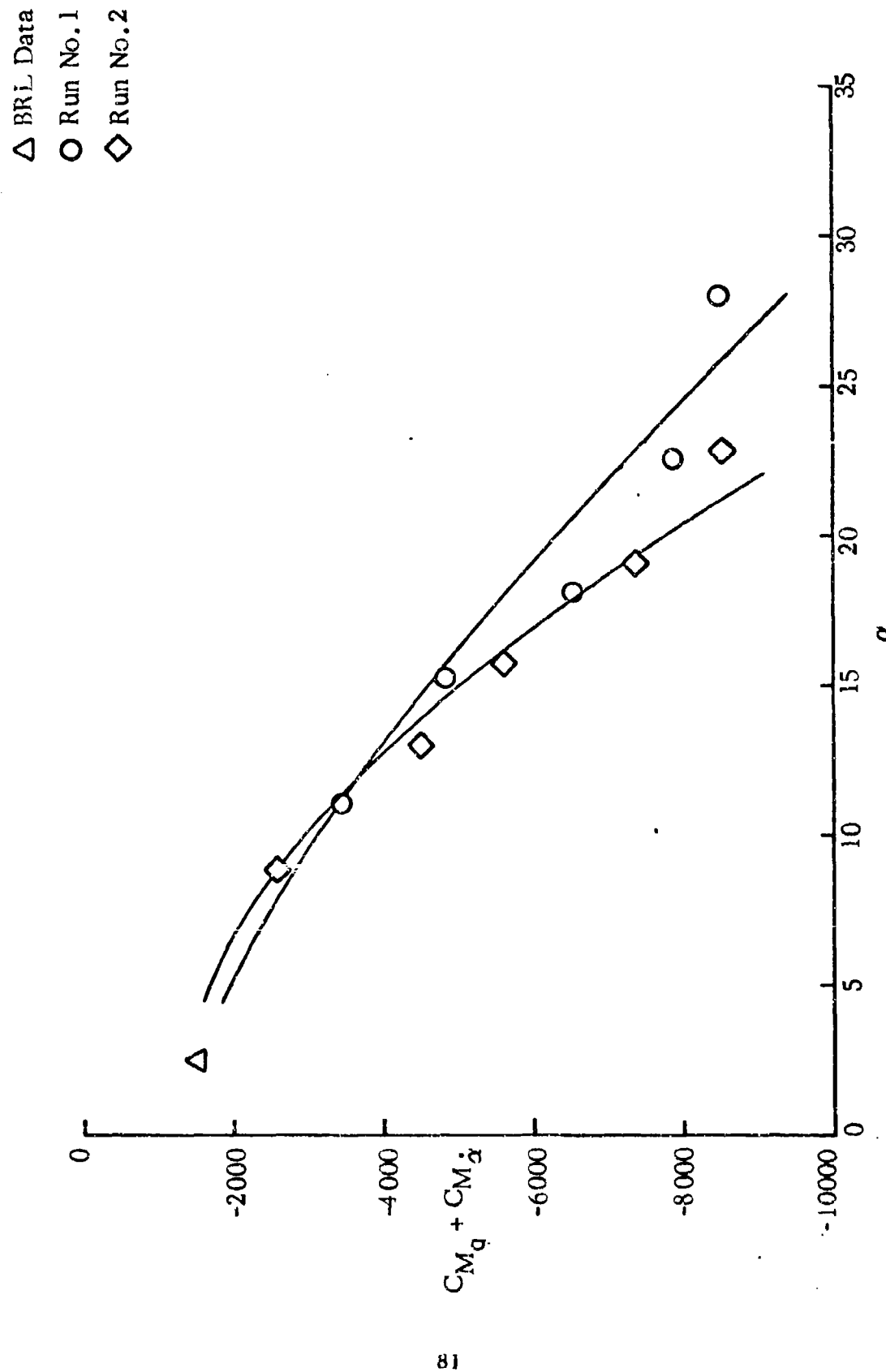


Figure 38. $C_{Mq} + CM\alpha$ vs. α (01In)

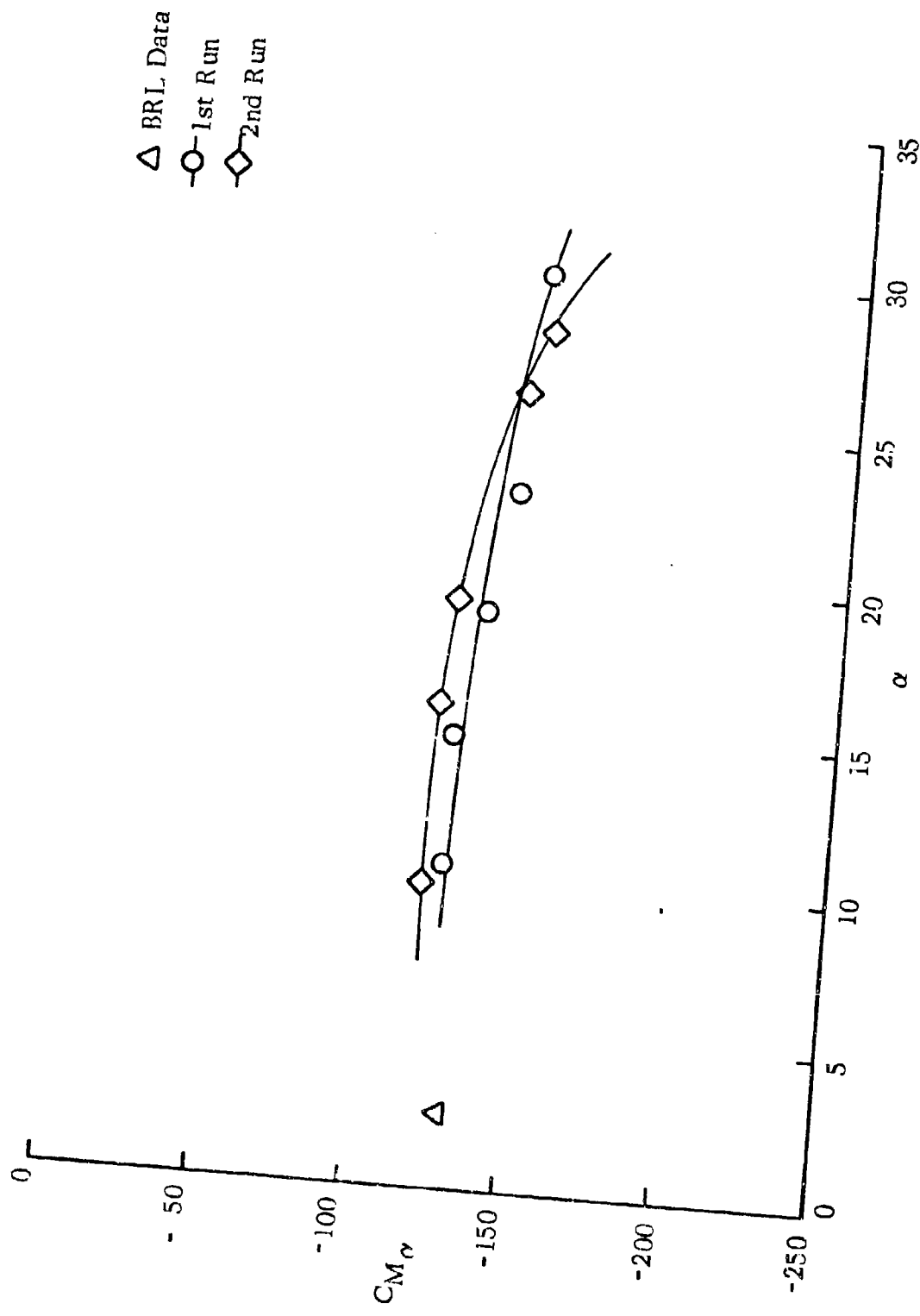


Figure 39. C_{M_α} vs α (Swaged Point)

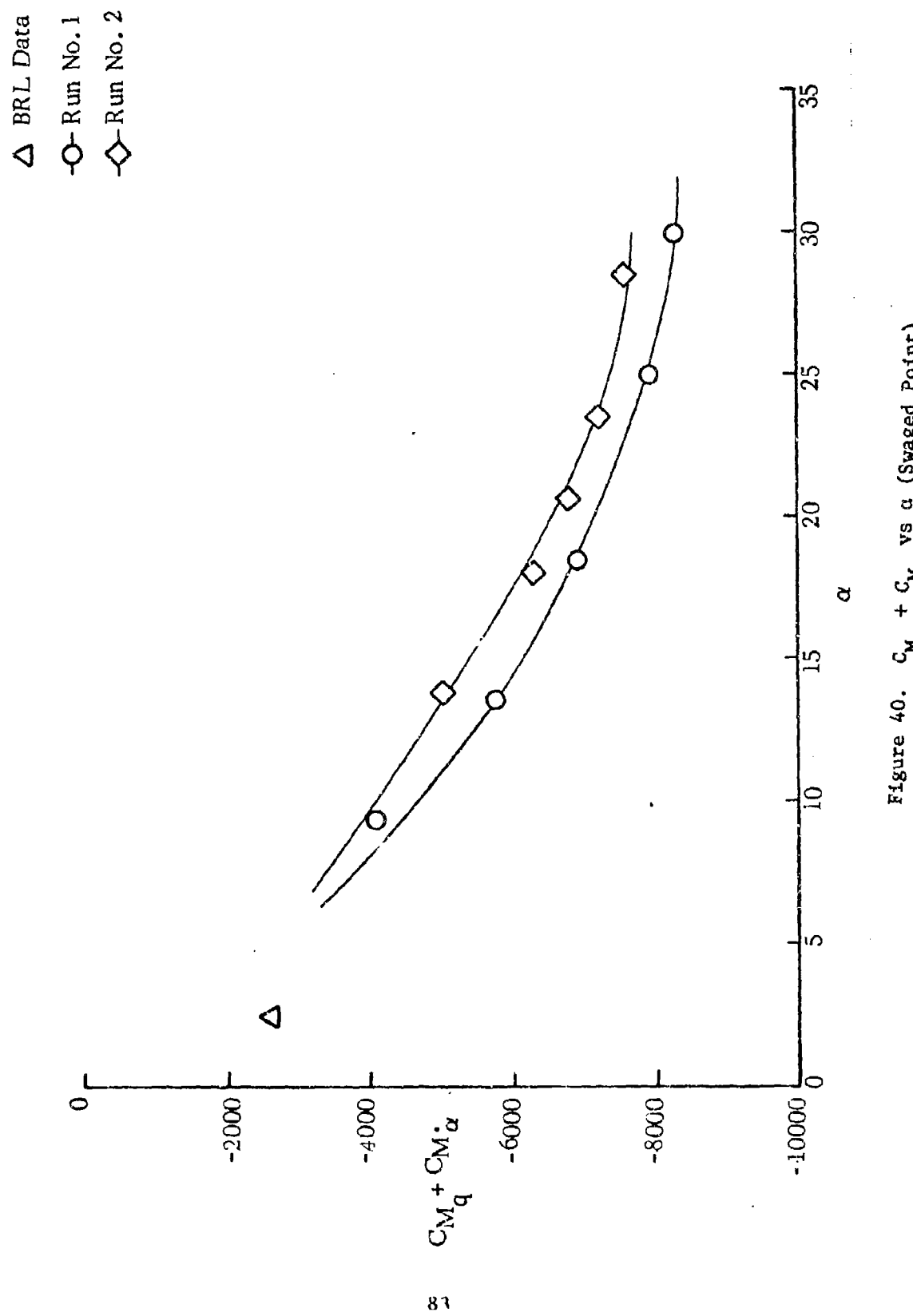


Figure 40. $C_{M_q} + C_{M_\alpha}$ vs α (Swaged Point)

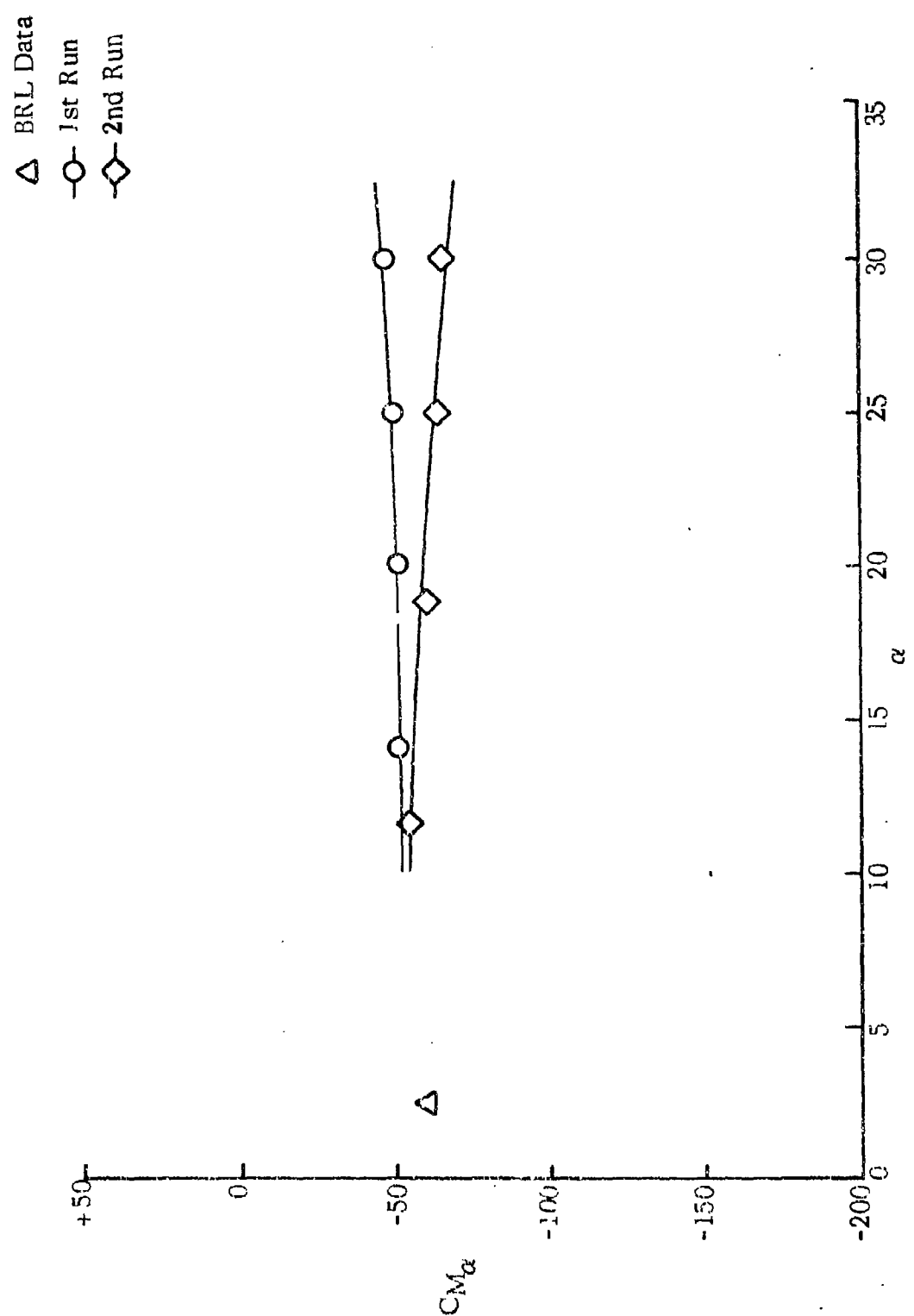


Figure 41. C_{M_α} vs α (Tracer)

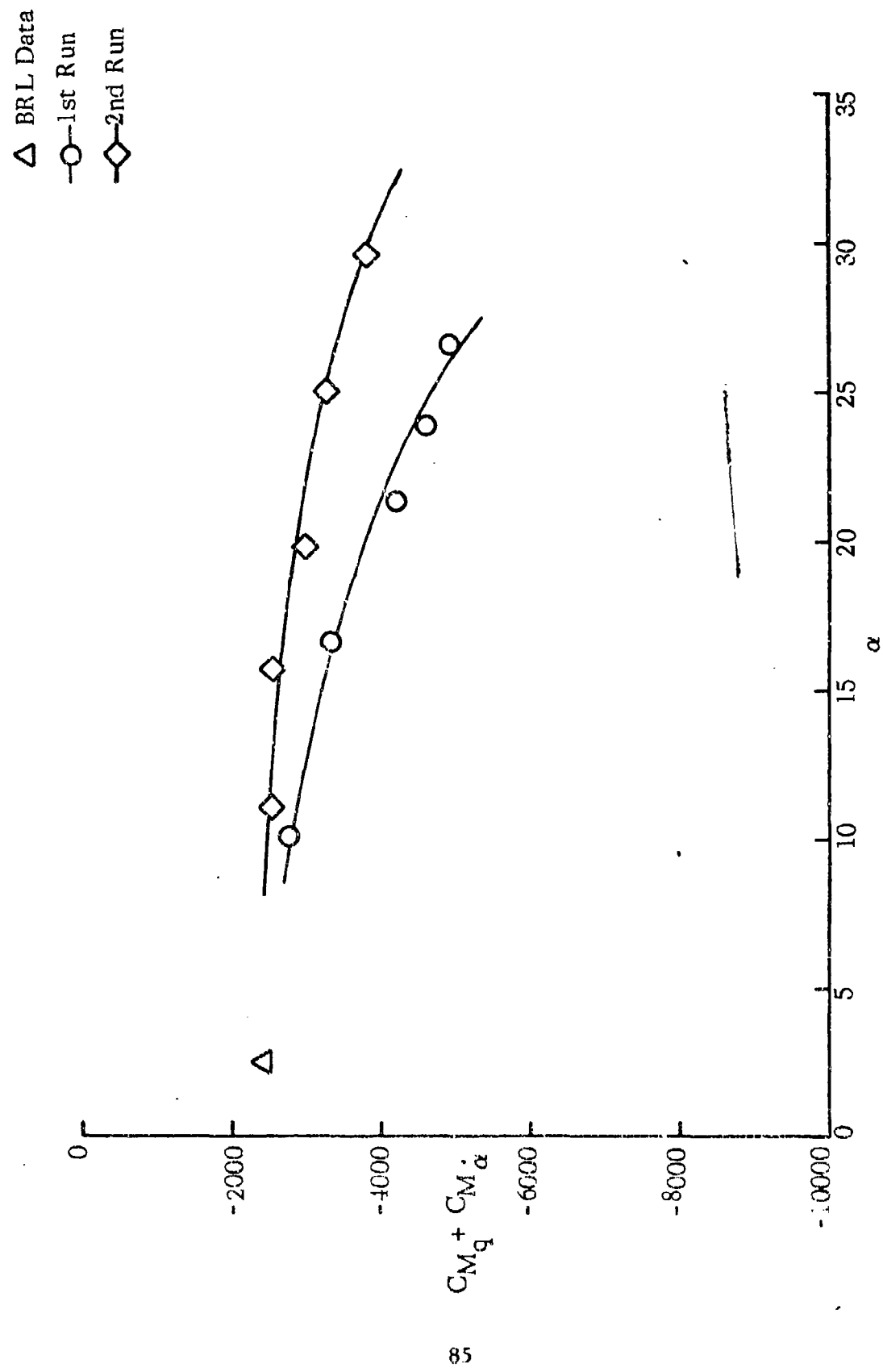


Figure 42. $C_{M_q} + C_{M_d}$ vs α (Tracer)

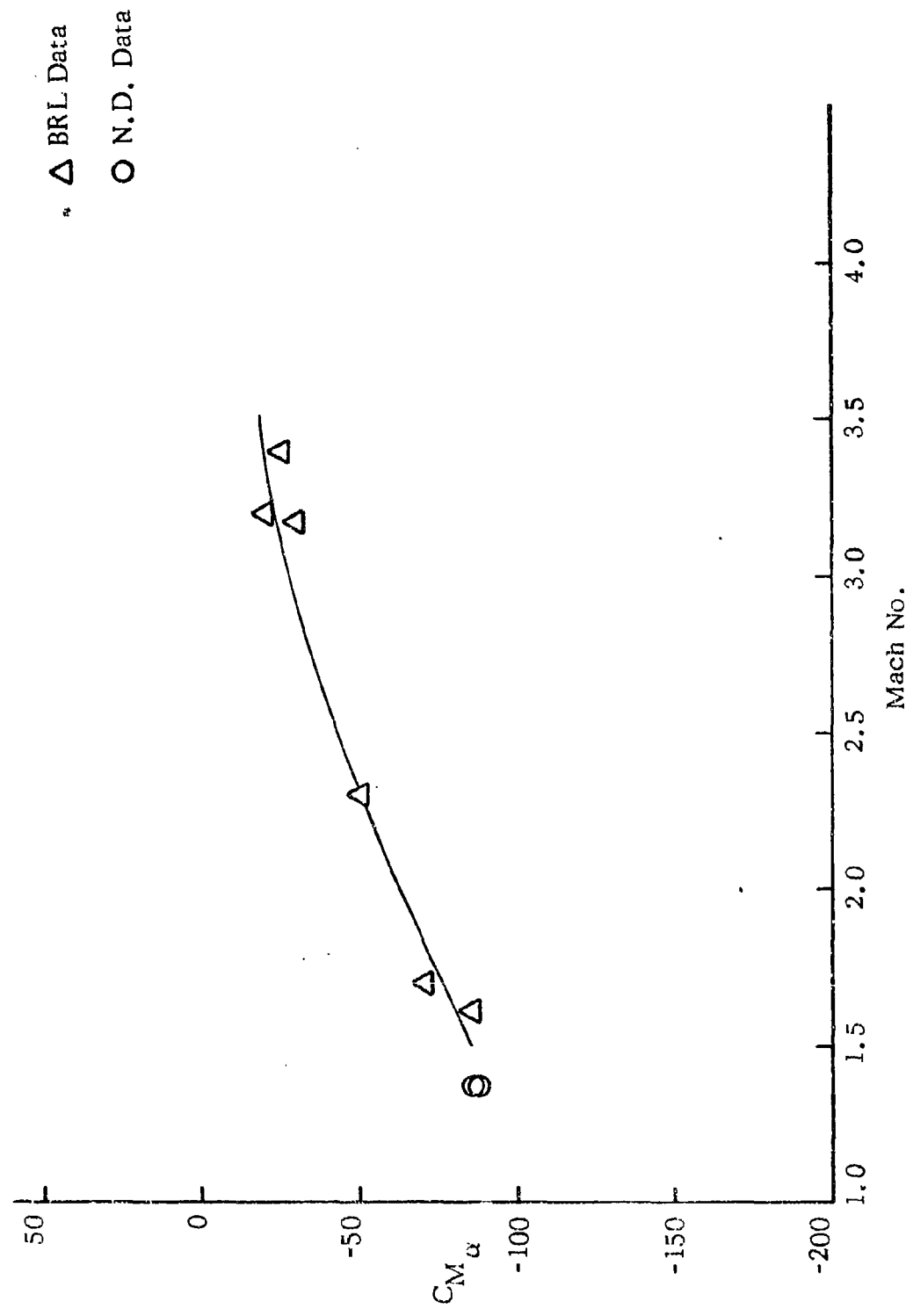


Figure 43. C_{M_α} vs Mach No. (Olin)

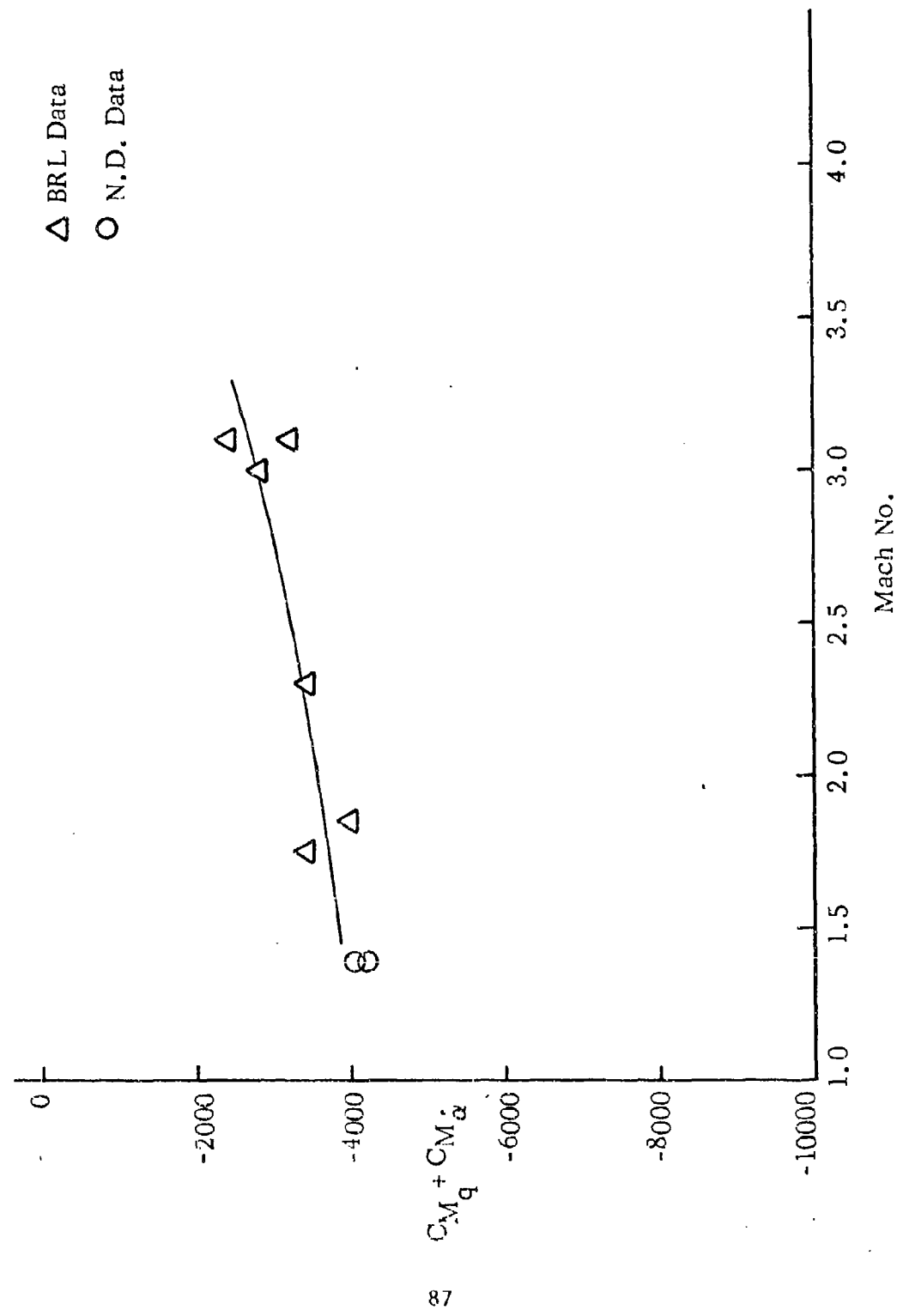


Figure 44. $(C_{M_q} + C_{M_\alpha})$ vs Mach No. (Ground Point)

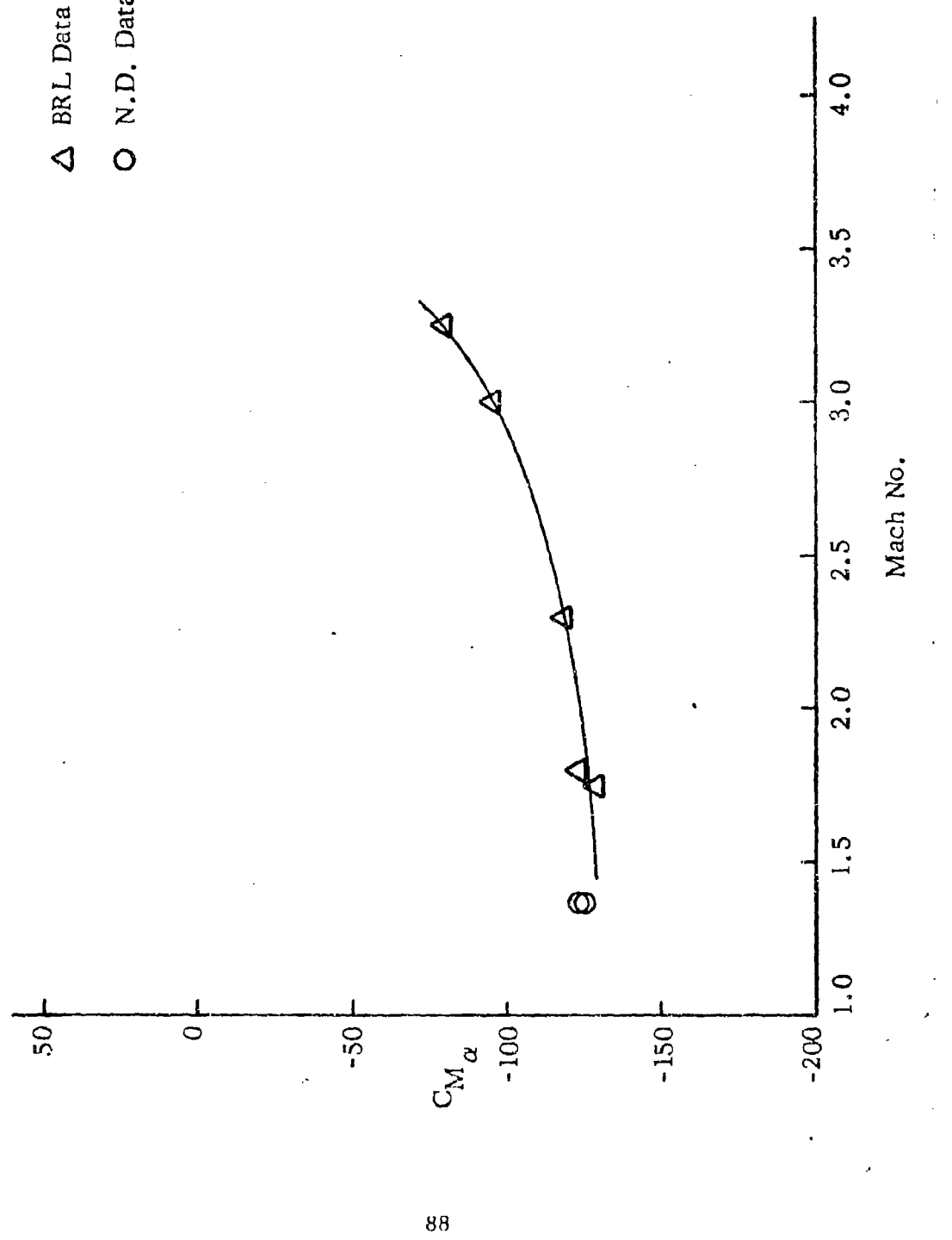


Figure 45. $C_{M\alpha}$ vs Mach No. (Ground Point)

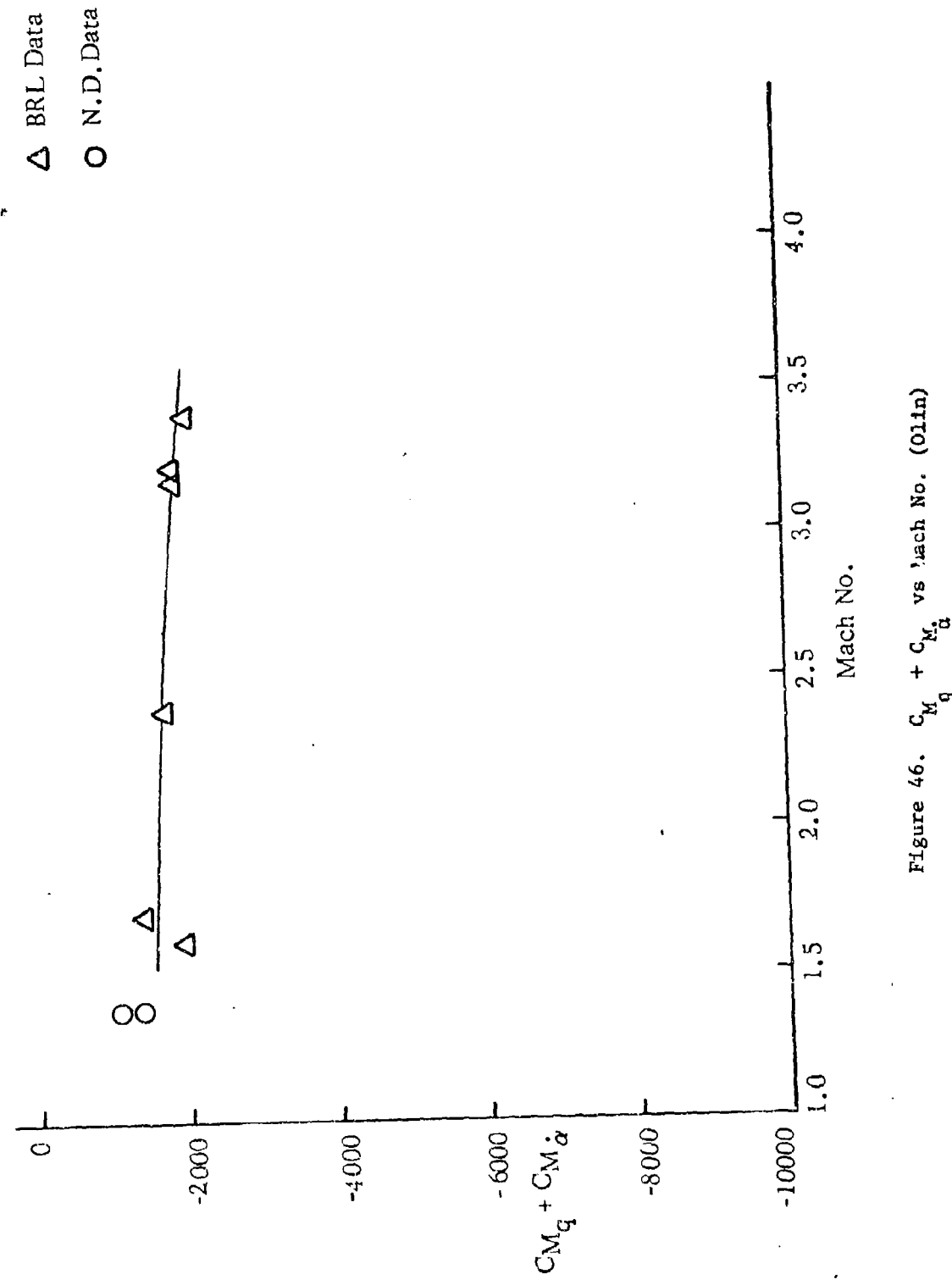


Figure 46. $C_{M_q} + C_{M\alpha}$ vs Mach No. (Olin)

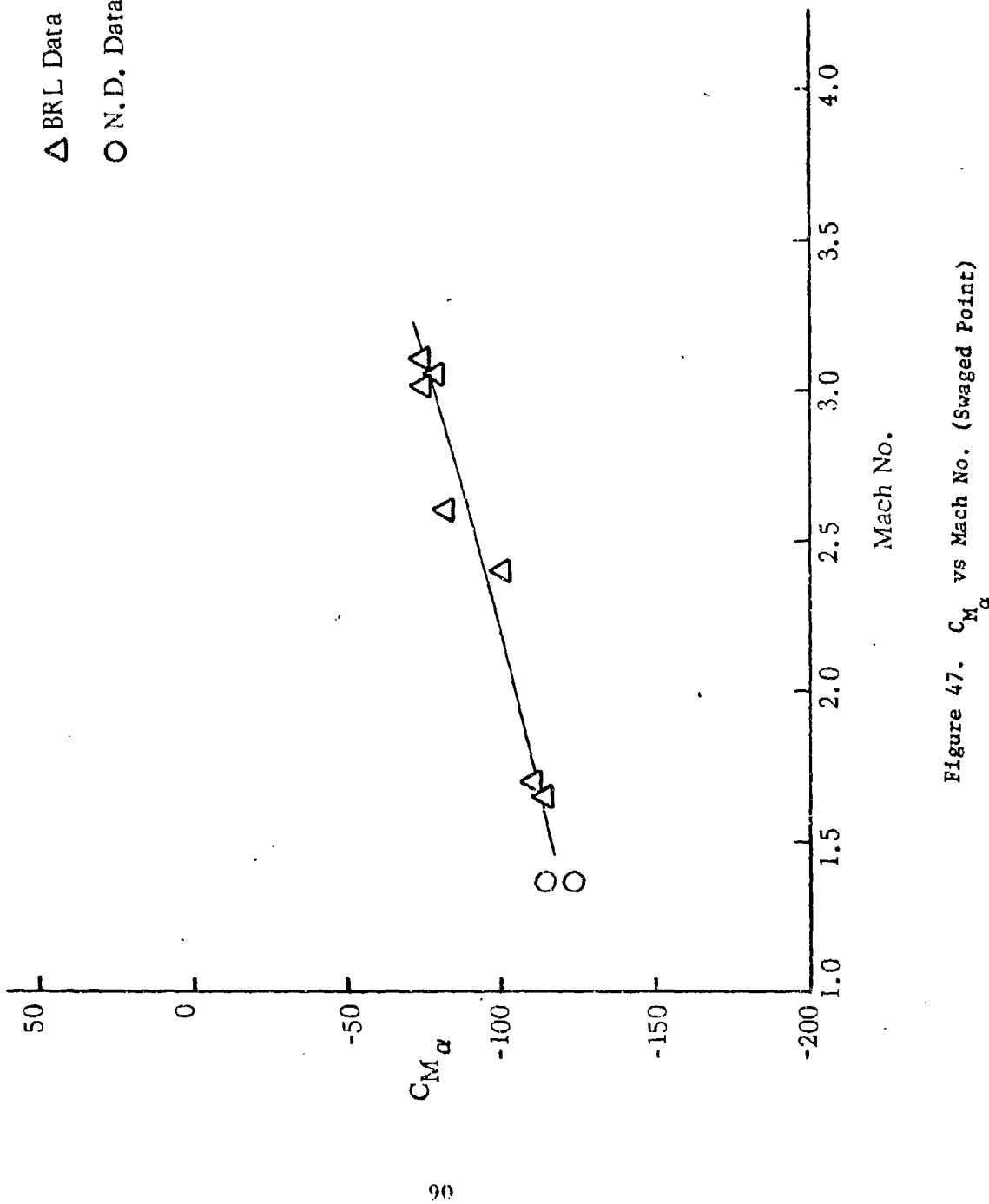


Figure 47. C_M vs Mach No. (Swaged Point)

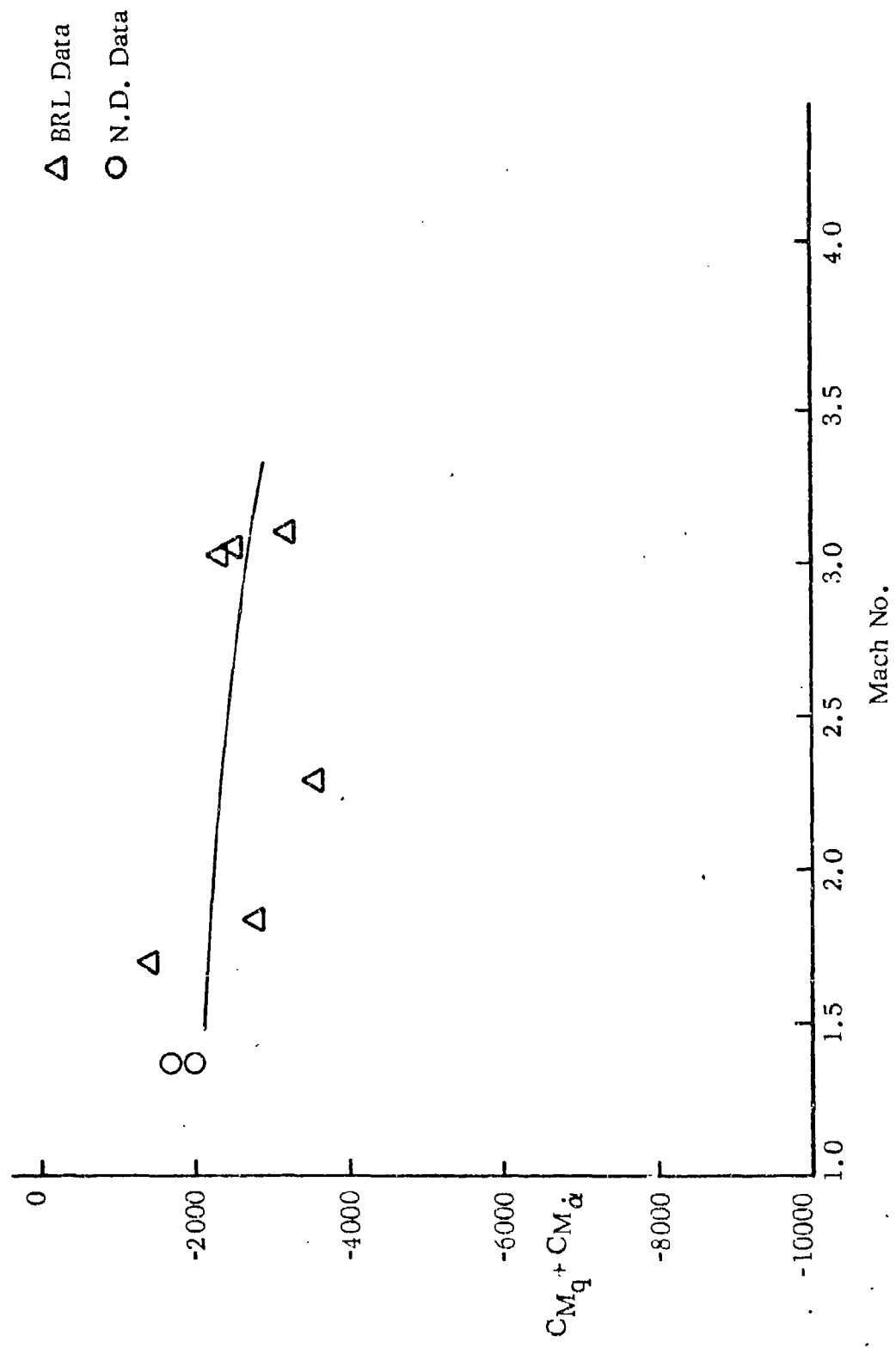


Figure 48. $(C_{Mq} + C_{Md})$ vs Mach No. (Swaged Point)

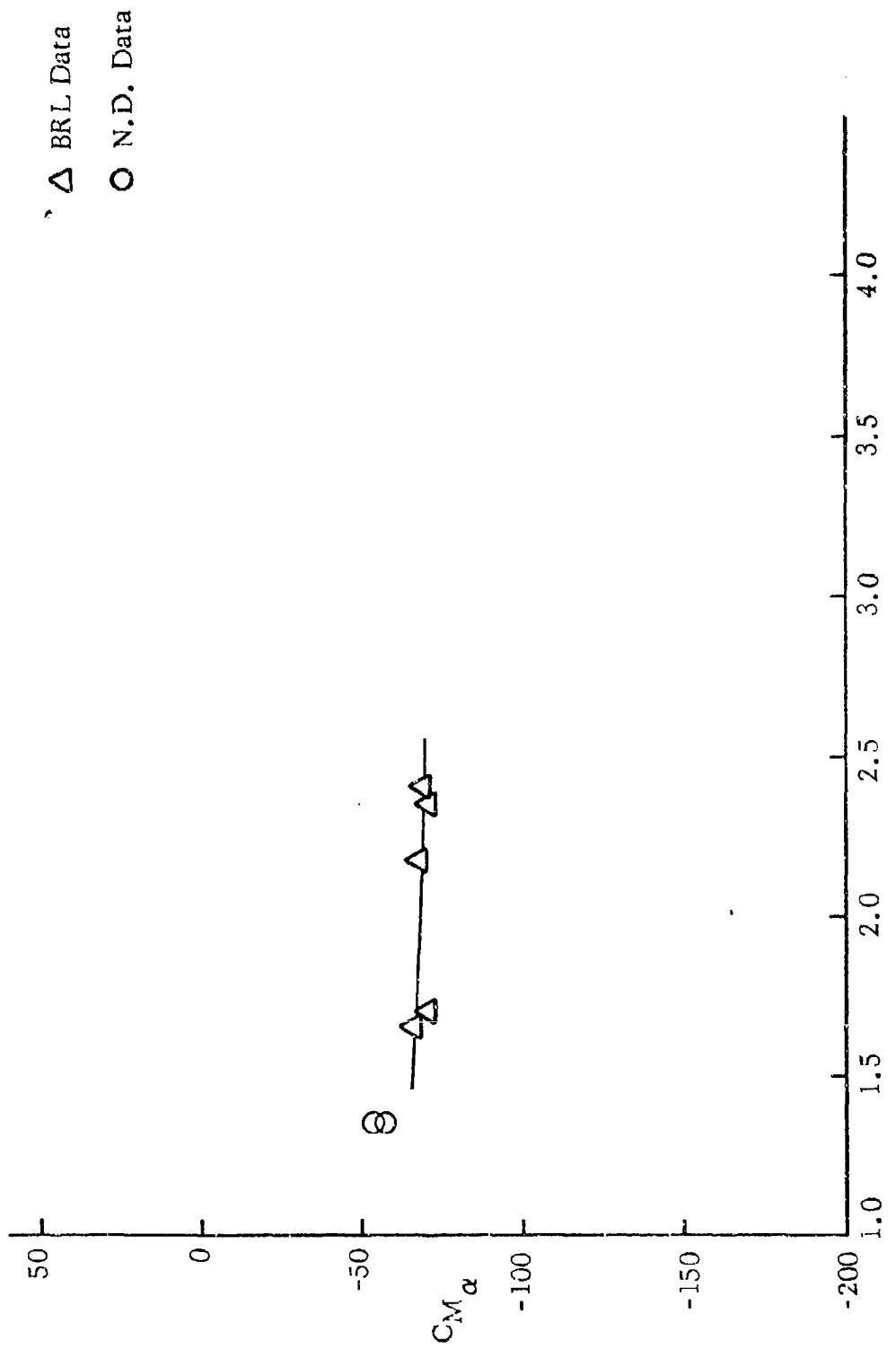


Figure 49. C_{M_α} vs Mach No. (Tracer)

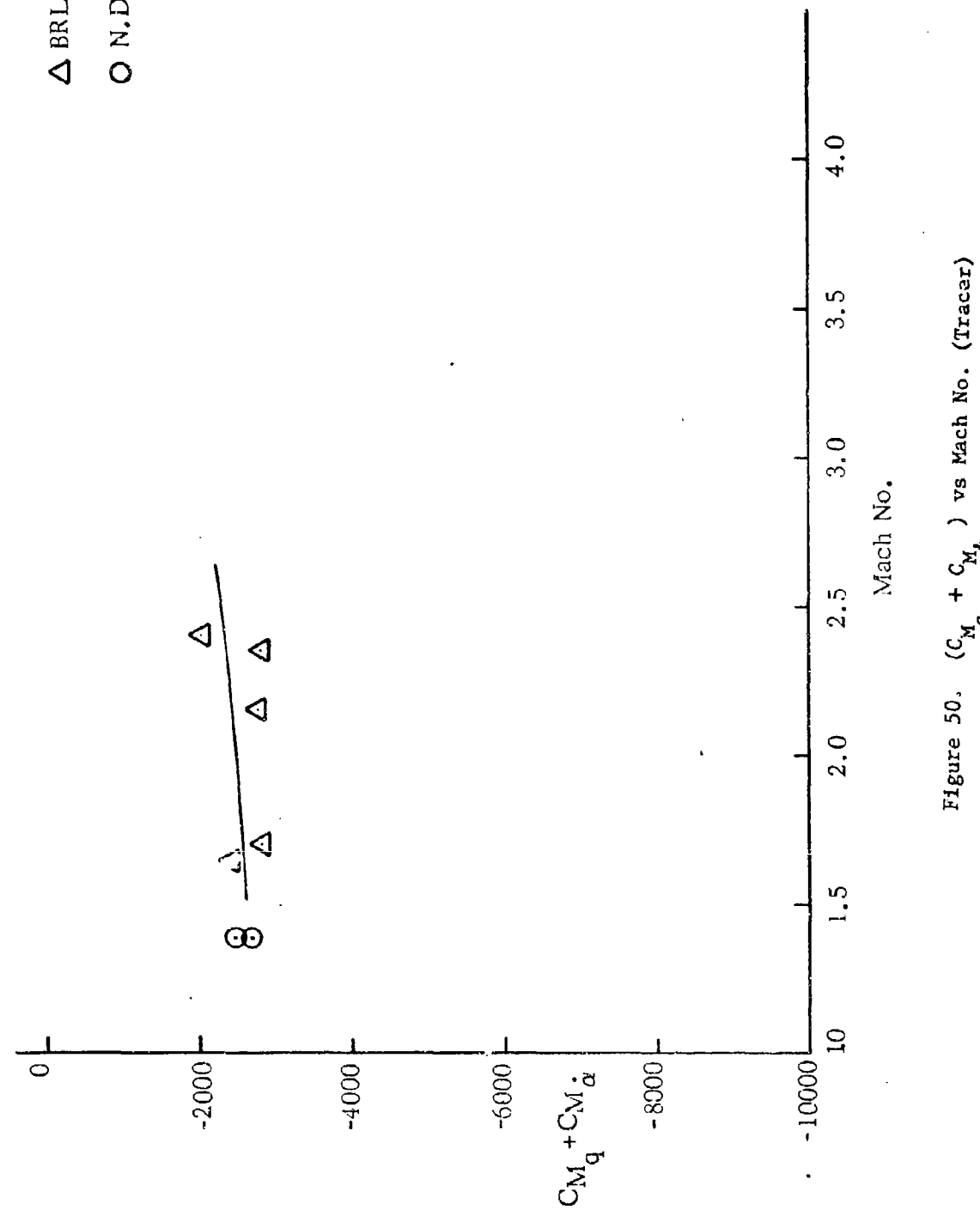


Figure 50. $(C_{M_q} + C_{M_\alpha})$ vs Mach No. (Tracar)

CONCLUSIONS

Single-degree-of-freedom dynamic supersonic wind tunnel tests of four flechette configurations has been presented. Linear values of $C_{M\alpha}$ and $(C_{Mq} + C_{M\dot{\alpha}})$ were determined from stability parameters acquired from the data taken during the tests. These values of $C_{M\dot{\alpha}}$ and $C_{Mq} + C_{M\dot{\alpha}}$ showed good repeatability and were compared to results from the Ballistics Range Laboratory (BRL) for the same designs at low angles of attack. Over the range of comparison the agreement between the two sets of data was shown to be quite good.

The repeatability of the results was a good indication of the absence of frictional effects and interference effects to the flow which might have been caused by the support system. In Reference 7 it was shown that this excellent one-degree-of-freedom dynamic testing technique can be easily extended to include the determination of nonlinear values of the static pitching and damping stability coefficients. Also, because the model is suspended at its center of gravity, there is no reason why this technique could not be moved into a horizontal supersonic wind tunnel if necessary.

APPENDIX A

MODEL PARAMETERS

Ground Point

Diameter = .012 ft.
 $I_y = .000004647 \text{ slugs}\cdot\text{ft}^2$
Mass = .0003647 slugs
Radius = 1.69 in.

Olin

Diameter = .0119 ft.
Mass = .000303 slugs
 $I_y = .000007040 \text{ slug}\cdot\text{ft}^2$
Radius = 1.52 in.

Tracer

Diameter = .01533 ft.
Mass = .0004520 slugs
 $I_y = .0000105570 \text{ slugs}\cdot\text{ft}^2$
Radius = 2.11 in.

Swaged Point

Diameter = .012 ft
Mass = .0003933 slugs
 $I_y = .000006041 \text{ slugs}\cdot\text{ft}^2$
Radius = 1.69 in.

APPENDIX B

SUPERSONIC WIND TUNNEL OPERATING PROCEDURE

Starting Procedure

1. Open valve to compressor manifold for wind tunnel to be used - make sure that the other wind tunnels are either shut off or blocked from the manifold.
2. Inform University Power Plant of intention to run compressors.
3. Turn cooling water on (one valve near wall inside laboratory).
4. Turn each compressor shaft to make sure they are free to rotate.
5. Check oil level for each compressor (oil level should be above gear).
6. Check oil pump for each compressor i.e. depress six plungers and observe oil bubbles.
7. Add a few squirts of No. 51 oil to hole in top of shaft bushing.
8. Check mercury manometer tubing in compressor room to make sure it is connected.
9. Turn master power switch on for each compressor.
10. Start one compressor - allow at least one minute after compressor comes up to speed before starting the second compressor and allow another one minute after this compressor comes up to speed before starting third compressor.
- 11.. If mercury manometer reads more than 18 inches, Shut Down Immediately.

Shut Down Procedure

1. Shut compressors off one at a time at one minute intervals.
2. Turn master power switch off for each compressor.
3. Shut compressor cooling water off.
4. Inform University Power Plant that compressors have been shut off.

APPENDIX C

ONE-DEGREE-OF-FREEDOM TEST RESULTS ON R&D FLECHETTES

The model* was initially disturbed to an angle of attack of approximately 180° and then allowed to oscillate freely. The resulting angular motions were then recorded by a high speed camera technique.

One-Degree-of-Freedom Data Reduction

The "Wobble" computer program was used to fit the one-degree-of-freedom Aeroballistic Theory to the angular oscillations obtained from the moving camera technique. This data was fitted in segments of 2.2 cycles with each segment containing approximately 25 points. The stability parameters K_1 , K_T , λ_1 , ω_1 , were determined by the Wobble program at a time interval of 0.015 seconds. The average percent error of the theory to the data showed an error of less than 3%. A representative plot of probable error of fit vs time is shown in Fig. 1a.

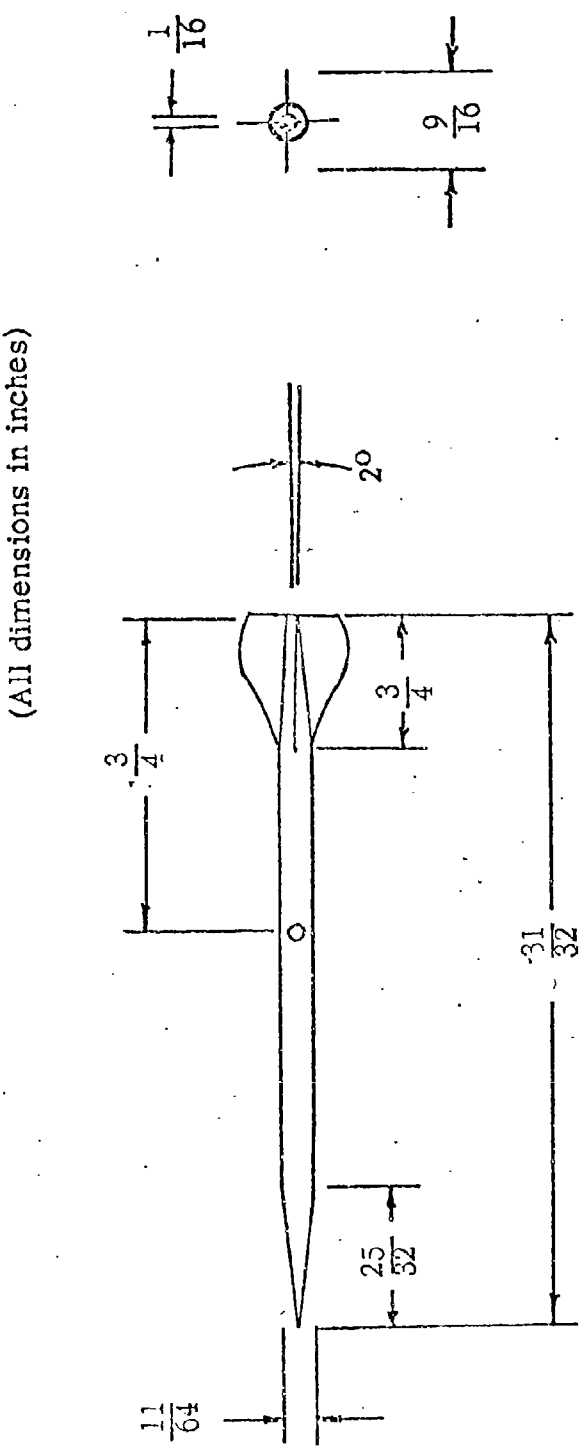
The stability parameters were obtained from the fits as functions of time, representative angular oscillations, probable errors of fit, and stability parameters are presented in Figs. 2 through 6. The resulting stability coefficients versus time are presented in Figs. 7 and 8.

One-Degree-of-Freedom Nonlinear Stability Coefficients

To get an indication of the nonlinearity of the stability coefficients

*Figure 1.

Figure 1. Schematic 1-D Pitch Model



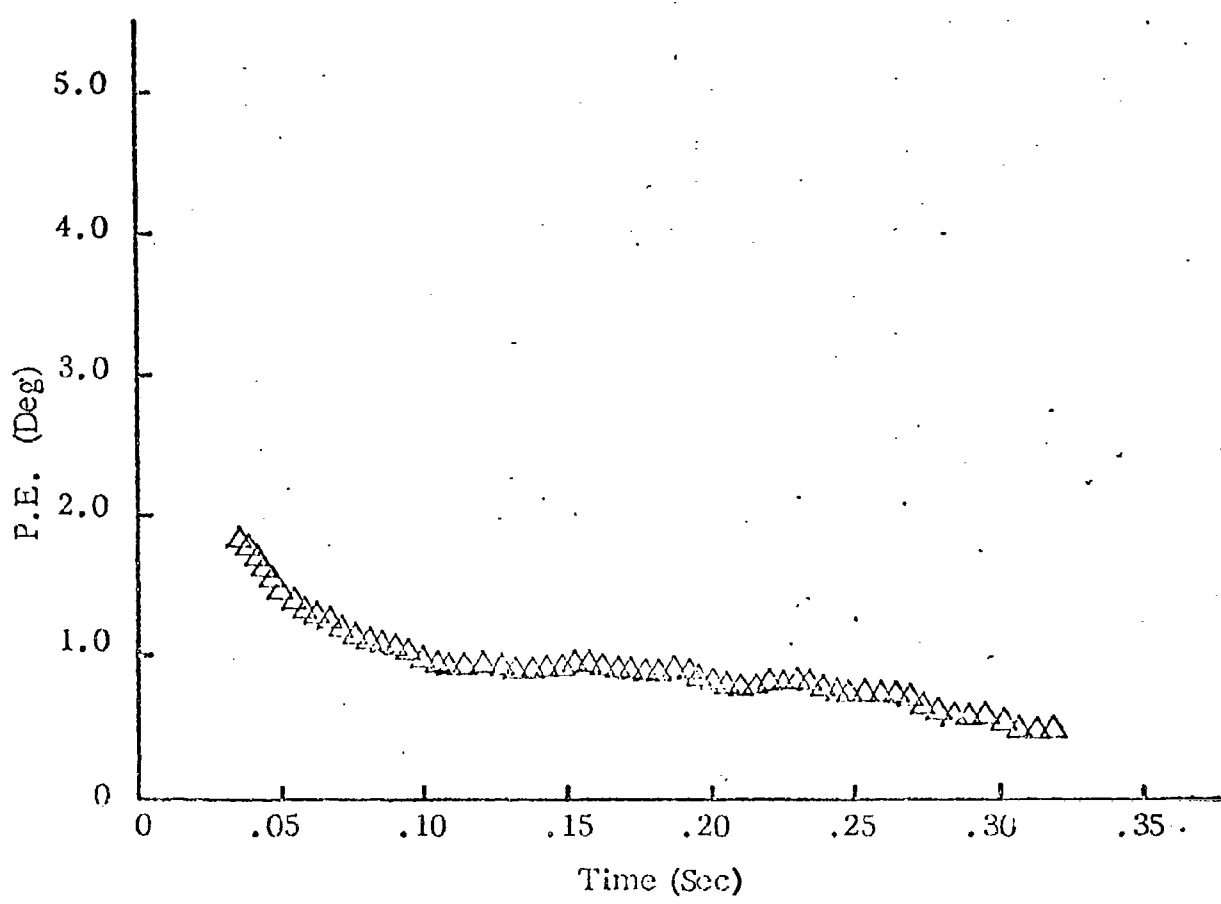


Figure 1a. Probable Error of Fit vs Time

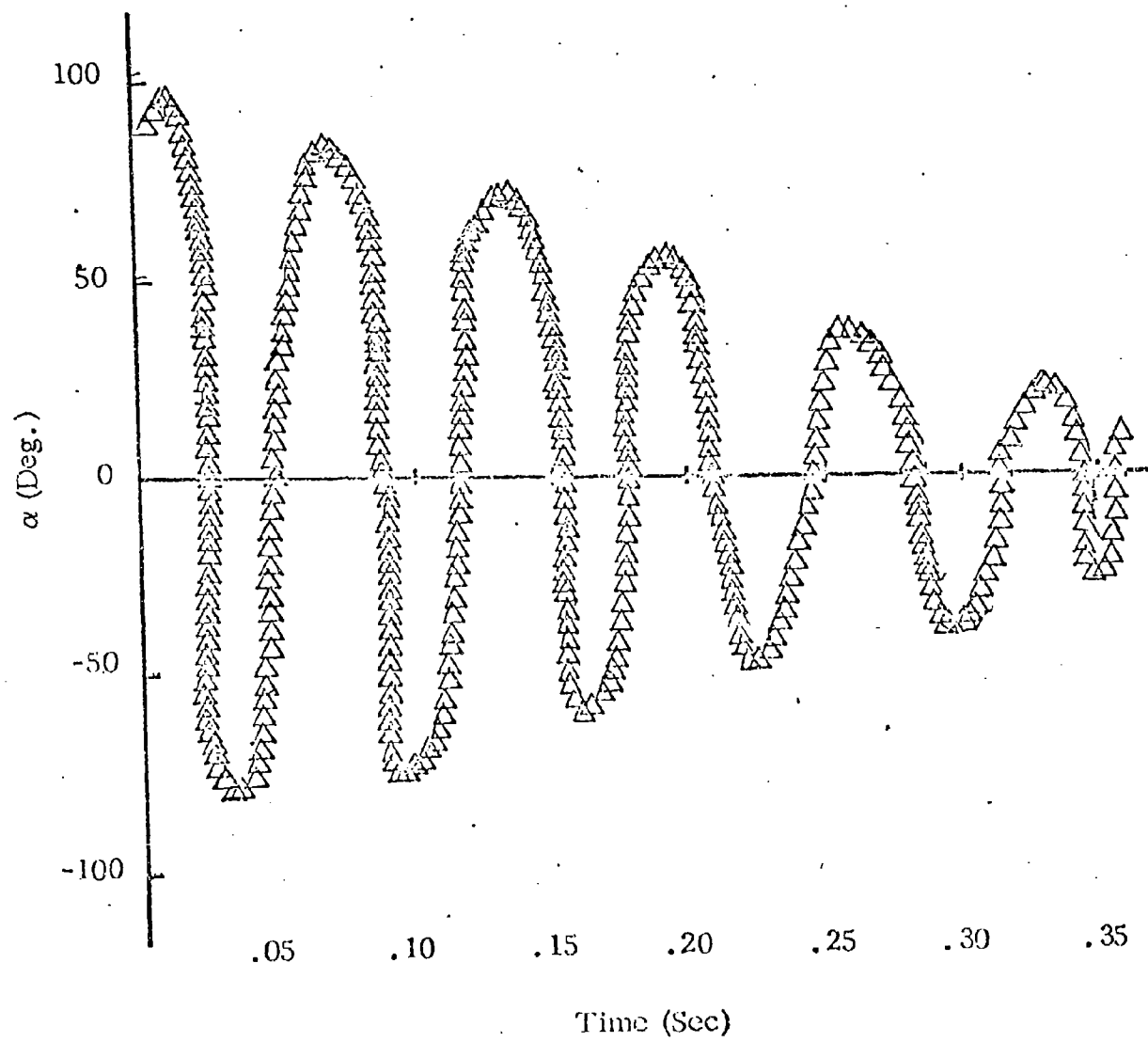


Figure 2. 1-D Oscillatory Motion

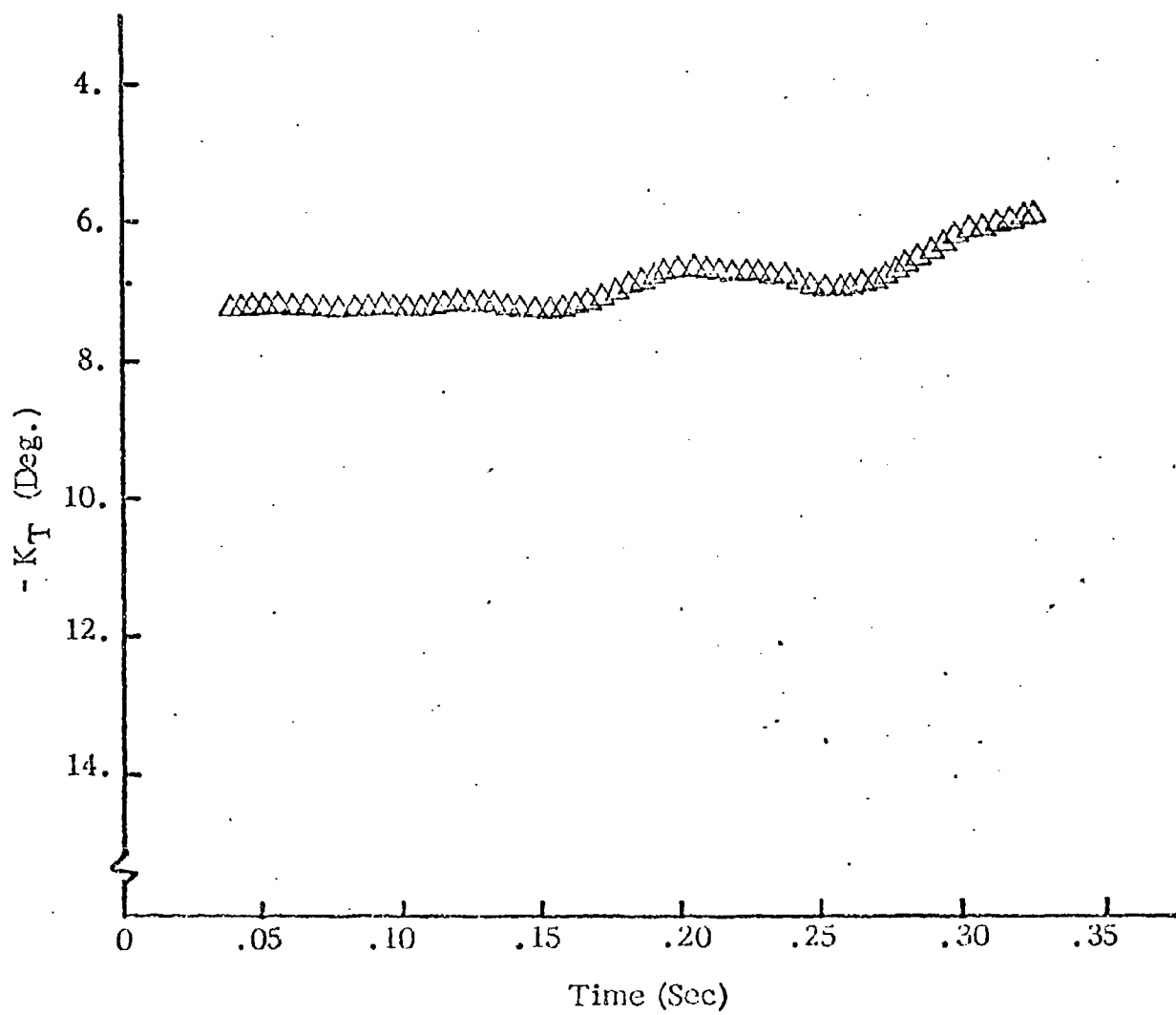


Figure 3. Trim Mode vs Time

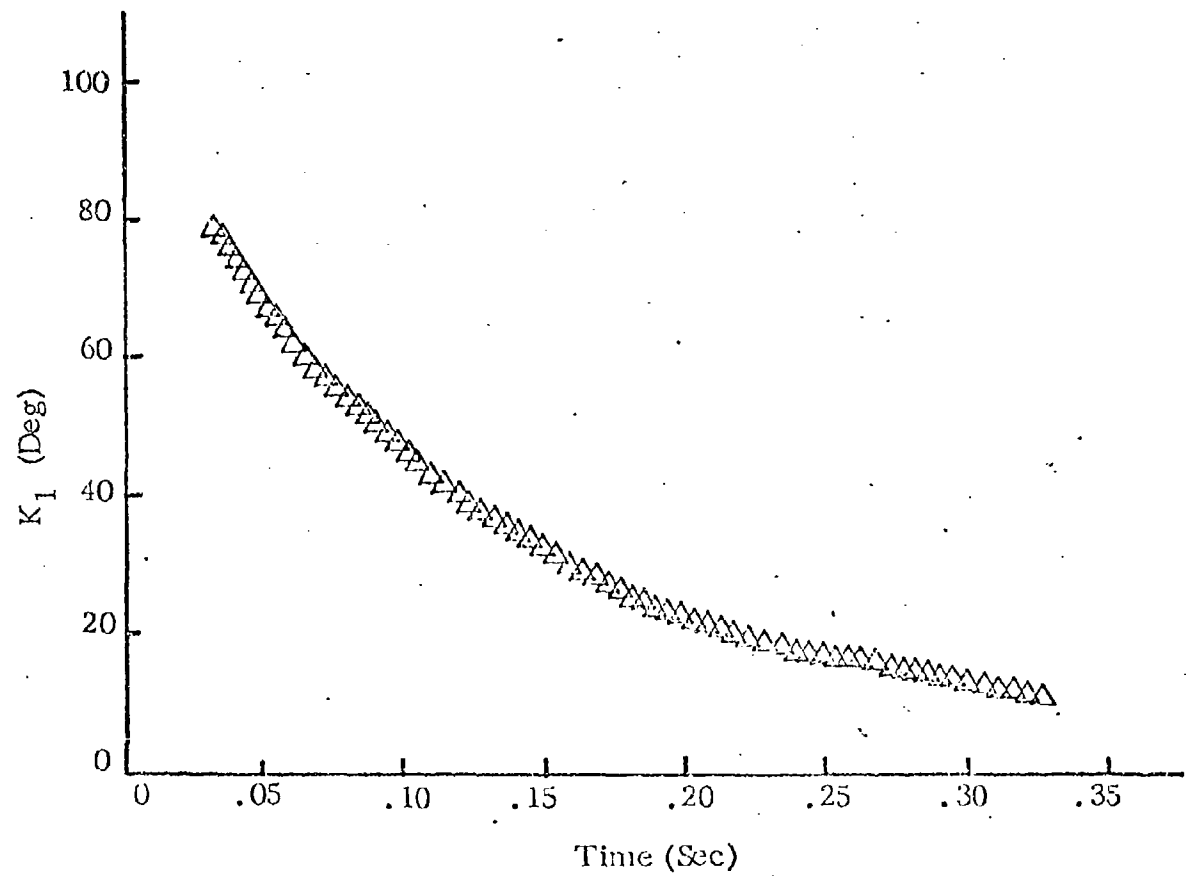


Figure 4. K_1 vs Time

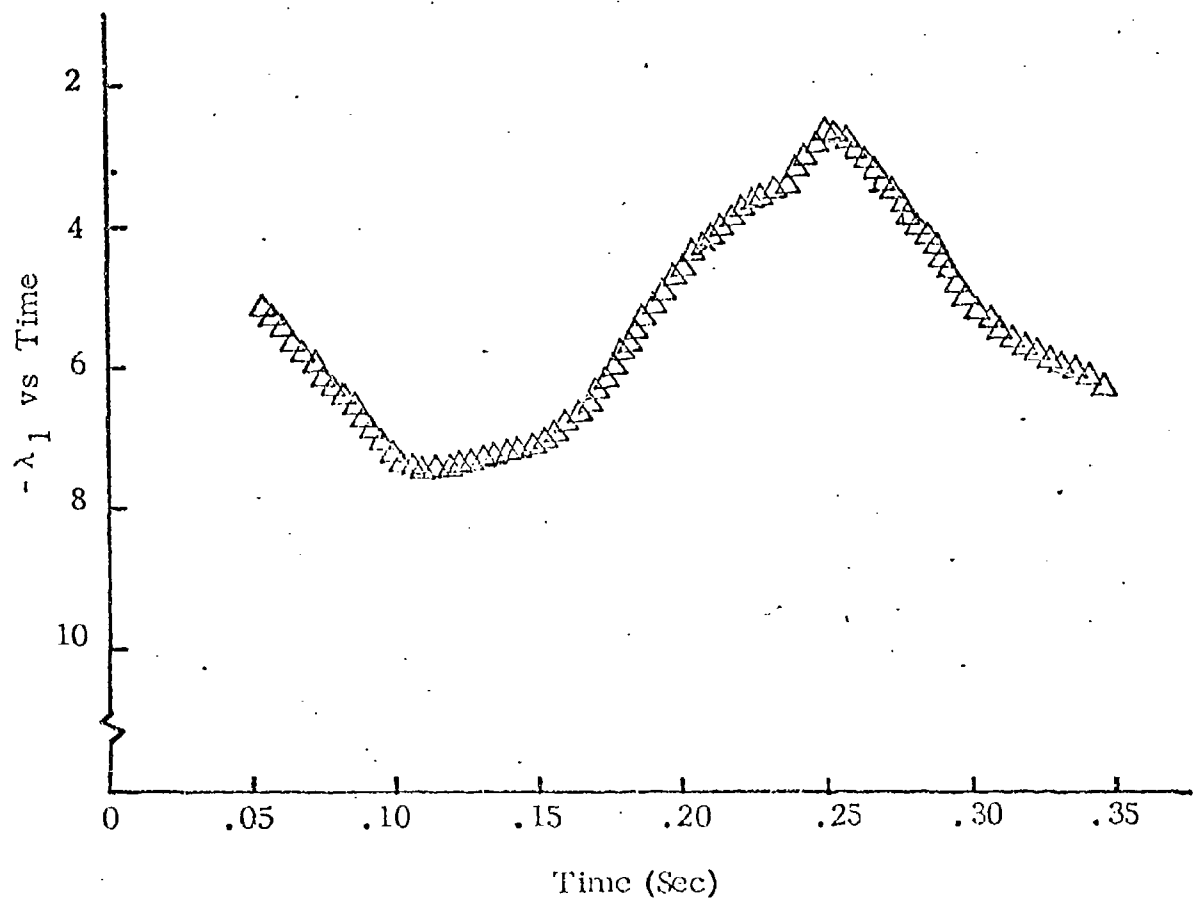


Figure 5. λ_1 vs Time

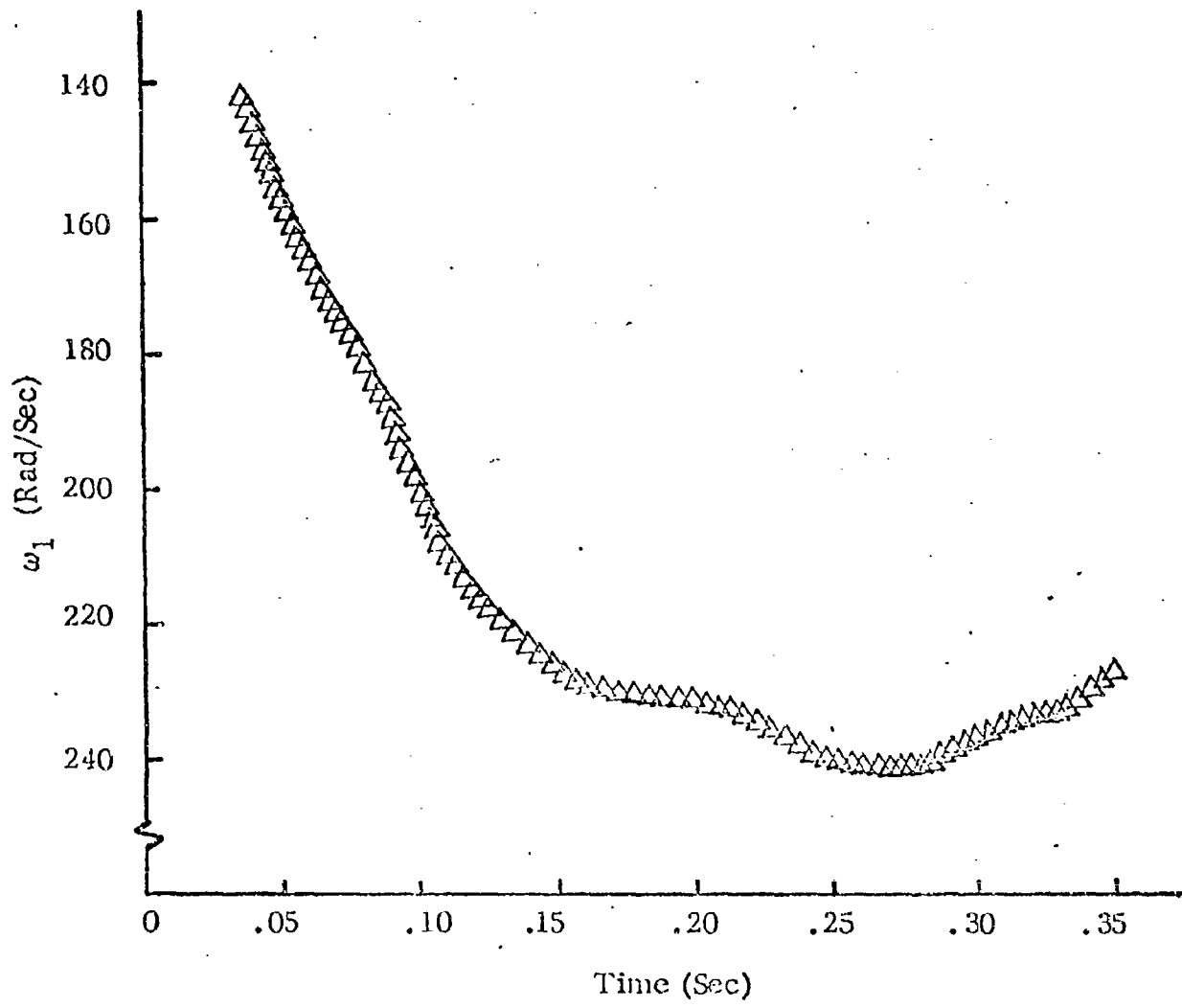


Figure 6. ω_1 vs Time

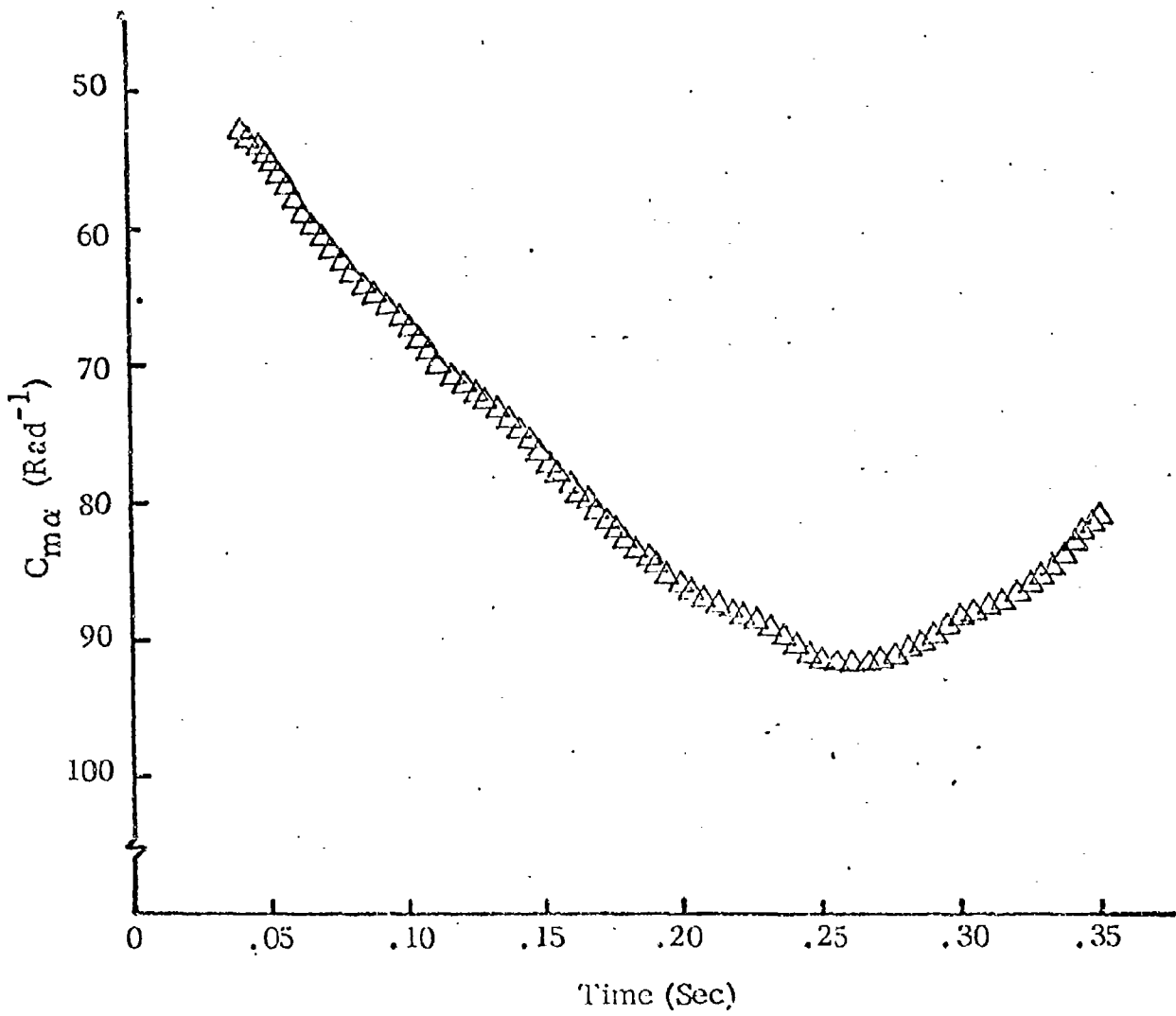


Figure 7. C_{ma} vs Time

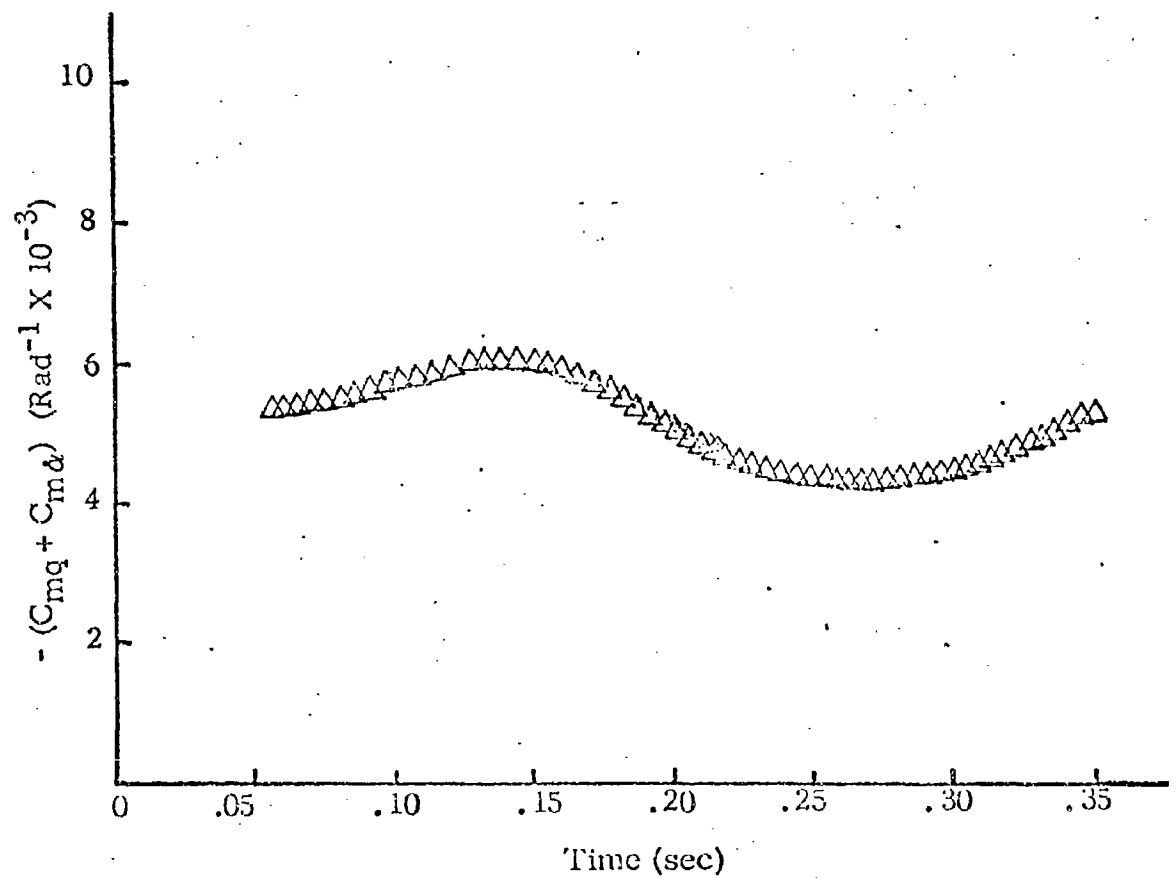


Figure 8. $(C_{mq} + C_{m\bar{a}})$ vs Time

$$C_{m\alpha}(\alpha) = C_{m\alpha_0} + C_{m\alpha_2} (\alpha)^2$$

△ Run 9
 ◎ Run 12
 □ Run 14

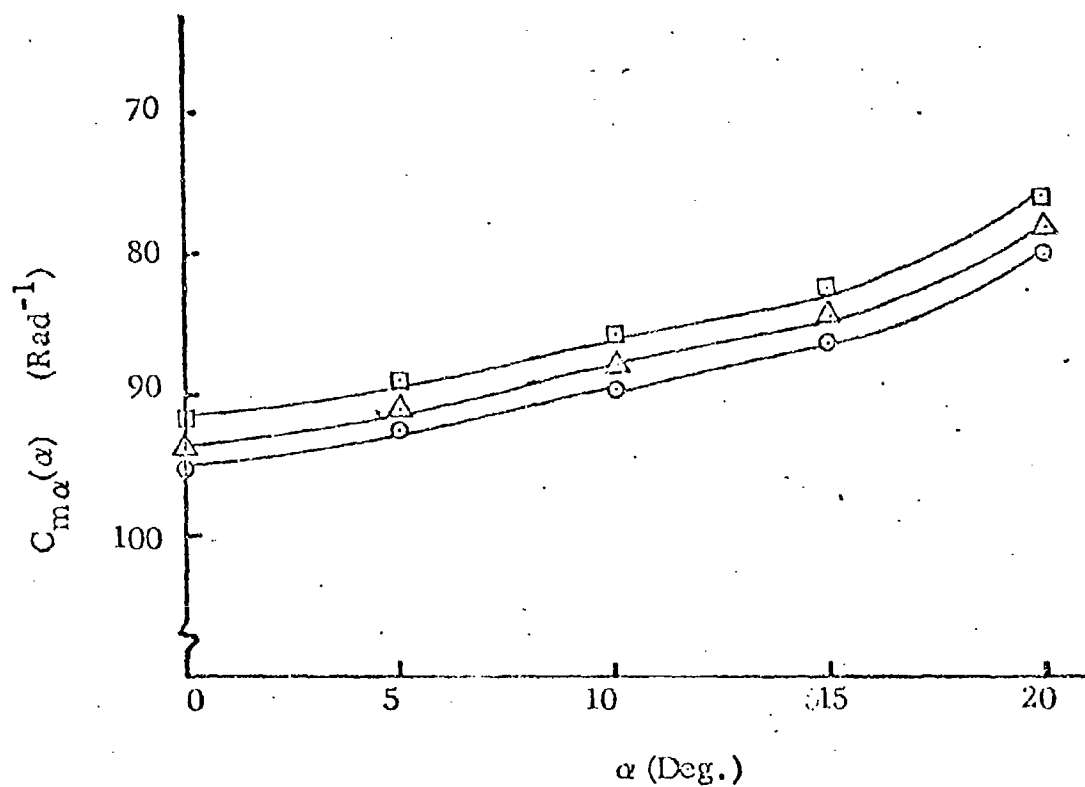


Figure 9. $C_{m\alpha}(\alpha)$ vs α

$$C_{mq}(\alpha) + C_{m\dot{\alpha}}(\alpha) = (C_{mq} + C_{m\dot{\alpha}})_0 + (C_{mq} + C_{m\dot{\alpha}})_2 (\alpha^2)$$

Δ Run 9

\circ Run 12

\square Run 14

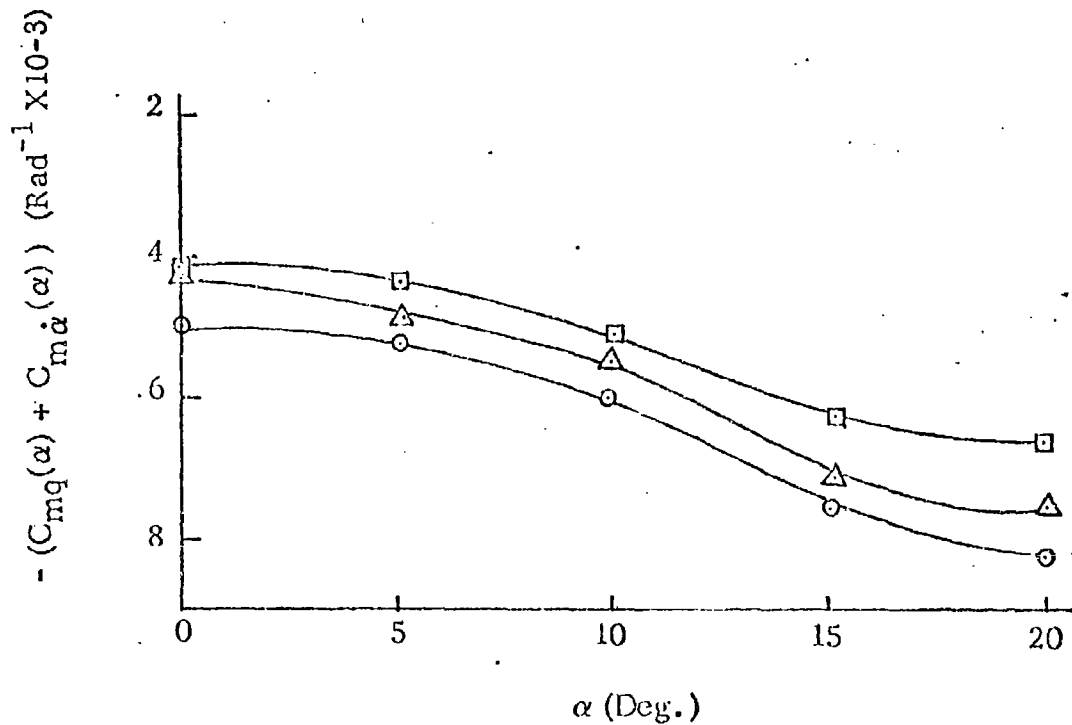


Figure 10. $(C_{mq}(\alpha) + C_{m\dot{\alpha}}(\alpha))$ vs α

with angle of attack, the one-degree-of-freedom Nonlinear Aeroballistic Theory was employed. Using this nonlinear theory, the stability coefficients were determined as polynomial functions of the angle of attack. Representative plots of runs made are presented in Figs. 9 and 10.

Both $C_{m\alpha}$, the pitching moment coefficient and $C_{mq} + C_{m\dot{\alpha}}$ the damping moment coefficient were found to vary nonlinearly with angle of attack. Both were found to be highly repeatable. $C_{m\alpha}$ varied no more than 2% about its mean while $C_{mq} + C_{m\dot{\alpha}}$ varied less than 5% about its mean.

APPENDIX C

DISPERSION THEORY OF HIGH FINENESS RATIO, CRUCIFORM FIN BODIES *

A complete Jump and Dispersion Theory is developed for free flight vehicles. Six-degree-of-freedom computer computations indicates that the theory accurately predicts the jump and dispersion of flechettes.

The initial conditions and dispersion values are established by range test firings. The raw data is fitted by least squares method and put into initial condition form. Initial conditions are applied to the theory and 6-D numerical computations to evaluate dispersion for eight test rounds. The results are compared to test firing target data. The agreement between the theory and test results indicate the data analysis and theory provide an accurate means of predicting dispersion of flechettes. Analysis of the firing data indicates that the initial conditions result from an impulse imparted to the flechette in the muzzle blast. The transverse impulse imparted to the flechette initially must be equal to the angular impulse to obtain zero dispersion. Other disturbances in the blast region such as sabot separation influence the initial conditions and hence dispersion. First maximum yaw theory is discussed and disproved.

*Prepared by Lawrence E. Lijewski.

TABLE OF CONTENTS

	Page
TABLE OF CONTENTS	112
LIST OF TABLES	114
LIST OF FIGURES	116
LIST OF SYMBOLS	122
INTRODUCTION	130
DISPERSION THEORY	134
High Roll Rate Theory	138
Low Roll Rate Theory	140
Very Slow Roll Rate Theory	142
VALIDATION OF THEORY	144
Phase I	145
Phase II	155
Phase III	160
Comparison: High, Low, Very Slow Roll Rate Theories	194
Phase IV	200
FREE FLIGHT DATA ANALYSIS	206
DISPERSION ANALYSIS	246
Free Flight vs Theory	246
Dispersion Theory vs First Maximum	
Yaw Hypothesis	266

TABLE OF CONTENTS (continued)

	Page
PHYSICAL EVALUATION OF DISPERSION	276
CONCLUSIONS	282
APPENDIX A-1	285
APPENDIX A-2	295
REFERENCES	337

LIST OF TABLES

Number		Page
I	Theory Validation, Restoring and Damping Moments, Cases 1-9	146
II	Theory Validation, Restoring and Damping Moments, Cases 10-18	147
III	Theory Validation, Restoring and Damping Moments, Cases 19-27	151
IV	Theory Validation, Restoring and Damping Mornents, Cases 28-36	152
V	Magnus Coefficients, at Mach 4.5	155
VI	Theory Validation, Magnus, Cases 37-57 . . .	157
VII	Theory Validation, Asymmetries, Cases 58-68	162
VIII	Theory Validation, Asymmetries, Cases 69-79	163
IX	Theory Validation, Asymmetries, Cases 80-90	164
X	Theory Validation, Asymmetries, Cases 91-101	172
XI	Theory Validation, Asymmetries, Cases 102-112	173
XII	Theory Validation, Asymmetries, Cases 113-123	174

LIST OF TABLES (continued)

Number		Page
XIII	Theory Validation, Asymmetries, Cases 124-134	181
XIV	Theory Validation, Asymmetries, Cases 135-145	182
XV	Theory Validation, Asymmetries, Cases 146-156	183
XVI	Theory Validation, Asymmetries, Cases 157-167	191
XVII	Theory Validation, Asymmetries, Cases 168-178	192
XVIII	Theory Validation, Asymmetries, Cases 179-189	193
XIX	Theory Validation, Gravity Cases 190-201	204
XX	Frankford Test Firing Data	209
XXI	Aerodynamic Parameters from Least Squares Fit	245
XXII	Dispersion Analysis Results	247

LIST OF FIGURES

Number		Page
1	Dispersion: Phase I Cases 10-18.	148
2	Trajectories, Cases 10-18	149
3	Dispersion: Phase I Cases 28-36	153
4	Trajectories, Cases 28-36	154
5	Dispersion: Phase II Cases 46,47,48,55,56, 57	158
6	Dispersion: Phase II Cases 38,41,44,47, 50,53,56	159
7	Dispersion: Phase III Cases 58-68	166
8	Dispersion: Phase III Cases 69-79	167
9	Dispersion: Phase III Cases 80-90	168
10	Dispersion: Phase III Theory, Cases 58-90 . .	169
11	Trajectory, Case 79	170
12	Dispersion: Phase III Cases 91-101	175
13	Dispersion: Phase III Cases 102-112	176
14	Dispersion: Phase III Cases 113-123	177
15	Dispersion: Phase III Theory, Cases 91-123 .	178
16	Trajectory, Case 101	179
17	Dispersion: Phase III Cases 124-134	185
18	Dispersion: Phase III Cases 135-145	186
19	Dispersion: Phase III Cases 146-156	187
20	Dispersion: Phase III Theory, Cases 124-156 .	188
21	Trajectory, Case 134	189

LIST OF FIGURES (continued)

Number		Page
22	Dispersion: Phase III Cases 157-167	195
23	Dispersion: Phase III Cases 168-178	196
24	Dispersion: Phase III Cases 179-189	197
25	Dispersion: Phase III Theory, Cases 157-189 .	198
26	Trajectory, Case 189	199
27	Phase III Theory Equations 24, 28, 30	201
28	Phase III Theory Effective Limits	202
29	Ground Point Flechette, With and Without Sabot	207
30	Free Flight Test Apparatus and Set-Up	208
31	Raw Translational Data Ground Point - Round 4	210
32	Raw Angular Data Ground Point - Round 4	211
33	Raw Translational Data Ground Point - Round 6	212
34	Raw Angular Data Ground Point- Round 6	213
35	Raw Translational Data Ground Point - Round 7	214
36	Raw Angular Data Groud Point - Round 7	215
37	Raw Translational Data Ground Point - Round 8	216

LIST OF FIGURES (continued)

Number		Page
38	Raw Angular Data Ground Point - Round 8 . . .	217
39	Raw Translational Data Ground Point -	
	Round 14	218
40	Raw Angular Data Ground Point -	
	Round 14	219
41	Raw Translational Data Ground Point -	
	Round 16	220
42	Raw Angular Data Ground Point - Round 16 . .	221
43	Raw Translational Data Ground Point -	
	Round 17	222
44	Raw Angular Data Ground Point - Round 17 . .	223
45	Raw Translational Data Ground Point -	
	Round 19	224
46	Raw Angular Data Ground Point - Round 19 . .	225
47	Axis Rotation Approximates Pure Pitching	
	Motion	227
48	Fitted Translational Data Ground Point -	
	Round 4	229
49	Fitted Angular Data Ground Point - Round 4 . .	230
50	Fitted Translational Data Ground Point -	
	Round 6	231
51	Fitted Angular Data Ground Point - Round 6 . .	232

LIST OF FIGURES (continued)

Number		Page
52	Fitted Translational Data Ground Point - Round 7	233
53	Fitted Angular Data Ground Point - Round 7	234
54	Fitted Translational Data Ground Point - Round 8	235
55	Fitted Angular Data Ground Point - Round 8 .	236
56	Fitted Translational Data Ground Point - Round 14	237
57	Fitted Angular Data Ground Point - Round 14	238
58	Fitted Translational Data Ground Point - Round 16	239
59	Fitted Angular Data Ground Point - Round 16	240
60	Fitted Translational Data Ground Point - Round 17	241
61	Fitted Angular Data Ground Point - Round 17	242
62	Fitted Translational Data Ground Point - Round 19	243

LIST OF FIGURES (continued)

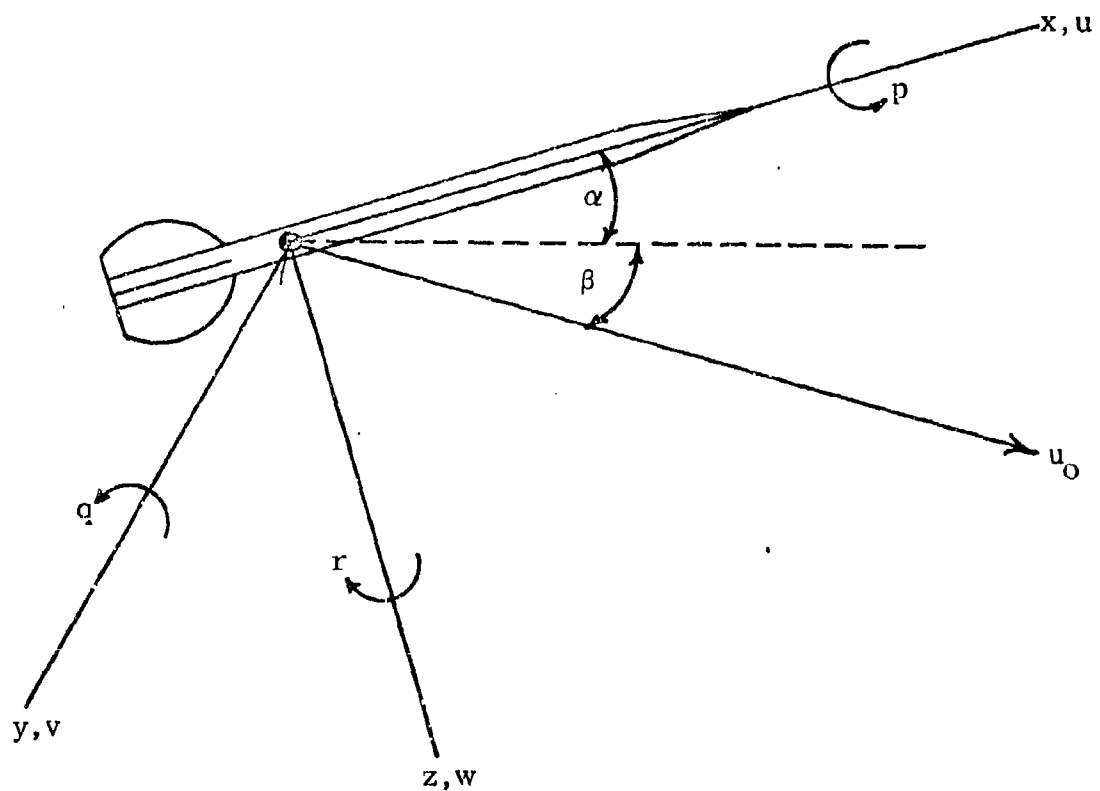
Number		Page
63	Fitted Angular Data Ground Point - Round 19 . . .	244
64	Dispersion: Ground Point - Round 4 Test	
	Firing vs Theory, at 50 ft. Downrange	248
65	Dispersion: Ground Point - Round 6 Test	
	Firing vs Theory, at 50 ft. Downrange	249
66	Dispersion: Ground Point - Round 7 Test	
	Firing vs Theory, at 50 ft. Downrange	250
67	Dispersion: Ground Point - Round 8 Test	
	Firing vs Theory, at 50 ft. Downrange	251
68	Dispersion: Ground Point - Round 14 Test	
	Firing vs Theory, at 50 ft. Downrange	252
69	Dispersion: Ground Point - Round 16 Test	
	Firing vs Theory, at 50 ft. Downrange	253
70	Dispersion: Ground Point - Round 17 Test	
	Firing vs Theory, at 50 ft. Downrange	254
71	Dispersion: Ground Point - Round 19 Test	
	Firing vs Theory, at 50 ft. Downrange	255
72	Flight Transition Sequence - Round 4	257
73	Flight Transition Sequence - Round 6	258
74	Flight Transition Sequence - Round 7	259
75	Flight Transition Sequence - Round 8	260

LIST OF FIGURES (concluded)

Number		Page
76	Flight Transition Sequence - Round 14	261
77	Flight Transition Sequence - Round 16	262
78	Flight Transition Sequence - Round 17	263
79	Flight Transition Sequence - Round 19	264
80	Dispersion vs First Maximum Yaw, Frankford Test Firing Results	267
81	Dispersion vs First Maximum Yaw, Theory - Initial Conditions, 1 ft. Downrange	269
82	Dispersion vs First Maximum Yaw, Theory - Initial Conditions, 3 ft. Downrange	270
83	Dispersion vs First Maximum Yaw, Theory - Initial Conditions, 5 ft. Downrange	271
84	Jump Angles for Various Initial Conditions . .	273
85	Flechette In-Bore Position	277
86	Typical Flechette Blast Region	279
87	Muzzle Blast Effects	280
88	Supersonic Free Flight, Ground Point Flechette	281

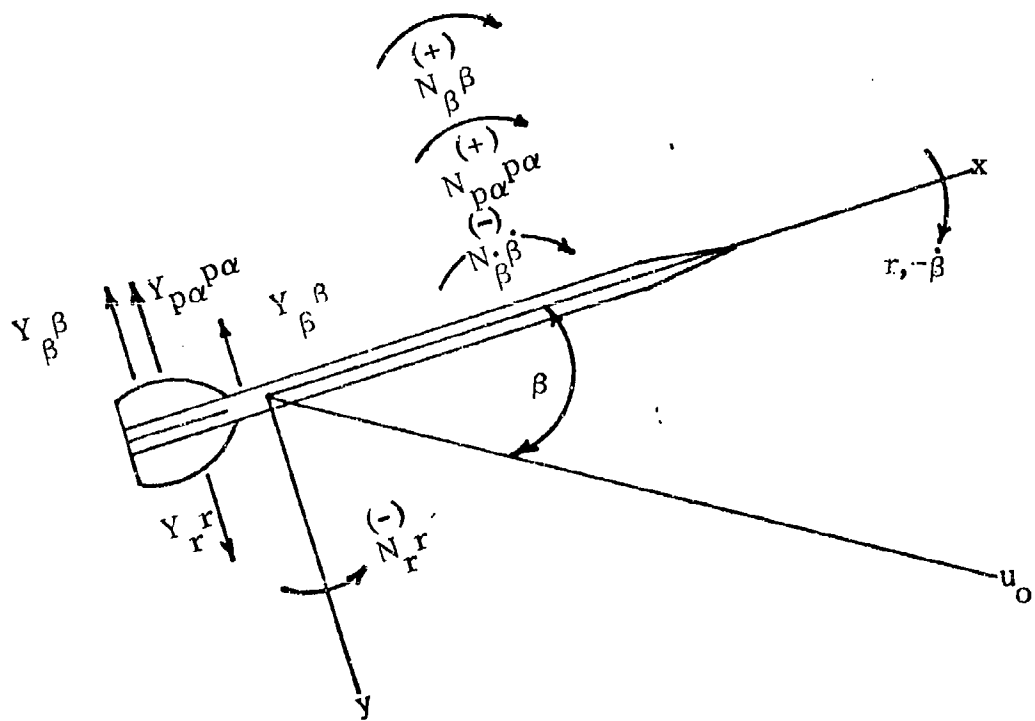
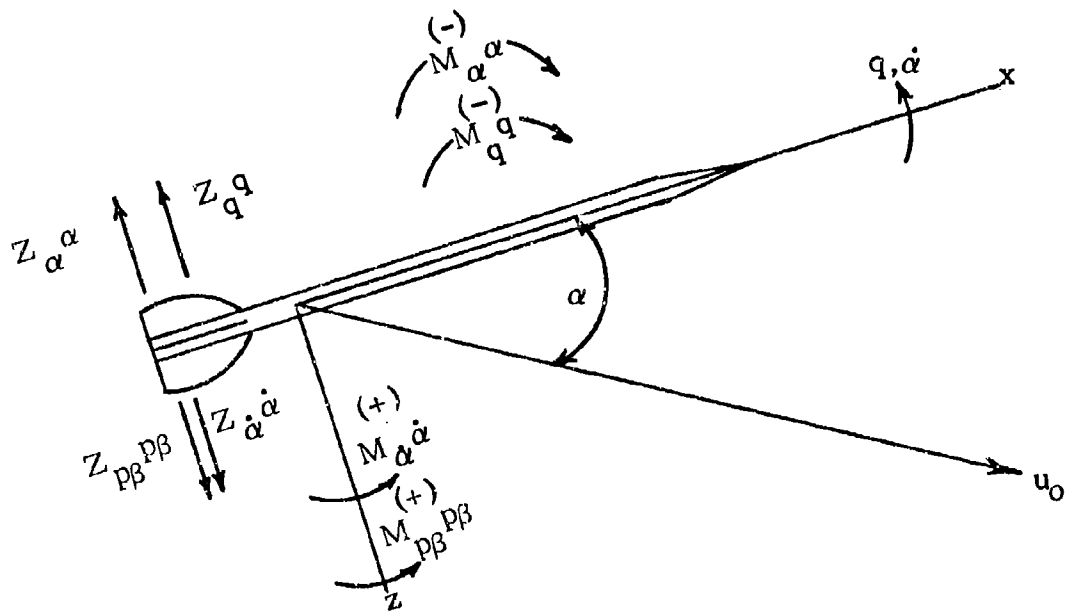
LIST OF SYMBOLS

Axis System



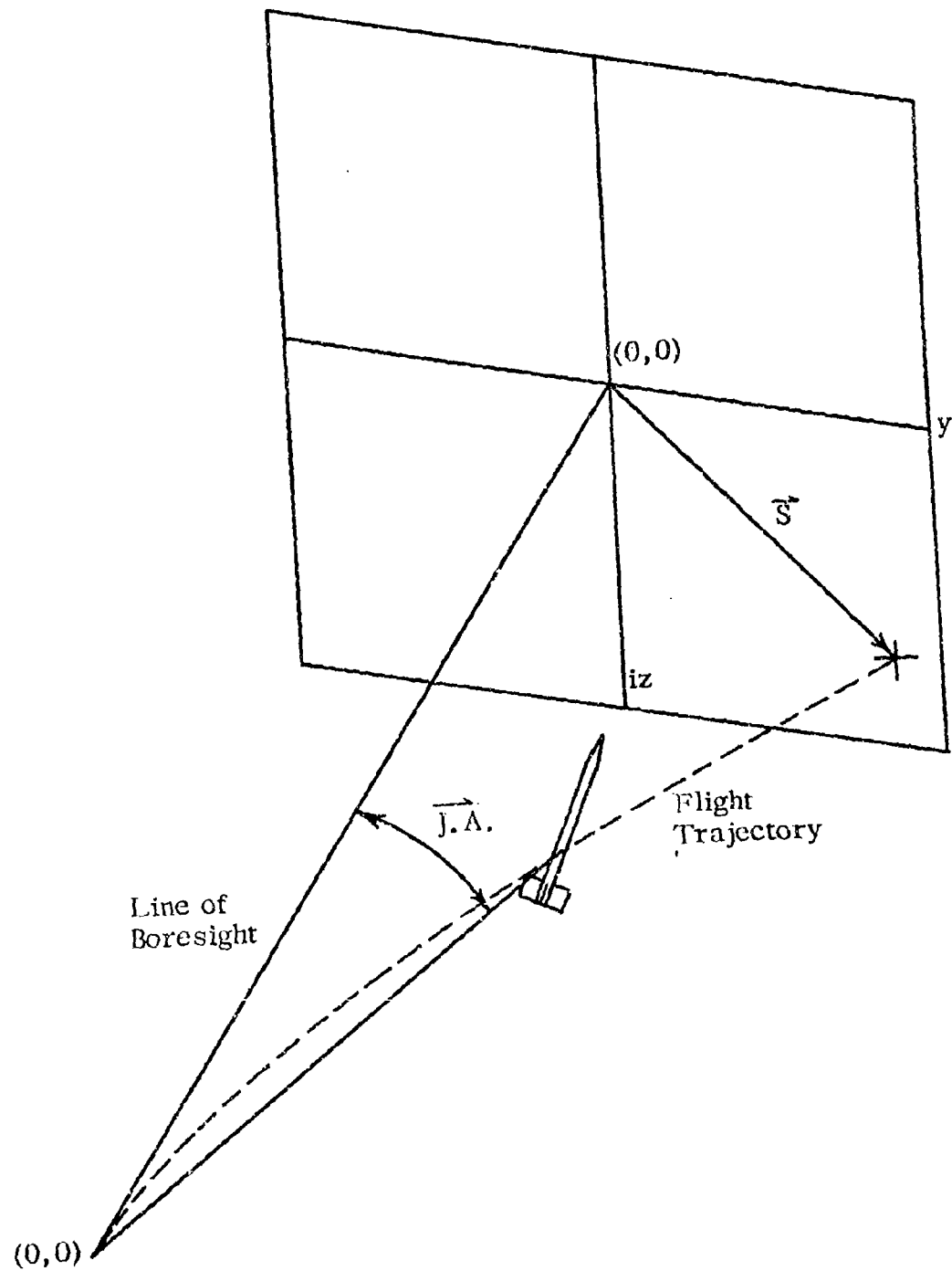
LIST OF SYMBOLS (continued)

Force and Moment Systems



LIST OF SYMBOLS (continued)

Jump Angle



LIST OF SYMBOLS (continued)

$\overline{\alpha}$	complex angle of attack (degrees or radians)
	$\overline{\alpha} = \beta + i\alpha$
α	pitch angle of attack
α_0	initial angle of attack
$\dot{\overline{\alpha}}_0$	initial angular rate (rad/sec)
	$\dot{\overline{\alpha}}_0 = \dot{\beta}_0 + i\dot{\alpha}_0$
β	yaw angle of attack
C_z	pitching force coefficients
	$C_z = \frac{Z}{QS}$
C_M	pitching moment coefficients
	$C_M = \frac{M}{QSd}$
C_{z_α}	static force stability coefficient (rad^{-1})
	$C_{z_\alpha} = \frac{\partial C_z}{\partial \alpha} = \frac{Z_\alpha \alpha}{\alpha QS} = \frac{Y_B \beta}{\beta QS}$
C_{M_α}	static moment stability coefficient (rad^{-1})
	$C_{M_\alpha} = \frac{\partial C_M}{\partial \alpha} = \frac{M_\alpha \alpha}{\alpha QSd} = -\frac{N_B \beta}{\beta QSd}$
C_{z_q}	damping force stability coefficient (rad^{-1})
	$C_{z_q} = \frac{\partial C_z}{\partial (\frac{qd}{2u})} = \frac{Z_q q}{(\frac{qd}{2u}) QS} = -\frac{Y_r r}{(\frac{rd}{2u}) QS}$

LIST OF SYMBOLS (continued)

$C_{Z\dot{\alpha}}$ lag force stability coefficient (rad^{-1})

$$C_{Z\dot{\alpha}} = \frac{\partial C_Z}{\partial \left(\frac{\dot{\alpha}d}{2u}\right)} = \frac{Z \dot{\alpha} \dot{\alpha}}{\left(\frac{\dot{\alpha}d}{2u}\right) Q_S} = \frac{Y_B \dot{\beta}}{\left(\frac{\beta d}{2u}\right) Q_S}$$

C_{M_q} damping moment stability coefficient (rad^{-1})

$$C_{M_q} = \frac{\partial C_M}{\partial \left(\frac{qd}{2u}\right)} = \frac{M_q q}{\left(\frac{qd}{2u}\right) Q_{Sd}} = \frac{N_r r}{\left(\frac{rd}{2u}\right) Q_{Sd}}$$

$C_{M\dot{\alpha}}$ lag moment stability coefficient (rad^{-1})

$$C_{M\dot{\alpha}} = \frac{\partial C_M}{\partial \left(\frac{\dot{\alpha}d}{2u}\right)} = \frac{M \dot{\alpha} \dot{\alpha}}{\left(\frac{\dot{\alpha}d}{2u}\right) Q_{Sd}} = \frac{N_B \dot{\beta}}{\left(\frac{\beta d}{2u}\right) Q_{Sd}}$$

$C_{Z_{p\beta}}$ magnus force stability coefficient (rad^{-2})

$$C_{Z_{p\beta}} = \frac{\partial C_Z}{\partial \beta \partial \left(\frac{pd}{2u}\right)} = \frac{Y_{p\alpha p\alpha}}{\left(\frac{pd}{2u}\right) \alpha Q_S} = \frac{Z_{p\beta p\beta}}{\left(\frac{pd}{2u}\right) \beta Q_S}$$

$C_{M_{p\beta}}$ magnus moment stability coefficient (rad^{-2})

$$C_{M_{p\beta}} = \frac{\partial C_M}{\partial \beta \partial \left(\frac{pd}{2u}\right)} = \frac{N_{p\alpha p\alpha}}{\left(\frac{pd}{2u}\right) \alpha Q_{Sd}} = \frac{M_{p\beta p\beta}}{\left(\frac{pd}{2u}\right) \beta Q_{Sd}}$$

$C_{Z_{\delta\epsilon}}^{\overrightarrow{\delta\epsilon}}$ aerodynamic asymmetry force, total coefficient

$$C_{Z_{\delta\epsilon}}^{\overrightarrow{\delta\epsilon}} = C_{Y_r} \delta_r + i C_{Z_\epsilon} \delta_\epsilon$$

$C_{M_{\delta\epsilon}}^{\overrightarrow{\delta\epsilon}}$ aerodynamic asymmetry moment, total coefficient

$$C_{M_{\delta\epsilon}}^{\overrightarrow{\delta\epsilon}} = C_{M_{\delta\epsilon}} \delta_\epsilon + i C_{N_{\delta_r}} \delta_r$$

LIST OF SYMBOLS (continued)

d	flechette body diameter (ft)
$\overrightarrow{\delta_\epsilon}$	complex aerodynamic asymmetry vector $\overline{\delta_\epsilon} = \delta_r + i\delta_\epsilon$
ϕ	phase angle (rad)
g	acceleration due to gravity 32.2 ft/sec ²
γ	rotation angle between α, β axis system and α', β' system to approximate pure pitching motion (deg.)
I_x	axial moment of inertia (slugs-ft ²)
I_y	transverse moment of inertia (slugs-ft ²)
$\overrightarrow{J.A.}$	jump angle vector (mils)
$\overrightarrow{K_1}$	nutation mode amplitude (deg)
$\overrightarrow{K_2}$	precession mode amplitude (deg)
$\overrightarrow{K_3}, k-T$	trim mode amplitude (deg)
$\overrightarrow{K_4}$	yaw of repose amplitude (deg)
$k_{1, 2, 3, 4, 5, 6}$	dispersion or jump angle amplitude coefficients
$\lambda_{1, 2} \lambda_{N, P}$	damping factors for nutation and precession modes respectively (rad/sec)
m	mass of flechette (slugs)
p	roll rate (rad/sec)
p_0	initial roll rate (rad/sec)
\overrightarrow{q}	complex angular velocity (rad/sec) $\overline{q} = q + ir$
q	pitching angular velocity (rad/sec)

LIST OF SYMBOLS (continued)

Q dynamic pressure $\frac{\text{slugs}}{\text{ft} \cdot \text{sec}^2}$

$$Q = \frac{1}{2} \rho u^2$$

r yawing angular velocity (rad/sec)

ρ density (slugs/ft³)

S reference area $S = \frac{\pi d^2}{4}$

\vec{s} complex translation (ft)

$$\vec{s} = y + iz$$

\vec{s}_o initial complex translation (ft)

$$\vec{s}_o = y_o + iz_o$$

\vec{s}'_o initial complex velocity (ft/sec)

$$\vec{s}'_o = \dot{y}_o + i\dot{z}_o$$

s gyroscopic stability factor

τ dynamic weight factor

t time (sec)

u axial velocity (ft/sec)

u_o initial axial velocity (ft/sec)

v, w transverse velocities (ft/sec)

\vec{w} complex transverse velocity (ft/sec)

$$\vec{w} = v + iw$$

LIST OF SYMBOLS (concluded)

$\omega, \omega_{N,P}$ nutation and precession mode frequencies (rad/sec)
 x,y,z position components

INTRODUCTION

The accuracy and dispersion of free flight vehicles has been a problem in aerodynamics and ballistics for many years. Until the present time, the primary investigations into causes and effects of jump (the angle between the line of boresight and the line connecting the point of launch with the instantaneous position on the trajectory,) and dispersion have been directed toward projectiles and, in particular, artillery rounds. A full program to investigate jump and dispersion characteristics of low trajectory finned bodies has been lacking and therefore is the subject of this dissertation. The purpose of this analysis is to develop a basic understanding of the parameters causing the jump and dispersion of flechettes. The flechette, being a gun launched finned body, requires a different approach to the problem. The old concept employed in the analysis of the dispersion of artillery rounds is that the dispersion results from initial launch disturbances imparted by the gun to the shell.^{1,2} This concept is no longer valid for flechettes since the flechette is a fin missile, sabot launched, and its dispersion must be tied to the disturbances it encounters when clearing the muzzle blast and sabot separation region. In addition, asymmetries are more prevalent in finned bodies than projectiles and a finned body is more apt to be influenced by the blast. These factors must be taken into account by a theory involving finned bodies.

In order to develop this new approach, (1) a theoretical expression for jump and dispersion had to be developed, (2) the theory had to be

validated, (3) free flight test firings had to be undertaken and initial condition data extracted, and (4) the test firing results had to be correlated with the validated theory. The Jump and Dispersion Theory was developed, in general, for both fin and spin stabilized missiles in air. The theory includes the effects of: initial conditions, Magnus, aerodynamic asymmetries, and gravity. In the past, theory development for projectiles included only initial angle of attack and initial angular rate.^{1,3} Initial transverse velocity was considered non-existent⁴ or negligible. Zaroodny⁵ included a linear momentum term to account for any transverse motion of the projectile but attributed it to the gun during recoil. Any transverse impulse imparted to the projectile by the blast was ignored. Other authors, including Sterne² attributed the jump only to bore clearance and therefore only included, effectively, the initial angle of attack. Magnus effects were always neglected in previous studies either due to lack of familiarity with the subject or lack of data. In general, all cross-forces, except lift, were neglected mainly for convenience sake. Zaroodny, however, cautioning against wholesale simplifying said "it would seem desirable that our formulas allow us to include these other forces as the experimental information on these forces becomes available." Aerodynamic asymmetries were neglected for projectiles but included in Murphy's work.⁶ It was not until Nicolaides^{7,8,9} that all four factors affecting dispersion; initial angle of attack, initial angular rate, initial transverse position and velocity, were put into one theory. The work presented here expands the work of Nicolaides to include all parameters affecting dispersion in detail. Three separate

equations comprise the theory to include the complete range of roll rates.

Before, only high roll rates were considered; with the study of finned bodies, the roll rate range extends down to zero roll and accurate theories had to be deduced from known aerodynamic equations.

To validate the theory, a six-degree-of-freedom trajectory computer program numerically integrating the equations of motion was utilized.^{10, 11, 12}

The validation consisted of four phases. The procedure began with the most basic theory equation and consecutively added terms to validate the entire theory. Initial conditions, magnus, asymmetries and gravity were successively validated with roll rate and velocity varied in each phase.

Before the advent of adequate photographic material, obtaining test data was often difficult. At first, jump target data was taken separate from yaw data. The thinking was that the yaw data was part of the projectile's characteristics and not affecting jump. As photographic methods improved, and theories developed, the data was correlated. The correlation of the data was often a problem. A fit of the motion to a least squares method was difficult. Fowler, Kent, and Hitchcock developed a method that would plot the magnitude of the yaw separately from the orientation and then fit the curves separately. A better method was developed by McShane-Charters-Turetsky approximated the yawing motion to a circle. For projectiles the method has been refined and is an excellent method. However, for finned bodies with not always circular angular motions, a different method of data analysis had to be devised. Utilizing the free flight data taken by test engineers at Frankford Arsenal on a number of flechettes, the least squares method was employed to fit the data pre-

sented here. The nearly planar oscillations of the flechette in the first few feet downrange were fit to a pure pitching motion^{13,14} and the position downrange fit to a third order polynomial. From these results, angle of attack, angular rate and transverse position and velocity were determined for the first few feet downrange. Before, there was some controversy as to whether or not the least squares fit could be extrapolated back to the muzzle. Zaroodny contended that the $x = 0$ position had to be taken out of the blast region to allow the aerodynamic equations to be valid. On the other hand, Kent, Hitchcock, Fowler and Sterne held to the fact that the free flight region began the instant the projectile left the bore. In the analysis of flechettes the position $x = 0$ is taken somewhere downrange after the sabot separation sequence has occurred. This is seen to be 3 to 5 feet downrange and assumed clear of any muzzle blast effects.

The striking shortcoming of previous works is the lack of correlation between test data and valid theory. For the flechette, correlation between the theory and test data was undertaken as well as correlation between test results and first maximum yaw data. Currently, the first maximum yaw theory¹⁵ is held by some to be an accurate method of predicting dispersion. This theory disallows any influence of initial angular rate, transverse position or velocity on dispersion. The dispersion analysis presented here disproves this theory with actual test data. The details of each of these aspects of this program are developed in the following sections.

DISPERSION THEORY

Dispersion relationships for free flight vehicles are embedded in the trajectory equation of any such aeroballistic body. To evaluate the trajectory equation and thus the dispersion, the linear second-order differential equation of angular motion is a logical starting point.

$$\ddot{\vec{w}} + N_1 \dot{\vec{w}} + N_2 \vec{w} = \vec{N}_3 e^{ipt} + \vec{N}_4 \quad (1)$$

where N_1 , N_2 , \vec{N}_3 , and \vec{N}_4 are constants.

$$N_1 = \left[\frac{Z_w + ipZ_{pv}}{Z_{\dot{w}} - m} \right] + \frac{M_w}{I_y} \left[\frac{mu + Z_q}{Z_{\dot{w}} - m} \right] - \left[\frac{ipI_x}{I_y} + \frac{M_q}{I_y} \right] \quad (2)$$

$$N_2 = \left[\frac{M_w + ipM_{pv}}{I_y} \right] \left[\frac{mu + Z_q}{Z_{\dot{w}} - m} \right] - \left[\frac{Z_w + ipZ_{pv}}{Z_{\dot{w}} - m} \right] \left[\frac{ipI_x}{I_y} + \frac{M_q}{I_y} \right] \quad (3)$$

$$\vec{N}_3 = \left[\frac{Z_{\delta_e} \vec{\delta}_e}{Z_{\dot{w}} - m} \right] \left[\frac{M_q}{I_y} + \frac{ipI_x}{I_y} - ip \right] - \frac{M_{\delta_e} \vec{\delta}_e}{I_y} \left[\frac{mu + Z_q}{Z_{\dot{w}} - m} \right] \quad (4)$$

$$\vec{N}_4 = \frac{img}{I_y} \left[\frac{M_q + ipI_x}{Z_{\dot{w}} - m} \right]. \quad (5)$$

In this discussion of dispersion theory, it is assumed that,

- (1) total velocity, u_0 , is constant, equal to u in the theory development.
- (2) all force and moment coefficients dependent on angle of attack are considered to be linear with angle of attack.
- (3) all force and moment coefficients independent of angle of attack are considered to be constant.

- (4) a linear relationship exists between x (distance down range) and time for the non-drag case.
- (5) roll rate, p , is considered to be constant.
- (6) products of force and moment derivatives are negligible, except those involving Z_{δ_e} and M_{δ_e} .

Utilizing these assumptions, and the binomial expansion of $(Z_w - m)^{-1}$,

2, 3, 4 and 5 become:

$$N_1 \approx - \left[\frac{Z_w + ipZ_{pv}}{m} \right] - \left[\frac{M_q + uM_w}{I_y} \right] - \frac{ipI_x}{I_y} \quad (2a)$$

$$N_2 \approx -u \left[\frac{M_w + ipM_{pv}}{I_y} \right] + \frac{ipI_x}{I_y} \left[\frac{Z_w + ipZ_{pv}}{m} \right] \quad (3a)$$

$$\vec{N}_3 \approx \frac{ipZ_{\delta_e} \vec{\delta}_e}{m} \left[1 - \frac{I_x}{I_y} \right] + \frac{uM_{\delta_e} \vec{\delta}_e}{I_y} \quad (4a)$$

$$\vec{N}_4 \approx g \left[\frac{pI_x}{I_y} \right] \quad (5a)$$

The solution to Equation 1 is that of tricyclic motion; that is,

$$\vec{w} = \vec{K}_1 e^{\phi_1 t} + \vec{K}_2 e^{\phi_2 t} + \vec{K}_3 e^{ipt} + \vec{K}_4 \quad (6)$$

where the complex coefficients are:

$$\vec{K}_{1,2} = \frac{\vec{w}_o - (\phi_{2,1}) \vec{w}_o + \vec{K}_3 (\phi_{2,1} - ip)}{\phi_{1,2} - \phi_{2,1}} \quad (7)$$

$$\vec{K}_3 = \frac{\vec{N}_3}{(ip - \phi_1)(ip - \phi_2)} \quad (8)$$

$$\vec{K}_4 = \frac{\vec{N}_4}{N_2} \quad (9)$$

and

$$\phi_{1,2} = -\frac{N_1}{2} \pm \frac{1}{2} \sqrt{N_1^2 - 4N_2} \quad (10)$$

The trajectory equation for free-flight motion:

$$\vec{S} = (\vec{w} - iu\vec{q}) \quad (11)$$

An expression for \vec{q} is obtained from the equations of motion

$$\begin{aligned} \vec{q} &= i\vec{w} \left[\frac{Z_w - m}{mu + Z_q} \right] + i\vec{w} \left[\frac{Z_w + ipZ_{pv}}{mu + Z_q} \right] + \left[\frac{iZ_\epsilon \vec{\delta}_\epsilon}{mu + Z_q} \right] e^{ipt} - \left[\frac{mg}{mu + Z_q} \right] \\ \vec{q} &\approx i\vec{w} \left[1 - \frac{Z_q + Z_w}{m} \right] + i\vec{w} \left[\frac{Z_w + ipZ_{pv}}{mu} \right] + \left[\frac{iZ_\epsilon \vec{\delta}_\epsilon}{mu} \right] e^{ipt} - \frac{g}{u} \end{aligned} \quad (12)$$

yielding a solution of the form:

$$\vec{S} = \vec{k}_1 e^{\phi_1 t} + \vec{k}_2 e^{\phi_2 t} + \vec{k}_3 e^{ipt} + \vec{k}_4 t^2 + \vec{k}_5 t + \vec{k}_6 \quad (13)$$

where the entire expression for the solution is:

$$\begin{aligned} \vec{S} &= \vec{k}_1 e^{\phi_1 t} \left[\frac{1}{\phi_1} \left(\frac{Z_q + uZ_w}{mu} \right) + \frac{u}{\phi_1^2} \left(\frac{Z_w + ipZ_{pv}}{mu} \right) \right] \\ &+ \vec{k}_2 e^{\phi_2 t} \left[\frac{1}{\phi_2} \left(\frac{Z_q + uZ_w}{mu} \right) + \frac{u}{\phi_2^2} \left(\frac{Z_w + ipZ_{pv}}{mu} \right) \right] \\ &+ \left[\frac{Z_w + ipZ_{pv}}{m} \vec{k}_3 + \frac{Z_\epsilon \vec{\delta}_\epsilon}{m} \right] \int_0^t \int_0^t e^{ipt} dt dt \\ &+ \left[\frac{Z_q + uZ_w}{mu} \right] \vec{k}_3 \int_0^t e^{ipt} + \left[\frac{\vec{k}_4}{2} \left(\frac{Z_w + ipZ_{pv}}{m} \right) + \frac{ig}{2} \right] t^2 \end{aligned}$$

$$+ t \left[\vec{S}_o + \left(\frac{Z_q + u Z_w}{mu} \right) (\vec{K}_4 \cdot \vec{w}_o) - \left(\frac{Z_w + ip Z_{pv}}{m} \right) \left(\frac{\vec{K}_1}{\phi_1} + \frac{\vec{K}_2}{\phi_2} \right) \right] \quad (14)$$

$$+ \left[\vec{S}_o - \left(\frac{Z_q + u Z_w}{mu} \right) \left(\frac{\vec{K}_1}{\phi_1} + \frac{\vec{K}_2}{\phi_2} \right) - \left(\frac{Z_w + ip Z_{pv}}{m} \right) \left(\frac{\vec{K}_1}{\phi_1^2} + \frac{\vec{K}_2}{\phi_2^2} \right) \right]$$

The term $\left(\frac{Z_q + u Z_w}{mu} \right)$ is of an order of magnitude 10^{-3} and thus is neglected from all further discussion. This reduces 14 to:

$$\vec{S} = \vec{K}_1 e^{\phi_1 t} \left[\frac{u}{\phi_1^2} \left(\frac{Z_w + ip Z_{pv}}{mu} \right) \right] + \vec{K}_2 e^{\phi_2 t} \left[\frac{u}{\phi_2^2} \left(\frac{Z_w + ip Z_{pv}}{mu} \right) \right] \quad (15)$$

$$+ \left[\frac{Z_w + ip Z_{pv}}{m} \vec{K}_3 + \frac{Z_{\delta_e} \vec{\delta}_e}{m} \right] \int_0^t \int_0^t e^{ipt} dt dt + \left[\frac{\vec{K}_4}{2} \left(\frac{Z_w + ip Z_{pv}}{m} \right) + \frac{ig}{2} \right] t^2$$

$$+ t \left[\vec{S}_o - \left(\frac{Z_w + ip Z_{pv}}{m} \right) \left(\frac{\vec{K}_1}{\phi_1} + \frac{\vec{K}_2}{\phi_2} \right) \right] + \left[\vec{S}_o - \left(\frac{Z_w + ip Z_{pv}}{m} \right) \left(\frac{\vec{K}_1}{\phi_1^2} + \frac{\vec{K}_2}{\phi_2^2} \right) \right]$$

By further inspection, terms with ϕ_1^2 and ϕ_2^2 will be negligible since they contain products of force and moment derivatives. Equation 15 becomes:

$$\vec{S} = \left[\frac{Z_w + ip Z_{pv}}{m} \vec{K}_3 + \frac{Z_{\delta_e} \vec{\delta}_e}{m} \right] \int_0^t \int_0^t e^{ipt} dt dt + \left[\frac{\vec{K}_4}{2} \left(\frac{Z_w + ip Z_{pv}}{m} \right) + \frac{ig}{2} \right] t^2$$

$$+ t \left[\vec{S}_o - \left(\frac{Z_w + ip Z_{pv}}{m} \right) \left(\frac{\vec{K}_1}{\phi_1} + \frac{\vec{K}_2}{\phi_2} \right) \right] + \vec{S}_o \quad (16)$$

Equation 16 contains only the significant terms in dispersion theory.

This equation is valid for all values of roll rate.

High Roll Rate Theory

For roll rates greater than 100 rad/sec, Equation 16 reduces to an approximate solution. Integration of the double integral gives:

$$\int_0^t \int_0^t e^{ipt} dt dt = \frac{e^{ipt}}{(ip)^2} - \frac{t}{ip} - \frac{1}{(ip)^2} \quad (17)$$

For high roll rates, the first and third terms go to zero, leaving only the second term to affect dispersion. Applying this approximation to Equation 16 :

$$\vec{S} = \left[\frac{\vec{K}_4}{2} \left(\frac{Z_w + ipZ_{pv}}{m} \right) + \frac{ig}{2} \right] t^2 + \left[\vec{S}_0 - \left(\frac{Z_w + ipZ_{pv}}{m} \right) \left(\frac{\vec{K}_1}{\phi_1} + \frac{\vec{K}_2}{\phi_2} + \frac{\vec{K}_3}{ip} \right) \right. \\ \left. + \frac{iZ_{\delta\epsilon} \vec{\delta\epsilon}}{mp} \right] t + \vec{S}_0 \quad (18)$$

where, by applying previous aerodynamic relationships:

$$\left(\frac{\vec{K}_1}{\phi_1} + \frac{\vec{K}_2}{\phi_2} + \frac{\vec{K}_3}{ip} \right) = \left[\frac{\vec{w}_o - \vec{w}_o (\phi_1 + \phi_2)}{-\phi_1 \phi_2} \right] + \left[\frac{\frac{u M_{\delta\epsilon} \vec{\delta\epsilon}}{l_y} + i \frac{p Z_{\delta\epsilon} \vec{\delta\epsilon}}{m} (1 - \frac{l_x}{l_y})}{(ip) \phi_1 \phi_2} \right] \quad (19)$$

$$\phi_1 + \phi_2 = -N_1$$

$$\phi_1 \phi_2 = N_2$$

$$\vec{K}_4 = -g p l_x \left[\left(\frac{1}{M_\alpha + \frac{p^2 l_x}{mu} Z_{p\beta}} \right) + i \left(p M_{p\beta} \cdot \frac{p l_x}{mu} Z_\alpha \right) \right] \quad (20)$$

Substituting 19 and 20 into 18 and expanding the various terms:

$$\begin{aligned}
 \vec{S} = & \frac{igt^2}{2} \left[1 + \frac{ipI_x}{mud} \left[\frac{C_{z\alpha} + i\left(\frac{pd}{2u}\right) C_{zp\beta}}{\left(C_{M\alpha} + \frac{pI_x}{mud} \frac{pd}{2u} C_{zp\beta}\right) + i\left(C_{Mp\beta} \frac{pd}{2u} - \frac{pI_x}{mud} C_{z\alpha}\right)} \right] \right] \\
 & + ut \left[\frac{\dot{S}_o}{u} + -\frac{I_y}{mud} \left[\frac{C_{z\alpha} + i\frac{pd}{2u} C_{zp\beta}}{\left(C_{M\alpha} + \frac{pI_x}{mud} \frac{pd}{2u} C_{zp\beta}\right) + i\left(C_{Mp\beta} \frac{pd}{2u} - \frac{pI_x}{mud} C_{z\alpha}\right)} \right] \right. \\
 & \quad \left. + i C_{z\delta\epsilon} \left[\frac{\rho u \pi d^2}{8mp} \right] \right] \\
 & \left[\vec{\alpha}_o - \vec{\alpha}_o \left(\frac{ipI_x}{I_y} \right) - C_{M\delta\epsilon} \vec{\delta\epsilon} \left(\frac{\rho u^2 \pi d^3}{8pI_y} \right) - C_{z\delta\epsilon} \vec{\delta\epsilon} \left(1 - \frac{I_x}{I_y} \right) \frac{\rho u \pi d^2}{8m} \right] + \vec{S}_o
 \end{aligned} \tag{21}$$

Employing assumption 6 ,

$$\begin{aligned}
 \vec{S} = & \frac{ig}{2} \left(\frac{x}{u} \right)^2 \left[1 + \frac{ipI_x}{mud} A \right] + (x) \left[\frac{\dot{S}_o}{u} + i C_{z\delta\epsilon} \vec{\delta\epsilon} \left(\frac{\rho u \pi d^2}{8mp} \right) \right. \\
 & - \frac{I_y}{mud} A \left[\vec{\alpha}_o - \vec{\alpha}_o \left(\frac{ipI_x}{I_y} \right) - C_{M\delta\epsilon} \vec{\delta\epsilon} \left(\frac{\rho u^2 \pi d^3}{8pI_y} \right) \right. \\
 & \quad \left. \left. - C_{z\delta\epsilon} \vec{\delta\epsilon} \left(1 - \frac{I_x}{I_y} \right) \frac{\rho u \pi d^2}{8m} \right] \right] + \vec{S}_o
 \end{aligned} \tag{22}$$

where

$$A = \frac{C_{z\alpha} + i\left(\frac{pd}{2u}\right) C_{zp\beta}}{\left(C_{M\alpha} + \frac{pI_x}{mud} \frac{pd}{2u} C_{zp\beta}\right) + i\left(C_{Mp\beta} \frac{pd}{2u} - \frac{pI_x}{mud} C_{z\alpha}\right)}$$

The mil-relation offers a method to define the Jump Angle from Equation 22.

$$\text{Jump Angle} = \frac{\overline{S}}{x} (10^3) \quad (23)$$

$$\begin{aligned} \overline{J.A.} = & \frac{ig}{2} \left(\frac{x}{u^2} \right) (10^3) \left[1 + \frac{ipL_x}{mud} A \right] + (10^3) \left[\frac{\overline{S}_o}{u} + i C_Z \overline{\delta}_e \left(\frac{\rho u \pi d^2}{8 mp} \right) \right. \\ & - \frac{l_y}{mud} A \left[\overline{\alpha}_o - \overline{\alpha}_o \left(\frac{ipL_x}{l_y} \right) - C_M \overline{\delta}_e \left(\frac{\rho u^2 \pi d^3}{8 p l_y} \right) \right. \\ & \left. \left. - C_Z \overline{\delta}_e \left(1 - \frac{l_x}{l_y} \right) \frac{\rho u \pi d^2}{8 m} \right] \right] + \frac{1000}{x} \overline{S}_o \end{aligned} \quad (24)$$

Equation 24 gives an approximation for the Jump Angle for high roll rate cases with gravity, at any position x down range.

Low Roll Rate Theory

For roll rates less than 100 rad/sec but having a parameter, pt , greater than 1, Equation 16 can be reduced to another approximation. As before, integration of the double integral yields Equation 17

$$\int_0^t \int_0^t e^{ipt} = \frac{e^{ipt}}{(ip)^2} - \frac{t}{ip} - \frac{1}{(ip)^2}$$

For low roll rates all three terms are significant to dispersion.

Equation 16 now becomes:

$$\begin{aligned} \overline{S} = & \left(\frac{Z_w + ipZ_{p\beta}}{m} \overline{K}_3 + \frac{Z_{\delta_e} \overline{\delta}_e}{m} \right) \left(1 - e^{ipt} \right) \frac{1}{p^2} + \left[\frac{\overline{K}_4}{2} \left(\frac{Z_w + ipZ_{p\beta}}{m} \right) + \frac{ig}{2} \right] t^2 \\ & + \left[\overline{S}_o \left(\frac{Z_w + ipZ_{p\beta}}{m} \right) \left(\frac{\overline{K}_1}{\phi_1} + \frac{\overline{K}_2}{\phi_2} \right) + \frac{\overline{K}_3}{ip} + \frac{i Z_{\delta_e} \overline{\delta}_e}{mp} \right] t + \overline{S}_o \end{aligned} \quad (25)$$

The \overline{K}_3 arm, or rolling trim vector must be separately examined.

From Equation 8,

$$\vec{K}_3 = \frac{\vec{N}_3}{(ip - \phi_1)(ip - \phi_2)}$$

or

$$\vec{K}_3 = \frac{\vec{N}_3}{(ip)^2 - ip(\phi_1 + \phi_2) + \phi_1\phi_2}$$

Numerical inspection of the three denominator terms indicates that the first two terms can be neglected. Each term is not only less than 1% of the third term but also they're subtracted from one another to make their contribution even more minimal. Thus K_3 is approximated by,

$$\vec{K}_3 = -\frac{I_y}{md} \left[\frac{ip C_{Z\delta\epsilon} \vec{\delta}_\epsilon \left(1 - \frac{I_x}{I_y} \right) + i \frac{mud}{I_y} C_{M\delta\epsilon} \vec{\delta}_\epsilon}{\left[C_{M\alpha} + \frac{pI_x}{mud} \left(\frac{pd}{2u} \right) C_{Zp\beta} \right] + i \left[C_{Mp\beta} \left(\frac{pd}{2u} \right) - \left(\frac{pI_x}{mud} \right) C_{Z\alpha} \right]} \right]$$

for low roll rates, the second term in the numerator and the first term in the denominator dominate all other terms and become the only significant terms. Thus,

$$\vec{K}_3 = -\frac{ui C_{M\delta\epsilon} \vec{\delta}_\epsilon}{C_{M\alpha}} \quad (26)$$

The same approximation holds true for applicable terms in Equation 25, thus reducing the jump angle equation to:

$$\begin{aligned} \vec{J.A.} = & \left\{ \frac{ig}{2} \left(\frac{x}{u^2} \right) + \frac{\rho u^2 \pi d^2}{8 mp^2} \left[C_{Z\delta\epsilon} \vec{\delta}_\epsilon - i \left(\frac{C_{Z\alpha}}{C_{M\alpha}} \right) C_{M\delta\epsilon} \vec{\delta}_\epsilon \right] (1 - e^{ipt}) \right. \\ & + \left[\frac{\vec{S}_0}{u} + i C_{Z\delta\epsilon} \vec{\delta}_\epsilon \left(\frac{\rho u \pi d^2}{8 mp} \right) - \frac{I_y}{mud} A \left[\vec{\dot{\alpha}}_0 - C_{M\delta\epsilon} \vec{\delta}_\epsilon \left(\frac{\rho u^2 \pi d^3}{8 p I_y} \right) \right. \right. \\ & \left. \left. - C_{Z\delta\epsilon} \vec{\delta}_\epsilon \left(1 - \frac{I_x}{I_y} \right) \frac{\rho u \pi d^2}{8 m} \right] \right] + \frac{\vec{S}_0}{x} \right\} (10^3) \end{aligned}$$

Combining terms and dropping the negligible second last term,

$$\begin{aligned}\overrightarrow{\text{J.A.}} = & \left[\frac{ig}{2} \left(\frac{x}{u^2} \right) + \frac{\rho u^2 \pi d^2}{8 m} \left[C_{Z\delta_e} \dot{\overline{\delta_e}} - i \left(\frac{C_{Z\alpha}}{C_{M\alpha}} \right) C_{M\delta_e} \dot{\overline{\delta_e}} \right] \left[\frac{1}{p^2 x} + \frac{i}{pu} - \frac{e^{ipt}}{p^2 x} \right] \right. \\ & \left. + \left[\frac{\dot{S}_o}{u} - \frac{I_y}{mud} \left(\frac{C_{Z\alpha}}{C_{M\alpha}} \right) \dot{\overline{\alpha_o}} \right] + \frac{\dot{\overline{S}_o}}{x} \right] (10^3) \quad (27)\end{aligned}$$

Expanding e^{ipt} to $\cos p \left(\frac{x}{u} \right) + i \sin p \left(\frac{x}{u} \right)$,

$$\begin{aligned}\overrightarrow{\text{J.A.}} = & \left\{ \frac{ig}{2} \left(\frac{x}{u^2} \right) + \frac{\rho u^2 \pi d^2}{8 mx} \left[C_{Z\delta_e} \dot{\overline{\delta_e}} - i \left(\frac{C_{Z\alpha}}{C_{M\alpha}} \right) C_{M\delta_e} \dot{\overline{\delta_e}} \right] \left[\frac{1}{p^2} \left(1 - \cos p \frac{x}{u} \right) \right. \right. \\ & \left. \left. + \frac{i}{p} \left(\frac{x}{u} - \frac{\sin p \frac{x}{u}}{p} \right) \right] + \left[\frac{\dot{S}_o}{u} - \frac{I_y}{mud} \left(\frac{C_{Z\alpha}}{C_{M\alpha}} \right) \dot{\overline{\alpha_o}} \right] + \frac{\dot{\overline{S}_o}}{x} \right\} (10^3) \quad (28)\end{aligned}$$

Equation 28 accurately approximates the jump angle for roll rates:

$$p > 100 \text{ rad/sec}$$

$$pt \geq 1.0$$

Very Slow Roll Rate Theory

For very low roll rates; that is, $p \geq 0$ and $pt \leq 1$, Equation 28 is again applicable.

One approximation is used, however, and that is that $\cos \left(\frac{px}{u} \right)$ and $\sin \left(\frac{px}{u} \right)$ are approximated by power series.

$$\cos \left(\frac{px}{u} \right) = 1 - \frac{(px)^2}{2u^2} + \frac{(px)^4}{24u^4} - \frac{(px)^6}{720u^6} + \dots \quad (29)$$

$$\sin \left(\frac{px}{u} \right) = \frac{px}{u} - \frac{(px)^3}{6u^3} + \frac{(px)^5}{120u^5} - \frac{(px)^7}{5040u^7} + \dots$$

Substituting and simplifying,

$$\begin{aligned}
 \vec{J} \cdot \vec{\Lambda}_+ = & \left\{ \frac{ig}{2} \left(\frac{x}{u^2} \right) + \frac{\rho \pi d^2 x}{16m} \left[C_{Z_\delta} \vec{\delta}_\epsilon - i \left(\frac{C_{Z_\alpha}}{C_{M_\alpha}} \right) C_{M_\delta} \vec{\delta}_\epsilon \right] \right\} \left[\left(1 - \frac{1}{12} \left(\frac{px}{u} \right)^2 \right. \right. \\
 & \left. \left. + \frac{1}{360} \left(\frac{px}{u} \right)^4 \right) + i \left(\frac{px}{3u} - \frac{1}{60} \left(\frac{px}{u} \right)^3 + \frac{1}{2520} \left(\frac{px}{u} \right)^5 \right) \right] \\
 & + \left[\frac{\vec{s}_o}{u} - \frac{L_y}{mud} \left(\frac{C_{Z_\alpha}}{C_{M_\alpha}} \right) \vec{\alpha}_o \right] + \frac{\vec{s}_o}{x} \Big\} (10^3) \quad (30)
 \end{aligned}$$

VALIDATION OF THEORY

The theoretical expressions for Jump Angle; Equations 24, 28 and 30; show that the dispersion depends on the initial conditions, aerodynamic coefficients, distance downrange , and mass parameters. Dispersion for this theoretical analysis is defined to be the deviation from the line of fire. By analyzing only one Flechette configuration to validate the theory, the producibility Ground Point, and taking all cases to be evaluated at 1000 feet downrange , then the expression for the Jump Angle can only be affected by the initial conditions and aerodynamic coefficients.

To assure that the three equations for Jump Angle are valid and to show the effects for various initial conditions and aerodynamic coefficients, the expressions for the Jump Angle were evaluated for a series of cases and compared to numerical integration of the six-degree-of-freedom equations of motion, (6-D). A sample case run can be found in Appendix A-2. The series of cases is broken down into various phases of development. Phase I considers various initial conditions but with only the restoring and damping aerodynamic coefficients. This phase validates the use of initial conditions alone. Phase II utilizes a set of constant initial conditions, except for roll rate, and constant restoring and damping coefficients, while varying Magnus coefficients to determine their influence. Phase III brings into consideration all the aerodynamic coefficients to include the configurational asymmetry coefficients. Different coefficients are used by varying the initial velocity and roll

rates are varied to evaluate high, low, and very low roll theories. Phase IV considers the effects of gravity for various initial velocities and roll rates. No configurational asymmetries are used in order to isolate the gravitational influence. Values for all coefficients are found in Appendix A1, as well as other data including mass parameters. Since computations were done at 1000 ft downrange, the Jump Angle in mils is equivalent to the deviation from the line of fire in feet for all presented cases. The axis system used throughout this analysis is illustrated in the list of symbols.

Phase I

To validate the effects of initial conditions with restoring and damping coefficients only, 36 cases were evaluated using the high roll rate theory, Equation 24. The cases are divided into 4 sections isolating different initial conditions and their effects.

Cases 1-9

The first section shows the effects of roll rate and velocity with zero \vec{s}_o , $\vec{\alpha}_o$ and $\vec{\dot{\alpha}}_o$

TABLE I
THEORY VALIDATION, RESTORING AND
DAMPING MOMENTS, CASES 1-9

C A S E	Initial Conditions					Coefficients				J. A (mils)	
	\vec{s}_o	$\vec{\alpha}_o$	$\vec{\dot{\alpha}}_o$	p_o	u_o	$C_{Z\alpha}$	$C_{Zp\beta}$	C_{YE}	C_{ZE}	6-D	Theory
						$C_{M\alpha}$	$C_{Mp\beta}$	C_{ME}	C_{NE}		
1	0	0	0	31416						0 + 0i	0 + 0i
2	0	0	0	18850	5000					0 + 0i	0 + 0i
3	0	0	0	6283						0 + 0i	0 + 0i
4	0	0	0	31416						0 + 0i	0 + 0i
5	0	0	0	18850	3000					0 + 0i	0 + 0i
6	0	0	0	6283		A1	0	0		0 + 0i	0 + 0i
7	0	0	0	31416						0 + 0i	0 + 0i
8	0	0	0	18850	1000					0 + 0i	0 + 0i
9	0	0	0	6283						0 + 0i	0 + 0i

Table I clearly indicates that no deviation from the line of fire occurs if \vec{s}_o , $\vec{\alpha}_o$, and $\vec{\dot{\alpha}}_o$ are set to zero. Roll rate and velocity changes have no effect on the Jump Angle for this particular situation. This is a trivial solution, it being obvious from inspection of Equation 24.

Cases 10-18

The second section gives the effects of initial translational velocity, $\vec{s}_o = \vec{y} + i\vec{z}$, with various roll rates and velocities. To assure the solution is correct in three dimensional space, the initial translation velocity is given in both y and iz directions. Equation 24 reduces to:

$$\overrightarrow{J.A.} = \frac{1000}{u} \vec{s}_o$$

TABLE II
THEORY VALIDATION, RESTORING AND
DAMPING MOMENTS, CASES 10-18

C A S E	Initial Conditions					Coefficients		$\overrightarrow{J.A.}$ (mils)		
	\dot{s}_o	$\dot{\alpha}_o$	$\dot{\dot{\alpha}}_o$	p_o	u_o	$C_{Z\alpha}$	$C_{Zp\beta}$			
						$C_{Mq} + C_{M\dot{\alpha}}$	$C_{Mp\beta}$	C_{YE}	6-D	Theory
10	100+	0	0	31416				20.002 +	20.000 +	
	100i							20.006 i	20.000 i	
11	100+	0	0	18850	5000			20.002 +	20.000 +	
	100i							20.006 i	20.000 i	
12	100+	0	0	6283				20.002 +	20.000 +	
	100i							20.006 i	20.000 i	
13	100+	0	0	31416				33.346 +	33.333 +	
	100i							33.368 i	33.333 i	
14	100+	0	0	18850	3000	A1	0	0	33.346 +	33.333 +
	100i								33.368 i	33.333 i
15	100+	0	0	6283				33.346 +	33.333 +	
	100i							33.368 i	33.333 i	
16	100+	0	0	31416				100.254 +	100.000 +	
	100i							100.765 i	100.000 i	
17	100+	0	0	18850	1000			100.254 +	100.000 +	
	100i							100.764 i	100.000 i	
18	100+	0	0	6283				100.257 +	100.000 +	
	100i							100.765 i	100.000 i	

The correlation between the theory and the 6-D integration for Cases 10-18 is excellent as shown in Table II. The Jump Angle is seen to be affected by velocity but not roll rate, as would be expected from the reduced Jump Angle equation. Figure I illustrates the deviation from the line of fire for initial velocities of 5000 ft/sec (Cases 10-12), 3000 ft/sec (Cases 13-15) and 1000 ft/sec (Cases 16-18). Since the theory and 6-D

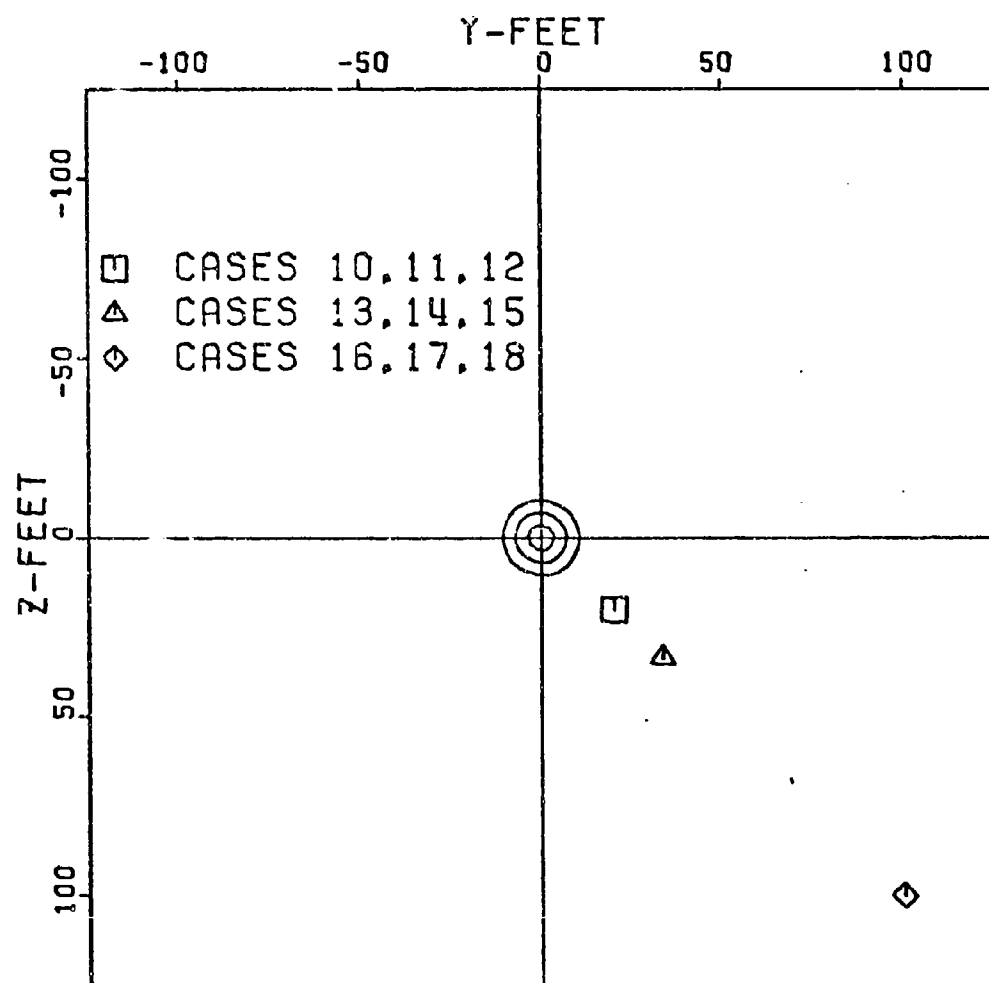


Figure 1. Dispersion: Phase I Cases 10-18

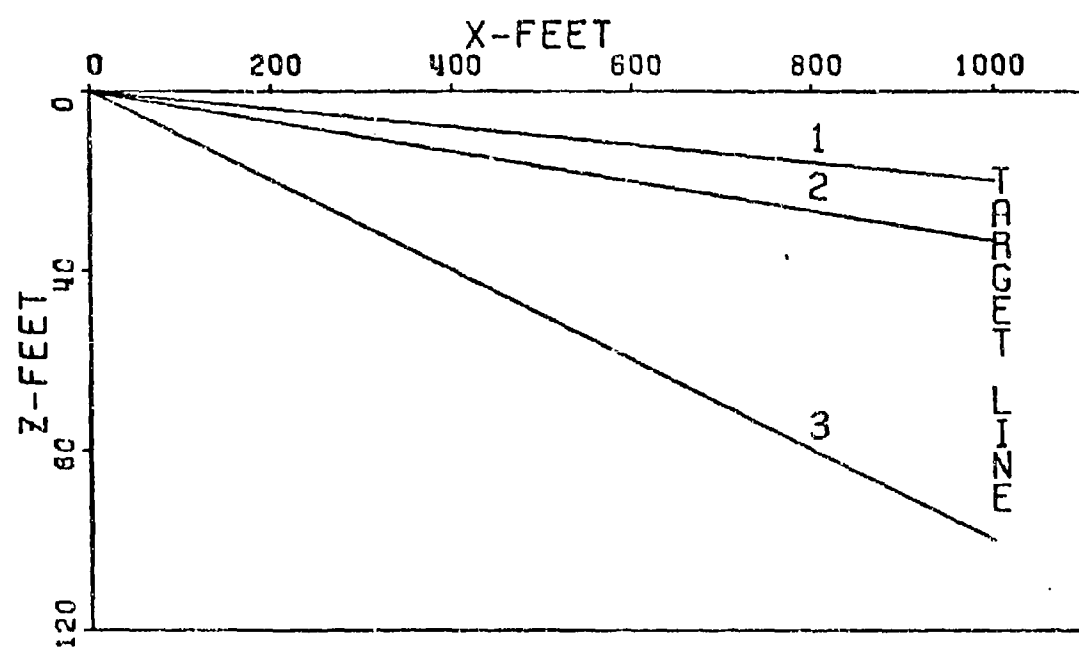
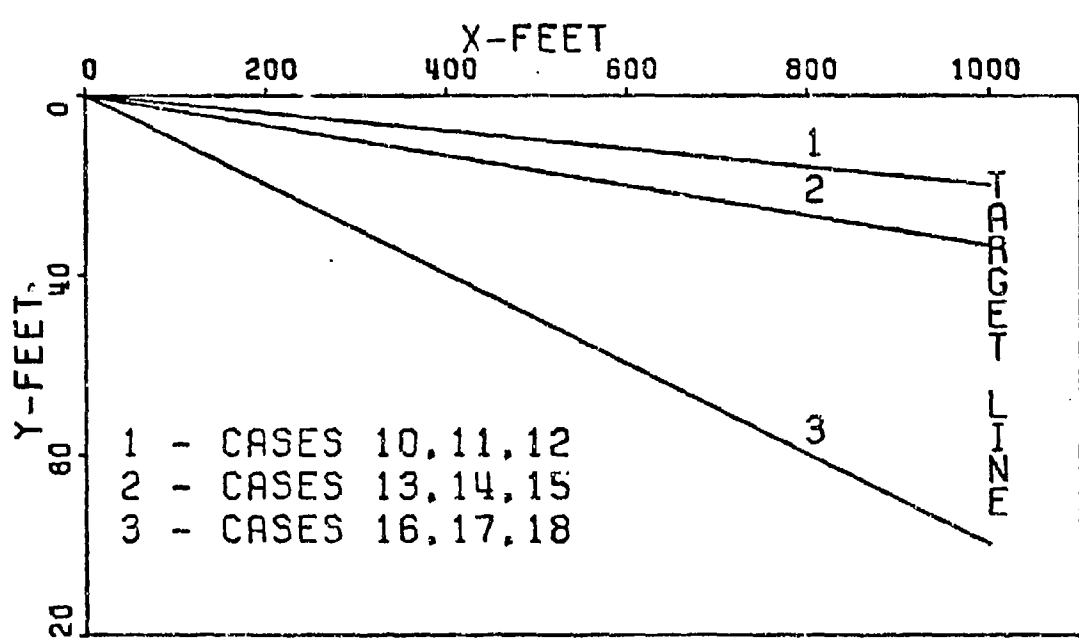


Figure 2. Trajectories, Cases 10-18

are so close, they are plotted as one point. Figure 2 illustrates the trajectory in both the x-y and x-z planes. The deviation from the line of fire is linear with distance downrange in both planes. This would be expected with no gravitational force acting.

Cases 19-27

The third section gives the effects of initial angle of attack, $\vec{\alpha}_0$, with various roll rates and velocities. Again a complex initial condition is used to validate the theory in three dimensional space. Equation 24 reduces to:

$$\overrightarrow{J.A.} = i\vec{\alpha}_0 \left(\frac{pI_x}{mud} \right) \left[\frac{C_{Z_\alpha}}{C_{M_\alpha} - i \left(\frac{pI_x}{mud} \right) C_{Z_\alpha}} \right] 1000$$

Table III shows the range of error between the 6-D computation and the theory to be 0.036 to 0.040 mils in the y-direction and 0.038 to 0.041 mils in the z-direction. Although the y-direction deviations differ in sign, the error between them is approximately 0.00225 degrees, an extremely small angle. This angle will give an approximate deviation of 0.04 feet from the line of fire at 1000 feet downrange. With the $\overrightarrow{J.A.}$ being so close to zero it can be expected that the signs may differ due to computational errors. The results do show Jump Angle variance with both roll rate and velocity. The largest changes occur as velocity goes to 1000 ft/sec.

TABLE III
THEORY VALIDATION, RESTORING AND
DAMPING MOMENTS, CASES 19-27

C A S E	Initial Conditions					Coefficients					$\overline{J.A.}$ (mils)	
	\vec{s}_o	$\vec{\alpha}_o$	$\dot{\vec{\alpha}}_o$	p_o	u_c	$C_{Z\alpha}$	$C_{Zp\beta}$	C_{YE}	C_{ZE}	6-D	Theory	
						$C_{M\alpha}$	$C_{Mq} + C_{M\dot{\alpha}}$	$C_{Mp\beta}$	C_{ME}			
19	0	$1+i$	0	31416						0.012+	-0.027	
										0.068i	+0.027i	
20	0	$1+i$	0	18850	5000					0.023+	-0.017	
										0.058i	+0.017i	
21	0	$1+i$	0	6283						0.034+	-0.006	
										0.047i	+0.006i	
22	0	$1+i$	0	31416						0.012+	-0.026	
										0.067+	+0.026i	
23	0	$1+i$	0	18850	3000	A1		0	0	0.022+	-0.016	
										0.056i	+0.016i	
24	0	$1+i$	0	6283						0.033+	-0.005	
										0.046i	+0.005i	
25	0	$1+i$	0	31416						-0.037+	-0.073	
										0.111i	+0.073i	
26	0	$1+i$	0	18850	1000					-0.008+	-0.044	
										0.082i	+0.044i	
27	0	$1+i$	0	6283						0.021+	-0.015	
										0.053i	+0.015i	

Cases 28-36

The fourth section gives the effects of initial angular rate $\vec{\alpha}_o$, with varying roll rate and velocity. An angular rate of 250 rad/sec is used in both directions of the complex plane to test validity in three dimensional space. Equation 24 reduces to:

$$\overrightarrow{J.A.} = -\vec{\alpha}_o \left(\frac{I_y}{\text{mud}} \right) \left[\frac{C_{Z\alpha}}{C_{M\alpha} - i \left(\frac{pI_x}{\text{mud}} \right) C_{Z\alpha}} \right] 1000$$

TABLE IV
THEORY VALIDATION, RESTORING AND
DAMPING MOMENTS, CASES 28-36

C A S E	Initial Conditions					Coefficients				J. A. (mils)	
	\vec{s}_o	$\vec{\alpha}_o$	$\dot{\vec{\alpha}}_o$	p_o	u_o	$C_{Z\alpha}$	$C_{Z\beta}$	C_{YE}	C_{ZE}	6-D	Theory
						$C_{M\alpha}$	$C_{M\beta}$	C_{ME}	C_{NE}		
28	0	0	$250+250i$	31416						-2.027	-2.073
										-2.034i	-2.073i
29	0	0	$250+250i$	18850	5900					-2.025	-2.073
										-2.030i	-2.073i
30	0	0	$250+250i$	6283						-2.027	-2.073
										-2.029i	-2.073i
31	0	0	$250+250i$	31416						-1.961	-1.970
										-1.967i	-1.970i
32	0	0	$250+250i$	18850	3000	A1	0	0		-1.962	-1.970
										-1.966i	-1.970i
33	0	0	$250+250i$	6283						-1.964	-1.970
										-1.964i	-1.970i
34	0	0	$250+250i$	31416						-5.238	-5.540
										-5.274i	-5.540i
35	0	0	$250+250i$	18850	1000					-5.243	-5.540
										-5.264i	-5.540i
36	0	0	$250+250i$	6283						-5.254	-5.540
										-5.260i	-5.540i

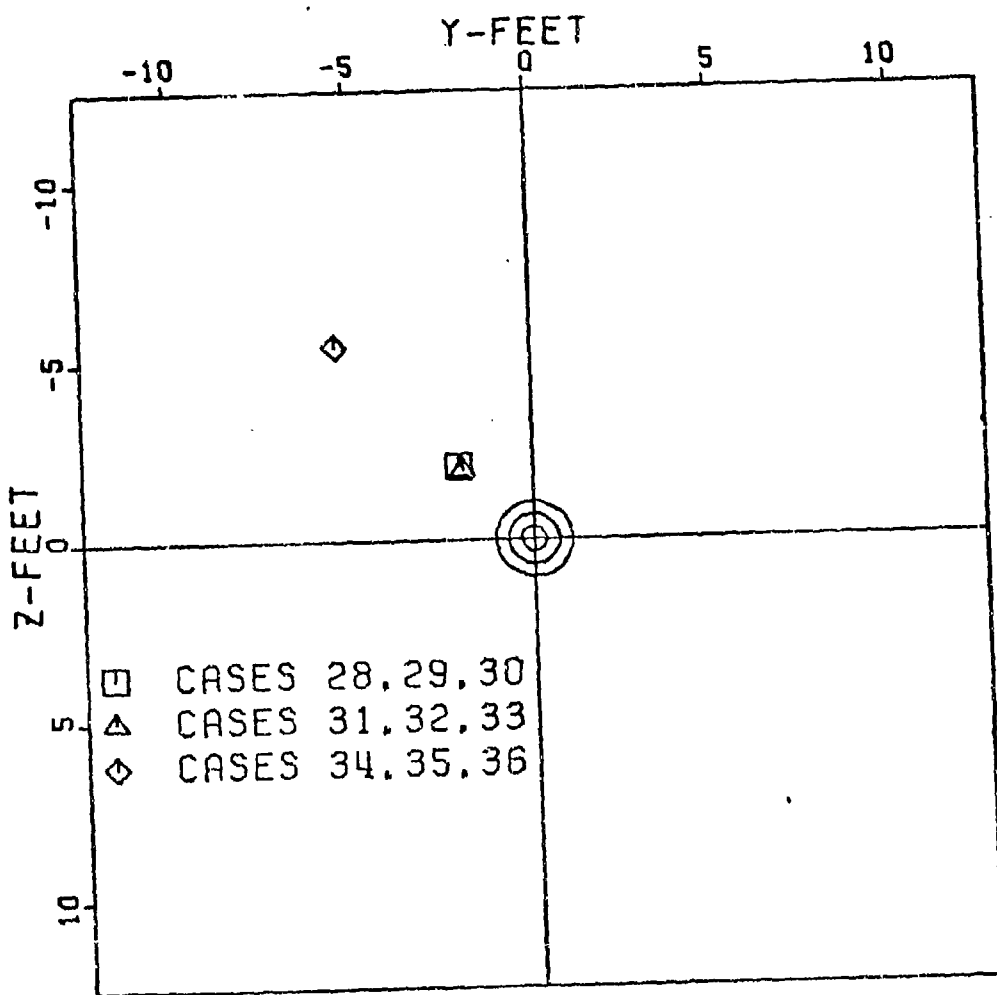


Figure 3. Dispersion: Phase I Cases 28-36

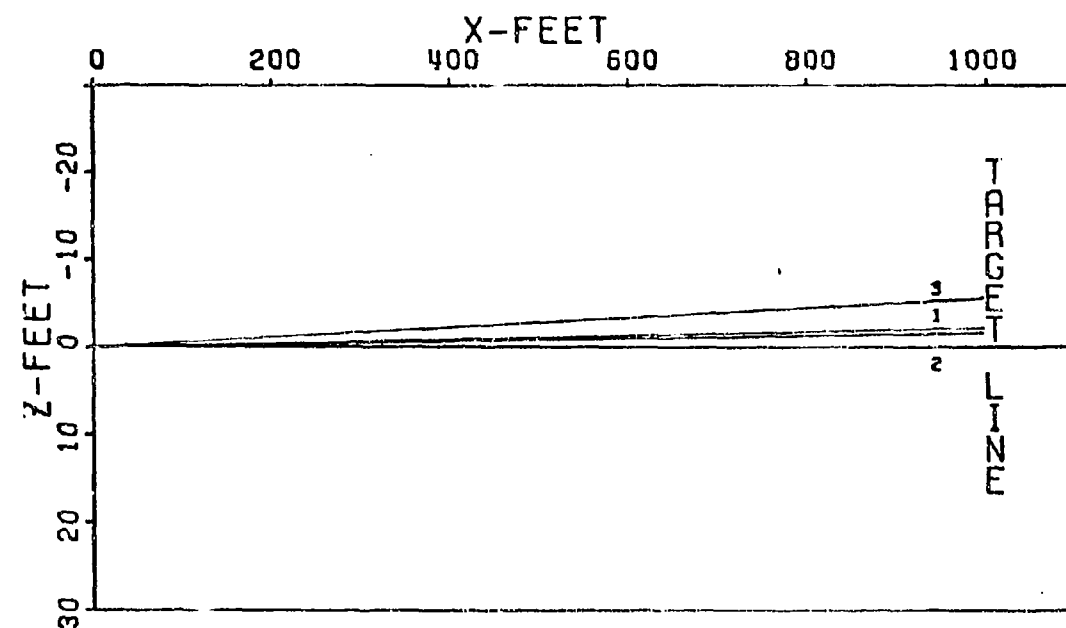
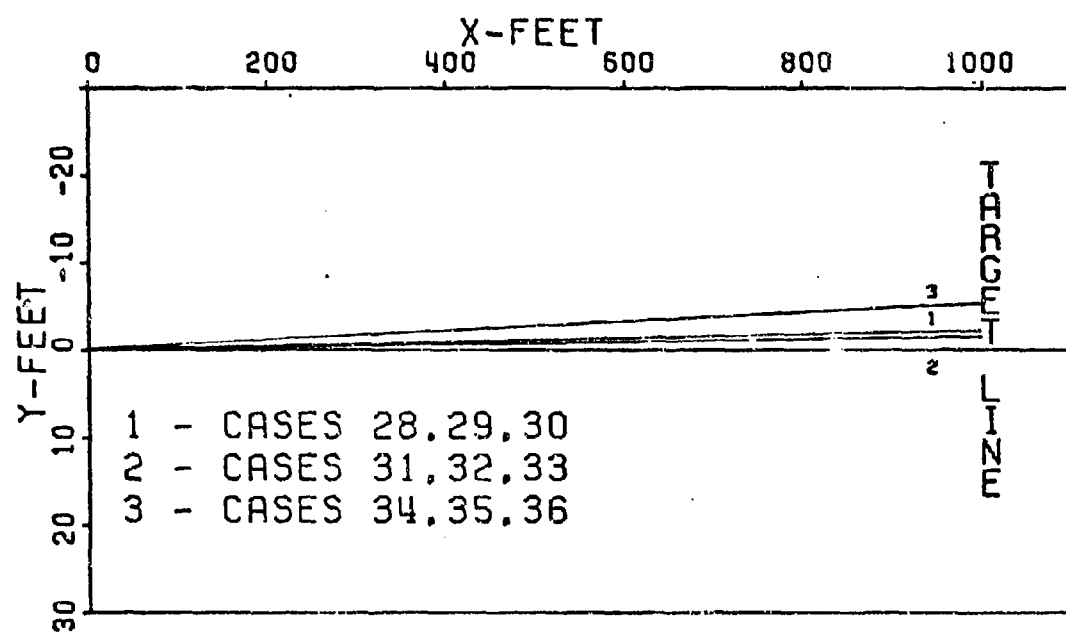


Figure 4. Trajectories, Cases 28-36

Table IV indicates excellent agreement between the theory and 6-D computations. Roll rate is found not to affect the Jump Angle appreciably but velocity does, as would be expected from the reduced Jump Angle equation. Figure 3 shows the dispersion pattern while Figure 4 illustrates the trajectories. Cases 28, 29, and 30 are plotted as one point due to the small difference between them. Cases 31, 32, 33 and 34, 35, and 36 are plotted similarly.

Phase II

To validate the effect of Magnus Forces and Moments on the dispersion of flechettes, 21 Cases were run varying the initial roll rate and Magnus Coefficients. All other conditions were held constant. The variance of Magnus coefficients with Mach number had to be chosen since no data was available. Arbitrarily, the ratio of $C_{Zp\beta}/C_{Mp\beta}$ was chosen to be the same as that of $C_{Z\alpha}/C_{M\alpha}$. The Magnus Coefficients used are presented as functions of Mach Number in Appendix A1 with only the values at Mach 4.5 tabulated here for identification sake:

TABLE V
MAGNUS COEFFICIENTS,
AT MACH 4.5

$C_{Zp\beta}$	$C_{Mp\beta}$
± 34.8	± 110.0
± 31.6	± 100.0
± 28.4	± 90.0

Equation 24 now becomes:

$$\overrightarrow{J.A.} = \left[\frac{\dot{\vec{S}}_o}{u} - \frac{I_y}{mud} \left[\vec{\alpha}_o - i\vec{\alpha}_o \left(\frac{pI_x}{I_y} \right) \right] \right. \\ \left. \left[C_{Z\alpha} + i \left(\frac{pd}{2u} \right) C_{Zp\beta} \right] \right] \frac{1000}{\left[C_{M\alpha} + \frac{pI_x}{mud} \frac{pd}{2u} C_{Zp\beta} \right] + i \left(C_{Mp\beta} \frac{pd}{2u} - \frac{pI_x}{mud} C_{Z\alpha} \right)}$$

Initial conditions used in this section are consistent with those of other sections to provide a basis for comparison. Three cases of zero Magnus were run, one at each roll rate to provide a standard to judge the influence of Magnus.

The effects of Magnus coefficients on dispersion are minimal as seen in Table VI. The variance between the zero Magnus cases and any other case is found not to be greater than 0.209 mils (or feet at 1000 feet of range). In order to obtain the maximum Magnus effects, the largest possible Magnus coefficients were used. Hence, $C_{Zp\beta} = 34.8$ and $C_{Mp\beta} = 110.0$ are the largest possible coefficients since cases 40 and 49 become unstable. Table VI indicates the effects (for positive Magnus coefficients)

- (1) increasing horizontal dispersion with increasing p
- (2) decreasing vertical dispersion with increasing p
- (3) increasing horizontal dispersion with increasing Magnus
- (4) decreasing vertical dispersion with increasing Magnus

TABLE VI
THEORY VALIDATION, MAGNUS, CASES 37-57

C A S E	Magnus Forces & Moments	Roll Rate	p_o 31416 rad/sec	p_o 18850 rad/sec	p_o 6283 rad/sec
37	$C_Z p\beta = 0.0$	(6-D) 17.994+ 18.042i	Theory	(6-D) 18.003+ 18.032i	Theory
38	$C_M p\beta = 0.0$			17.900+ 17.944i	18.013+ 18.022i
39				17.910+ 17.944i	Theory 17.921+ 17.933i
40	$C_Z p\beta = 34.8$			18.141+ 17.903i	18.057+ 17.979i
41	$C_M p\beta = 110.0$		Unstable		17.920+ 17.931i
42				17.909+ 17.942i	
43	$C_Z p\beta = 31.6$	18.203+ 17.849i		18.123+ 17.915i	18.053+ 17.982i
44	$C_M p\beta = 100.0$		17.899		17.920+ 17.931i
45		17.954i		17.909 17.942i	
46	$C_Z p\beta = 28.4$	18.183+ 17.869i		18.114+ 17.925i	18.050+ 17.987i
47	$C_M p\beta = 90.0$		17.899		17.920+ 17.931i
48		17.954i		17.909 17.942i	
49	$C_Z p\beta = -34.8$			17.877+ 18.170i	17.969+ 18.067i
50	$C_M p\beta = -110.0$		Unstable		17.920+ 17.931i
51				17.090+ 17.942i	
52	$C_Z p\beta = -31.6$	17.807+ 18.258i		17.888+ 18.158i	17.973+ 18.063i
53	$C_M p\beta = -100.0$		17.899+ 17.954i		17.920+ 17.931i
54				17.909+ 17.942i	
55	$C_Z p\beta = -28.4$	17.826+ 18.233i		17.900+ 18.144i	17.977+ 18.059i
56	$C_M p\beta = -90.0$		17.899+ 17.954i		17.820+ 17.931i
57				17.909+ 17.942i	

CMP 8 = ± 90.0

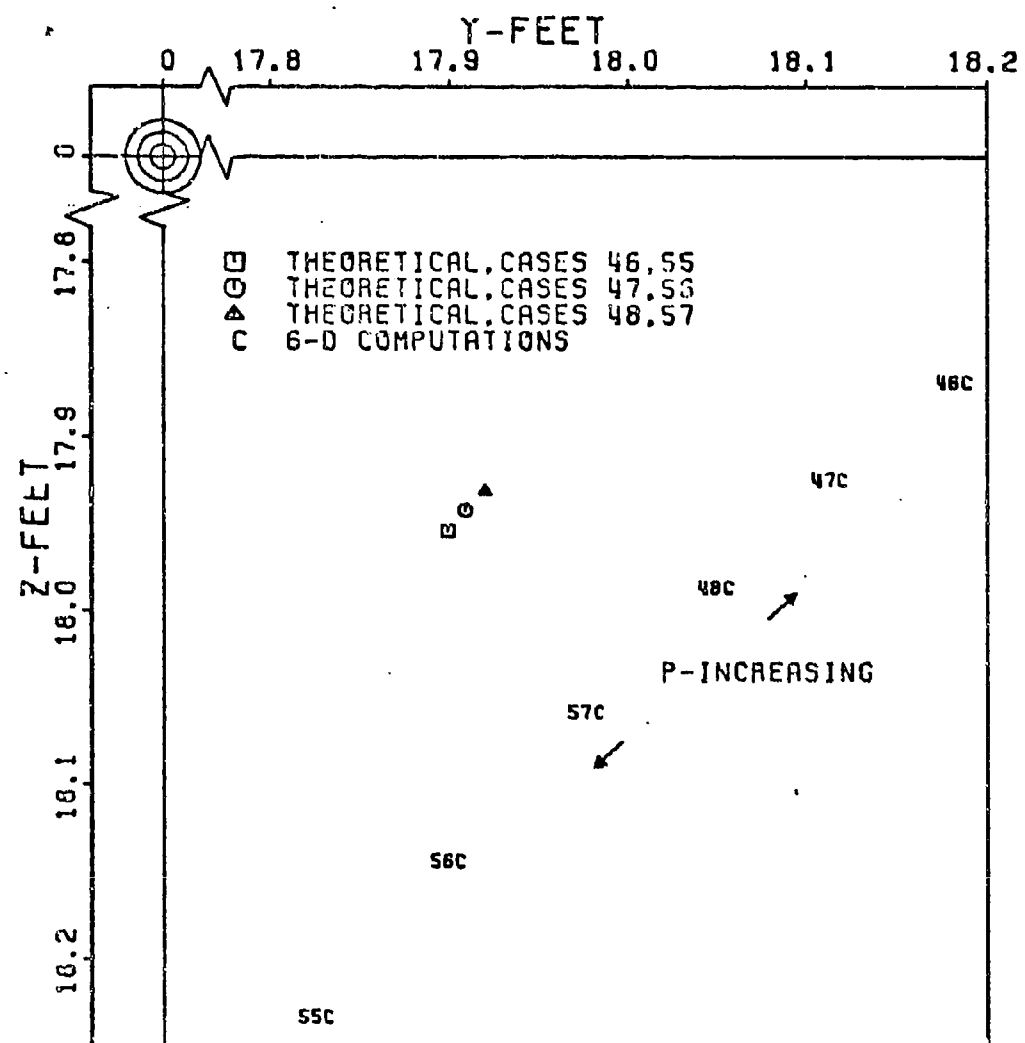


Figure 5. Dispersion: Phase II Cases 46,47,48,55,56,57

$P=18850$ RAD/SEC

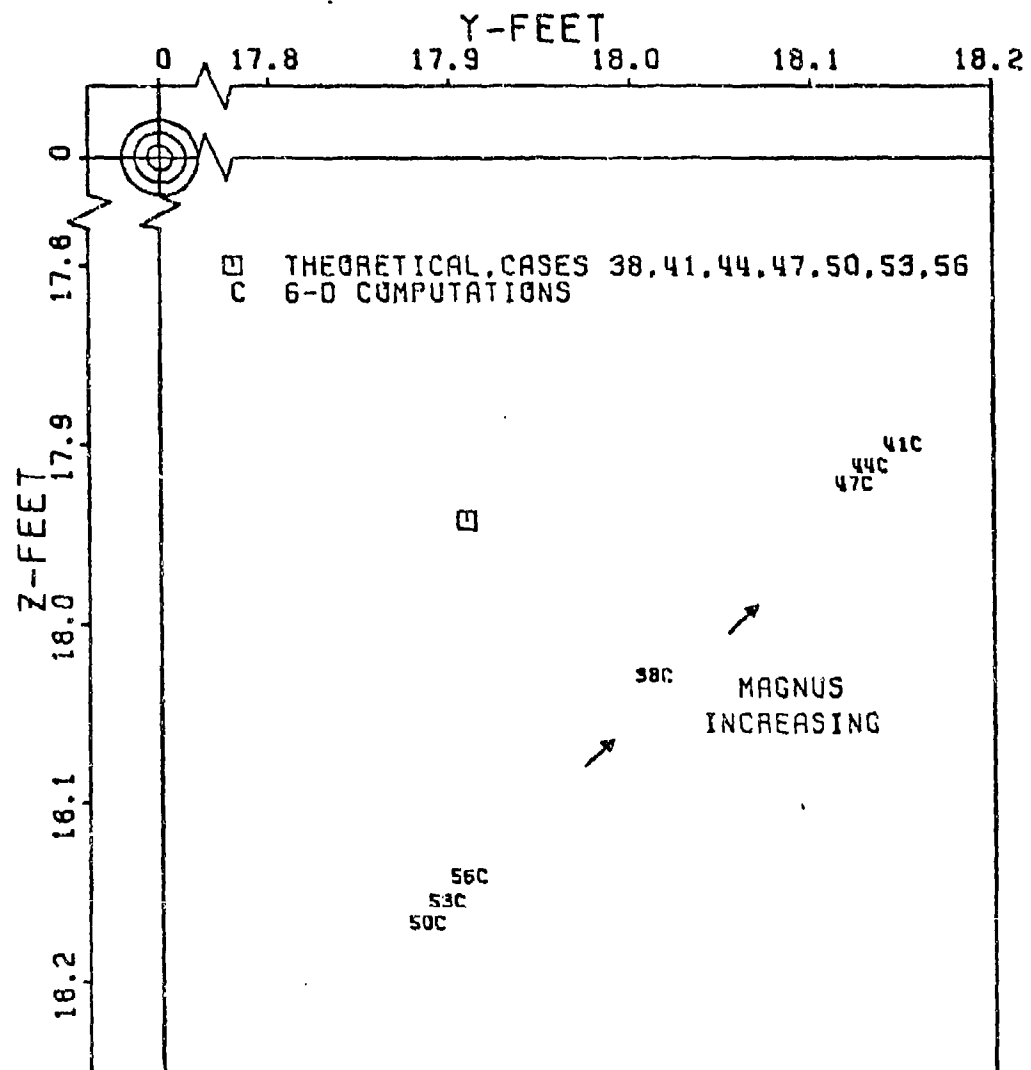


Figure 6. Dispersion: Phase II Cases 38,41,44,47,50,53,56

(for negative Magnus coefficients)

- (5) decreasing horizontal dispersion with increasing p
- (6) increasing vertical dispersion with increasing p
- (7) decreasing horizontal dispersion with decreasing Magnus
- (8) increasing vertical dispersion with decreasing Magnus

For example, Figure 5 illustrates the effects of roll rate for constant Magnus coefficients of $\pm 90^\circ$ (1,2,5,6 above). Figure 6 illustrates the effects of Magnus for a constant sample roll rate (3,4,7,8 above).

Obviously, when only a 0.209 mil maximum deviation due to Magnus occurs when the situation is geared toward finding the largest effect due to Magnus, smaller deviations due to Magnus would be found in actual situations. It can be concluded that Magnus has no large effect on dispersion although it could be significant if the total dispersion is close to zero.

Phase III

To validate the effects of aerodynamic asymmetries on dispersion of flechettes, a large number of cases were run varying roll rate, velocity, and initial conditions while holding the asymmetry coefficients constant. The asymmetries coefficients were selected to allow 10° of non-rolling trim to exist while the flechette was in flight. The asymmetry coefficients, C_{YE} , C_{ZE} , C_{ME} and C_{NE} are presented in Appendix A-1 as a function of Mach number. The variance with Mach number was chosen arbitrarily: the ratio of asymmetry force to asymmetry moment identical to the ratio

of $C_{Z\alpha}$ to $C_{M\alpha}$. The wide range of roll rates makes mandatory use of all three dispersion theories. The governing equations are presented as they apply.

Cases 58-90

The first set of cases utilizes zero initial disturbances while varying velocity and roll rate. For roll rates of 31416 rad/sec down to 100 rad/sec the High Roll Rate Theory yields the governing equation,

$$\overrightarrow{J.A.} = \frac{\rho u \pi d^2}{8m} \left[C_{M\delta\epsilon} \vec{\delta}_\epsilon \left(\frac{A}{p} \right) + C_{Z\delta\epsilon} \vec{\delta}_\epsilon \left(\frac{I_y - I_x}{mud} A + \frac{i}{p} \right) \right] 1000$$

For roll rates: $p < 100$ rad/sec and $pt \geq 1.0$, the Low Roll Rate Theory takes effect:

$$\begin{aligned} \overrightarrow{J.A.} = & \frac{\rho u^2 \pi d^2}{8mx} \left[C_{Z\delta\epsilon} \vec{\delta}_\epsilon \cdot i \left(\frac{C_{Z\alpha}}{C_{M\alpha}} \right) C_{M\delta\epsilon} \vec{\delta}_\epsilon \right] \left[\frac{1}{p^2} \left(1 - \cos \frac{px}{u} \right) \right. \\ & \left. + \frac{1}{p} \left(\frac{x}{u} - \frac{1}{p} \sin \frac{px}{u} \right) \right] 1000 \end{aligned}$$

Finally, the very Slow Roll Rate Theory applies for values of $pt < 1.0$:

$$\begin{aligned} \overrightarrow{J.A.} = & \frac{\rho \pi d^2 x}{16m} \left[C_{Z\delta\epsilon} \vec{\delta}_\epsilon \cdot i \left(\frac{C_{Z\alpha}}{C_{M\alpha}} \right) C_{M\delta\epsilon} \vec{\delta}_\epsilon \right] \left[\left(1 - \frac{1}{12} \left(\frac{px}{u} \right)^2 + \frac{1}{360} \left(\frac{px}{u} \right)^4 \right) \right. \\ & \left. + i \left(\frac{px}{3u} - \frac{1}{60} \left(\frac{px}{u} \right)^3 + \frac{1}{2520} \left(\frac{px}{u} \right)^5 \right) \right] 1000 \end{aligned}$$

Tables 7, 8, and 9 list Cases 58-90:

TABLE VII
THEORY VALIDATION, ASYMMETRIES,
CASES 58-68

C A S E	Initial Conditions					Coefficients					$\overrightarrow{J.A.}$ (mils)		
	\vec{s}_o	$\vec{\alpha}_o$	$\vec{\dot{\alpha}}_o$	p_o	u_o	$C_{Z\alpha}$	$C_{Z\beta}$	C_{YE}	C_{ZE}	C_{ME}	C_{NE}	6-D	Theory
58	0	0	0	31416								0.018-	0.018-
												0.013i	0.014i
59	0	0	0	18850								0.030-	0.029-
												0.027i	0.025i
60	0	0	0	6283								0.060-	0.064-
												0.127i	0.130i
61	0	0	0	500								0.997-	1.013-
												0.992i	1.009i
62	0	0	0	300								1.620-	1.688-
												1.721i	1.683i
63	0	0	0	100	5000	A1	A1	A1	A1	A1	A1	4.574-	4.675-
												4.896i	4.975i
64	0	0	0	50								8.666-	8.780-
												12.280i	12.489i
65	0	0	0	25								20.669-	21.150-
												26.418i	26.927i
66	0	0	0	10								-7.973	-8.210
												-62.197i	-63.210i
67	0	0	0	5								-29.857	-30.372
												-61.459i	-62.353i
68	0	0	0	0								-49.706	-50.427
												-49.706i	-50.427i

TABLE VIII
THEORY VALIDATION, ASYMMETRIES,
CASES 69-79

C A S E	Initial Conditions					Coefficients					<u>J.A.</u> (mils)	
						$C_{Z\alpha}$	$C_{M\alpha}$	$C_{Zp\beta}$	C_{YE}	C_{ZE}		
	\dot{S}_o	$\dot{\alpha}_o$	$\ddot{\alpha}_o$	p_o	u_o	$C_{Mq} + C_{M\dot{\alpha}}$	$C_{Mp\beta}$	A1	A1	A1	6-D	Theory
69	0	0	0	31416							0.008- 0.004i	0.009- 0.004i
70	0	0	0	18850							0.013- 0.008i	0.013- 0.008i
71	0	0	0	6283							0.033- 0.028i	0.034- 0.029i
72	0	0	0	500							0.394- 0.398i	0.401- 0.395i
73	0	0	0	300							0.663- 0.659i	0.666- 0.662i
74	0	0	0	100	3000		A1		A1	A1	1.841- 1.998i	1.994- 1.984i
75	0	0	0	50							3.780- 4.513i	3.411- 4.164i
76	0	0	0	25							5.676- 8.457i	5.721- 8.516i
77	0	0	0	10							9.203- 32.628i	9.217 32.897i
78	0	0	0	5							-41.029- -41.985i	-42.273i -42.273i
79	0	0	0	0							-33.014- -33.014i	-33.194 -33.194i

TABLE IX
THEORY VALIDATION, ASYMMETRIES,
CASES 80-90

C A S E	Initial Conditions					Coefficients					J.A. (mils)					
	\dot{S}_o	$\dot{\alpha}_o$	$\dot{\alpha}_o$	p_o	u_o	$C_{Z\alpha}$	$C_{M\alpha}$	$C_{Zp\beta}$	$C_{Mq} + C_{M\dot{\alpha}}$	C_{YE}	C_{ZE}	C_{ME}	C_{NE}	6-D	Theory	
80	0	0	0	31416											Unstable	
81	0	0	0	18850											Unstable	
82	0	0	0	6283											0.025 - 0.010i	0.023 - 0.014i
83	0	0	0	500											0.241 - 0.229i	0.238 - 0.229i
84	0	0	0	300											0.396 - 0.380i	0.394 - 0.385i
85	0	0	0	100	1000	A1		A1		A1					1.177 - 1.160i	1.174 - 1.165i
86	0	0	0	50											2.346 - 2.329i	2.349 - 2.352i
87	0	0	0	25											4.684 - 4.672i	4.699 - 4.702i
88	0	0	0	10											10.224 - 14.447i	10.177 - 14.476i
89	0	0	0	5											24.402 - 31.013i	24.516 - 31.212i
90	0	0	0	0											-58.711 -58.711i	-58.450 -58.450i

Evident from Tables VII, VIII, IX is the fact that roll rate has tremendous influence on the dispersion of flechettes with aerodynamic asymmetries. Figures 7, 8, and 9 illustrate the dispersion pattern for these cases. The 6-D computations and theory are in very good agreement considering the large deviations involved. It should be noted that the actual flechette with its velocity approaching 5000 ft/sec is affected very little by aerodynamic asymmetries. However, if the flechette were only to roll very slowly, large dispersion ranges in excess of 60 mils could occur. Velocity also has a noticeable effect on dispersion. Figure 10 shows the three theory curves from Figures 7, 8, 9 in composite to illustrate velocity effects. A sample trajectory, Case 79, is shown in Figure 11, illustrating the curved path of flight. This is typical of trajectories involving aerodynamic asymmetries.

Cases 91-123

To show the relation between the effects on dispersion for initial transverse velocity and aerodynamic asymmetries a second set of cases were run. Roll rate and velocity were varied as in the first set of cases, but \dot{S}_o was set at $(100 + 100i)$ ft/sec with $\dot{\alpha}_o = 0$ and $\dot{\alpha}_{\epsilon} = 0$. Tables X, XI, and XII list the results. For high roll rate cases, Equation 24 becomes:

$$\overline{J.A.} = \left[\frac{\dot{S}_o}{u} + \frac{\rho u \pi d^2}{8m} \left[C_M \overline{\delta}_{\epsilon} \left(\frac{A}{p} \right) + C_Z \overline{\delta}_{\epsilon} \left(\frac{I_y - I_x}{mud} A + \frac{i}{p} \right) \right] \right] 1000$$

For low rate cases, Equation 28 becomes:

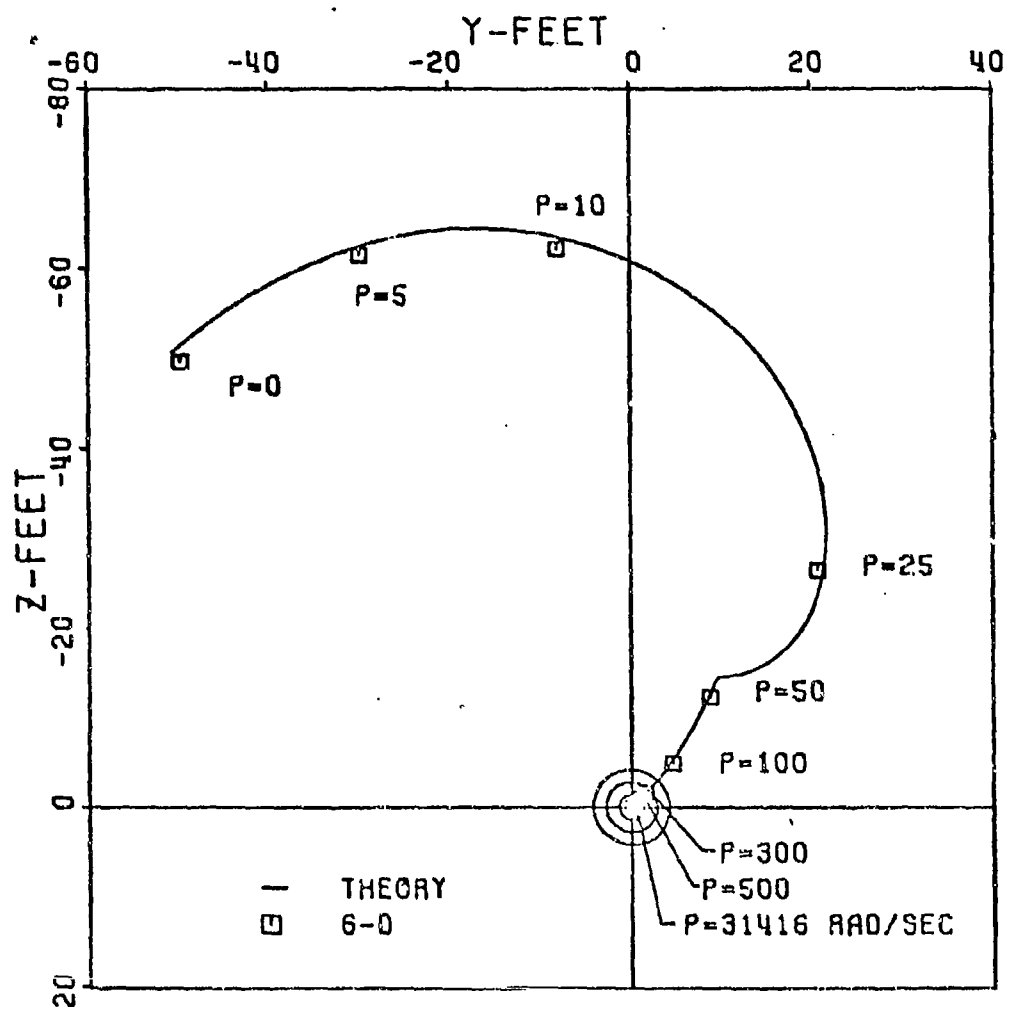


Figure 7. Dispersion: Phase III Cases 58-68

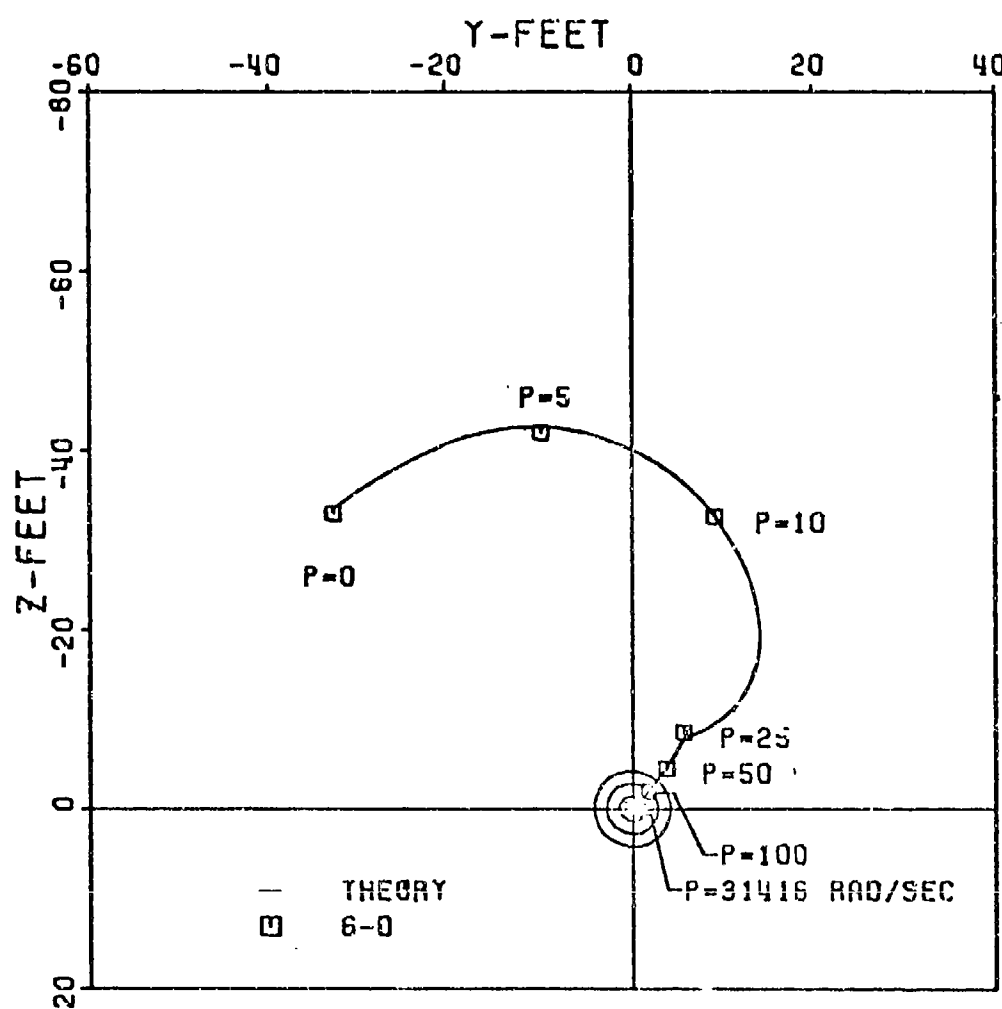


Figure 8. Dispersion: Phase III Cases 69-79

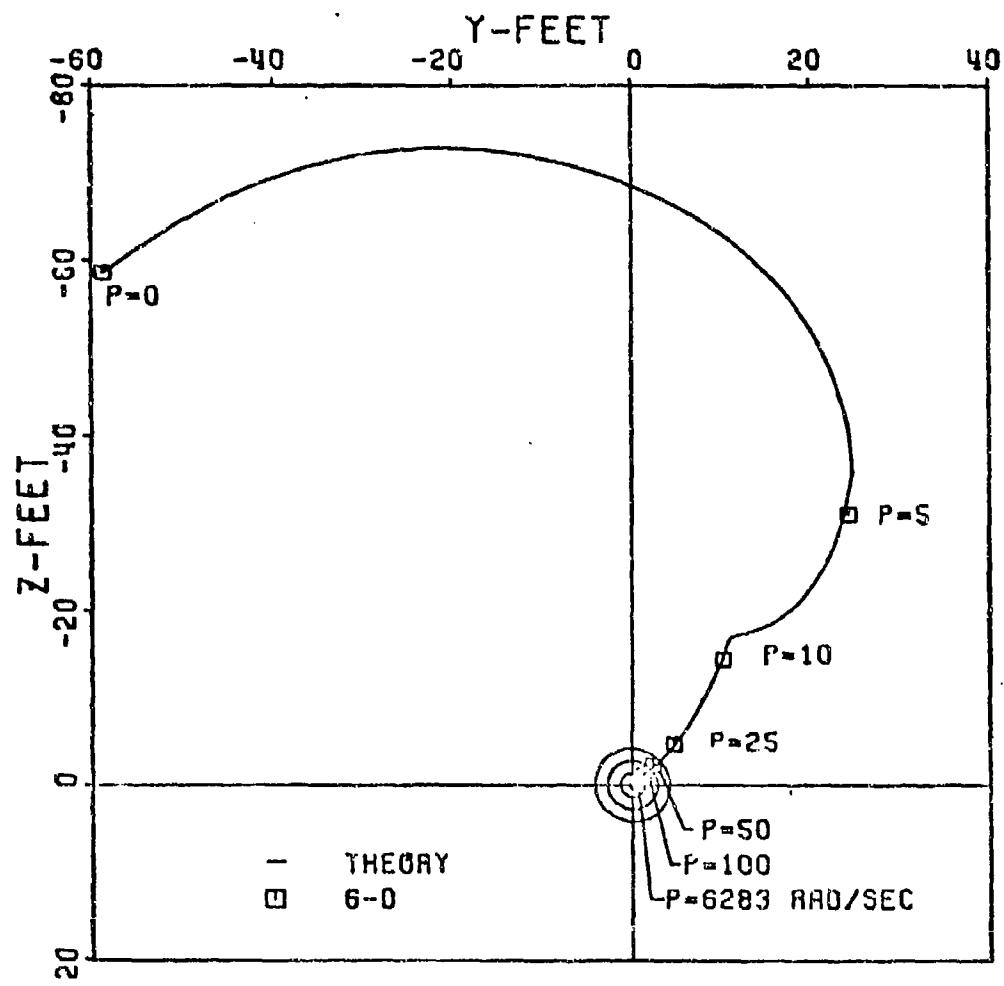


Figure 9. Dispersion: Phase III Cases 80-90

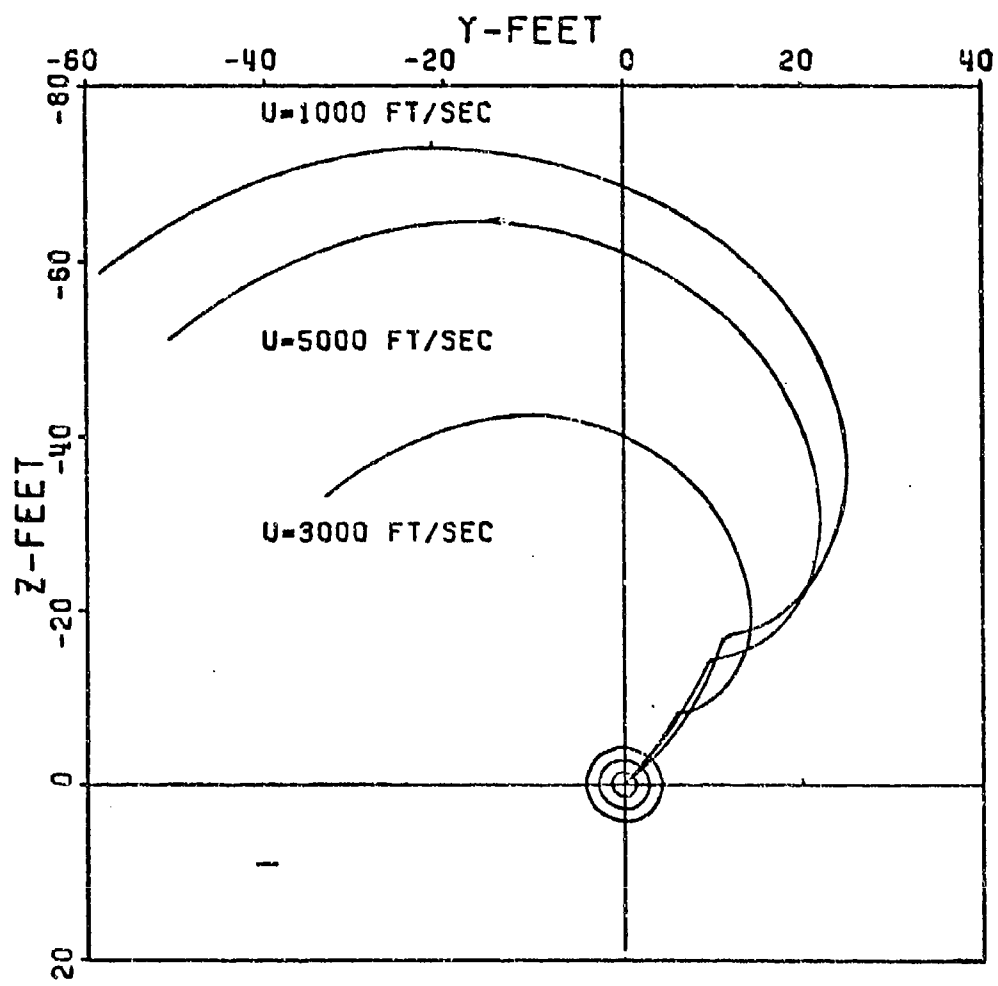


Figure 10. Dispersion: Phase III Theory, Cases 58-90

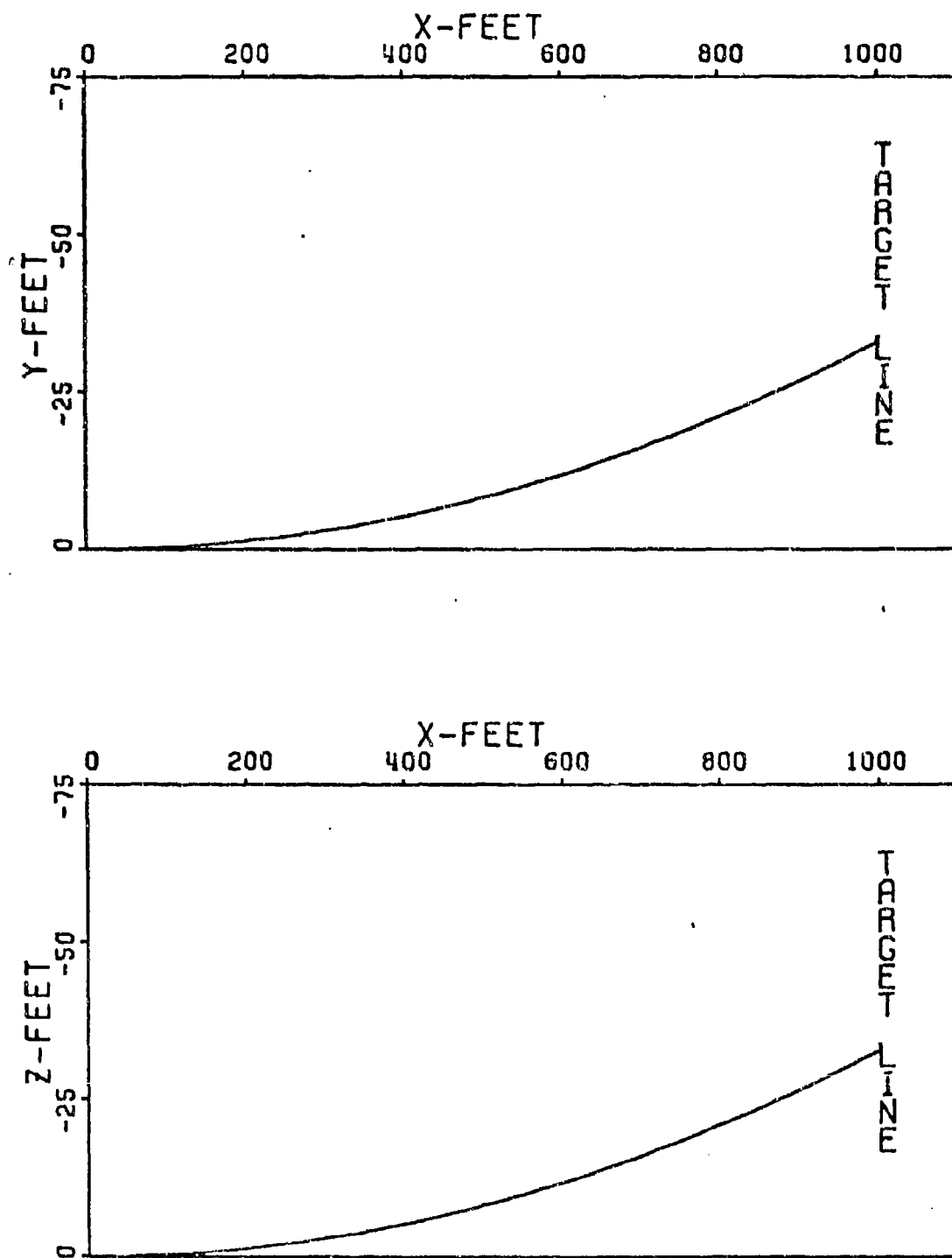


Figure 11. Trajectory, Case 79

$$\overrightarrow{J.A.} = \left[\frac{\vec{S}_0}{u} + \frac{\rho u^2 \pi d^2}{8mx} \left[C_Z \vec{\delta}_\epsilon - i \left(\frac{C_Z \alpha}{C_M \alpha} \right) C_M \vec{\delta}_\epsilon \right] \left[\frac{1}{p^2} (1 - \cos \frac{px}{u}) \right. \right. \\ \left. \left. + \frac{i}{p} \left(\frac{x}{u} - \frac{1}{p} \sin \frac{px}{u} \right) \right] \right] 1000$$

For very slow roll cases, Equation 30 becomes:

$$\overrightarrow{J.A.} = \left[\frac{\vec{S}_0}{u} + \frac{\rho \pi d^2 x}{16m} \left[C_Z \vec{\delta}_\epsilon - i \left(\frac{C_Z \alpha}{C_M \alpha} \right) C_M \vec{\delta}_\epsilon \right] \left[\left(1 - \frac{1}{12} \left(\frac{px}{u} \right)^2 \right. \right. \right. \right. \\ \left. \left. \left. \left. + \frac{1}{360} \left(\frac{px}{u} \right)^4 \right) + i \left(\frac{px}{3u} - \frac{1}{60} \left(\frac{px}{u} \right)^3 + \frac{1}{2520} \left(\frac{px}{u} \right)^5 \right) \right] \right] 1000$$

Comparing Cases 91, 92, 93 in Table X with Cases 10, 11, 12 in Table II and Cases 58, 59, 60 in Table VII it can be concluded that; except for possible computational error, Cases 91, 92 and 93 are the algebraic sum of Cases 10, 11, 12 and 58, 59, 60; that is, for example, Case 91 equals Case 10 plus Case 58. This fact is obviously true of the theory equations and is here shown to be the case for the 6-D computations as well. Similar comparisons can be made with corresponding cases in Tables II, VIII, XI and II, IX, XII. Thus, the effects of aerodynamic asymmetries and those of initial transverse velocity are independent of one another.

Figures 12, 13 and 14 illustrate the Cases 91-123. The curves are of the same form as Figures 7, 8 and 9 but differ with the addition of \vec{S}_0 . Maximum effect of all parameters is desired. Cases 113, 114 and 115 show the limit of parameter combinations by 113 and 114 going unstable. Roll rate effects are again large and velocity effects are larger than in Cases 58-90. Figure 15 shows this to be true and also shows the cases involving

TABLE X
THEORY VALIDATION, ASYMMETRIES,
CASES 91-101

C A S E	Initial Conditions					Coefficients				J. A. (mils)	
	\vec{s}_o	$\vec{\alpha}_o$	$\vec{\dot{\alpha}}_o$	p_o	u_o	$C_{Z\alpha}$	$C_{Zp\beta}$	C_{YE}	$J.A.$	6-D	Theory
				$C_{Mq} + C_{M\dot{\alpha}}$		$C_{Mp\beta}$	C_{ZE}	C_{ME}			
91				31416						20.011+	20.018+
92				18850						19.987i	19.986i
93				6283						20.026+	20.029+
94				500						19.972i	19.975i
95				300						20.056+	20.083+
96	100+ 100i	0	0	100	5000	A1	A1	A1		19.872i	19.922i
97				50						21.004+	21.013+
98				25						19.012i	18.991i
99				10						21.626+	21.688+
100				5						18.286i	18.317i
101				0						24.593+	24.675+
										15.099i	15.025i
										28.702+	28.780+
										7.687i	7.511i
										40.766-	41.150-
										6.492i	6.927i
										11.983-	11.790-
										42.325i	43.210i
										-9.908-	-10.372
										41.503i	-42.353i
										-29.727	-30.427
										-29.743i	-30.427i

TABLE XI
THEORY VALIDATION, ASYMMETRIES,
CASES 102-112

C A S E	Initial Conditions					Coefficients				J.A. (mils)	
						$C_{Z\alpha}$	$C_{Z\beta}$	C_{YE}			
	\dot{S}_0	$\dot{\alpha}_0$	$\dot{\alpha}_0$	p_0	u_0	$C_{M\alpha} + C_M\dot{\alpha}$	$C_{M\beta}$	C_{ZE}	C_{ME}	6-D	Theory
102				31416						33.352+	33.342+
				18850						33.362i	33.329i
103				6283						33.366+	33.345+
				500						33.364i	33.325i
104				300						33.388+	33.367+
				100	3000	A1	A1	A1		33.347i	33.304i
105				50						33.740+	33.734+
				25						32.964i	32.937i
106				10						34.009+	34.000+
				5						33.705i	32.761i
107	100+	0	0	0						35.188+	35.327+
	100i									31.361i	31.344i
108										37.139+	36.744+
										28.850i	29.169i
109										39.029+	39.054+
										24.892i	24.817i
110										42.575+	42.550+
										0.716i	0.436i
111										23.312-	23.159-
										8.612i	8.940i
112				0						0.380+	0.139+
										0.362i	0.139i

TABLE XII
THEORY VALIDATION, ASYMMETRIES,
CASES 113-123

C A S E	Initial Conditions					Coefficients				J. A. (mils)	
						$C_{Z\alpha}$	C_{YE}	C_{ZE}	C_{ME}	6-D	Theory
	\vec{s}_o	$\vec{\alpha}_o$	$\vec{\dot{\alpha}}_o$	p_o	u_o	$C_{Mq} + C_M\dot{\alpha}$	$C_{M\beta}$	C_{NE}	$C_{Mp\beta}$		
113				31416							Unstable
114				18850							Unstable
115				6283							100.351+ 100.814i
116				500							100.559+ 100.587i
117				300							100.710+ 100.431i
118	100+ 100i	0	0	100	1000	A1	A1	A1			101.492+ 99.658i
119				50							102.668+ 98.495i
120				25							105.019+ 96.164i
121				10							110.862+ 86.275i
122				5							125.216+ 69.958i
123				0							41.499+ 41.413i
											41.550+ 41.550i

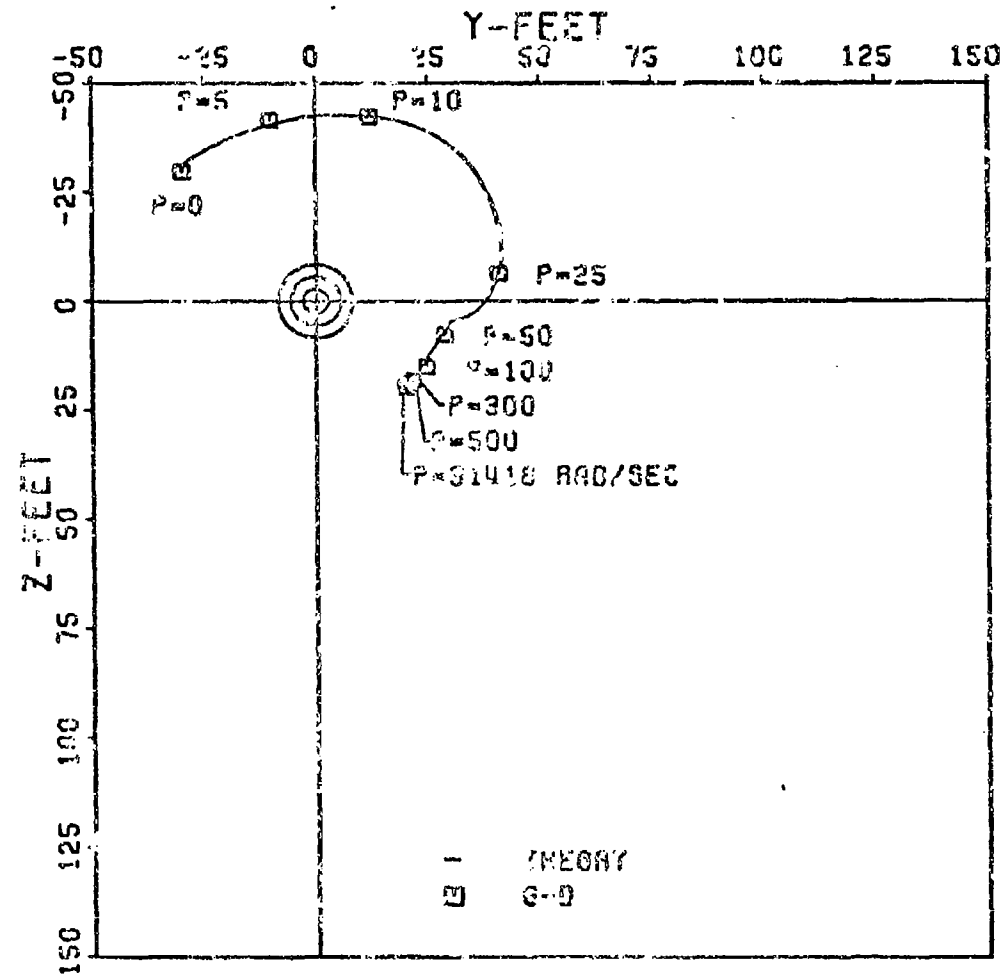


Figure 12. Dispersion: Case III Cases 91-101

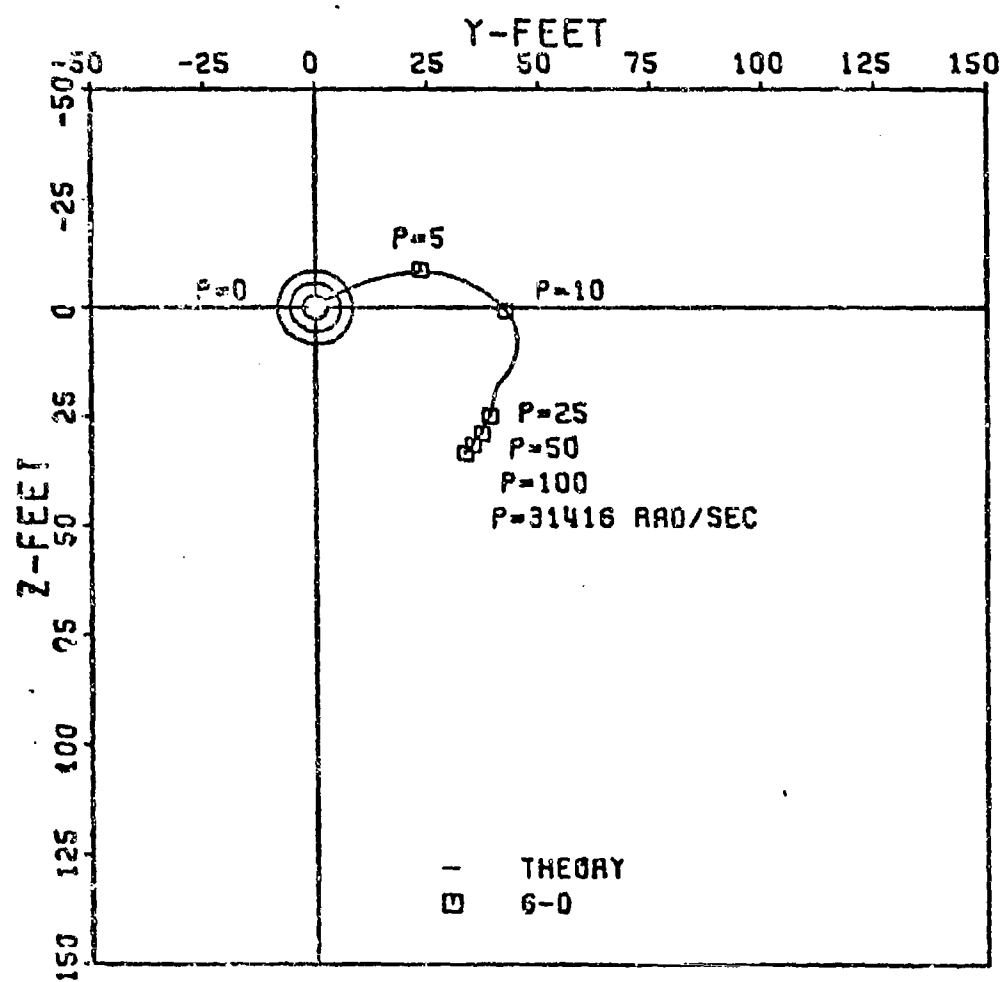


Figure 13. Dispersion: Phase III Cases 102-112

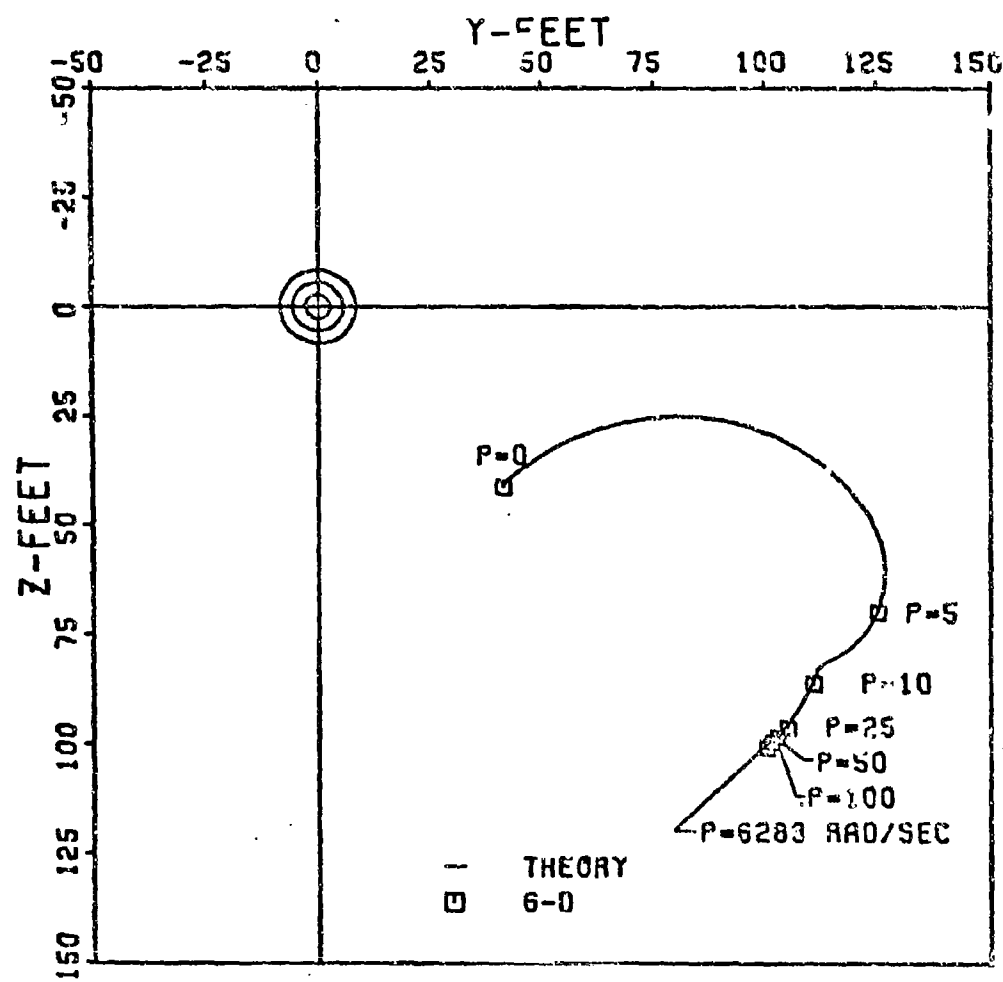


Figure 14. Dispersion: Phase III Cases 113-123

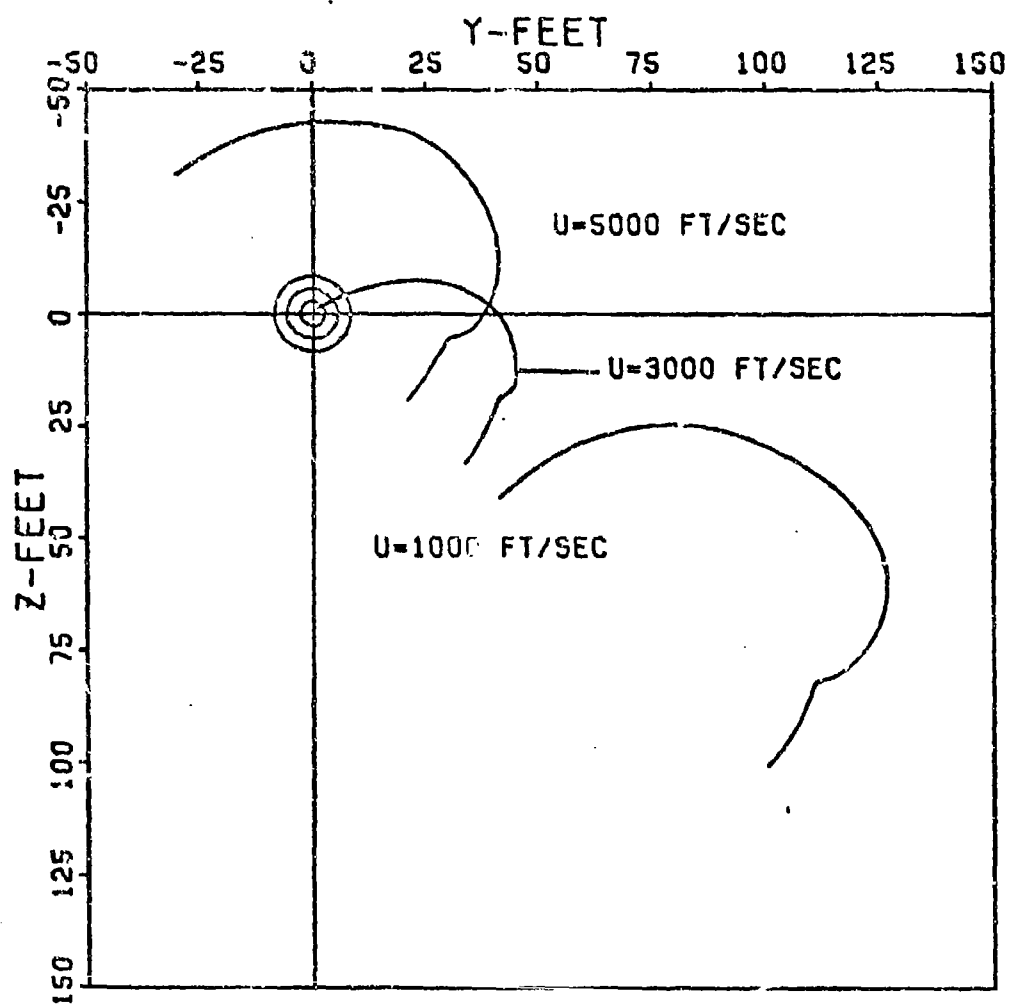


Figure 15. Dispersion: Phase III Theory, Cases 91-123

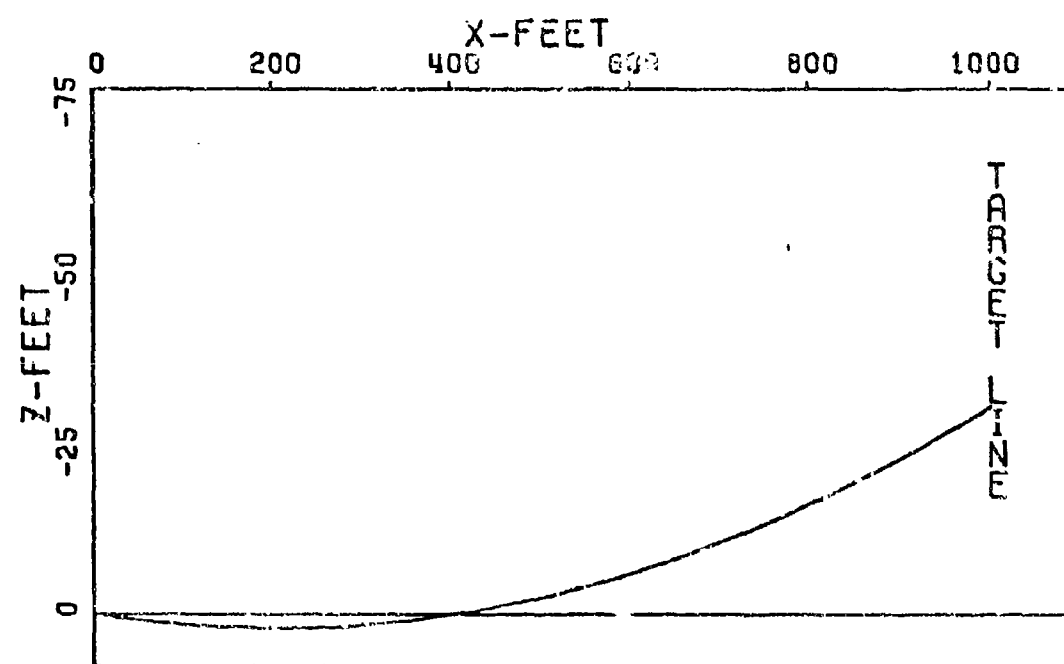
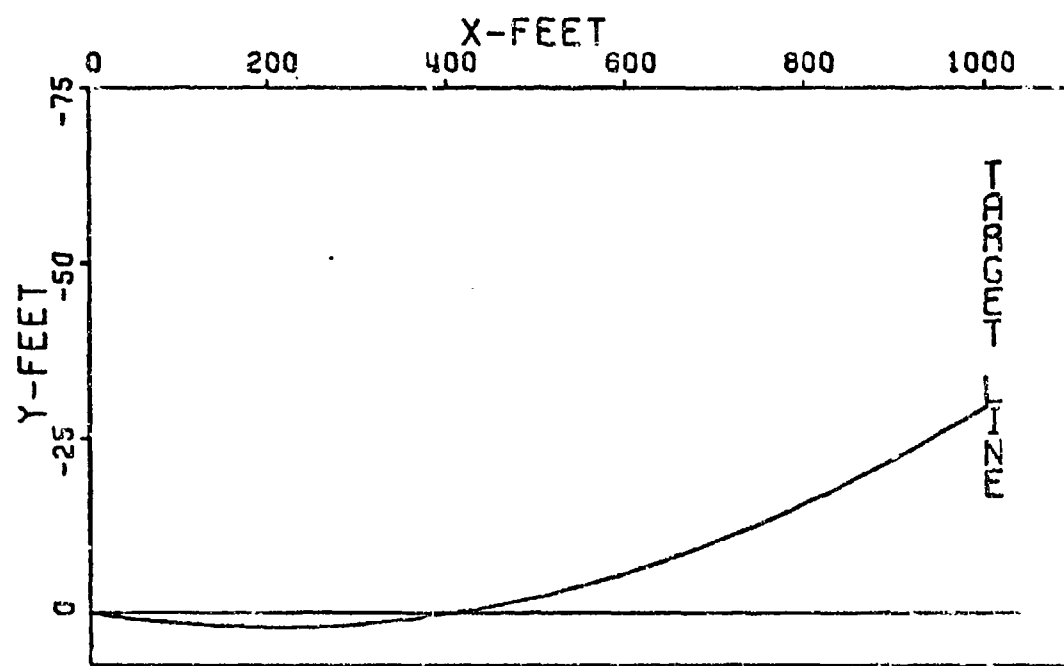


Figure 16. Trajectory, Case 101

$U = 3000$ ft/sec to be ones of smallest dispersion. Such was the case in Figure 10. Figure 16 illustrates a sample trajectory, Case 101.

Cases 124-156

To establish the relationship between the effects on dispersion for aerodynamic asymmetries and initial angle of attack, a third set of cases were run. Again roll rate and velocity were varied as done previously but $\vec{\alpha}_0$ was set at $(1+i)$ degrees with $\dot{\vec{S}}_0=0$ and $\dot{\vec{\alpha}}_0=0$. Tables XIII, XIV, and XV tabulate the results. For all high roll rate cases, Equation 24 reduces to:

$$\overline{J.A.} = \left[\frac{ipI_x}{mud} A\vec{\alpha}_0 + \frac{\rho u^2 d^2}{8m} \left[C_M \vec{\delta}_e \left(\frac{A}{p} \right) + C_Z \vec{\delta}_e \left(\frac{I_y - I_x}{mud} A + \frac{i}{p} \right) \right] \right] 1000$$

For low roll rate cases, Equation 28 reduces to:

$$\begin{aligned} \overline{J.A.} = & \frac{\rho u^2 \pi d^2}{8mx} \left[C_Z \vec{\delta}_e - i \left(\frac{C_Z \alpha}{C_M \alpha} \right) C_M \vec{\delta}_e \right] \left[\frac{1}{p^2} \left(1 - \cos \frac{px}{u} \right) \right. \\ & \left. + \frac{i}{p} \left(\frac{x}{u} - \frac{1}{p} \sin \frac{px}{u} \right) \right] 1000 \end{aligned}$$

For very low roll rates, Equation 30 reduces to:

$$\begin{aligned} \overline{J.A.} = & \frac{\rho v^2 d^2 x}{16m} \left[C_Z \vec{\delta}_e - i \left(\frac{C_Z \alpha}{C_M \alpha} \right) C_M \vec{\delta}_e \right] \left[\left(1 - \frac{1}{12} \left(\frac{px}{u} \right)^2 + \frac{1}{360} \left(\frac{px}{u} \right)^4 \right) \right. \\ & \left. + i \left(\frac{px}{3u} - \frac{1}{60} \left(\frac{px}{u} \right)^3 + \frac{1}{2520} \left(\frac{px}{u} \right)^5 \right) \right] 1000 \end{aligned}$$

Only for high roll rates does the $\vec{\alpha}_0$ term appear. $\vec{\alpha}_0$ should have no noticeable effect on dispersion for $p < 100$ rad/sec.

TABLE XIII
THEORY VALIDATION, ASYMMETRIES,
CASES 124-134

C A S E	Initial Conditions					Coefficients					$\overline{J.A.}$ (mils)		
	\vec{s}_o	$\vec{\alpha}_o$	$\vec{\dot{\alpha}}_o$	p_o	u_o	$C_{Z\alpha}$	C_{ZE}	C_{YE}	$C_{Z\beta}$	C_{ME}	C_{NE}	6-D	Theory
						$C_{M\alpha}$	$C_{M\beta}$					6-D	Theory
124				31416								0.028+	0.009-
												0.052i	0.013i
125				18850								0.052+	0.013-
												0.029i	0.009i
126				6283								0.094-	0.078-
												0.080i	0.073i
127				500								1.040-	1.013-
												0.954i	1.009i
128				300								1.660-	1.688-
												1.680i	1.683i
129	0	1+i	0	100	5000	A1	A1	A1	A1	A1	A1	4.628-	4.675-
												4.868i	4.975i
130				50								8.732-	8.780-
												12.279i	12.489i
131				25								20.784-	21.150-
												26.468i	26.927i
132				10								-7.954-	-8.210-
												62.367i	63.210i
133				5								-29.912	-30.372
												-61.629i	-62.353i
134				0								-49.828	-50.427
												-49.840i	-50.427i

TABLE XIV
THEORY VALIDATION, ASYMMETRIES,
CASES 135-145

C A S E	Initial Conditions					Coefficients			$\vec{J.A.}$ (mils)	
	\dot{s}_o	$\dot{\alpha}_o$	$\dot{\dot{\alpha}}_o$	p_o	u_o	$C_{Z\alpha}$	C_{YE}	C_{ZE}	6-D	Theory
135				31416					Unstable	
136				18850					0.035+	-0.003
137				6283					0.046i	+0.008i
138				500					0.066+	0.029-
139				300					0.017i	0.024i
140	0	!+i	0	100	3000	A1	A1	A1	1.879-	1.994-
141				50					1.958i	1.989i
142				25					3.819-	3.411-
143				10					4.473i	4.164i
144				.5					5.714-	5.721-
145				0					8.416i	8.516i
									9.247-	9.217-
									32.586i	32.897i
									-9.985-	-10.174
									41.948i	-42.273i
									-32.973	-33.194
									-32.981i	-33.194i

TABLE XV
THEORY VALIDATION, ASYMMETRIES,
CASES 146-156

C A S E	Initial Conditions					Coefficients					$\overline{J}.$ A. (mils)	
						$C_{Z\alpha}$	$C_{M\alpha}$	$C_Z p\beta$	C_{YE}			
	$C_{Mq} + C_{M\alpha}$	$C_M p\beta$	C_{ZE}	C_{ME}	C_{NE}	6-D	Theory					
146				31416								Unstable
147				18850								Unstable
148				6283								0.046+ 0.039i
149				500								0.275- 0.188i
150				300								0.432- 0.342i
151	0	1+i	0	100	1000	A1	A1	A1				1.213- 1.123i
152				50								2.381- 2.294i
153				25								4.719- 4.637i
154				10								10.258- 14.411i
155				5								24.440- 30.976i
156				0								-58.669 -58.684i
												-58.450 -58.450i

Comparing Cases 124, 125, 126 in Table XIII with Cases 19, 20, 21 in Table III and Cases 58, 59, 60 in Table VII it can be concluded that Cases 124, 125 and 126 are the algebraic sum of Cases 19, 20, 21 and 58, 59, 60; that is, for example, Case 124 equals Case 19 plus Case 58. This is obvious from the reduced theoretical equations for Cases 124-156. It is shown here to be also true for the 6-D computations; allowing for some computational error. Similar comparisons can be made with corresponding cases in Tables III, VIII, XIV and III, IX, XV. Thus the effects of aerodynamic asymmetries and those of initial angle of attack are independent of one another.

Figures 17, 18 and 19 illustrate Cases 124-156. The curves are very similar to those in Figures 7, 8, and 9 with the only difference being the very small $\vec{\alpha}_0$ contribution in Figures 17, 18, and 19. Cases 135, 146, and 147 result in instabilities, indicating that maximum effect of the various parameters has been accomplished. Effects of roll rate are essentially the same as in Case 58-90 and effects of velocity, Figure 20, the same as in Figure 10. Cases with $U = 3000$ ft/sec again have the smallest dispersion. Figure 21 shows a typical trajectory, Case 134.

Cases 157-189

To validate the relationship between the effects on dispersion for aerodynamic asymmetries and those of initial angular rate, a fourth set of cases were run. As before, roll rate and velocity were varied, but $\vec{\dot{\alpha}}_0$ set at $(250 + 250i)$ rad/sec with $\vec{S}_0 = 0$ and $\vec{\alpha}_0 = 0$. Tables XVI, XVII,

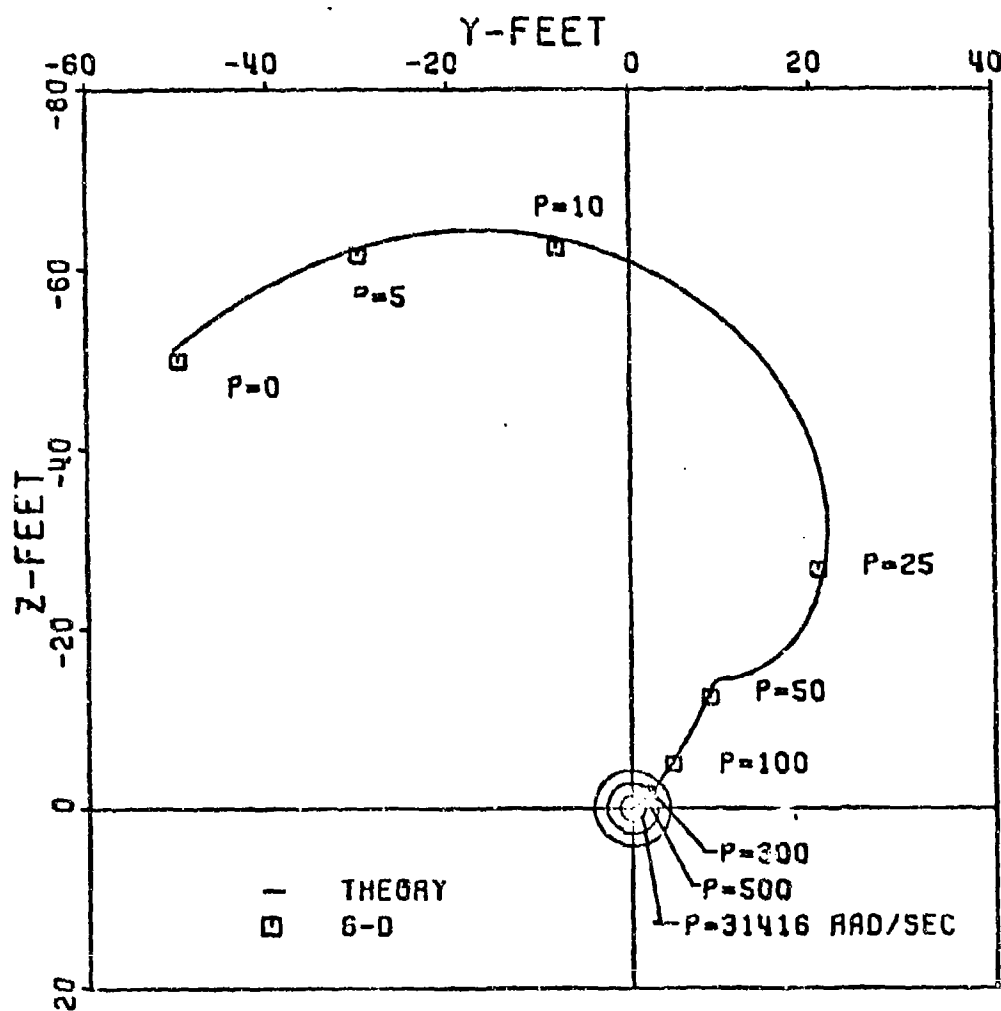


Figure 17. Dispersion: Phase III Cases 124-134

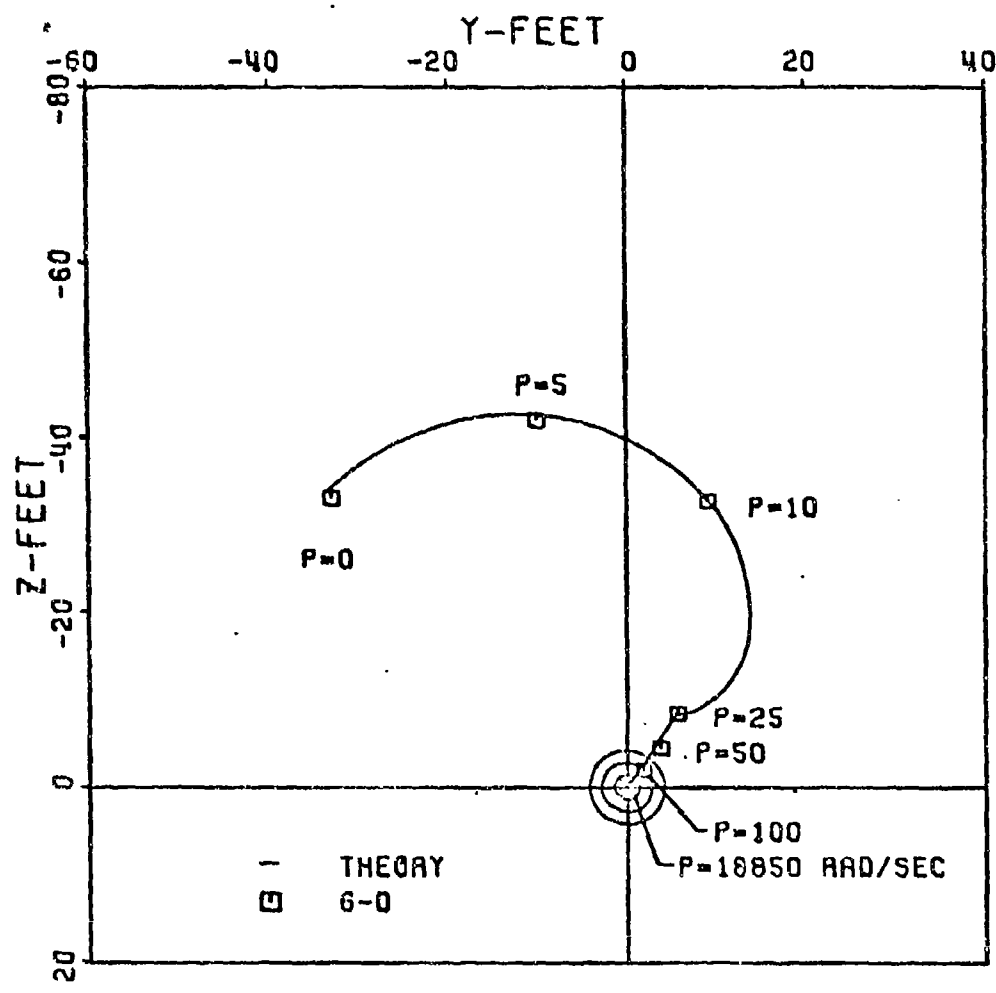


Figure 18. Dispersion: Phase III Cases 135-145

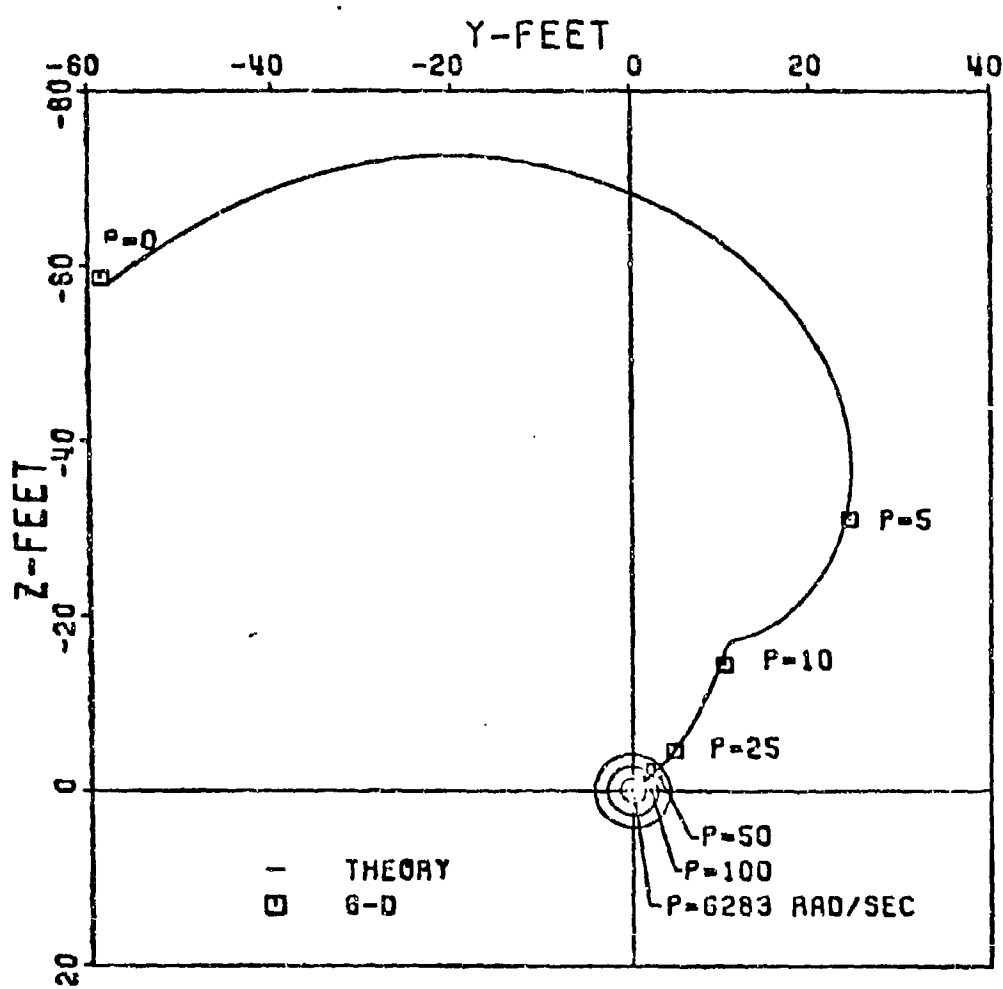


Figure 19. Dispersion: Phase III Cases 146-156

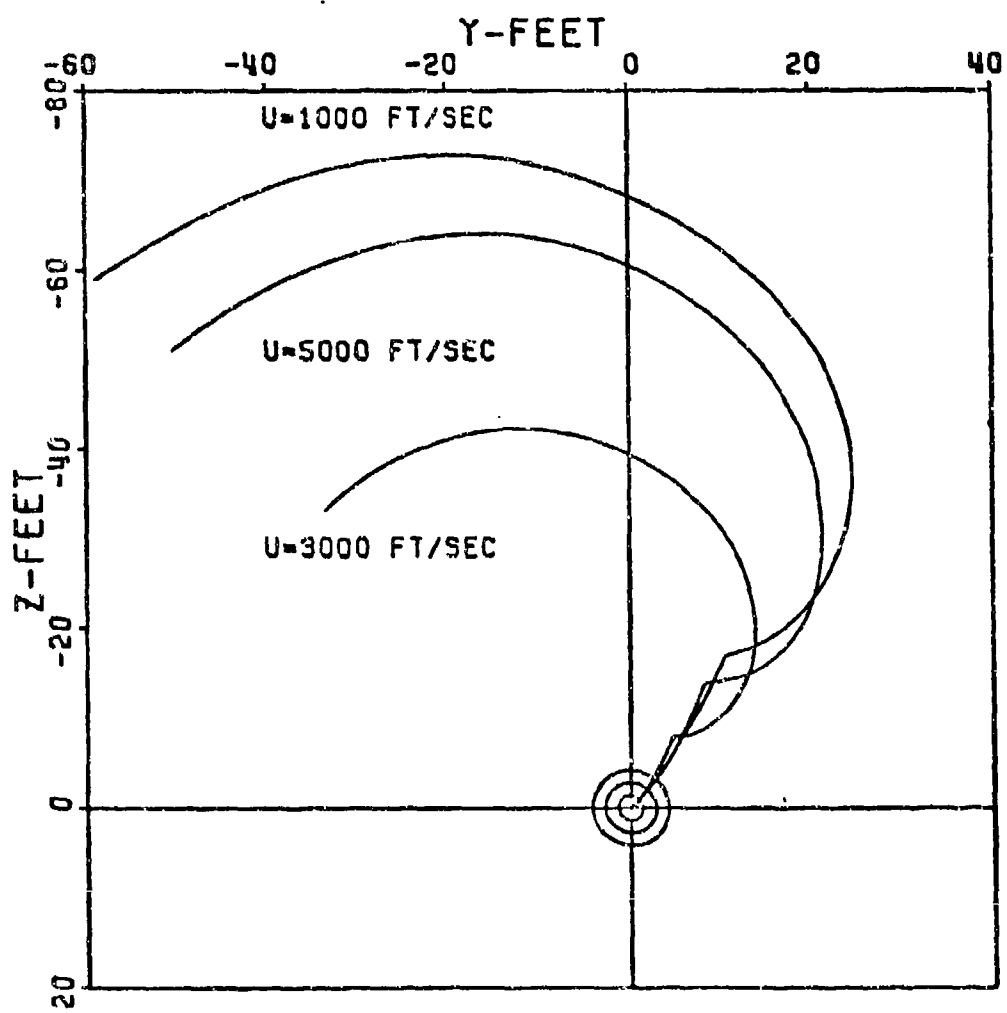


Figure 20. Dispersion: Phase III Theory, Cases 124-156

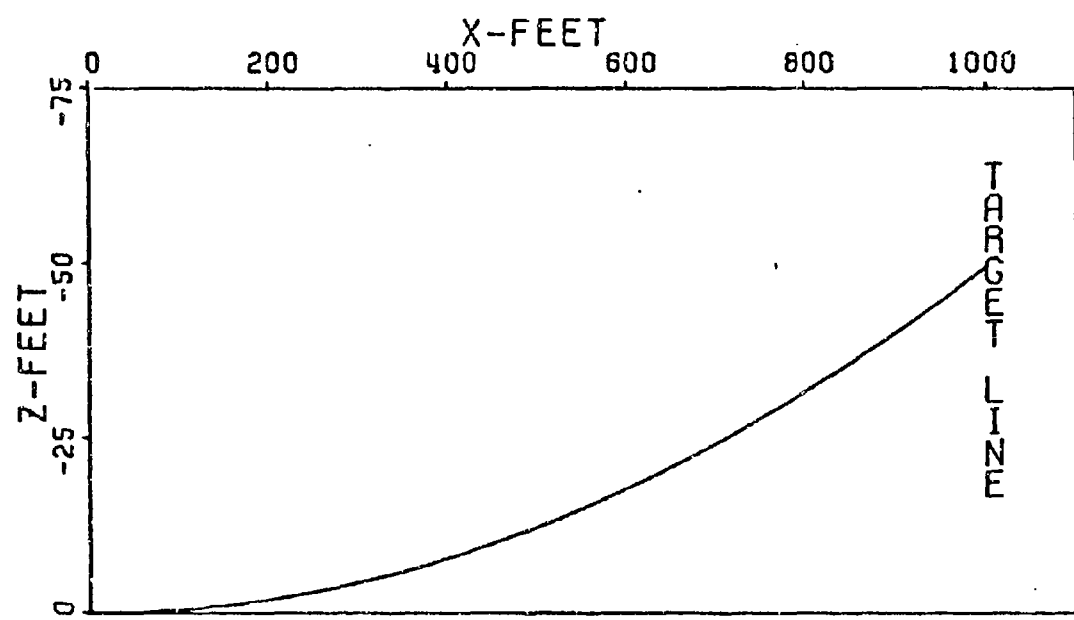
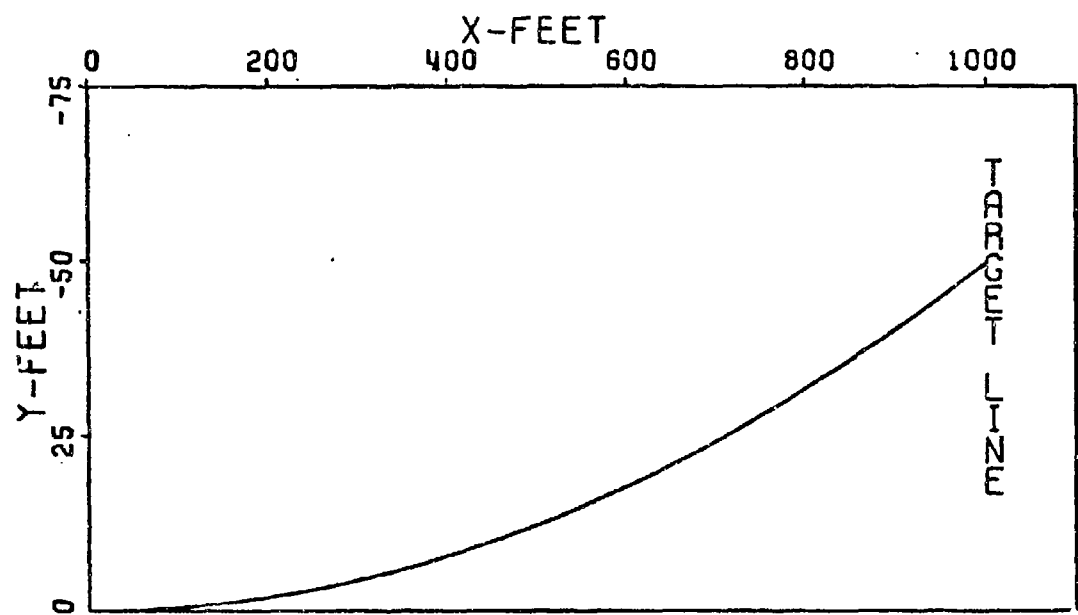


Figure 21. Trajectory, Case 134

XVIII gives the results. For high roll rates, the governing equation becomes:

$$\vec{J} \cdot \vec{\Lambda} = \left[\frac{\rho u \pi d^2}{8m} \left[C_{M_{\delta_e}} \vec{\delta}_e \left(\frac{\Lambda}{p} \right) + C_{Z_{\delta_e}} \vec{\delta}_e \left(\frac{I_y - I_x}{mud} \Lambda + \frac{i}{p} \right) \right] - \frac{I_y}{mud} \Lambda \vec{\alpha}_o \right] 1000$$

For low roll rates, the governing equation:

$$\begin{aligned} \vec{J} \cdot \vec{\Lambda} = & \left[\frac{\rho u^2 \pi d^2}{8 mx} \left[C_{Z_{\delta_e}} \vec{\delta}_e - i \left(\frac{C_Z \alpha}{C_M \alpha} \right) C_{M_{\delta_e}} \vec{\delta}_e \right] \left[\left(1 - \cos \frac{px}{u} \right) \right. \right. \\ & \left. \left. + \frac{i}{p} \left(\frac{x}{u} - \frac{1}{p} \sin \frac{px}{u} \right) \right] - \frac{I_y}{mud} \left(\frac{C_Z \alpha}{C_M \alpha} \right) \vec{\alpha}_o \right] 1000 \end{aligned}$$

For very slow roll, the governing equation:

$$\begin{aligned} \vec{J} \cdot \vec{\Lambda} = & \left[\frac{\rho \pi d^2 x}{16m} \left[C_{Z_{\delta_e}} \vec{\delta}_e - i \left(\frac{C_Z \alpha}{C_M \alpha} \right) C_{M_{\delta_e}} \vec{\delta}_e \right] \left[\left(1 - \frac{1}{12} \left(\frac{px}{u} \right)^2 + \frac{1}{360} \left(\frac{px}{u} \right)^4 \right) \right. \right. \\ & \left. \left. + i \left(\frac{px}{3u} - \frac{1}{60} \left(\frac{px}{u} \right)^3 + \frac{1}{2520} \left(\frac{px}{u} \right)^5 \right) \right] - \frac{I_y}{mud} \left(\frac{C_Z \alpha}{C_M \alpha} \right) \vec{\alpha}_o \right] 1000 \end{aligned}$$

Comparing Cases 157, 158, 159 in Table XVI with Cases 28, 29, 30 in Table IV and Cases 58, 59, 60 in Table VII, it can be concluded that Cases 157, 158, and 159 are the algebraic sum of Cases 28, 29, 30 and 58, 59, 60; that is, for example, Case 157 equals Case 28 plus Case 58. This is obvious from the reduced theoretical equations for Cases 157-189. Here it is shown to be true for 6-D computations also. Any discrepancy can be attributed to computational error. Similar comparisons can be made with corresponding cases in Table IV, VIII, and XVII. Thus the effects of aerodynamic asymmetries and those of initial angular rate are independent of one another.

TABLE XVI
THEORY VALIDATION, ASYMMETRIES,
CASES 157-167

C A S E	Initial Conditions					Coefficients					\vec{J}_A (mils)	
						$C_{Z\alpha}$	$C_{M\alpha}$	$C_{Zp\beta}$	C_{YE}	C_{ZE}		
	\dot{S}_O	$\vec{\alpha}_O$	$\vec{\dot{\alpha}}_O$	p_O	u_O	$C_{Mq} + C_{M\dot{\alpha}}$	$C_{Mp\beta}$	C_{ZE}	C_{ME}	C_{NE}	6-D	Theory
157				31416							-1.799	-2.055
											-2.236i	-2.087i
158				18850							-1.873	-2.044
											-2.169i	-2.098i
159				6283							-1.924	-1.990
											-2.190i	-2.151i
160				500							-1.049	-1.060
											-3.000i	-3.082i
161				300							-0.419	-0.385
											-3.716i	-3.756i
162	0	0	250+ 250i	100	5000	A1	A1	A1			2.457-	2.602-
											6.836i	7.048i
163				50							6.576-	6.707-
											14.075i	14.562i
164				25							18.366-	19.077-
											27.827i	29.000i
165				10							-9.690-	-10.283
											63.387	-65.283i
166				5							-31.387	-32.445
											-62.730i	-64.426i
167				0							-51.094	-52.500
											-51.094i	-52.500i

TABLE XVII
THEORY VALIDATION, ASYMMETRIES,
CASES 168-178

C A S E	Initial Conditions					Coefficients				J.A. (mils)	
						$C_{Z\alpha}$	$C_{M\alpha}$	$C_{Zp\beta}$	C_{YE}		
	\dot{S}_0	$\dot{\alpha}_0$	$\dot{\alpha}_0$	p_0	u_0	$C_{Mq} + C_{M\dot{\alpha}}$	$C_{Mp\beta}$	C_{ZE}	C_{ME}	6-D	Theory
168				31415						Unstable	
169				18850						-1.755	-1.957
170				6283						-2.154i	-1.978i
171				500						-1.866	-1.936
172				300						-2.054i	-1.999i
173	0	0	250+ 250i	100	3000	A1	A1	A1		-1.572	-1.569
174				50						-2.351i	-2.366i
175				25						-1.308	-1.304
176				10						-2.595i	-2.632i
177				5						-0.114	-0.024
178				0						-3.912i	-3.959i
										1.873-	1.441-
										6.399i	6.134i
										3.755-	3.751-
										10.393i	10.486i
										7.435-	7.247-
										34.530i	34.867i
										-11.870	-12.144
										-44.054i	-44.243i
										-35.054	-35.164
										-35.053i	-35.164i

TABLE XVIII
THEORY VALIDATION, ASYMMETRIES,
CASES 179-189

C, A S E	Initial Conditions					Coefficients					$\vec{J}.$ A. (mils)		
	s_o	$\dot{\alpha}_o$	$\ddot{\alpha}_o$	p_o	u_o	$C_{M_q} + C_{M\dot{\alpha}}$	$C_Z \alpha$	$C_Z p\beta$	C_{YE}	C_{ZE}	C_{ME}	C_{NE}	6-D
179				31416									Unstable
180				18850									Unstable
181				6283									Unstable
182				500									-5.015 -5.503i
183				300									-4.884 -5.572i
184	0	0	250+ 250i	100	1000	A1	A1	A1					-4.208 -6.135i
185				50									-3.056 -7.031i
186				25									-0.741 -9.079i
187				10									5.244- 18.344i
188				5									18.563- 33.158i
189				0									-61.894 -61.894i
													-63.990 -63.990i

Figures 22, 23 and 24 illustrate Cases 157-189. The curves are similar to those in Figures 7, 8 and 9 but are displaced by the $\vec{\alpha}_0$ contribution. Cases 168, 179, 180 and 181 indicate that maximum effects of the various parameters has been achieved in other stable cases. The effects of roll rate and velocity follow the same trends as those in Cases 58-60. Figure 25 shows the effects of velocity for Cases 157-189. Cases with $U = 3000$ ft/sec exhibit the smallest dispersion. A sample trajectory, Case 189, is shown in Figure 26.

Comparison: High, Low, Very Slow

Roll Rate Theories

In Cases 58-189 the High, Low, and Very Slow Roll Rate Theories are validated for various initial conditions and parameters. The theories have been applied for certain ranges in roll rate and roll rate times time (pt) The range of pt , ($pt \leq 1.0$) are governed by the inherent requirements of power series expansion. However, the ranges of p are arbitrary (to a certain extent) and are based on accuracy of the theories themselves. Each theory approximates the solution very well for a certain range of p and then begins to diverge and become inaccurate. The range of p for which the very slow roll rate theory is accurate is fairly well cut and dried; $p \geq 0$, $pt \leq 1.0$. For any $pt > 1.0$ we must now use the low roll rate theory. The question now arises, how high a roll rate can this theory accommodate? At what value of p must we change to the high roll rate theory? These questions are answered by a plot of sample 6-D computations, Figure 27

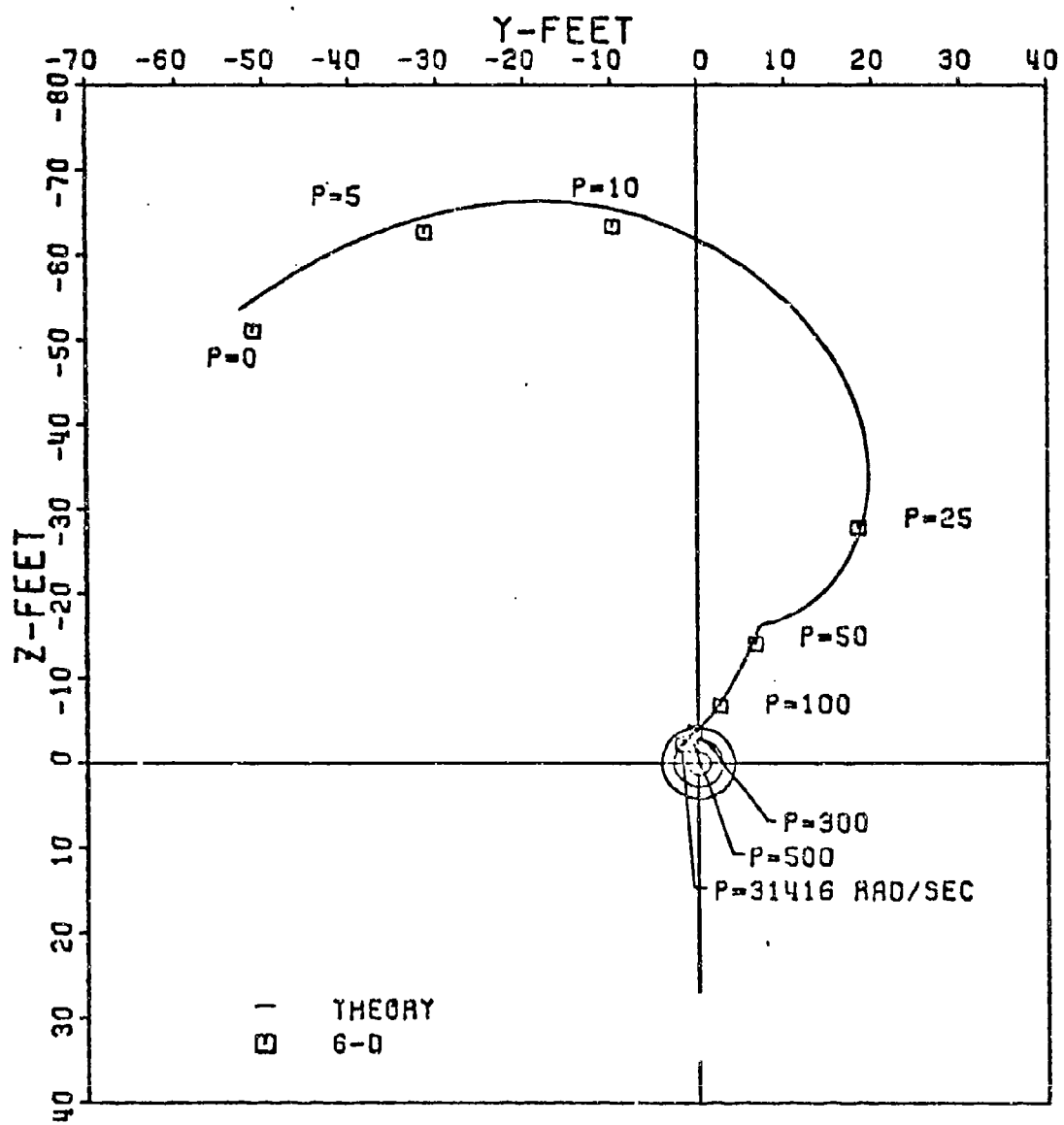


Figure 22. Dispersion: Phase III Cases 157-167

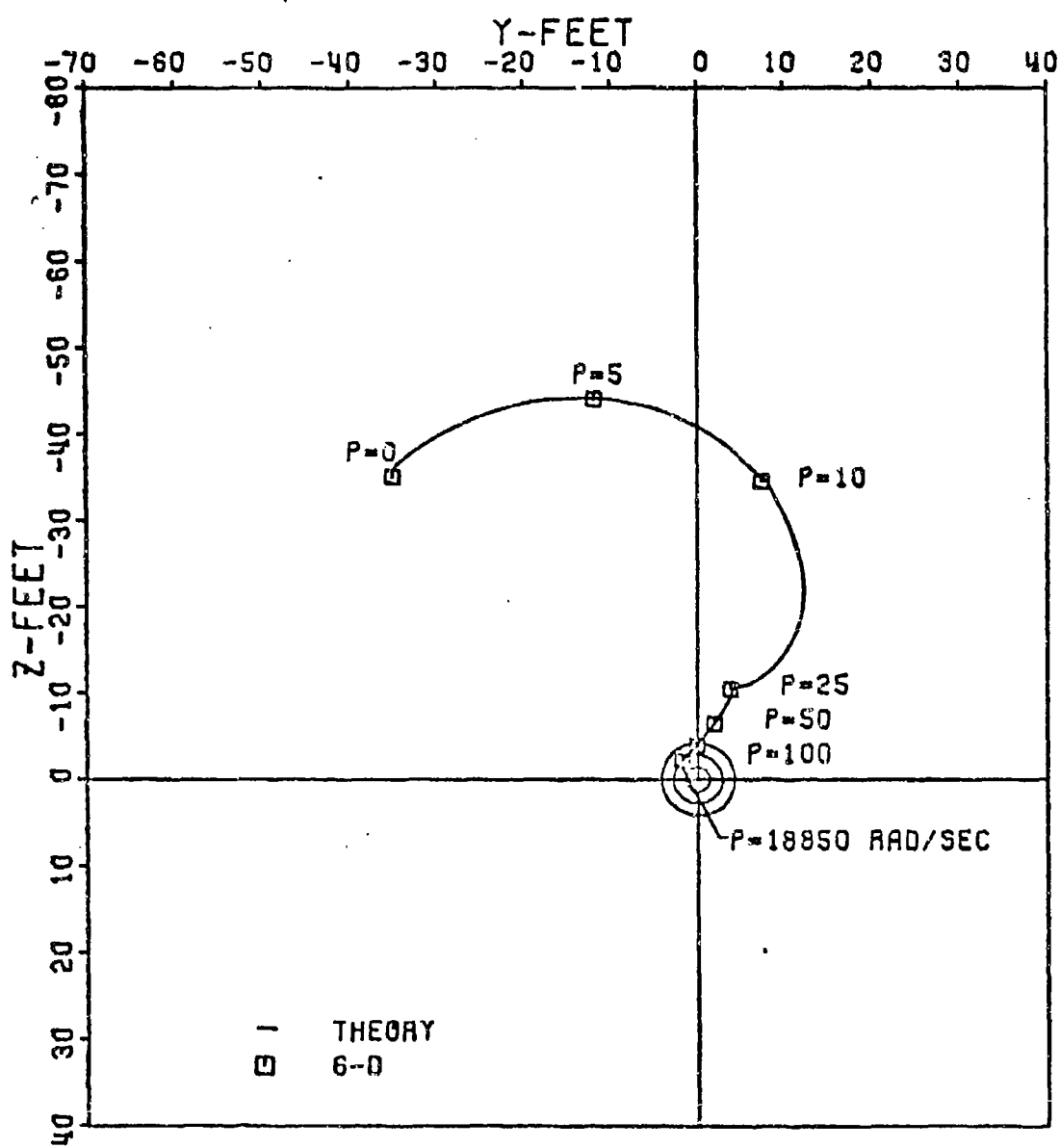


Figure 23. Dispersion: Phase III Cases 168-178

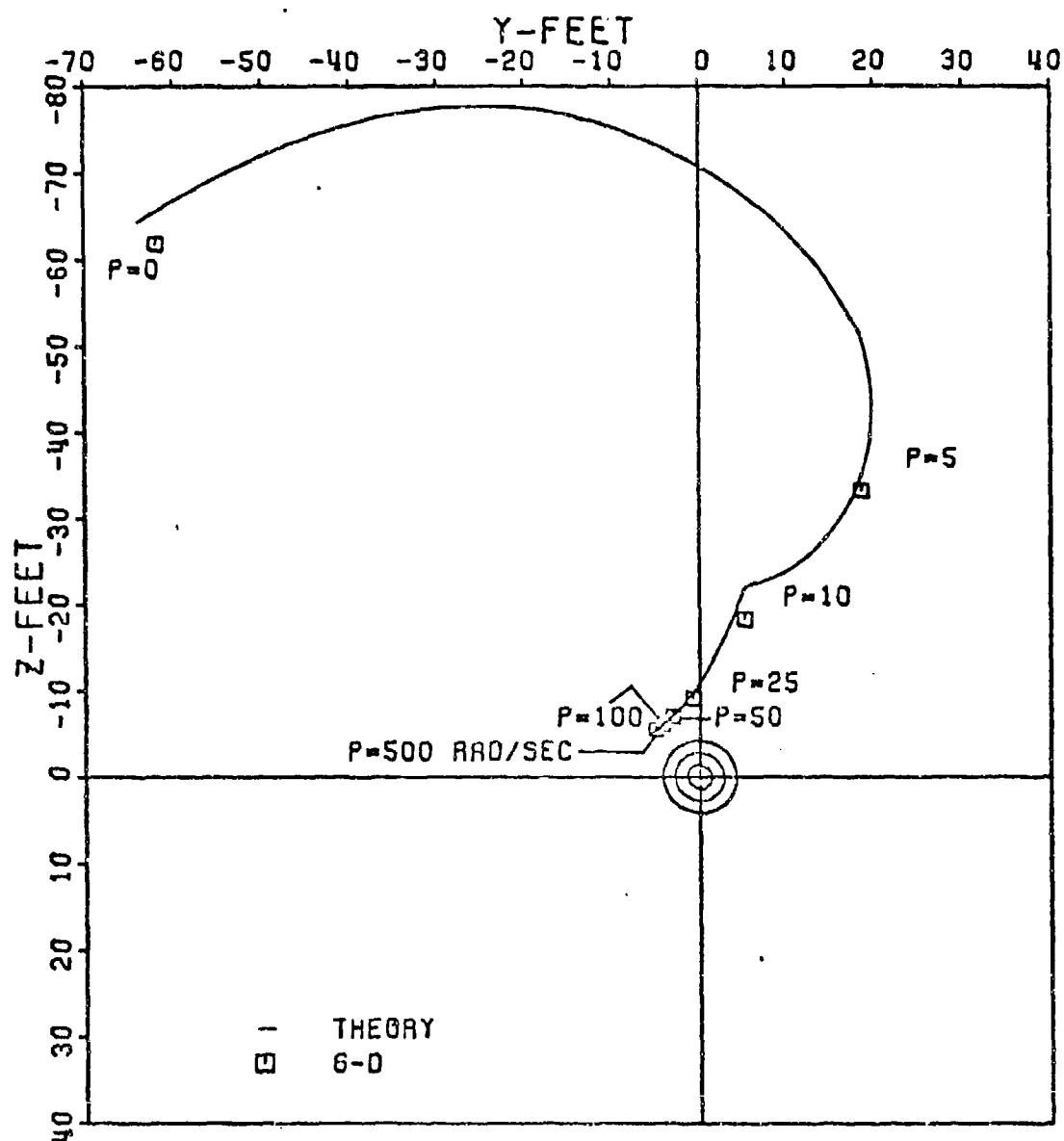


Figure 24. Dispersion: Phase III Cases 179-189

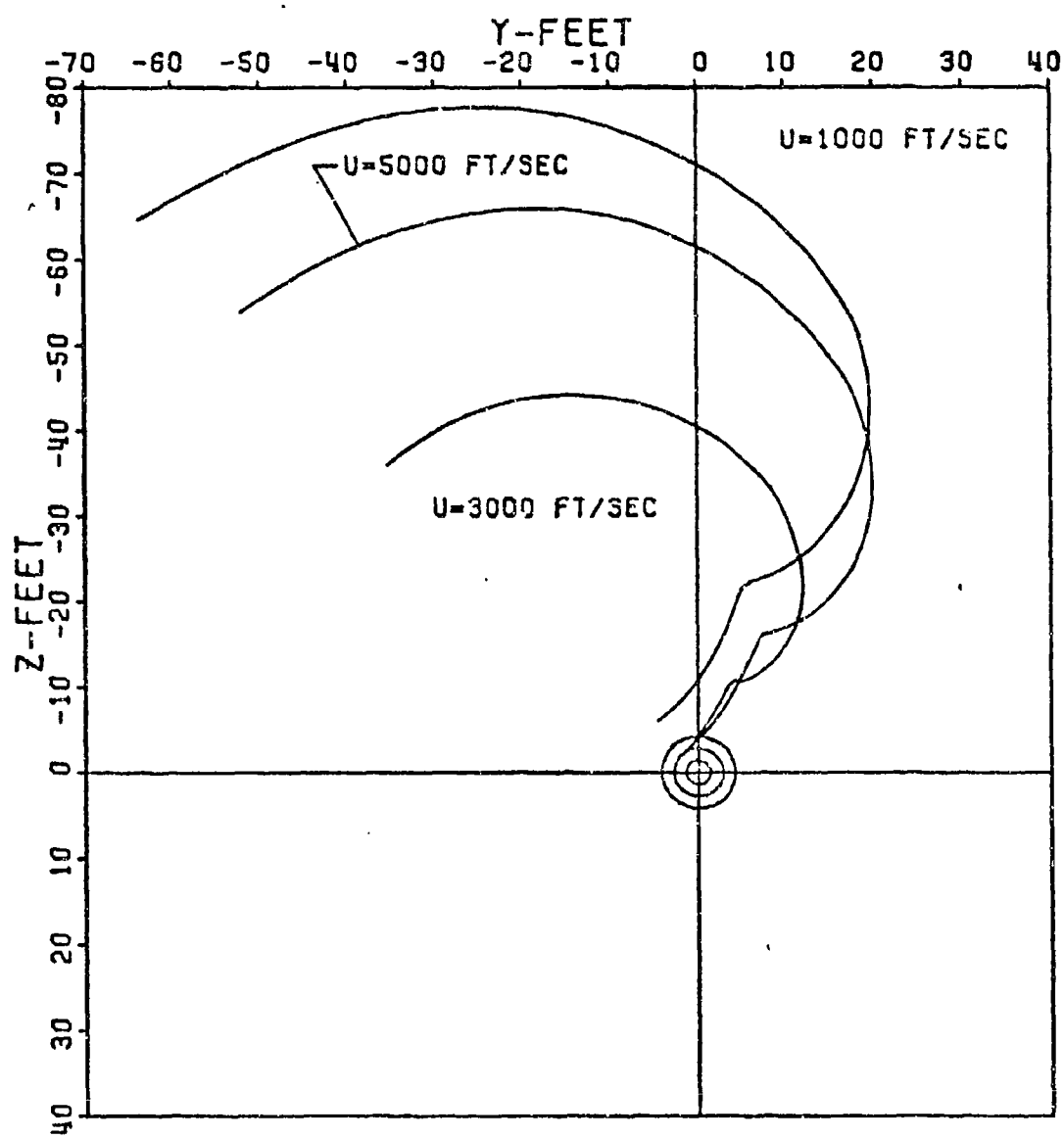


Figure 25. Dispersion: Phase III Theory, Cases 157-189

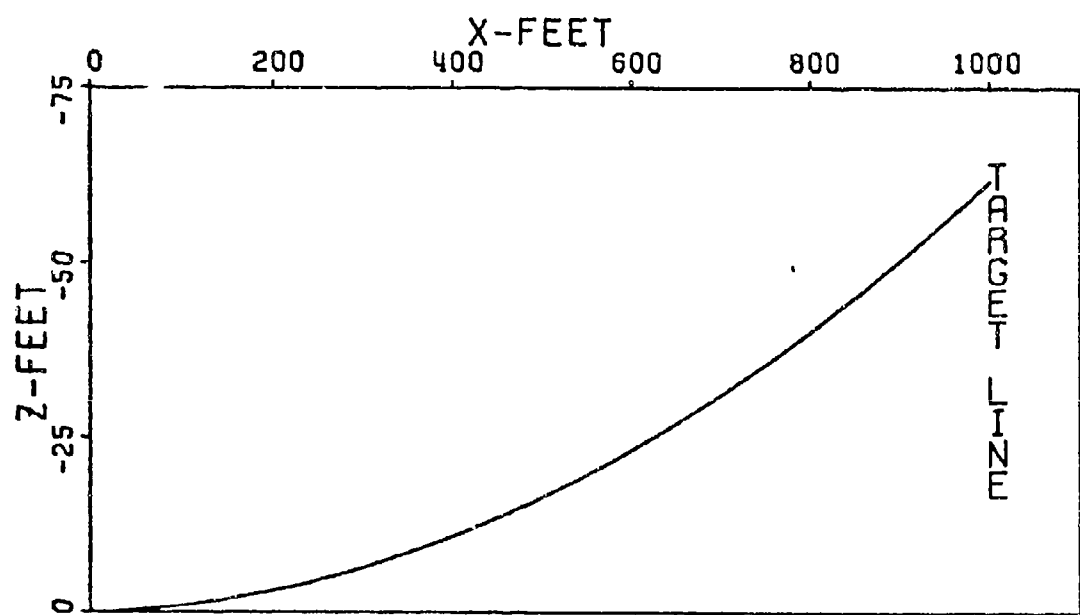
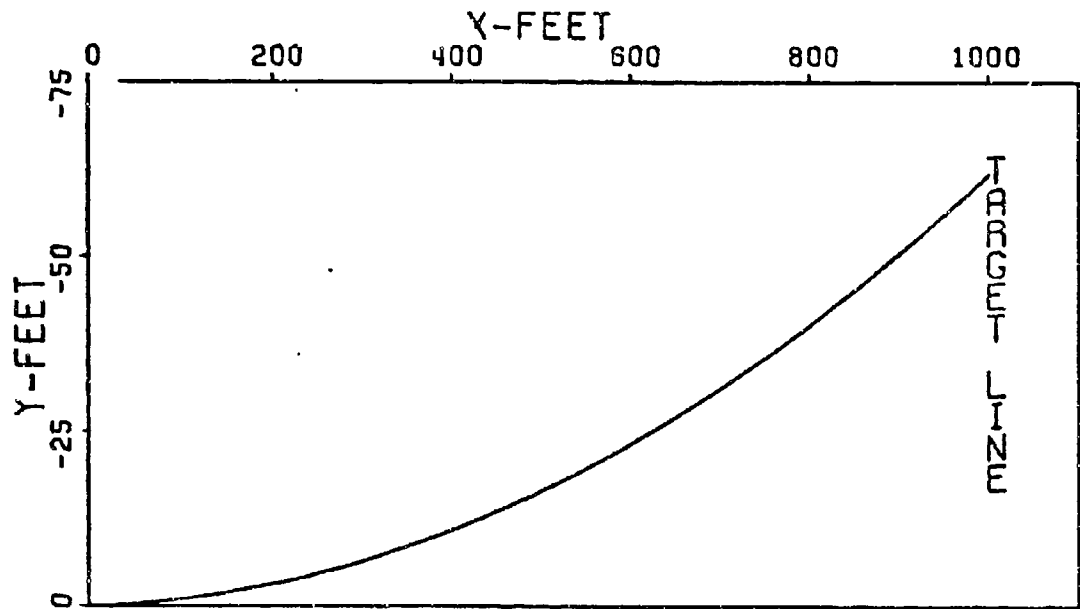


Figure 26. Trajectory, Case 189

and all three theories extended beyond the limits used in the previous validation. The high roll rate theory is a straight line going off to infinity as p goes to zero. Although the length of the curve in which it is an effective theory is short graphically, the range of roll rates it encompasses is tremendous. Figure 28 illustrates the effective limits of each theory; that is, on the spectrum of possible roll rates it shows where each theory is the most effective. The low roll rate theory handles the largest graphical area but only roll rates less than 100 rad/sec and greater than 5 rad/sec. The upper limit of 100 rad/sec was chosen since here the low roll theory attaches itself to the 6-D results while the high roll theory diverges. The lower limit of 5 rad/sec corresponds to $pt \leq 1.0$. Figures 27 and 28 depict Cases 58-68 where $u_0 = 5000$ ft/sec or $t = 0.2$ sec. Therefore $p = 5$ rad/sec corresponds to $pt = 1.0$. The very low roll rate theory has the smallest range but is essential in predicting dispersion as the roll rate goes to zero. As $pt > 1$, the theory diverges as would be expected from a power series; Equation 29. The sharp turn occurs at $p \approx 20$ rad/sec or $pt \approx 4$ for Cases 58-68. Although Cases 58-68 were illustrated here, this analysis of the effective limits of the roll theories was found to be similar for all other cases. For the $u_0 = 3000$ ft/sec cases the low roll theory limits were $3.0 < p < 50$ for $u_0 = 1000$ ft/sec cases: $1.0 < p < 25.0$.

Phase IV

To validate the effects of gravity on dispersion, a final set of cases were run using the high roll rate theory, Equation 24. Ordinarily, one would think that gravity would only introduce a constant term; one

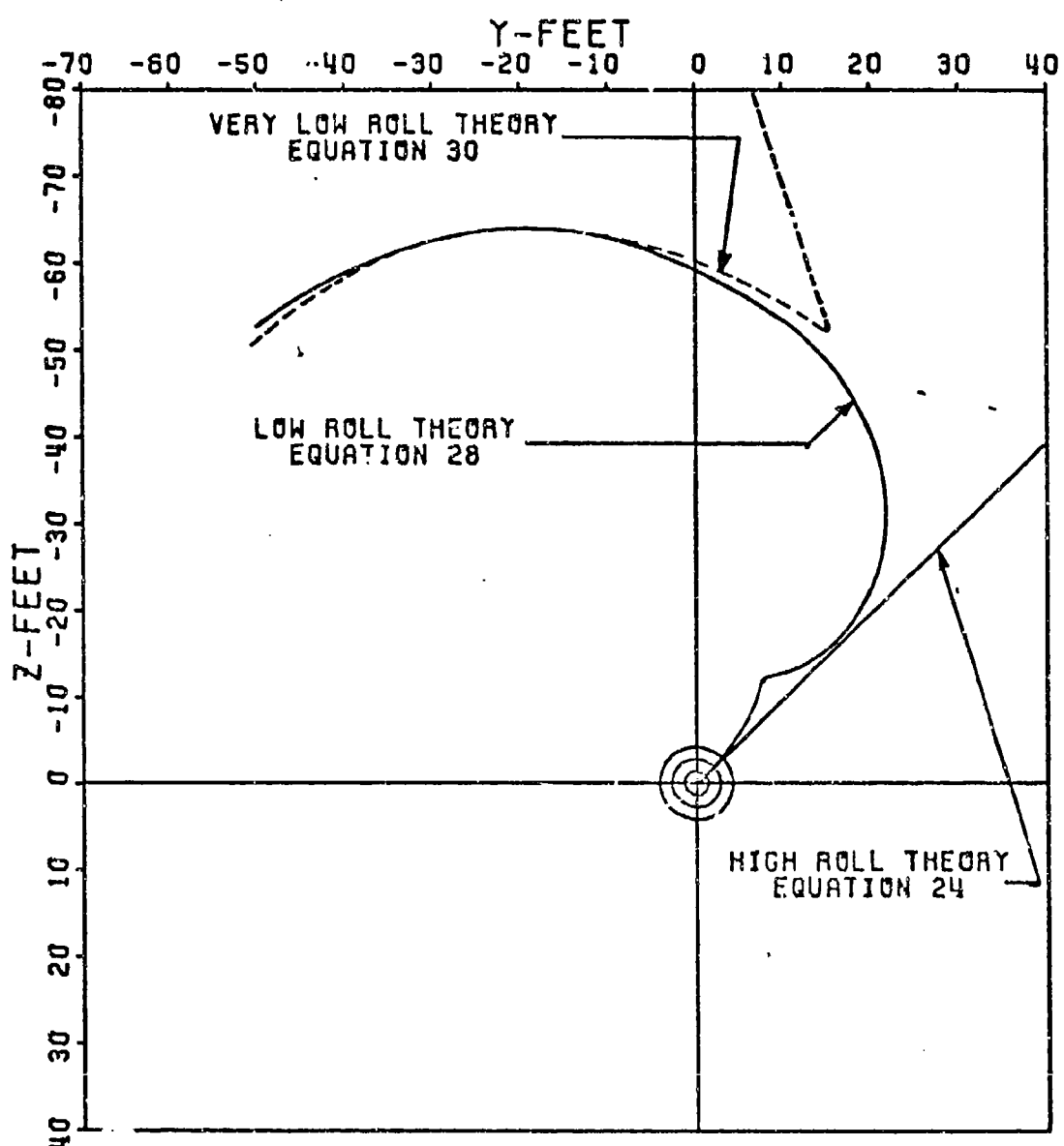


Figure 27. Phase III Theory Equations 24, 28, 30

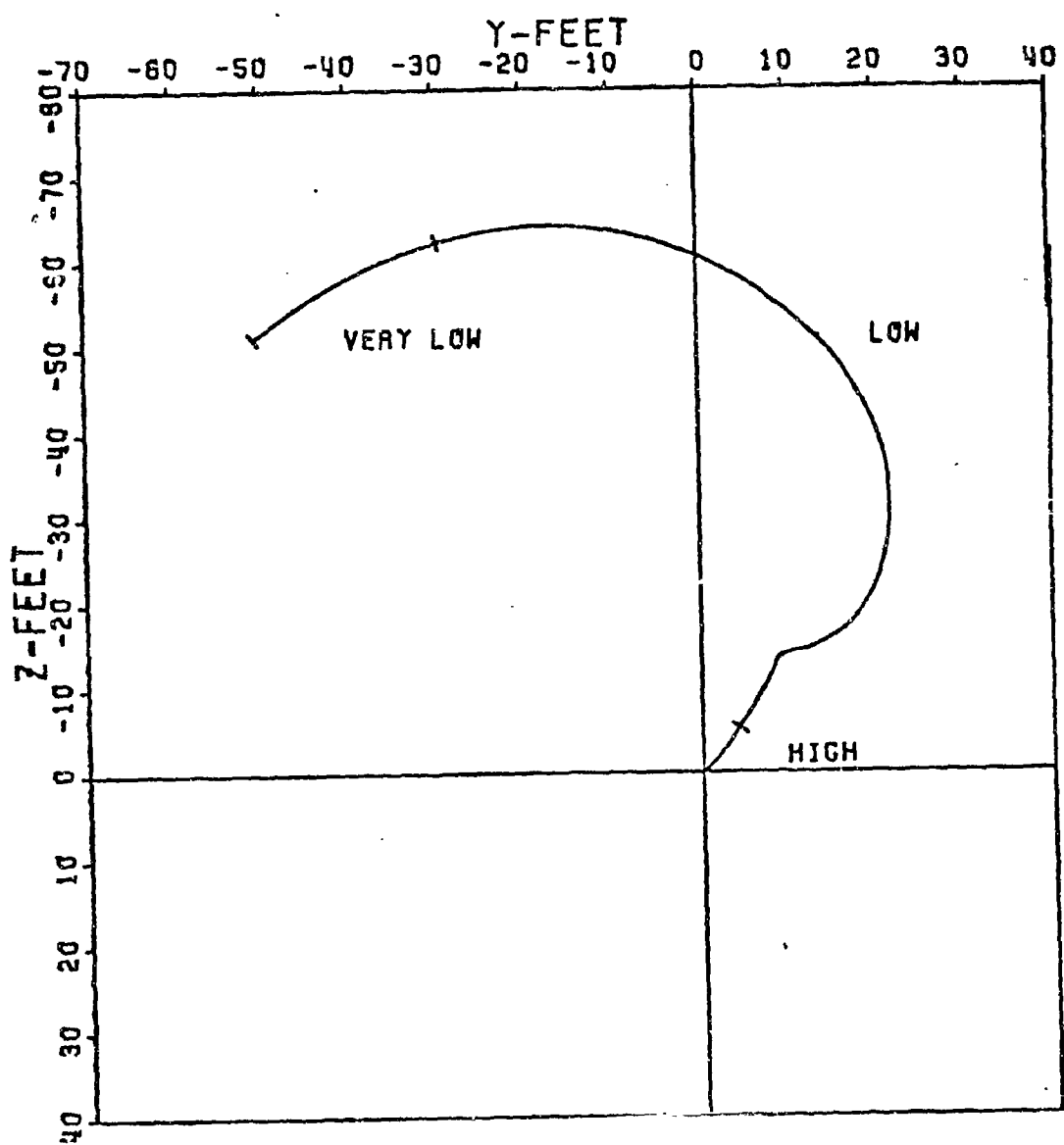


Figure 28. Phase III Theory Effective Limits

that could be factored out. However integration of the equations of motion produce a gravity term dependent upon roll rate. Determination of its validity and consequence is what is important here. \vec{S}_o , $\vec{\alpha}_o$, and $\dot{\vec{\alpha}}_o$ were set to zero in order to allow determination of the effects due to roll rate and velocity. The reduced governing equation becomes:

$$\overline{J.A.} = \frac{ig}{2} \left(\frac{x}{u^2} \right) \left[1 + \frac{ipl_x}{mud} A \right] 1000$$

No aerodynamic asymmetries were present and the effects of gravity were assumed independent of effects due to \vec{S}_o , $\vec{\alpha}_o$, $\dot{\vec{\alpha}}_o$; a logical assumption.

Table XIX lists the results.

Table XIX indicates that the effects due to gravity occur largely in the vertical plane, as would be expected. The transverse contribution is minimal but is affected by both velocity and roll rate. The vertical contribution is only affected by velocity. The unstable cases indicate maximum use of Magnus and thus maximum transverse effects on dispersion. It can be concluded from this brief but thorough treatment that gravity effects dispersion only in the vertical plane (for all practical purposes) and that its contribution is constant with velocity. The roll dependent term, $\frac{ipl_x}{mud} A$, has been shown to exist but become negligible for the flechette. This term would possibly become important for projectile dispersion and other missile applications. Projectile motion with gravity is typified by a cocking right of the projectile in flight with a positive $C_{M\alpha}$ but negative $C_{Z\alpha}$; the parameter A would become negative and the entire roll dependent term, positive; that is, cocked to the right, dispersion to

TABLE XIX
THEORY VALIDATION, GRAVITY
CASES 190-201

C A S E	Initial Conditions					Coefficients					J. A. (mils)	
						$C_{Z\alpha}$	$C_{M\alpha}$	$C_{Zp\beta}$	C_{YE}	C_{ZE}		
						$C_{Mq} + C_M \dot{\alpha}$	$C_{Mp\beta}$	C_{ME}	C_{NE}	6-D	Theory	
190	↑	↑	↑	↑	31416					-0.001 +0.644i	-0.001 +0.644i	
191					18850	5000				-0.001 +0.644i	-0.001 +0.644i	
192					6283					-0.001 +0.644i	-0.001 +0.644i	
193					0					0.000 +0.644i	0.000 +0.644i	
194					31416					-0.002 +1.788i	-0.003 +1.789i	
195	0	0	0		18850	3000	A1	A1	0	-0.001 +1.789i	-0.002 +1.789i	
196					6283					0.000 +1.788i	-0.001 +1.789i	
197					0					0.000 +1.788i	0.000 +1.789i	
198					31416					Unstable		
199					18850	1000				Unstable		
200					6283					0.001+ 16.100i	0.001+ 16.100i	
201					0					0.000+ 16.100i	0.000+ 16.100i	

the right. For a finned missile the opposite would occur due to the agreement in sign between $C_{M\alpha}$ and $C_{z\alpha}$.

FREE FLIGHT DATA ANALYSIS

In order to analyze actual test firings as to jump and dispersion and correlate them with the validated theory, the initial conditions of each test firing must be obtained and put into the proper form. To obtain raw experimental data, test firings were conducted by the U.S. Army, Frankford Arsenal. The configuration tested was the Producibility Ground Point Flechette, Figure 29. The raw data required was both translational and angular; that is, data was needed to determine position as a function of time and angle of attack of the flechette as a function of time. To accomplish this, Frankford Arsenal devised the test apparatus shown in Figure 30. The gun barrel was mounted on a steel girder and a laser beam was used to obtain the aim point on a target 50 meters down range. At positions, 1, 3, 5, 7, 9, and 11 feet downrange, orthogonal flash x-ray tubes were placed to photograph the flechette as it passed its station. One tube was placed to allow a top view at each station and provide a means of obtaining swerve and yaw data. The other tube allowed a side view at each station to obtain heave and pitch data. At each station reference marks oriented the flechette as to its exact position downrange. This was to allow for any timing error and/or variation in muzzle velocity. The photographs were taken using special soft flash x-ray tubes which permit the photographing of the low density sabot pieces and analyzing the separation in addition to the motion of the flechette.

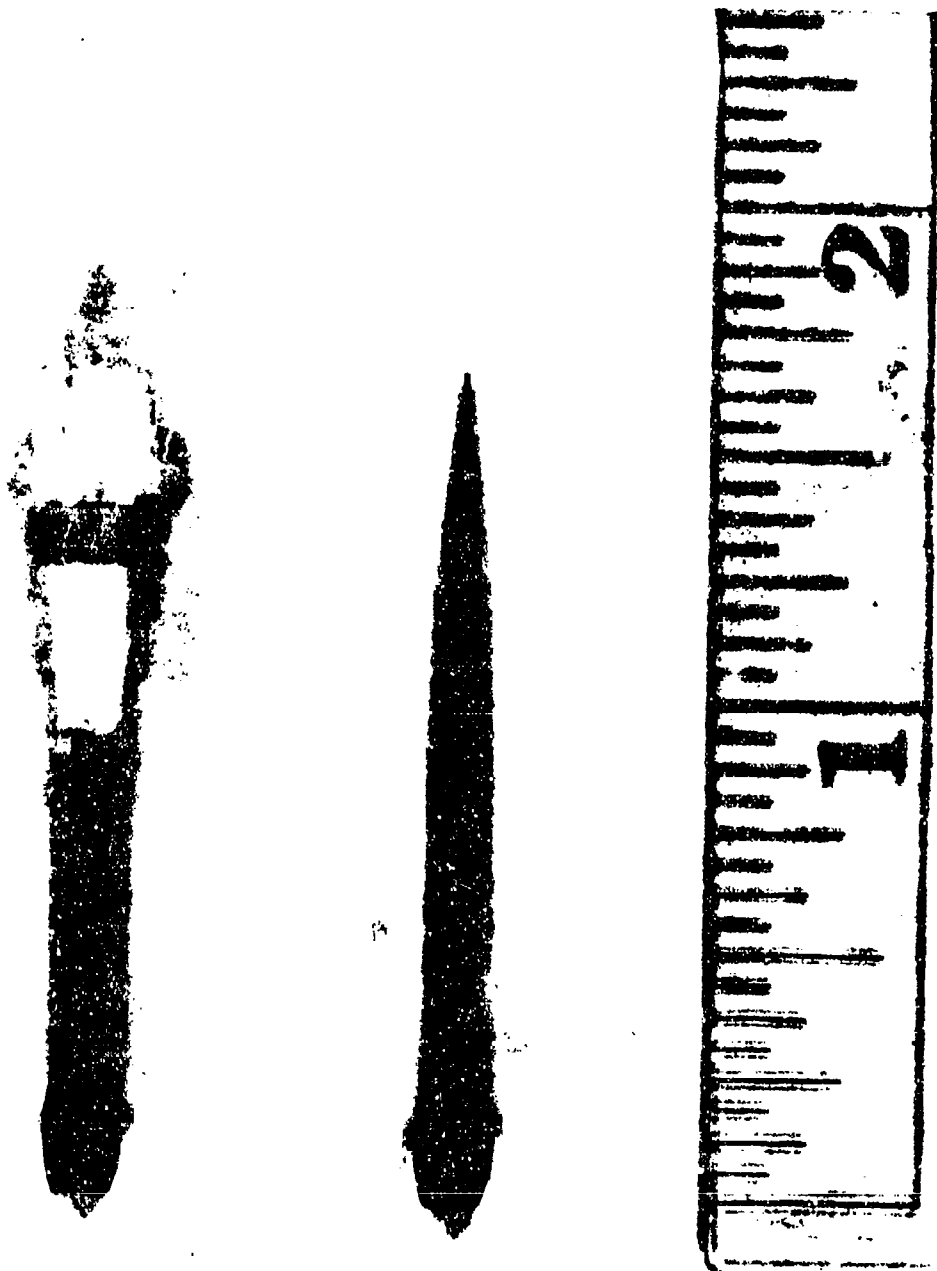
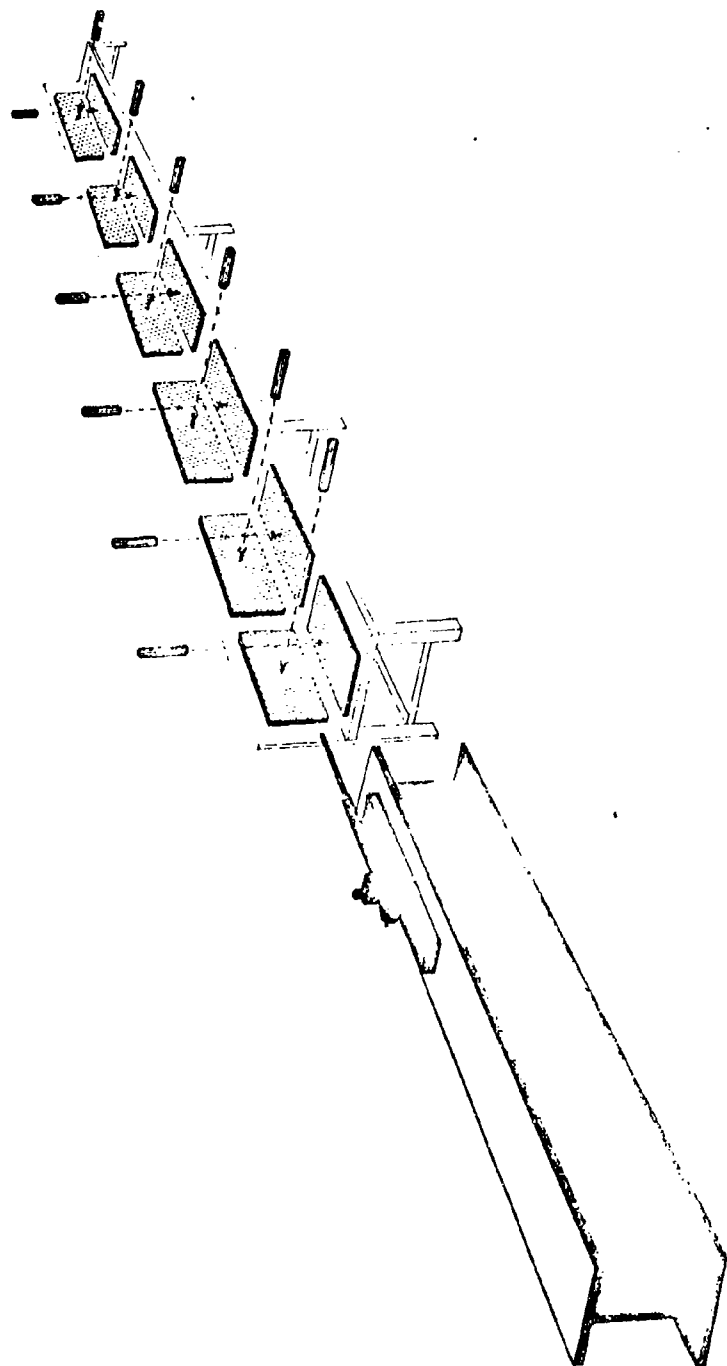


Figure 29. Ground Point Flechette, With and Without Sabot

Figure 30. Free Flight Test Apparatus and Set-up



From the battery of test firings of 20 rounds of each type (which included tests of the ground point, and swayed point producibility flechette as well as the R&D version), 8 of the ground point producibility rounds were selected to be analyzed. The eight rounds along with velocity, roll rates and target positions are given in Table XX.

Raw translational and angular data are shown in Figures 31 through 46. The figures illustrate the position and complex angle of attack of the flechette for each station.

TABLE XX
FRANKFORD TEST FIRING DATA

R O U N D	u_0	p_0	Target at 50 ft.	
			Y (ft)	iZ (ft)
4	4747	11,454	0.117	-0.038
6	4662	13,201	0.053	-0.010
7	4642	14,219	0.141	-0.004
8	4662	13,000	0.053	0.099
14	4758	13,289	0.053	0.016
16	4753	17,354	0.084	-0.004
17	4677	16,613	0.070	-0.019
19	4679	11,913	0.089	0.059

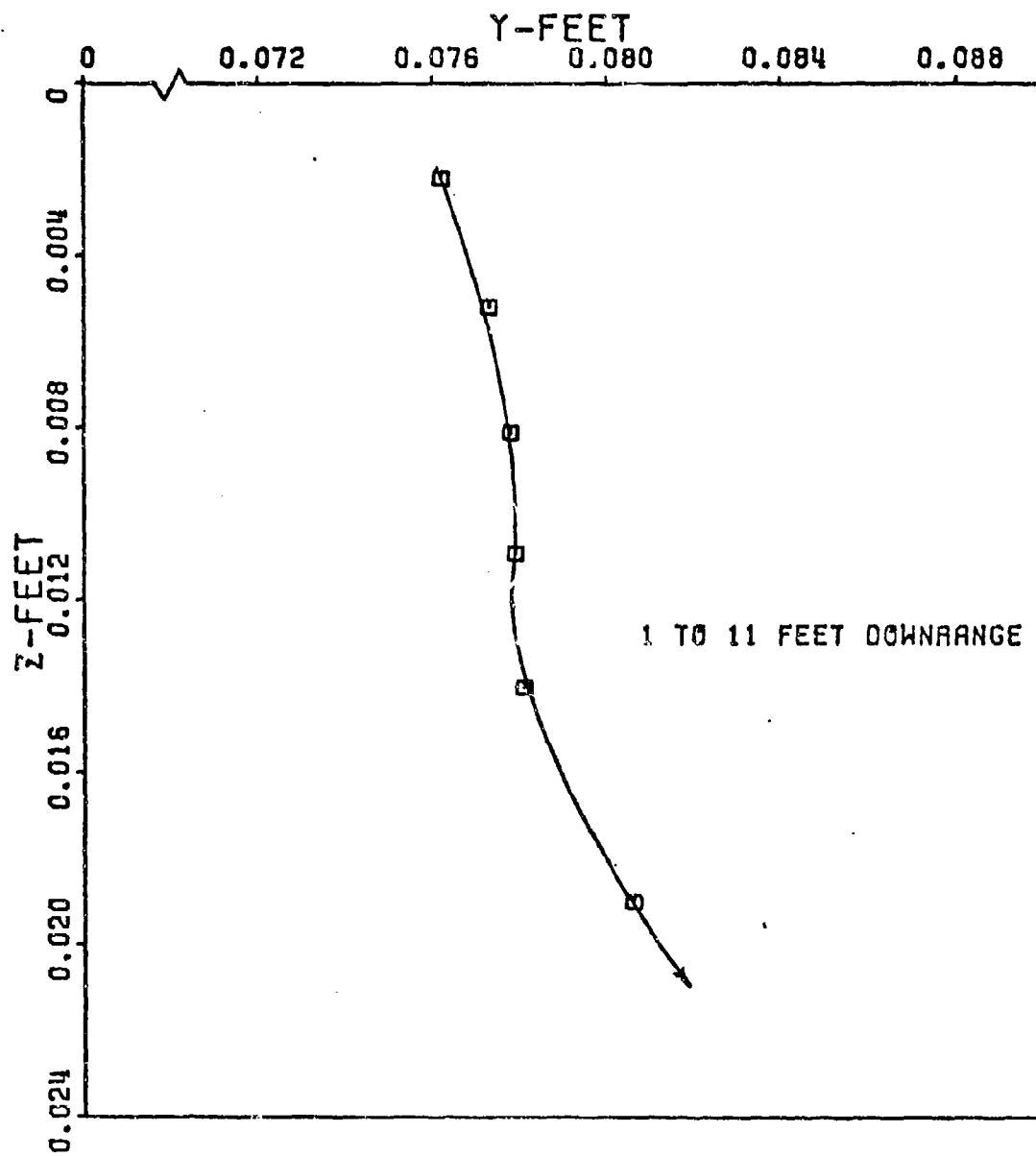


Figure 31. Raw Translational Data Ground Point - Round 4

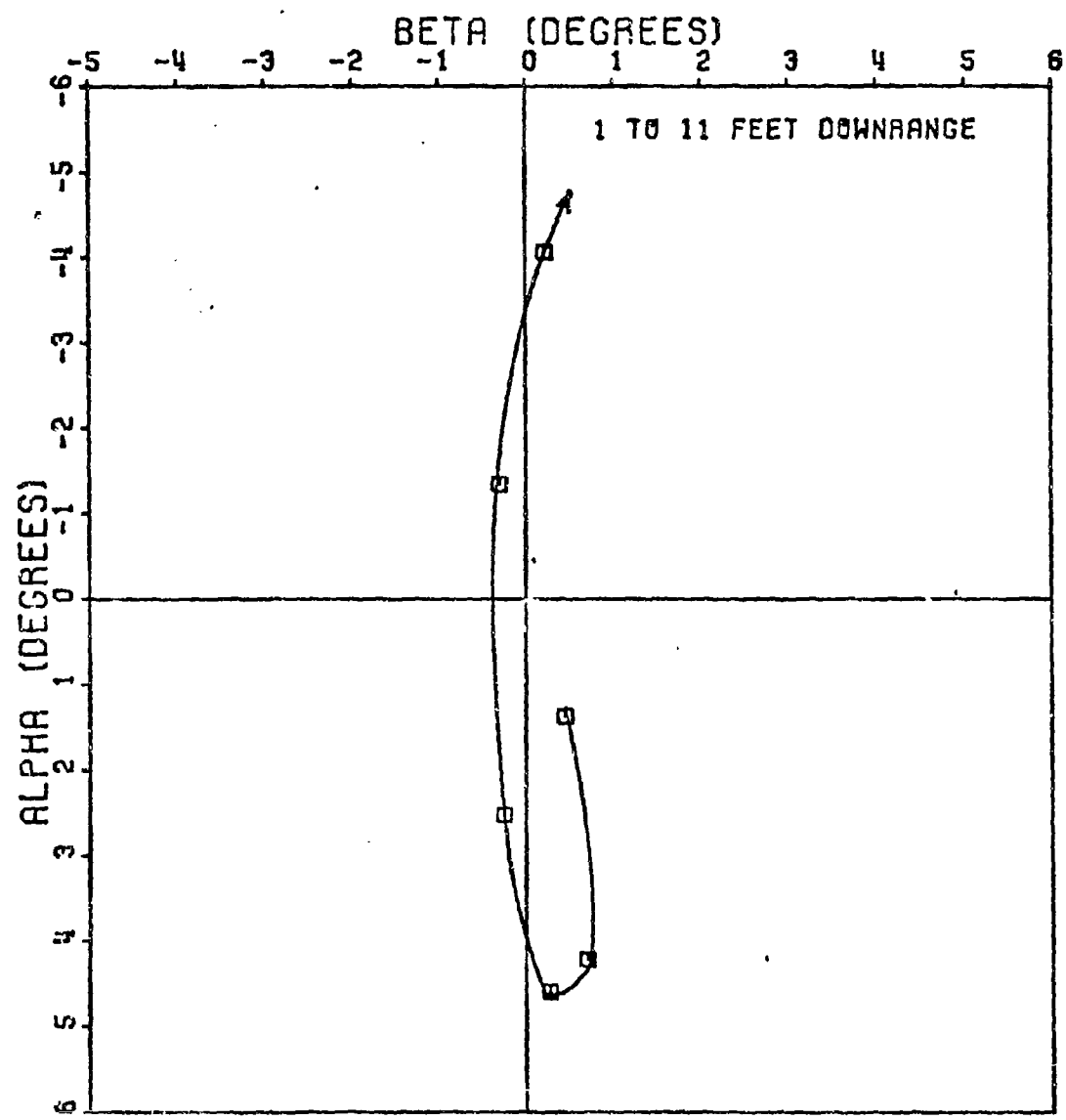


Figure 32. Raw Angular Data Ground Point - Round 4

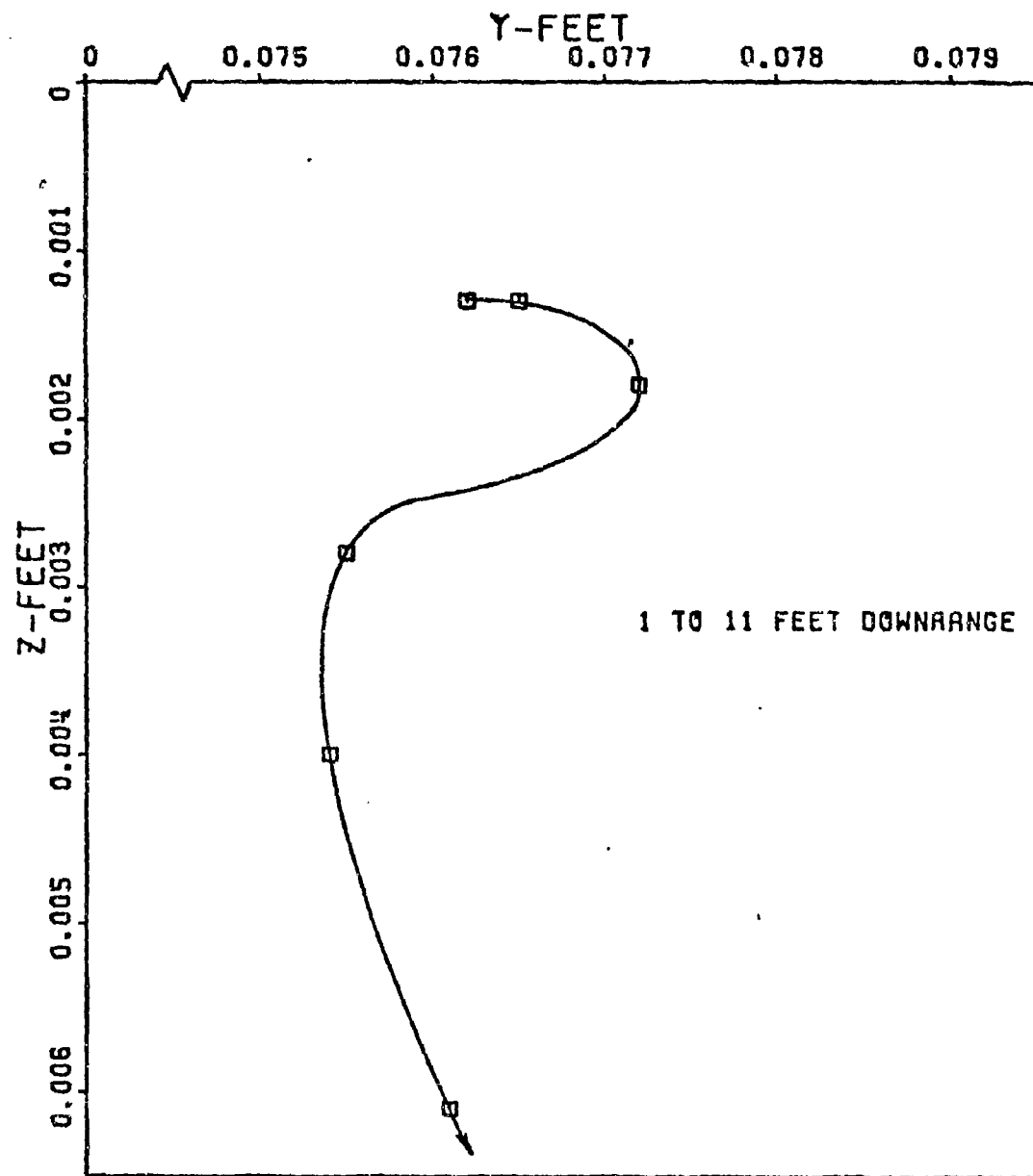


Figure 33. Raw Translational Data Ground Point - Round 6

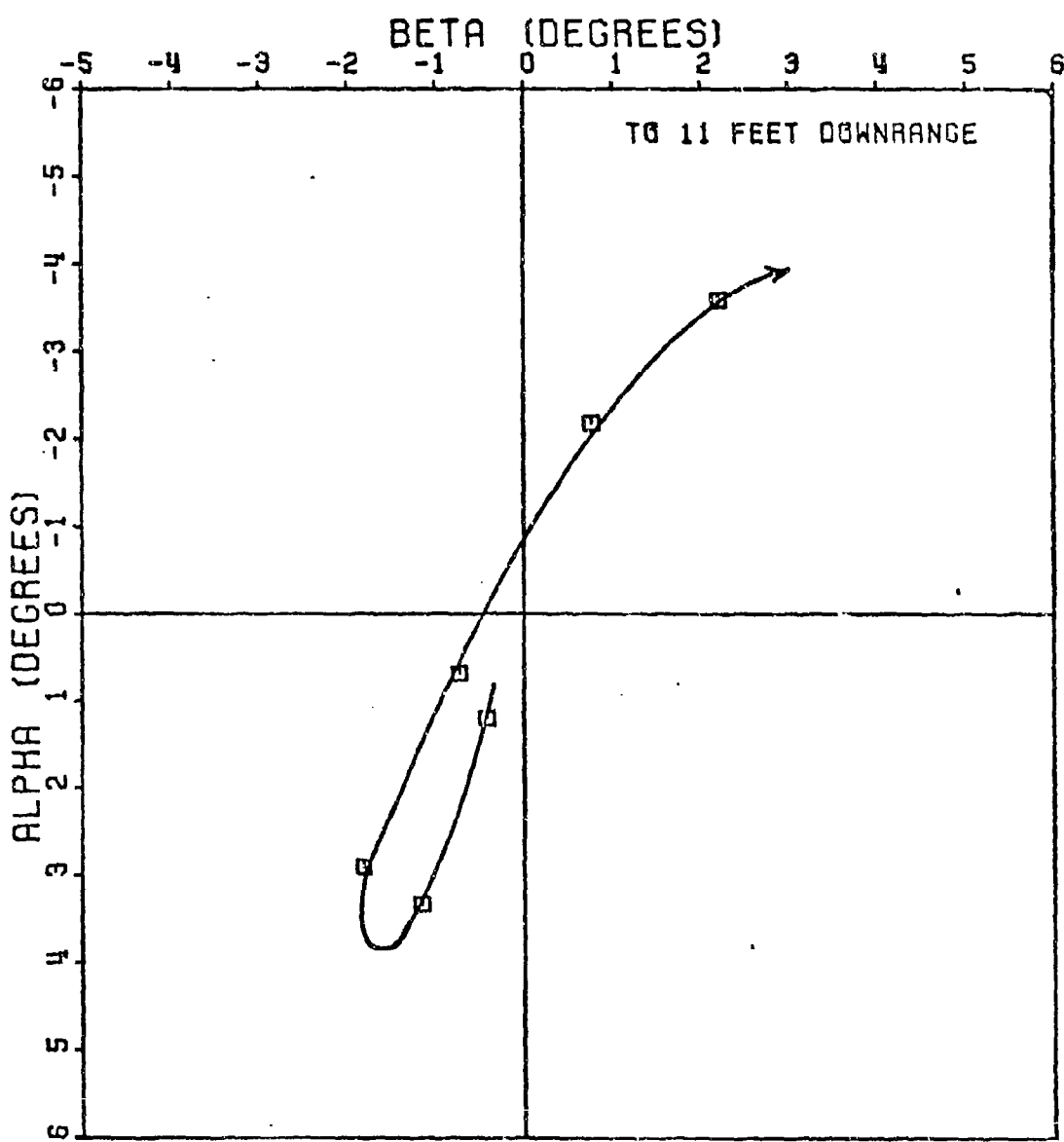


Figure 34. Raw Angular Data Ground Point - Round 6

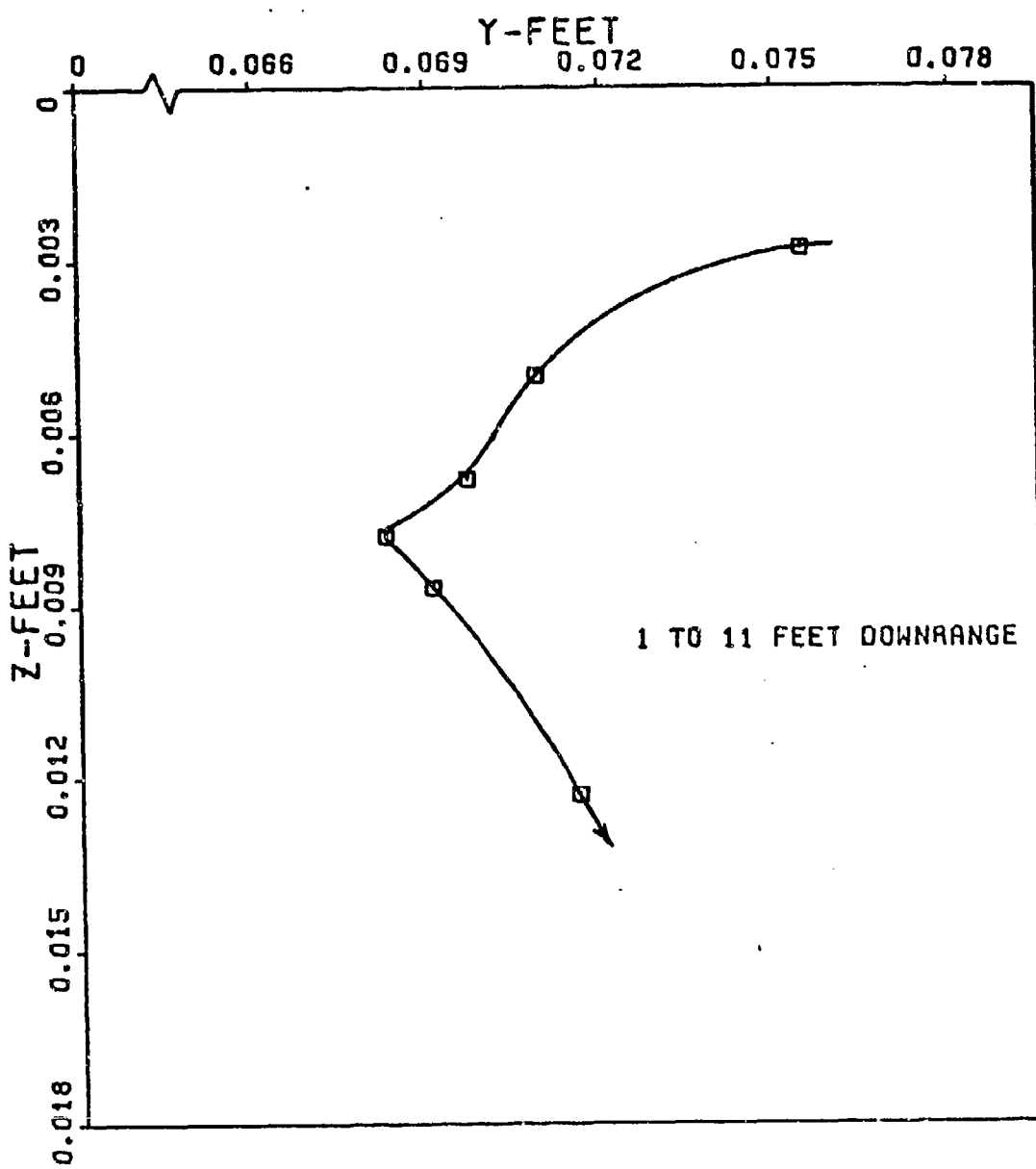


Figure 35. Raw Translational Data Ground Point - Round 7

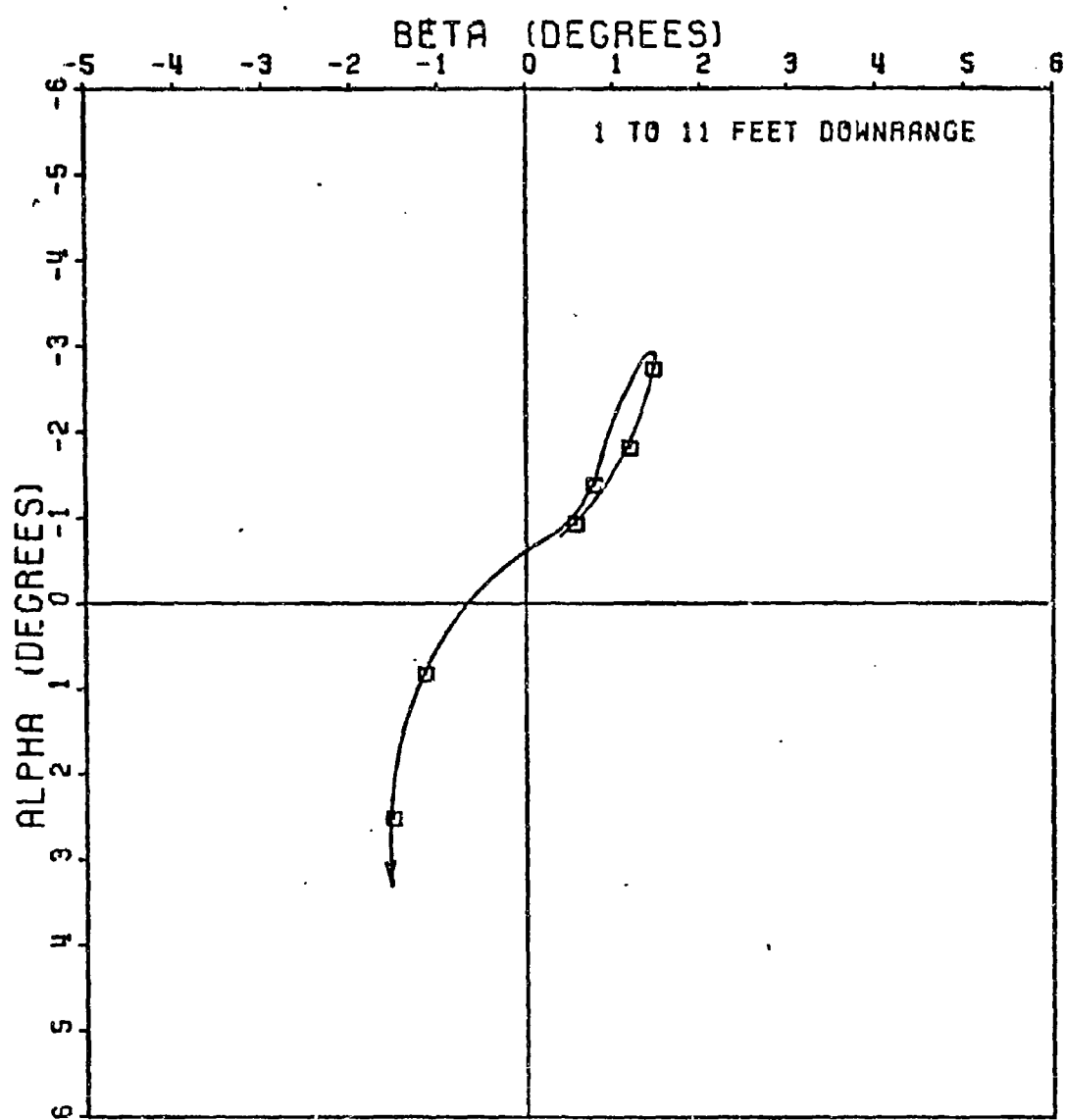


Figure 36. Raw Angular Data Ground Point - Round 7

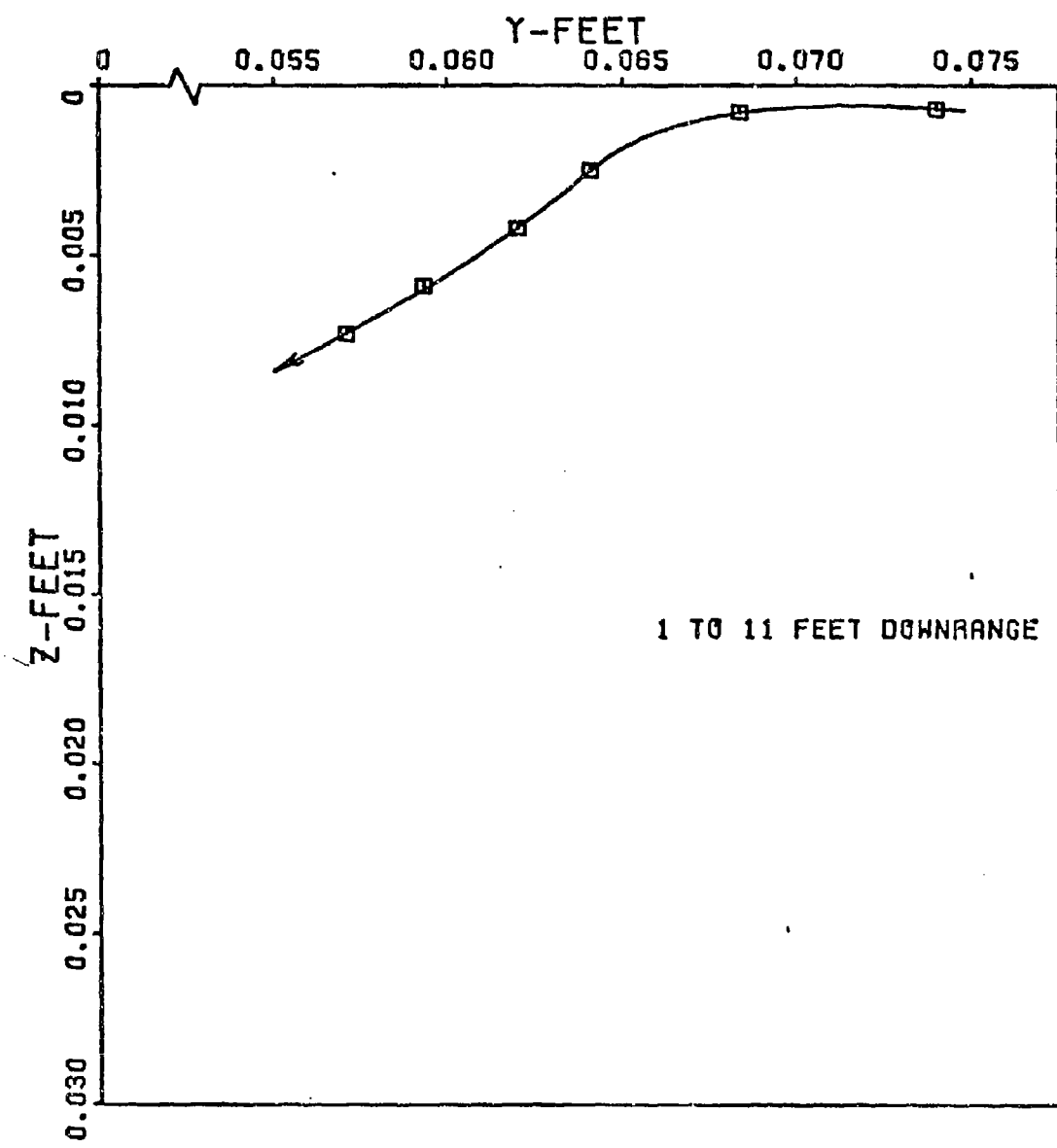


Figure 37. Raw Translational Data Ground Point - Round 8

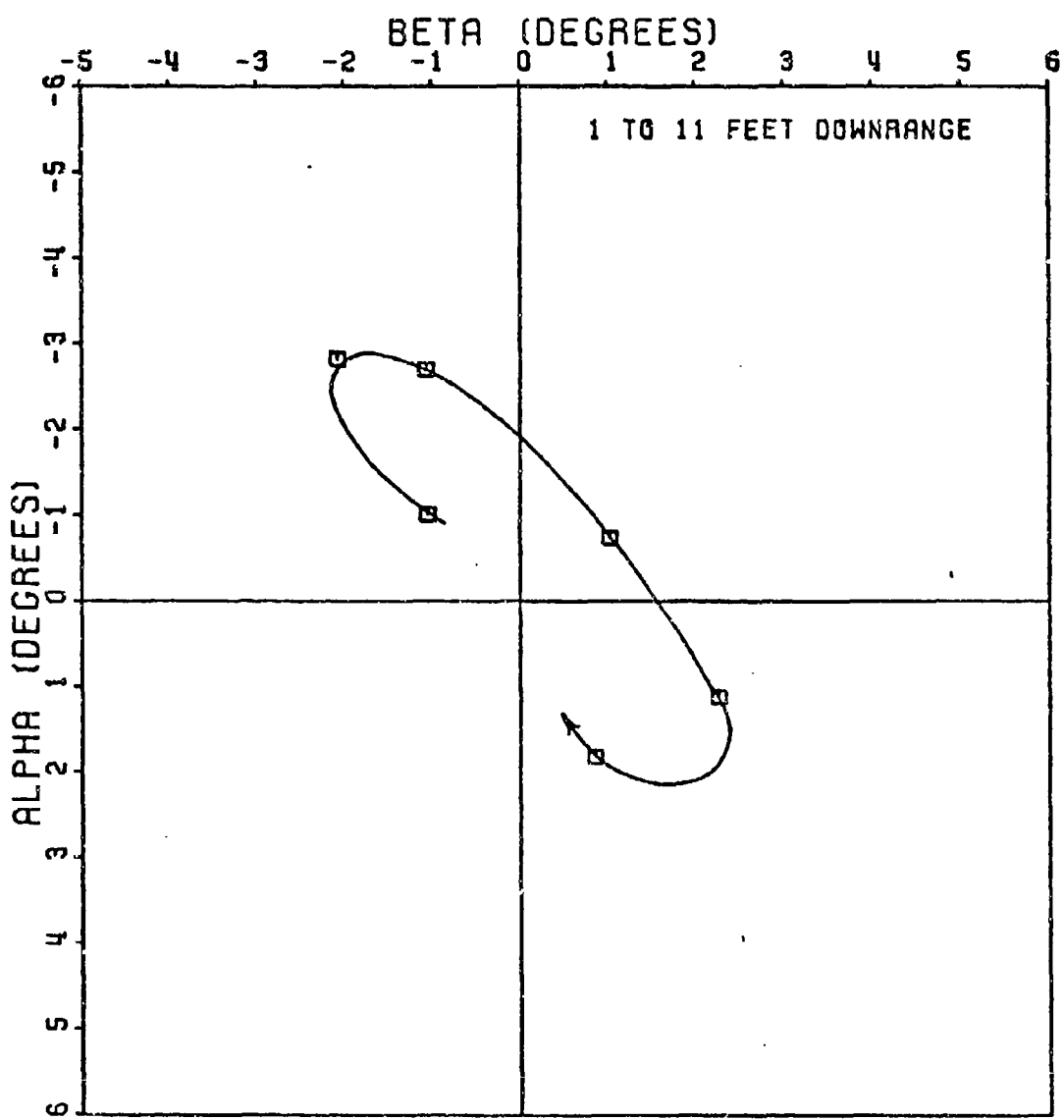


Figure 38. Raw Angular Data Ground Point - Round 8

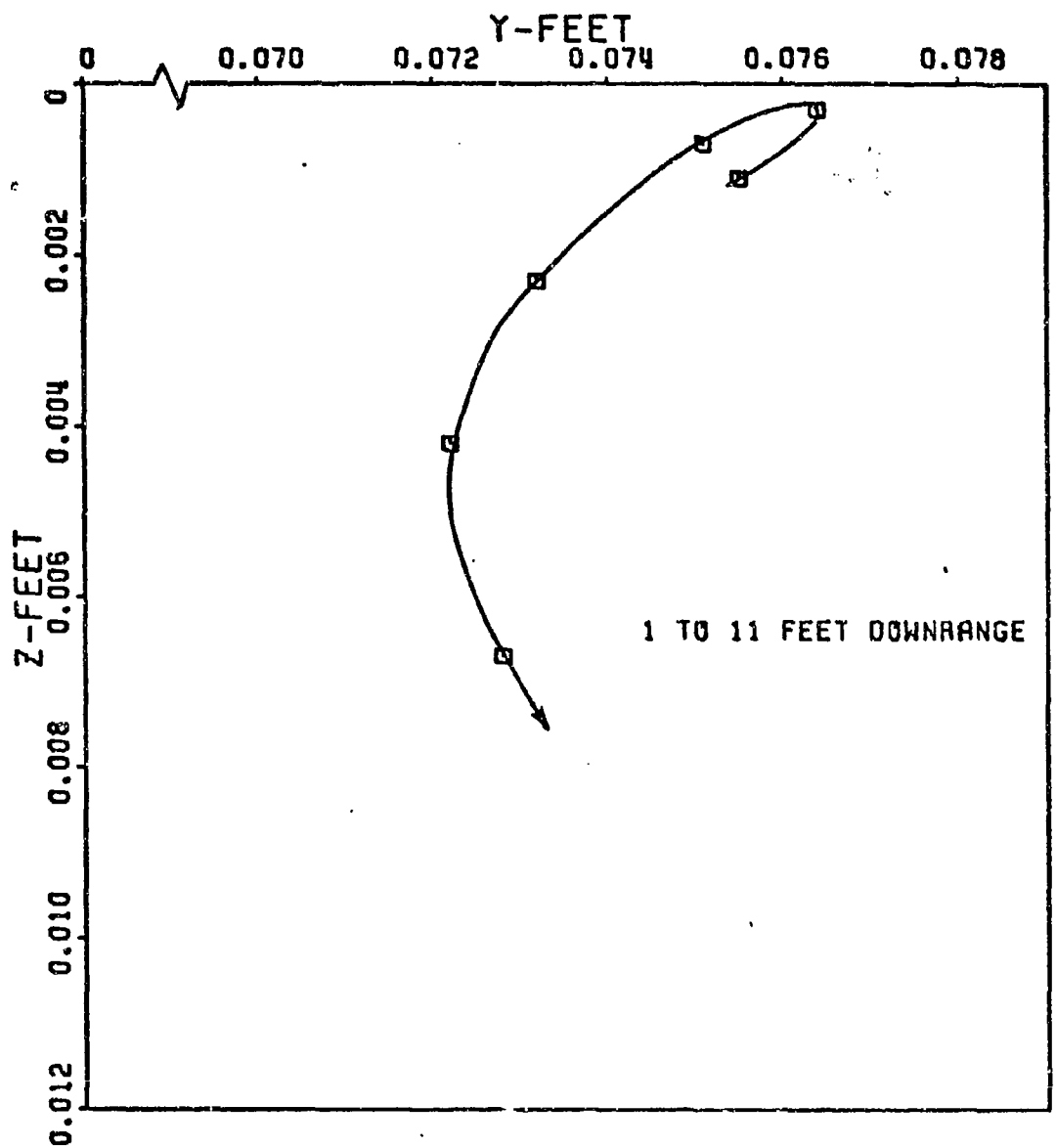


Figure 39. Raw Tranlational Data Ground Point - Round 14

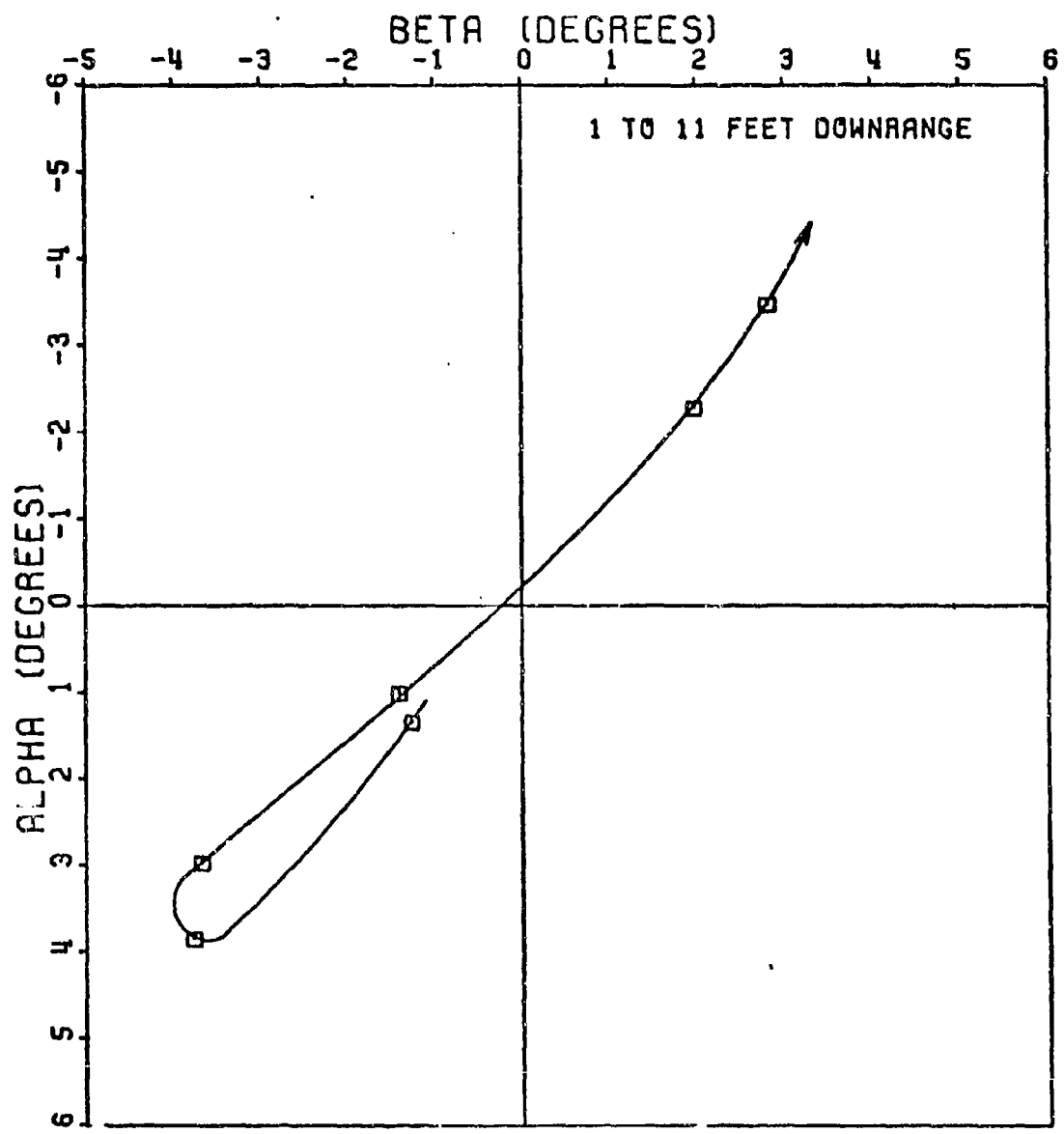


Figure 40. Raw Angular Data Ground Point - Round 14

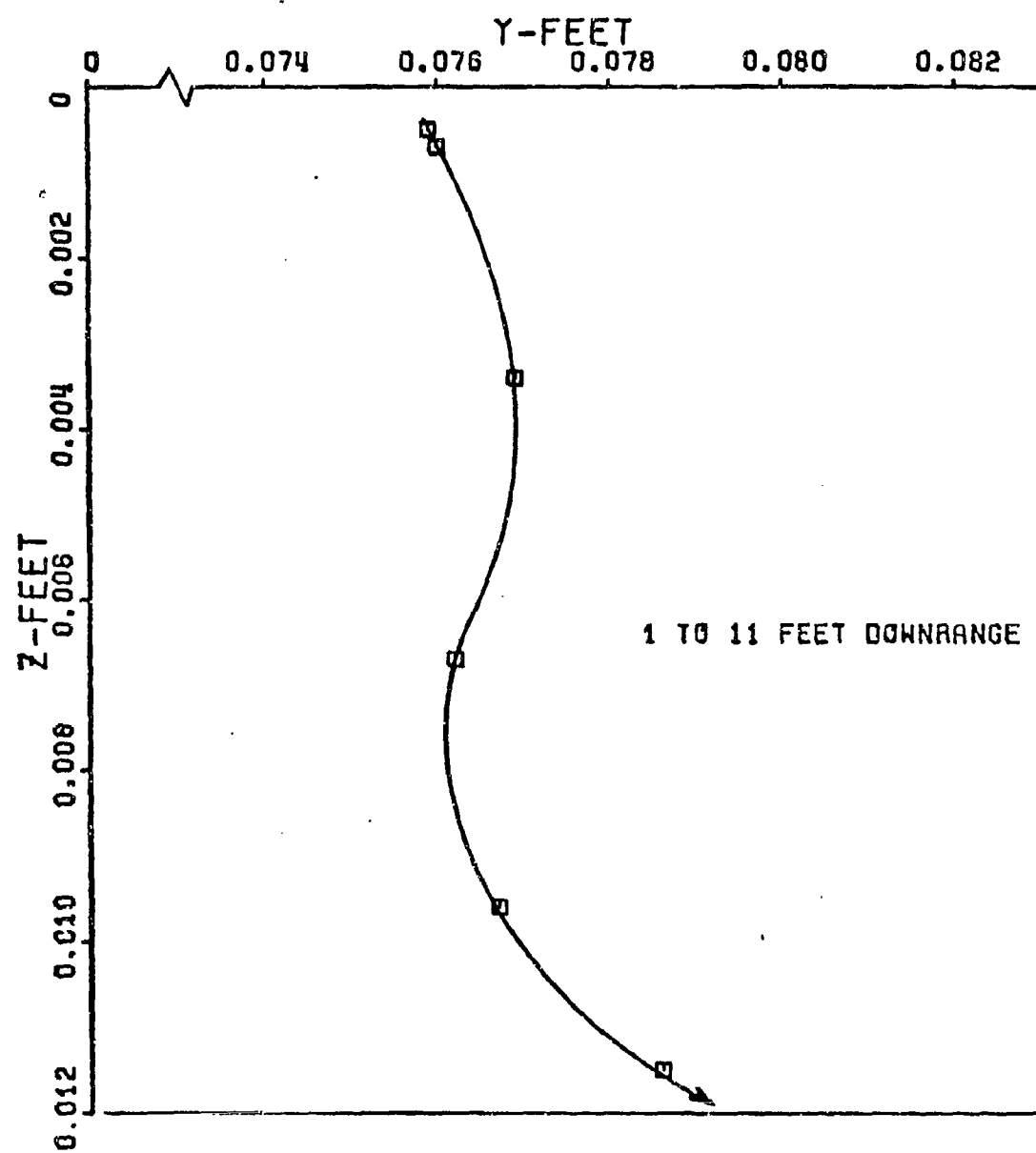


Figure 41. Raw Translational Data Ground Point - Round 16

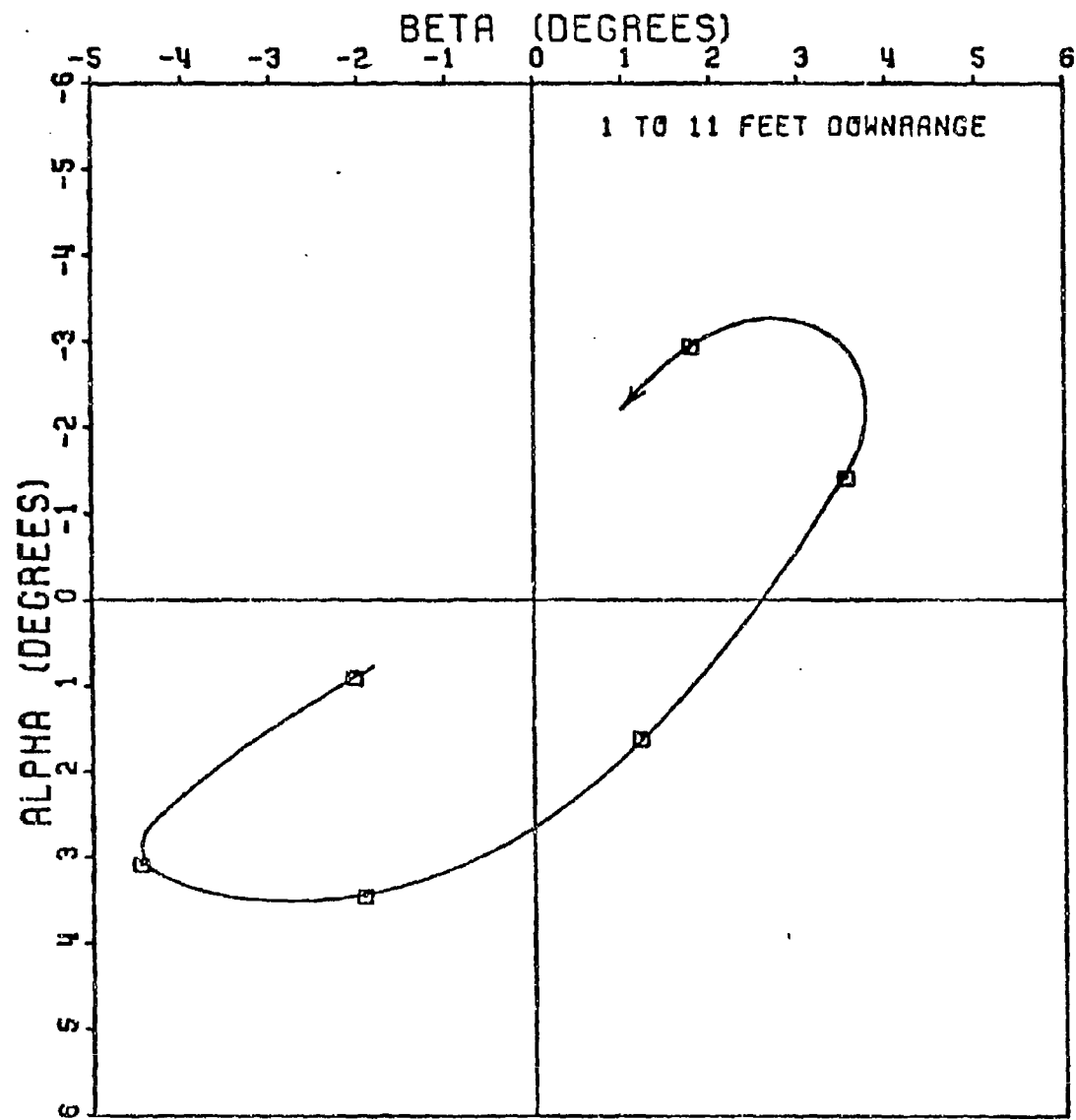


Figure 42. Raw Angular Data Ground Point - Round 16

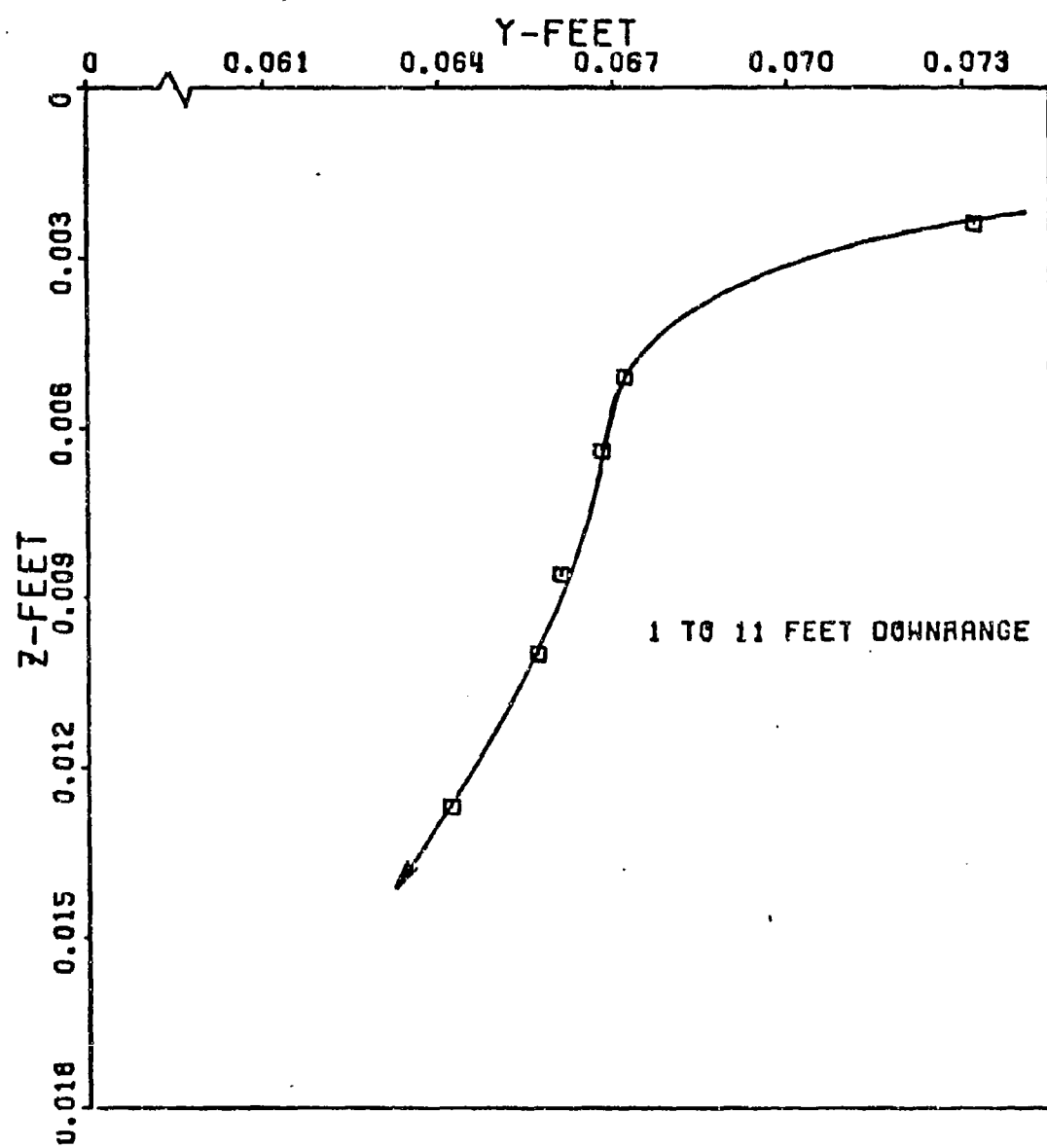


Figure 43. Raw Translational Data Ground Point - Round 17

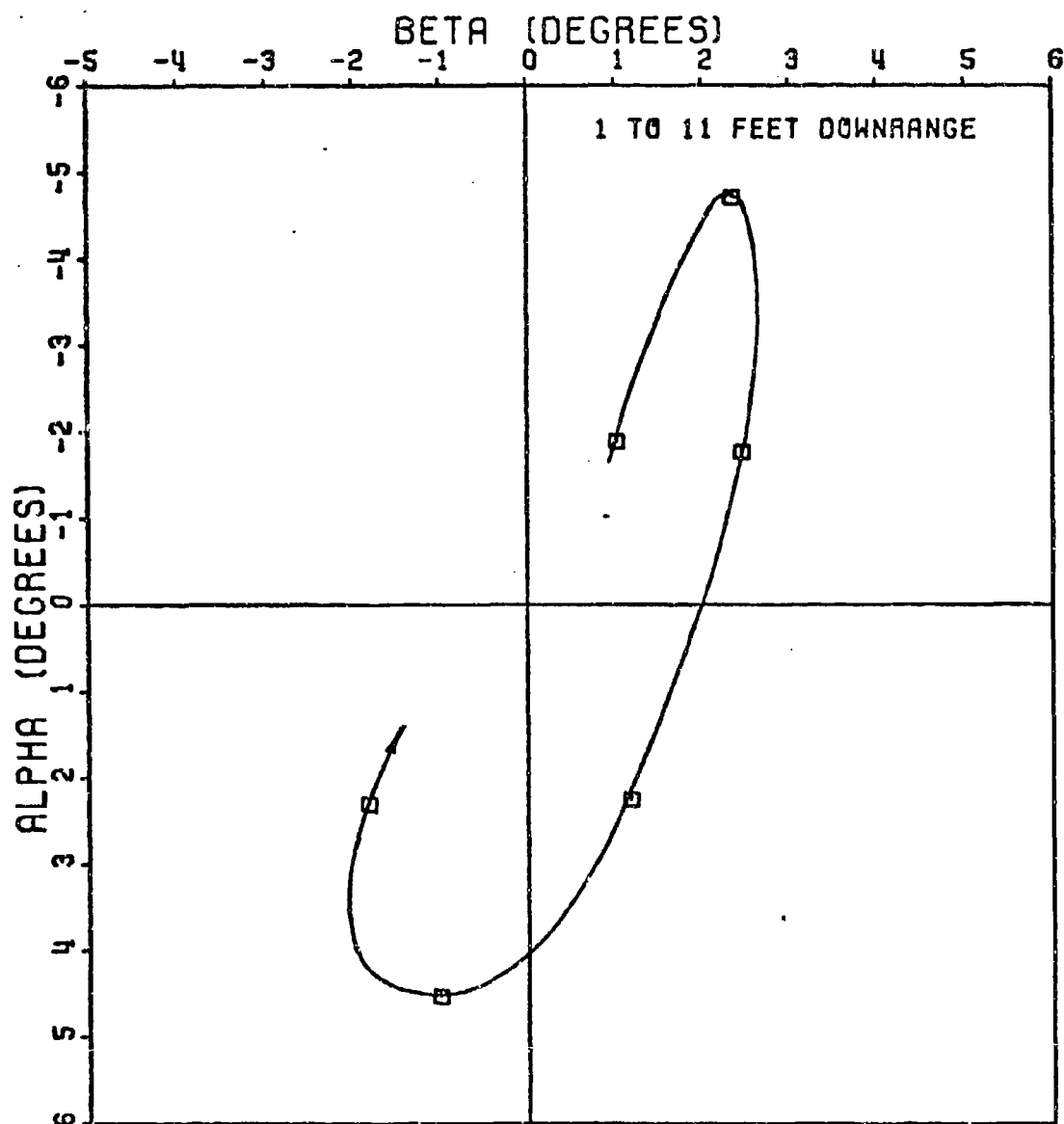


Figure 44. Raw Angular Data Ground Point - Round 17

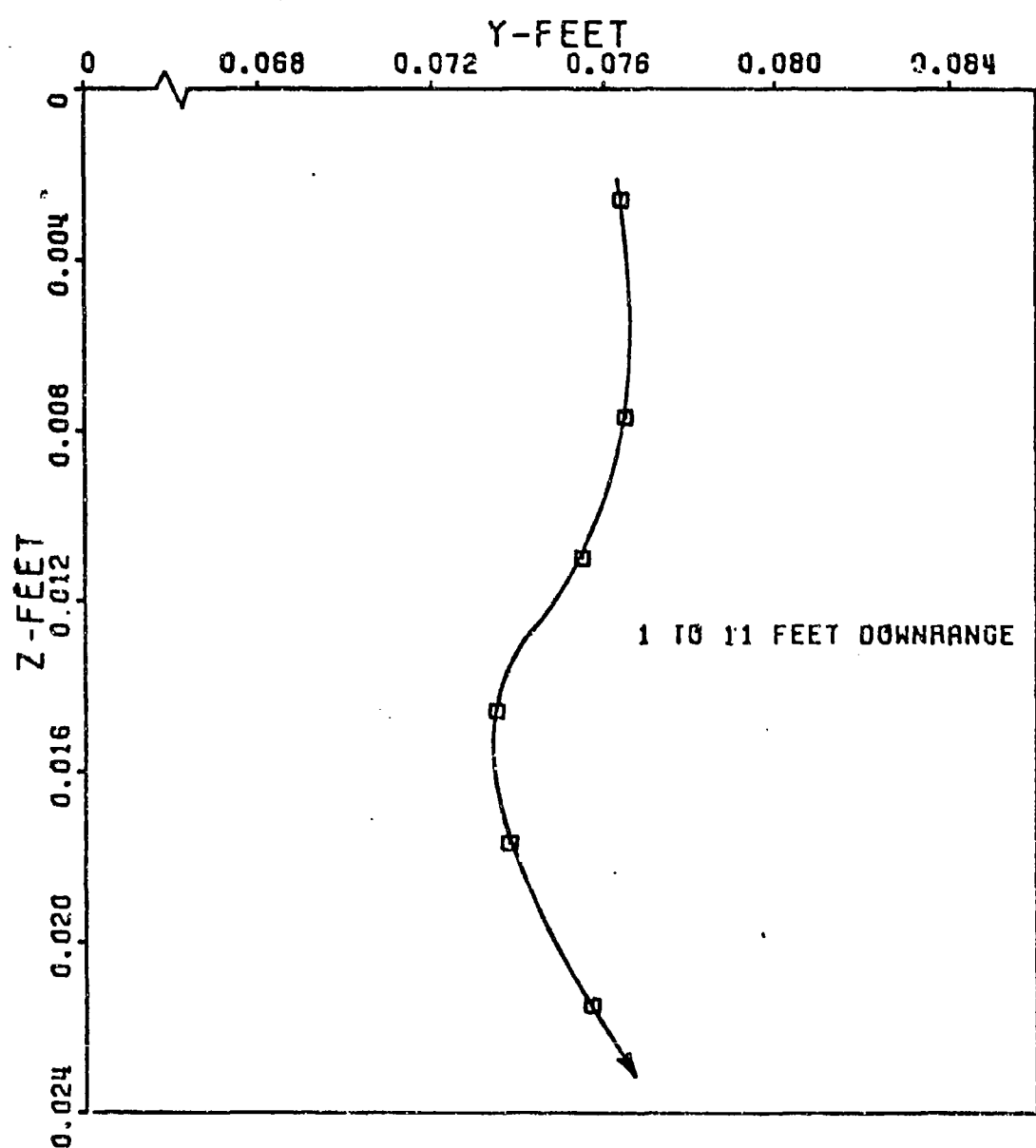


Figure 45. Raw Translational Data Ground Point - Round 19

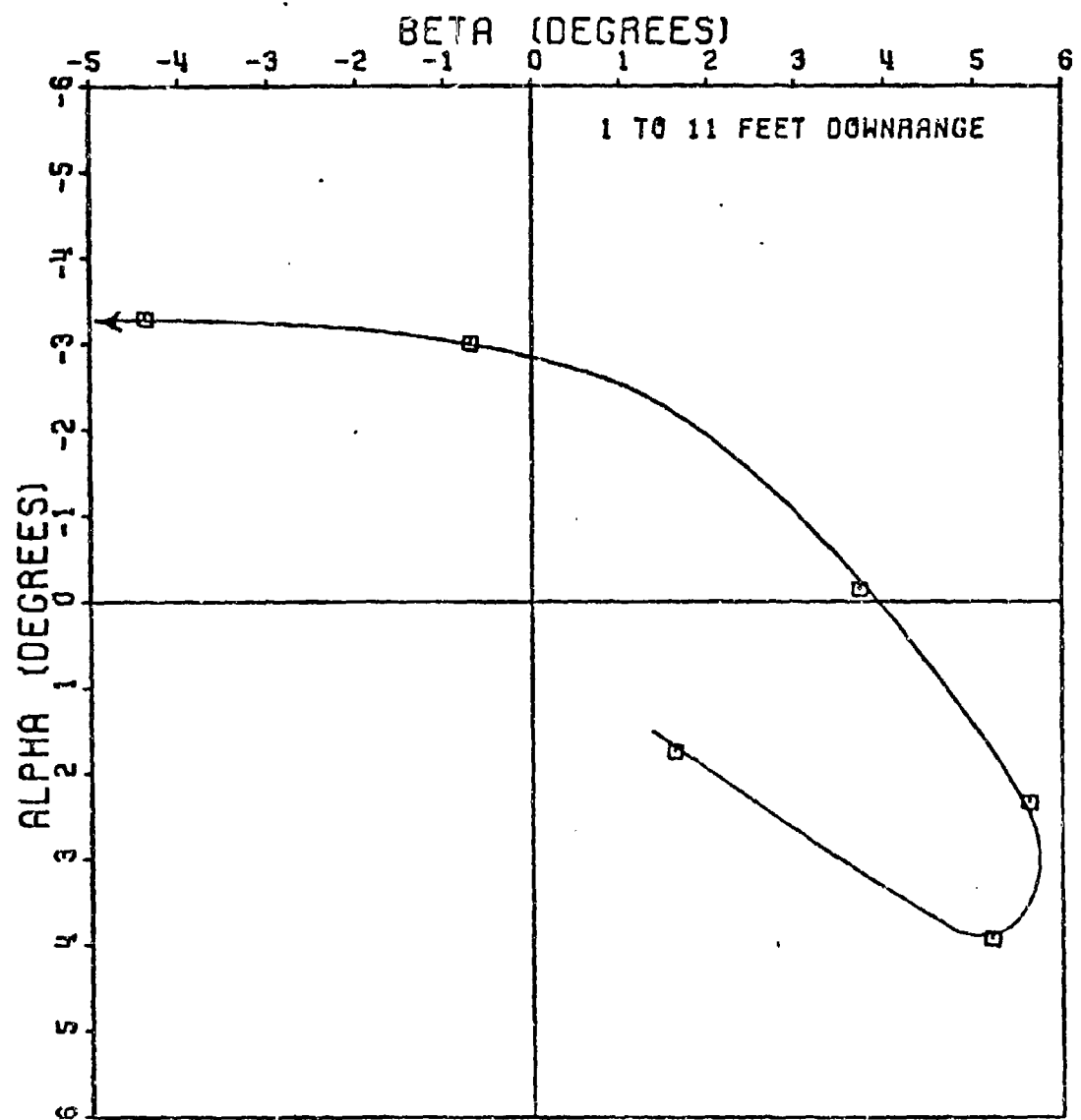


Figure 46. Raw Angular Data Ground Point - Round 19

Once the raw data was obtained, it had to be converted into a form such that initial conditions \vec{S}_o , $\dot{\vec{S}}_o$, $\vec{\alpha}_o$ and $\dot{\vec{\alpha}}_o$ could be extracted from it. To eventually arrive at values for \vec{S}_o and $\dot{\vec{S}}_o$, the translational parameters, the raw position or translational data had to be approximated by equations. The raw data was fitted to a polynomial equation of third degree by a least squares method. The data in the y-direction was fit separately from that in the z-direction to distinguish between the swerve and heave contributions. With the equations obtained, a simple differentiation yielded equations for the velocities in the y and z directions. The initial conditions \vec{S}_o and $\dot{\vec{S}}_o$ are now readily obtainable:

$$\begin{aligned}\vec{S}_o \text{ (ft)} &= y_o + iz_o \\ \dot{\vec{S}}_o \text{ (ft/sec)} &= \dot{y}_o + i\dot{z}_o\end{aligned}$$

Obtaining $\vec{\alpha}_o$ and $\dot{\vec{\alpha}}_o$ from the raw angular data was more difficult. The traditional way of analyzing any missile motion with pitch, yaw, and roll is by a three-degree-of-freedom least squares fit to the tricyclic motion, Equation 6. However, the availability of only 6 data points made this technique impossible, so another, approximate method, had to be employed. The solution was to approximate the pitching and yawing motion to one-degree-of-freedom while holding the roll rate constant. In order to do this, the $\beta - \alpha$ axis system had to be rotated to coincide with the more dominant angular mode. Figure 47 illustrates a typical raw angular data plot. Since the angular motion of the flechette tends to approximate an ellipse, the $\beta - \alpha$ axes are rotated some angle γ to coincide with the

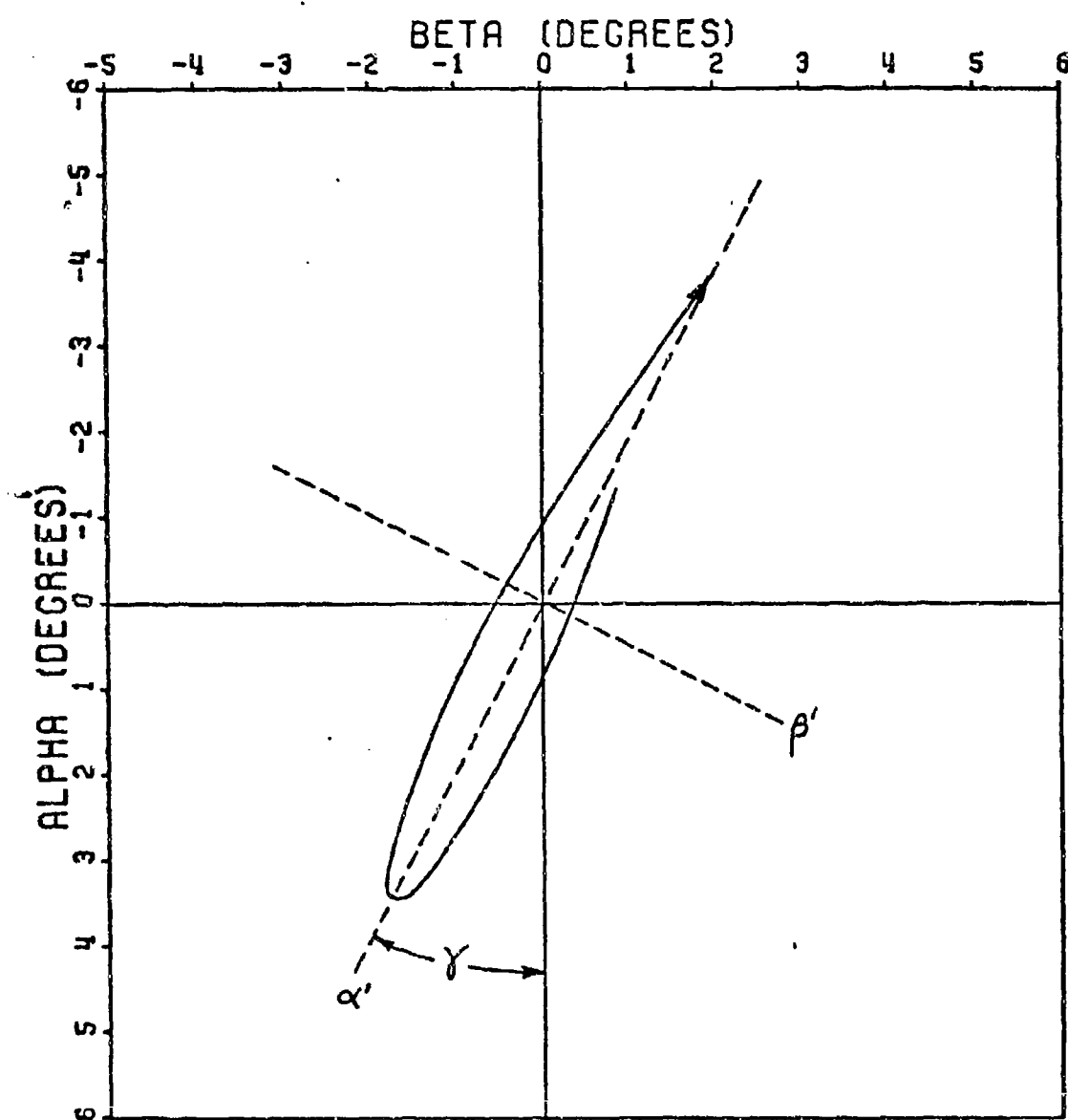


Figure 47. Axis Rotation Approximates Pure Pitching Motion

major and minor axes of the ellipse, as shown. The angular data is retabulated for this new axes system, $\beta' - \alpha'$. To fit the data to the one-degree-of-freedom equation:

$$\alpha = K_1 e^{\lambda t} \cos(\omega t + \delta)$$

only the dominant mode can be considered. For example, in Figure 47 the dominant mode occurs along the α' axis; therefore, only α' coordinates are utilized in the least squares fit, corresponding β' coordinates are ignored. Table XXI lists the parameters obtained for the eight flechette rounds. Once an equation for α' is obtained, it represents one dimensional oscillatory motion along the α' axis. A simple differentiating of the α' equation yields an equation for $\dot{\alpha}'$. The initial conditions $\overrightarrow{\alpha}_0$ and $\overrightarrow{\dot{\alpha}}_0$, however, are complex whereas α' and $\dot{\alpha}'$ are only one dimensional. Therefore, the rotation angle γ is taken into account and the α' equation is projected back into the β , α axes system:

$$\alpha = \alpha' \cos \gamma$$

$$\dot{\alpha} = \dot{\alpha}' \cos \gamma$$

$$\beta = \alpha' \sin \gamma$$

$$\dot{\beta} = \dot{\alpha}' \sin \gamma$$

Thus the complex initial conditions are approximated.

$$\overrightarrow{\alpha}_0 = \beta_0 + i\alpha_0$$

$$\overrightarrow{\dot{\alpha}}_0 = \dot{\beta}_0 + i\dot{\alpha}_0$$

Figures 48-63 illustrate the fitted data both translational and angular for the eight rounds. The transitional data includes the pertinent equations.

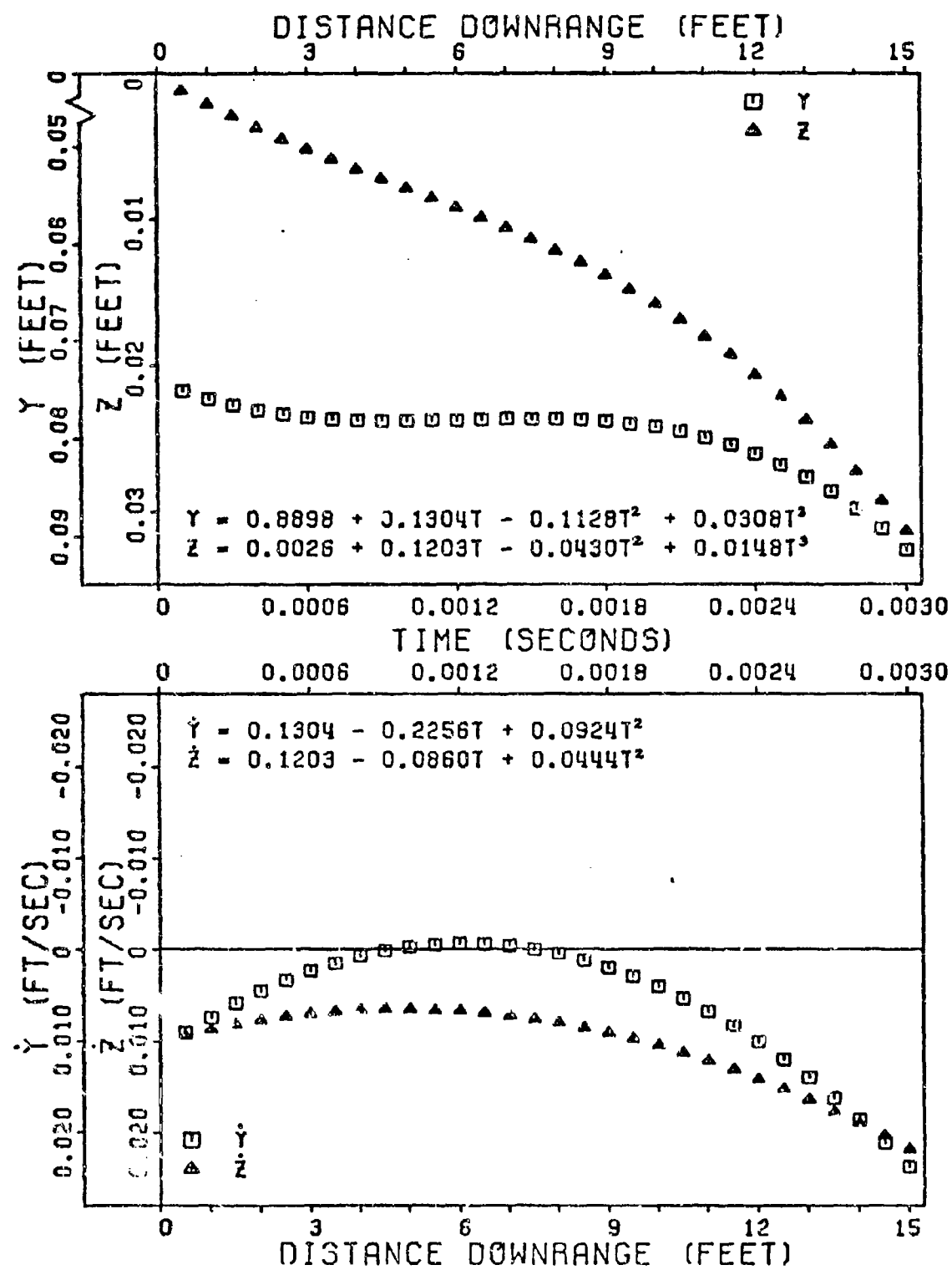


Figure 48. Fitted Translational Data Ground Point - Round 4

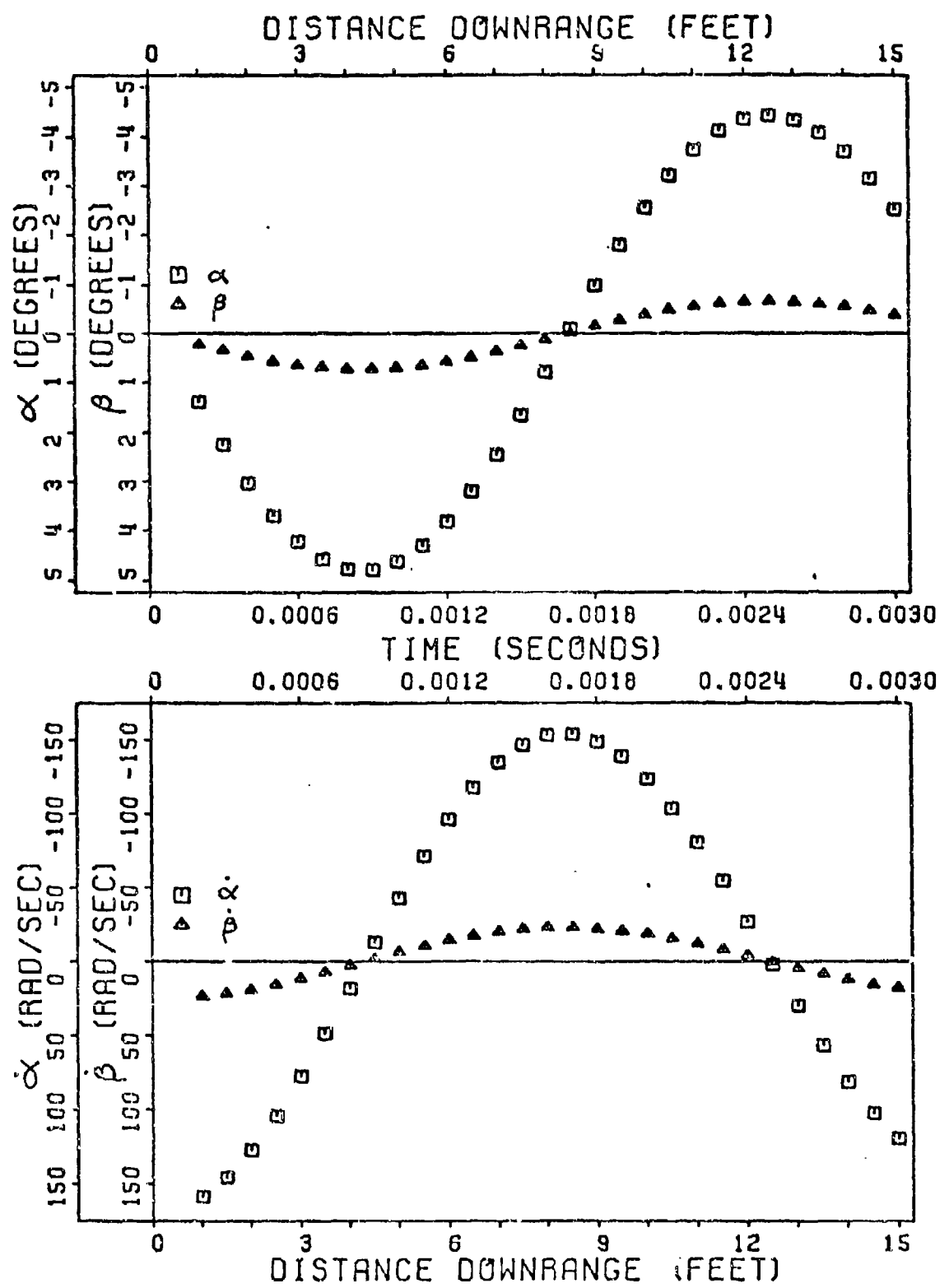


Figure 49. Fitted Angular Data Ground Point - Round 4

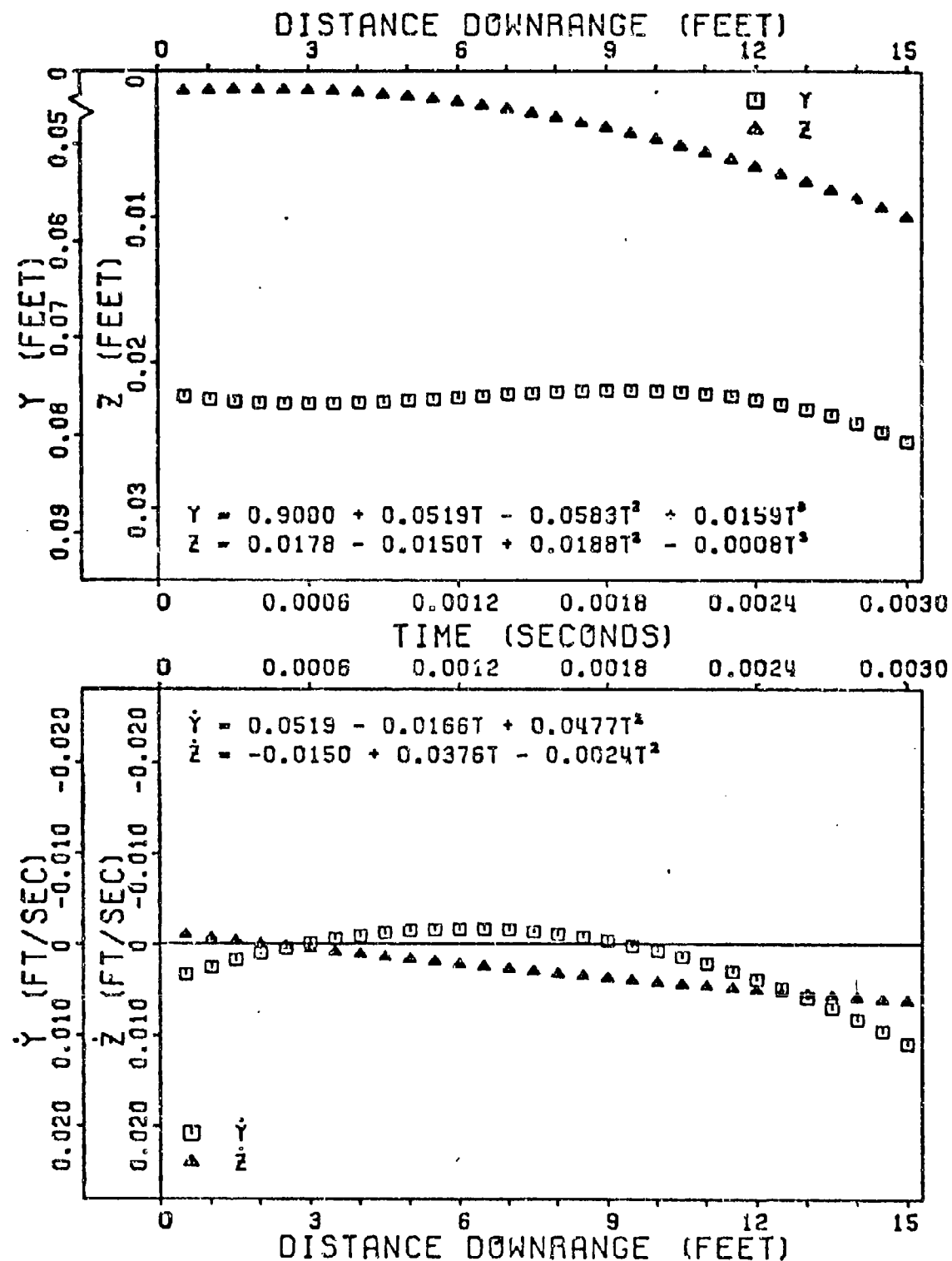


Figure 50. Fitted Translational Data Ground Point - Round 6

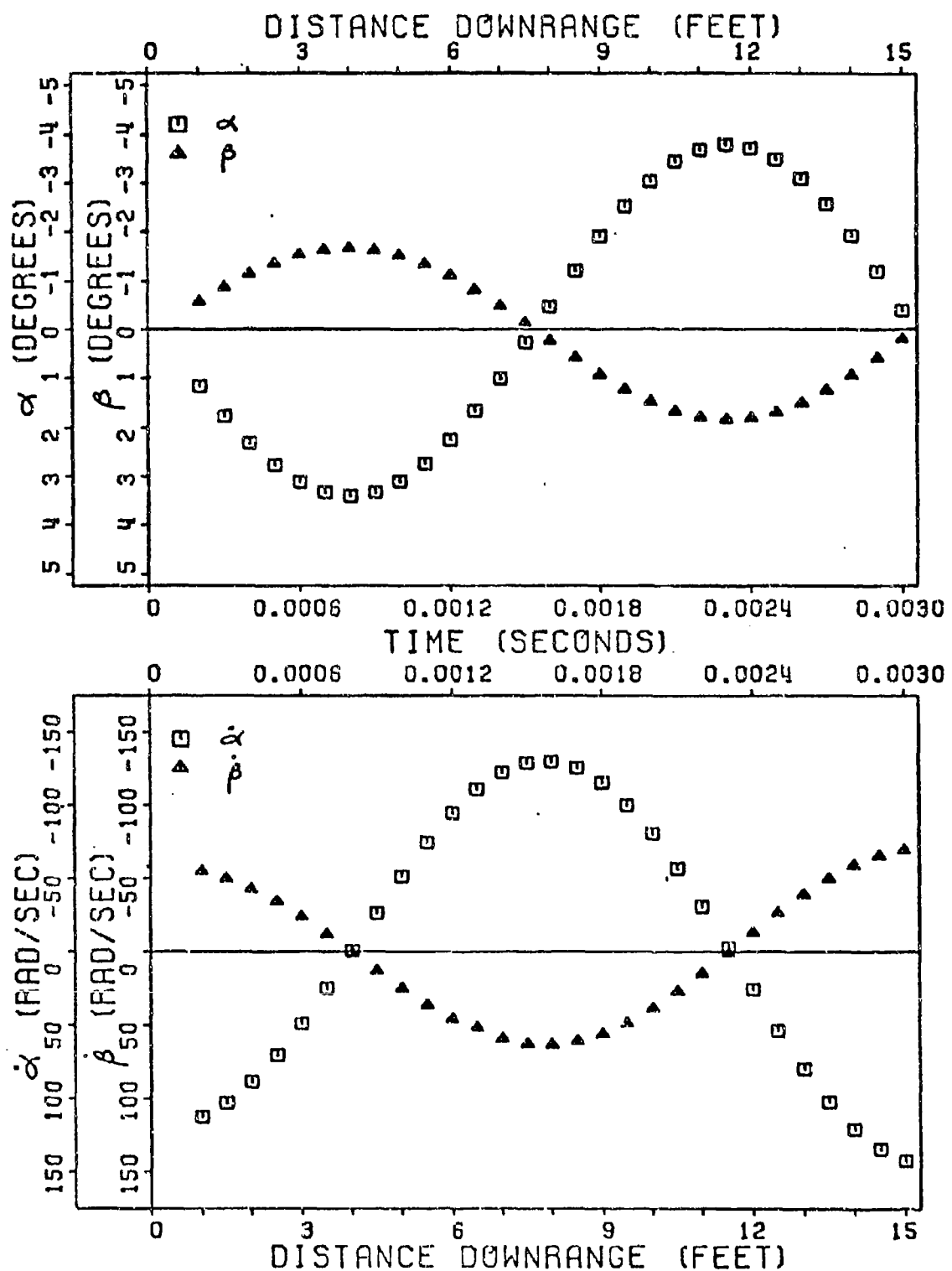


Figure 51. Fitted Angular Data Ground Point - Round 6

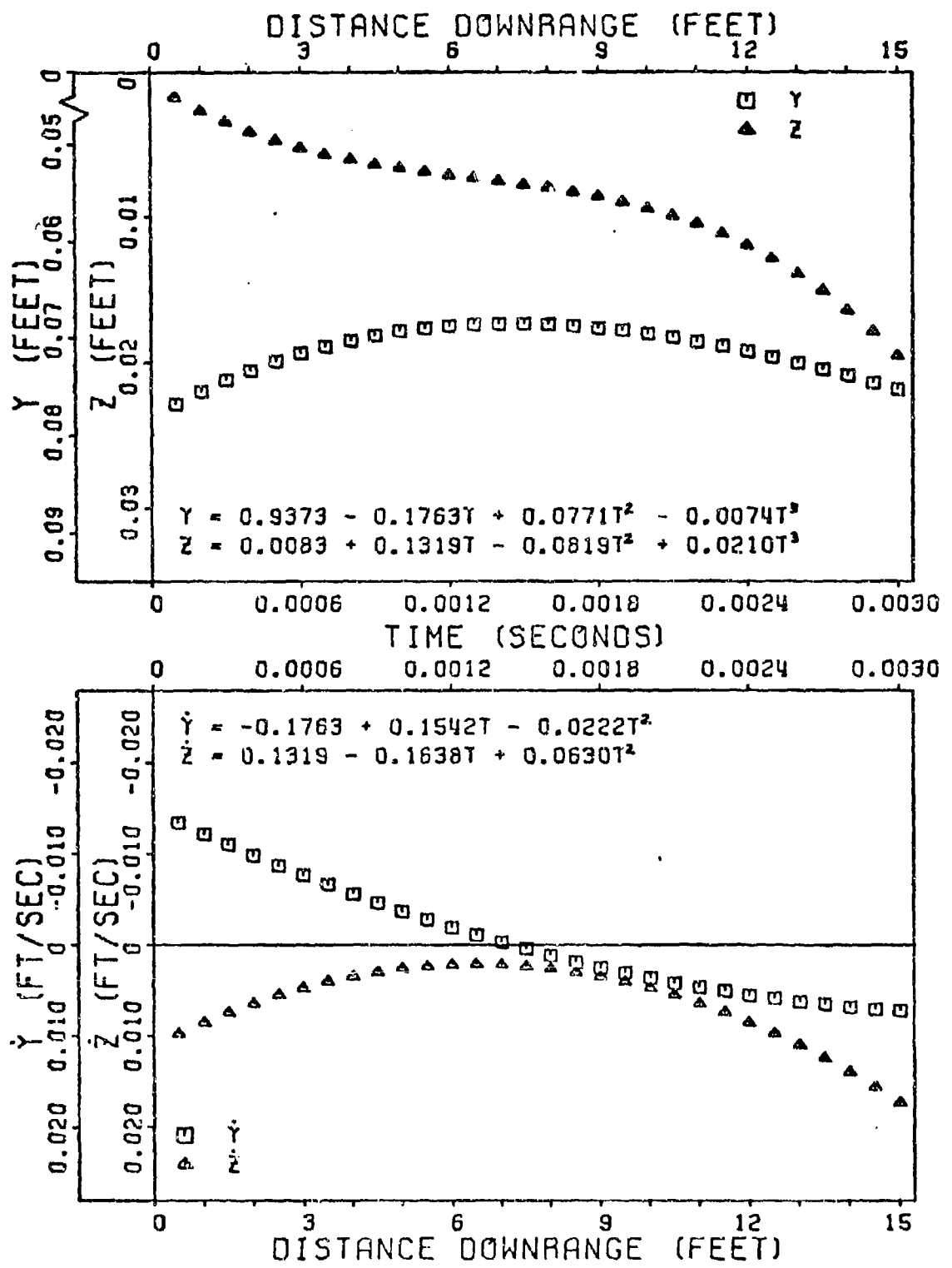


Figure 52. Fitted Translational Data Ground Point - Round 7

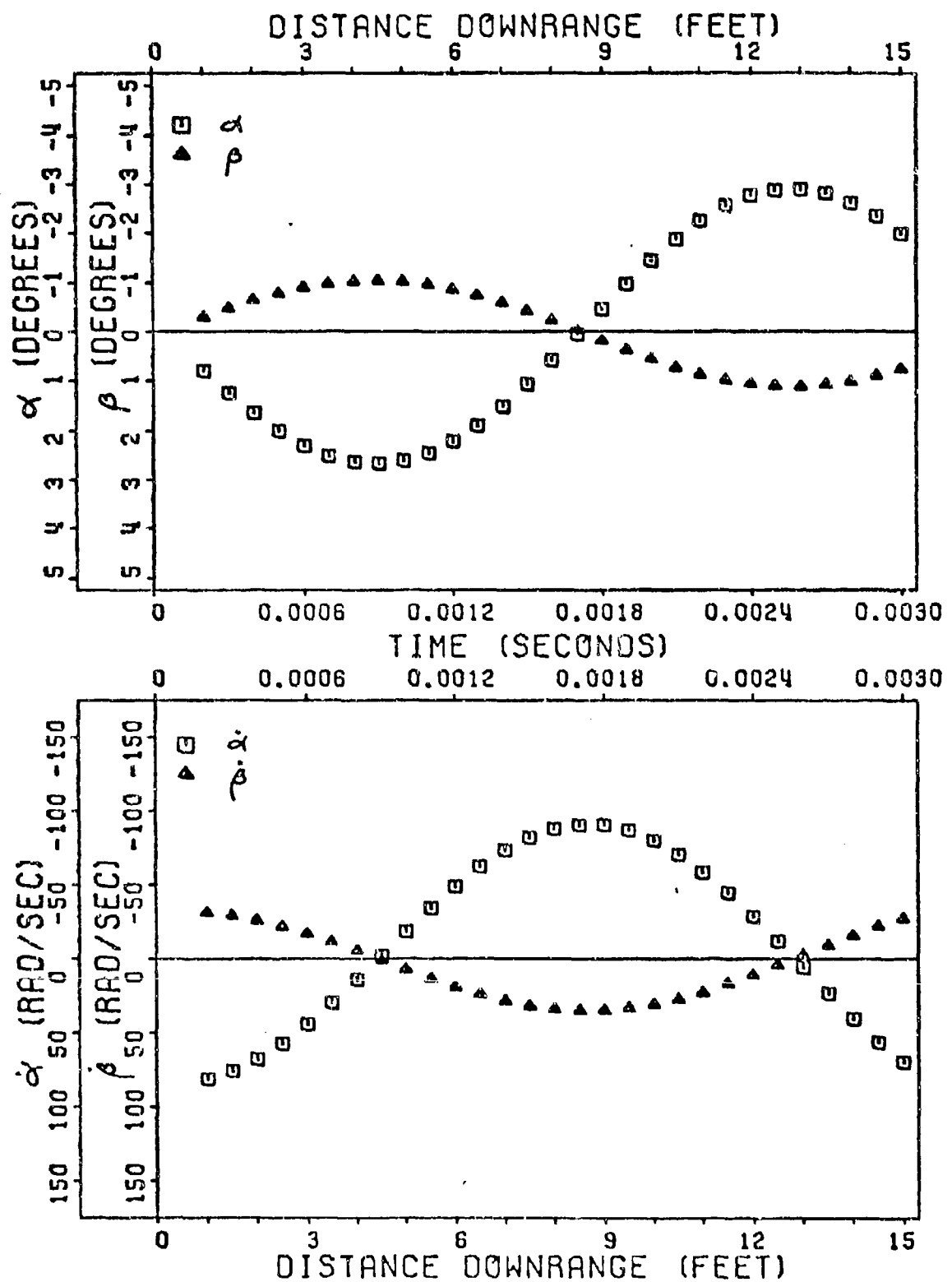


Figure 53. Fitted Angular Data Ground Point - Round 7

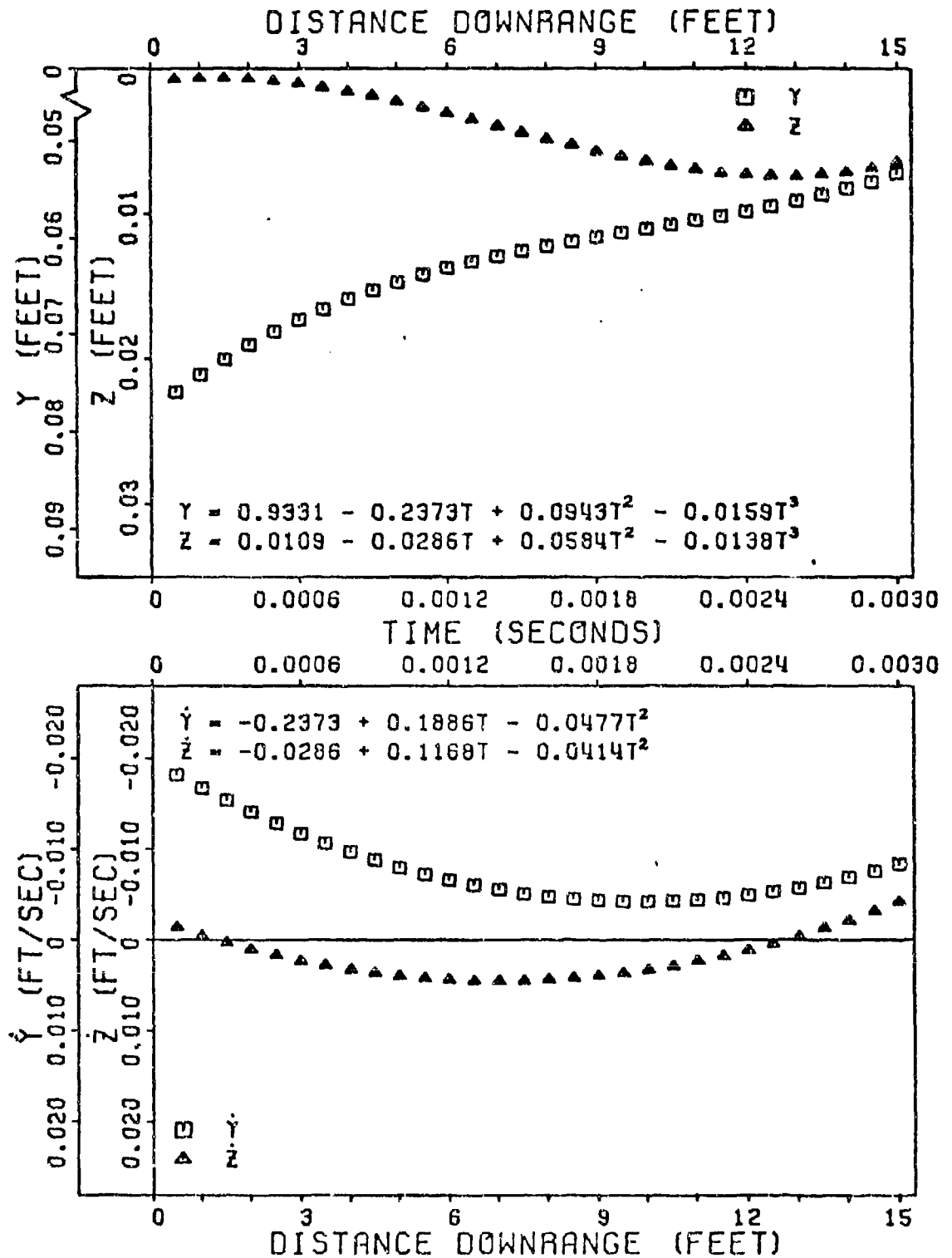


Figure 54. Fitted Translational Data Ground Point - Round 8

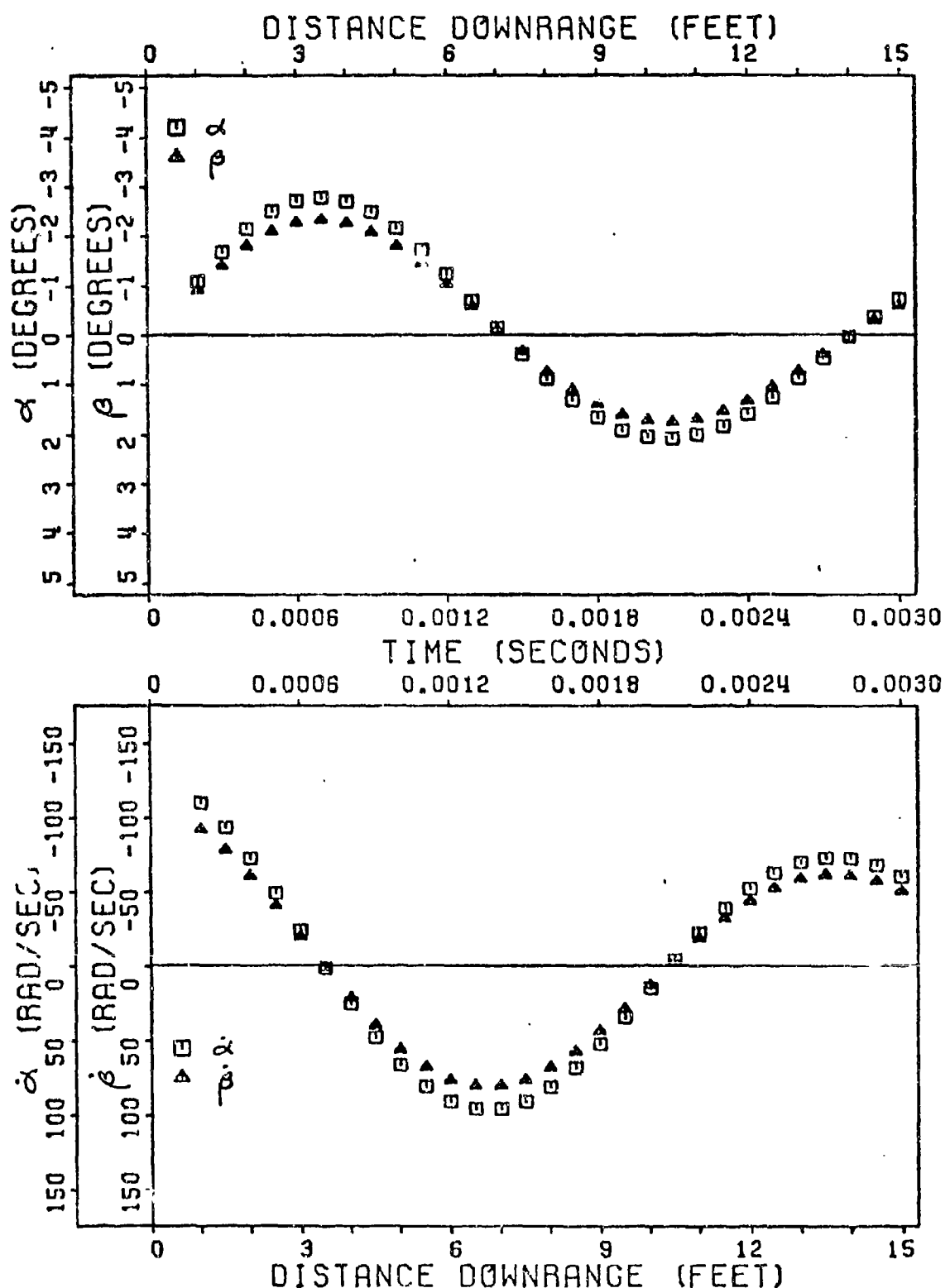


Figure 55. Fitted Angular Data Ground Point - Round 8

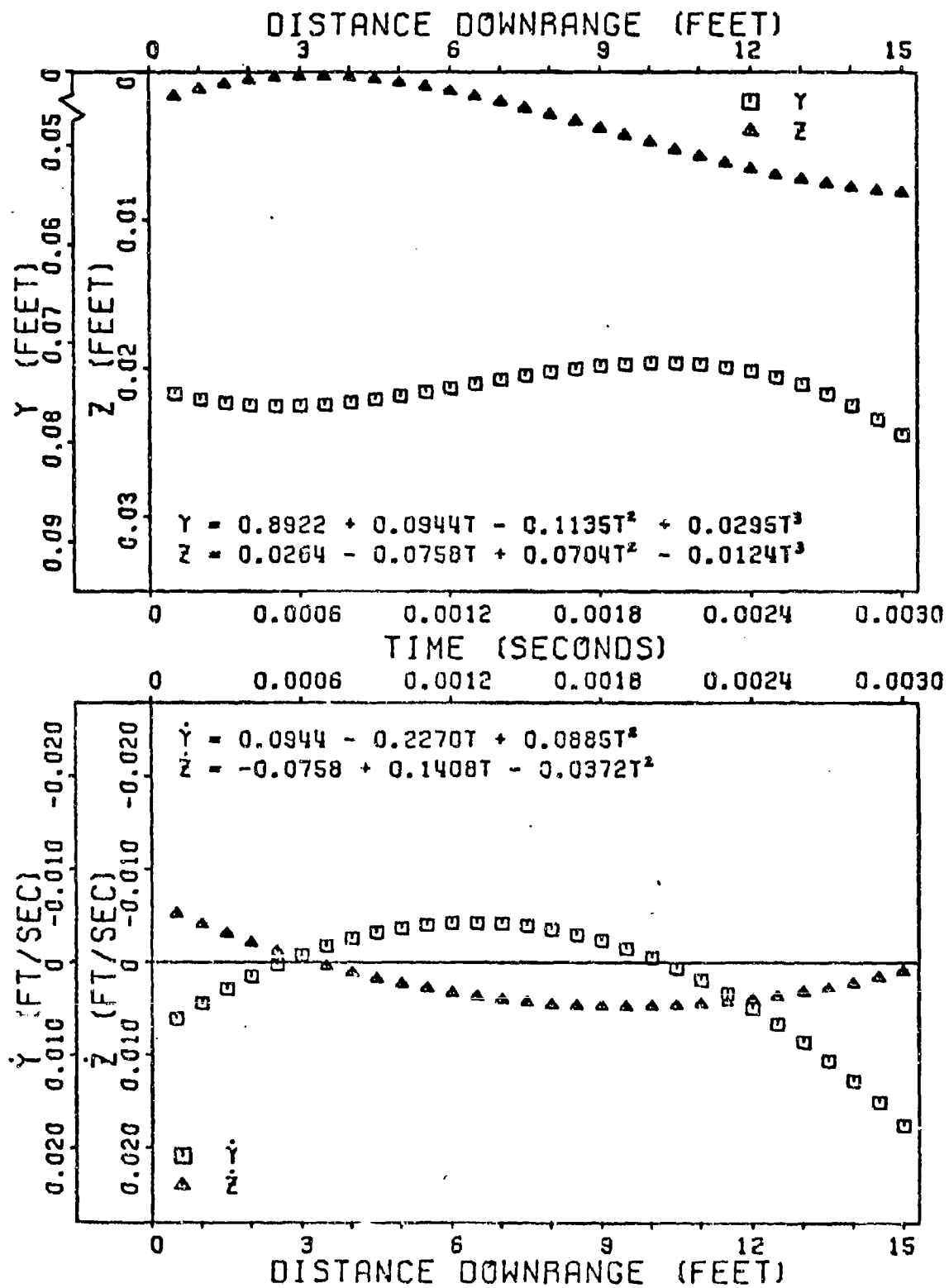


Figure 56. Fitted Translational Data Ground Point -- Round 14

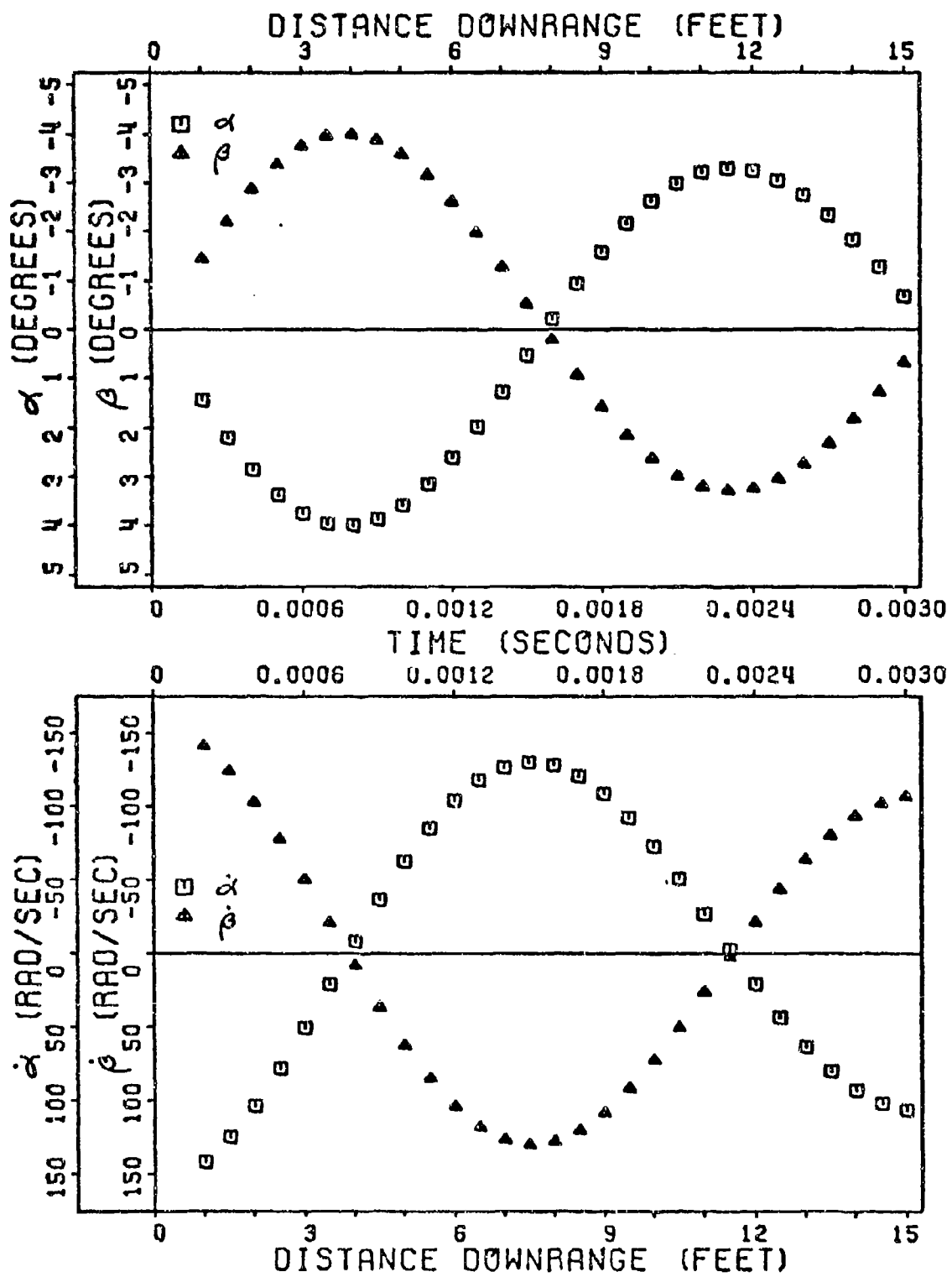


Figure 57. Fitted Angular Data Ground Point - Round 14

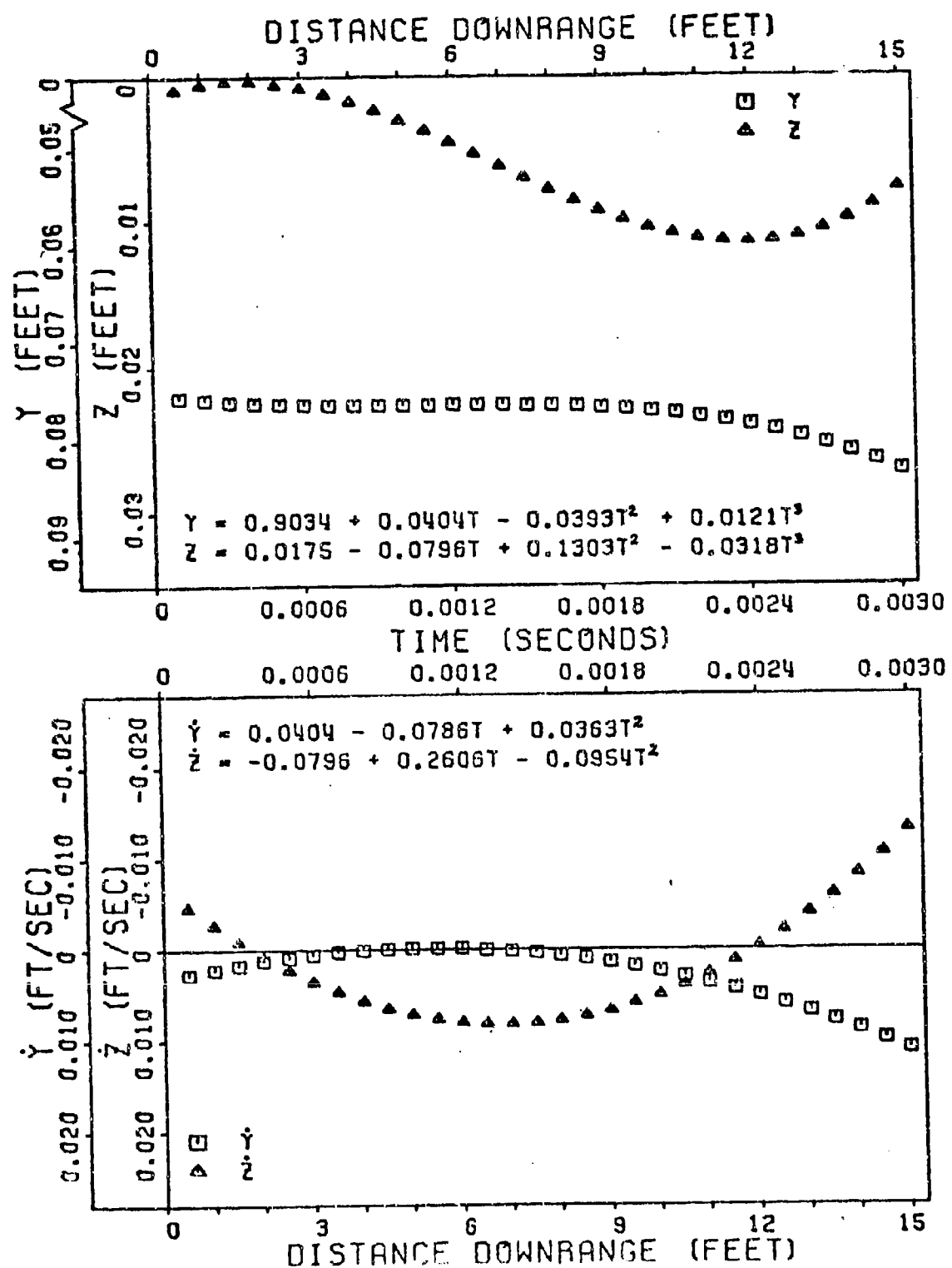


Figure 58. Fitted Translational Data Ground Point - Round 16

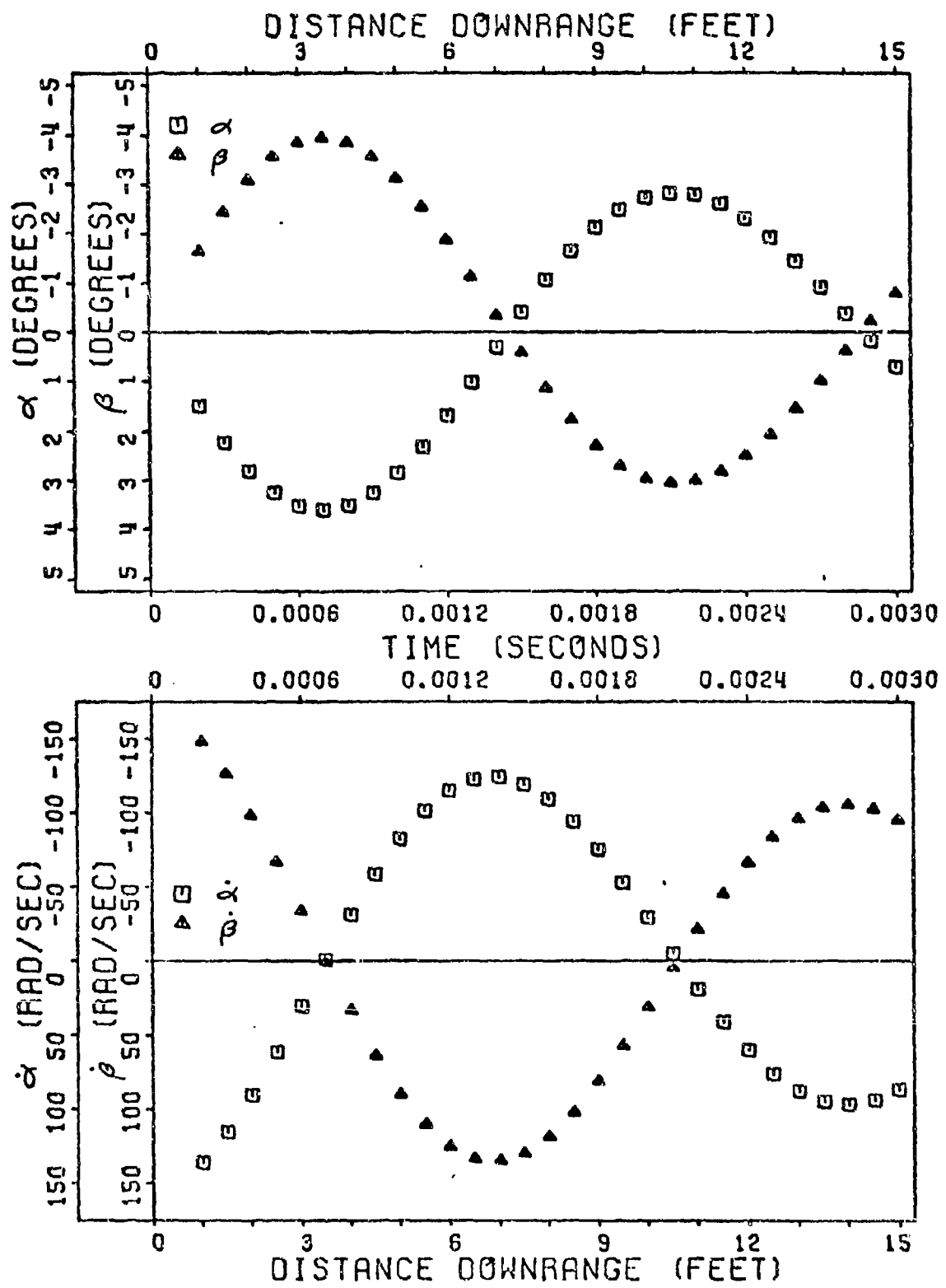


Figure 59. Fitted Angular Data Ground Point - Round 16

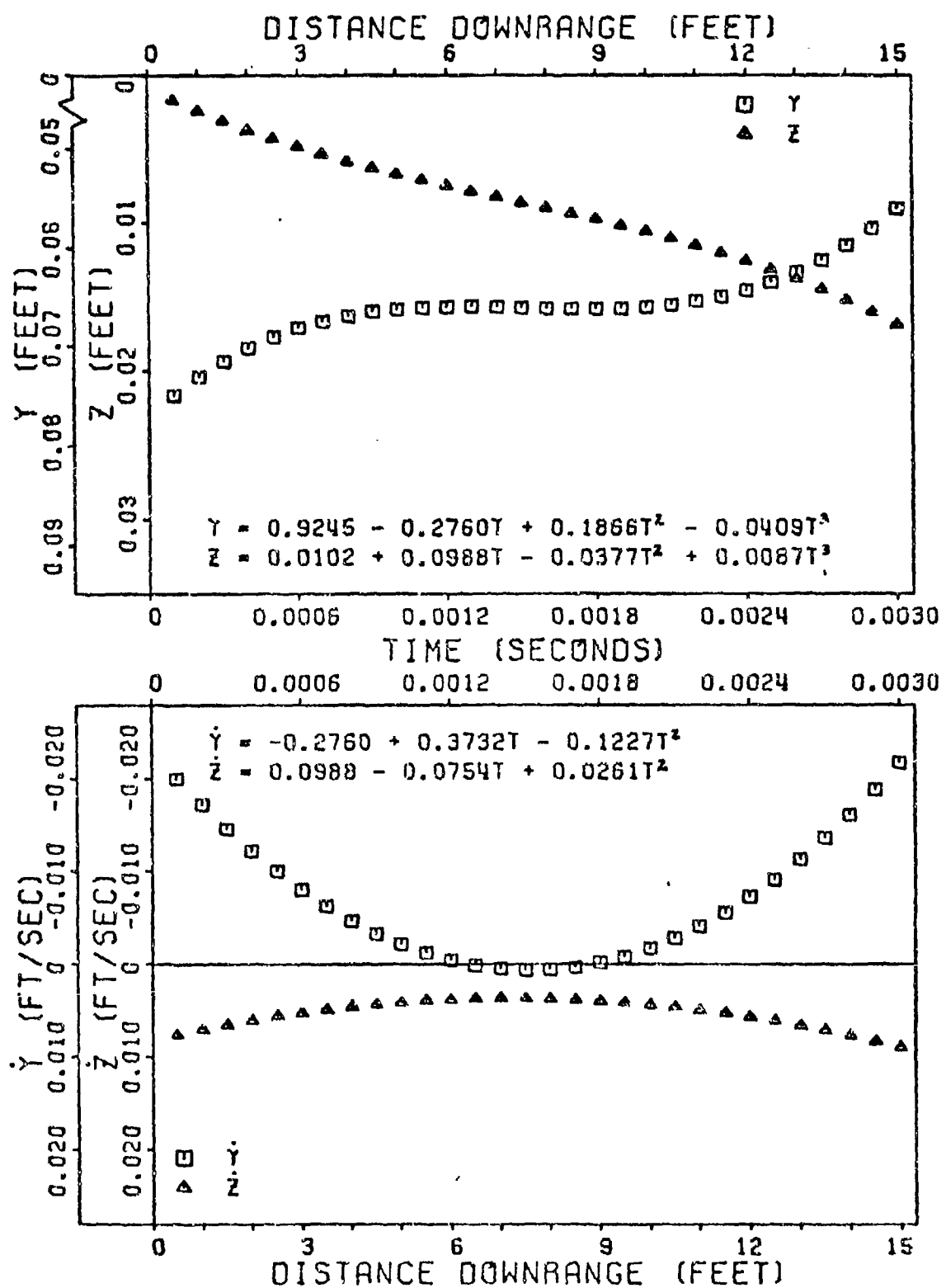


Figure 60. Fitted Translational Data Ground Point - Round 17

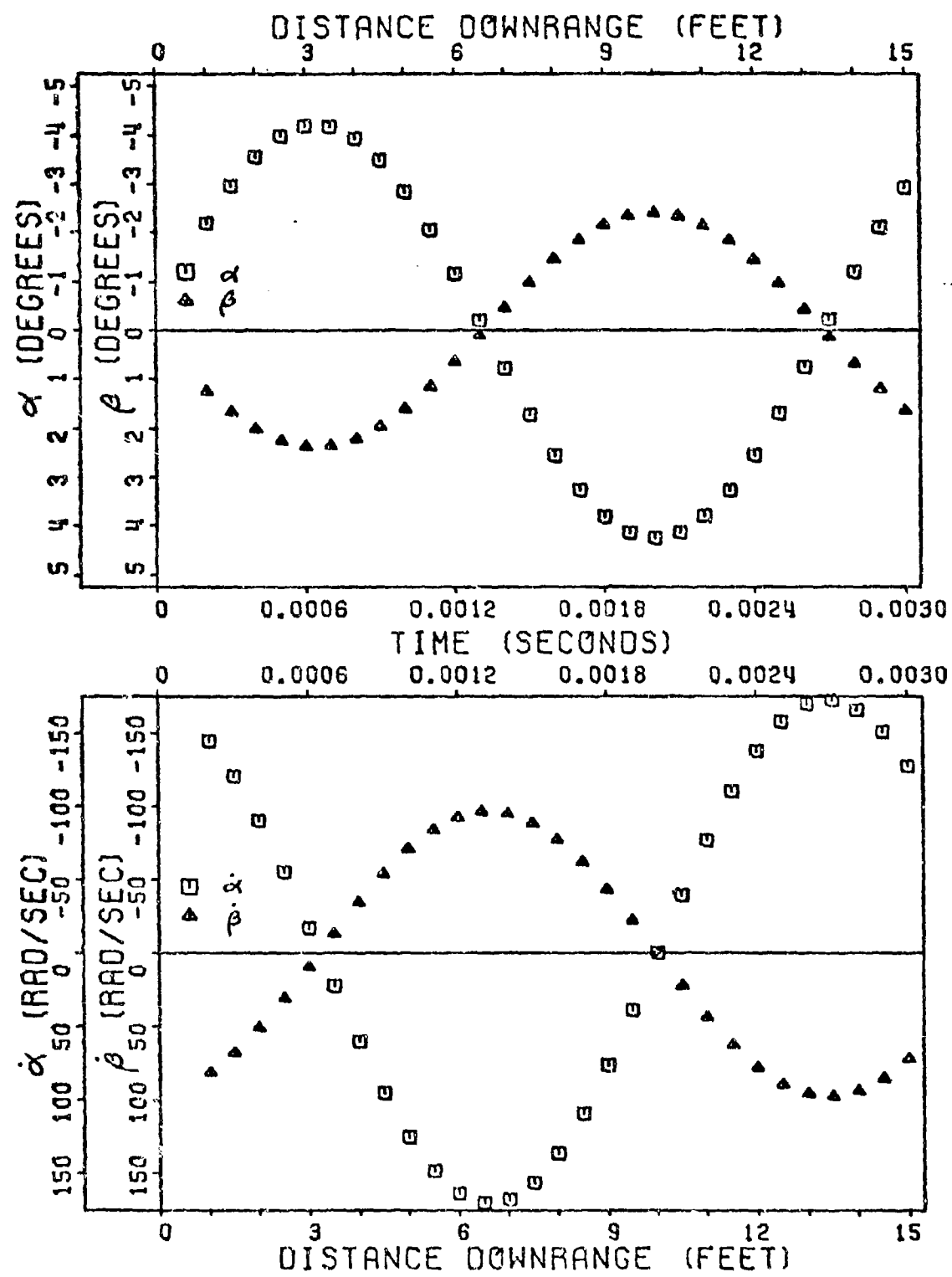


Figure 61. Fitted Angular Data Ground Point - Round 17

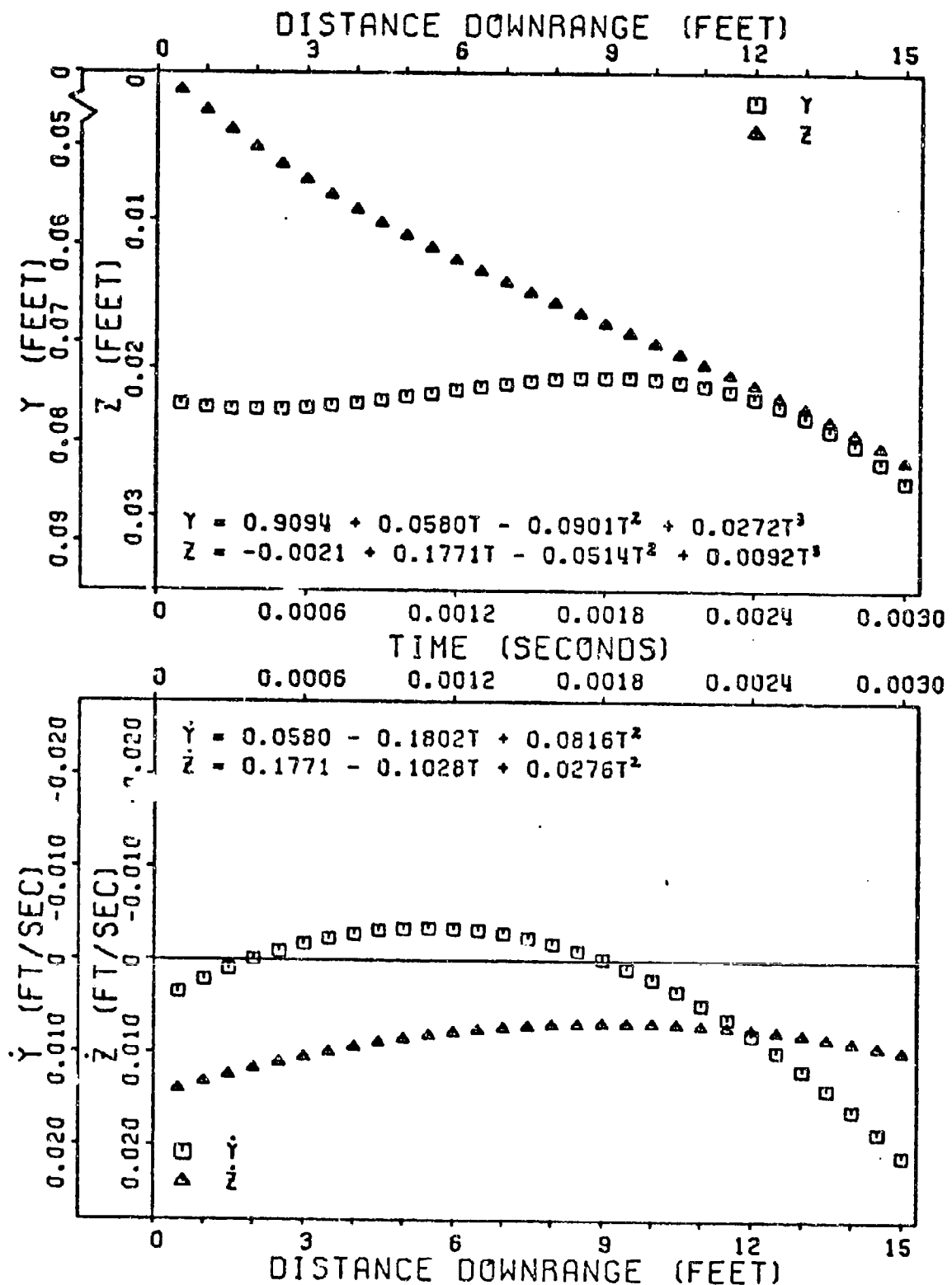


Figure 62. Fitted Translational Data Ground Point - Round 19

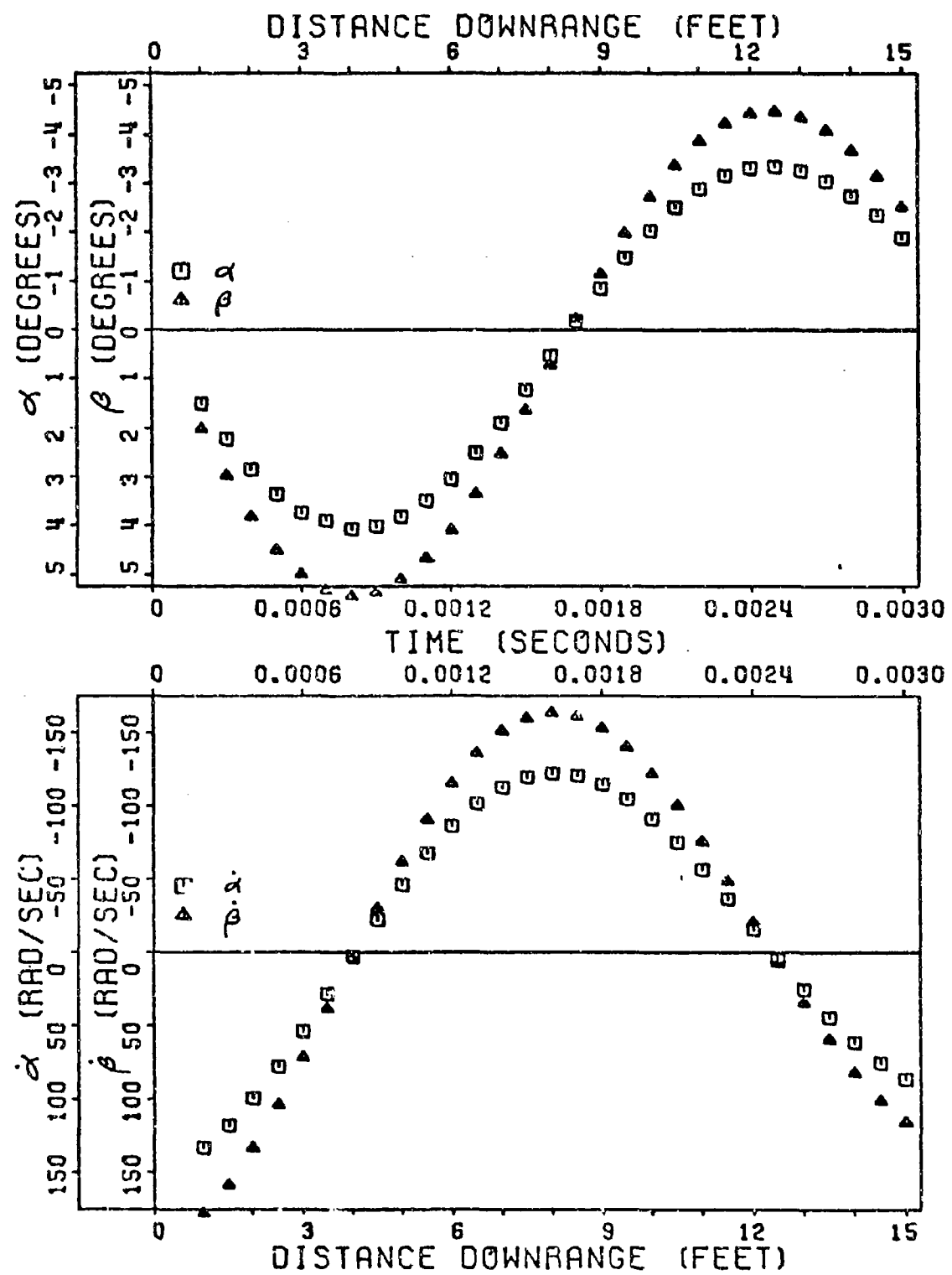


Figure 63. Fitted Angular Data Ground Point - Round 19

TABLE XXI
AERODYNAMIC PARAMETERS FROM LEAST SQUARES FIT

R O U N D	K ₁ (degrees)	λ (rad/sec)	ω (rad/sec)	δ (rad)
4	5.01	-49.48	1921.3	-1.29
6	3.64	68.24	2079.8	-1.21
7	-2.78	46.48	1871.4	-1.26
8	-4.02	-203.19	2267.6	-1.21
14	6.09	-126.37	2042.0	-1.23
16	5.84	-174.7	2211.7	-1.18
17	-4.81	8.53	2314.5	-1.02
19	7.35	-121.62	1889.9	-1.22

$$\alpha = K_1 e^{\lambda t} \cos(\omega t + \delta)$$

$$\dot{\alpha} = K_1 e^{\lambda t} \left[\lambda \cos(\omega t + \delta) - \omega \sin(\omega t + \delta) \right]$$

DISPERSION ANALYSIS

Free Flight vs Theory

Once the initial conditions are determined as in the previous section, they are applied to the theory and compared to the dispersion of each test fired round. To utilize the theory, the fitted data must be chosen for a given time; that is, \overrightarrow{S}_0 , $\overrightarrow{\dot{S}}_0$, $\overrightarrow{\alpha}_0$, $\overrightarrow{\dot{\alpha}}_0$ must be selected for one given point in time - position downrange. Since the question of what point in time do the initial conditions occur, 3 sets of initial conditions were chosen to correspond with positions 1, 3, 5 feet downrange. This span of position downrange may or may not be sufficient to include the actual time corresponding to the initial conditions for each round. The following analysis will determine each round's effective time for its initial conditions.

For each set of initial conditions, theory and 6-D computations were done and compared to target data for the Frankford test firings. The results are tabulated in Table XXII in mils and plotted in Figures 64-71 in feet; deviation from the time of fire at 50 ft. downrange. The relationship between the deviations in feet and mils at 50 ft. downrange is:

$$\overline{J.A.} \text{ (mils)} = \frac{\overline{S} \text{ (ft)}}{x} (1000)$$

or $\overline{J.A.} \text{ (mils)} = (20) \overline{S} \text{ (ft)}$

To accurately and concisely analyze the complex and large amount of data in Table XXII, the positions downrange in which the initial conditions were selected must be simultaneously analyzed with the dispersion results at 50 ft downrange. The problem in choosing initial conditions is where they should be taken; at what point downrange. Normally, one would think

TABLE XXII
DISPERSION ANALYSIS RESULTS

R O U N D	P O S I T I O N (ft)	D O W N R A N G E	Initial Conditions						Frankford Dispersion		Theory Dispersion		6-D Dispersion	
			u_0 (ft/sec)	ρ_0 (rad/sec)	\vec{S}_0 (ft)	\vec{s}_0 (ft/sec)	$\vec{\alpha}_0$ (deg)	$\vec{\dot{\alpha}}_0$ (rad/sec)	mils	mils	mils	mils	mils	mils
4	1	4747	11454	0.075968+	0.007415+	0.2045+	23.60+		2.333- 0.7501	2.451	1.329- 1.3021	1.861	1.300-	1.703
				0.0020881	0.0087401	1.37321	158.461				1.413- 0.5291	1.508	1.380-	1.461
				0.077840+	0.002359+	0.62734	11.54+				1.571+ 0.5781	1.674	1.520+	1.577
6	3	4662	13201	0.078183+	-0.000233+	0.6877+	-6.41		1.050- 0.2001	1.069	2.001- 0.9441	2.213	2.100-	2.293
				0.0052081	0.0070571	4.21251	77.571				1.709- 0.3901	1.753	1.760-	1.796
				0.0782921	0.0065581	4.61841	-43.041				1.268+ 0.5091	1.367	1.340+	1.361
7	5	4642	14219	0.076348+	0.002541+	-0.5633+	-54.86+		2.817- 0.0831	2.818	1.777- 0.6381	1.820-	1.820-	1.893
				0.0012951	0.0006311	1.15501	112.481				1.550- 0.2631	1.572	1.560-	1.573
				0.076799+	0.000704+	-1.5239+	-23.78+				1.285+ 0.5201	1.386	1.340+	1.358
8	1	4662	12998	0.075422+	-0.0121964	-0.3073+	-31.50+		1.067+ 1.9831	2.249	2.314+ 1.0181	2.527	2.000+	2.225
				0.0026311	0.0084721	0.79271	81.241				1.577+ 0.2421	1.596	1.600+	1.621
				0.0714734	-0.0076484	-0.89284	-17.09+				0.819- 0.5301	0.975-	0.980-	1.037
14	3	4756	13289	0.069225+	-0.003692+	-1.01384	7.18-		1.067+ 0.3171	1.113	2.727- 1.1921	2.976	2.620-	2.804
				0.0052081	0.0046921	2.30271	44.081				1.917- 0.4421	1.967	1.960-	1.993
				0.066436+	-0.011776+	-2.2737-	-20.06-				0.917+ 0.5501	1.069	1.280+	1.310
16	5	4753	17354	0.075365+	0.004378-	-1.4392+	-141.45+		1.683- 0.0831	1.685	2.790- 1.1681	3.024	2.740-	2.884
				0.0011631	0.0040941	1.43941	141.471				1.762- 0.2751	1.784	1.960-	1.983
				0.076196-	-0.000828-	-3.7492+	-50.31+				0.699+	1.037	1.000+	1.093
17	1	4677	16613	0.076383+	-0.000158+	-3.1123+	89.81-		1.400- 0.3831	1.451	2.790- 1.3851	3.024	2.740-	2.884
				0.0030331	0.0071331	2.85221	82.311				1.342+ 0.3181	1.379	1.180+	1.223
				0.073036+	-0.0171894	1.2395-	81.70-				1.996- 0.9151	2.195	1.860-	1.931
19	3	4679	11913	0.0764681	0.002102+	2.0237+	178.11+		1.783+ 1.1831	2.140	-0.063- 1.0631	1.065	0.180-	0.937
				0.0026111	0.0131371	1.51141	133.021				0.849- 0.2371	0.881	0.780-	0.805
				0.0764704	-0.0017294	5.0161+	72.16+				2.010+ 0.7231	2.136	1.620+	1.728

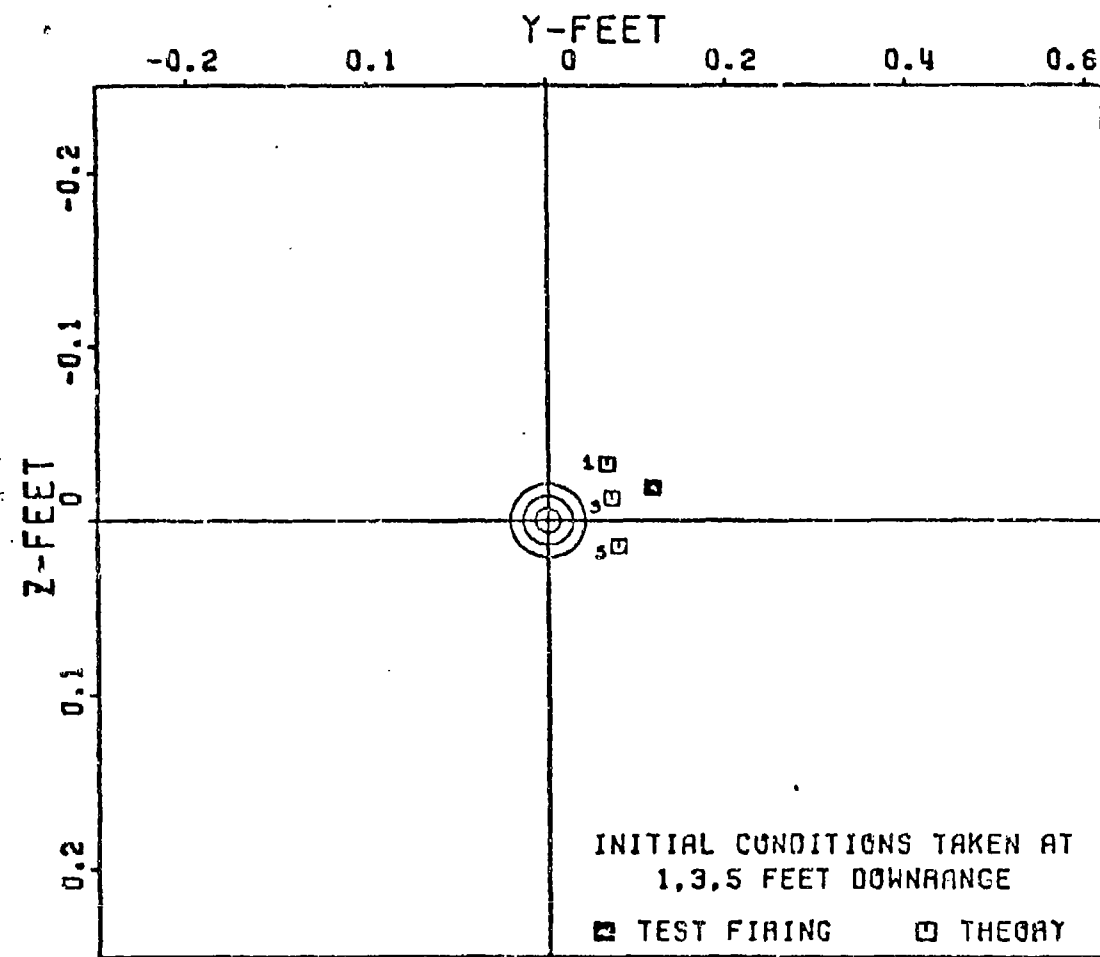


Figure 64. Dispersion: Ground Point - Round 4 Test Firing vs Theory,
at 50 ft. Downrange

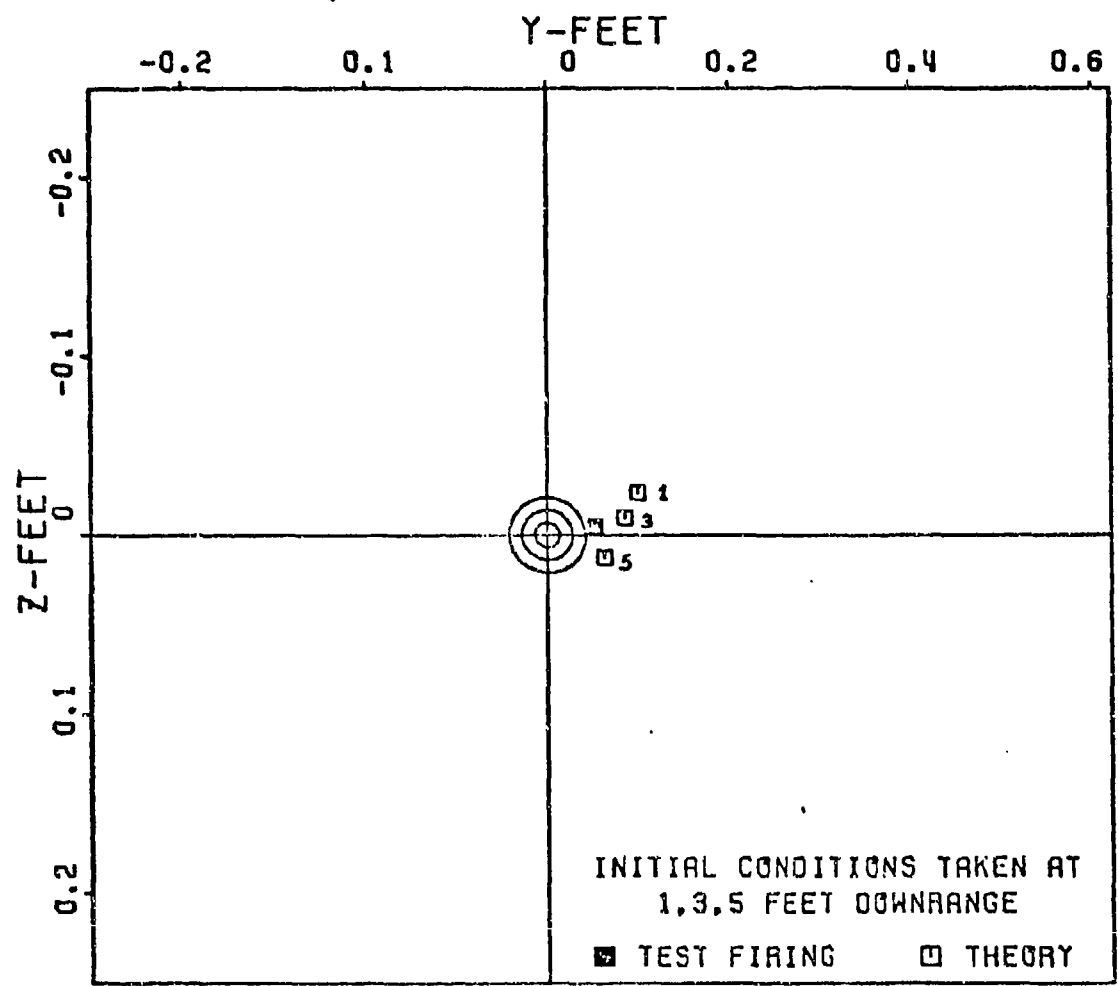


Figure 65. Dispersion: Ground Point - Round 6 Test Firing vs Theory,
at 50 ft. Downrange

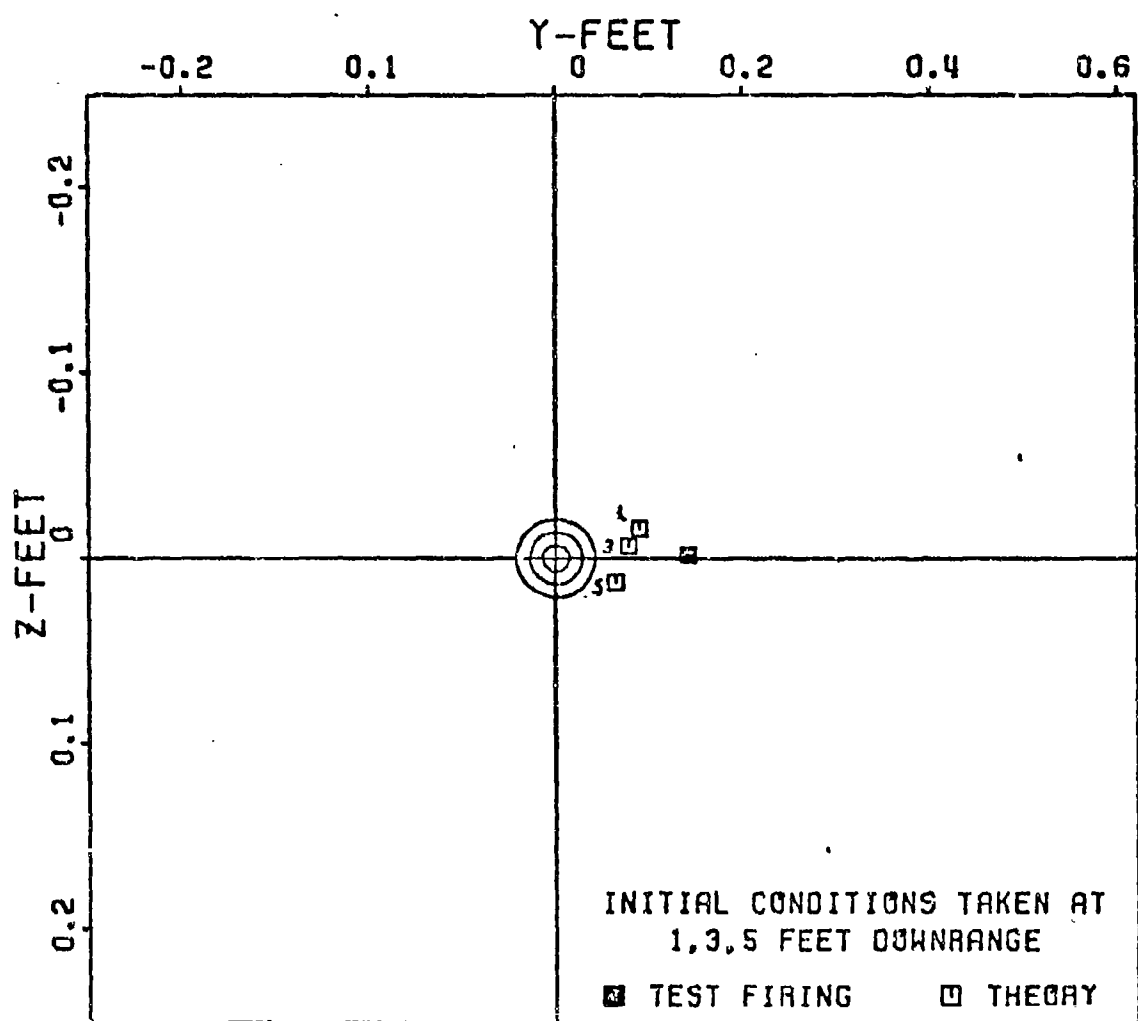


Figure 6. Dispersion: Ground Point - Round 7 Test Firing vs Theory,
at 50 ft. Downrange

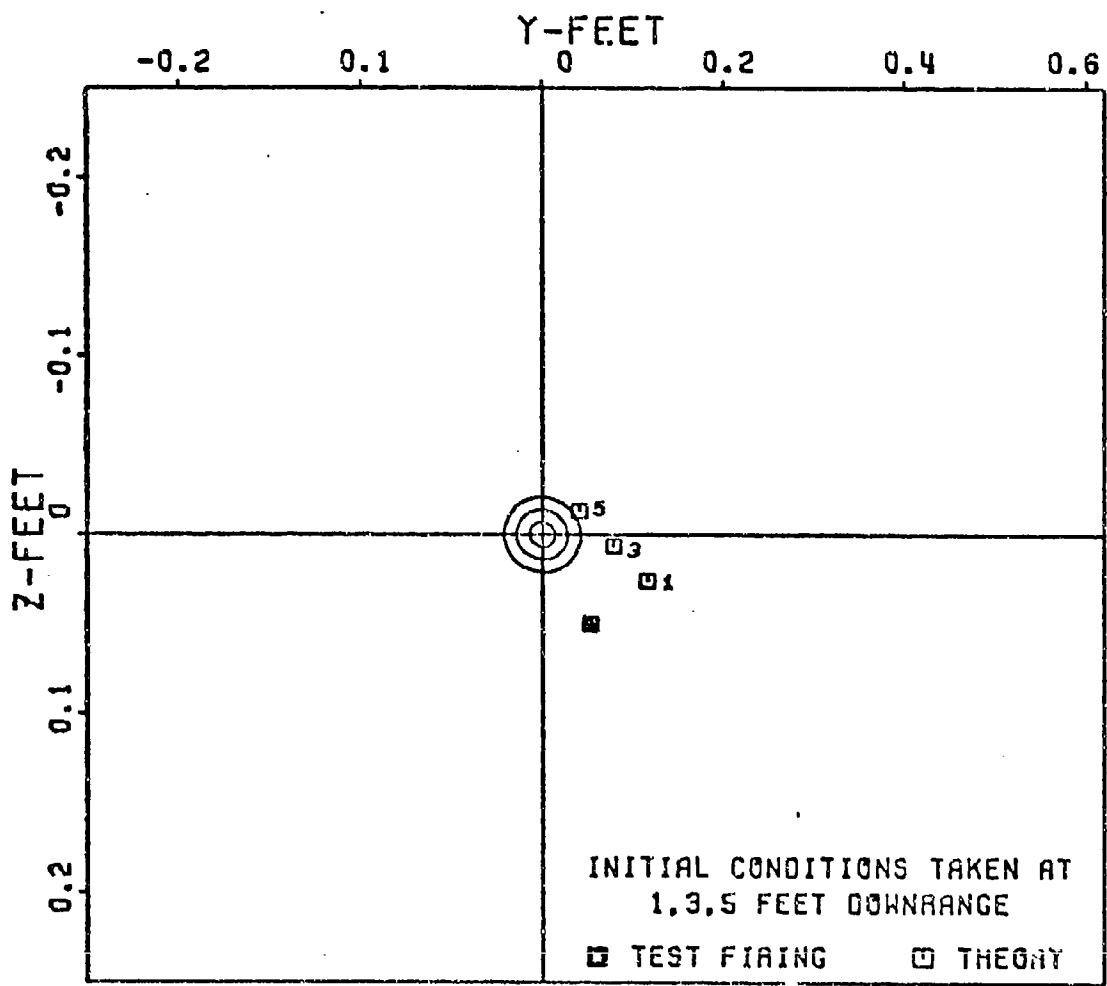


Figure 67. Dispersion: Ground Point - Round 8 Test Firing vs Theory,
at 50 ft. Downrange

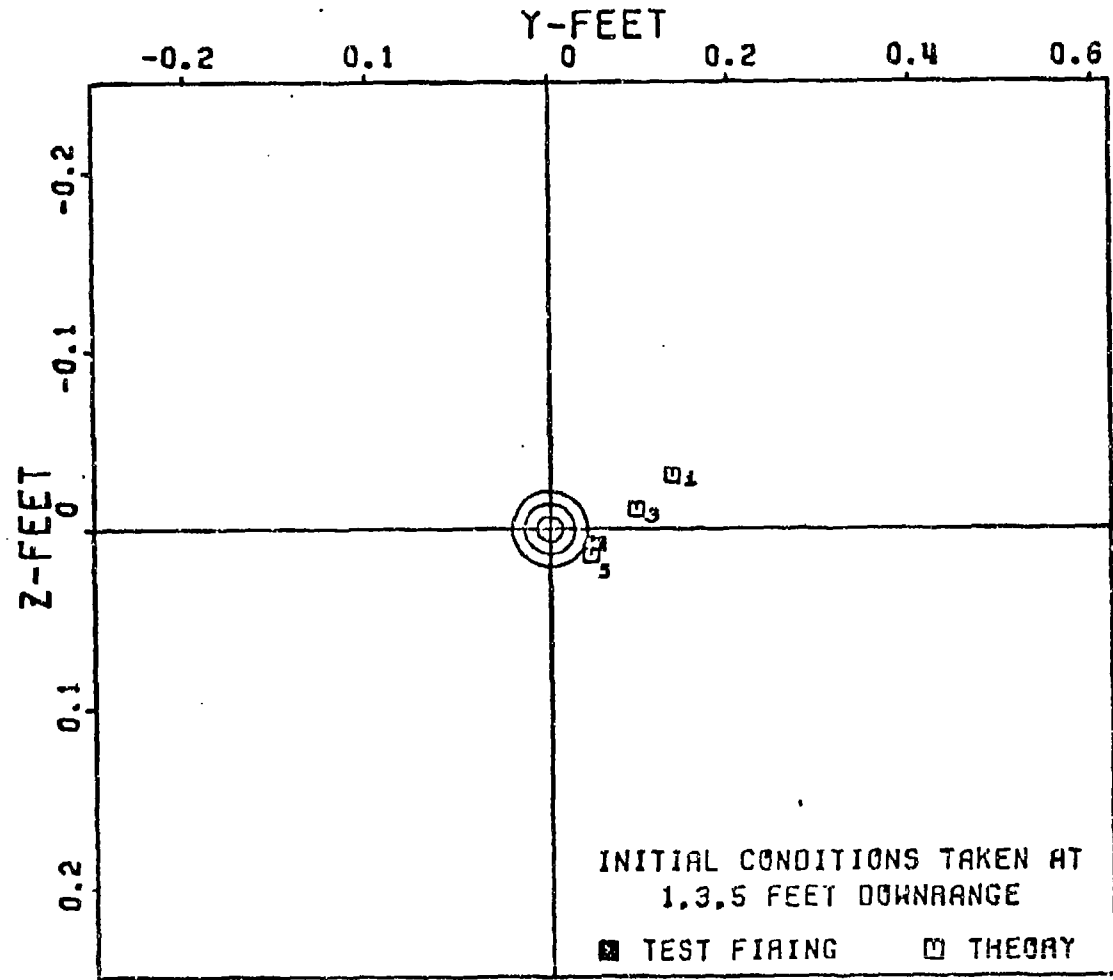


Figure 68. Dispersion: Ground Point - Round 14 Test Firing vs Theory,
at 50 ft. Downrange

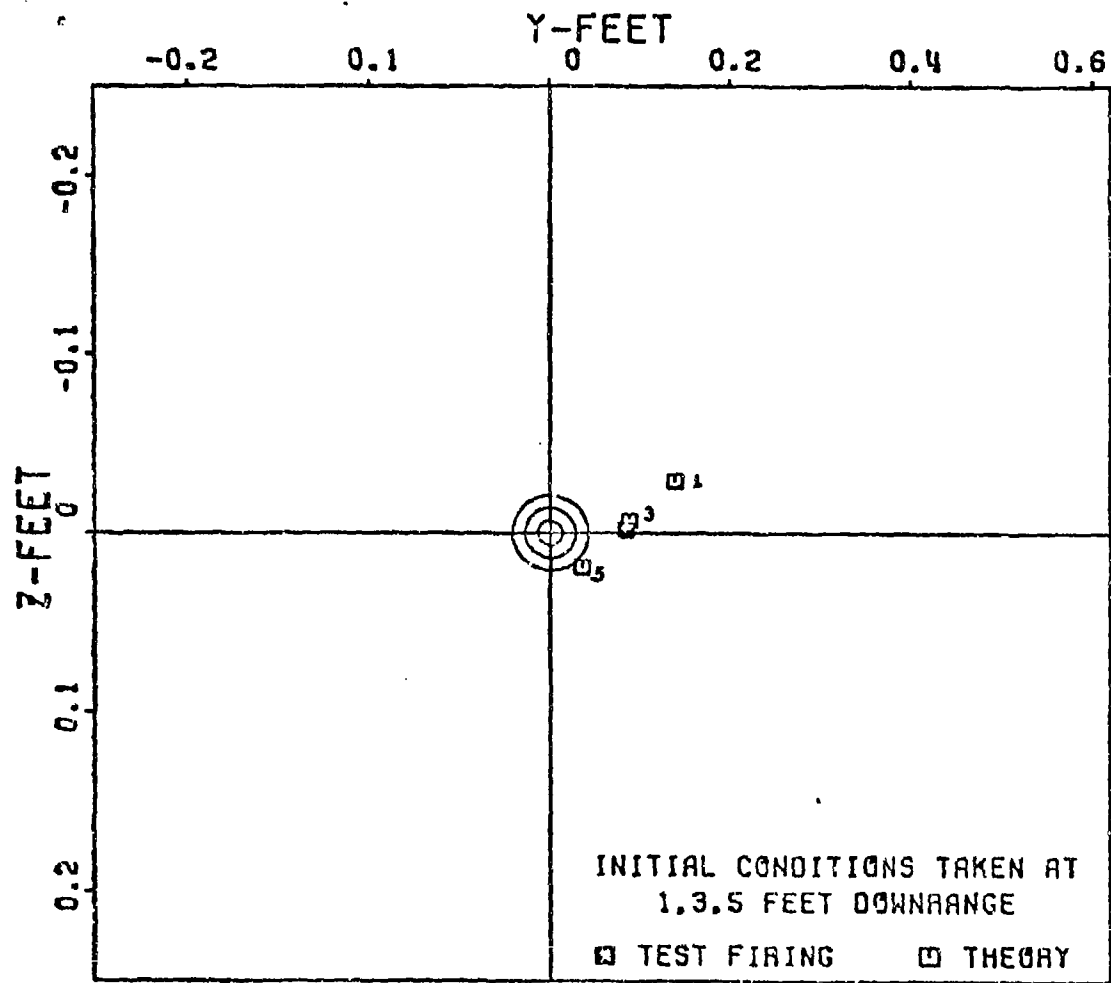


Figure 69. Dispersion: Ground Point - Round 16 Test Firing vs Theory,
at 50 ft. Downrange

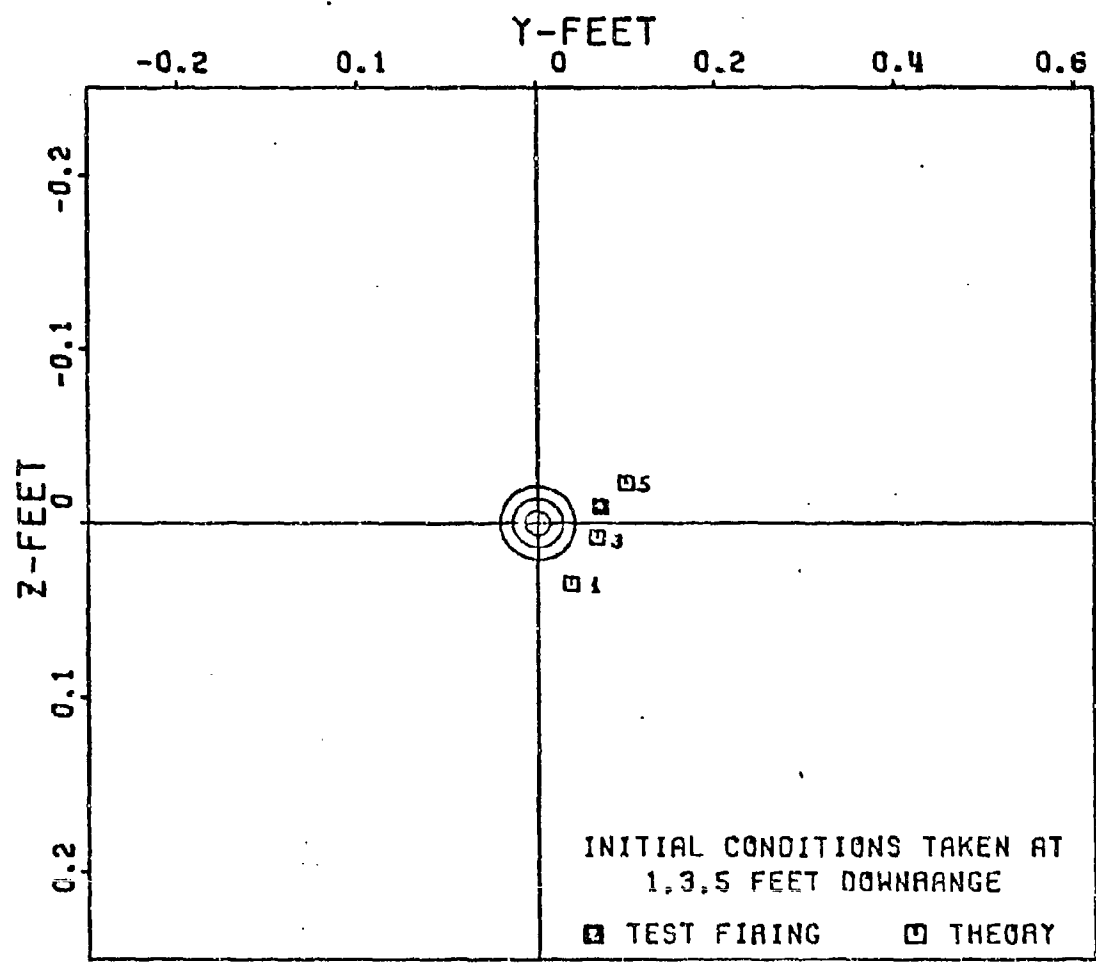


Figure 70. Dispersion: Ground Point - Round 17 Test Firing vs Theory,
at 50 ft. Downrange

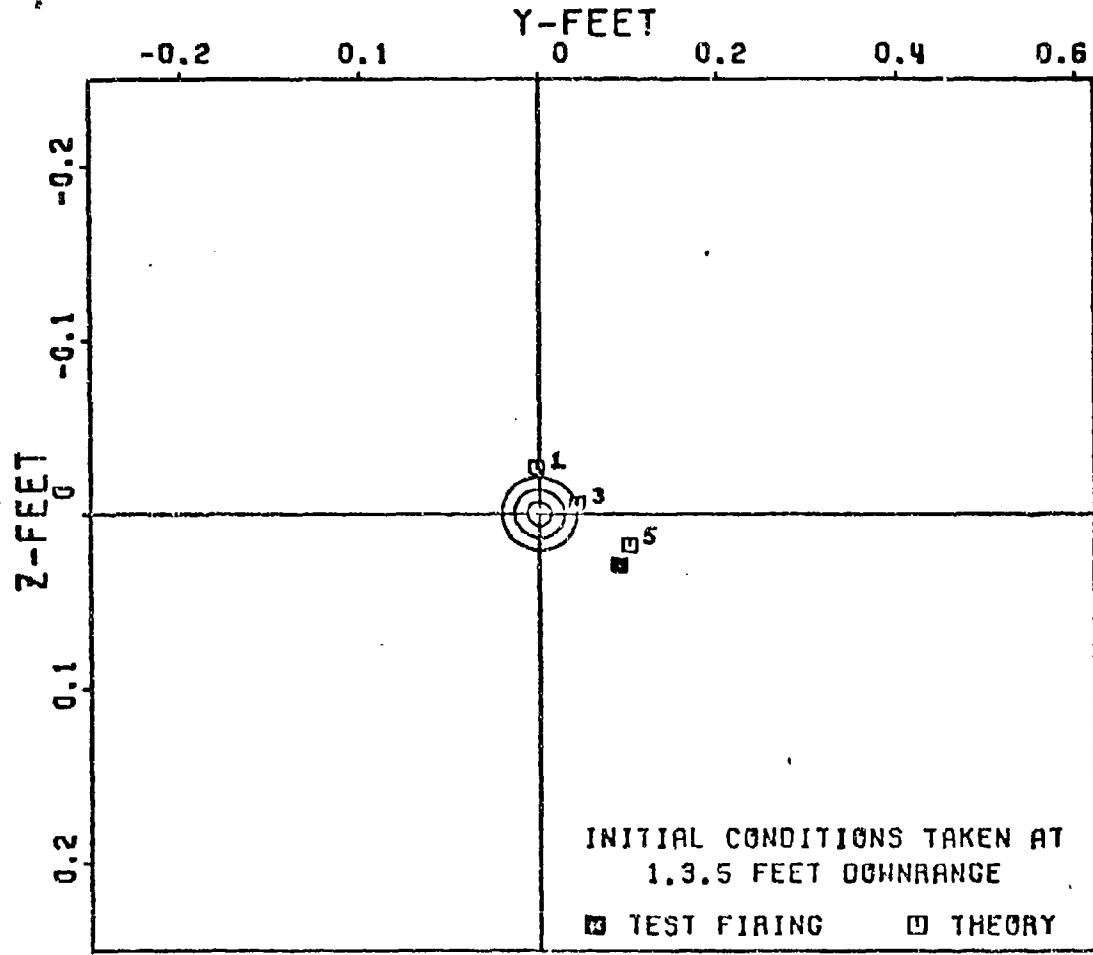
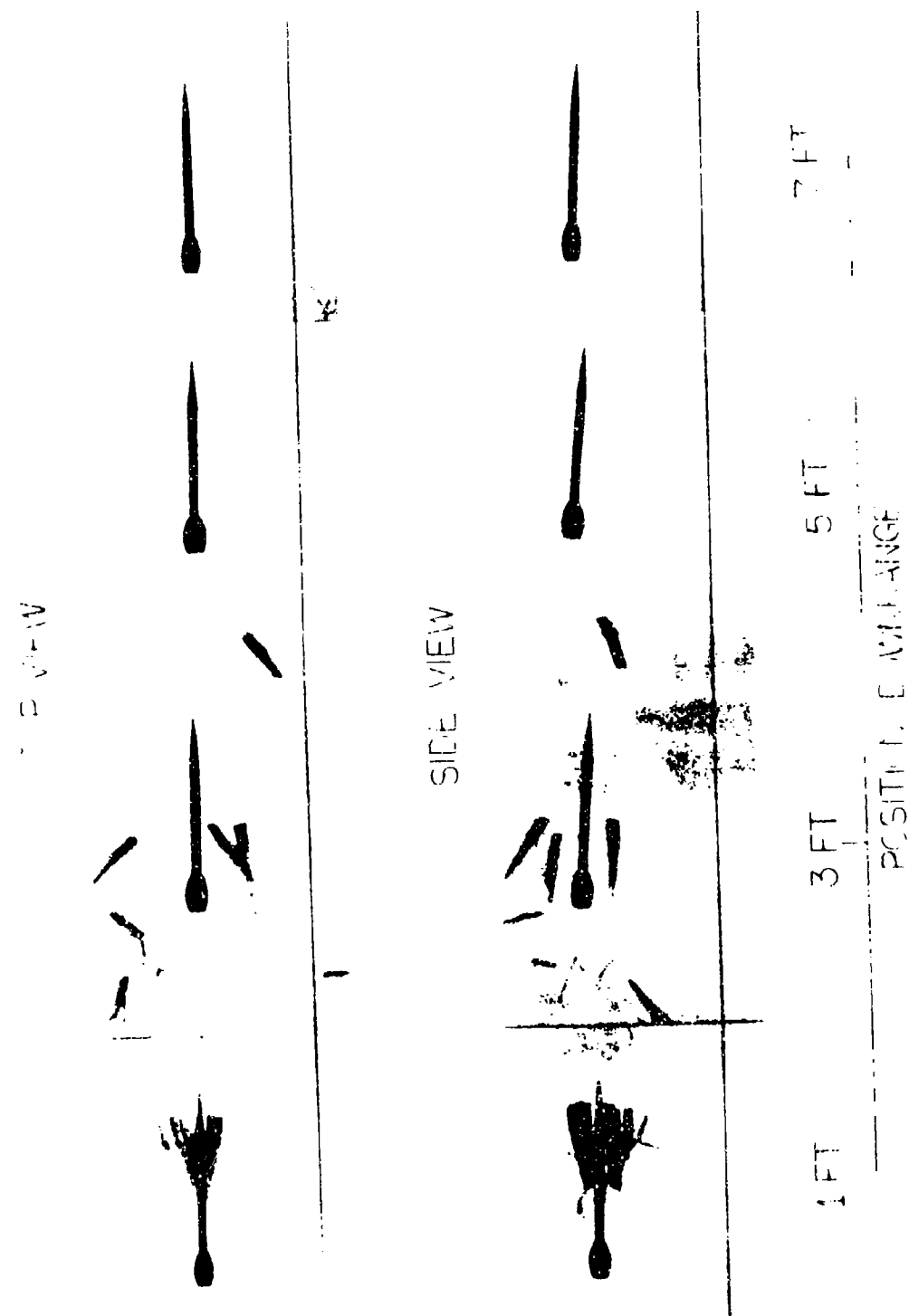


Figure 71. Dispersion: Ground Point - Round 19 Test Firing vs Theory,
at 50 ft. Downrange

that the initial conditions would occur immediately after leaving the gun barrel. However, the flechette being a finned body needs a sabot configuration to guide it down the barrel, Figure 29. The sabot causes the initial condition location problem since the sabot must separate from the flechette outside of the gun barrel. The exact time and place where this occurs is not constant; varying from round to round. Not only does the sabot separate from the flechette instantaneously different every time, the sabot may not separate cleanly or the same way every time. Interference with the fins after sabot separation can cause disturbances to the flechette and alter the initial conditions. In addition, asymmetric sabot separation can influence the initial conditions. Figures 72-79 illustrate the flight transition sequence for the 8 flechette test rounds. In every sequence the sabot begins to separate, in varying degrees, 1 ft. downrange. At 3 ft. downrange, the sabot is nearly completely separated, but in some cases the sabot particles pose interference problems with the fins. By 5 and 7 ft. downrange the sabot has completely separated and the flechette is in free flight. The correspondence between the flight transition sequence and dispersion results can be seen in each individual round. Figure 64 indicates that the initial conditions for round 4 occur somewhere between 1 and 3 ft. downrange judging by the dispersion of the actual tested round. Figure 72 verifies this fact in that the sabot has separated from the flechette between 1 and 3 ft. downrange. The y-coordinate in the dispersion vector does not

Figure 72. Flight Transition Sequence - Round 4



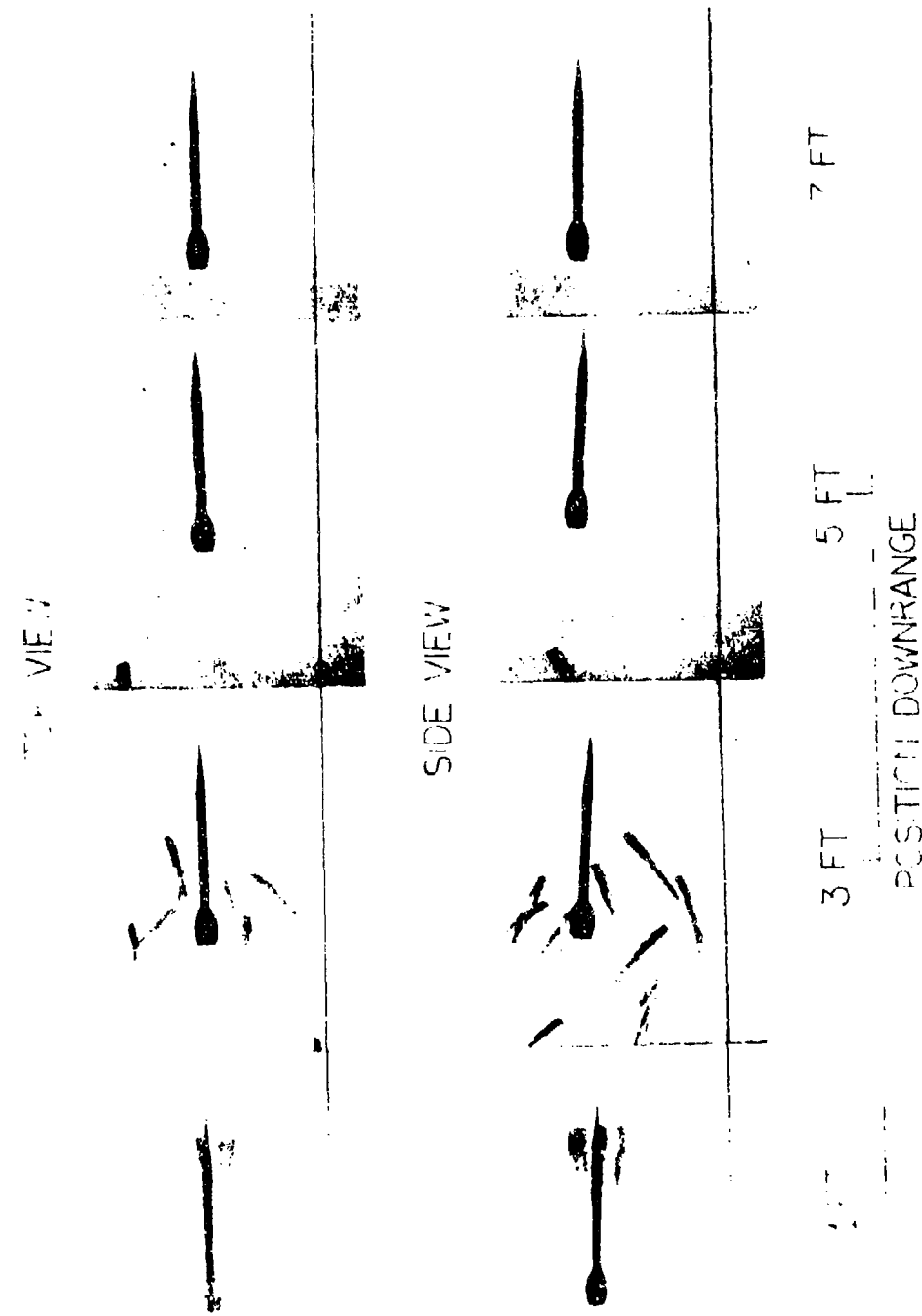
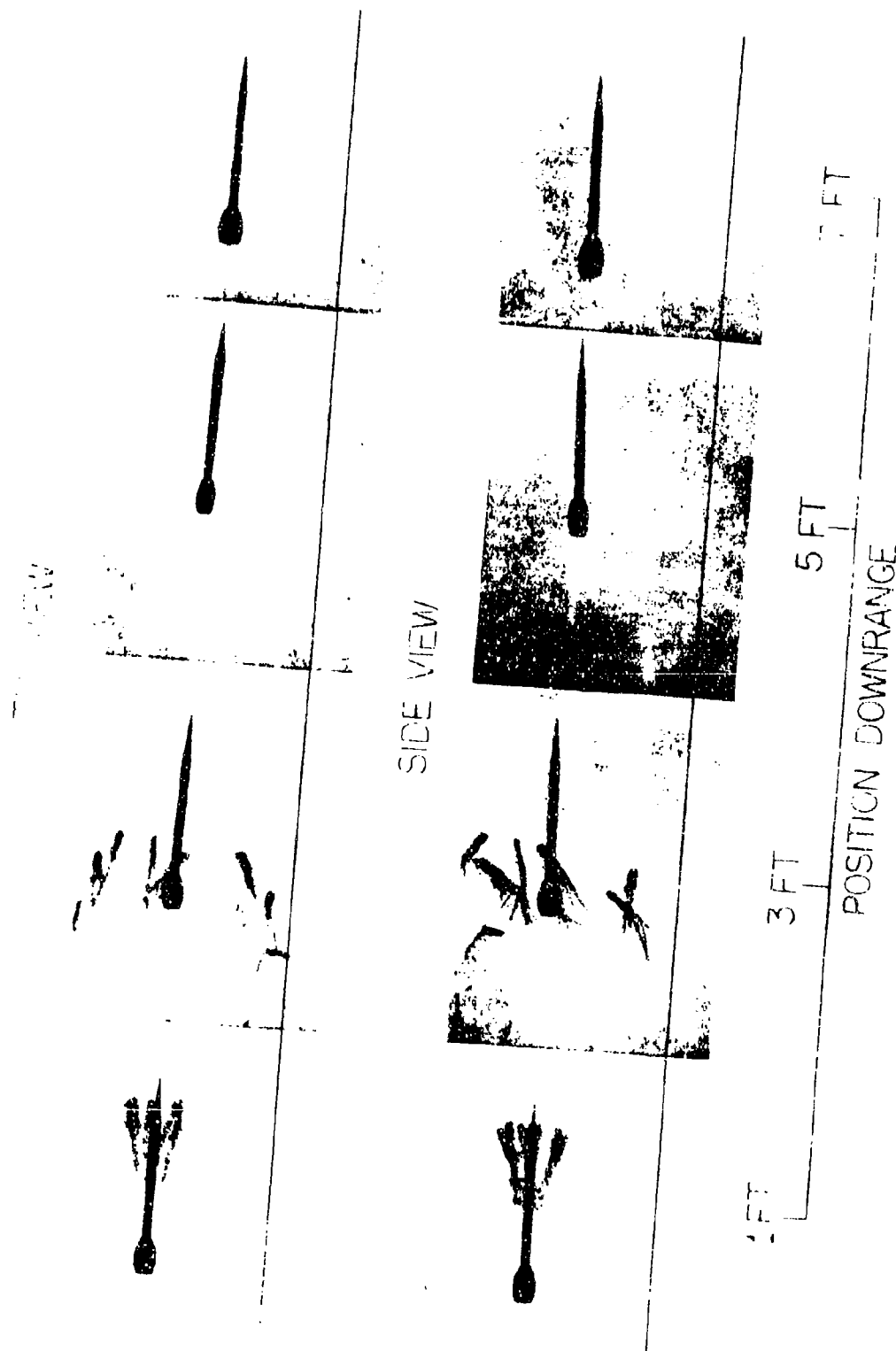


Figure 73. Flight Transition Sequence - Round 6

Figure 74. Flight Transition Sequence - Round 7



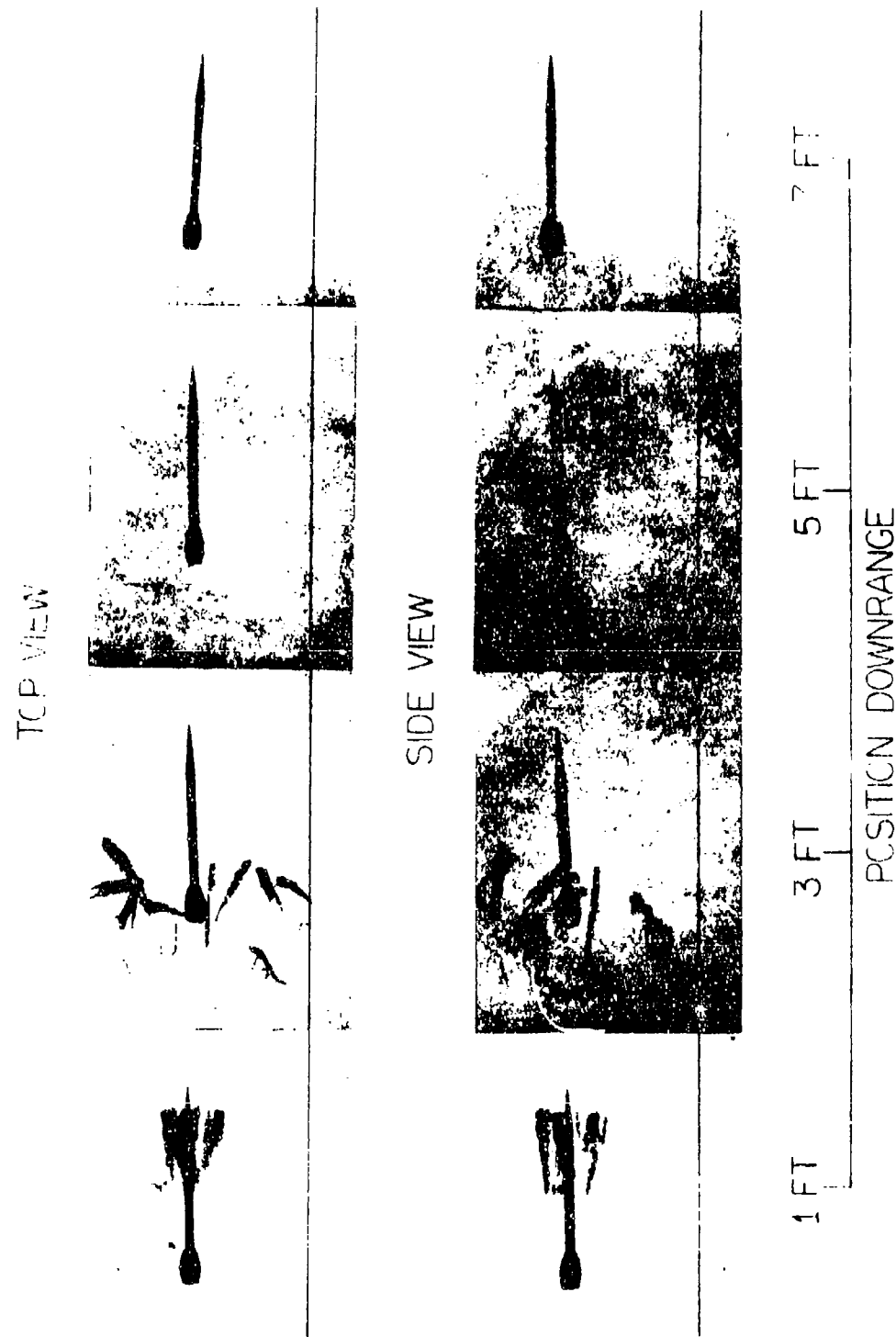


Figure 75. Flight Transition Sequence - Round 8

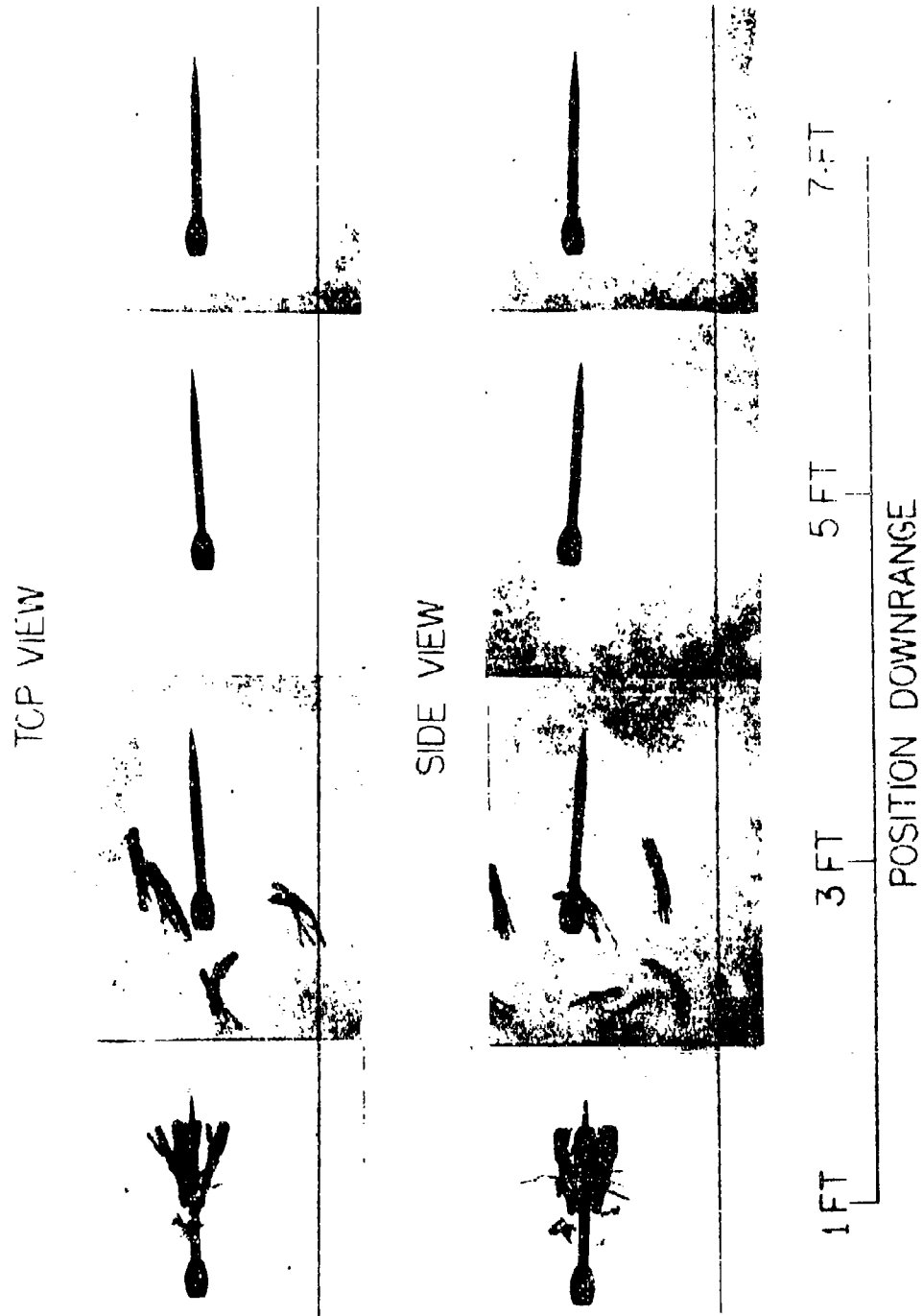


Figure 76. Flight Transition Sequence - Round 14

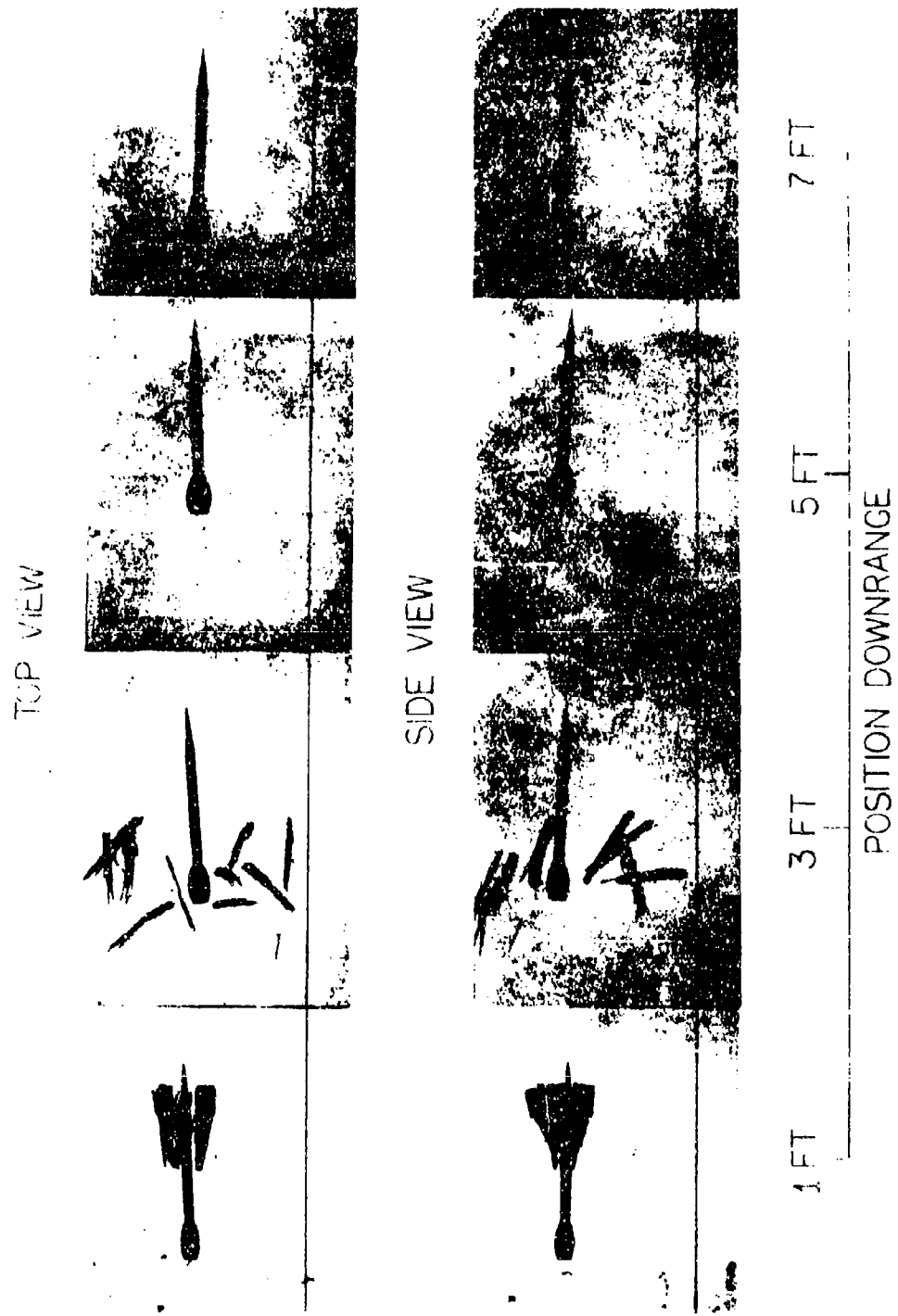


Figure 77. Flight Transition Sequence - Round 16

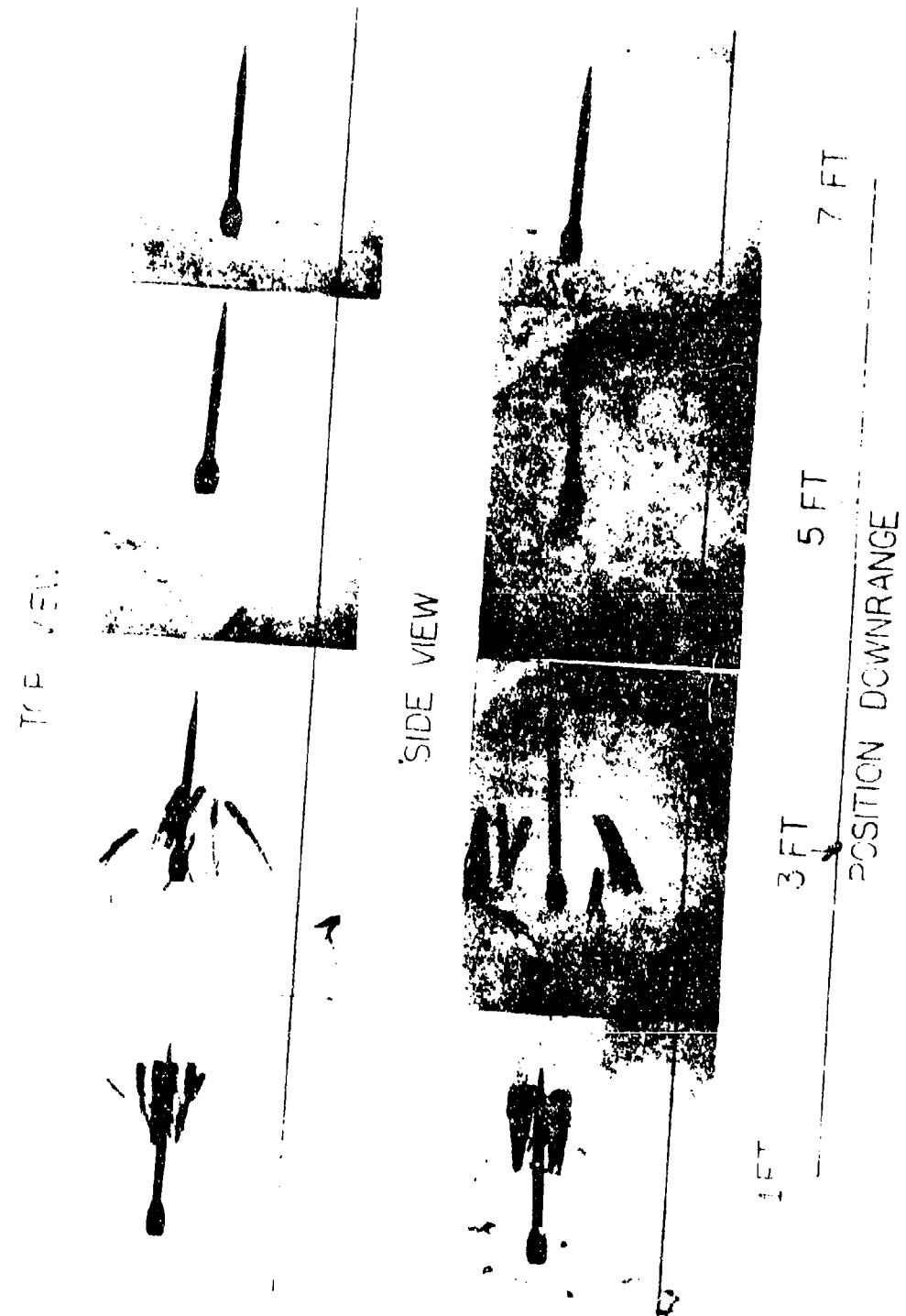


Figure 78. Flight Transition Sequence - Round 17

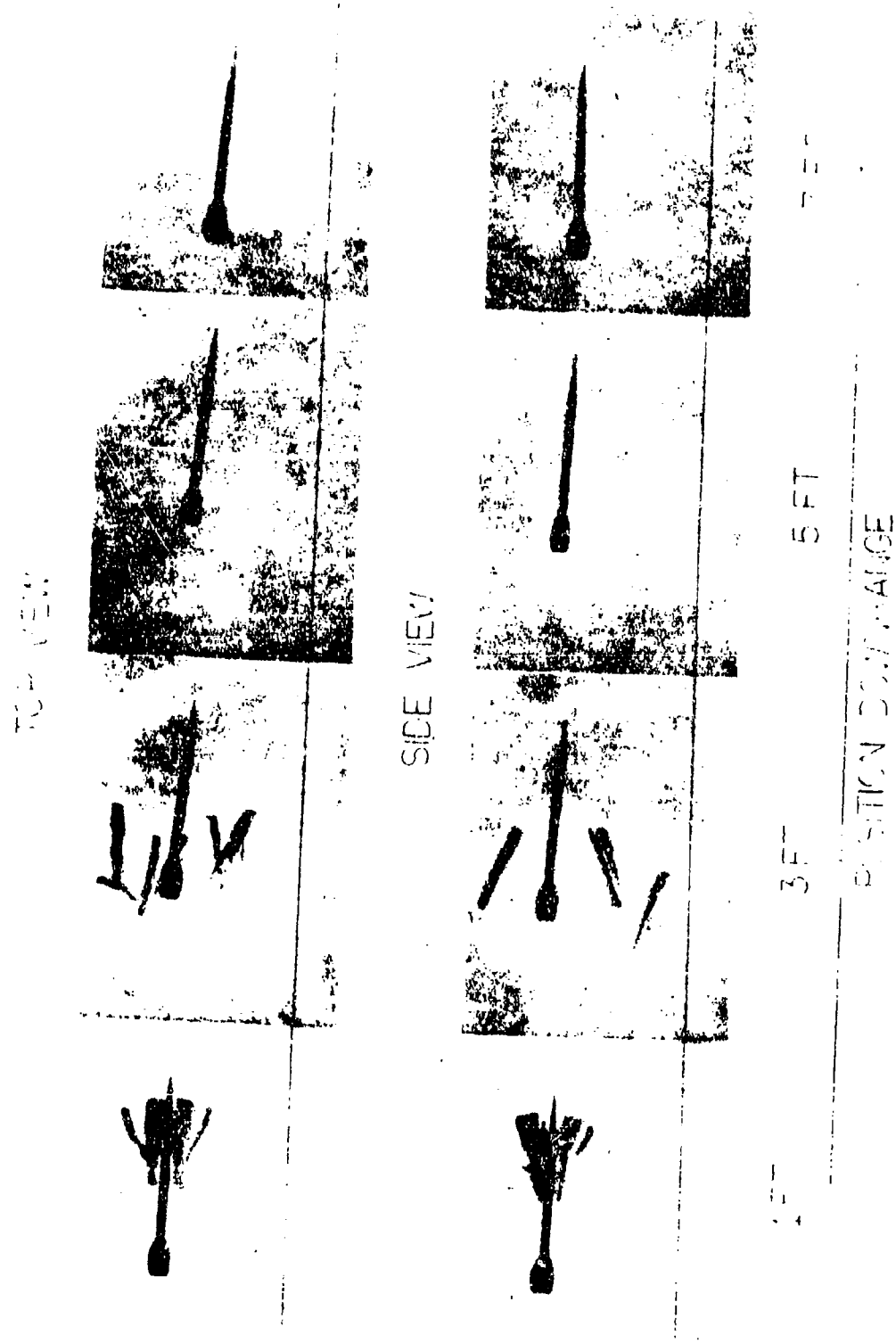


Figure 79. Flight Transition Sequence - Round 19

accurately agree with the theory for this case. However, besides computational error other physical factors can influence dispersion. Contributions by fin asymmetries and other configurational asymmetries can be important but are unable to be detected or accounted for. Throughout this analysis this must be kept in mind to partially account for any discrepancy between the actual test firing and the theory and 6-D computations. Figure 65 indicates the initial conditions for round 6 occur between 3 and 5 ft. downrange. Figure 73 verifies this choice showing separation occurring around 3 ft but with sabot particles very close to the fins causing possible interference and delaying the initial conditions location. The initial conditions location for round 7 is difficult to accurately choose since the y-coordinate does not accurately agree, Figure 66. It is safe to say that the initial conditions occur sometime around 3 ft and Figure 74 verifies this choice. The z-coordinate for round 8 is not as accurate as would be desired, Figure 7, but the y-coordinate indicates initial conditions occurring between 3 and 5 ft downrange. Figure 75 agrees with this choice indicated interference with the fins at 3 ft delaying the initial conditions. Initial conditions for round 14 are chosen between 3 and 5 ft. downrange, Figure 68. Figure 76 indicates possible fin interference tending to verify the choice. Figures 69 and 77 indicate and verify the choice of initial conditions in the immediate vicinity of 3 ft downrange for round 16. Possible fin interference at 3 ft downrange, Figure 78, round 17, verifies a choice of initial conditions between 3 and 5 ft, Figure 70. A similar situation occurs for round 19 in Figures 71 and 79. It is often difficult to

choose initial condition positions accurately due to slight discrepancies between theory and test firings. However, the discrepancies are of the order 0.05 ft, which shows up large in Figures 64-71 due to the scale chosen, but is within the error expected from the validation of theory section.

The influence of sabot separation can be readily seen by inspection of Figures 72-79, 1 and 3 ft downrange. In every case, the flechette and sabot are at nearly a zero angle of attack at 1 ft, but has changed angle of attack noticeably by 3 ft downrange. This would indicate that fin interference or asymmetric sabot separation is causing the noticeable effect. It can be concluded that dispersion is dependent upon the initial conditions that the initial conditions are a function of sabot separation and that the theory can predict what the initial conditions are and where they occur.

Dispersion Theory vs. First Maximum Yaw Hypothesis

A popular theory to predict the dispersion of flechettes is the First Maximum Yaw Hypothesis. This theory relates the dispersion magnitude to the first maximum yaw magnitude by a nearly linear relationship. Other initial conditions such as angular rate, $\dot{\alpha}_0$ and translational velocity, \dot{S}_0 are said not to effect dispersion. To disprove this theory and strengthen the position of the theory ascribing to dispersion due to initial conditions \dot{S}_0 , $\dot{\alpha}_0$, $\ddot{\alpha}_0$, the First Maximum Yaw theory was applied to Frankford Arsenal data. Figure 80 shows a plot of dispersion magnitude vs. first maximum yaw magnitude. Clearly no linear relationship exists between

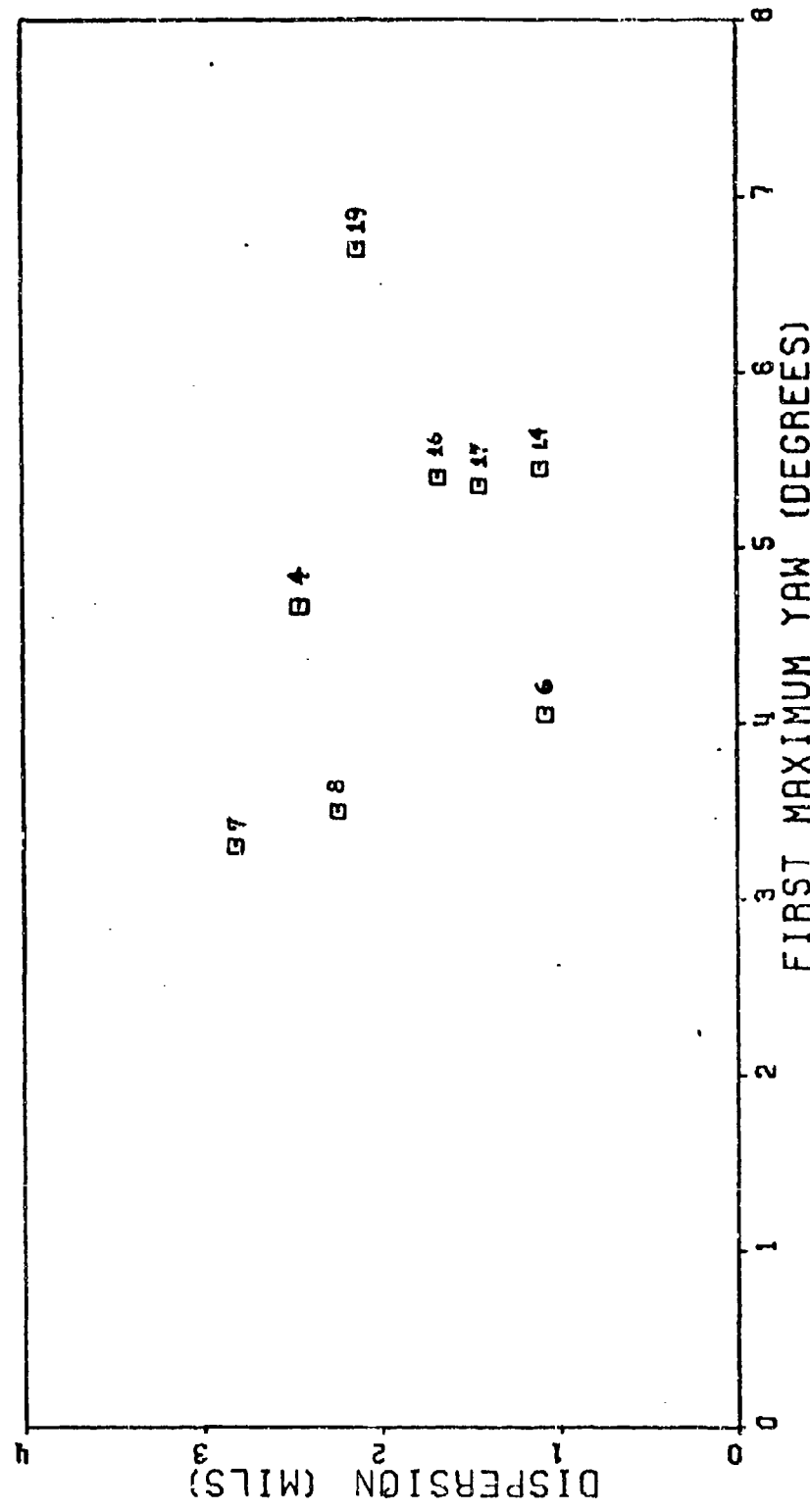


Figure 80. Dispersion vs First Maximum Yaw, Frankford Test Firing Results

dispersion and first maximum yaw. In fact, the plotted data resembles a random shotgun blast. Figures 81, 82 and 83 employ the theory to the first maximum yaw hypothesis. Again the plot substantiates the findings of Figure 80. The disproval of the first maximum yaw hypothesis comes as no surprise since the dispersion theory contradicts it and the 6-D computations, which integrate the actual equations of motion, validated the dispersion theory. Therefore, dispersion could never accurately be predicted by a theory involving only first maximum yaw.

The influence of initial conditions, \dot{S}_o , $\dot{\alpha}_o$, and $\ddot{\alpha}_o$ and dispersion for the actual test firings are expected to be different from that in the validation of theory section because of the different ranges in the initial conditions. For example, \dot{S}_o in the validation section was $(100 + 100i)$ ft/sec. In the actual test firings, \dot{S}_o only ranged as high as 0.017 ft/sec. Of course, the large value was only to validate the theory. Here \dot{S}_o is very small and its contribution is accordingly smaller. In the reduced equation 24, employed to calculate the theory column in Table XXII,

$$\overline{J.A.} \text{ (mils)} = 1000 \left[\frac{\dot{S}_o}{x} + \frac{\dot{S}_o}{u} - \frac{l_y}{mud} A \left(\dot{\alpha}_o - \ddot{\alpha}_o \frac{ipI_x}{l_y} \right) \right]$$

for round 4, 1 ft downrange,

$$1000 \frac{\dot{S}_o}{u} = (0.001562 + 0.001841i) \text{ mils}$$

where as,

$$\overline{J.A.} = (1.329 - 1.302i) \text{ mils}$$

Since this is typical of the 8 rounds tested, \dot{S}_o has little effect on dispersion for these rounds.

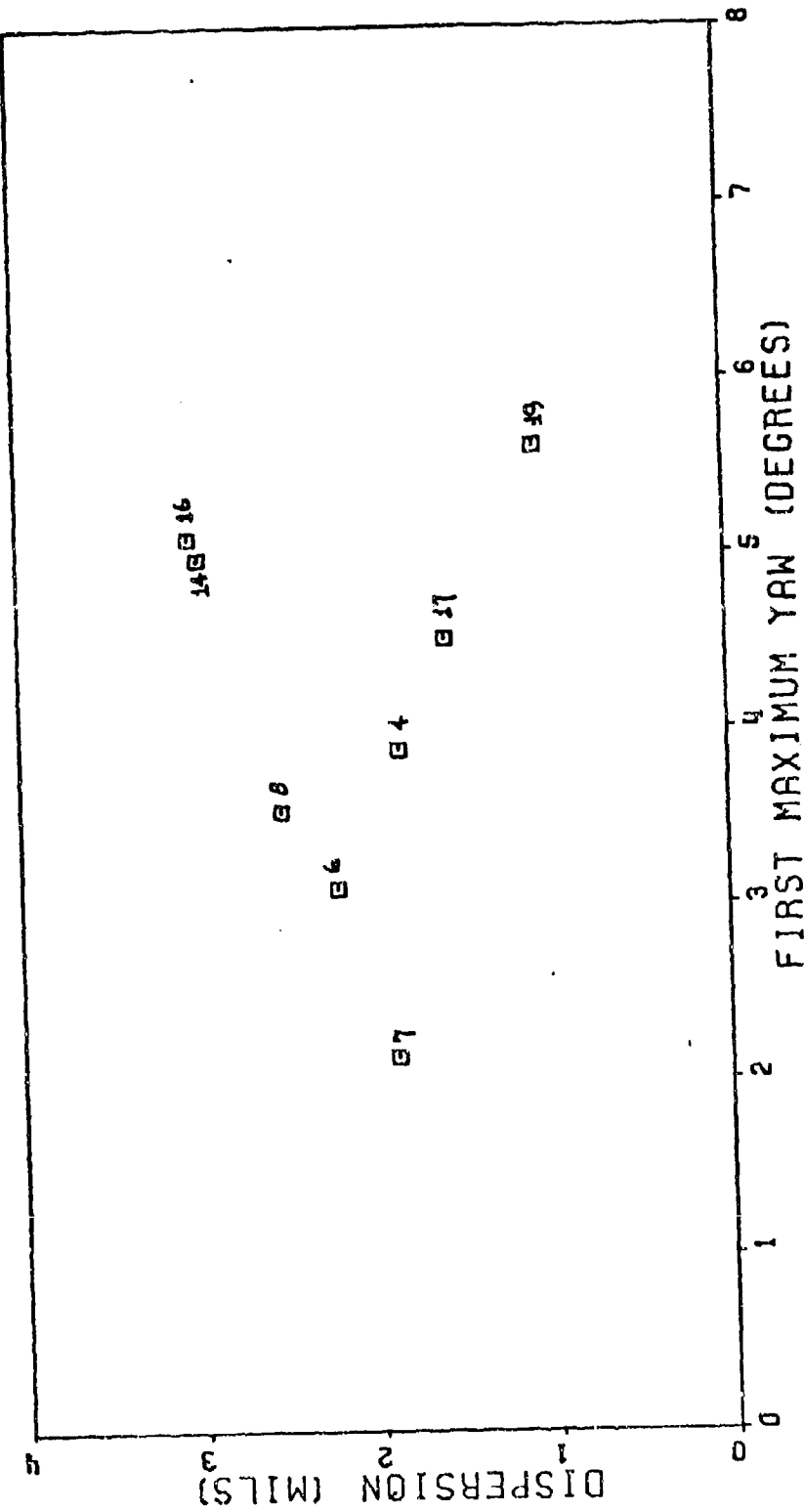


Figure 81. Dispersion vs First Maximum Yaw, Theory - Initial Conditions,
1 ft Downrange

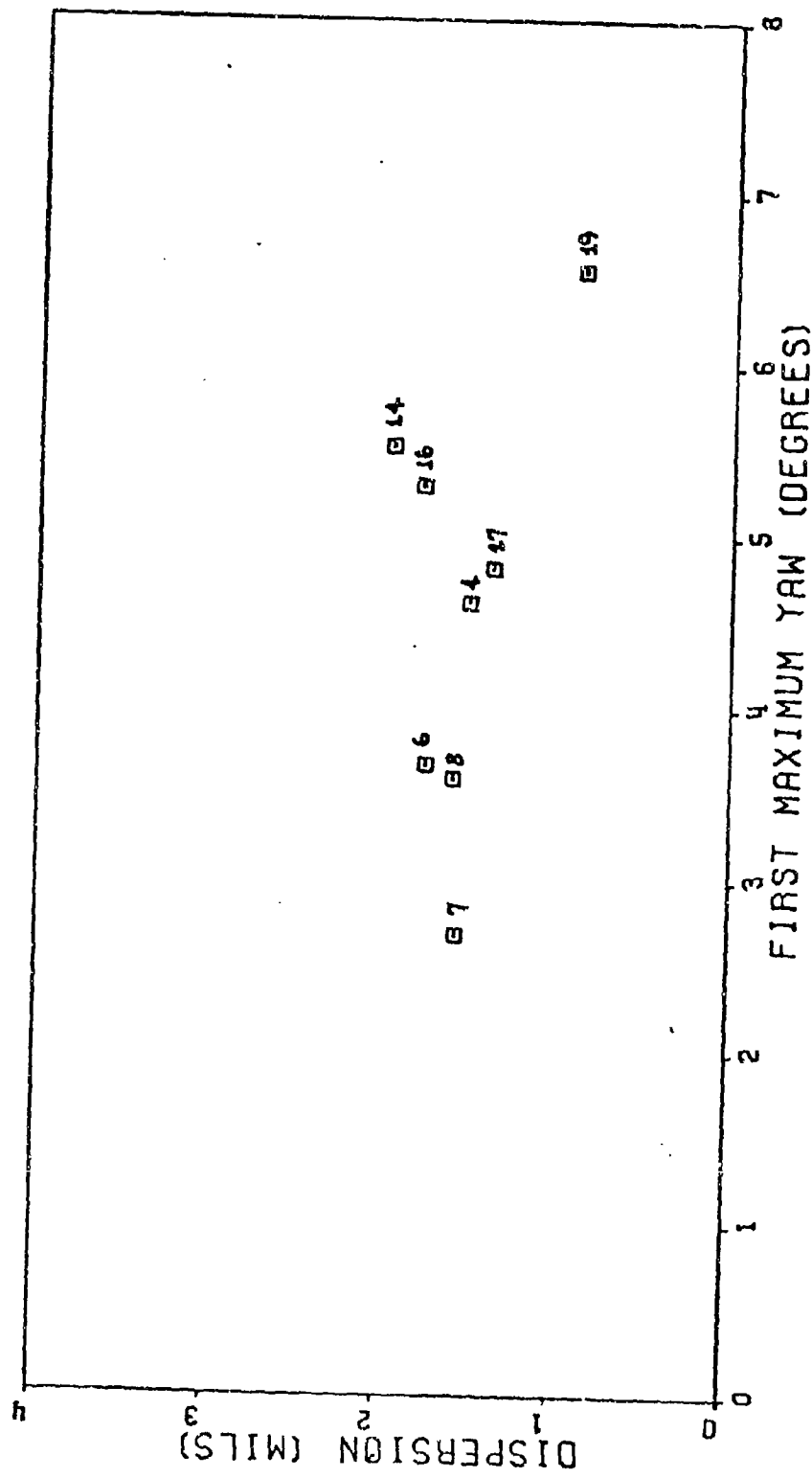


Figure 82. Dispersion vs First Maximum Yaw, Theory - Initial Conditions,
3 ft. Downrange

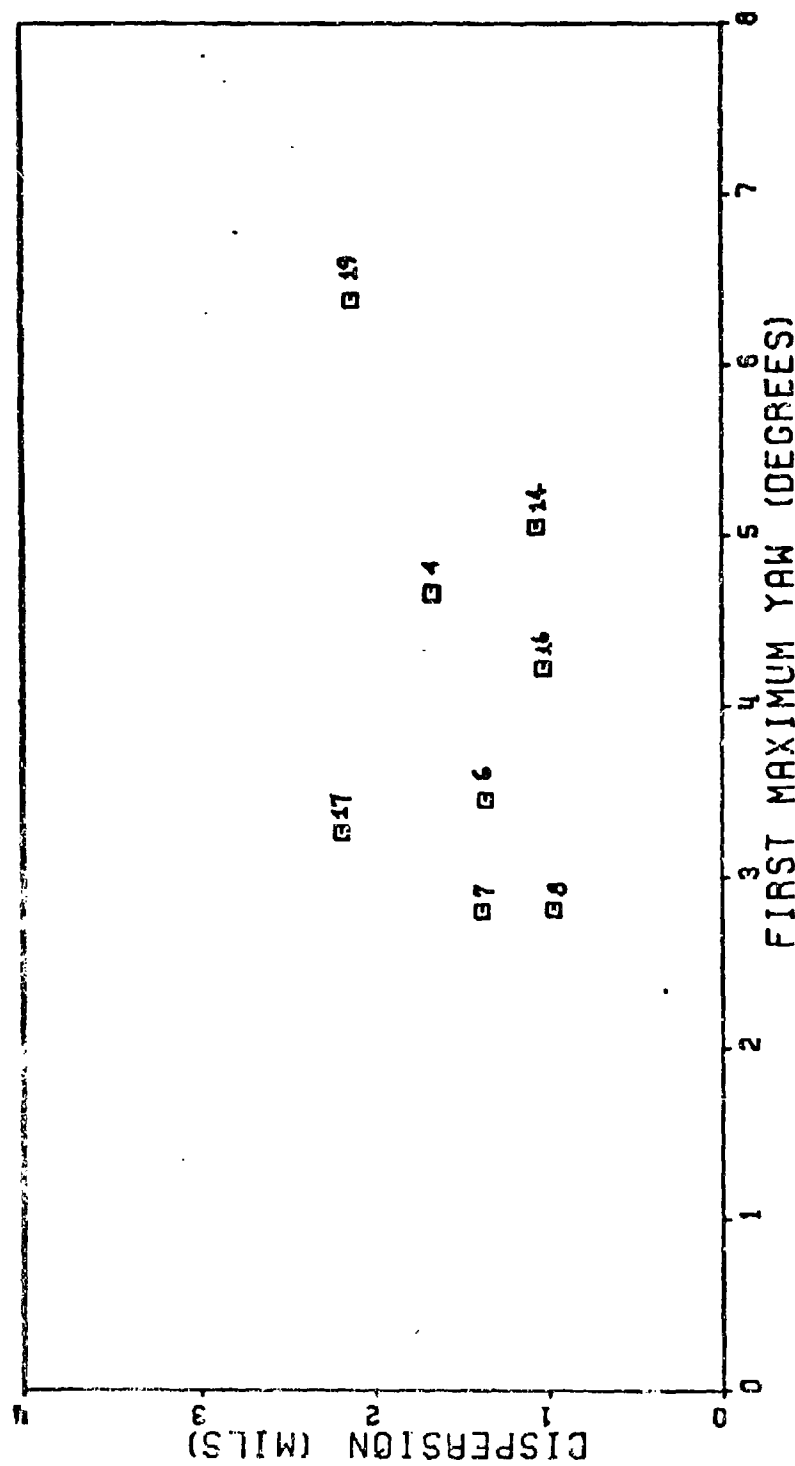


Figure 63. Dispersion vs First Maximum Yaw, Theory - Initial Conditions,
5 ft. Downrange

Similarly, for this particular case,

$$1000 \frac{\vec{S}_o}{x} = (1.519360 + 0.041760i) \text{ mils}$$

$$1000 \vec{\alpha}_o \frac{ipLA}{mud} = (-0.01437 + 0.00214i) \text{ mils}$$

$$-1000 \vec{\dot{\alpha}}_o \frac{LyA}{mud} = (-0.206075 - 1.383672i) \text{ mils}$$

Obviously, \vec{S}_o and $\vec{\alpha}_o$ are by far the greatest contributors to dispersion for this case. Inspection of all the other 23 cases in Table XXII agrees with this general pattern. \vec{S}_o can be nearly eliminated, of course, by accurate setup of the test equipment so that the gun barrel is set exactly at coordinates (0,0). Any \vec{S}_o then would occur from displacement due to the blast. This leaves the major culprit in dispersion to be $\vec{\alpha}_o$.

Figure 84 illustrates the dependence of the Jump Angle, and hence dispersion, upon angular rate and angle of attack.

Although $\vec{\alpha}_o$ contributes the most to the Jump Angle, the combination of \vec{S}_o and $\vec{\alpha}_o$ also has a noticeable influence. From the test firings, \vec{S}_o was found to have a negligible effect on dispersion. Therefore, it is neglected in Figure 84 to simplify the plot. It is evident from Figure 84 that various combinations of $\vec{\alpha}_o$ and $\vec{\dot{\alpha}}_o$ yield zero dispersion. It is possible that large values of $\vec{\alpha}_o$ and $\vec{\dot{\alpha}}_o$ can combine to yield zero dispersion; an impossibility with the first maximum yaw hypothesis. If α_o and $\dot{\alpha}_o$ are able to balance to give zero dispersion, then this idea can be expanded to include the entire equation.

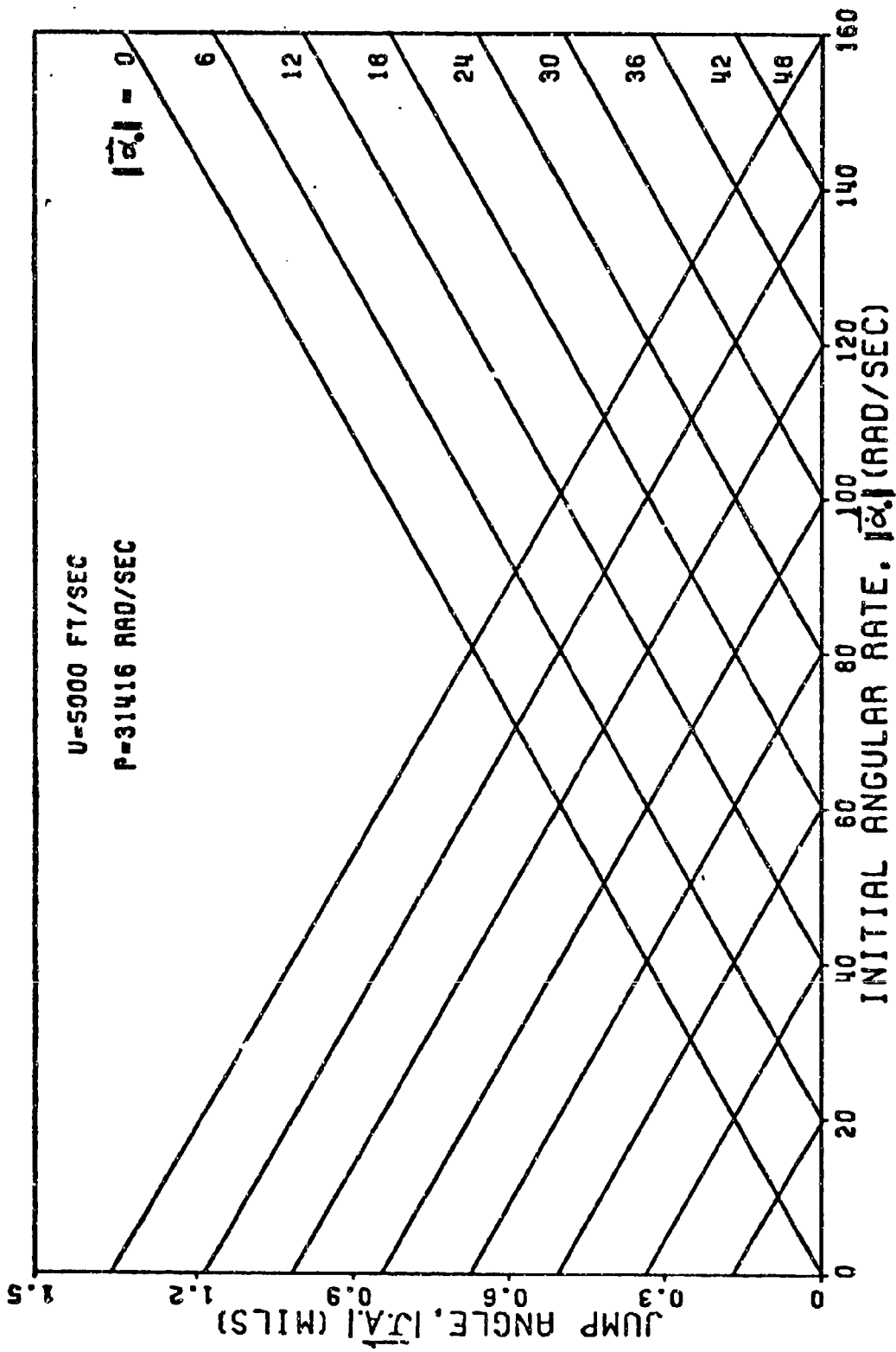


Figure 24. Jump Angles for Various Initial Conditions

The governing equation used throughout this dispersion analysis section is:

$$\overrightarrow{J.A.} = 1000 \left[\frac{\overrightarrow{S}_o}{x} + \frac{\dot{\overrightarrow{S}}_o}{u} - \frac{I_y}{mud} A \left(\overrightarrow{\dot{\alpha}}_o - \overrightarrow{\alpha}_o \frac{ipI_x}{I_y} \right) + \frac{ig}{2} \left(\frac{x}{u^2} \right) \right]$$

Eliminating the constant gravity term,

$$\overrightarrow{J.A.} = 1000 \left[\frac{\overrightarrow{S}_o}{x} + \frac{\dot{\overrightarrow{S}}_o}{u} - \frac{I_y}{mud} A \left(\overrightarrow{\dot{\alpha}}_o - \overrightarrow{\alpha}_o \frac{ipI_x}{I_y} \right) \right]$$

Setting $\overrightarrow{J.A.}$ to zero, the idea behind Figure 84 is expanded to include \overrightarrow{S}_o , $\dot{\overrightarrow{S}}_o$.

$$\frac{\overrightarrow{S}_o}{x} + \frac{\dot{\overrightarrow{S}}_o}{u} = \frac{I_y}{mud} A \left(\overrightarrow{\dot{\alpha}}_o - \overrightarrow{\alpha}_o \frac{ipI_x}{I_y} \right)$$

rearranging

$$m \left[\overrightarrow{S}_o \left(\frac{u}{x} \right) + \dot{\overrightarrow{S}}_o \right] = \frac{A}{d} \left(\overrightarrow{\dot{\alpha}}_o I_y - \overrightarrow{\alpha}_o ipI_x \right)$$

A dimensional analysis of the equations finds that both sides have units of momentum or impulse. Going one step farther it can be said that to obtain zero dispersion:

initial transverse momentum = initial angular momentum

Therefore it is the imbalance in the initial momentums that causes dispersion. The size of initial conditions can be huge, Figure 84, but if they can combine to balance, zero dispersion results. The way the initial conditions combine, determine the magnitude of the imbalance or dispersion. It should be noted that this dispersion discussed is round to round dispersion and that the inconsistency of the momentum imbalance

from round to round causes a dispersion pattern (a set of rounds). The next section will highlight this principle in the evaluation of physical factors affecting dispersion.

PHYSICAL EVALUATION OF DISPERSION

Initial momentum imbalance has been shown to cause dispersion.

Initial conditions determine the magnitude of the imbalance. What causes these initial conditions to occur is the subject of this final section. Initial conditions occur somewhere between zero and five feet downrange to different degrees of magnitude due to various conditions. These conditions are:

1. Fin or body asymmetry
2. In-bore mal-alignment
3. Asymmetric blast
4. Asymmetric sabot separation
5. Sabot-fin interference
6. Fin or body damage

Fin or body asymmetries can cause dispersion magnitudes to range as much or greater than those in the Validation of Theory section for aerodynamic asymmetries. These asymmetries can be overcanted or bent fins, damaged nose cone, or even body deformities. Figure 85 which shows in-bore mal-alignment also shows a slightly bent body, concave downward. In-bore mal-alignment can be attributed to warping and/or the entire flechette at some angle of attack. Clearly, if this flechette were fired, the in-bore angle of attack would produce an $\vec{\alpha}_0$ outside the gun barrel even before sabot separation. With the flechette at some angle of attack, the blast can cause a large $\vec{\alpha}_0$ and an \vec{S}_0 and $\dot{\vec{S}}_0$. The blast itself

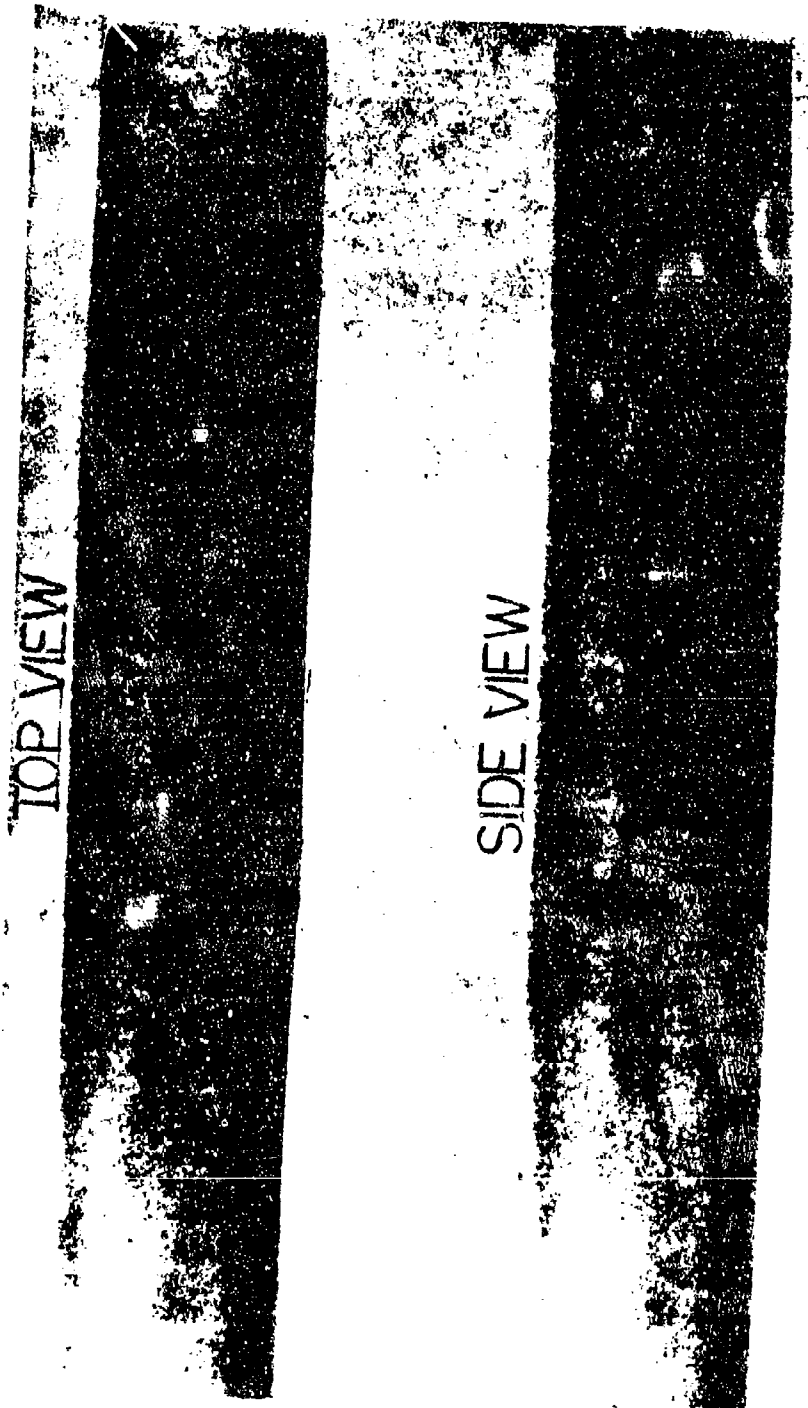


Figure 85. Flechette In-Bore Position

is a chief catalyst in causing the initial conditions. An asymmetric blast can indeed impart influence on the initial conditions, but symmetric blast can also. Given an initial angle of attack due to some disturbances the symmetric blast can cause significant $\vec{\alpha}_0$, $\dot{\vec{\alpha}}_0$, \vec{S}_0 and $\dot{\vec{S}}_0$. Figure 86 shows a typical blast region with the flechette outlined in the picture. The momentum principle discussed in the previous section goes hand-in-hand with this blast region. It is here that the transverse and angular-momentum is imparted to the flechette. Figure 87 illustrates a typical flechette in the blast region. Coming out of the barrel at some angle of attack, the blast catches the flechette and induces some angular rate. At the same time, the flechette is translated laterally giving an \vec{S}_0 and $\dot{\vec{S}}_0$. If these contributions cancel each other out; that is, if initial transverse momentum equals initial angular momentum then the dispersion is zero. If they do not cancel, dispersion results. The sketch is highly simplified in that the blast itself is all-engulfing as in Figure 86. Of course, the transition sequence of sabot separation, fin interference, and possible fin damage must not be forgotten. The transition sequence occurs in the blast region, however, and is not considered separate from the blast. When separation occurs, the sabot particles are apt to interfere with the fin section and cause possible damage. Once the sabot has separated and cleared the fins the blast has had its greatest effect and the initial conditions can be determined. After the flechette has moved downrange, it assumes supersonic free flight, Figure 88.



Figure 86. Typical Flechette Blast Region

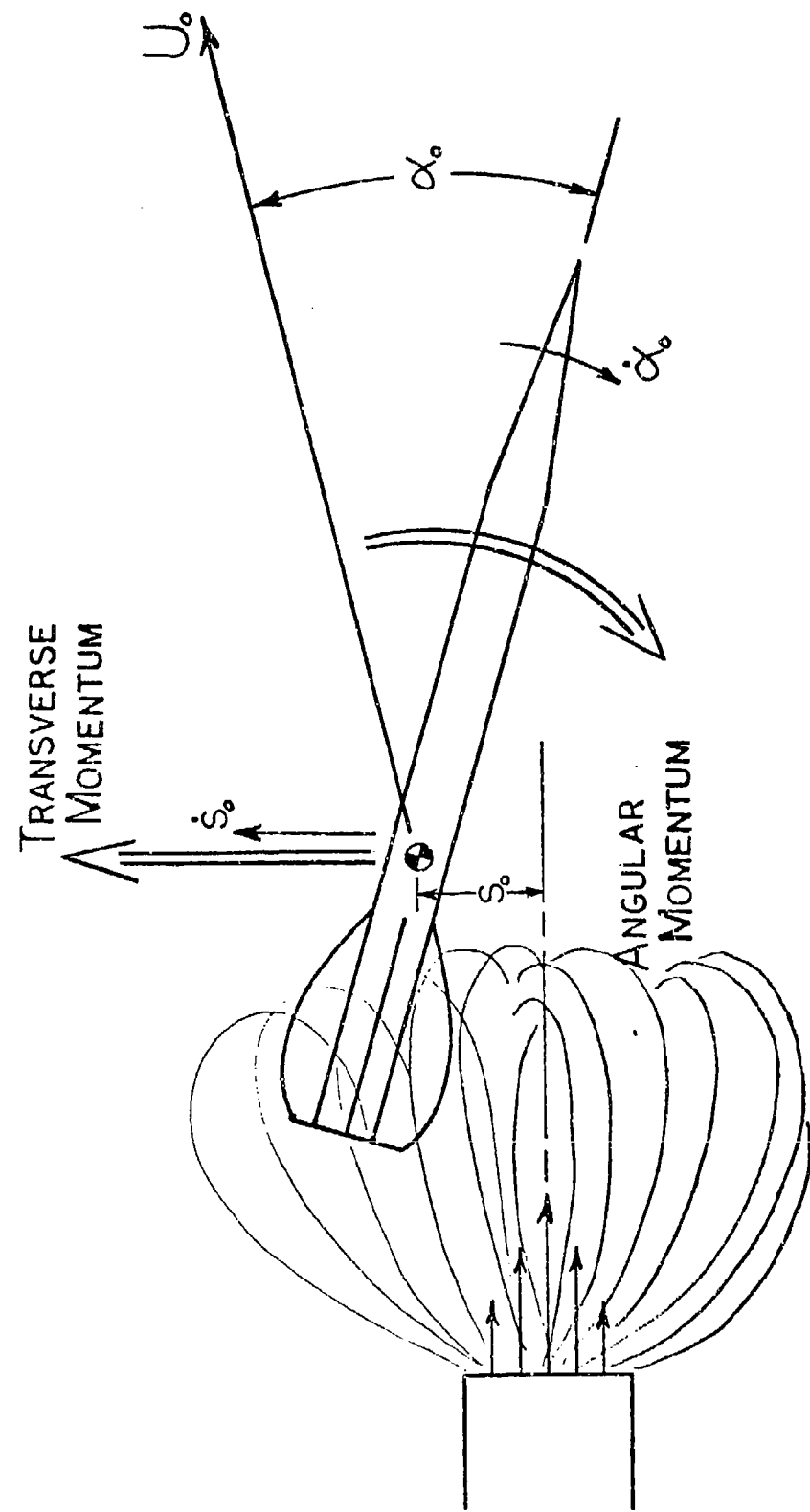


Figure 87. Muzzle Blast Effects

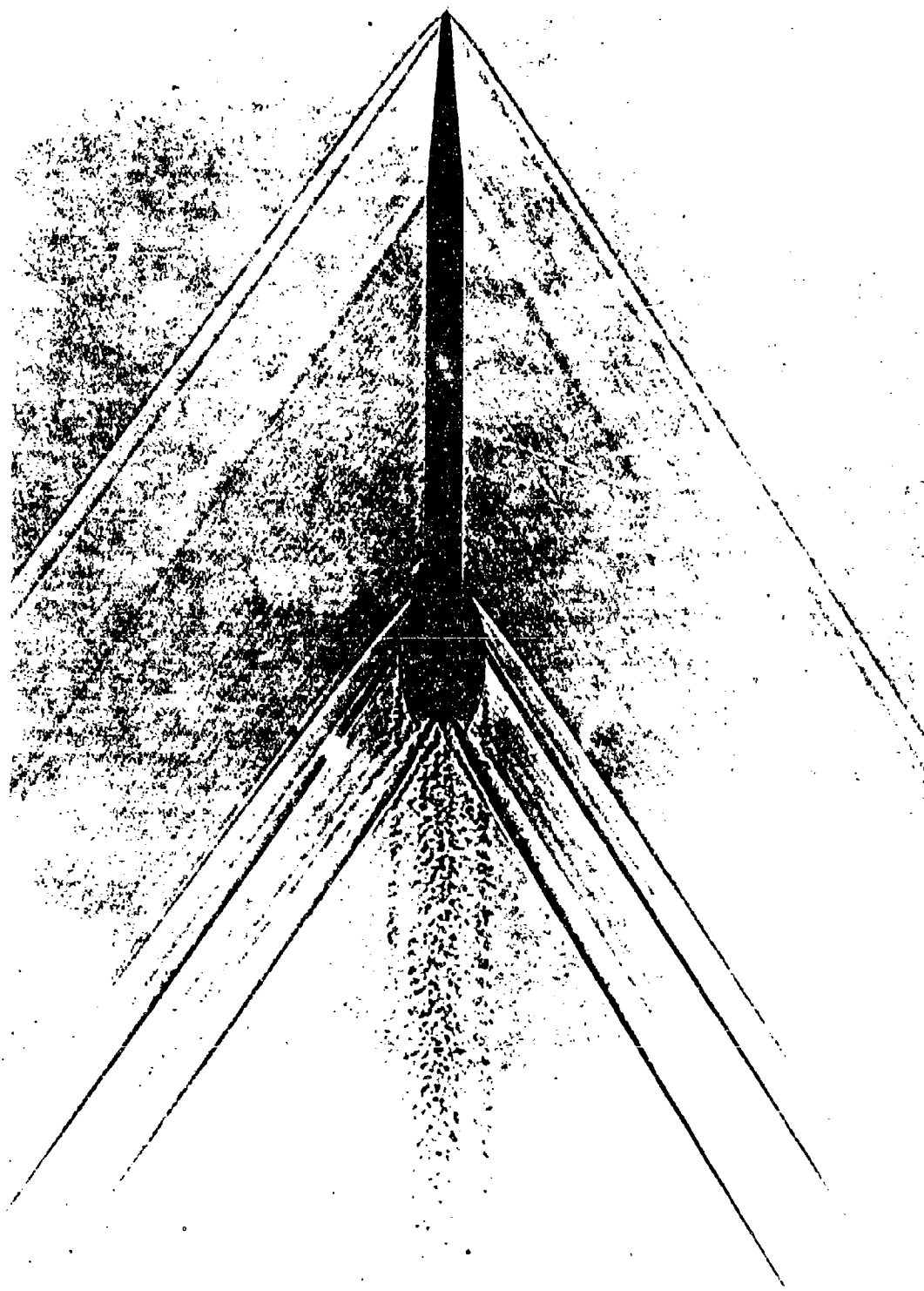


Figure 88. Supersonic Free Flight, Ground Point Flechette

CONCLUSIONS

A complete Jump and Dispersion Theory has been developed for free flight vehicles. Three governing equations have been determined to accommodate high, low, and very low roll rates. The theories were found to be accurate with six-degree-of-freedom numerical computations of the equations of motion and therefore reliably predict the jump and dispersion of flechettes. The theory validation included 201 case runs in four phases. The first phase validated the theory with respect to restoring and damping moments. The effect of these moments on dispersion was found to depend on the initial conditions. The second phase validated the theory with respect to Magnus forces and moments. The effect of Magnus was found to be very small and not to be of any consequence unless the total dispersion of any given round was of the same order of magnitude as the Magnus effect. Phase three validates the theory with respect to aerodynamic asymmetries and roll rate. All three theories were validated in this phase and found to be quite accurate considering the large dispersions encountered. Aerodynamic asymmetries causing a trim angle of 1° had little effect on the dispersion of flechettes. Slower rolling bodies were shown to have, in general, increasingly larger dispersion values as roll rate decreased. It can be concluded that for free flight vehicles that are prone to aerodynamic asymmetries and fin damage, a high roll rate is essential to lower dispersion and increase accuracy. The fourth phase validates the theory with respect to gravity. The theory indicates a lateral contribution to dispersion from gravity in addition to the obvious vertical contribution.

For the flechette, the lateral contribution was found to be minimal and was neglected in this analysis.

Free flight data was obtained from Frankford Arsenal to correlate with the theory. Angular and translational data was fitted and put into initial condition form. The initial condition data was applied to the theory and compared to target data for the rounds tested. The theory was found to agree favorably in magnitude with the test firings. As a result, the method used to analyze the data can be considered a valid method. Photographs of the test firings were taken to include the flight transition sequence in the blast region. The pictures further verify the analysis method of the initial conditions by allowing agreement between the chosen initial conditions and the position downrange where they were selected.

The evaluation of the free flight dispersion against the theory also disproves the First Maximum Yaw hypothesis. A plot of jump angle vs. first maximum yaw of actual test data produced a shotgun blast pattern with no relationship evident between dispersion and first maximum yaw. In addition, a plot of jump angle versus angular rate for various initial angles of attack indicates an infinite amount of combinations of initial conditions to yield a given jump angle. Thus, zero dispersion has an infinite set of possible initial conditions. It was found for zero dispersion that a unique physical condition holds: to obtain zero dispersion, initial transverse momentum = initial angular momentum. These impulses are imparted to the flechette in the blast region where the body and especially the fins are subject to disturbances. Momentum imbalance is the reason

dispersion occurs. The initial conditions only determine the magnitude of imbalance or dispersion. This dispersion is round to round dispersion. Inconsistency in the imbalance results in a dispersion pattern. The initial conditions were found not to occur until after the sabot separation and the blast has had its greatest effect. The factors causing the existence of initial conditions were found to be not only the blast and sabot separation sequence, but also fin and body asymmetries and bore mal-alignment. In order to decrease dispersion, these physical factors causing initial conditions must be kept at a minimum. The most important aspect would be to protect the fins from asymmetries, damage, and interference from the separating sabot. Initial conditions can never realistically be eliminated but if kept minimal, dispersion is reduced.

APPENDIX

A-1

Appendix A1 contains mass parameters and stability coefficients for the Ground Point Flechette. Table A1-1 lists values for mass, diameter, axial and transverse moments of inertia. Figures A1-1 through A1-8 present stability coefficients used in this analysis versus Mach number.

$C_{z\alpha}$, $C_{M\alpha}$, $C_{Mq} + C_{M\dot{\alpha}}$ were provided by Frankford Arsenal. $C_{zp\beta}$, $C_{Mp\beta}$, C_{YE} , C_{ZE} , C_{ME} , C_{NE} were nominal values of the coefficients following the same trends of $C_{z\alpha}$ and $C_{M\alpha}$ for Mach number. $C_{M\alpha}$ and C_{Mq} , $C_{M\dot{\alpha}}$ were verified in the University of Notre Dame supersonic wind tunnel.¹⁶

TABLE A1-1
FLECHETTE PARAMETERS

mass = 0.000046 slugs
diameter = 0.006 ft.
 I_x = 0.00000000217 slugs-ft²
 I_y = 0.00000036421 slugs-ft²

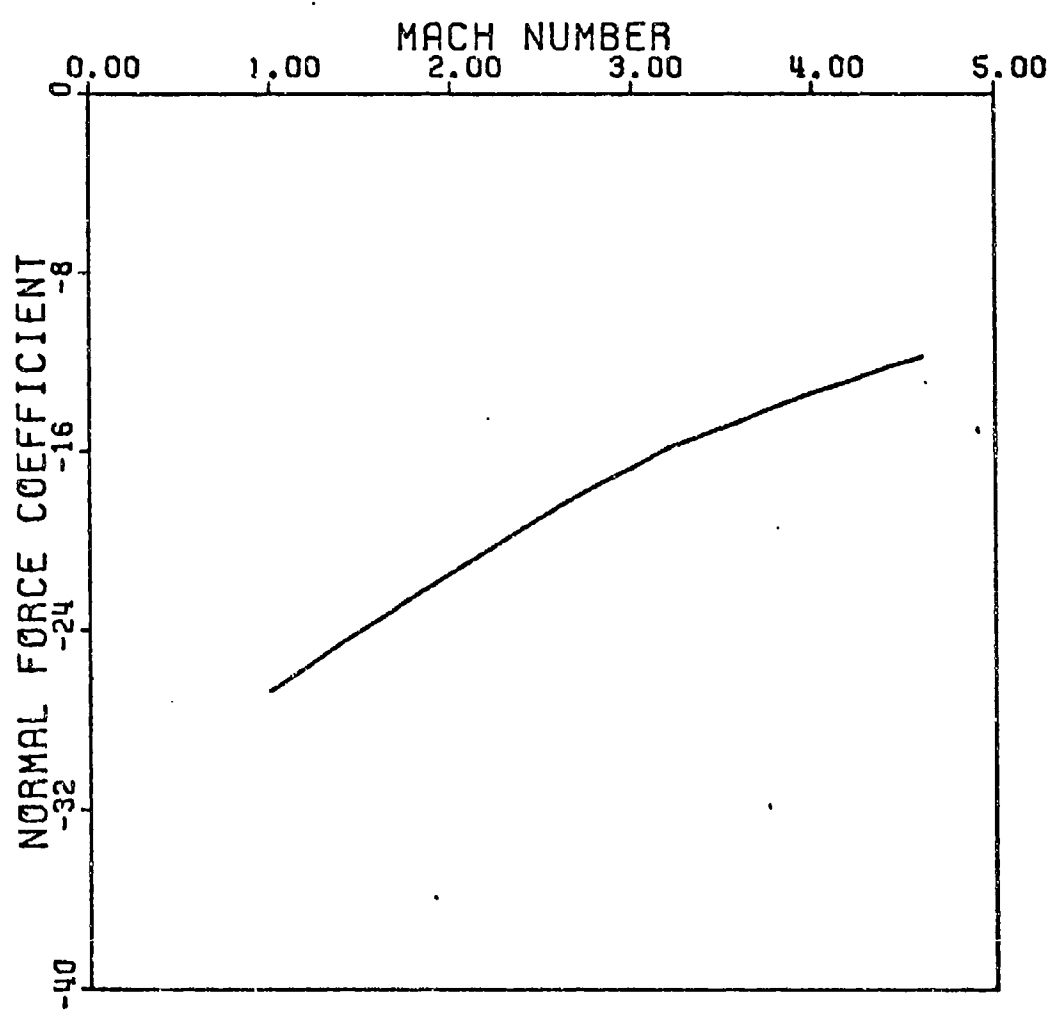


Figure A1-1. $CZ\alpha$ vs Mach Number Producibility Ground Point

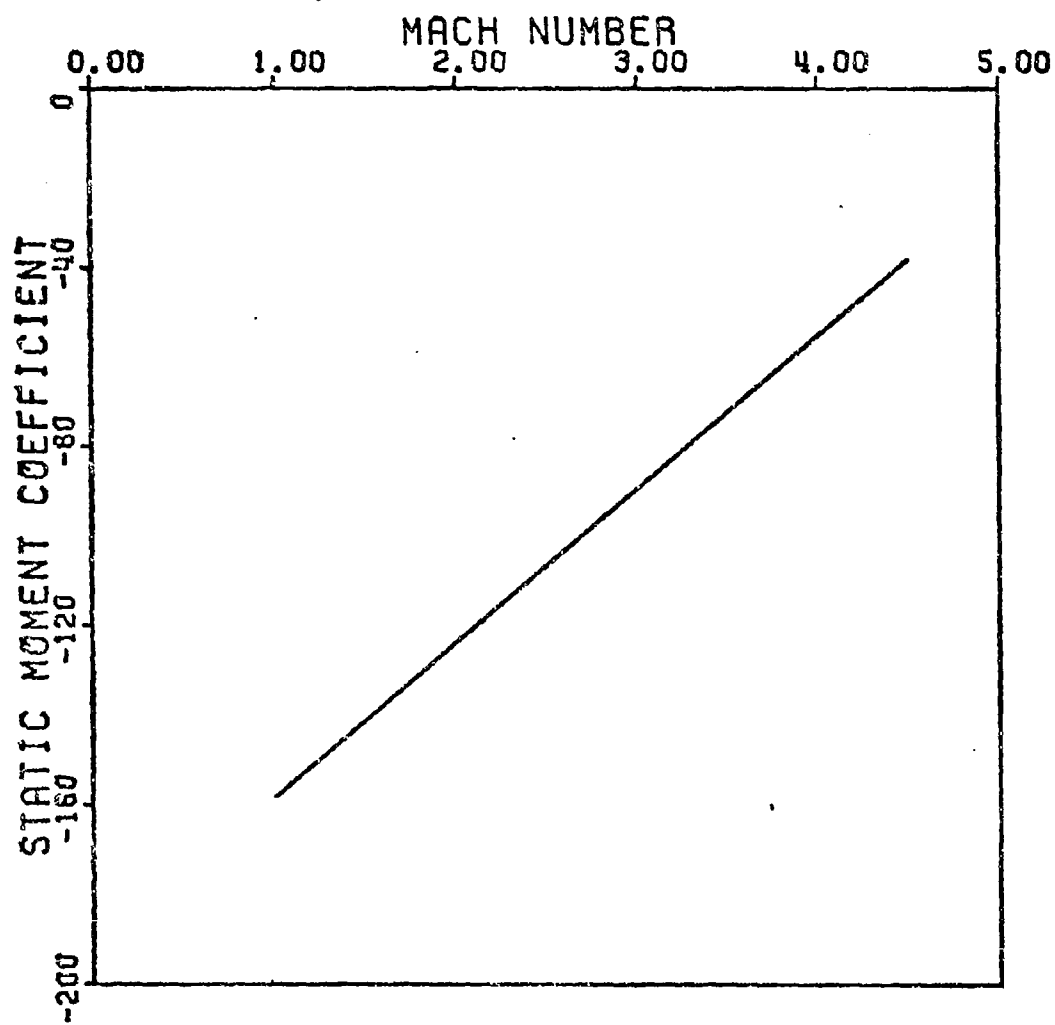


Figure A1-2. CM_{α} vs Mach Number Producibility Ground Point

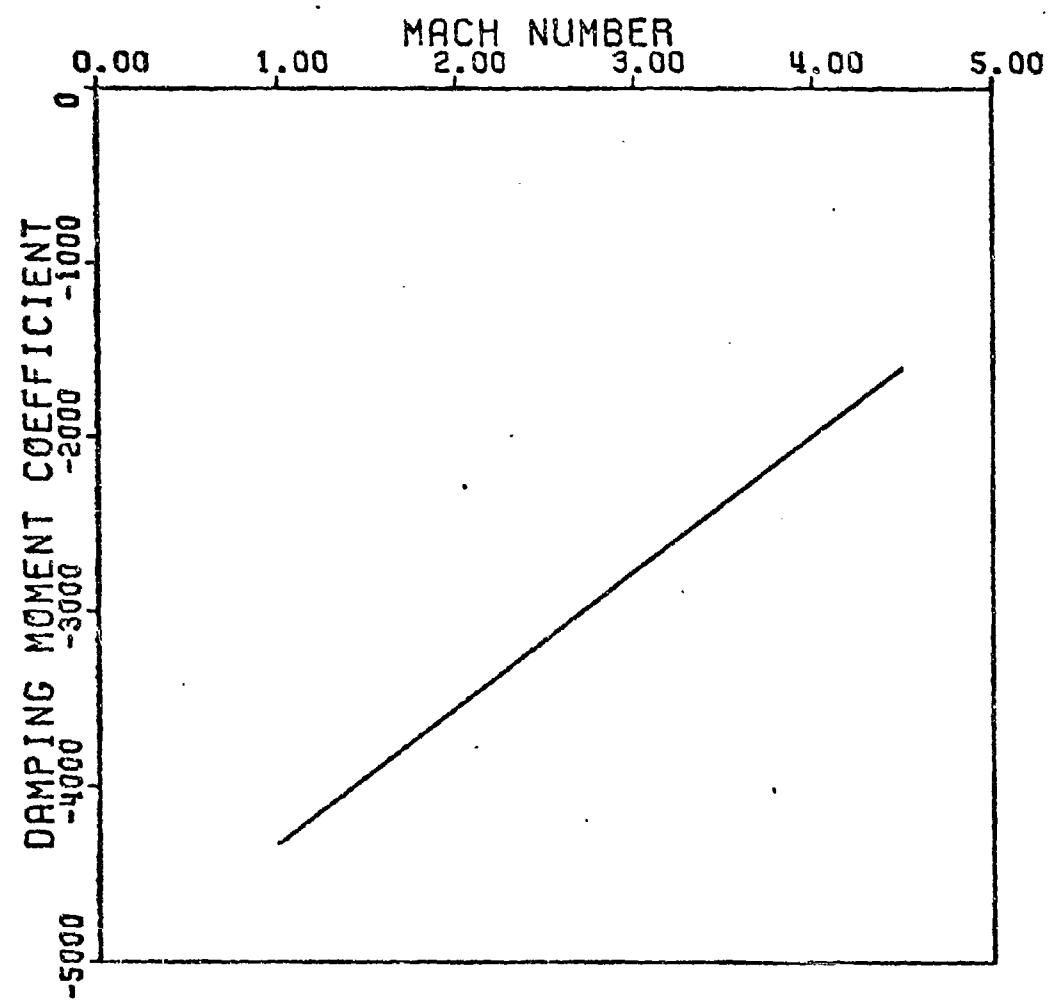


Figure A1-3. $CM_q + CM_d$ vs Mach Number Producibility Ground Point

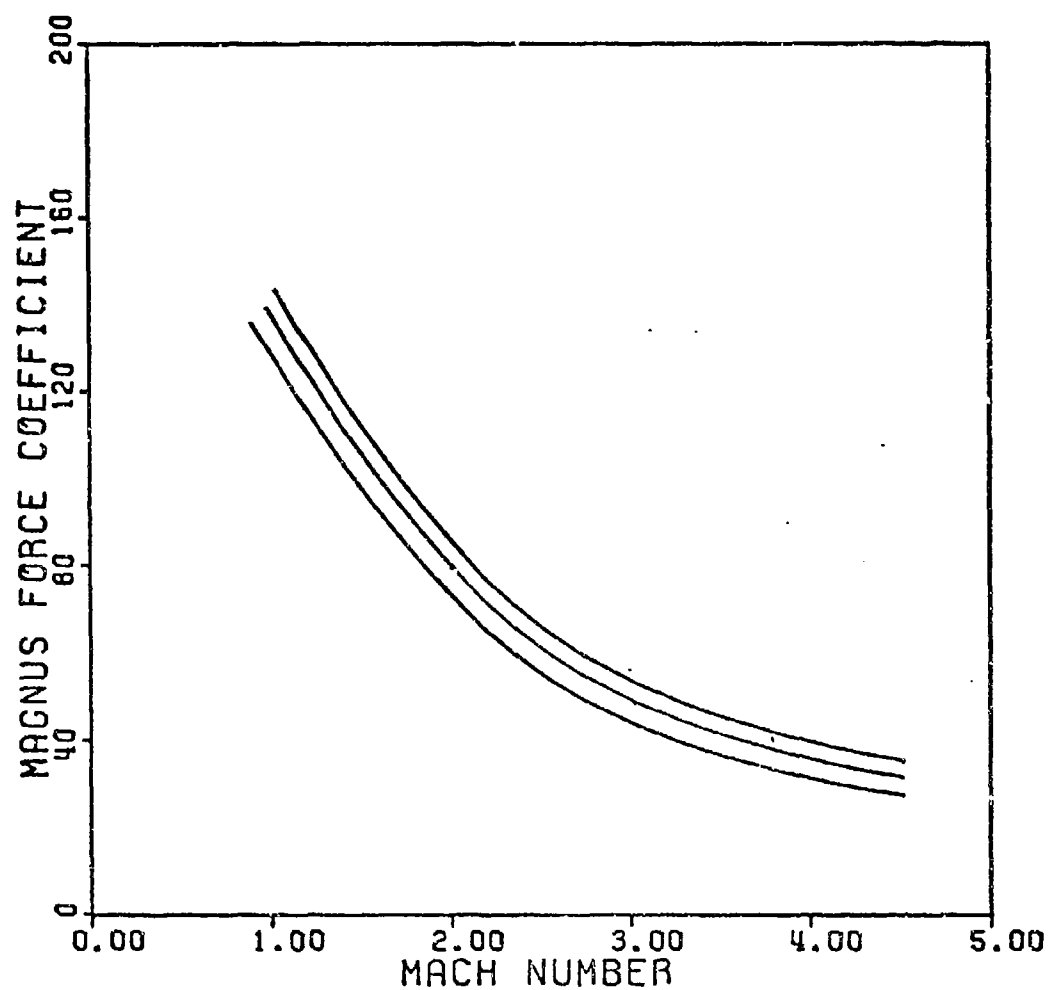


Figure A1-4. CZpb vs Mach Number Producibility Ground Point

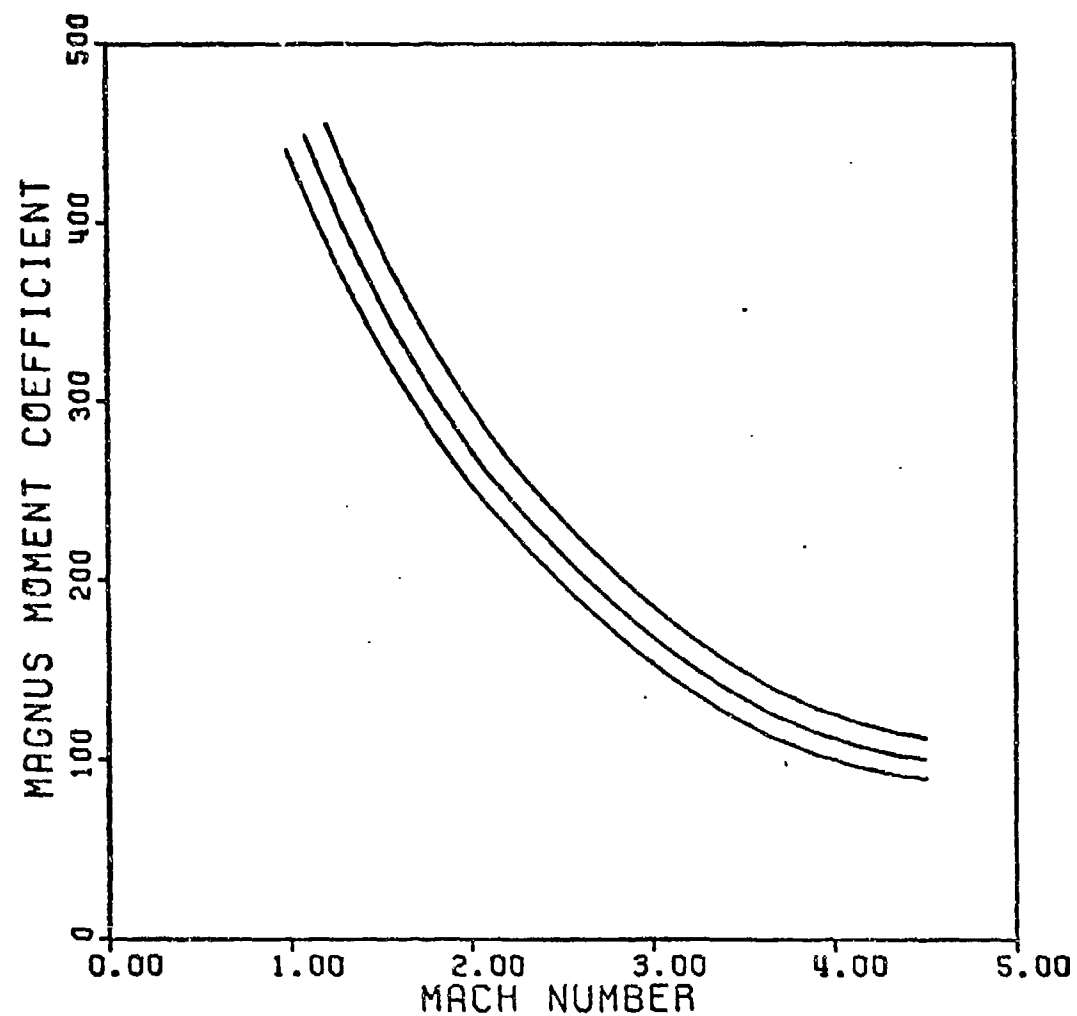


Figure Al-5. CMpb vs Mach Number Producibility Ground Point

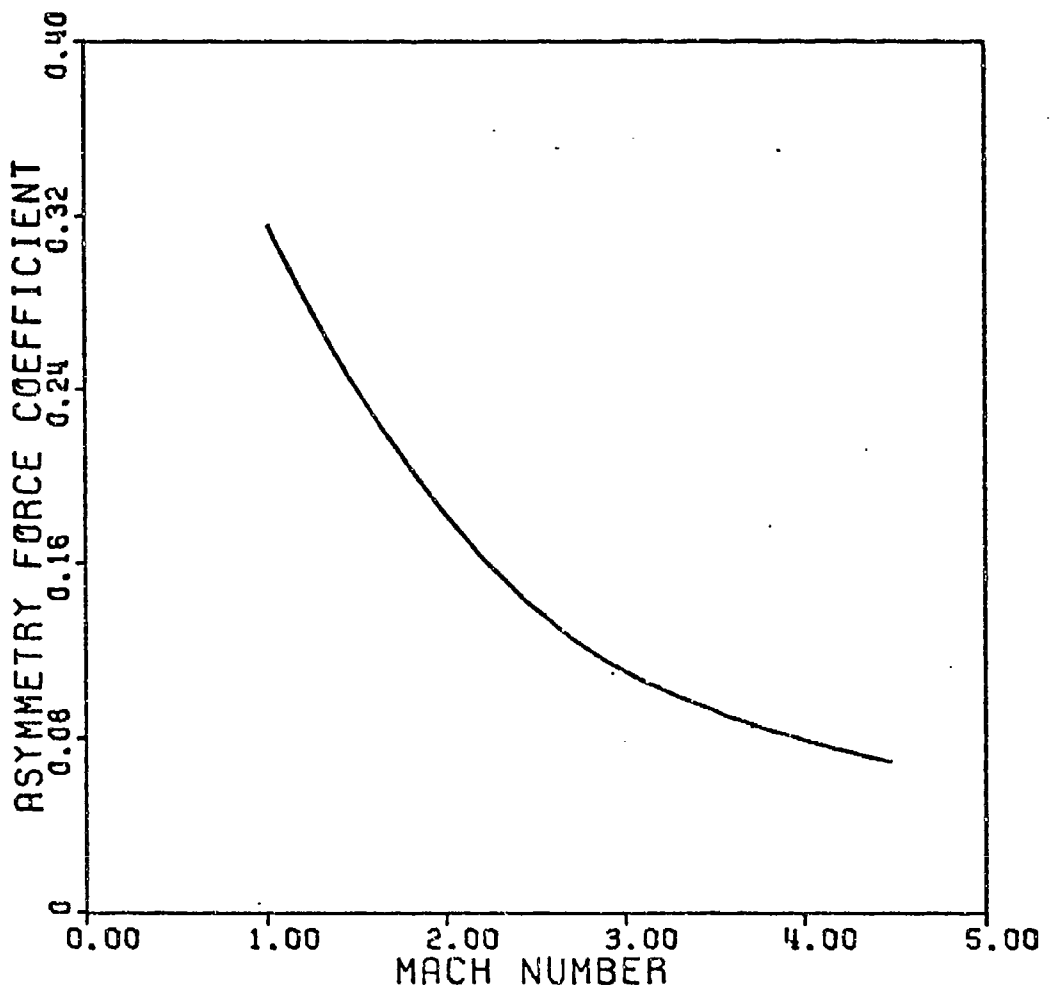


Figure Al-6. CYE, CZE vs Mach Number Producibility Ground Point

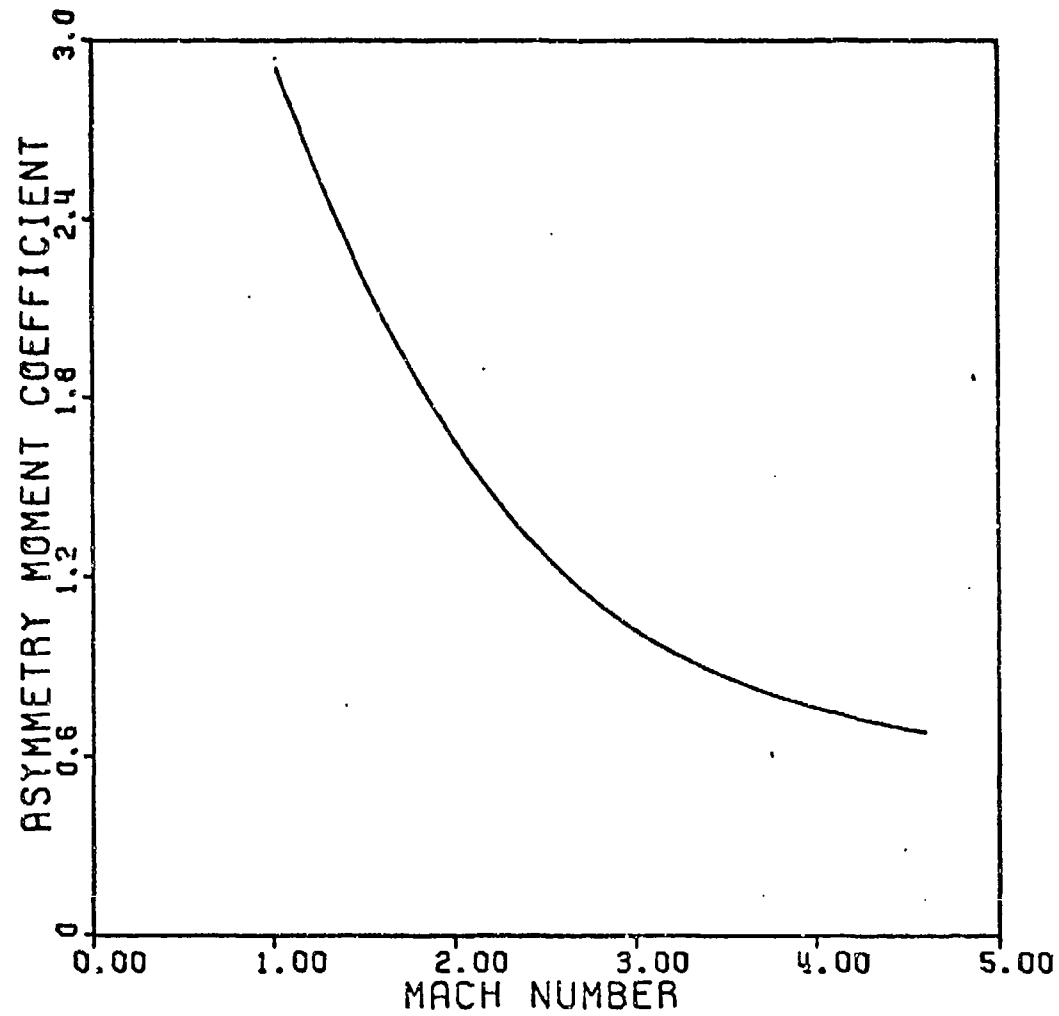


Figure Al-7. CME vs Mach Number Producibility Ground Point

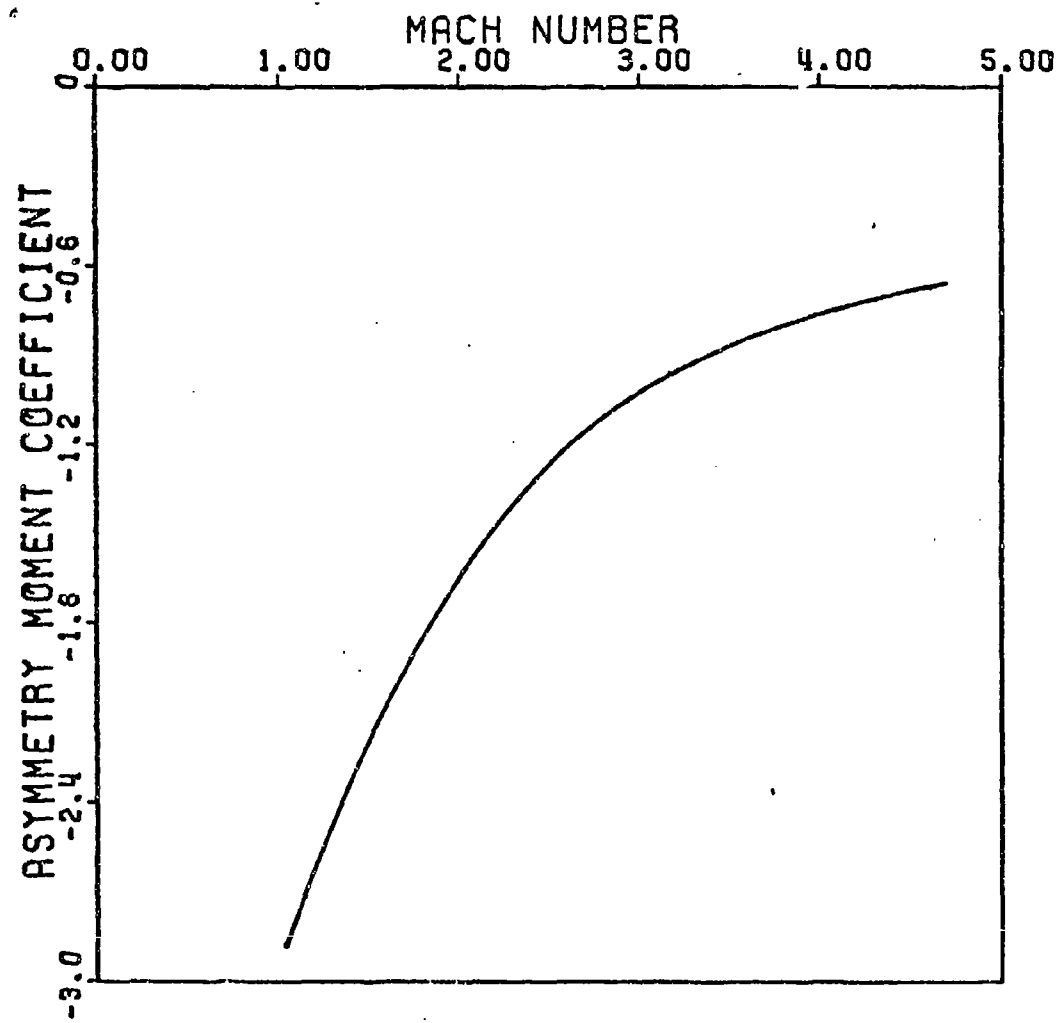


Figure A1-8. CNE vs Mach Number Producibility Ground Point

APPENDIX

A-2

Appendix A-2 contains the complete print-out of the results from a typical 6-D computer program run. The results give the time from launch, position coordinates x, y, z , velocity, roll rate, the magnitude of the complex angle of attack, Mach number, roll orientation angle, angles of pitch and yaw, nutation and precession damping factors, nutation and precession mode frequency rates, the gyroscopic stability factor, dynamic weight factor, and trim angle.

The program is divided into various subroutines to eliminate any superfluous calculations. These subroutines read in aerodynamic coefficients in tabular form as functions of Mach number and angle of attack, initialize the data, and integrate the six-degrees-of-freedom differential equations of motion using a four-step Runge-Kutta scheme to obtain the vehicle trajectory.

FLECHETTE GROUND POINT

PAGE 1

	T SEC	X FT	Y FT	Z FT	V FT/SEC	RAD/SEC	DEC SEC	PHI SEC	ALPHA SEC	BETA SEC	DEL SEC	TAU SEC	R SEC
0.00001	0.0	0.0	0.0	5000.0	0.0	4.09	0.0	-6.0	-6.0	-6.0	-6.0	-6.0	-6.0
0.00002	0.0050	0.0000	-0.0000	5000.00	2.07	4.09	1.74	-1.44	-5.55	-5.55	-5.55	-5.55	-5.55
0.00003	1.400	0.0000	-0.0000	4295.49	0.91	4.05	5.04	2.84	2.83	-4.65	-4.65	-4.65	-4.65
0.00004	1.500	0.0000	-0.0000	4300.00	5.93	4.09	5.14	4.14	4.11	-4.55	-4.55	-4.55	-4.55
0.00005	2.000	0.0000	-0.0000	4300.50	7.19	4.09	5.12	5.25	5.25	-4.55	-4.55	-4.55	-4.55
0.00006	3.000	0.0000	-0.0000	4295.46	5.00	4.05	5.01	3.99	6.77	-4.55	-4.55	-4.55	-4.55
0.00007	3.500	0.0000	-0.0000	4294.60	5.01	4.05	5.02	5.08	6.92	-4.55	-4.55	-4.55	-4.55
0.00008	4.000	0.0000	-0.0000	4297.44	5.01	4.05	5.02	5.08	6.91	-4.55	-4.55	-4.55	-4.55
0.00009	4.500	0.0000	-0.0000	4298.94	501.00	4.05	5.02	5.08	7.19	-4.55	-4.55	-4.55	-4.55
0.00010	5.000	0.0000	-0.0000	4298.35	501.00	4.05	5.02	5.08	7.19	-4.55	-4.55	-4.55	-4.55
0.00011	5.500	0.0000	-0.0000	4298.69	501.00	4.05	5.02	5.08	7.19	-4.55	-4.55	-4.55	-4.55
0.00012	6.000	0.0000	-0.0000	4295.72	501.00	4.05	5.02	5.08	7.19	-4.55	-4.55	-4.55	-4.55
0.00013	6.500	0.0000	-0.0000	4295.5	501.00	4.05	5.02	5.08	7.19	-4.55	-4.55	-4.55	-4.55
0.00014	7.000	0.0000	-0.0000	4297.4	501.00	4.05	5.02	5.08	7.19	-4.55	-4.55	-4.55	-4.55
0.00015	7.500	0.0000	-0.0000	4298.5	501.00	4.05	5.02	5.08	7.19	-4.55	-4.55	-4.55	-4.55
0.00016	8.000	0.0000	-0.0000	4298.3	501.00	4.05	5.02	5.08	7.19	-4.55	-4.55	-4.55	-4.55
0.00017	8.500	0.0000	-0.0000	4298.6	501.00	4.05	5.02	5.08	7.19	-4.55	-4.55	-4.55	-4.55
0.00018	9.000	0.0000	-0.0000	4295.2	501.00	4.05	5.02	5.08	7.19	-4.55	-4.55	-4.55	-4.55
0.00019	9.400	0.0000	-0.0000	4295.0	501.00	4.05	5.02	5.08	7.19	-4.55	-4.55	-4.55	-4.55
0.00020	9.800	0.0000	-0.0000	4295.4	501.00	4.05	5.02	5.08	7.19	-4.55	-4.55	-4.55	-4.55
0.00021	10.200	0.0000	-0.0000	4295.3	501.00	4.05	5.02	5.08	7.19	-4.55	-4.55	-4.55	-4.55
0.00022	10.600	0.0000	-0.0000	4295.6	501.00	4.05	5.02	5.08	7.19	-4.55	-4.55	-4.55	-4.55
0.00023	11.100	0.0000	-0.0000	4295.3	501.00	4.05	5.02	5.08	7.19	-4.55	-4.55	-4.55	-4.55
0.00024	11.900	0.0000	-0.0000	4295.3	501.00	4.05	5.02	5.08	7.19	-4.55	-4.55	-4.55	-4.55
0.00025	12.600	0.0000	-0.0000	4295.2	501.00	4.05	5.02	5.08	7.19	-4.55	-4.55	-4.55	-4.55
0.00026	12.900	0.0000	-0.0000	4295.7	501.00	4.05	5.02	5.08	7.19	-4.55	-4.55	-4.55	-4.55
0.00027	13.400	0.0000	-0.0000	4295.4	501.00	4.05	5.02	5.08	7.19	-4.55	-4.55	-4.55	-4.55
0.00028	13.900	0.0000	-0.0000	4295.3	501.00	4.05	5.02	5.08	7.19	-4.55	-4.55	-4.55	-4.55
0.00029	14.400	0.0000	-0.0000	4295.4	501.00	4.05	5.02	5.08	7.19	-4.55	-4.55	-4.55	-4.55
0.00030	14.900	0.0000	-0.0000	4295.0	501.00	4.05	5.02	5.08	7.19	-4.55	-4.55	-4.55	-4.55
0.00031	15.400	0.0000	-0.0000	4295.2	501.00	4.05	5.02	5.08	7.19	-4.55	-4.55	-4.55	-4.55
0.00032	15.900	0.0000	-0.0000	4295.7	501.00	4.05	5.02	5.08	7.19	-4.55	-4.55	-4.55	-4.55
0.00033	16.400	0.0000	-0.0000	4295.3	501.00	4.05	5.02	5.08	7.19	-4.55	-4.55	-4.55	-4.55
0.00034	16.900	0.0000	-0.0000	4295.0	501.00	4.05	5.02	5.08	7.19	-4.55	-4.55	-4.55	-4.55
0.00035	17.400	0.0000	-0.0000	4295.6	501.00	4.05	5.02	5.08	7.19	-4.55	-4.55	-4.55	-4.55
0.00036	17.900	0.0000	-0.0000	4295.1	501.00	4.05	5.02	5.08	7.19	-4.55	-4.55	-4.55	-4.55
0.00037	18.400	0.0000	-0.0000	4295.8	501.00	4.05	5.02	5.08	7.19	-4.55	-4.55	-4.55	-4.55
0.00038	18.900	0.0000	-0.0000	4295.6	501.00	4.05	5.02	5.08	7.19	-4.55	-4.55	-4.55	-4.55
0.00039	19.400	0.0000	-0.0000	4295.3	501.00	4.05	5.02	5.08	7.19	-4.55	-4.55	-4.55	-4.55
0.00040	19.900	0.0000	-0.0000	4295.7	501.00	4.05	5.02	5.08	7.19	-4.55	-4.55	-4.55	-4.55
0.00041	20.400	0.0000	-0.0000	4295.1	501.00	4.05	5.02	5.08	7.19	-4.55	-4.55	-4.55	-4.55
0.00042	20.900	0.0000	-0.0000	4295.7	501.00	4.05	5.02	5.08	7.19	-4.55	-4.55	-4.55	-4.55
0.00043	21.400	0.0000	-0.0000	4295.6	501.00	4.05	5.02	5.08	7.19	-4.55	-4.55	-4.55	-4.55
0.00044	21.900	0.0000	-0.0000	4295.3	501.00	4.05	5.02	5.08	7.19	-4.55	-4.55	-4.55	-4.55
0.00045	22.400	0.0000	-0.0000	4295.0	501.00	4.05	5.02	5.08	7.19	-4.55	-4.55	-4.55	-4.55
0.00046	22.900	0.0000	-0.0000	4295.6	501.00	4.05	5.02	5.08	7.19	-4.55	-4.55	-4.55	-4.55
0.00047	23.400	0.0000	-0.0000	4295.2	501.00	4.05	5.02	5.08	7.19	-4.55	-4.55	-4.55	-4.55
0.00048	23.900	0.0000	-0.0000	4295.7	501.00	4.05	5.02	5.08	7.19	-4.55	-4.55	-4.55	-4.55
0.00049	24.400	0.0000	-0.0000	4295.3	501.00	4.05	5.02	5.08	7.19	-4.55	-4.55	-4.55	-4.55

FLECHETTE GROUND POINT

PAGE 2

T SEC	X FT	Y FT	Z FT	V FT/SEC	P FT/SEC	ALPHA DEG	MACH PER	PHI DEG	L-N SEC	L-P SEC	L-S SEC	S INSEC	TAU SEC	R-T SEC
0.0050	26.97	0.189	-0.053	4988.5	500.00	7.32	4.47	16.33	-4.42	-5.24	-5.5	-57.	2324-2324	-5
0.0051	6.041	0.054	-0.053	4988.5	500.00	6.52	4.47	19.36	-3.62	-5.21	-5.5	-57.	2323-2323	-5
0.0052	25.97	0.192	-0.053	4988.0	500.00	5.45	4.47	22.13	-3.24	-4.39	-5.5	-57.	2323-2324	-5
0.0053	26.47	0.026	-0.053	4987.8	500.00	2.17	4.47	26.32	-1.51	-1.41	-5.5	-57.	2323-2324	-5
0.0054	27.95	0.192	-0.053	4987.8	500.00	2.76	4.47	26.32	-1.46	-2.33	-5.5	-57.	2323-2324	-5
0.0055	27.45	0.197	-0.052	4987.7	500.00	1.31	4.47	45.12	-0.41	-1.21	-5.5	-57.	2322-2322	-5
0.0056	27.95	0.193	-0.052	4987.7	500.00	0.47	4.47	19.82	-0.25	-0.19	-5.5	-57.	2322-2322	-5
0.0057	28.45	0.110	-0.051	4987.7	500.00	1.66	4.47	19.82	-0.31	-0.25	-5.5	-57.	2322-2322	-5
0.0058	28.95	0.192	-0.051	4987.7	500.00	2.61	4.47	21.71	-0.33	-0.23	-5.5	-57.	2322-2321	-5
0.0059	29.46	0.104	-0.051	4987.6	500.00	3.76	4.47	212.31	-2.71	-2.67	-5.5	-57.	2323-2321	-5
0.0060	29.56	0.105	-0.050	4987.5	500.00	4.42	4.47	216.4	-1.11	-1.09	-5.5	-57.	2323-2321	-5
0.0061	30.46	0.107	-0.050	4987.3	500.00	4.76	4.47	220.12	-3.37	-3.36	-5.5	-57.	2323-2324	-5
0.0062	30.95	0.109	-0.050	4987.1	500.00	4.89	4.47	223.47	-3.45	-3.45	-5.5	-57.	2323-2324	-5
0.0063	31.45	0.111	-0.050	4987.0	500.00	4.69	4.47	227.23	-3.43	-3.43	-5.5	-57.	2323-2321	-5
0.0064	31.45	0.114	-0.050	4986.9	500.00	3.57	4.47	230.41	-2.61	-2.61	-5.5	-57.	2322-2321	-5
0.0065	32.45	0.116	-0.051	4986.7	500.00	2.62	4.47	235.15	-1.65	-2.25	-5.5	-57.	2322-2321	-5
0.0066	32.95	0.118	-0.051	4986.5	500.00	1.67	4.47	241.6	-1.11	-1.09	-5.5	-57.	2322-2321	-5
0.0067	33.45	0.121	-0.052	4986.7	500.00	0.66	4.47	262.75	0.21	0.21	-5.5	-57.	2322-2321	-5
0.0068	33.95	0.123	-0.052	4986.7	500.00	0.65	4.47	262.75	0.21	0.21	-5.5	-57.	2322-2321	-5
0.0069	34.45	0.126	-0.053	4986.5	500.00	2.20	4.47	53.81	-0.28	-0.28	-5.5	-57.	2322-2321	-5
0.0070	34.45	0.129	-0.053	4986.6	500.00	3.51	4.47	56.26	-2.74	-2.74	-5.5	-57.	2322-2321	-5
0.0071	35.45	0.131	-0.052	4986.5	500.00	4.70	4.47	63.18	-3.62	-3.62	-5.5	-57.	2322-2321	-5
0.0072	35.95	0.133	-0.052	4986.7	500.00	5.45	4.47	65.92	-3.36	-3.36	-5.5	-57.	2322-2321	-5
0.0073	36.45	0.135	-0.052	4986.7	500.00	6.10	4.47	59.22	-4.22	-4.22	-5.5	-57.	2322-2321	-5
0.0074	36.95	0.137	-0.052	4986.7	500.00	6.60	4.47	71.57	-5.12	-5.12	-5.5	-57.	2322-2321	-5
0.0075	37.45	0.139	-0.051	4986.5	500.00	7.26	4.47	76.31	-5.46	-5.46	-5.5	-57.	2322-2321	-5
0.0076	37.93	0.141	-0.051	4986.6	500.00	6.50	4.47	76.15	-5.32	-5.32	-5.5	-57.	2322-2321	-5
0.0077	38.43	0.142	-0.052	4986.7	500.00	6.45	4.47	78.18	-5.12	-5.12	-5.5	-57.	2322-2321	-5
0.0078	38.93	0.143	-0.053	4986.7	500.00	5.71	4.47	79.13	-6.51	-6.51	-5.5	-57.	2322-2321	-5
0.0079	39.43	0.145	-0.053	4986.1	500.00	6.70	4.47	79.39	-6.54	-6.54	-5.5	-57.	2322-2321	-5
0.0080	39.93	0.145	-0.052	4986.5	500.00	3.43	4.47	75.12	-3.23	-3.23	-5.5	-57.	2322-2321	-5
0.0081	40.43	0.146	-0.051	4986.5	500.00	2.45	4.46	65.61	-2.35	-2.35	-5.5	-57.	2322-2321	-5
0.0082	40.93	0.147	-0.052	4986.2	500.00	1.65	4.46	72.72	-1.45	-1.45	-5.5	-57.	2322-2321	-5
0.0083	41.42	0.148	-0.052	4986.7	500.00	1.42	4.46	72.51	-0.31	-0.31	-5.5	-57.	2322-2321	-5
0.0084	41.92	0.148	-0.053	4986.7	500.00	0.71	4.46	72.51	-0.31	-0.31	-5.5	-57.	2322-2321	-5
0.0085	42.42	0.149	-0.053	4986.2	500.00	3.24	4.46	74.45	-5.05	-5.05	-5.5	-57.	2322-2321	-5
0.0086	42.92	0.150	-0.052	4986.5	500.00	4.10	4.46	312.37	1.63	1.63	-5.5	-57.	2322-2321	-5
0.0087	43.42	0.151	-0.051	4986.5	500.00	4.76	4.45	312.46	2.14	2.14	-5.5	-57.	2322-2321	-5
0.0088	43.92	0.152	-0.051	4986.6	500.00	5.12	4.45	314.30	2.31	2.31	-5.5	-57.	2322-2321	-5
0.0089	44.41	0.153	-0.052	4986.7	500.00	1.42	4.46	316.59	1.62	1.62	-5.5	-57.	2322-2321	-5
0.0090	44.91	0.154	-0.053	4986.7	500.00	0.65	4.46	316.59	2.42	2.42	-5.5	-57.	2322-2321	-5
0.0091	45.41	0.155	-0.053	4986.3	500.00	4.62	4.46	324.61	2.04	2.04	-5.5	-57.	2322-2321	-5
0.0092	45.91	0.157	-0.052	4986.2	500.00	2.92	4.45	310.53	1.57	1.57	-5.5	-57.	2322-2321	-5
0.0093	46.41	0.158	-0.051	4986.1	500.00	3.14	4.46	336.33	0.63	0.63	-5.5	-57.	2322-2321	-5
0.0094	46.91	0.160	-0.051	4986.1	500.00	2.25	4.46	363.64	0.21	0.21	-5.5	-57.	2322-2321	-5
0.0095	47.40	0.161	-0.052	4986.1	500.00	1.54	4.46	22.59	-0.53	-0.53	-5.5	-57.	2322-2321	-5
0.0096	47.89	0.163	-0.052	4986.1	500.00	1.45	4.46	26.83	-1.31	-1.31	-5.5	-57.	2322-2321	-5
0.0097	48.40	0.164	-0.052	4986.0	500.00	2.07	4.46	102.69	-2.07	-2.07	-5.5	-57.	2322-2321	-5
0.0098	48.50	0.166	-0.053	4986.0	500.00	2.38	4.46	112.65	-0.85	-0.85	-5.5	-57.	2322-2321	-5
0.0099	49.40	0.167	-0.051	4986.2	500.00	3.62	4.46	127.75	-3.31	-3.31	-5.5	-57.	2322-2321	-5

LECTURE 10: CONVERGENCE TESTS FOR SERIES

298

**COPY AVAILABLE TO FED AGES NOT
PERMIT FULLY LEGIBLE PRODUCTION**

FLECHETTE GROUND POINT

PAGE

T SFC	X FT	Y FT	Z FT	V FT/SEC	P ALPHA	MACH	PHI	ALPHA	PHT	L-N DEC	W-N DEC	L-P DEC	W-P DEC	S DEC	TAU DEC	W-T DEC
										CDS	CDG	1/SEC	1/SEC	1/SEC	1/SEC	1/SEC
0.0150	74.60	0.221	-0.154	4676.7	500.00	1.43	4.44	25.30	1.00	-6.94	-75.	-2.27	-2.27	-0.	-0.	-1.
0.0151	75.30	0.223	-0.056	4978.7	500.00	1.67	4.46	355.37	0.45	-1.21	-22.	-57.	-227.	-0.	-0.	-1.
0.0152	75.79	0.225	-0.059	4978.7	500.00	1.66	4.46	312.94	-2.15	-2.23	-56.	-57.	-227.	-0.	-0.	-1.
0.0153	76.29	0.227	-0.059	4978.6	500.00	2.84	4.45	335.23	-0.46	-2.75	-55.	-57.	-227.	-0.	-0.	-1.
0.0154	76.19	0.223	-0.103	4977.6	500.00	2.25	4.46	323.61	-1.07	-3.13	-55.	-57.	-227.	-0.	-0.	-1.
0.0155	77.29	0.234	-0.131	4979.5	500.00	3.72	4.46	312.84	-1.34	-3.46	-55.	-57.	-227.	-0.	-0.	-1.
0.0156	77.79	0.234	-0.102	4978.4	500.00	2.52	4.46	336.44	-1.52	-3.21	-55.	-57.	-227.	-0.	-0.	-1.
0.0157	78.28	0.235	-0.103	4978.3	500.00	3.62	4.46	317.93	-1.54	-3.61	-55.	-57.	-227.	-0.	-0.	-1.
0.0158	78.78	0.238	-0.105	4978.2	500.00	3.75	4.46	365.66	-1.62	-3.27	-55.	-57.	-227.	-0.	-0.	-1.
0.0159	79.29	0.240	-0.105	4978.1	500.00	3.41	4.46	365.52	-1.13	-3.29	-55.	-57.	-227.	-0.	-0.	-1.
0.0160	79.78	0.241	-0.195	4979.2	500.00	2.65	4.46	321.15	-0.34	-2.41	-55.	-57.	-227.	-0.	-0.	-1.
0.0161	80.27	0.243	-0.137	4978.0	500.00	2.39	4.46	1.77	-0.41	-2.15	-55.	-57.	-227.	-0.	-0.	-1.
0.0162	80.77	0.245	-0.197	4978.0	500.00	1.92	4.46	17.07	0.93	-1.42	-55.	-57.	-227.	-0.	-0.	-1.
0.0163	81.27	0.247	-0.104	4978.3	500.00	1.40	4.46	42.79	0.63	-1.26	-55.	-57.	-227.	-0.	-0.	-1.
0.0164	81.77	0.248	-0.168	4977.5	500.00	1.32	4.46	77.49	1.11	-0.71	-55.	-57.	-227.	-0.	-0.	-1.
0.0165	82.27	0.249	-0.193	4977.9	500.00	1.61	4.46	185.80	1.59	-0.20	-55.	-57.	-227.	-0.	-0.	-1.
0.0166	82.76	0.252	-0.102	4977.9	500.00	2.13	4.46	123.02	2.01	-0.25	-55.	-57.	-227.	-0.	-0.	-1.
0.0167	83.26	0.254	-0.103	4977.9	500.00	2.42	4.46	143.46	2.34	-0.42	-55.	-57.	-227.	-0.	-0.	-1.
0.0168	83.76	0.256	-0.119	4977.2	500.00	2.70	4.46	149.35	2.54	-0.47	-55.	-57.	-227.	-0.	-0.	-1.
0.0169	84.26	0.259	-0.111	4977.5	500.00	2.84	4.46	145.12	2.70	1.03	-55.	-57.	-227.	-0.	-0.	-1.
0.0170	84.75	0.263	-0.111	4977.7	500.00	2.81	4.46	141.39	2.62	1.01	-55.	-57.	-227.	-0.	-0.	-1.
0.0171	85.25	0.264	-0.112	4977.7	500.00	2.61	4.46	149.93	2.46	0.99	-55.	-57.	-227.	-0.	-0.	-1.
0.0172	85.75	0.265	-0.113	4977.5	500.00	2.27	4.46	152.46	2.01	0.25	-55.	-57.	-227.	-0.	-0.	-1.
0.0173	86.25	0.267	-0.113	4977.0	500.00	1.80	4.46	155.25	1.70	0.23	-55.	-57.	-227.	-0.	-0.	-1.
0.0174	86.75	0.270	-0.114	4977.6	500.00	1.29	4.46	132.47	1.25	-0.14	-55.	-57.	-227.	-0.	-0.	-1.
0.0175	87.25	0.272	-0.115	4977.6	500.00	0.97	4.46	101.43	0.73	-0.34	-55.	-57.	-227.	-0.	-0.	-1.
0.0176	87.74	0.275	-0.115	4977.6	500.00	1.17	4.46	65.77	0.13	-1.17	-55.	-57.	-227.	-0.	-0.	-1.
0.0177	88.24	0.277	-0.112	4977.7	500.00	2.61	4.46	149.93	2.46	0.99	-55.	-57.	-227.	-0.	-0.	-1.
0.0178	88.74	0.275	-0.113	4977.5	500.00	2.27	4.46	152.46	2.17	0.64	-55.	-57.	-227.	-0.	-0.	-1.
0.0179	89.23	0.279	-0.115	4977.5	500.00	1.80	4.46	155.25	1.70	0.23	-55.	-57.	-227.	-0.	-0.	-1.
0.0180	89.73	0.285	-0.118	4977.4	500.00	2.71	4.46	31.19	-2.12	-2.14	-55.	-57.	-227.	-0.	-0.	-1.
0.0181	90.23	0.287	-0.119	4977.3	500.00	3.19	4.46	2.51	-3.32	-3.32	-55.	-57.	-227.	-0.	-0.	-1.
0.0182	90.73	0.280	-0.115	4977.2	500.00	4.47	4.46	33.12	-2.79	-3.69	-55.	-57.	-227.	-0.	-0.	-1.
0.0183	91.22	0.292	-0.120	4977.1	500.00	4.49	4.46	36.73	-2.45	-3.23	-55.	-57.	-227.	-0.	-0.	-1.
0.0184	91.72	0.291	-0.120	4977.5	500.00	2.46	4.46	31.67	-1.95	-2.21	-55.	-57.	-227.	-0.	-0.	-1.
0.0185	92.22	0.292	-0.120	4977.5	500.00	3.13	4.46	31.61	-1.65	-2.67	-55.	-57.	-227.	-0.	-0.	-1.
0.0186	92.72	0.294	-0.123	4977.6	500.00	3.99	4.46	49.35	2.72	2.33	-55.	-57.	-227.	-0.	-0.	-1.
0.0187	93.22	0.300	-0.117	4977.5	500.00	3.19	4.46	62.15	-2.12	-2.12	-55.	-57.	-227.	-0.	-0.	-1.
0.0188	93.71	0.302	-0.119	4977.6	500.00	2.80	4.46	63.51	-2.13	-2.13	-55.	-57.	-227.	-0.	-0.	-1.
0.0189	94.21	0.313	-0.119	4977.6	500.00	2.21	4.46	24.31	-1.53	-1.49	-55.	-57.	-227.	-0.	-0.	-1.
0.0190	94.71	0.305	-0.118	4977.5	500.00	1.51	4.46	36.55	-2.5	-3.25	-55.	-57.	-227.	-0.	-0.	-1.
0.0191	95.21	0.316	-0.118	4977.5	500.00	1.34	4.46	32.47	-2.1	-2.4	-55.	-57.	-227.	-0.	-0.	-1.
0.0192	95.70	0.318	-0.113	4977.5	500.00	0.33	4.46	35.22	-0.73	-0.68	-55.	-57.	-227.	-0.	-0.	-1.
0.0193	96.20	0.310	-0.117	4977.5	500.00	0.62	4.46	31.42	-0.30	-0.34	-55.	-57.	-227.	-0.	-0.	-1.
0.0194	96.70	0.311	-0.117	4977.6	500.00	1.09	4.46	24.36	-0.37	-0.43	-55.	-57.	-227.	-0.	-0.	-1.
0.0195	97.20	0.313	-0.117	4977.5	500.00	1.44	4.46	25.91	0.61	1.30	-55.	-57.	-227.	-0.	-0.	-1.
0.0196	97.69	0.315	-0.116	4977.5	500.00	1.65	4.46	28.53	0.73	1.59	-55.	-57.	-227.	-0.	-0.	-1.
0.0197	98.19	0.316	-0.116	4977.6	500.00	1.74	4.46	26.97	0.74	1.32	-55.	-57.	-227.	-0.	-0.	-1.
0.0198	98.69	0.318	-0.116	4977.6	500.00	1.67	4.46	27.75	0.54	1.25	-55.	-57.	-227.	-0.	-0.	-1.
0.0199	99.19	0.320	-0.116	4977.6	500.00	1.48	4.46	23.44	0.43	1.41	-55.	-57.	-227.	-0.	-0.	-1.

FLECHETTE GROUND POINT

PAGE 5

	X	Y	Z	P	V	FT	FT	FT/SEC	PADSEC	REG	ALPHA	BETA	DEC	DEC	1/SEC	1/SEC	AG/SIC	AG/SIC	H-V	H-P	S	TAN	N-T	E-S
0.0200	99.68	0.322	-0.116	4976.4	2976.4	500.00	0.51	4.46	2556.78	0.14	1.18	-55.	-57.	2324	-2325	-	-	0*	0*	-	-	1*	-	
0.0201	100.18	0.321	-0.115	4975.4	2975.4	500.00	0.51	4.46	321.25	-0.24	0.43	-55.	-57.	2324	-2325	-	-	0*	0*	-	-	1*	-	
0.0202	100.58	0.325	-0.116	4975.4	2975.4	500.00	0.51	4.46	0.91	-0.57	0.52	-55.	-57.	2323	-2325	-	-	0*	0*	-	-	1*	-	
0.0203	101.18	0.328	-0.116	4974.4	2974.4	500.00	1.14	4.46	35.16	-1.13	0.13	-55.	-57.	2323	-2325	-	-	0*	0*	-	-	1*	-	
0.0204	101.68	0.329	-0.116	4974.4	2974.4	500.00	1.42	4.46	54.03	-1.63	0.63	-55.	-57.	2323	-2325	-	-	0*	0*	-	-	1*	-	
0.0205	102.17	0.331	-0.116	4975.3	2975.3	500.00	2.15	4.46	67.64	-2.35	0.24	-55.	-57.	2323	-2325	-	-	0*	0*	-	-	1*	-	
0.0206	102.67	0.333	-0.117	4975.3	2975.3	500.00	2.65	4.46	72.37	-2.47	0.37	-55.	-57.	2324	-2325	-	-	0*	0*	-	-	1*	-	
0.0207	103.17	0.325	-0.117	4976.3	2976.3	500.00	3.04	4.46	77.25	-2.52	1.25	-55.	-57.	2324	-2325	-	-	0*	0*	-	-	1*	-	
0.0208	103.67	0.335	-0.117	4976.2	2976.2	500.00	2.71	4.46	81.72	-3.04	1.64	-55.	-57.	2324	-2325	-	-	0*	0*	-	-	1*	-	
0.0209	104.16	0.318	-0.117	4977.1	2977.1	500.00	3.60	4.46	54.32	-3.26	1.56	-45.	-57.	2324	-2325	-	-	0*	0*	-	-	1*	-	
0.0210	104.65	0.320	-0.114	4975.3	2975.3	500.00	3.66	4.46	56.67	-3.33	1.53	-45.	-57.	2324	-2325	-	-	0*	0*	-	-	1*	-	
0.0211	105.16	0.310	-0.115	4975.9	2975.9	500.00	2.58	4.46	98.23	-1.23	1.21	-55.	-57.	2324	-2325	-	-	0*	0*	-	-	1*	-	
0.0212	105.56	0.312	-0.115	4975.2	2975.2	500.00	3.37	4.46	69.82	-3.14	1.21	-55.	-57.	2324	-2325	-	-	0*	0*	-	-	1*	-	
0.0213	105.15	0.343	-0.114	4975.4	2975.4	500.00	2.04	4.46	83.05	-2.40	0.51	-55.	-57.	2323	-2324	-	-	0*	0*	-	-	1*	-	
0.0214	105.65	0.344	-0.115	4975.5	2975.5	500.00	2.62	4.46	85.21	-2.54	0.53	-55.	-57.	2323	-2324	-	-	0*	0*	-	-	1*	-	
0.0215	107.15	0.354	-0.115	4975.7	2975.7	500.00	2.17	4.46	76.45	-2.15	0.18	-55.	-57.	2323	-2324	-	-	0*	0*	-	-	1*	-	
0.0216	107.45	0.345	-0.115	4975.7	2975.7	500.00	1.76	4.46	69.52	-1.72	0.32	-55.	-57.	2323	-2324	-	-	0*	0*	-	-	1*	-	
0.0217	105.14	0.345	-0.114	4975.0	2975.0	500.00	1.55	4.46	26.33	-1.24	3.67	-55.	-57.	2323	-2324	-	-	0*	0*	-	-	1*	-	
0.0218	105.44	0.367	-0.113	4975.7	2975.7	500.00	1.55	4.46	26.29	-1.36	3.65	-55.	-57.	2323	-2324	-	-	0*	0*	-	-	1*	-	
0.0219	109.12	0.347	-0.113	4975.7	2975.7	500.00	1.94	4.46	77.43	-0.31	1.21	-55.	-57.	2323	-2324	-	-	0*	0*	-	-	1*	-	
0.0220	105.64	0.349	-0.113	4975.5	2975.5	500.00	2.22	4.46	357.92	2.11	2.21	-55.	-57.	2323	-2324	-	-	0*	0*	-	-	1*	-	
0.0221	110.13	0.345	-0.113	4975.4	2975.4	500.00	2.59	4.46	365.33	0.45	2.79	-55.	-57.	2323	-2324	-	-	0*	0*	-	-	1*	-	
0.0222	110.63	0.350	-0.113	4975.5	2975.5	500.00	2.85	4.46	351.70	0.73	2.79	-55.	-57.	2323	-2324	-	-	0*	0*	-	-	1*	-	
0.0223	111.13	0.351	-0.113	4975.5	2975.5	500.00	3.35	4.46	351.93	0.52	2.65	-55.	-57.	2323	-2324	-	-	0*	0*	-	-	1*	-	
0.0224	111.63	0.351	-0.113	4975.7	2975.7	500.00	3.16	4.46	353.49	1.36	3.65	-55.	-57.	2323	-2324	-	-	0*	0*	-	-	1*	-	
0.0225	112.12	0.352	-0.113	4975.7	2975.7	500.00	3.12	4.46	353.49	1.21	3.65	-55.	-57.	2323	-2324	-	-	0*	0*	-	-	1*	-	
0.0226	112.62	0.353	-0.113	4975.3	2975.3	500.00	2.96	4.46	365.15	0.92	2.81	-55.	-57.	2323	-2324	-	-	0*	0*	-	-	1*	-	
0.0227	113.12	0.354	-0.114	4975.5	2975.5	500.00	2.65	4.46	37.76	0.70	2.79	-55.	-57.	2323	-2324	-	-	0*	0*	-	-	1*	-	
0.0228	113.62	0.355	-0.114	4975.2	2975.2	500.00	2.35	4.46	31.43	1.42	0.51	-55.	-57.	2323	-2324	-	-	0*	0*	-	-	1*	-	
0.0229	114.11	0.355	-0.115	4975.2	2975.2	500.00	1.96	4.46	29.48	1.20	1.65	-55.	-57.	2323	-2324	-	-	0*	0*	-	-	1*	-	
0.0230	114.61	0.357	-0.115	4975.2	2975.2	500.00	1.56	4.46	33.93	-0.12	1.52	-55.	-57.	2323	-2324	-	-	0*	0*	-	-	1*	-	
0.0231	115.11	0.352	-0.113	4975.2	2975.2	500.00	1.25	4.46	355.42	1.51	1.51	-55.	-57.	2323	-2324	-	-	0*	0*	-	-	1*	-	
0.0232	115.61	0.349	-0.117	4975.2	2975.2	500.00	1.18	4.46	53.46	0.21	1.29	-55.	-57.	2323	-2324	-	-	0*	0*	-	-	1*	-	
0.0233	116.10	0.354	-0.114	4975.3	2975.3	500.00	1.16	4.46	102.44	-0.73	3.55	-55.	-57.	2323	-2324	-	-	0*	0*	-	-	1*	-	
0.0234	116.60	0.342	-0.113	4975.3	2975.3	500.00	1.35	4.46	127.12	-1.31	3.20	-55.	-57.	2323	-2324	-	-	0*	0*	-	-	1*	-	
0.0235	117.10	0.342	-0.119	4975.1	2975.1	500.00	1.78	4.46	136.46	-1.43	0.32	-55.	-57.	2323	-2324	-	-	0*	0*	-	-	1*	-	
0.0236	117.61	0.363	-0.116	4975.1	2975.1	500.00	1.55	4.46	172.53	-1.57	0.16	-55.	-57.	2323	-2324	-	-	0*	0*	-	-	1*	-	
J-0.0237	118.09	0.364	-0.120	4975.1	2975.1	500.00	1.59	4.46	53.29	-0.23	0.23	-55.	-57.	2323	-2324	-	-	0*	0*	-	-	1*	-	
0.0238	121.08	0.359	-0.123	4975.0	2975.0	500.00	1.00	4.46	72.01	-0.73	0.73	-55.	-57.	2323	-2324	-	-	0*	0*	-	-	1*	-	
0.0239	118.58	0.345	-0.120	4975.1	2975.1	500.00	1.56	4.46	145.92	-1.43	0.12	-55.	-57.	2323	-2324	-	-	0*	0*	-	-	1*	-	
0.0240	121.58	0.356	-0.121	4975.1	2975.1	500.00	1.32	4.46	149.56	-1.32	0.93	-55.	-57.	2323	-2324	-	-	0*	0*	-	-	1*	-	
0.0241	122.05	0.369	-0.124	4975.0	2975.0	500.00	1.02	4.46	62.37	-0.35	1.07	-55.	-57.	2323	-2324	-	-	0*	0*	-	-	1*	-	
0.0242	122.55	0.370	-0.125	4975.0	2975.0	500.00	2.41	4.46	50.44	-1.47	1.47	-55.	-57.	2323	-2324	-	-	0*	0*	-	-	1*	-	
0.0243	123.07	0.370	-0.125	4975.0	2975.0	500.00	2.84	4.46	43.37	1.75	2.24	-55.	-57.	2323	-2324	-	-	0*	0*	-	-	1*	-	
0.0244	123.57	0.371	-0.125	4975.0	2975.0	500.00	3.20	4.46	40.53	-2.02	2.32	-55.	-57.	2323	-2324	-	-	0*	0*	-	-	1*	-	
0.0245	124.06	0.372	-0.127	4975.5	2975.5	500.00	3.46	4.46	41.72	2.32	2.32	-55.	-57.	2323	-2324	-	-	0*	0*	-	-	1*	-	

300 COPY AVAILABLE TO DDC DOES NOT PERMIT FULLY LEGIBLE PRODUCTION

FLECHETTE GROUND POINT

T	X	Y	Z	FT	FT	PT/SEF	RAD/SEC	PRG	ALPHA MACH	PHI ALPHAI	PCT	DEG	DSC	DEG	W/N SEC	W/P SEC	S	TAN	F	G
SEC	124.56	3.113	-0.129	4.674	7	500.00	3.61	7.6	63.59	2.13	2.51	-5.5	-5.5	-5.5	232.5	222.5	-10	0	-	-
0.0250	125.05	0.377	-0.125	4.974	7	500.00	3.61	4.15	66.57	2.57	2.57	-5.5	-5.5	-5.5	232.5	222.5	-10	0	-	-
0.0251	125.54	0.315	-0.130	4.974	6	500.00	3.54	4.65	62.05	2.53	2.45	-6.5	-6.5	-6.5	232.5	222.5	-10	0	-	-
0.0252	125.56	0.377	-0.130	4.974	5	500.00	3.34	4.56	47.41	2.49	2.24	-5.5	-5.5	-5.5	232.5	222.5	-10	0	-	-
0.0253	126.05	0.377	-0.131	4.974	5	500.00	3.34	4.56	47.41	2.49	2.24	-5.5	-5.5	-5.5	232.5	222.5	-10	0	-	-
0.0254	126.55	0.377	-0.132	4.974	5	500.00	3.04	4.15	43.85	2.31	2.07	-5.5	-5.5	-5.5	232.5	222.5	-10	0	-	-
0.0255	127.05	0.378	-0.134	4.974	4	500.00	2.55	4.44	4.93	2.05	1.93	-5.5	-5.5	-5.5	232.5	222.5	-10	0	-	-
0.0256	127.55	0.377	-0.135	4.974	4	500.00	2.21	4.15	15.51	1.92	1.25	-5.5	-5.5	-5.5	232.5	222.5	-10	0	-	-
0.0257	128.04	0.361	-0.126	4.974	3	500.00	1.74	6.45	46.17	1.51	0.95	-5.5	-5.5	-5.5	232.5	222.5	-10	0	-	-
0.0258	128.54	0.352	-0.134	4.974	3	500.00	1.24	4.45	49.35	1.13	0.75	-5.5	-5.5	-5.5	232.5	222.5	-10	0	-	-
0.0259	129.04	0.344	-0.130	4.974	3	500.00	0.56	4.16	25.73	0.14	0.15	-5.5	-5.5	-5.5	232.5	222.5	-10	0	-	-
0.0260	129.54	0.345	-0.130	4.974	3	500.00	0.56	4.16	25.73	0.14	0.15	-5.5	-5.5	-5.5	232.5	222.5	-10	0	-	-
0.0261	130.03	0.355	-0.142	4.974	3	500.00	0.73	4.15	32.71	0.35	0.63	-5.5	-5.5	-5.5	232.5	222.5	-10	0	-	-
0.0262	130.53	0.358	-0.143	4.974	3	500.00	0.81	6.45	31.11	0.16	0.79	-5.5	-5.5	-5.5	232.5	222.5	-10	0	-	-
0.0263	131.03	0.369	-0.165	4.974	3	500.00	1.09	4.75	30.57	0.14	0.99	-5.5	-5.5	-5.5	232.5	222.5	-10	0	-	-
0.0264	131.53	0.361	-0.134	4.974	3	500.00	1.21	4.45	30.57	0.12	1.21	-5.5	-5.5	-5.5	232.5	222.5	-10	0	-	-
0.0265	132.02	0.372	-0.147	4.974	3	500.00	1.25	4.45	30.37	0.09	1.75	-5.5	-5.5	-5.5	232.5	222.5	-10	0	-	-
0.0266	132.52	0.334	-0.133	4.974	3	500.00	1.22	4.75	217.5	0.12	2.21	-5.5	-5.5	-5.5	232.5	222.5	-10	0	-	-
0.0267	133.02	0.355	-0.152	4.974	3	500.00	1.14	4.16	32.3	0.26	1.11	-4.5	-4.5	-4.5	232.5	222.5	-10	0	-	-
0.0268	133.52	0.356	-0.151	4.974	3	500.00	1.07	4.45	32.45	0.15	0.95	-5.5	-5.5	-5.5	232.5	222.5	-10	0	-	-
0.0269	134.01	0.358	-0.152	4.974	3	500.00	1.06	6.16	6.01	0.73	0.73	-5.5	-5.5	-5.5	232.5	222.5	-10	0	-	-
0.0270	134.51	0.369	-0.155	4.974	3	500.00	1.16	4.15	27.17	1.01	2.51	-5.5	-5.5	-5.5	232.5	222.5	-10	0	-	-
0.0271	135.01	0.363	-0.154	4.974	3	500.00	1.22	4.75	217.5	0.12	2.21	-5.5	-5.5	-5.5	232.5	222.5	-10	0	-	-
0.0272	135.52	0.355	-0.152	4.974	3	500.00	1.14	4.16	32.3	0.26	1.11	-4.5	-4.5	-4.5	232.5	222.5	-10	0	-	-
0.0273	136.02	0.356	-0.151	4.974	3	500.00	1.07	4.45	32.45	0.15	0.95	-5.5	-5.5	-5.5	232.5	222.5	-10	0	-	-
0.0274	136.52	0.358	-0.152	4.974	3	500.00	1.06	6.16	6.01	0.73	0.73	-5.5	-5.5	-5.5	232.5	222.5	-10	0	-	-
0.0275	137.02	0.369	-0.155	4.974	3	500.00	1.16	4.15	27.17	1.01	2.51	-5.5	-5.5	-5.5	232.5	222.5	-10	0	-	-
0.0276	137.52	0.361	-0.154	4.974	3	500.00	1.22	4.75	217.5	0.12	2.21	-5.5	-5.5	-5.5	232.5	222.5	-10	0	-	-
0.0277	137.99	0.362	-0.154	4.974	2	500.00	1.38	4.15	45.53	1.15	0.27	-5.5	-5.5	-5.5	232.5	222.5	-10	0	-	-
0.0278	138.49	0.402	-0.155	4.974	2	500.00	1.66	4.16	87.35	2.53	0.62	-5.5	-5.5	-5.5	232.5	222.5	-10	0	-	-
0.0279	138.99	0.413	-0.156	4.974	2	500.00	1.66	4.16	87.35	2.53	0.62	-5.5	-5.5	-5.5	232.5	222.5	-10	0	-	-
0.0280	139.48	0.415	-0.155	4.974	2	500.00	2.35	4.45	22.3	0.45	0.25	-5.5	-5.5	-5.5	232.5	222.5	-10	0	-	-
0.0281	139.99	0.416	-0.156	4.974	2	500.00	2.45	4.45	69.00	2.01	0.43	-5.5	-5.5	-5.5	232.5	222.5	-10	0	-	-
0.0282	140.49	0.421	-0.155	4.974	2	500.00	1.56	4.16	95.16	2.12	0.43	-5.5	-5.5	-5.5	232.5	222.5	-10	0	-	-
0.0283	140.99	0.422	-0.156	4.974	2	500.00	1.56	4.16	95.16	2.12	0.43	-5.5	-5.5	-5.5	232.5	222.5	-10	0	-	-
0.0284	141.47	0.424	-0.161	4.974	2	500.00	2.64	4.46	53.95	2.54	0.36	-5.5	-5.5	-5.5	232.5	222.5	-10	0	-	-
0.0285	141.47	0.424	-0.162	4.974	0	500.00	2.47	4.46	47.45	2.11	0.44	-5.5	-5.5	-5.5	232.5	222.5	-10	0	-	-
0.0286	141.47	0.424	-0.163	4.974	0	500.00	1.53	4.45	47.45	2.11	0.44	-5.5	-5.5	-5.5	232.5	222.5	-10	0	-	-
0.0287	142.07	0.424	-0.171	4.974	0	500.00	2.47	4.46	47.45	2.11	0.44	-5.5	-5.5	-5.5	232.5	222.5	-10	0	-	-
0.0288	142.97	0.431	-0.172	4.974	0	500.00	1.53	4.45	47.45	2.11	0.44	-5.5	-5.5	-5.5	232.5	222.5	-10	0	-	-
0.0289	143.46	0.432	-0.173	4.974	0	500.00	1.53	4.45	47.45	2.11	0.44	-5.5	-5.5	-5.5	232.5	222.5	-10	0	-	-
0.0290	143.96	0.436	-0.174	4.974	0	500.00	2.64	4.46	53.95	2.54	0.36	-5.5	-5.5	-5.5	232.5	222.5	-10	0	-	-
0.0291	144.46	0.439	-0.175	4.974	0	500.00	1.53	4.45	47.45	2.11	0.44	-5.5	-5.5	-5.5	232.5	222.5	-10	0	-	-
0.0292	144.96	0.449	-0.175	4.974	0	500.00	2.47	4.46	47.45	2.11	0.44	-5.5	-5.5	-5.5	232.5	222.5	-10	0	-	-
0.0293	145.45	0.452	-0.177	4.974	0	500.00	1.53	4.45	47.45	2.11	0.44	-5.5	-5.5	-5.5	232.5	222.5	-10	0	-	-
0.0294	145.95	0.454	-0.177	4.974	0	500.00	2.64	4.46	53.95	2.54	0.36	-5.5	-5.5	-5.5	232.5	222.5	-10	0	-	-
0.0295	146.45	0.447	-0.178	4.974	0	500.00	2.17	4.45	15.47	2.71	2.36	-5.5	-5.5	-5.5	232.5	222.5	-10	0	-	-
0.0296	146.94	0.454	-0.178	4.974	0	500.00	2.26	4.45	20.53	0.57	2.18	-5.5	-5.5	-5.5	232.5	222.5	-10	0	-	-
0.0297	147.44	0.451	-0.173	4.974	0	500.00	2.09	4.45	20.53	0.57	2.18	-5.5	-5.5	-5.5	232.5	222.5	-10	0	-	-
0.0298	147.94	0.453	-0.173	4.974	0	500.00	1.71	4.45	31.57	1.23	1.70	-5.5	-5.5	-5.5	232.5	222.5	-10	0	-	-
0.0299	148.43	0.455	-0.170	4.974	0	500.00	1.17	4.45	4.45	0.22	0.43	-5.5	-5.5	-5.5	232.5	222.5	-10	0	-	-
0.0300	148.93	0.457	-0.169	4.974	0	500.00	0.93	4.45	56.93	0.19	1.16	-5.5	-5.5	-5.5	232.5	222.5	-10	0	-	-

#FLFCHEETE GROUP PCINIT

一
二
三
四

FLECHETTE GROUND POINT

PAGE

5

	X	Y	Z	N	P	ALPHA	MAGN	PHI	ALPHA	BETA	LEP	HIP	S	TAU	K-1
SEC	FT	FT	FT	SEC	RAD/SEC	SEC	SEC	SEC	SEC	SEC	SEC	SEC	SEC	SEC	SEC
0.0350	174.30	0.541	-0.150	4972.6	.509.00	1.49	4.45	63.23	-1.22	0.65	-55.	-57.	23.0	-2327.	0.
0.0351	174.79	0.442	-0.180	4672.6	.503.00	1.45	4.45	57.57	-0.45	1.00	-55.	-57.	22.28	-2327.	0.
0.0352	175.29	0.542	-0.150	4972.6	.507.00	1.68	4.15	25.74	-0.62	1.32	-55.	-57.	23.50	-2327.	0.
0.0353	175.70	0.543	-0.180	4972.6	.506.00	1.60	4.15	35.91	-0.41	1.14	-55.	-57.	23.30	-2327.	0.
0.0354	176.20	0.544	-0.150	4972.6	.506.00	1.67	4.45	23.51	-0.15	0.45	-55.	-57.	23.30	-2327.	0.
0.0355	176.70	0.545	-0.180	4972.6	.507.00	1.86	4.45	24.74	2.11	1.34	-55.	-57.	23.30	-2327.	0.
0.0356	177.20	0.545	-0.181	4672.6	.500.00	2.11	4.95	21.99	0.21	2.03	-55.	-57.	23.41	-2327.	0.
0.0357	177.70	0.546	-0.150	4972.5	.500.00	2.24	4.45	20.77	2.19	2.19	-55.	-57.	23.30	-2327.	0.
0.0358	178.20	0.546	-0.181	4972.5	.500.00	2.33	4.45	20.74	0.52	2.25	-55.	-57.	23.30	-2327.	0.
0.0359	178.70	0.547	-0.182	4772.5	.510.00	2.37	4.45	21.42	0.71	2.26	-55.	-57.	23.30	-2327.	0.
0.0360	179.20	0.548	-0.182	4672.5	.500.00	2.35	4.45	21.25	0.75	2.22	-55.	-57.	23.30	-2327.	0.
0.0361	179.70	0.549	-0.183	4772.4	.500.00	2.27	4.45	25.53	0.75	2.14	-55.	-57.	23.30	-2327.	0.
0.0362	180.20	0.550	-0.183	4972.4	.500.00	2.31	4.45	25.41	0.79	2.22	-55.	-57.	23.30	-2327.	0.
0.0363	180.70	0.551	-0.184	4672.4	.500.00	1.97	4.45	31.91	2.53	1.55	-55.	-57.	23.30	-2327.	0.
0.0364	181.20	0.551	-0.185	4972.3	.510.00	1.76	4.45	36.69	0.52	1.59	-55.	-57.	24.31	-2327.	0.
0.0365	181.70	0.552	-0.185	4772.3	.500.00	1.54	4.45	41.00	0.61	1.63	-55.	-57.	23.30	-2327.	0.
0.0366	182.20	0.553	-0.185	4672.3	.500.00	1.32	4.45	45.21	1.25	1.25	-55.	-57.	23.30	-2327.	0.
0.0367	182.70	0.554	-0.187	4972.3	.500.00	1.11	4.45	53.61	0.18	1.39	-55.	-57.	23.30	-2327.	0.
0.0368	183.20	0.555	-0.188	4972.3	.500.00	0.91	4.45	61.39	2.95	0.91	-55.	-57.	23.30	-2327.	0.
0.0369	183.70	0.556	-0.189	4972.3	.500.00	0.76	4.45	69.75	0.93	0.93	-55.	-57.	23.30	-2327.	0.
0.0370	184.20	0.557	-0.191	4772.3	.500.00	0.63	4.45	77.16	0.93	0.53	-55.	-57.	23.30	-2327.	0.
0.0371	184.70	0.558	-0.191	4572.3	.500.00	0.54	4.45	83.41	0.53	0.53	-55.	-57.	23.30	-2327.	0.
0.0372	185.20	0.559	-0.191	4972.3	.500.00	0.40	4.45	84.19	0.37	0.17	-55.	-57.	23.30	-2327.	0.
0.0373	185.70	0.560	-0.192	4972.3	.500.00	0.34	4.45	79.11	0.39	0.45	-55.	-57.	23.30	-2327.	0.
0.0374	186.20	0.560	-0.193	4772.3	.500.00	0.26	4.45	62.93	0.11	0.47	-55.	-57.	23.30	-2327.	0.
0.0375	186.70	0.561	-0.194	4972.3	.500.00	0.20	4.45	59.40	0.25	0.53	-55.	-57.	23.30	-2327.	0.
0.0376	187.20	0.562	-0.195	4772.3	.500.00	0.15	4.45	57.14	0.13	0.61	-55.	-57.	23.30	-2327.	0.
0.0377	187.70	0.563	-0.196	4972.3	.500.00	0.95	4.45	7.35	0.64	0.71	-55.	-57.	23.30	-2327.	0.
0.0378	188.20	0.564	-0.197	4972.3	.500.00	1.19	4.45	47.16	0.55	0.32	-55.	-57.	23.30	-2327.	0.
0.0379	188.70	0.565	-0.198	4972.2	.500.00	1.43	4.45	67.12	1.03	0.51	-55.	-57.	23.30	-2327.	0.
0.0380	189.20	0.566	-0.198	4972.2	.500.00	1.62	4.45	47.75	1.31	1.15	-55.	-57.	23.30	-2327.	0.
0.0381	189.70	0.567	-0.200	4972.2	.500.00	1.09	4.45	7.61	1.52	1.24	-55.	-57.	23.30	-2327.	0.
0.0382	190.20	0.568	-0.201	4672.2	.500.00	2.19	4.45	57.13	1.71	1.22	-55.	-57.	23.30	-2327.	0.
0.0383	190.70	0.569	-0.202	4572.2	.500.00	2.26	4.45	51.61	1.57	1.27	-55.	-57.	23.30	-2327.	0.
0.0384	191.20	0.570	-0.202	4972.1	.500.00	2.37	4.45	53.21	2.93	1.25	-55.	-57.	23.30	-2327.	0.
0.0385	191.70	0.571	-0.203	4572.1	.500.00	2.12	4.45	51.45	2.13	1.25	-55.	-57.	23.30	-2327.	0.
0.0386	192.20	0.572	-0.203	4972.1	.500.00	2.42	4.45	55.47	2.12	1.13	-55.	-57.	23.30	-2327.	0.
0.0387	192.65	0.573	-0.204	4972.1	.500.00	2.37	4.45	55.13	2.14	1.07	-55.	-57.	23.30	-2327.	0.
0.0388	193.15	0.575	-0.204	4972.0	.500.00	1.45	4.45	55.30	2.97	1.22	-55.	-57.	23.30	-2327.	0.
0.0389	193.59	0.576	-0.204	4972.0	.500.00	2.02	4.45	51.61	1.63	1.25	-55.	-57.	23.30	-2327.	0.
0.0390	194.19	0.578	-0.211	4972.0	.500.00	1.64	4.45	54.34	1.56	1.25	-55.	-57.	23.30	-2327.	0.
0.0391	194.69	0.579	-0.212	4971.9	.500.00	1.75	4.45	51.55	1.72	1.33	-55.	-57.	23.30	-2327.	0.
0.0392	195.18	0.581	-0.213	4971.9	.500.00	1.56	4.45	67.35	1.55	1.10	-55.	-57.	23.30	-2327.	0.
0.0393	195.68	0.582	-0.215	4971.9	.500.00	1.49	4.45	51.22	1.39	1.13	-55.	-57.	23.30	-2327.	0.
0.0394	196.17	0.584	-0.215	4971.9	.500.00	1.27	4.45	33.55	1.22	0.35	-55.	-57.	24.31	-2327.	0.
0.0395	196.67	0.586	-0.217	4971.9	.500.00	1.21	4.45	1.36	1.17	0.36	-55.	-57.	23.30	-2327.	0.
0.0396	197.17	0.587	-0.219	4971.9	.500.00	1.19	4.45	15.38	0.93	0.74	-55.	-57.	23.30	-2327.	0.
0.0397	197.67	0.589	-0.220	4971.9	.500.00	1.21	4.45	11.36	0.31	0.55	-55.	-57.	23.30	-2327.	0.
0.0398	198.16	0.591	-0.221	4971.9	.500.00	1.25	4.45	9.27	0.73	1.92	-55.	-57.	23.30	-2327.	0.
0.0399	198.66	0.592	-0.223	4971.9	.500.00	1.30	4.45	5.03	0.84	1.11	-55.	-57.	23.30	-2327.	0.

COPY AVAILABLE TO FDR AGES NOT
PERMIT FULLY LEGIBLE PRODUCTION

ELEPHETTE GROUND POINT

PAGE 9

T	X	Y	Z	V	P	ALPHA	MACH	PHI	ALPHA	BETA	GAMMA	W-E	N-S	E-W	S	TAU	K-T
SEC	FT	FT	FT	FT/SEC	RADIANS	DEG	DEG	DEG	SEC	SEC	SEC	SEC	SEC	SEC	SEC	SEC	SEC
0.0400	198.16	0.624	4.971.4	500.00	1.33	4.45	6.11	0.46	-1.16	-55.	-57.	2330.	-2327.	-0.	0.	1.	
0.0401	198.65	0.6225	4.971.6	500.00	1.35	4.43	6.25	0.57	-1.17	-55.	-57.	2330.	-2327.	-0.	0.	1.	
0.0402	200.15	0.593	4.971.8	500.00	1.36	4.45	6.20	0.72	-1.15	-55.	-57.	2330.	-2327.	-0.	0.	1.	
0.0403	200.65	0.559	4.971.8	500.00	1.36	4.45	6.69	0.73	-1.11	-55.	-57.	2330.	-2327.	-0.	0.	1.	
0.0404	201.15	0.621	4.971.5	500.00	1.37	4.45	22.45	2.32	-1.16	-55.	-57.	2330.	-2327.	-0.	0.	1.	
0.0405	201.64	0.663	4.971.8	500.00	1.36	4.45	38.45	0.79	-0.95	-55.	-57.	2330.	-2327.	-0.	0.	1.	
0.0406	202.14	0.605	4.971.4	500.00	1.41	4.45	45.53	1.11	-0.97	-55.	-57.	2330.	-2327.	-0.	0.	1.	
0.0407	202.64	0.607	4.971.2	500.00	1.44	4.45	53.96	1.22	-0.74	-55.	-57.	2330.	-2327.	-0.	0.	1.	
0.0408	203.13	0.609	4.971.3	500.00	1.49	4.45	61.61	1.32	-0.70	-55.	-57.	2330.	-2327.	-0.	0.	1.	
0.0409	203.53	0.610	4.971.2	500.00	1.53	4.45	67.77	1.39	-0.64	-55.	-57.	2330.	-2327.	-0.	0.	1.	
0.0410	204.13	0.612	4.971.7	500.00	1.55	4.45	72.91	1.43	-0.59	-55.	-57.	2330.	-2327.	-0.	0.	1.	
0.0411	204.63	0.614	4.971.7	500.00	1.55	4.45	75.56	1.47	-0.57	-55.	-57.	2330.	-2327.	-0.	0.	1.	
0.0412	205.12	0.615	4.971.6	500.00	1.57	4.45	76.04	1.42	-0.58	-55.	-57.	2330.	-2327.	-0.	0.	1.	
0.0413	205.62	0.619	4.971.7	500.00	1.55	4.45	79.33	1.41	-0.63	-55.	-57.	2330.	-2327.	-0.	0.	1.	
0.0414	206.12	0.621	4.971.7	500.00	1.59	4.45	79.92	1.22	-0.70	-55.	-57.	2330.	-2327.	-0.	0.	1.	
0.0415	206.61	0.523	4.971.7	500.00	1.14	4.45	79.92	1.22	-0.70	-55.	-57.	2330.	-2327.	-0.	0.	1.	
0.0416	207.11	0.625	4.971.0	500.00	1.35	4.45	79.13	1.22	-0.79	-55.	-57.	2330.	-2327.	-0.	0.	1.	
0.0417	207.61	0.627	4.971.5	500.00	1.37	4.45	64.62	1.25	-0.61	-55.	-57.	2330.	-2327.	-0.	0.	1.	
0.0418	208.11	0.592	4.971.6	500.00	1.38	4.45	57.37	0.27	-0.27	-55.	-57.	2330.	-2327.	-0.	0.	1.	
0.0419	208.60	0.632	4.971.6	500.00	1.43	4.45	42.78	0.46	-1.36	-55.	-57.	2330.	-2327.	-0.	0.	1.	
0.0420	209.10	0.634	4.971.8	500.00	1.50	4.45	47.00	0.45	-0.70	-55.	-57.	2330.	-2327.	-0.	0.	1.	
0.0421	209.59	0.623	4.971.7	500.00	1.54	4.45	79.45	1.22	-0.79	-55.	-57.	2330.	-2327.	-0.	0.	1.	
0.0422	210.09	0.639	4.971.6	500.00	1.55	4.45	79.13	1.22	-0.79	-55.	-57.	2330.	-2327.	-0.	0.	1.	
0.0423	210.59	0.541	4.971.6	500.00	1.91	4.45	71.32	1.25	-0.31	-55.	-57.	2330.	-2327.	-0.	0.	1.	
0.0424	211.09	0.624	4.971.5	500.00	1.37	4.45	64.62	1.22	-0.67	-55.	-57.	2330.	-2327.	-0.	0.	1.	
0.0425	211.59	0.586	4.971.5	500.00	2.02	4.45	50.37	0.33	-1.93	-55.	-57.	2330.	-2327.	-0.	0.	1.	
0.0426	212.09	0.629	4.971.5	500.00	1.65	4.45	43.03	0.25	-1.51	-55.	-57.	2330.	-2327.	-0.	0.	1.	
0.0427	212.59	0.624	4.971.6	500.00	1.65	4.45	37.63	0.23	-1.65	-55.	-57.	2330.	-2327.	-0.	0.	1.	
0.0428	213.09	0.639	4.971.6	500.00	1.75	4.45	26.12	2.1	-1.77	-55.	-57.	2330.	-2327.	-0.	0.	1.	
0.0429	213.57	0.652	4.971.6	500.00	1.91	4.45	31.78	0.3	-1.23	-55.	-57.	2330.	-2327.	-0.	0.	1.	
0.0430	214.07	0.624	4.971.6	500.00	2.02	4.45	50.93	0.21	-1.93	-55.	-57.	2330.	-2327.	-0.	0.	1.	
0.0431	214.57	0.659	4.971.4	500.00	1.74	4.45	36.45	0.22	-1.72	-55.	-57.	2330.	-2327.	-0.	0.	1.	
0.0432	215.07	0.561	4.971.4	500.00	1.74	4.45	37.18	0.24	-1.58	-55.	-57.	2330.	-2327.	-0.	0.	1.	
0.0433	215.56	0.624	4.971.4	500.00	1.60	4.45	41.65	1.72	-1.43	-55.	-57.	2330.	-2327.	-0.	0.	1.	
0.0434	216.05	0.665	4.971.3	500.00	1.43	4.45	44.19	0.35	-0.55	-55.	-57.	2330.	-2327.	-0.	0.	1.	
0.0435	216.54	0.577	4.971.2	500.00	2.04	4.45	44.66	1.22	-0.47	-55.	-57.	2330.	-2327.	-0.	0.	1.	
0.0436	217.04	0.647	4.971.3	500.00	2.02	4.45	48.97	0.51	-0.97	-55.	-57.	2330.	-2327.	-0.	0.	1.	
0.0437	217.53	0.659	4.971.4	500.00	0.83	4.45	50.42	0.42	-1.72	-55.	-57.	2330.	-2327.	-0.	0.	1.	
0.0438	218.05	0.573	4.971.3	500.00	0.74	4.45	51.43	0.42	-1.74	-55.	-57.	2330.	-2327.	-0.	0.	1.	
0.0439	218.55	0.675	4.971.2	500.00	0.49	4.45	48.87	0.43	-0.24	-55.	-57.	2330.	-2327.	-0.	0.	1.	
0.0440	219.04	0.657	4.971.3	500.00	0.58	4.45	47.44	0.47	-0.47	-55.	-57.	2330.	-2327.	-0.	0.	1.	
0.0441	219.54	0.579	4.971.2	500.00	0.72	4.45	41.99	0.54	-1.92	-55.	-57.	2330.	-2327.	-0.	0.	1.	
0.0442	220.04	0.651	4.971.3	500.00	0.75	4.45	42.21	0.54	-1.54	-55.	-57.	2330.	-2327.	-0.	0.	1.	
0.0443	220.53	0.582	4.971.3	500.00	0.63	4.45	51.49	0.43	-0.71	-55.	-57.	2330.	-2327.	-0.	0.	1.	
0.0444	221.03	0.665	4.971.3	500.00	1.05	4.45	43.14	0.53	-0.55	-55.	-57.	2330.	-2327.	-0.	0.	1.	
0.0445	221.53	0.687	4.971.3	500.00	1.18	4.45	46.28	1.01	-0.41	-55.	-57.	2330.	-2327.	-0.	0.	1.	
0.0446	222.03	0.689	4.971.3	500.00	1.35	4.45	45.97	1.22	-0.47	-55.	-57.	2330.	-2327.	-0.	0.	1.	
0.0447	222.52	0.641	4.971.3	500.00	1.52	4.45	47.70	1.35	-0.63	-55.	-57.	2330.	-2327.	-0.	0.	1.	
0.0448	223.02	0.653	4.971.3	500.00	1.67	4.45	49.60	1.51	-0.72	-55.	-57.	2330.	-2327.	-0.	0.	1.	
0.0449	223.52	0.695	4.971.2	500.00	1.91	4.45	51.47	1.65	-0.75	-55.	-57.	2330.	-2327.	-0.	0.	1.	

FLECHETTE GROUND POINT

PAGE 10

	X	Y	Z	P	ALPHA	MACH	PHI	BETA	W-N	L-P	W-P	S	TAU	K-T
SEC	FT	FT	FT	FT/SEC	DEG/SEC	DIG	DEG	DEG	FT/SEC	FT/SEC	FT/SEC	FT/SEC	FT/SEC	DEG
0.0450	224.01	0.248	4.671.2	501.04	-1.02	4.45	32.1	-1.74	0.75	5.55	-57.	23.31	-2325.	1.
0.0451	224.51	0.249	4.671.2	501.04	-1.02	4.45	54.79	-1.96	0.76	5.55	-57.	23.31	-2325.	1.
0.0452	225.01	0.248	4.671.2	500.60	-2.03	4.45	56.10	-1.92	0.77	5.55	-57.	23.31	-2325.	1.
0.0453	225.51	0.248	4.671.2	500.60	-2.03	4.45	57.96	-1.95	0.78	5.55	-57.	23.31	-2325.	1.
0.0454	226.01	0.248	4.671.2	500.60	-2.03	4.45	57.96	-1.95	0.78	5.55	-57.	23.31	-2325.	1.
0.0455	226.51	0.248	4.671.2	500.60	-2.03	4.45	57.96	-1.95	0.78	5.55	-57.	23.31	-2325.	1.
0.0456	227.01	0.248	4.671.2	500.60	-2.03	4.45	57.96	-1.95	0.78	5.55	-57.	23.31	-2325.	1.
0.0457	227.51	0.248	4.671.2	500.60	-2.03	4.45	57.96	-1.95	0.78	5.55	-57.	23.31	-2325.	1.
0.0458	227.99	0.247	4.671.1	500.60	-1.79	4.45	55.49	-1.76	0.77	5.55	-57.	23.31	-2325.	1.
0.0459	228.47	0.247	4.671.1	500.60	-1.79	4.45	52.71	-1.59	0.71	5.55	-57.	23.31	-2325.	1.
0.0460	228.95	0.247	4.671.1	500.60	-1.79	4.45	52.71	-1.59	0.71	5.55	-57.	23.31	-2325.	1.
0.0461	229.43	0.247	4.671.1	500.60	-1.79	4.45	52.71	-1.59	0.71	5.55	-57.	23.31	-2325.	1.
0.0462	229.91	0.247	4.671.1	500.60	-1.79	4.45	52.71	-1.59	0.71	5.55	-57.	23.31	-2325.	1.
0.0463	230.41	0.247	4.671.1	500.60	-1.79	4.45	52.71	-1.59	0.71	5.55	-57.	23.31	-2325.	1.
0.0464	230.89	0.245	4.671.1	500.60	-1.35	4.45	23.62	-1.33	0.77	5.55	-57.	23.31	-2325.	1.
0.0465	231.37	0.245	4.671.0	500.60	-1.35	4.45	23.62	-1.33	0.77	5.55	-57.	23.31	-2325.	1.
0.0466	231.85	0.245	4.671.0	500.60	-1.35	4.45	23.62	-1.33	0.77	5.55	-57.	23.31	-2325.	1.
0.0467	232.33	0.245	4.671.0	500.60	-1.35	4.45	23.62	-1.33	0.77	5.55	-57.	23.31	-2325.	1.
0.0468	232.81	0.245	4.671.0	500.60	-1.35	4.45	23.62	-1.33	0.77	5.55	-57.	23.31	-2325.	1.
0.0469	233.29	0.245	4.671.0	500.60	-1.35	4.45	23.62	-1.33	0.77	5.55	-57.	23.31	-2325.	1.
0.0470	233.77	0.245	4.671.0	500.60	-1.35	4.45	23.62	-1.33	0.77	5.55	-57.	23.31	-2325.	1.
0.0471	234.25	0.245	4.671.0	500.60	-1.35	4.45	23.62	-1.33	0.77	5.55	-57.	23.31	-2325.	1.
0.0472	234.73	0.245	4.671.0	500.60	-1.35	4.45	23.62	-1.33	0.77	5.55	-57.	23.31	-2325.	1.
0.0473	235.21	0.245	4.671.0	500.60	-1.35	4.45	23.62	-1.33	0.77	5.55	-57.	23.31	-2325.	1.
0.0474	235.69	0.245	4.671.0	500.60	-1.35	4.45	23.62	-1.33	0.77	5.55	-57.	23.31	-2325.	1.
0.0475	236.17	0.245	4.671.0	500.60	-1.35	4.45	23.62	-1.33	0.77	5.55	-57.	23.31	-2325.	1.
0.0476	236.65	0.245	4.671.0	500.60	-1.35	4.45	23.62	-1.33	0.77	5.55	-57.	23.31	-2325.	1.
0.0477	237.13	0.245	4.671.0	500.60	-1.35	4.45	23.62	-1.33	0.77	5.55	-57.	23.31	-2325.	1.
0.0478	237.61	0.245	4.671.0	500.60	-1.35	4.45	23.62	-1.33	0.77	5.55	-57.	23.31	-2325.	1.
0.0479	238.09	0.245	4.671.0	500.60	-1.35	4.45	23.62	-1.33	0.77	5.55	-57.	23.31	-2325.	1.
0.0480	238.57	0.245	4.671.0	500.60	-1.35	4.45	23.62	-1.33	0.77	5.55	-57.	23.31	-2325.	1.
0.0481	239.05	0.245	4.671.0	500.60	-1.35	4.45	23.62	-1.33	0.77	5.55	-57.	23.31	-2325.	1.
0.0482	239.53	0.245	4.671.0	500.60	-1.35	4.45	23.62	-1.33	0.77	5.55	-57.	23.31	-2325.	1.
0.0483	240.01	0.245	4.671.0	500.60	-1.35	4.45	23.62	-1.33	0.77	5.55	-57.	23.31	-2325.	1.
0.0484	240.49	0.245	4.671.0	500.60	-1.35	4.45	23.62	-1.33	0.77	5.55	-57.	23.31	-2325.	1.
0.0485	240.97	0.245	4.671.0	500.60	-1.35	4.45	23.62	-1.33	0.77	5.55	-57.	23.31	-2325.	1.
0.0486	241.45	0.245	4.671.0	500.60	-1.35	4.45	23.62	-1.33	0.77	5.55	-57.	23.31	-2325.	1.
0.0487	241.93	0.245	4.671.0	500.60	-1.35	4.45	23.62	-1.33	0.77	5.55	-57.	23.31	-2325.	1.
0.0488	242.41	0.245	4.671.0	500.60	-1.35	4.45	23.62	-1.33	0.77	5.55	-57.	23.31	-2325.	1.
0.0489	242.89	0.245	4.671.0	500.60	-1.35	4.45	23.62	-1.33	0.77	5.55	-57.	23.31	-2325.	1.
0.0490	243.37	0.245	4.671.0	500.60	-1.35	4.45	23.62	-1.33	0.77	5.55	-57.	23.31	-2325.	1.
0.0491	243.85	0.245	4.671.0	500.60	-1.35	4.45	23.62	-1.33	0.77	5.55	-57.	23.31	-2325.	1.
0.0492	244.33	0.245	4.671.0	500.60	-1.35	4.45	23.62	-1.33	0.77	5.55	-57.	23.31	-2325.	1.
0.0493	244.81	0.245	4.671.0	500.60	-1.35	4.45	23.62	-1.33	0.77	5.55	-57.	23.31	-2325.	1.
0.0494	245.29	0.245	4.671.0	500.60	-1.35	4.45	23.62	-1.33	0.77	5.55	-57.	23.31	-2325.	1.
0.0495	245.77	0.245	4.671.0	500.60	-1.35	4.45	23.62	-1.33	0.77	5.55	-57.	23.31	-2325.	1.
0.0496	246.25	0.245	4.671.0	500.60	-1.35	4.45	23.62	-1.33	0.77	5.55	-57.	23.31	-2325.	1.
0.0497	246.73	0.245	4.671.0	500.60	-1.35	4.45	23.62	-1.33	0.77	5.55	-57.	23.31	-2325.	1.
0.0498	247.21	0.245	4.671.0	500.60	-1.35	4.45	23.62	-1.33	0.77	5.55	-57.	23.31	-2325.	1.
0.0499	247.69	0.245	4.671.0	500.60	-1.35	4.45	23.62	-1.33	0.77	5.55	-57.	23.31	-2325.	1.

COPY AVAILABLE TO DDC USES NOT
PERMIT FULLY LEGIBLE PRODUCTION

FLECHETTE GROUND POINT

PAGE 11

T SEC	X FT	Y FT	Z FT	V FT/SEC	P RAD/SEC	ALPHA REG	BETA REG	PHI REG	ALPHA MACH	BETA MACH	PHI MACH	L-N SEC	L-P SEC	L-V SEC	W-P SEC	S-JAU SEC
0.0500	248.87	0.745	-0.2250	4970.5	500.00	1.00	4.45	0.00	4.45	0.00	4.45	1.15	-55.	-57.	231.1-2325.	-0.
0.0501	248.36	0.750	-0.2260	4970.5	500.00	1.01	4.45	0.01	4.45	0.01	4.45	1.03	-55.	-57.	231.1-2325.	-0.
0.0502	249.86	0.755	-0.2261	4970.5	500.00	1.02	4.45	0.02	4.45	0.02	4.45	1.02	-55.	-57.	231.1-2325.	-0.
0.0503	250.36	0.751	-0.2262	4970.5	500.00	1.03	4.45	0.03	4.45	0.03	4.45	1.03	-55.	-57.	231.1-2325.	-0.
0.0504	250.86	0.752	-0.2263	4970.5	500.00	1.04	4.45	0.04	4.45	0.04	4.45	1.04	-55.	-57.	231.1-2325.	-0.
0.0505	251.35	0.753	-0.2264	4970.5	500.00	1.05	4.45	0.05	4.45	0.05	4.45	1.05	-55.	-57.	231.1-2325.	-0.
0.0506	251.85	0.754	-0.2265	4970.5	500.00	1.06	4.45	0.06	4.45	0.06	4.45	1.06	-55.	-57.	231.1-2325.	-0.
0.0507	252.35	0.755	-0.2266	4970.5	500.00	1.07	4.45	0.07	4.45	0.07	4.45	1.07	-55.	-57.	231.1-2325.	-0.
0.0508	252.84	0.756	-0.2267	4970.5	500.00	1.08	4.45	0.08	4.45	0.08	4.45	1.08	-55.	-57.	231.1-2325.	-0.
0.0509	253.34	0.757	-0.2268	4970.5	500.00	1.09	4.45	0.09	4.45	0.09	4.45	1.09	-55.	-57.	231.1-2325.	-0.
0.0510	253.84	0.758	-0.2269	4970.5	500.00	1.10	4.45	0.10	4.45	0.10	4.45	1.10	-55.	-57.	231.1-2325.	-0.
0.0511	254.33	0.759	-0.2270	4970.5	500.00	1.11	4.45	0.11	4.45	0.11	4.45	1.11	-55.	-57.	231.1-2325.	-0.
0.0512	254.83	0.761	-0.2271	4970.5	500.00	1.12	4.45	0.12	4.45	0.12	4.45	1.12	-55.	-57.	231.1-2325.	-0.
0.0513	255.33	0.762	-0.2272	4970.5	500.00	1.13	4.45	0.13	4.45	0.13	4.45	1.13	-55.	-57.	231.1-2325.	-0.
0.0514	255.82	0.763	-0.2273	4970.5	500.00	1.14	4.45	0.14	4.45	0.14	4.45	1.14	-55.	-57.	231.1-2325.	-0.
0.0515	256.32	0.764	-0.2274	4970.5	500.00	1.15	4.45	0.15	4.45	0.15	4.45	1.15	-55.	-57.	231.1-2325.	-0.
0.0516	256.82	0.765	-0.2275	4970.5	500.00	1.16	4.45	0.16	4.45	0.16	4.45	1.16	-55.	-57.	231.1-2325.	-0.
0.0517	257.32	0.766	-0.2276	4970.5	500.00	1.17	4.45	0.17	4.45	0.17	4.45	1.17	-55.	-57.	231.1-2325.	-0.
0.0518	257.81	0.767	-0.2277	4970.5	500.00	1.18	4.45	0.18	4.45	0.18	4.45	1.18	-55.	-57.	231.1-2325.	-0.
0.0519	258.31	0.768	-0.2278	4970.5	500.00	1.19	4.45	0.19	4.45	0.19	4.45	1.19	-55.	-57.	231.1-2325.	-0.
0.0520	258.80	0.769	-0.2279	4970.5	500.00	1.20	4.45	0.20	4.45	0.20	4.45	1.20	-55.	-57.	231.1-2325.	-0.
0.0521	259.30	0.770	-0.2280	4970.5	500.00	1.21	4.45	0.21	4.45	0.21	4.45	1.21	-55.	-57.	231.1-2325.	-0.
0.0522	259.80	0.771	-0.2281	4970.5	500.00	1.22	4.45	0.22	4.45	0.22	4.45	1.22	-55.	-57.	231.1-2325.	-0.
0.0523	260.30	0.772	-0.2282	4970.5	500.00	1.23	4.45	0.23	4.45	0.23	4.45	1.23	-55.	-57.	231.1-2325.	-0.
0.0524	260.79	0.773	-0.2283	4970.5	500.00	1.24	4.45	0.24	4.45	0.24	4.45	1.24	-55.	-57.	231.1-2325.	-0.
0.0525	261.29	0.774	-0.2284	4970.5	500.00	1.25	4.45	0.25	4.45	0.25	4.45	1.25	-55.	-57.	231.1-2325.	-0.
0.0526	261.79	0.775	-0.2285	4970.5	500.00	1.26	4.45	0.26	4.45	0.26	4.45	1.26	-55.	-57.	231.1-2325.	-0.
0.0527	262.28	0.776	-0.2286	4970.5	500.00	1.27	4.45	0.27	4.45	0.27	4.45	1.27	-55.	-57.	231.1-2325.	-0.
0.0528	262.78	0.777	-0.2287	4970.5	500.00	1.28	4.45	0.28	4.45	0.28	4.45	1.28	-55.	-57.	231.1-2325.	-0.
0.0529	263.27	0.778	-0.2288	4970.5	500.00	1.29	4.45	0.29	4.45	0.29	4.45	1.29	-55.	-57.	231.1-2325.	-0.
0.0530	263.76	0.779	-0.2289	4970.5	500.00	1.30	4.45	0.30	4.45	0.30	4.45	1.30	-55.	-57.	231.1-2325.	-0.
0.0531	264.25	0.780	-0.2290	4970.5	500.00	1.31	4.45	0.31	4.45	0.31	4.45	1.31	-55.	-57.	231.1-2325.	-0.
0.0532	264.75	0.781	-0.2291	4970.5	500.00	1.32	4.45	0.32	4.45	0.32	4.45	1.32	-55.	-57.	231.1-2325.	-0.
0.0533	265.25	0.782	-0.2292	4970.5	500.00	1.33	4.45	0.33	4.45	0.33	4.45	1.33	-55.	-57.	231.1-2325.	-0.
0.0534	265.74	0.783	-0.2293	4970.5	500.00	1.34	4.45	0.34	4.45	0.34	4.45	1.34	-55.	-57.	231.1-2325.	-0.
0.0535	266.24	0.784	-0.2294	4970.5	500.00	1.35	4.45	0.35	4.45	0.35	4.45	1.35	-55.	-57.	231.1-2325.	-0.
0.0536	266.73	0.785	-0.2295	4970.5	500.00	1.36	4.45	0.36	4.45	0.36	4.45	1.36	-55.	-57.	231.1-2325.	-0.
0.0537	267.22	0.786	-0.2296	4970.5	500.00	1.37	4.45	0.37	4.45	0.37	4.45	1.37	-55.	-57.	231.1-2325.	-0.
0.0538	267.71	0.787	-0.2297	4970.5	500.00	1.38	4.45	0.38	4.45	0.38	4.45	1.38	-55.	-57.	231.1-2325.	-0.
0.0539	268.20	0.788	-0.2298	4970.5	500.00	1.39	4.45	0.39	4.45	0.39	4.45	1.39	-55.	-57.	231.1-2325.	-0.
0.0540	268.69	0.789	-0.2299	4970.5	500.00	1.40	4.45	0.40	4.45	0.40	4.45	1.40	-55.	-57.	231.1-2325.	-0.
0.0541	269.18	0.790	-0.2300	4970.5	500.00	1.41	4.45	0.41	4.45	0.41	4.45	1.41	-55.	-57.	231.1-2325.	-0.
0.0542	269.67	0.791	-0.2301	4970.5	500.00	1.42	4.45	0.42	4.45	0.42	4.45	1.42	-55.	-57.	231.1-2325.	-0.
0.0543	270.16	0.792	-0.2302	4970.5	500.00	1.43	4.45	0.43	4.45	0.43	4.45	1.43	-55.	-57.	231.1-2325.	-0.
0.0544	270.65	0.793	-0.2303	4970.5	500.00	1.44	4.45	0.44	4.45	0.44	4.45	1.44	-55.	-57.	231.1-2325.	-0.
0.0545	271.14	0.794	-0.2304	4970.5	500.00	1.45	4.45	0.45	4.45	0.45	4.45	1.45	-55.	-57.	231.1-2325.	-0.
0.0546	271.63	0.795	-0.2305	4970.5	500.00	1.46	4.45	0.46	4.45	0.46	4.45	1.46	-55.	-57.	231.1-2325.	-0.
0.0547	272.12	0.796	-0.2306	4970.5	500.00	1.47	4.45	0.47	4.45	0.47	4.45	1.47	-55.	-57.	231.1-2325.	-0.
0.0548	272.61	0.797	-0.2307	4970.5	500.00	1.48	4.45	0.48	4.45	0.48	4.45	1.48	-55.	-57.	231.1-2325.	-0.
0.0549	273.20	0.798	-0.2308	4970.5	500.00	1.49	4.45	0.49	4.45	0.49	4.45	1.49	-55.	-57.	231.1-2325.	-0.

FLECHETTE GROUND PENNY

12

**COPY AVAILABLE TO LAW ENFORCEMENT
PERMIT FULLY LEGIBLE PROSECUTION**

FLECHETTE GROUND POINT

PAGE 13

T SEC	X FT	Y FT	Z FT	V FT/SEC	RAD/SEC	DIG	PHI DEG	MAGN DEG	BETA DEG	ALPHA DEG	W-P DEG	N-S DEG	E-W DEG	W-N DEG	S-E DEG	E-W DEG	N-S DEG	E-W DEG
0.0500	293.55	0.314	-0.310	456.0	500.0	1.51	6.45	36.39	-2.53	1.37	-55.	-57.	232.1	-212.8	-9.	2.	1.	1.
0.0501	299.55	0.715	-0.310	456.0	500.0	1.52	6.45	33.92	-2.54	1.42	-55.	-57.	232.1	-222.8	-9.	2.	1.	1.
0.0502	299.55	0.915	-0.311	456.0	500.0	1.53	6.45	31.32	-2.53	1.43	-1.15	-57.	232.1	-222.8	-9.	2.	1.	1.
0.0503	300.04	0.917	-0.311	456.5	510.0	1.53	6.45	34.90	-3.42	1.47	-45.	-57.	232.1	-222.8	-9.	2.	1.	1.
0.0504	300.54	0.918	-0.311	456.0	510.0	1.53	6.45	24.23	-2.19	1.48	-55.	-57.	242.1	-222.4	-9.	2.	1.	1.
0.0505	301.04	0.918	-0.311	456.5	500.0	1.52	6.45	37.63	-3.16	1.47	-52.	-57.	223.1	-232.4	-9.	2.	1.	1.
0.0506	301.53	0.912	-0.311	456.0	500.0	1.50	6.45	37.58	-3.32	1.46	-45.	-57.	232.1	-222.8	-9.	2.	1.	1.
0.0507	302.03	0.920	-0.312	456.5	500.0	1.47	6.45	41.93	-3.31	1.44	-55.	-57.	232.1	-222.8	-9.	2.	1.	1.
0.0508	302.53	0.921	-0.312	456.0	500.0	1.44	6.45	44.30	-2.23	1.41	-55.	-57.	232.1	-222.8	-9.	2.	1.	1.
0.0509	303.02	0.922	-0.313	456.5	500.0	1.41	6.45	46.55	-2.27	1.38	-55.	-57.	232.1	-222.8	-9.	2.	1.	1.
0.0510	303.52	0.923	-0.313	456.0	500.0	1.37	6.45	43.37	-2.25	1.35	-55.	-57.	232.1	-222.8	-9.	2.	1.	1.
0.0511	304.52	0.923	-0.313	456.0	500.0	1.34	6.45	51.94	-2.13	1.32	-53.	-57.	232.1	-222.8	-9.	2.	1.	1.
0.0512	304.52	0.924	-0.313	456.5	500.0	1.32	6.45	51.32	-1.19	1.29	-55.	-57.	232.1	-222.8	-9.	2.	1.	1.
0.0513	305.01	0.925	-0.315	456.0	500.0	1.29	6.45	53.79	-0.15	1.27	-45.	-57.	232.1	-222.8	-9.	2.	1.	1.
0.0514	305.51	0.926	-0.315	456.5	500.0	1.26	6.45	54.37	-0.19	1.25	-45.	-57.	232.1	-222.8	-9.	2.	1.	1.
0.0515	306.01	0.927	-0.316	456.0	500.0	1.24	6.45	54.35	-0.07	1.24	-45.	-57.	232.1	-222.8	-9.	2.	1.	1.
0.0516	306.50	0.927	-0.316	456.0	500.0	1.24	6.45	53.77	0.05	1.24	-45.	-57.	232.1	-222.8	-9.	2.	1.	1.
0.0517	307.00	0.928	-0.317	456.0	500.0	1.25	6.45	51.12	-0.12	1.24	-45.	-57.	232.1	-222.8	-9.	2.	1.	1.
0.0518	307.50	0.929	-0.316	456.5	500.0	1.27	6.45	51.35	0.22	1.25	-52.	-57.	232.1	-222.8	-9.	2.	1.	1.
0.0519	307.69	0.930	-0.316	456.0	500.0	1.30	6.45	49.42	-0.32	1.25	-45.	-57.	232.1	-222.8	-9.	2.	1.	1.
0.0520	308.49	0.910	-0.315	456.0	500.0	1.35	4.45	56.36	-1.13	1.28	-45.	-57.	232.1	-222.8	-9.	2.	1.	1.
0.0521	308.49	0.927	-0.316	456.0	500.0	1.24	6.45	47.02	0.34	1.23	-55.	-57.	232.1	-222.8	-9.	2.	1.	1.
0.0522	309.49	0.922	-0.321	456.0	500.0	1.26	6.45	47.05	0.56	1.30	-55.	-57.	232.1	-222.8	-9.	2.	1.	1.
0.0523	109.68	0.923	-0.321	456.0	500.0	1.52	6.45	51.16	0.77	1.31	-45.	-57.	222.1	-232.6	-9.	2.	1.	1.
0.0524	310.68	0.929	-0.316	456.0	500.0	1.52	6.45	47.45	-1.31	1.31	-45.	-57.	232.1	-222.8	-9.	2.	1.	1.
0.0525	310.97	0.924	-0.323	456.5	500.0	1.62	6.45	44.44	0.37	1.30	-45.	-57.	232.1	-222.8	-9.	2.	1.	1.
0.0526	311.47	0.925	-0.324	456.0	500.0	1.67	6.45	45.72	-1.33	1.28	-45.	-57.	232.1	-222.8	-9.	2.	1.	1.
0.0527	311.77	0.936	-0.324	456.0	500.0	1.65	6.45	41.50	1.29	1.25	-55.	-57.	232.1	-222.8	-9.	2.	1.	1.
0.0528	312.46	0.937	-0.324	456.0	500.0	1.71	6.45	44.35	1.21	1.21	-55.	-57.	232.1	-222.8	-9.	2.	1.	1.
0.0529	312.96	0.938	-0.327	456.0	500.0	1.71	6.45	45.16	1.26	1.15	-55.	-57.	232.1	-222.8	-9.	2.	1.	1.
0.0530	313.46	0.939	-0.324	456.5	500.0	1.66	6.45	45.45	1.34	1.12	-45.	-57.	232.1	-222.8	-9.	2.	1.	1.
0.0531	313.46	0.940	-0.323	456.0	500.0	1.67	6.45	45.72	1.33	1.11	-45.	-57.	232.1	-222.8	-9.	2.	1.	1.
0.0532	314.55	0.940	-0.324	456.0	500.0	1.67	6.45	44.43	1.16	1.26	-55.	-57.	212.1	-222.8	-9.	2.	1.	1.
0.0533	314.55	0.942	-0.324	456.0	500.0	1.65	6.45	41.50	1.12	1.25	-55.	-57.	232.1	-222.8	-9.	2.	1.	1.
0.0534	315.45	0.943	-0.324	456.0	500.0	1.62	6.45	44.35	1.08	1.21	-55.	-57.	232.1	-222.8	-9.	2.	1.	1.
0.0535	315.94	0.945	-0.326	456.0	500.0	1.67	6.45	45.08	1.08	1.33	-62.	-57.	232.1	-222.8	-9.	2.	1.	1.
0.0536	316.35	0.945	-0.345	456.0	500.0	1.61	6.45	44.34	1.04	1.31	-55.	-57.	232.1	-222.8	-9.	2.	1.	1.
0.0537	316.44	0.945	-0.345	456.0	500.0	1.67	6.45	45.72	1.02	1.31	-55.	-57.	232.1	-222.8	-9.	2.	1.	1.
0.0538	317.43	0.945	-0.349	456.0	500.0	1.61	6.45	44.37	0.98	1.31	-55.	-57.	232.1	-222.8	-9.	2.	1.	1.
0.0539	317.93	0.940	-0.349	456.0	500.0	1.60	6.45	41.28	0.95	1.22	-55.	-57.	232.1	-222.8	-9.	2.	1.	1.
0.0540	320.51	0.945	-0.340	456.0	500.0	1.51	6.45	44.35	0.94	1.23	-55.	-57.	232.1	-222.8	-9.	2.	1.	1.
0.0541	320.51	0.945	-0.340	456.0	500.0	1.51	6.45	40.18	0.94	1.23	-55.	-57.	232.1	-222.8	-9.	2.	1.	1.
0.0542	321.50	0.945	-0.343	456.0	500.0	1.25	6.45	39.35	1.02	1.25	-55.	-57.	232.1	-222.8	-9.	2.	1.	1.
0.0543	321.50	0.945	-0.343	456.0	500.0	1.25	6.45	39.28	1.02	1.22	-55.	-57.	232.1	-222.8	-9.	2.	1.	1.
0.0544	321.50	0.945	-0.343	456.0	500.0	1.26	6.45	39.82	1.02	1.22	-55.	-57.	232.1	-222.8	-9.	2.	1.	1.
0.0545	321.50	0.945	-0.343	456.0	500.0	1.26	6.45	39.82	1.02	1.22	-55.	-57.	232.1	-222.8	-9.	2.	1.	1.
0.0546	322.40	0.943	-0.350	456.0	500.0	1.49	6.45	46.62	1.37	0.91	-22.	-57.	232.1	-222.8	-9.	2.	1.	1.
0.0547	322.90	0.945	-0.351	456.0	500.0	1.47	6.45	45.19	1.39	0.91	-22.	-57.	232.1	-222.8	-9.	2.	1.	1.

FLECHETTE GROUND POINT

PAGE 1

	T	X	Y	Z	V	P	ALPHA	BETA	GAMMA	H-H	L-N	L-P	S	T-AU	K-T
SEC	FT	FT	FT	FT	FT	FT	DEG	DEG	DEG	DEG	DEG	DEG	DEG	DEG	DEG
0.0550	323.39	0.256	-0.153	4.756	500.00	1.47	4.45	37.83	1.62	-0.39	-55	-57	232.2	-222.5	
0.0550	323.89	0.253	-0.355	4.656	500.00	1.49	4.45	69.62	1.43	-0.62	-53	-57	232.2	-222.5	
0.0552	324.39	0.270	-0.355	4.656	500.00	1.51	4.45	51.10	1.41	-0.45	-55	-57	232.2	-222.5	
0.0553	324.89	0.272	-0.355	4.656	500.00	1.52	4.45	52.32	1.44	-0.52	-55	-57	232.2	-222.5	
0.0554	325.38	0.273	-0.357	4.656	500.00	1.53	4.45	53.21	1.42	-0.55	-55	-57	232.2	-222.5	
0.0555	325.88	0.275	-0.357	4.656	500.00	1.54	4.45	53.73	1.40	-0.51	-55	-57	232.2	-222.5	
0.0555	326.38	0.277	-0.360	4.656	500.00	1.52	4.45	54.93	1.35	-0.57	-55	-57	232.2	-222.5	
0.0557	326.87	0.277	-0.361	4.656	500.00	1.51	4.45	54.49	1.31	-0.75	-55	-57	232.2	-222.5	
0.0558	327.37	0.271	-0.361	4.656	500.00	1.45	4.45	52.59	1.25	-0.52	-55	-57	232.2	-222.5	
0.0559	327.87	0.263	-0.363	4.656	500.00	1.43	4.45	51.43	1.13	-0.57	-55	-57	232.2	-222.5	
0.0560	328.36	0.265	-0.364	4.656	500.00	1.47	4.45	46.91	1.05	-0.47	-55	-57	232.2	-222.5	
0.0564	328.85	0.267	-0.367	4.656	500.00	1.46	4.45	48.01	1.01	-0.51	-55	-57	232.2	-222.5	
0.0565	329.36	0.272	-0.367	4.656	500.00	1.50	4.45	46.92	1.14	-0.35	-55	-57	232.2	-222.5	
0.0565	329.85	0.261	-0.367	4.656	500.00	1.46	4.45	44.11	0.92	-0.21	-55	-57	232.2	-222.5	
0.0566	330.35	0.263	-0.369	4.656	500.00	1.45	4.45	42.57	0.75	-0.23	-55	-57	232.2	-222.5	
0.0566	330.85	0.266	-0.365	4.656	500.00	1.45	4.45	43.53	0.52	-0.35	-55	-57	232.2	-222.5	
0.0567	331.34	0.263	-0.373	45.56	500.00	1.50	4.45	39.44	0.53	-1.12	-55	-57	232.2	-222.5	
0.0567	331.84	0.260	-0.371	45.56	500.00	1.52	4.45	38.59	0.41	-1.02	-55	-57	232.2	-222.5	
0.0568	332.34	0.262	-0.371	45.56	500.00	1.53	4.45	38.15	0.35	-1.02	-55	-57	232.2	-222.5	
0.0569	332.83	0.264	-0.372	45.56	500.00	1.54	4.45	38.12	0.23	-1.01	-55	-57	232.2	-222.5	
0.0570	333.33	0.266	-0.373	45.56	500.00	1.54	4.45	35.47	0.22	-1.02	-55	-57	232.2	-222.5	
0.0571	333.83	0.269	-0.374	45.56	500.00	1.50	4.45	39.15	0.15	-1.02	-55	-57	232.2	-222.5	
0.0572	334.32	0.271	-0.374	45.56	500.00	1.53	4.45	39.12	0.11	-1.02	-55	-57	232.2	-222.5	
0.0573	334.82	0.273	-0.375	45.56	500.00	1.51	4.45	38.59	0.04	-1.02	-55	-57	232.2	-222.5	
0.0574	335.32	0.274	-0.376	45.56	500.00	1.48	4.45	42.43	0.02	-1.02	-55	-57	232.2	-222.5	
0.0575	335.82	0.271	-0.376	45.56	500.00	1.46	4.45	41.95	-0.01	-1.01	-55	-57	232.2	-222.5	
0.0576	336.31	0.270	-0.375	45.56	500.00	1.43	4.45	44.91	-0.01	-1.01	-55	-57	232.2	-222.5	
0.0577	336.81	0.272	-0.377	45.56	500.00	1.45	4.45	45.78	-0.03	-1.02	-55	-57	232.2	-222.5	
0.0578	337.31	0.274	-0.377	45.56	500.00	1.46	4.45	47.35	-0.12	-1.02	-55	-57	232.2	-222.5	
0.0579	337.80	0.276	-0.378	45.56	500.00	1.33	4.45	42.82	-0.17	-1.01	-55	-57	232.2	-222.5	
0.0580	338.30	0.277	-0.375	45.56	500.00	1.31	4.45	43.95	-0.21	-1.02	-55	-57	232.2	-222.5	
0.0581	338.80	0.271	-0.374	45.56	500.00	1.29	4.45	46.93	-0.21	-1.02	-55	-57	232.2	-222.5	
0.0582	339.29	0.273	-0.375	45.56	500.00	1.29	4.45	45.45	-0.05	-1.02	-55	-57	232.2	-222.5	
0.0583	339.79	0.275	-0.375	45.56	500.00	1.27	4.45	45.78	-0.12	-1.02	-55	-57	232.2	-222.5	
0.0584	340.29	0.276	-0.376	45.56	500.00	1.26	4.45	47.35	-0.12	-1.02	-55	-57	232.2	-222.5	
0.0585	341.28	0.264	-0.370	45.56	500.00	1.32	4.45	47.75	-0.53	-1.02	-55	-57	232.2	-222.5	
0.0587	341.79	0.264	-0.370	45.56	500.00	1.35	4.45	47.07	-0.72	-1.02	-55	-57	232.2	-222.5	
0.0588	342.29	0.265	-0.370	45.56	500.00	1.25	4.45	45.92	-0.42	-1.01	-55	-57	232.2	-222.5	
0.0589	342.77	0.264	-0.370	45.56	500.00	1.23	4.45	45.52	-0.32	-1.01	-55	-57	232.2	-222.5	
0.0590	343.27	0.262	-0.370	45.56	500.00	1.20	4.45	45.81	-0.32	-1.01	-55	-57	232.2	-222.5	
0.0591	343.76	0.264	-0.372	45.56	500.00	1.19	4.45	45.75	-0.53	-1.01	-55	-57	232.2	-222.5	
0.0592	344.26	0.254	-0.370	45.56	500.00	1.15	4.45	45.73	-1.05	-1.01	-55	-57	232.2	-222.5	
0.0593	344.76	0.256	-0.370	45.56	500.00	1.15	4.45	45.38	-1.22	-1.01	-55	-57	232.2	-222.5	
0.0594	345.25	0.252	-0.370	45.56	500.00	1.11	4.45	45.50	-1.01	-1.01	-55	-57	232.2	-222.5	
0.0595	345.75	0.250	-0.370	45.56	500.00	1.12	4.45	45.34	-1.36	-1.01	-55	-57	232.2	-222.5	
0.0596	346.25	0.249	-0.370	45.56	500.00	1.02	4.45	45.52	-1.32	-1.01	-55	-57	232.2	-222.5	
0.0597	346.75	0.248	-0.370	45.56	500.00	1.02	4.45	45.79	-1.71	-1.01	-55	-57	232.2	-222.5	
0.0598	347.24	0.245	-0.370	45.56	500.00	1.02	4.45	46.83	-1.13	-1.01	-55	-57	232.2	-222.5	
0.0599	347.74	0.247	-0.370	45.56	500.00	1.02	4.45	46.78	-0.63	-1.01	-55	-57	232.2	-222.5	

FLECHETTE GROUND FLOOR

310 COPY AVAILABLE TO FEDERAL BUREAU OF INVESTIGATION
NOT AT FULLY LEGIBLE

ELECHETTE GROUND POINT

PAGE 16

T SEC	X FT	Y FT	Z FT	V SEC	P SEC	ALPHA RADISTC	PHI SEC	MACH SEC	LW 1/5 SEC	LP 1/5 SEC	PAW 1/5 SEC	PAW 1/5 SEC	S IAU	K-T CG
0.0750	373.06	1.121	-0.342	4957.7	510.69	1.31 4.45	4.14	0.70	1.11	-0.53	233.00	232.00	0	1.
0.0751	373.56	1.122	-0.349	4957.7	500.00	1.32 4.45	4.14	0.70	1.07	-0.52	232.00	232.00	0	1.
0.0752	374.06	1.123	-0.349	4957.7	500.00	1.33 4.45	4.14	0.70	1.07	-0.52	232.00	232.00	0	1.
0.0753	374.55	1.124	-0.341	4957.7	500.00	1.34 4.45	4.14	0.70	1.07	-0.52	232.00	232.00	0	1.
0.0754	375.05	1.125	-0.332	4957.7	500.00	1.37 4.45	4.14	0.70	1.07	-0.52	232.00	232.00	0	1.
0.0755	375.55	1.126	-0.333	4957.7	500.00	1.35 4.45	4.14	0.70	1.07	-0.52	232.00	232.00	0	1.
0.0756	376.04	1.127	-0.342	4957.7	500.00	1.32 4.45	4.14	0.70	1.07	-0.52	232.00	232.00	0	1.
0.0757	376.54	1.128	-0.345	4957.7	500.00	1.35 4.45	4.14	0.70	1.07	-0.52	232.00	232.00	0	1.
0.0758	377.04	1.129	-0.346	4957.7	500.00	1.34 4.45	4.14	0.70	1.07	-0.52	232.00	232.00	0	1.
0.0759	377.53	1.130	-0.358	4957.6	500.00	1.31 4.45	4.14	0.70	1.07	-0.52	232.00	232.00	0	1.
0.0760	378.03	1.131	-0.345	4957.6	500.00	1.33 4.45	4.14	0.70	1.07	-0.52	232.00	232.00	0	1.
0.0761	378.53	1.133	-0.400	4957.6	500.00	1.35 4.45	4.14	0.70	1.07	-0.52	232.00	232.00	0	1.
0.0762	379.02	1.134	-0.491	4957.6	500.00	1.32 4.45	4.14	0.70	1.07	-0.52	232.00	232.00	0	1.
0.0763	379.52	1.135	-0.492	4957.6	500.00	1.35 4.45	4.14	0.70	1.07	-0.52	232.00	232.00	0	1.
0.0764	380.02	1.136	-0.494	4957.6	500.00	1.36 4.45	4.14	0.70	1.07	-0.52	232.00	232.00	0	1.
0.0765	380.51	1.137	-0.446	4957.6	500.00	1.33 4.45	4.14	0.70	1.07	-0.52	232.00	232.00	0	1.
0.0766	381.01	1.139	-0.396	4957.5	500.00	1.33 4.45	4.14	0.70	1.07	-0.52	232.00	232.00	0	1.
0.0767	381.51	1.140	-0.407	4957.5	500.00	1.32 4.45	4.14	0.70	1.07	-0.52	232.00	232.00	0	1.
0.0768	382.00	1.142	-0.405	4957.5	500.00	1.34 4.45	4.14	0.70	1.07	-0.52	232.00	232.00	0	1.
0.0769	382.50	1.143	-0.410	4957.5	500.00	1.37 4.45	4.14	0.70	1.07	-0.52	232.00	232.00	0	1.
0.0770	383.00	1.145	-0.411	4957.5	500.00	1.35 4.45	4.14	0.70	1.07	-0.52	232.00	232.00	0	1.
0.0771	383.44	1.146	-0.412	4957.5	500.00	1.36 4.45	4.14	0.70	1.07	-0.52	232.00	232.00	0	1.
0.0772	383.99	1.147	-0.413	4957.5	500.00	1.34 4.45	4.14	0.70	1.07	-0.52	232.00	232.00	0	1.
0.0773	384.00	1.147	-0.405	4957.5	500.00	1.34 4.45	4.14	0.70	1.07	-0.52	232.00	232.00	0	1.
0.0774	384.58	1.148	-0.410	4957.5	500.00	1.35 4.45	4.14	0.70	1.07	-0.52	232.00	232.00	0	1.
0.0775	385.48	1.149	-0.415	4957.4	500.00	1.36 4.45	4.14	0.70	1.07	-0.52	232.00	232.00	0	1.
0.0776	385.98	1.150	-0.415	4957.4	500.00	1.35 4.45	4.14	0.70	1.07	-0.52	232.00	232.00	0	1.
0.0777	386.67	1.154	-0.420	4957.4	500.00	1.33 4.45	4.14	0.70	1.07	-0.52	232.00	232.00	0	1.
0.0778	387.07	1.158	-0.421	4957.4	500.00	1.32 4.45	4.14	0.70	1.07	-0.52	232.00	232.00	0	1.
0.0779	387.47	1.160	-0.422	4957.4	500.00	1.34 4.45	4.14	0.70	1.07	-0.52	232.00	232.00	0	1.
0.0780	387.98	1.162	-0.423	4957.4	500.00	1.35 4.45	4.14	0.70	1.07	-0.52	232.00	232.00	0	1.
0.0781	388.45	1.163	-0.425	4957.4	500.00	1.36 4.45	4.14	0.70	1.07	-0.52	232.00	232.00	0	1.
0.0782	388.95	1.165	-0.425	4957.4	500.00	1.37 4.45	4.14	0.70	1.07	-0.52	232.00	232.00	0	1.
0.0783	389.45	1.166	-0.427	4957.4	500.00	1.35 4.45	4.14	0.70	1.07	-0.52	232.00	232.00	0	1.
0.0784	389.95	1.167	-0.428	4957.4	500.00	1.34 4.45	4.14	0.70	1.07	-0.52	232.00	232.00	0	1.
0.0785	390.44	1.171	-0.428	4957.3	500.00	1.33 4.45	4.14	0.70	1.07	-0.52	232.00	232.00	0	1.
0.0786	390.94	1.173	-0.430	4957.3	500.00	1.32 4.45	4.14	0.70	1.07	-0.52	232.00	232.00	0	1.
0.0787	391.44	1.175	-0.431	4957.3	500.00	1.31 4.45	4.14	0.70	1.07	-0.52	232.00	232.00	0	1.
0.0788	391.93	1.177	-0.432	4957.3	500.00	1.30 4.45	4.14	0.70	1.07	-0.52	232.00	232.00	0	1.
0.0789	392.43	1.178	-0.432	4957.3	500.00	1.29 4.45	4.14	0.70	1.07	-0.52	232.00	232.00	0	1.
0.0790	392.93	1.181	-0.434	4957.3	500.00	1.28 4.45	4.14	0.70	1.07	-0.52	232.00	232.00	0	1.
0.0791	393.42	1.184	-0.434	4957.3	500.00	1.27 4.45	4.14	0.70	1.07	-0.52	232.00	232.00	0	1.
0.0792	393.92	1.186	-0.435	4957.3	500.00	1.26 4.45	4.14	0.70	1.07	-0.52	232.00	232.00	0	1.
0.0793	394.42	1.188	-0.436	4957.3	500.00	1.25 4.45	4.14	0.70	1.07	-0.52	232.00	232.00	0	1.
0.0794	394.91	1.191	-0.437	4957.3	500.00	1.24 4.45	4.14	0.70	1.07	-0.52	232.00	232.00	0	1.
0.0795	395.41	1.195	-0.438	4957.3	500.00	1.23 4.45	4.14	0.70	1.07	-0.52	232.00	232.00	0	1.
0.0796	395.91	1.197	-0.439	4957.2	500.00	1.22 4.45	4.14	0.70	1.07	-0.52	232.00	232.00	0	1.
0.0797	396.40	1.201	-0.440	4957.2	500.00	1.21 4.45	4.14	0.70	1.07	-0.52	232.00	232.00	0	1.
0.0798	396.50	1.201	-0.440	4957.2	500.00	1.20 4.45	4.14	0.70	1.07	-0.52	232.00	232.00	0	1.
0.0799	397.40	1.201	-0.440	4957.2	500.00	1.19 4.45	4.14	0.70	1.07	-0.52	232.00	232.00	0	1.

COPY AVAILABLE
PERMIT FULLY LEGIBLE PRODUCTION

FLECHETTE GROUND POINT

PAGE 17

	X	Y	Z	V	FT	FT/SEC	KM/SEC	SEC	ALPHA	BETA	GAMMA	W-N	W-E	N-S	E-W	IAU	E-T
	FT	FT	FT	FT	FT	FT	FT	SEC	DEG	DEG	DEG	SEC	SEC	SEC	SEC	SEC	SEC
0.0630	307.85	1.203	-0.441	4957.2	500.00	1.46	6.45	43.64	-1.49	-0.02	-1.49	-57.	2332.	2326.	-9.	0.	-
0.0631	198.39	1.227	-0.442	4957.2	500.00	1.45	6.45	43.23	-1.45	-0.02	-1.45	-57.	2332.	2326.	-9.	0.	-
0.0632	198.89	1.205	-0.442	4957.2	500.00	1.51	6.45	42.78	-0.15	-1.49	-1.49	-57.	2332.	2326.	-9.	0.	-
0.0633	303.31	1.211	-0.442	4957.2	500.00	1.51	6.45	42.43	-1.22	-1.50	-1.50	-57.	2332.	2326.	-9.	0.	-
0.0634	325.63	1.212	-0.443	4957.1	500.00	1.52	6.45	42.45	-1.37	-1.47	-1.47	-57.	2332.	2326.	-9.	0.	-
0.0635	201.19	1.215	-0.443	4957.1	500.00	1.52	6.45	43.13	-0.37	-1.47	-1.47	-57.	2332.	2326.	-9.	0.	-
0.0636	403.87	1.217	-0.443	4957.1	500.00	1.51	6.45	43.42	-0.43	-1.45	-1.45	-57.	2332.	2326.	-9.	0.	-
0.0637	401.37	1.217	-0.444	4957.1	500.00	1.52	6.45	43.79	-0.43	-1.42	-1.42	-57.	2332.	2326.	-9.	0.	-
0.0638	401.87	1.221	-0.444	4957.1	500.00	1.49	6.45	44.16	-0.45	-1.36	-1.36	-57.	2332.	2326.	-9.	0.	-
0.0639	402.15	1.223	-0.444	4957.1	500.00	1.47	6.45	44.69	-0.43	-1.34	-1.34	-57.	2332.	2326.	-9.	0.	-
0.0640	402.86	1.225	-0.445	4957.1	500.00	1.45	6.45	45.09	-0.53	-1.30	-1.30	-57.	2332.	2326.	-9.	0.	-
0.0641	403.36	1.227	-0.445	4957.1	500.00	1.43	6.45	45.35	-0.65	-1.25	-1.25	-57.	2332.	2326.	-9.	0.	-
0.0642	403.65	1.230	-0.445	4957.1	500.00	1.21	6.45	45.53	-0.74	-1.20	-1.20	-57.	2332.	2326.	-9.	0.	-
0.0643	404.35	1.232	-0.445	4957.0	500.00	1.35	6.45	45.92	-0.74	-1.15	-1.15	-57.	2332.	2326.	-9.	0.	-
0.0644	404.25	1.223	-0.445	4957.0	500.00	1.24	6.45	45.93	-0.83	-1.05	-1.05	-57.	2332.	2326.	-9.	0.	-
0.0645	405.34	1.236	-0.445	4957.0	500.00	1.36	6.45	45.95	-0.87	-1.05	-1.05	-57.	2332.	2326.	-9.	0.	-
0.0646	405.44	1.235	-0.445	4957.0	500.00	1.35	6.45	45.85	-0.85	-1.02	-1.02	-57.	2332.	2326.	-9.	0.	-
0.0647	406.34	1.243	-0.445	4957.0	500.00	1.35	6.45	46.79	-0.57	-0.93	-0.93	-57.	2332.	2326.	-9.	0.	-
0.0648	405.83	1.242	-0.445	4957.0	500.00	1.35	6.45	45.96	-0.51	-0.99	-0.99	-57.	2332.	2326.	-9.	0.	-
0.0649	407.13	1.242	-0.445	4957.0	500.00	1.36	6.45	45.95	-0.56	-0.94	-0.94	-57.	2332.	2326.	-9.	0.	-
0.0650	407.83	1.242	-0.445	4957.0	500.00	1.37	6.45	45.45	-0.53	-0.83	-0.83	-57.	2332.	2326.	-9.	0.	-
0.0651	408.32	1.246	-0.445	4957.0	500.00	1.36	6.45	45.46	-0.57	-0.87	-0.87	-57.	2332.	2326.	-9.	0.	-
0.0652	408.82	1.249	-0.445	4957.0	500.00	1.40	6.45	45.42	-0.57	-0.87	-0.87	-57.	2332.	2326.	-9.	0.	-
0.0653	409.31	1.241	-0.445	4956.9	500.00	1.42	6.45	45.42	-0.57	-0.87	-0.87	-57.	2332.	2326.	-9.	0.	-
0.0654	409.83	1.242	-0.445	4957.0	500.00	1.35	6.45	45.96	-0.51	-0.99	-0.99	-57.	2332.	2326.	-9.	0.	-
0.0655	407.13	1.242	-0.445	4957.0	500.00	1.36	6.45	45.54	-0.56	-0.94	-0.94	-57.	2332.	2326.	-9.	0.	-
0.0656	407.83	1.246	-0.445	4957.0	500.00	1.37	6.45	45.53	-0.51	-0.94	-0.94	-57.	2332.	2326.	-9.	0.	-
0.0657	408.32	1.249	-0.445	4957.0	500.00	1.40	6.45	45.42	-0.51	-0.94	-0.94	-57.	2332.	2326.	-9.	0.	-
0.0658	408.82	1.250	-0.445	4957.0	500.00	1.40	6.45	45.42	-0.51	-0.94	-0.94	-57.	2332.	2326.	-9.	0.	-
0.0659	410.31	1.243	-0.445	4957.0	500.00	1.40	6.45	45.42	-0.51	-0.94	-0.94	-57.	2332.	2326.	-9.	0.	-
0.0660	410.80	1.243	-0.445	4957.0	500.00	1.40	6.45	45.42	-0.51	-0.94	-0.94	-57.	2332.	2326.	-9.	0.	-
0.0661	412.29	1.262	-0.445	4956.9	500.00	1.42	6.45	45.97	-0.51	-0.99	-0.99	-57.	2332.	2326.	-9.	0.	-
0.0662	402.21	1.253	-0.445	4956.9	500.00	1.42	6.45	45.97	-0.51	-0.99	-0.99	-57.	2332.	2326.	-9.	0.	-
0.0663	402.71	1.244	-0.445	4956.9	500.00	1.42	6.45	45.97	-0.51	-0.99	-0.99	-57.	2332.	2326.	-9.	0.	-
0.0664	403.21	1.244	-0.445	4956.9	500.00	1.42	6.45	45.97	-0.51	-0.99	-0.99	-57.	2332.	2326.	-9.	0.	-
0.0665	403.71	1.245	-0.445	4956.9	500.00	1.42	6.45	45.97	-0.51	-0.99	-0.99	-57.	2332.	2326.	-9.	0.	-
0.0666	404.21	1.245	-0.445	4956.9	500.00	1.42	6.45	45.97	-0.51	-0.99	-0.99	-57.	2332.	2326.	-9.	0.	-
0.0667	404.71	1.245	-0.445	4956.9	500.00	1.42	6.45	45.97	-0.51	-0.99	-0.99	-57.	2332.	2326.	-9.	0.	-
0.0668	405.21	1.245	-0.445	4956.9	500.00	1.42	6.45	45.97	-0.51	-0.99	-0.99	-57.	2332.	2326.	-9.	0.	-
0.0669	405.71	1.245	-0.445	4956.9	500.00	1.42	6.45	45.97	-0.51	-0.99	-0.99	-57.	2332.	2326.	-9.	0.	-
0.0670	406.21	1.245	-0.445	4956.9	500.00	1.42	6.45	45.97	-0.51	-0.99	-0.99	-57.	2332.	2326.	-9.	0.	-
0.0671	406.71	1.245	-0.445	4956.9	500.00	1.42	6.45	45.97	-0.51	-0.99	-0.99	-57.	2332.	2326.	-9.	0.	-
0.0672	407.21	1.245	-0.445	4956.9	500.00	1.42	6.45	45.97	-0.51	-0.99	-0.99	-57.	2332.	2326.	-9.	0.	-
0.0673	407.71	1.245	-0.445	4956.9	500.00	1.42	6.45	45.97	-0.51	-0.99	-0.99	-57.	2332.	2326.	-9.	0.	-
0.0674	408.21	1.245	-0.445	4956.9	500.00	1.42	6.45	45.97	-0.51	-0.99	-0.99	-57.	2332.	2326.	-9.	0.	-
0.0675	408.71	1.245	-0.445	4956.9	500.00	1.42	6.45	45.97	-0.51	-0.99	-0.99	-57.	2332.	2326.	-9.	0.	-
0.0676	409.21	1.245	-0.445	4956.9	500.00	1.42	6.45	45.97	-0.51	-0.99	-0.99	-57.	2332.	2326.	-9.	0.	-
0.0677	411.30	1.255	-0.445	4956.9	500.00	1.42	6.45	45.97	-0.51	-0.99	-0.99	-57.	2332.	2326.	-9.	0.	-
0.0678	411.80	1.243	-0.445	4956.9	500.00	1.42	6.45	45.97	-0.51	-0.99	-0.99	-57.	2332.	2326.	-9.	0.	-
0.0679	412.29	1.262	-0.445	4956.9	500.00	1.42	6.45	45.97	-0.51	-0.99	-0.99	-57.	2332.	2326.	-9.	0.	-
0.0680	412.79	1.262	-0.445	4956.9	500.00	1.42	6.45	45.97	-0.51	-0.99	-0.99	-57.	2332.	2326.	-9.	0.	-
0.0681	413.29	1.265	-0.445	4956.9	500.00	1.42	6.45	45.97	-0.51	-0.99	-0.99	-57.	2332.	2326.	-9.	0.	-
0.0682	413.78	1.265	-0.445	4956.9	500.00	1.42	6.45	45.97	-0.51	-0.99	-0.99	-57.	2332.	2326.	-9.	0.	-
0.0683	414.28	1.262	-0.445	4956.9	500.00	1.42	6.45	45.97	-0.51	-0.99	-0.99	-57.	2332.	2326.	-9.	0.	-
0.0684	414.78	1.265	-0.445	4956.9	500.00	1.42	6.45	45.97	-0.51	-0.99	-0.99	-57.	2332.	2326.	-9.	0.	-
0.0685	415.27	1.261	-0.445	4956.9	500.00	1.42	6.45	45.97	-0.51	-0.99	-0.99	-57.	2332.	2326.	-9.	0.	-
0.0686	415.77	1.272	-0.445	4956.9	500.00	1.42	6.45	45.97	-0.51	-0.99	-0.99	-57.	2332.	2326.	-9.	0.	-
0.0687	416.27	1.273	-0.445	4956.9	500.00	1.42	6.45	45.97	-0.51	-0.99	-0.99	-57.	2332.	2326.	-9.	0.	-
0.0688	416.76	1.273	-0.445	4956.9	500.00	1.42	6.45	45.97	-0.51	-0.99	-0.99	-57.	2332.	2326.	-9.	0.	-
0.0689	417.26	1.274	-0.445	4956.9	500.00	1.42	6.45	45.97	-0.51	-0.99	-0.99	-57.	2332.	2326.	-9.	0.	-
0.0690	417.76	1.277	-0.445	4956.9	500.00	1.42	6.45	45.97	-0.51	-0.99	-0.99	-57.	2332.	2326.	-9.	0.	-
0.0691	418.25	1.278	-0.445	4956.9	500.00	1.42	6.45	45.97	-0.51	-0.99	-0.99	-57.	2332.	2326.	-9.	0.	-
0.0692	418.75	1.281	-0.445	4956.9	500.00	1.42	6.45	45.97	-0.51	-0.99	-0.99	-57.	2332.	2326.	-9.	0.	-
0.0693	419.25	1.281	-0.445	4956.9	500.00	1.42	6.45	45.97	-0.51	-0.99	-0.99	-57.	2332.	2326.	-9.	0.	-
0.0694	419.74	1.281	-0.445	4956.9	500.00	1.42	6.45	45.97	-0.51</								

FLECHETTE GROUND POINT

PAGE 13

T SEC	X FT	Y FT	Z FT	V FT/SEC	P FT/SEC	ALPHABETIC CHAR	PHT SEC	STH SEC	L-P SEC	W-N SEC	W-E SEC	E-T SEC	R-T SEC	S SEC	T-A SEC	TAU SEC
0.0850	422.72	1.283	-2.661	423.22	1.289	-2.641	423.72	1.295	0.65	44.76	44.76	44.76	44.76	0.5	1.12	-0.95
0.0851	423.22	1.295	-2.641	423.72	1.295	-2.641	424.22	1.305	0.65	45.25	45.25	45.25	45.25	0.5	1.15	-0.95
0.0852	423.72	1.305	-2.641	424.22	1.305	-2.641	424.72	1.315	0.65	45.74	45.74	45.74	45.74	0.5	1.15	-0.95
0.0853	424.22	1.315	-2.641	424.72	1.315	-2.641	425.22	1.325	0.65	46.23	46.23	46.23	46.23	0.5	1.15	-0.95
0.0854	424.72	1.325	-2.641	425.22	1.325	-2.641	425.72	1.335	0.65	46.72	46.72	46.72	46.72	0.5	1.15	-0.95
0.0855	425.22	1.335	-2.641	425.72	1.335	-2.641	426.22	1.345	0.65	47.21	47.21	47.21	47.21	0.5	1.15	-0.95
0.0856	425.72	1.345	-2.641	426.22	1.345	-2.641	426.72	1.355	0.65	47.7	47.7	47.7	47.7	0.5	1.15	-0.95
0.0857	426.22	1.355	-2.641	426.72	1.355	-2.641	427.22	1.365	0.65	48.19	48.19	48.19	48.19	0.5	1.15	-0.95
0.0858	426.72	1.365	-2.641	427.22	1.365	-2.641	427.72	1.375	0.65	48.68	48.68	48.68	48.68	0.5	1.15	-0.95
0.0859	427.22	1.375	-2.641	427.72	1.375	-2.641	428.22	1.385	0.65	49.17	49.17	49.17	49.17	0.5	1.15	-0.95
0.0860	427.72	1.385	-2.641	428.22	1.385	-2.641	428.72	1.395	0.65	49.66	49.66	49.66	49.66	0.5	1.15	-0.95
0.0861	428.22	1.395	-2.641	428.72	1.395	-2.641	429.22	1.405	0.65	50.15	50.15	50.15	50.15	0.5	1.15	-0.95
0.0862	428.72	1.405	-2.641	429.22	1.405	-2.641	429.72	1.415	0.65	50.64	50.64	50.64	50.64	0.5	1.15	-0.95
0.0863	429.22	1.415	-2.641	429.72	1.415	-2.641	430.22	1.425	0.65	51.13	51.13	51.13	51.13	0.5	1.15	-0.95
0.0864	429.72	1.425	-2.641	430.22	1.425	-2.641	430.72	1.435	0.65	51.62	51.62	51.62	51.62	0.5	1.15	-0.95
0.0865	430.22	1.435	-2.641	430.72	1.435	-2.641	431.22	1.445	0.65	52.11	52.11	52.11	52.11	0.5	1.15	-0.95
0.0866	430.72	1.445	-2.641	431.22	1.445	-2.641	431.72	1.455	0.65	52.6	52.6	52.6	52.6	0.5	1.15	-0.95
0.0867	431.22	1.455	-2.641	431.72	1.455	-2.641	432.22	1.465	0.65	53.09	53.09	53.09	53.09	0.5	1.15	-0.95
0.0868	431.72	1.465	-2.641	432.22	1.465	-2.641	432.72	1.475	0.65	53.58	53.58	53.58	53.58	0.5	1.15	-0.95
0.0869	432.22	1.475	-2.641	432.72	1.475	-2.641	433.22	1.485	0.65	54.07	54.07	54.07	54.07	0.5	1.15	-0.95
0.0870	432.72	1.485	-2.641	433.22	1.485	-2.641	433.72	1.495	0.65	54.56	54.56	54.56	54.56	0.5	1.15	-0.95
0.0871	433.22	1.495	-2.641	433.72	1.495	-2.641	434.22	1.505	0.65	55.05	55.05	55.05	55.05	0.5	1.15	-0.95
0.0872	433.72	1.505	-2.641	434.22	1.505	-2.641	434.72	1.515	0.65	55.54	55.54	55.54	55.54	0.5	1.15	-0.95
0.0873	434.22	1.515	-2.641	434.72	1.515	-2.641	435.22	1.525	0.65	56.03	56.03	56.03	56.03	0.5	1.15	-0.95
0.0874	434.72	1.525	-2.641	435.22	1.525	-2.641	435.72	1.535	0.65	56.52	56.52	56.52	56.52	0.5	1.15	-0.95
0.0875	435.22	1.535	-2.641	435.72	1.535	-2.641	436.22	1.545	0.65	57.01	57.01	57.01	57.01	0.5	1.15	-0.95
0.0876	435.72	1.545	-2.641	436.22	1.545	-2.641	436.72	1.555	0.65	57.5	57.5	57.5	57.5	0.5	1.15	-0.95
0.0877	436.22	1.555	-2.641	436.72	1.555	-2.641	437.22	1.565	0.65	58.09	58.09	58.09	58.09	0.5	1.15	-0.95
0.0878	436.72	1.565	-2.641	437.22	1.565	-2.641	437.72	1.575	0.65	58.58	58.58	58.58	58.58	0.5	1.15	-0.95
0.0879	437.22	1.575	-2.641	437.72	1.575	-2.641	438.22	1.585	0.65	59.07	59.07	59.07	59.07	0.5	1.15	-0.95
0.0880	437.72	1.585	-2.641	438.22	1.585	-2.641	438.72	1.595	0.65	59.56	59.56	59.56	59.56	0.5	1.15	-0.95
0.0881	438.22	1.595	-2.641	438.72	1.595	-2.641	439.22	1.605	0.65	60.05	60.05	60.05	60.05	0.5	1.15	-0.95
0.0882	438.72	1.605	-2.641	439.22	1.605	-2.641	439.72	1.615	0.65	60.54	60.54	60.54	60.54	0.5	1.15	-0.95
0.0883	439.22	1.615	-2.641	439.72	1.615	-2.641	440.22	1.625	0.65	61.03	61.03	61.03	61.03	0.5	1.15	-0.95
0.0884	439.72	1.625	-2.641	440.22	1.625	-2.641	440.72	1.635	0.65	61.52	61.52	61.52	61.52	0.5	1.15	-0.95
0.0885	440.22	1.635	-2.641	440.72	1.635	-2.641	441.22	1.645	0.65	62.01	62.01	62.01	62.01	0.5	1.15	-0.95
0.0886	440.72	1.645	-2.641	441.22	1.645	-2.641	441.72	1.655	0.65	62.5	62.5	62.5	62.5	0.5	1.15	-0.95
0.0887	441.22	1.655	-2.641	441.72	1.655	-2.641	442.22	1.665	0.65	63.0	63.0	63.0	63.0	0.5	1.15	-0.95
0.0888	441.72	1.665	-2.641	442.22	1.665	-2.641	442.72	1.675	0.65	63.49	63.49	63.49	63.49	0.5	1.15	-0.95
0.0889	442.22	1.675	-2.641	442.72	1.675	-2.641	443.22	1.685	0.65	63.98	63.98	63.98	63.98	0.5	1.15	-0.95
0.0890	442.72	1.685	-2.641	443.22	1.685	-2.641	443.72	1.695	0.65	64.47	64.47	64.47	64.47	0.5	1.15	-0.95
0.0891	443.22	1.695	-2.641	443.72	1.695	-2.641	444.22	1.705	0.65	64.96	64.96	64.96	64.96	0.5	1.15	-0.95
0.0892	443.72	1.705	-2.641	444.22	1.705	-2.641	444.72	1.715	0.65	65.45	65.45	65.45	65.45	0.5	1.15	-0.95
0.0893	444.22	1.715	-2.641	444.72	1.715	-2.641	445.22	1.725	0.65	65.94	65.94	65.94	65.94	0.5	1.15	-0.95
0.0894	444.72	1.725	-2.641	445.22	1.725	-2.641	445.72	1.735	0.65	66.43	66.43	66.43	66.43	0.5	1.15	-0.95
0.0895	445.22	1.735	-2.641	445.72	1.735	-2.641	446.22	1.745	0.65	66.92	66.92	66.92	66.92	0.5	1.15	-0.95
0.0896	445.72	1.745	-2.641	446.22	1.745	-2.641	446.72	1.755	0.65	67.41	67.41	67.41	67.41	0.5	1.15	-0.95
0.0897	446.22	1.755	-2.641	446.72	1.755	-2.641	447.22	1.765	0.65	67.9	67.9	67.9	67.9	0.5	1.15	-0.95
0.0898	446.72	1.765	-2.641	447.22	1.765	-2.641	447.72	1.775	0.65	68.39	68.39	68.39	68.39	0.5	1.15	-0.95
0.0899	447.22	1.775	-2.641	447.72	1.775	-2.641	448.22	1.785	0.65	68.88	68.88	68.88	68.88	0.5	1.15	-0.95
0.0900	447.72	1.785	-2.641	448.22	1.785	-2.641	448.72	1.795	0.65	69.37	69.37	69.37	69.37	0.5	1.15	-0.95
0.0901	448.22	1.795	-2.641	448.72	1.795	-2.641	449.22	1.805	0.65	69.86	69.86	69.86	69.86	0.5	1.15	-0.95
0.0902	448.72	1.805	-2.641	449.22	1.805	-2.641	449.72	1.815	0.65	70.35	70.35	70.35	70.35	0.5	1.15	-0.95
0.0903	449.22	1.815	-2.641	449.72	1.815	-2.641	450.22	1.825	0.65	70.84	70.84	70.84	70.84	0.5	1.15	-0.95
0.0904	449.72	1.825	-2.641	450.22	1.825	-2.641	450.72	1.835	0.65	71.33	71.33	71.33	71.33	0.5	1.15	-0.95
0.0905	450.22	1.835	-2.641	450.72	1.835	-2.641	451.22	1.845	0.65	71.82	71.82	71.82	71.82	0.5	1.15	-0.95
0.0906	450.72	1.845	-2.641	451.22	1.845	-2.641	451.72	1.855	0.65	72.31	72.31	72.31	72.31	0.5	1.15	-0.95
0.0907	451.22	1.855	-2.641	451.72	1.855	-2.641	452.22	1.865	0.65	72.8	72.8	72.8	72.8	0.5	1.15	-0.95
0.0908	451.72	1.865	-2.641	452.22	1.865	-2.641	452.72	1.875	0.65	73.29	73.29	73.29	73.29	0.5	1.15	-0.95
0.0909	452.22	1.875	-2.641	452.72	1.875	-2.641	453.22	1.885	0.65	73.78	73.78	73.78	73.78	0.5	1.15	-0.95
0.0910	452.72	1.885	-2.641	453.22	1.885	-2.641	453.72	1.895	0.65	74.27	74.27	74.27	74.27	0.5	1.15	-0.95
0.0911	453.22	1.895	-2.641	453.72	1.895	-2.641	454.22	1.905	0.65	74.76	74.76	74.76	74.76	0.5	1.15	-0.95
0.0912	453.72	1.905	-2.641	454.22	1.905	-2.641	454.72	1.915	0.65	75.25	75.25	75.25	75.25	0.5	1.15	-0.95
0.0913	454.22	1.915	-2.641	454.72	1.915	-2.641	455.22	1.925	0.65	75.74						

FLECHETTE GROUND POINT

PAGE 12

	X	Y	Z	FT	V	FT/SEC	RAD/SEC	MFG	PHI	ALPHA	BETA	L-N	L-P	L-S	L-T	W-P	W-Q	W-R	W-S
0-0.930	447.55	1.339	-0.422	4965.1	500.00	1.48	4.45	47.39	1.43	0.31	-55	-57	2333.-2333.	-55	0	1	0	1	0
0-0.931	449.05	1.341	-0.432	4968.1	500.00	1.47	4.45	46.63	1.42	-0.34	-55	-57	2333.-2333.	-55	0	1	0	1	0
0-0.932	449.54	1.342	-0.451	4965.1	510.00	1.46	4.45	45.93	1.42	-0.46	-55	-57	2333.-2333.	-55	0	1	0	1	0
0-0.933	126.04	1.374	-0.425	4965.1	510.00	1.46	4.45	45.27	1.35	-0.54	-55	-57	2333.-2333.	-55	0	1	0	1	0
0-0.935	469.56	1.376	-0.437	4965.0	520.00	1.45	4.45	45.14	1.32	-0.41	-55	-57	2333.-2333.	-55	0	1	0	1	0
0-0.936	450.03	1.378	-0.485	4965.0	510.00	1.45	4.45	45.35	1.27	-0.59	-55	-57	2333.-2333.	-55	0	1	0	1	0
0-0.937	450.53	1.350	-0.187	4965.0	500.00	1.47	4.45	45.39	1.23	-0.76	-55	-57	2333.-2333.	-55	0	1	0	1	0
0-0.938	451.03	1.351	-0.449	4965.0	510.00	1.44	4.45	46.14	1.18	-0.62	-55	-57	2333.-2333.	-55	0	1	0	1	0
0-0.939	451.52	1.353	-0.491	4965.0	500.00	1.44	4.45	46.43	1.13	-0.53	-55	-57	2333.-2333.	-55	0	1	0	1	0
0-0.940	452.02	1.355	-0.492	4965.0	500.00	1.44	4.45	46.83	1.05	-0.63	-55	-57	2333.-2333.	-55	0	1	0	1	0
0-0.941	452.52	1.357	-0.493	4965.0	510.00	1.44	4.45	47.35	1.02	-1.01	-55	-57	2333.-2333.	-55	0	1	0	1	0
0-0.942	453.01	1.359	-0.494	4965.0	500.00	1.44	4.45	47.32	0.97	-1.06	-55	-57	2333.-2333.	-55	0	1	0	1	0
0-0.943	453.51	1.351	-0.475	4965.0	500.00	1.44	4.45	47.30	0.92	-1.11	-55	-57	2333.-2333.	-55	0	1	0	1	0
0-0.944	454.01	1.353	-0.496	4965.0	510.00	1.44	4.45	47.31	0.89	-1.15	-55	-57	2333.-2333.	-55	0	1	0	1	0
0-0.945	454.50	1.374	-0.497	4965.0	510.00	1.44	4.45	47.32	0.85	-1.17	-55	-57	2333.-2333.	-55	0	1	0	1	0
0-0.946	455.00	1.365	-0.498	4965.0	510.00	1.44	4.45	47.33	0.78	-1.23	-55	-57	2333.-2333.	-55	0	1	0	1	0
0-0.947	455.50	1.367	-0.499	4965.0	510.00	1.44	4.45	47.34	0.73	-1.26	-55	-57	2333.-2333.	-55	0	1	0	1	0
0-0.948	455.90	1.370	-0.499	4965.0	510.00	1.44	4.45	47.35	0.68	-1.29	-55	-57	2333.-2333.	-55	0	1	0	1	0
0-0.949	456.30	1.372	-0.501	4965.0	510.00	1.44	4.45	47.36	0.63	-1.31	-55	-57	2333.-2333.	-55	0	1	0	1	0
0-0.950	456.70	1.374	-0.502	4965.0	510.00	1.43	4.45	47.37	0.58	-1.33	-55	-57	2333.-2333.	-55	0	1	0	1	0
0-0.951	457.10	1.376	-0.502	4965.0	510.00	1.43	4.45	47.38	0.53	-1.34	-55	-57	2333.-2333.	-55	0	1	0	1	0
0-0.952	457.50	1.377	-0.503	4965.0	510.00	1.43	4.45	47.39	0.48	-1.35	-55	-57	2333.-2333.	-55	0	1	0	1	0
0-0.953	457.90	1.379	-0.503	4965.0	510.00	1.43	4.45	47.40	0.43	-1.36	-55	-57	2333.-2333.	-55	0	1	0	1	0
0-0.954	458.30	1.381	-0.504	4965.0	510.00	1.43	4.45	47.41	0.38	-1.37	-55	-57	2333.-2333.	-55	0	1	0	1	0
0-0.955	458.70	1.382	-0.504	4965.0	510.00	1.43	4.45	47.42	0.33	-1.38	-55	-57	2333.-2333.	-55	0	1	0	1	0
0-0.956	459.10	1.384	-0.505	4965.0	510.00	1.43	4.45	47.43	0.28	-1.39	-55	-57	2333.-2333.	-55	0	1	0	1	0
0-0.957	459.50	1.385	-0.505	4965.0	510.00	1.43	4.45	47.44	0.23	-1.40	-55	-57	2333.-2333.	-55	0	1	0	1	0
0-0.958	459.80	1.387	-0.506	4965.0	510.00	1.43	4.45	47.45	0.18	-1.41	-55	-57	2333.-2333.	-55	0	1	0	1	0
0-0.959	460.10	1.388	-0.506	4965.0	510.00	1.43	4.45	47.46	0.13	-1.42	-55	-57	2333.-2333.	-55	0	1	0	1	0
0-0.960	460.40	1.389	-0.507	4965.0	510.00	1.43	4.45	47.47	0.08	-1.43	-55	-57	2333.-2333.	-55	0	1	0	1	0
0-0.961	460.70	1.391	-0.507	4965.0	510.00	1.43	4.45	47.48	0.03	-1.44	-55	-57	2333.-2333.	-55	0	1	0	1	0
0-0.962	461.00	1.392	-0.508	4965.0	510.00	1.43	4.45	47.49	-0.01	-1.45	-55	-57	2333.-2333.	-55	0	1	0	1	0
0-0.963	461.30	1.393	-0.508	4965.0	510.00	1.43	4.45	47.50	-0.06	-1.46	-55	-57	2333.-2333.	-55	0	1	0	1	0
0-0.964	461.60	1.394	-0.509	4965.0	510.00	1.43	4.45	47.51	-0.11	-1.47	-55	-57	2333.-2333.	-55	0	1	0	1	0
0-0.965	461.90	1.395	-0.509	4965.0	510.00	1.43	4.45	47.52	-0.16	-1.48	-55	-57	2333.-2333.	-55	0	1	0	1	0
0-0.966	462.20	1.396	-0.509	4965.0	510.00	1.43	4.45	47.53	-0.21	-1.49	-55	-57	2333.-2333.	-55	0	1	0	1	0
0-0.967	462.50	1.397	-0.509	4965.0	510.00	1.43	4.45	47.54	-0.26	-1.50	-55	-57	2333.-2333.	-55	0	1	0	1	0
0-0.968	462.80	1.398	-0.509	4965.0	510.00	1.43	4.45	47.55	-0.31	-1.51	-55	-57	2333.-2333.	-55	0	1	0	1	0
0-0.969	463.10	1.399	-0.509	4965.0	510.00	1.43	4.45	47.56	-0.36	-1.52	-55	-57	2333.-2333.	-55	0	1	0	1	0
0-0.970	463.40	1.400	-0.509	4965.0	510.00	1.43	4.45	47.57	-0.41	-1.53	-55	-57	2333.-2333.	-55	0	1	0	1	0
0-0.971	463.70	1.401	-0.509	4965.0	510.00	1.43	4.45	47.58	-0.46	-1.54	-55	-57	2333.-2333.	-55	0	1	0	1	0
0-0.972	464.00	1.402	-0.509	4965.0	510.00	1.43	4.45	47.59	-0.51	-1.55	-55	-57	2333.-2333.	-55	0	1	0	1	0
0-0.973	464.30	1.403	-0.509	4965.0	510.00	1.43	4.45	47.60	-0.56	-1.56	-55	-57	2333.-2333.	-55	0	1	0	1	0
0-0.974	464.60	1.404	-0.509	4965.0	510.00	1.43	4.45	47.61	-0.61	-1.57	-55	-57	2333.-2333.	-55	0	1	0	1	0
0-0.975	464.90	1.405	-0.509	4965.0	510.00	1.43	4.45	47.62	-0.66	-1.58	-55	-57	2333.-2333.	-55	0	1	0	1	0
0-0.976	465.20	1.406	-0.509	4965.0	510.00	1.43	4.45	47.63	-0.71	-1.59	-55	-57	2333.-2333.	-55	0	1	0	1	0
0-0.977	465.50	1.407	-0.509	4965.0	510.00	1.43	4.45	47.64	-0.76	-1.60	-55	-57	2333.-2333.	-55	0	1	0	1	0
0-0.978	465.80	1.408	-0.509	4965.0	510.00	1.43	4.45	47.65	-0.81	-1.61	-55	-57	2333.-2333.	-55	0	1	0	1	0
0-0.979	466.10	1.409	-0.509	4965.0	510.00	1.43	4.45	47.66	-0.86	-1.62	-55	-57	2333.-2333.	-55	0	1	0	1	0
0-0.980	466.40	1.410	-0.509	4965.0	510.00	1.43	4.45	47.67	-0.91	-1.63	-55	-57	2333.-2333.	-55	0	1	0	1	0
0-0.981	466.70	1.411	-0.509	4965.0	510.00	1.43	4.45	47.68	-0.96	-1.64	-55	-57	2333.-2333.	-55	0	1	0	1	0
0-0.982	467.00	1.412	-0.509	4965.0	510.00	1.43	4.45	47.69	-1.01	-1.65	-55	-57	2333.-2333.	-55	0	1	0	1	0
0-0.983	467.30	1.413	-0.509	4965.0	510.00	1.43	4.45	47.70	-1.06	-1.66	-55	-57	2333.-2333.	-55	0	1	0	1	0
0-0.984	467.60	1.414	-0.509	4965.0	510.00	1.43	4.45	47.71	-1.11	-1.67	-55	-57	2333.-2333.	-55	0	1	0	1	0
0-0.985	467.90	1.415	-0.509	4965.0	510.00	1.43	4.45	47.72	-1.16	-1.68	-55	-57	2333.-2333.	-55	0	1	0	1	0
0-0.986	468.20	1.416	-0.509	4965.0	510.00	1.43	4.45	47.73	-1.21	-1.69	-55	-57	2333.-2333.	-55	0	1	0	1	0
0-0.987	468.50	1.417	-0.509	4965.0	510.00	1.43	4.45	47.74	-1.26	-1.70	-55	-57	2333.-2333.	-55	0	1	0	1	0
0-0.988	468.80	1.418	-0.509	4965.0	510.00	1.43	4.45	47.75	-1.31	-1.71	-55	-57	2333.-2333.	-55	0	1	0	1	0
0-0.989	469.10	1.419	-0.509	4965.0	510.00	1.43	4.45	47.76	-1.36	-1.72	-55	-57	2333.-2333.	-55	0	1	0	1	0
0-0.990	469.40	1.420	-0.509	4965.0	510.00	1.43	4.45	47.77	-1.41	-1.73	-55	-57	2333.-2333.	-55	0	1	0	1	0
0-0.991	469.70	1.421	-0.509	4965.0	510.00	1.43	4.45	47.78	-1.46	-1.74	-55	-57	2333.-2333.	-55	0	1	0	1	0
0-0.992	470.00	1.422	-0.509	4965.0	510.00	1.43	4.45	47.79	-1.51	-1.75	-55	-57	2						

FLICETTE GROUND FOIST

PAGE 20

T	X	Y	Z	V	P	ALPHA	BETA	GAMMA	U-N	U-P	U-I	K-P	K-I
SFC	FT	FT	FT	FT/SEC									
0.0950	472.37	1.421	-0.510	500.00	1.040	4.045	44.49	1.129	-0.53	-0.53	0	1	
0.0951	472.87	1.423	-0.510	496.55	1.040	4.045	44.93	1.122	-0.53	-0.53	0	1	
0.0952	473.37	1.425	-0.510	493.55	1.040	4.045	44.96	1.134	-0.53	-0.55	0	1	
0.0953	473.86	1.426	-0.510	490.55	1.040	4.045	44.99	1.135	-0.53	-0.55	0	1	
0.0954	474.35	1.428	-0.510	485.55	1.040	4.045	45.03	1.138	-0.53	-0.55	0	1	
0.0955	474.85	1.429	-0.510	482.55	1.040	4.045	45.06	1.142	-0.53	-0.55	0	1	
0.0956	475.35	1.430	-0.509	479.55	1.040	4.045	45.10	1.145	-0.53	-0.55	0	1	
0.0957	475.85	1.431	-0.509	476.55	1.040	4.045	45.13	1.148	-0.53	-0.55	0	1	
0.0958	476.35	1.432	-0.509	473.55	1.040	4.045	45.17	1.152	-0.53	-0.55	0	1	
0.0959	476.84	1.433	-0.509	470.55	1.040	4.045	45.20	1.155	-0.53	-0.55	0	1	
0.0960	477.34	1.434	-0.509	467.55	1.040	4.045	45.24	1.158	-0.53	-0.55	0	1	
0.0961	477.83	1.435	-0.509	464.55	1.040	4.045	45.28	1.162	-0.53	-0.55	0	1	
0.0962	478.33	1.436	-0.509	461.55	1.040	4.045	45.32	1.165	-0.53	-0.55	0	1	
0.0963	478.83	1.437	-0.509	458.55	1.040	4.045	45.36	1.168	-0.53	-0.55	0	1	
0.0964	479.32	1.438	-0.509	455.55	1.040	4.045	45.40	1.172	-0.53	-0.55	0	1	
0.0965	479.82	1.439	-0.509	452.55	1.040	4.045	45.44	1.175	-0.53	-0.55	0	1	
0.0966	480.31	1.440	-0.509	449.55	1.040	4.045	45.48	1.178	-0.53	-0.55	0	1	
0.0967	480.81	1.441	-0.509	446.55	1.040	4.045	45.52	1.182	-0.53	-0.55	0	1	
0.0968	481.31	1.442	-0.509	443.55	1.040	4.045	45.56	1.185	-0.53	-0.55	0	1	
0.0969	481.81	1.443	-0.509	440.55	1.040	4.045	45.60	1.188	-0.53	-0.55	0	1	
0.0970	482.31	1.444	-0.509	437.55	1.040	4.045	45.64	1.192	-0.53	-0.55	0	1	
0.0971	482.80	1.445	-0.509	434.55	1.040	4.045	45.68	1.195	-0.53	-0.55	0	1	
0.0972	483.29	1.446	-0.509	431.55	1.040	4.045	45.72	1.198	-0.53	-0.55	0	1	
0.0973	483.79	1.447	-0.509	428.55	1.040	4.045	45.76	1.202	-0.53	-0.55	0	1	
0.0974	484.29	1.448	-0.509	425.55	1.040	4.045	45.80	1.205	-0.53	-0.55	0	1	
0.0975	484.78	1.449	-0.509	422.55	1.040	4.045	45.84	1.208	-0.53	-0.55	0	1	
0.0976	485.28	1.450	-0.509	419.55	1.040	4.045	45.88	1.212	-0.53	-0.55	0	1	
0.0977	485.77	1.451	-0.509	416.55	1.040	4.045	45.92	1.215	-0.53	-0.55	0	1	
0.0978	486.27	1.452	-0.509	413.55	1.040	4.045	45.96	1.218	-0.53	-0.55	0	1	
0.0979	486.76	1.453	-0.509	410.55	1.040	4.045	46.00	1.222	-0.53	-0.55	0	1	
0.0980	487.26	1.454	-0.509	407.55	1.040	4.045	46.04	1.225	-0.53	-0.55	0	1	
0.0981	487.75	1.455	-0.509	404.55	1.040	4.045	46.08	1.228	-0.53	-0.55	0	1	
0.0982	488.25	1.456	-0.509	401.55	1.040	4.045	46.12	1.232	-0.53	-0.55	0	1	
0.0983	488.75	1.457	-0.509	398.55	1.040	4.045	46.16	1.235	-0.53	-0.55	0	1	
0.0984	489.23	1.458	-0.509	395.55	1.040	4.045	46.20	1.238	-0.53	-0.55	0	1	
0.0985	489.73	1.459	-0.509	392.55	1.040	4.045	46.24	1.242	-0.53	-0.55	0	1	
0.0986	490.22	1.460	-0.509	389.55	1.040	4.045	46.28	1.245	-0.53	-0.55	0	1	
0.0987	490.72	1.461	-0.509	386.55	1.040	4.045	46.32	1.248	-0.53	-0.55	0	1	
0.0988	491.21	1.462	-0.509	383.55	1.040	4.045	46.36	1.252	-0.53	-0.55	0	1	
0.0989	491.70	1.463	-0.509	380.55	1.040	4.045	46.40	1.255	-0.53	-0.55	0	1	
0.0990	492.19	1.464	-0.509	377.55	1.040	4.045	46.44	1.258	-0.53	-0.55	0	1	
0.0991	492.69	1.465	-0.509	374.55	1.040	4.045	46.48	1.262	-0.53	-0.55	0	1	
0.0992	493.17	1.466	-0.509	371.55	1.040	4.045	46.52	1.265	-0.53	-0.55	0	1	
0.0993	493.66	1.467	-0.509	368.55	1.040	4.045	46.56	1.268	-0.53	-0.55	0	1	
0.0994	494.15	1.468	-0.509	365.55	1.040	4.045	46.60	1.272	-0.53	-0.55	0	1	
0.0995	494.64	1.469	-0.509	362.55	1.040	4.045	46.64	1.275	-0.53	-0.55	0	1	
0.0996	495.13	1.470	-0.509	359.55	1.040	4.045	46.68	1.278	-0.53	-0.55	0	1	
0.0997	495.62	1.471	-0.509	356.55	1.040	4.045	46.72	1.282	-0.53	-0.55	0	1	
0.0998	496.11	1.472	-0.509	353.55	1.040	4.045	46.76	1.285	-0.53	-0.55	0	1	
0.0999	496.60	1.473	-0.509	350.55	1.040	4.045	46.80	1.288	-0.53	-0.55	0	1	
0.0999	496.69	1.474	-0.509	347.55	1.040	4.045	46.84	1.292	-0.53	-0.55	0	1	
0.0999	497.18	1.475	-0.509	344.55	1.040	4.045	46.88	1.295	-0.53	-0.55	0	1	
0.0999	497.67	1.476	-0.509	341.55	1.040	4.045	46.92	1.298	-0.53	-0.55	0	1	
0.0999	498.16	1.477	-0.509	338.55	1.040	4.045	46.96	1.302	-0.53	-0.55	0	1	
0.0999	498.65	1.478	-0.509	335.55	1.040	4.045	47.00	1.305	-0.53	-0.55	0	1	
0.0999	499.14	1.479	-0.509	332.55	1.040	4.045	47.04	1.308	-0.53	-0.55	0	1	
0.0999	499.63	1.480	-0.509	329.55	1.040	4.045	47.08	1.312	-0.53	-0.55	0	1	
0.0999	500.12	1.481	-0.509	326.55	1.040	4.045	47.12	1.315	-0.53	-0.55	0	1	
0.0999	500.61	1.482	-0.509	323.55	1.040	4.045	47.16	1.318	-0.53	-0.55	0	1	
0.0999	501.10	1.483	-0.509	320.55	1.040	4.045	47.20	1.322	-0.53	-0.55	0	1	
0.0999	501.59	1.484	-0.509	317.55	1.040	4.045	47.24	1.325	-0.53	-0.55	0	1	
0.0999	502.08	1.485	-0.509	314.55	1.040	4.045	47.28	1.328	-0.53	-0.55	0	1	
0.0999	502.57	1.486	-0.509	311.55	1.040	4.045	47.32	1.332	-0.53	-0.55	0	1	
0.0999	503.06	1.487	-0.509	308.55	1.040	4.045	47.36	1.335	-0.53	-0.55	0	1	
0.0999	503.55	1.488	-0.509	305.55	1.040	4.045	47.40	1.338	-0.53	-0.55	0	1	
0.0999	504.04	1.489	-0.509	302.55	1.040	4.045	47.44	1.342	-0.53	-0.55	0	1	
0.0999	504.53	1.490	-0.509	299.55	1.040	4.045	47.48	1.345	-0.53	-0.55	0	1	
0.0999	505.02	1.491	-0.509	296.55	1.040	4.045	47.52	1.348	-0.53	-0.55	0	1	
0.0999	505.51	1.492	-0.509	293.55	1.040	4.045	47.56	1.352	-0.53	-0.55	0	1	
0.0999	505.99	1.493	-0.509	290.55	1.040	4.045	47.60	1.355	-0.53	-0.55	0	1	
0.0999	506.48	1.494	-0.509	287.55	1.040	4.045	47.64	1.358	-0.53	-0.55	0	1	
0.0999	506.97	1.495	-0.509	284.55	1.040	4.045	47.68	1.362	-0.53	-0.55	0	1	
0.0999	507.46	1.496	-0.509	281.55	1.040	4.045	47.72	1.365	-0.53	-0.55	0	1	
0.0999	507.95	1.497	-0.509	278.55	1.040	4.045	47.76	1.368	-0.53	-0.55	0	1	
0.0999	508.44	1.498	-0.509	275.55	1.040	4.045	47.80	1.372	-0.53	-0.55	0	1	
0.0999	508.93	1.499	-0.509	272.55	1.040	4.045	47.84	1.375	-0.53	-0.55	0	1	
0.0999	509.42	1.500	-0.509	269.55	1.040	4.045	47.88	1.378	-0.53	-0.55	0	1	
0.0999	509.91	1.501	-0.509	266.55	1.040	4.045	47.92	1.382	-0.53	-0.55	0	1	
0.0999	509.40	1.502	-0.509	263.55	1.040	4.045	47.96	1.385	-0.53	-0.55	0	1	
0.0999	509.89	1.503	-0.509	260.55	1.040	4.045	48.00	1.388	-0.53	-0.55	0	1	
0.0999	509.38	1.504	-0.509	257.55	1.040	4.045	48.04	1.392	-0.53	-0.55	0	1	
0.0999	509.87	1.505	-0.509	254.55	1.040	4.045	48.08	1.395	-0.53	-0.55	0	1	
0.0999	509.37	1.506											

**316 COPY AVAILABLE TO DEC BUSES NOT
PERMIT FULLY LEGIBLE PRODUCTION**

FLECHETTE GROUND POINT

PAGE 22

	X	Y	Z	P	ALPHA	MACH	PHI	ALPHAI	PHII	L-O	H-N	N-P	S	TAU	R-I	
T	FT	FT	FT	FT/SEC	PSI/SEC	PSI	DEG	DEG	DEG	PSI	PSI/SEC	PSI	PSI	PSI	D-G	
SEC	FT	FT	FT	FT/SEC	PSI/SEC	PSI	DEG	DEG	DEG	PSI	PSI/SEC	PSI	PSI	PSI	D-G	
0.1050	522.01	1.575	-0.571	426.5	500.00	1.05	4.45	4.45	3.14	-55	-57	233.0	-233.0	-0	1.	
0.1051	522.50	1.577	-0.571	426.6	500.00	1.04	4.45	4.45	2.17	-45	-57	233.0	-233.0	-0	1.	
0.1052	523.00	1.572	-0.571	426.6	500.00	1.04	4.45	4.45	4.21	-55	-57	233.0	-233.0	-0	1.	
0.1053	523.50	1.582	-0.572	426.6	500.00	1.04	4.45	4.45	4.21	-54	-57	233.0	-233.0	-0	1.	
-	0.1054	523.69	1.584	-0.573	426.6	4.45	500.00	1.03	4.45	4.55	-55	-57	233.0	-233.0	-0	1.
-	0.1055	524.46	1.586	-0.573	426.6	4.45	500.00	1.03	4.45	4.55	-42	-57	233.0	-233.0	-0	1.
-	0.1056	524.99	1.583	-0.571	426.6	4.45	500.00	1.03	4.45	4.55	-32	-57	233.0	-233.0	-0	1.
-	0.1057	525.08	1.591	-0.571	426.6	4.45	500.00	1.02	4.45	4.55	-32	-57	233.0	-233.0	-0	1.
-	0.1058	525.98	1.593	-0.576	426.6	4.45	500.00	1.02	4.45	4.55	-32	-57	233.0	-233.0	-0	1.
-	0.1059	526.47	1.595	-0.575	426.6	4.45	500.00	1.02	4.45	4.55	-32	-57	233.0	-233.0	-0	1.
-	0.1060	526.97	1.597	-0.575	426.6	4.45	500.00	1.02	4.45	4.55	-32	-57	233.0	-233.0	-0	1.
-	0.1061	527.7	1.598	-0.575	426.6	4.45	500.00	1.02	4.45	4.55	-32	-57	233.0	-233.0	-0	1.
-	0.1062	527.95	1.602	-0.571	426.6	4.45	500.00	1.02	4.45	4.55	-22	-57	233.0	-233.0	-0	1.
-	0.1063	528.45	1.604	-0.576	426.6	4.45	500.00	1.02	4.45	4.55	-22	-57	233.0	-233.0	-0	1.
-	0.1064	529.06	1.606	-0.576	426.6	4.45	500.00	1.02	4.45	4.55	-22	-57	233.0	-233.0	-0	1.
-	0.1065	529.45	1.609	-0.575	426.6	4.45	500.00	1.02	4.45	4.55	-22	-57	233.0	-233.0	-0	1.
-	0.1066	529.55	1.610	-0.575	426.6	4.45	500.00	1.02	4.45	4.55	-22	-57	233.0	-233.0	-0	1.
-	0.1067	531.46	1.612	-0.576	426.6	4.45	500.00	1.02	4.45	4.55	-22	-57	233.0	-233.0	-0	1.
-	0.1068	531.94	1.614	-0.576	426.6	4.45	500.00	1.02	4.45	4.55	-22	-57	233.0	-233.0	-0	1.
-	0.1069	531.64	1.616	-0.576	426.6	4.45	500.00	1.02	4.45	4.55	-22	-57	233.0	-233.0	-0	1.
-	0.1070	531.93	1.615	-0.576	426.6	4.45	500.00	1.02	4.45	4.55	-22	-57	233.0	-233.0	-0	1.
-	0.1071	532.43	1.620	-0.576	426.6	4.45	500.00	1.02	4.45	4.55	-22	-57	233.0	-233.0	-0	1.
-	0.1072	532.93	1.622	-0.576	426.6	4.45	500.00	1.02	4.45	4.55	-22	-57	233.0	-233.0	-0	1.
-	0.1073	533.42	1.624	-0.576	426.6	4.45	500.00	1.02	4.45	4.55	-22	-57	233.0	-233.0	-0	1.
-	0.1074	533.92	1.625	-0.576	426.6	4.45	500.00	1.02	4.45	4.55	-22	-57	233.0	-233.0	-0	1.
-	0.1075	534.42	1.627	-0.575	426.6	4.45	500.00	1.02	4.45	4.55	-22	-57	233.0	-233.0	-0	1.
-	0.1076	534.51	1.629	-0.575	426.6	4.45	500.00	1.02	4.45	4.55	-22	-57	233.0	-233.0	-0	1.
-	0.1077	535.41	1.631	-0.575	426.6	4.45	500.00	1.02	4.45	4.55	-22	-57	233.0	-233.0	-0	1.
-	0.1078	535.30	1.632	-0.575	426.6	4.45	500.00	1.02	4.45	4.55	-22	-57	233.0	-233.0	-0	1.
-	0.1079	535.40	1.634	-0.575	426.6	4.45	500.00	1.02	4.45	4.55	-22	-57	233.0	-233.0	-0	1.
-	0.1080	535.90	1.635	-0.575	426.6	4.45	500.00	1.02	4.45	4.55	-22	-57	233.0	-233.0	-0	1.
-	0.1081	537.39	1.637	-0.574	426.6	4.45	500.00	1.02	4.45	4.55	-22	-57	233.0	-233.0	-0	1.
-	0.1082	537.59	1.639	-0.574	426.6	4.45	500.00	1.02	4.45	4.55	-22	-57	233.0	-233.0	-0	1.
-	0.1083	538.19	1.642	-0.574	426.6	4.45	500.00	1.02	4.45	4.55	-22	-57	233.0	-233.0	-0	1.
-	0.1084	538.39	1.642	-0.574	426.6	4.45	500.00	1.02	4.45	4.55	-22	-57	233.0	-233.0	-0	1.
-	0.1085	539.38	1.643	-0.574	426.6	4.45	500.00	1.02	4.45	4.55	-22	-57	233.0	-233.0	-0	1.
-	0.1086	540.31	1.645	-0.574	426.6	4.45	500.00	1.02	4.45	4.55	-22	-57	233.0	-233.0	-0	1.
-	0.1087	540.67	1.647	-0.573	426.6	4.45	500.00	1.02	4.45	4.55	-22	-57	233.0	-233.0	-0	1.
-	0.1088	541.36	1.649	-0.573	426.6	4.45	500.00	1.02	4.45	4.55	-22	-57	233.0	-233.0	-0	1.
-	0.1089	541.86	1.650	-0.573	426.6	4.45	500.00	1.02	4.45	4.55	-22	-57	233.0	-233.0	-0	1.
-	0.1090	542.14	1.651	-0.572	426.6	4.45	500.00	1.02	4.45	4.55	-22	-57	233.0	-233.0	-0	1.
-	0.1091	542.85	1.653	-0.572	426.6	4.45	500.00	1.02	4.45	4.55	-22	-57	233.0	-233.0	-0	1.
-	0.1092	543.37	1.656	-0.573	426.6	4.45	500.00	1.02	4.45	4.55	-22	-57	233.0	-233.0	-0	1.
-	0.1093	543.79	1.659	-0.573	426.6	4.45	500.00	1.02	4.45	4.55	-22	-57	233.0	-233.0	-0	1.
-	0.1094	544.33	1.660	-0.572	426.6	4.45	500.00	1.02	4.45	4.55	-22	-57	233.0	-233.0	-0	1.
-	0.1095	544.84	1.667	-0.572	426.6	4.45	500.00	1.02	4.45	4.55	-22	-57	233.0	-233.0	-0	1.
-	0.1096	545.33	1.669	-0.572	426.6	4.45	500.00	1.02	4.45	4.55	-22	-57	233.0	-233.0	-0	1.
-	0.1097	545.93	1.670	-0.572	426.6	4.45	500.00	1.02	4.45	4.55	-22	-57	233.0	-233.0	-0	1.
-	0.1098	546.33	1.670	-0.572	426.6	4.45	500.00	1.02	4.45	4.55	-22	-57	233.0	-233.0	-0	1.
-	0.1099	546.69	1.672	-0.572	426.6	4.45	500.00	1.02	4.45	4.55	-22	-57	233.0	-233.0	-0	1.

FLECHETTE GROUP POINT

۲۳

318 COPY AVAILABLE TO EDC DOES NOT
PERMIT FULLY LEGIBLE PRODUCTION

FLECHETTE GROUND POINT

PAGE 21

	X	Y	Z	V	FIT SEC	RAD/SEC	DEG	PHS	ALPHA	BETA	GAMMA	L-P	L-S	L-C	P-H	H-T	E-L
0.1150	571.64	-1.711	-0.611	4653.4	512.30	1.673	4.45	46.21	1.071	-0.126	-0.177	23.3	-2331.	-0.1	1.6	-	-
0.1151	572.14	-1.713	-0.612	4653.4	511.30	1.673	4.45	45.16	1.079	-0.233	-0.177	23.0	-2321.	-0.1	1.6	-	-
0.1152	572.63	-1.715	-0.613	4653.4	509.30	1.673	4.45	45.07	1.077	-0.341	-0.177	23.0	-2321.	-0.1	1.6	-	-
0.1153	573.13	-1.714	-0.613	4653.4	508.30	1.673	4.45	45.02	1.077	-0.449	-0.177	23.0	-2321.	-0.1	1.6	-	-
0.1154	573.62	-1.715	-0.614	4653.4	507.30	1.673	4.45	45.03	1.077	-0.557	-0.177	23.0	-2321.	-0.1	1.6	-	-
0.1155	574.12	-1.715	-0.614	4653.4	506.30	1.673	4.45	45.01	1.077	-0.665	-0.177	23.0	-2321.	-0.1	1.6	-	-
0.1156	574.62	-1.722	-0.617	4653.4	505.30	1.673	4.45	45.04	1.077	-0.773	-0.177	23.0	-2321.	-0.1	1.6	-	-
0.1157	575.11	-1.722	-0.613	4653.3	504.30	1.673	4.45	45.05	1.077	-0.881	-0.177	23.0	-2321.	-0.1	1.6	-	-
0.1158	575.61	-1.723	-0.619	4653.3	503.30	1.673	4.45	45.07	1.077	-0.989	-0.177	23.0	-2321.	-0.1	1.6	-	-
0.1159	576.10	-1.728	-0.523	4653.3	502.30	1.674	4.45	45.03	1.077	-1.097	-0.177	23.0	-2321.	-0.1	1.6	-	-
0.1160	576.59	-1.731	-0.624	4653.4	501.30	1.674	4.45	45.01	1.077	-1.205	-0.177	23.0	-2321.	-0.1	1.6	-	-
0.1161	577.09	-1.733	-0.525	4653.2	501.30	1.674	4.45	45.03	1.077	-1.313	-0.177	23.0	-2321.	-0.1	1.6	-	-
0.1162	577.59	-1.735	-0.625	4653.2	501.30	1.674	4.45	45.05	1.077	-1.421	-0.177	23.0	-2321.	-0.1	1.6	-	-
0.1163	578.09	-1.735	-0.625	4653.2	501.30	1.674	4.45	45.07	1.077	-1.529	-0.177	23.0	-2321.	-0.1	1.6	-	-
0.1164	578.59	-1.737	-0.627	4653.2	501.30	1.674	4.45	45.03	1.077	-1.637	-0.177	23.0	-2321.	-0.1	1.6	-	-
0.1165	579.09	-1.739	-0.623	4653.2	501.30	1.674	4.45	45.02	1.077	-1.745	-0.177	23.0	-2321.	-0.1	1.6	-	-
0.1166	579.58	-1.741	-0.525	4653.2	501.30	1.674	4.45	45.03	1.077	-1.853	-0.177	23.0	-2321.	-0.1	1.6	-	-
0.1167	580.07	-1.743	-0.629	4653.2	501.30	1.674	4.45	45.01	1.077	-1.961	-0.177	23.0	-2321.	-0.1	1.6	-	-
0.1168	580.57	-1.746	-0.531	4653.2	501.30	1.674	4.45	45.03	1.077	-2.069	-0.177	23.0	-2321.	-0.1	1.6	-	-
0.1169	581.07	-1.747	-0.531	4653.2	501.30	1.674	4.45	45.05	1.077	-2.177	-0.177	23.0	-2321.	-0.1	1.6	-	-
0.1170	581.56	-1.750	-0.632	4653.2	501.30	1.674	4.45	45.07	1.077	-2.285	-0.177	23.0	-2321.	-0.1	1.6	-	-
0.1171	582.06	-1.752	-0.633	4653.2	501.30	1.674	4.45	45.03	1.077	-2.393	-0.177	23.0	-2321.	-0.1	1.6	-	-
0.1172	582.55	-1.754	-0.535	4653.2	501.30	1.674	4.45	45.02	1.077	-2.501	-0.177	23.0	-2321.	-0.1	1.6	-	-
0.1173	583.05	-1.756	-0.535	4653.1	501.30	1.674	4.45	45.03	1.077	-2.609	-0.177	23.0	-2321.	-0.1	1.6	-	-
0.1174	583.55	-1.759	-0.635	4653.1	501.30	1.674	4.45	45.05	1.077	-2.717	-0.177	23.0	-2321.	-0.1	1.6	-	-
0.1175	584.05	-1.761	-0.636	4653.1	501.30	1.674	4.45	45.07	1.077	-2.825	-0.177	23.0	-2321.	-0.1	1.6	-	-
0.1176	584.54	-1.764	-0.632	4653.1	501.30	1.674	4.45	45.03	1.077	-2.933	-0.177	23.0	-2321.	-0.1	1.6	-	-
0.1177	585.03	-1.766	-0.533	4653.1	501.30	1.674	4.45	45.02	1.077	-3.041	-0.177	23.0	-2321.	-0.1	1.6	-	-
0.1178	585.53	-1.769	-0.637	4653.1	501.30	1.674	4.45	45.03	1.077	-3.149	-0.177	23.0	-2321.	-0.1	1.6	-	-
0.1179	586.03	-1.770	-0.533	4653.1	501.30	1.674	4.45	45.05	1.077	-3.257	-0.177	23.0	-2321.	-0.1	1.6	-	-
0.1180	586.52	-1.772	-0.637	4653.1	501.30	1.674	4.45	45.07	1.077	-3.365	-0.177	23.0	-2321.	-0.1	1.6	-	-
0.1181	587.02	-1.774	-0.538	4653.0	501.30	1.674	4.45	45.03	1.077	-3.473	-0.177	23.0	-2321.	-0.1	1.6	-	-
0.1182	587.52	-1.776	-0.633	4653.0	501.30	1.674	4.45	45.02	1.077	-3.581	-0.177	23.0	-2321.	-0.1	1.6	-	-
0.1183	588.02	-1.778	-0.535	4653.0	501.30	1.674	4.45	45.03	1.077	-3.689	-0.177	23.0	-2321.	-0.1	1.6	-	-
0.1184	588.51	-1.780	-0.637	4653.0	501.30	1.674	4.45	45.05	1.077	-3.797	-0.177	23.0	-2321.	-0.1	1.6	-	-
0.1185	589.00	-1.783	-0.537	4653.0	501.30	1.674	4.45	45.07	1.077	-3.905	-0.177	23.0	-2321.	-0.1	1.6	-	-
0.1186	589.50	-1.785	-0.635	4653.0	501.30	1.674	4.45	45.03	1.077	-4.013	-0.177	23.0	-2321.	-0.1	1.6	-	-
0.1187	590.00	-1.787	-0.641	4653.0	501.30	1.674	4.45	45.02	1.077	-4.121	-0.177	23.0	-2321.	-0.1	1.6	-	-
0.1188	590.49	-1.789	-0.541	4653.0	501.30	1.674	4.45	45.03	1.077	-4.229	-0.177	23.0	-2321.	-0.1	1.6	-	-
0.1189	590.97	-1.791	-0.641	4653.0	501.30	1.674	4.45	45.05	1.077	-4.337	-0.177	23.0	-2321.	-0.1	1.6	-	-
0.1190	591.46	-1.793	-0.541	4653.0	501.30	1.674	4.45	45.07	1.077	-4.445	-0.177	23.0	-2321.	-0.1	1.6	-	-
0.1191	591.95	-1.795	-0.641	4653.0	501.30	1.674	4.45	45.03	1.077	-4.553	-0.177	23.0	-2321.	-0.1	1.6	-	-
0.1192	592.44	-1.797	-0.541	4653.0	501.30	1.674	4.45	45.02	1.077	-4.661	-0.177	23.0	-2321.	-0.1	1.6	-	-
0.1193	592.93	-1.799	-0.641	4653.0	501.30	1.674	4.45	45.03	1.077	-4.769	-0.177	23.0	-2321.	-0.1	1.6	-	-
0.1194	593.42	-1.801	-0.541	4653.0	501.30	1.674	4.45	45.05	1.077	-4.877	-0.177	23.0	-2321.	-0.1	1.6	-	-
0.1195	593.91	-1.803	-0.641	4653.0	501.30	1.674	4.45	45.07	1.077	-4.985	-0.177	23.0	-2321.	-0.1	1.6	-	-
0.1196	594.40	-1.805	-0.541	4653.0	501.30	1.674	4.45	45.03	1.077	-5.093	-0.177	23.0	-2321.	-0.1	1.6	-	-
0.1197	594.89	-1.807	-0.641	4653.0	501.30	1.674	4.45	45.02	1.077	-5.201	-0.177	23.0	-2321.	-0.1	1.6	-	-
0.1198	595.38	-1.809	-0.541	4653.0	501.30	1.674	4.45	45.03	1.077	-5.309	-0.177	23.0	-2321.	-0.1	1.6	-	-
0.1199	595.87	-1.811	-0.641	4653.0	501.30	1.674	4.45	45.05	1.077	-5.417	-0.177	23.0	-2321.	-0.1	1.6	-	-
0.1200	596.36	-1.813	-0.541	4653.0	501.30	1.674	4.45	45.07	1.077	-5.525	-0.177	23.0	-2321.	-0.1	1.6	-	-
0.1201	596.85	-1.815	-0.641	4653.0	501.30	1.674	4.45	45.03	1.077	-5.633	-0.177	23.0	-2321.	-0.1	1.6	-	-
0.1202	597.34	-1.817	-0.541	4653.0	501.30	1.674	4.45	45.02	1.077	-5.741	-0.177	23.0	-2321.	-0.1	1.6	-	-
0.1203	597.83	-1.819	-0.641	4653.0	501.30	1.674	4.45	45.03	1.077	-5.849	-0.177	23.0	-2321.	-0.1	1.6	-	-
0.1204	598.32	-1.821	-0.541	4653.0	501.30	1.674	4.45	45.05	1.077	-5.957	-0.177	23.0	-2321.	-0.1	1.6	-	-
0.1205	598.81	-1.823	-0.641	4653.0	501.30	1.674	4.45	45.07	1.077	-6.065	-0.177	23.0	-2321.	-0.1	1.6	-	-
0.1206	599.30	-1.825	-0.541	4653.0	501.30	1.674	4.45	45.03	1.077	-6.173	-0.177	23.0	-2321.	-0.1	1.6	-	-
0.1207	599.79	-1.827	-0.641	4653.0	501.30	1.674	4.45	45.02	1.077	-6.281	-0.177	23.0	-2321.	-0.1	1.6	-	-
0.1208	600.28	-1.829	-0.541	4653.0	501.30	1.674	4.45	45.03	1.077	-6.389	-0.177	23.0	-2321.	-0.1	1.6	-	-
0.1209	600.77	-1.831	-0.641	4653.0	501.30	1.674	4.45	45.05	1.077	-6.497	-0.177	23.0	-2321.	-0.1	1.6	-	-
0.1210	601.26	-1.833	-0.541	4653.0	501.30	1.674	4.45	45.07	1.077	-6.605	-0.177	23.0	-2321.	-0.1	1.6	-	-
0.1211	601.75	-1.835	-0.641	4653.0	501.30	1.674	4.45	45.03	1.077	-6.713	-0.177	23.0	-2321.	-0.1	1.6	-	-
0.1212	602.24	-1.837	-0.541	4653.0	501.30	1.674	4.45	45.02	1.077	-6.821	-0.177	23.0	-2321.	-0.1	1.6	-	-
0.1213	602.73	-1.839	-0.641	4653.0	501.30	1.674	4.45	45.03	1.077	-6.929	-0.177	23.0	-2321.	-0.1	1.6	-	-
0.1214	603.22	-1.841	-0.541	4653.0	501.30	1.674	4.45	45.05	1.077	-7.037	-0.177	23.0	-2321.	-0.1	1.6	-	-
0.1215	603.71	-1.843	-0.641	4653.0	501.30	1.674	4.45										

FIECHETTE GROUND POINT

PAGE 25

	X	Y	Z	V	P	ALPHA	BETA	PHI	U-G	B-G	G-R	R-I	I-J	J-H	H-P	P-T	T-U	U-G
SEC	FT	FT	FT	FT/SEC	FT/SEC	SEC	SEC	SEC	SEC	SEC	SEC	SEC	SEC	SEC	SEC	SEC	SEC	SEC
0.1200	566.44	1.813	-0.541	5952.8	500.00	1.44	4.45	45.51	-1.29	-0.64	-0.55	-0.57	23.36	-2321.	-0.6	0.6	0.6	
0.1201	566.94	1.815	-0.541	5952.8	500.00	1.44	4.45	45.53	-1.12	-0.53	-0.55	-0.57	23.36	-2321.	-0.6	0.6	0.6	
0.1202	567.44	1.817	-0.541	5952.8	500.00	1.44	4.45	45.55	-1.03	-0.51	-0.55	-0.57	23.36	-2321.	-0.6	0.6	0.6	
0.1203	567.93	1.818	-0.540	5952.8	500.00	1.44	4.45	45.58	-1.37	-0.44	-0.55	-0.57	23.36	-2321.	-0.6	0.6	0.6	
0.1204	568.43	1.820	-0.540	5952.8	500.00	1.44	4.45	45.61	-1.30	-0.42	-0.55	-0.57	23.36	-2321.	-0.6	0.6	0.6	
0.1205	568.92	1.822	-0.539	5952.8	500.00	1.44	4.45	45.64	-1.41	-0.31	-0.55	-0.57	23.36	-2321.	-0.6	0.6	0.6	
0.1206	569.42	1.824	-0.539	5952.8	500.00	1.45	4.45	45.67	-1.43	-0.24	-0.55	-0.57	23.36	-2321.	-0.6	0.6	0.6	
0.1207	569.92	1.825	-0.539	5952.8	500.00	1.45	4.45	45.70	-1.44	-0.17	-0.55	-0.57	23.36	-2321.	-0.6	0.6	0.6	
0.1208	600.41	1.827	-0.533	6252.7	510.00	1.45	4.45	45.71	-1.04	-0.17	-0.55	-0.57	23.36	-2321.	-0.6	0.6	0.6	
0.1209	600.61	1.829	-0.530	6252.7	510.00	1.45	4.45	45.71	-1.05	-0.12	-0.55	-0.57	23.36	-2321.	-0.6	0.6	0.6	
0.1210	601.61	1.831	-0.533	6252.7	510.00	1.45	4.45	45.72	-1.35	-0.15	-0.55	-0.57	23.36	-2321.	-0.6	0.6	0.6	
0.1211	601.61	1.831	-0.533	6252.7	510.00	1.45	4.45	45.75	-1.36	-0.12	-0.55	-0.57	23.36	-2321.	-0.6	0.6	0.6	
0.1212	602.50	1.833	-0.533	6252.7	510.00	1.45	4.45	45.76	-1.43	-0.21	-0.55	-0.57	23.36	-2321.	-0.6	0.6	0.6	
0.1213	602.81	1.834	-0.533	6252.7	510.00	1.45	4.45	45.76	-1.42	-0.27	-0.55	-0.57	23.36	-2321.	-0.6	0.6	0.6	
0.1214	603.11	1.835	-0.533	6252.7	510.00	1.45	4.45	45.71	-1.04	-0.17	-0.55	-0.57	23.36	-2321.	-0.6	0.6	0.6	
0.1215	603.59	1.837	-0.530	6252.7	510.00	1.45	4.45	45.71	-1.05	-0.12	-0.55	-0.57	23.36	-2321.	-0.6	0.6	0.6	
0.1216	604.35	1.838	-0.533	6252.7	510.00	1.45	4.45	45.72	-1.35	-0.15	-0.55	-0.57	23.36	-2321.	-0.6	0.6	0.6	
0.1217	604.83	1.840	-0.534	6252.7	510.00	1.45	4.45	45.73	-1.35	-0.12	-0.55	-0.57	23.36	-2321.	-0.6	0.6	0.6	
0.1218	605.37	1.841	-0.534	6242.4	510.00	1.45	4.45	45.73	-1.39	-0.32	-0.55	-0.57	23.36	-2321.	-0.6	0.6	0.6	
0.1219	605.47	1.841	-0.537	6242.4	510.00	1.45	4.45	45.74	-1.43	-0.26	-0.55	-0.57	23.36	-2321.	-0.6	0.6	0.6	
0.1220	605.55	1.843	-0.537	6242.4	510.00	1.45	4.45	45.75	-1.43	-0.25	-0.55	-0.57	23.36	-2321.	-0.6	0.6	0.6	
0.1221	605.55	1.844	-0.537	6242.4	510.00	1.45	4.45	45.75	-1.37	-0.32	-0.55	-0.57	23.36	-2321.	-0.6	0.6	0.6	
0.1222	607.36	1.845	-0.537	6242.4	510.00	1.45	4.45	45.76	-1.43	-0.26	-0.55	-0.57	23.36	-2321.	-0.6	0.6	0.6	
0.1223	607.95	1.846	-0.537	6242.4	510.00	1.45	4.45	45.77	-1.43	-0.25	-0.55	-0.57	23.36	-2321.	-0.6	0.6	0.6	
0.1224	608.35	1.847	-0.537	6242.4	510.00	1.45	4.45	45.77	-1.43	-0.25	-0.55	-0.57	23.36	-2321.	-0.6	0.6	0.6	
0.1225	608.65	1.848	-0.537	6242.4	510.00	1.45	4.45	45.78	-1.43	-0.25	-0.55	-0.57	23.36	-2321.	-0.6	0.6	0.6	
0.1226	609.34	1.849	-0.537	6242.4	510.00	1.45	4.45	45.78	-1.43	-0.25	-0.55	-0.57	23.36	-2321.	-0.6	0.6	0.6	
0.1227	609.64	1.850	-0.537	6242.4	510.00	1.45	4.45	45.79	-1.43	-0.25	-0.55	-0.57	23.36	-2321.	-0.6	0.6	0.6	
0.1228	610.33	1.851	-0.537	6242.4	510.00	1.45	4.45	45.80	-1.43	-0.25	-0.55	-0.57	23.36	-2321.	-0.6	0.6	0.6	
0.1229	610.83	1.851	-0.537	6242.4	510.00	1.45	4.45	45.81	-1.43	-0.25	-0.55	-0.57	23.36	-2321.	-0.6	0.6	0.6	
0.1230	611.33	1.851	-0.537	6242.4	510.00	1.45	4.45	45.81	-1.43	-0.25	-0.55	-0.57	23.36	-2321.	-0.6	0.6	0.6	
0.1231	611.92	1.853	-0.531	6242.4	510.00	1.44	4.45	45.79	-1.37	-0.27	-0.55	-0.57	23.36	-2321.	-0.6	0.6	0.6	
0.1232	612.32	1.853	-0.538	6242.4	510.00	1.44	4.45	45.80	-1.37	-0.27	-0.55	-0.57	23.36	-2321.	-0.6	0.6	0.6	
0.1233	612.82	1.855	-0.535	6242.4	510.00	1.44	4.45	45.81	-1.37	-0.27	-0.55	-0.57	23.36	-2321.	-0.6	0.6	0.6	
0.1234	613.31	1.855	-0.534	6242.4	510.00	1.44	4.45	45.82	-1.37	-0.27	-0.55	-0.57	23.36	-2321.	-0.6	0.6	0.6	
0.1235	613.81	1.856	-0.534	6242.4	510.00	1.44	4.45	45.83	-1.37	-0.27	-0.55	-0.57	23.36	-2321.	-0.6	0.6	0.6	
0.1236	614.30	1.857	-0.534	6242.4	510.00	1.44	4.45	45.84	-1.37	-0.27	-0.55	-0.57	23.36	-2321.	-0.6	0.6	0.6	
0.1237	614.80	1.858	-0.534	6242.4	510.00	1.44	4.45	45.85	-1.37	-0.27	-0.55	-0.57	23.36	-2321.	-0.6	0.6	0.6	
0.1238	615.39	1.858	-0.534	6242.4	510.00	1.44	4.45	45.86	-1.37	-0.27	-0.55	-0.57	23.36	-2321.	-0.6	0.6	0.6	
0.1239	615.89	1.859	-0.534	6242.4	510.00	1.44	4.45	45.87	-1.37	-0.27	-0.55	-0.57	23.36	-2321.	-0.6	0.6	0.6	
0.1240	616.29	1.860	-0.534	6242.4	510.00	1.44	4.45	45.88	-1.37	-0.27	-0.55	-0.57	23.36	-2321.	-0.6	0.6	0.6	
0.1241	616.79	1.861	-0.534	6242.4	510.00	1.44	4.45	45.89	-1.37	-0.27	-0.55	-0.57	23.36	-2321.	-0.6	0.6	0.6	
0.1242	617.28	1.862	-0.542	6262.4	510.00	1.44	4.45	45.90	-1.37	-0.27	-0.55	-0.57	23.36	-2321.	-0.6	0.6	0.6	
0.1243	617.78	1.863	-0.542	6262.4	510.00	1.44	4.45	45.91	-1.37	-0.27	-0.55	-0.57	23.36	-2321.	-0.6	0.6	0.6	
0.1244	618.27	1.863	-0.543	6262.4	510.00	1.44	4.45	45.92	-1.37	-0.27	-0.55	-0.57	23.36	-2321.	-0.6	0.6	0.6	
0.1245	618.77	1.864	-0.543	6262.4	510.00	1.44	4.45	45.93	-1.37	-0.27	-0.55	-0.57	23.36	-2321.	-0.6	0.6	0.6	
0.1246	619.26	1.865	-0.543	6262.4	510.00	1.44	4.45	45.94	-1.37	-0.27	-0.55	-0.57	23.36	-2321.	-0.6	0.6	0.6	
0.1247	619.76	1.866	-0.543	6262.4	510.00	1.44	4.45	45.95	-1.37	-0.27	-0.55	-0.57	23.36	-2321.	-0.6	0.6	0.6	
0.1248	620.25	1.866	-0.546	6262.4	510.00	1.45	4.45	45.96	-1.37	-0.27	-0.55	-0.57	23.36	-2321.	-0.6	0.6	0.6	
0.1249	620.75	1.867	-0.547	6262.4	510.00	1.45	4.45	45.97	-1.37	-0.27	-0.55	-0.57	23.36	-2321.	-0.6	0.6	0.6	

FLÉCHETTE GROUND PECIINT

PPG 26

321

**COPY AVAILABLE TO LAW ENFORCEMENT
PERMIT FULL LEGAL PRODUCTION**

ELDERCHEMIST GRADING POINT

PAGE 21

322

**COPY AVAILABLE TO REC ECRS NOT
PERMIT FULLY LEGIBLE PRODUCTION**

FLECHETTE GROUND POINT

PAGE 25

	T SEC	X FT	Y FT	Z FT	V FT/SEC	R/SEC	ALPHA SEC	BETA SEC	W FT/SEC	G FT/SEC	L FT/SEC	M FT/SEC	N FT/SEC	O FT/SEC	P FT/SEC	Q FT/SEC	R FT/SEC	S FT/SEC	T FT/SEC	U FT/SEC	V FT/SEC	W FT/SEC	W FT/SEC
0.1350	670.95	2.034	-0.752	4561.2	.500.00	1.34	6.24	1.546	-1.042	6.99	-5.51	21.1	-2322.	-6.0	1.0	-	-	-	-	-	-	-	-
0.1351	671.35	2.035	-0.752	4741.2	.500.00	1.44	6.34	1.542	-1.042	6.94	-5.54	21.1	-2322.	-6.0	1.0	-	-	-	-	-	-	-	-
0.1352	671.65	2.035	-0.752	4941.2	.500.00	1.44	6.44	1.535	-0.976	1.14	-5.54	21.1	-2322.	-6.0	1.0	-	-	-	-	-	-	-	-
0.1353	672.35	2.037	-0.752	4761.1	.500.00	1.44	6.44	1.532	-0.976	1.13	-5.54	21.1	-2322.	-6.0	1.0	-	-	-	-	-	-	-	-
0.1354	672.84	2.038	-0.753	4581.1	.500.00	1.44	6.56	1.532	-0.976	1.13	-5.54	21.1	-2322.	-6.0	1.0	-	-	-	-	-	-	-	-
0.1355	673.34	2.038	-0.753	4661.1	.500.00	1.44	6.64	1.531	-0.975	1.22	-5.54	21.1	-2322.	-6.0	1.0	-	-	-	-	-	-	-	-
0.1356	673.63	2.038	-0.753	4931.1	.500.00	1.44	6.64	1.530	-0.975	1.22	-5.54	21.1	-2322.	-6.0	1.0	-	-	-	-	-	-	-	-
0.1357	674.33	2.041	-0.753	4681.1	.500.00	1.44	6.74	1.531	-0.964	1.23	-5.55	21.1	-2322.	-6.0	1.0	-	-	-	-	-	-	-	-
0.1358	674.93	2.041	-0.753	4761.1	.500.00	1.44	6.74	1.532	-0.957	1.32	-5.55	21.1	-2322.	-6.0	1.0	-	-	-	-	-	-	-	-
0.1359	675.32	2.042	-0.753	4551.1	.500.00	1.44	6.84	1.534	-0.956	1.35	-5.55	21.1	-2322.	-6.0	1.0	-	-	-	-	-	-	-	-
0.1360	675.82	2.043	-0.753	4531.1	.500.00	1.44	6.84	1.537	-0.954	1.37	-5.55	21.1	-2322.	-6.0	1.0	-	-	-	-	-	-	-	-
0.1361	676.32	2.044	-0.753	4761.1	.500.00	1.44	6.94	1.541	-0.937	1.37	-5.55	21.1	-2322.	-6.0	1.0	-	-	-	-	-	-	-	-
0.1362	676.81	2.045	-0.754	4681.1	.500.00	1.44	6.94	1.542	-0.933	1.41	-5.55	21.1	-2322.	-6.0	1.0	-	-	-	-	-	-	-	-
0.1363	677.31	2.045	-0.754	4761.1	.500.00	1.44	6.94	1.543	-0.932	1.42	-5.55	21.1	-2322.	-6.0	1.0	-	-	-	-	-	-	-	-
0.1364	677.90	2.049	-0.754	4831.0	.500.00	1.44	6.94	1.544	-0.915	1.43	-5.55	21.1	-2322.	-6.0	1.0	-	-	-	-	-	-	-	-
0.1365	678.30	2.049	-0.754	4731.0	.500.00	1.44	6.94	1.544	-0.905	1.43	-5.55	21.1	-2322.	-6.0	1.0	-	-	-	-	-	-	-	-
0.1366	678.39	2.049	-0.754	4791.0	.500.00	1.44	6.94	1.544	-0.905	1.43	-5.55	21.1	-2322.	-6.0	1.0	-	-	-	-	-	-	-	-
0.1367	679.29	2.051	-0.754	4511.0	.500.00	1.45	6.94	1.545	-0.905	1.43	-5.55	21.1	-2322.	-6.0	1.0	-	-	-	-	-	-	-	-
0.1368	679.73	2.051	-0.754	4761.0	.500.00	1.45	6.94	1.545	-0.905	1.43	-5.55	21.1	-2322.	-6.0	1.0	-	-	-	-	-	-	-	-
0.1369	680.24	2.052	-0.754	4751.0	.500.00	1.45	6.94	1.545	-0.905	1.43	-5.55	21.1	-2322.	-6.0	1.0	-	-	-	-	-	-	-	-
0.1370	680.73	2.051	-0.754	4761.0	.500.00	1.45	6.94	1.545	-0.905	1.43	-5.55	21.1	-2322.	-6.0	1.0	-	-	-	-	-	-	-	-
0.1371	681.23	2.052	-0.754	4731.0	.500.00	1.45	6.94	1.545	-0.905	1.43	-5.55	21.1	-2322.	-6.0	1.0	-	-	-	-	-	-	-	-
0.1372	681.77	2.052	-0.754	4711.0	.500.00	1.45	6.94	1.545	-0.905	1.43	-5.55	21.1	-2322.	-6.0	1.0	-	-	-	-	-	-	-	-
0.1373	682.27	2.053	-0.754	4761.0	.500.00	1.45	6.94	1.545	-0.905	1.43	-5.55	21.1	-2322.	-6.0	1.0	-	-	-	-	-	-	-	-
0.1374	682.75	2.054	-0.754	4651.0	.500.00	1.45	6.94	1.545	-0.905	1.43	-5.55	21.1	-2322.	-6.0	1.0	-	-	-	-	-	-	-	-
0.1375	683.24	2.055	-0.754	4751.0	.500.00	1.45	6.94	1.545	-0.905	1.43	-5.55	21.1	-2322.	-6.0	1.0	-	-	-	-	-	-	-	-
0.1376	683.73	2.055	-0.754	4761.0	.500.00	1.45	6.94	1.545	-0.905	1.43	-5.55	21.1	-2322.	-6.0	1.0	-	-	-	-	-	-	-	-
0.1377	684.23	2.056	-0.754	4731.0	.500.00	1.45	6.94	1.545	-0.905	1.43	-5.55	21.1	-2322.	-6.0	1.0	-	-	-	-	-	-	-	-
0.1378	684.75	2.056	-0.754	4711.0	.500.00	1.45	6.94	1.545	-0.905	1.43	-5.55	21.1	-2322.	-6.0	1.0	-	-	-	-	-	-	-	-
0.1379	685.21	2.056	-0.754	4761.0	.500.00	1.45	6.94	1.545	-0.905	1.43	-5.55	21.1	-2322.	-6.0	1.0	-	-	-	-	-	-	-	-
0.1380	685.74	2.056	-0.754	4751.0	.500.00	1.45	6.94	1.545	-0.905	1.43	-5.55	21.1	-2322.	-6.0	1.0	-	-	-	-	-	-	-	-
0.1381	686.23	2.056	-0.754	4761.0	.500.00	1.45	6.94	1.545	-0.905	1.43	-5.55	21.1	-2322.	-6.0	1.0	-	-	-	-	-	-	-	-
0.1382	686.73	2.057	-0.754	4651.0	.500.00	1.45	6.94	1.545	-0.905	1.43	-5.55	21.1	-2322.	-6.0	1.0	-	-	-	-	-	-	-	-
0.1383	687.23	2.057	-0.754	4621.0	.500.00	1.45	6.94	1.545	-0.905	1.43	-5.55	21.1	-2322.	-6.0	1.0	-	-	-	-	-	-	-	-
0.1384	687.72	2.058	-0.754	4721.0	.500.00	1.45	6.94	1.545	-0.905	1.43	-5.55	21.1	-2322.	-6.0	1.0	-	-	-	-	-	-	-	-
0.1385	688.22	2.058	-0.754	4711.0	.500.00	1.45	6.94	1.545	-0.905	1.43	-5.55	21.1	-2322.	-6.0	1.0	-	-	-	-	-	-	-	-
0.1386	688.71	2.059	-0.754	4761.0	.500.00	1.45	6.94	1.545	-0.905	1.43	-5.55	21.1	-2322.	-6.0	1.0	-	-	-	-	-	-	-	-
0.1387	689.21	2.059	-0.754	4651.0	.500.00	1.45	6.94	1.545	-0.905	1.43	-5.55	21.1	-2322.	-6.0	1.0	-	-	-	-	-	-	-	-
0.1388	689.71	2.059	-0.754	4621.0	.500.00	1.45	6.94	1.545	-0.905	1.43	-5.55	21.1	-2322.	-6.0	1.0	-	-	-	-	-	-	-	-
0.1389	690.20	2.059	-0.754	4591.0	.500.00	1.45	6.94	1.545	-0.905	1.43	-5.55	21.1	-2322.	-6.0	1.0	-	-	-	-	-	-	-	-
0.1390	690.68	2.059	-0.754	4551.0	.500.00	1.45	6.94	1.545	-0.905	1.43	-5.55	21.1	-2322.	-6.0	1.0	-	-	-	-	-	-	-	-
0.1391	691.18	2.059	-0.754	4521.0	.500.00	1.45	6.94	1.545	-0.905	1.43	-5.55	21.1	-2322.	-6.0	1.0	-	-	-	-	-	-	-	-
0.1392	691.68	2.059	-0.754	4501.0	.500.00	1.45	6.94	1.545	-0.905	1.43	-5.55	21.1	-2322.	-6.0	1.0	-	-	-	-	-	-	-	-
0.1393	692.18	2.059	-0.754	4461.0	.500.00	1.45	6.94	1.545	-0.905	1.43	-5.55	21.1	-2322.	-6.0	1.0	-	-	-	-	-	-	-	-
0.1394	692.68	2.059	-0.754	4431.0	.500.00	1.45	6.94	1.545	-0.905	1.43	-5.55	21.1	-2322.	-6.0	1.0	-	-	-	-	-	-	-	-
0.1395	693.18	2.059	-0.754	4401.0	.500.00	1.45	6.94	1.545	-0.905	1.43	-5.55	21.1	-2322.	-6.0	1.0	-	-	-	-	-	-	-	-
0.1396	693.67	2.059	-0.754	4371.0	.500.00	1.45	6.94	1.545	-0.905	1.43	-5.55	21.1	-2322.	-6.0	1.0	-	-	-	-	-	-	-	-
0.1397	694.16	2.059	-0.754	4341.0	.500.00	1.45	6.94	1.545	-0.905	1.43	-5.55	21.1	-2322.	-6.0	1.0	-	-	-	-	-	-	-	-
0.1398	694.66	2.059	-0.754	4311.0	.500.00	1.45	6.94	1.545	-0.905	1.43	-5.55	21.1	-2322.	-6.0	1.0	-	-	-	-	-	-	-	-
0.1399	695.16	2.059	-0.754	4281.0	.500.00	1.45	6.94	1.545	-0.905	1.43	-5.55	21.1	-2322.	-6.0	1.0	-	-	-	-	-	-	-	-

PRINT FULL PAGE
PRINT FULL PAGE
PRINT FULL PAGE

FLECHETTE GROUND POINT

PAGE 25

T	X	Y	Z	L	V	FITSES	PADSEC	ALPHA	MACH	PHI	BETA	L-H	L-P	R-H	R-P	S-TAYL	K-T
SFC	FT	FT	FT	FT	FT	SEC	SEC	DEC	DEC	DEC	DEC	SEC	SEC	SEC	SEC	SEC	SEC
0.1410	695.66	2.024	-6.740	4.915	4.915	4.44	4.44	45.43	45.43	-0.17	-0.17	0.0	0.0	-0.0	-0.0	-0.0	-0.0
2.1401	695.65	2.035	-6.741	4.916	4.916	4.44	4.44	45.44	45.44	-0.17	-0.17	0.0	0.0	-0.0	-0.0	-0.0	-0.0
0.1402	695.65	2.047	-6.742	4.916	4.916	4.44	4.44	45.45	45.45	-0.17	-0.17	0.0	0.0	-0.0	-0.0	-0.0	-0.0
0.1403	697.14	2.020	-6.743	4.916	4.916	4.44	4.44	45.46	45.46	-0.17	-0.17	0.0	0.0	-0.0	-0.0	-0.0	-0.0
2.1404	697.14	2.039	-6.743	4.916	4.916	4.44	4.44	45.47	45.47	-0.17	-0.17	0.0	0.0	-0.0	-0.0	-0.0	-0.0
0.1405	699.63	2.022	-6.744	4.916	4.916	4.44	4.44	45.48	45.48	-0.17	-0.17	0.0	0.0	-0.0	-0.0	-0.0	-0.0
2.1406	699.63	2.042	-6.744	4.916	4.916	4.44	4.44	45.49	45.49	-0.17	-0.17	0.0	0.0	-0.0	-0.0	-0.0	-0.0
2.1407	699.63	2.054	-6.745	4.916	4.916	4.44	4.44	45.50	45.50	-0.17	-0.17	0.0	0.0	-0.0	-0.0	-0.0	-0.0
2.1418	735.62	2.057	-6.753	4.916	4.916	4.44	4.44	45.51	45.51	-0.17	-0.17	0.0	0.0	-0.0	-0.0	-0.0	-0.0
2.1409	769.12	2.069	-6.751	4.916	4.916	4.44	4.44	45.52	45.52	-0.17	-0.17	0.0	0.0	-0.0	-0.0	-0.0	-0.0
2.1410	783.61	2.111	-6.752	4.916	4.916	4.44	4.44	45.53	45.53	-0.17	-0.17	0.0	0.0	-0.0	-0.0	-0.0	-0.0
2.1411	783.61	2.113	-6.753	4.916	4.916	4.44	4.44	45.54	45.54	-0.17	-0.17	0.0	0.0	-0.0	-0.0	-0.0	-0.0
2.1412	791.61	2.105	-6.754	4.916	4.916	4.44	4.44	45.55	45.55	-0.17	-0.17	0.0	0.0	-0.0	-0.0	-0.0	-0.0
2.1413	792.10	2.115	-6.755	4.916	4.916	4.44	4.44	45.56	45.56	-0.17	-0.17	0.0	0.0	-0.0	-0.0	-0.0	-0.0
2.1414	792.60	2.119	-6.755	4.916	4.916	4.44	4.44	45.57	45.57	-0.17	-0.17	0.0	0.0	-0.0	-0.0	-0.0	-0.0
2.1415	793.09	2.111	-6.755	4.916	4.916	4.44	4.44	45.58	45.58	-0.17	-0.17	0.0	0.0	-0.0	-0.0	-0.0	-0.0
2.1416	793.59	2.113	-6.756	4.916	4.916	4.44	4.44	45.59	45.59	-0.17	-0.17	0.0	0.0	-0.0	-0.0	-0.0	-0.0
2.1417	793.59	2.115	-6.756	4.916	4.916	4.44	4.44	45.60	45.60	-0.17	-0.17	0.0	0.0	-0.0	-0.0	-0.0	-0.0
2.1418	793.59	2.117	-6.756	4.916	4.916	4.44	4.44	45.61	45.61	-0.17	-0.17	0.0	0.0	-0.0	-0.0	-0.0	-0.0
2.1419	793.59	2.119	-6.756	4.916	4.916	4.44	4.44	45.62	45.62	-0.17	-0.17	0.0	0.0	-0.0	-0.0	-0.0	-0.0
2.1420	795.08	2.115	-6.761	4.916	4.916	4.44	4.44	45.63	45.63	-0.17	-0.17	0.0	0.0	-0.0	-0.0	-0.0	-0.0
2.1421	795.57	2.121	-6.762	4.916	4.916	4.44	4.44	45.64	45.64	-0.17	-0.17	0.0	0.0	-0.0	-0.0	-0.0	-0.0
2.1422	795.56	2.124	-6.763	4.916	4.916	4.44	4.44	45.65	45.65	-0.17	-0.17	0.0	0.0	-0.0	-0.0	-0.0	-0.0
2.1423	795.56	2.126	-6.763	4.916	4.916	4.44	4.44	45.66	45.66	-0.17	-0.17	0.0	0.0	-0.0	-0.0	-0.0	-0.0
2.1424	797.06	2.128	-6.764	4.916	4.916	4.44	4.44	45.67	45.67	-0.17	-0.17	0.0	0.0	-0.0	-0.0	-0.0	-0.0
2.1425	797.06	2.130	-6.764	4.916	4.916	4.44	4.44	45.68	45.68	-0.17	-0.17	0.0	0.0	-0.0	-0.0	-0.0	-0.0
2.1426	798.55	2.132	-6.765	4.916	4.916	4.44	4.44	45.69	45.69	-0.17	-0.17	0.0	0.0	-0.0	-0.0	-0.0	-0.0
2.1427	799.05	2.137	-6.765	4.916	4.916	4.44	4.44	45.70	45.70	-0.17	-0.17	0.0	0.0	-0.0	-0.0	-0.0	-0.0
2.1428	799.55	2.139	-6.766	4.916	4.916	4.44	4.44	45.71	45.71	-0.17	-0.17	0.0	0.0	-0.0	-0.0	-0.0	-0.0
2.1429	799.55	2.141	-6.766	4.916	4.916	4.44	4.44	45.72	45.72	-0.17	-0.17	0.0	0.0	-0.0	-0.0	-0.0	-0.0
2.1430	799.55	2.143	-6.766	4.916	4.916	4.44	4.44	45.73	45.73	-0.17	-0.17	0.0	0.0	-0.0	-0.0	-0.0	-0.0
2.1431	799.55	2.145	-6.766	4.916	4.916	4.44	4.44	45.74	45.74	-0.17	-0.17	0.0	0.0	-0.0	-0.0	-0.0	-0.0
2.1432	799.55	2.147	-6.767	4.916	4.916	4.44	4.44	45.75	45.75	-0.17	-0.17	0.0	0.0	-0.0	-0.0	-0.0	-0.0
2.1433	799.55	2.150	-6.767	4.916	4.916	4.44	4.44	45.76	45.76	-0.17	-0.17	0.0	0.0	-0.0	-0.0	-0.0	-0.0
2.1434	799.55	2.152	-6.768	4.916	4.916	4.44	4.44	45.77	45.77	-0.17	-0.17	0.0	0.0	-0.0	-0.0	-0.0	-0.0
2.1435	799.55	2.154	-6.768	4.916	4.916	4.44	4.44	45.78	45.78	-0.17	-0.17	0.0	0.0	-0.0	-0.0	-0.0	-0.0
2.1436	799.55	2.157	-6.771	4.916	4.916	4.44	4.44	45.79	45.79	-0.17	-0.17	0.0	0.0	-0.0	-0.0	-0.0	-0.0
2.1437	799.55	2.160	-6.771	4.916	4.916	4.44	4.44	45.80	45.80	-0.17	-0.17	0.0	0.0	-0.0	-0.0	-0.0	-0.0
2.1438	799.55	2.162	-6.771	4.916	4.916	4.44	4.44	45.81	45.81	-0.17	-0.17	0.0	0.0	-0.0	-0.0	-0.0	-0.0
2.1439	799.55	2.163	-6.771	4.916	4.916	4.44	4.44	45.82	45.82	-0.17	-0.17	0.0	0.0	-0.0	-0.0	-0.0	-0.0
2.1440	799.55	2.165	-6.772	4.916	4.916	4.44	4.44	45.83	45.83	-0.17	-0.17	0.0	0.0	-0.0	-0.0	-0.0	-0.0
2.1441	799.55	2.167	-6.772	4.916	4.916	4.44	4.44	45.84	45.84	-0.17	-0.17	0.0	0.0	-0.0	-0.0	-0.0	-0.0
2.1442	799.55	2.169	-6.773	4.916	4.916	4.44	4.44	45.85	45.85	-0.17	-0.17	0.0	0.0	-0.0	-0.0	-0.0	-0.0
2.1443	799.55	2.171	-6.773	4.916	4.916	4.44	4.44	45.86	45.86	-0.17	-0.17	0.0	0.0	-0.0	-0.0	-0.0	-0.0
2.1444	799.55	2.173	-6.773	4.916	4.916	4.44	4.44	45.87	45.87	-0.17	-0.17	0.0	0.0	-0.0	-0.0	-0.0	-0.0
2.1445	799.55	2.175	-6.774	4.916	4.916	4.44	4.44	45.88	45.88	-0.17	-0.17	0.0	0.0	-0.0	-0.0	-0.0	-0.0
2.1446	799.55	2.177	-6.774	4.916	4.916	4.44	4.44	45.89	45.89	-0.17	-0.17	0.0	0.0	-0.0	-0.0	-0.0	-0.0
2.1447	799.55	2.179	-6.775	4.916	4.916	4.44	4.44	45.90	45.90	-0.17	-0.17	0.0	0.0	-0.0	-0.0	-0.0	-0.0
2.1448	799.55	2.181	-6.775	4.916	4.916	4.44	4.44	45.91	45.91	-0.17	-0.17	0.0	0.0	-0.0	-0.0	-0.0	-0.0
2.1449	799.55	2.183	-6.776	4.916	4.916	4.44	4.44	45.92	45.92	-0.17	-0.17	0.0	0.0	-0.0	-0.0	-0.0	-0.0

LECHETTE GUNN POINT

三

FLD 325HETTE GROUND COUNT

FLESHETTE GROUND POINT											
T	X	Y	Z	P	ALPHA	BETA	GAMMA	L-N	L-E	L-S	S-JAU
SEC	FT	FT	FT	FT SEC	D-G	D-G	D-G	1/SEC	1/SEC	1/SEC	1/SEC
0.1500	745.24	2.241	-0.777	4955.6	1.44	4.44	4.44	-557.	223.	-233.	-10
0.1501	745.74	2.242	-0.775	4955.6	1.44	4.44	4.44	-557.	213.	-223.	-10
0.1502	746.23	2.243	-0.770	4253.6	500.00	1.44	4.44	-557.	213.	-223.	-10
0.1503	746.73	2.244	-0.772	795.44	500.00	1.44	4.44	-557.	213.	-223.	-10
0.1504	747.22	2.245	-0.769	4955.6	500.00	1.43	4.44	-557.	213.	-223.	-10
0.1505	747.72	2.246	-0.766	500.00	1.43	4.44	4.44	-557.	213.	-223.	-10
0.1506	748.22	2.247	-0.763	4955.6	1.43	4.44	4.44	-557.	213.	-223.	-10
0.1507	748.72	2.248	-0.760	4955.6	1.43	4.44	4.44	-557.	213.	-223.	-10
0.1508	749.21	2.249	-0.757	1259.4	500.00	1.44	4.44	-557.	213.	-223.	-10
0.1509	749.70	2.250	-0.755	250.00	1.44	4.44	4.44	-557.	213.	-223.	-10
0.1510	750.20	2.251	-0.752	4955.6	500.00	1.45	5.52	-557.	213.	-223.	-10
0.1511	750.69	2.251	-0.749	4955.6	500.00	1.45	5.52	-557.	213.	-223.	-10
0.1512	751.19	2.252	-0.746	4955.6	500.00	1.45	5.51	-557.	213.	-223.	-10
0.1513	751.69	2.253	-0.743	4955.6	500.00	1.45	5.51	-557.	213.	-223.	-10
0.1514	752.18	2.254	-0.740	4955.6	500.00	1.45	5.51	-557.	213.	-223.	-10
0.1515	752.68	2.255	-0.737	4955.6	500.00	1.45	5.51	-557.	213.	-223.	-10
0.1516	753.17	2.256	-0.734	4955.6	500.00	1.45	5.51	-557.	213.	-223.	-10
0.1517	753.67	2.257	-0.731	4955.6	500.00	1.45	5.51	-557.	213.	-223.	-10
0.1518	754.17	2.258	-0.728	4955.6	500.00	1.45	5.51	-557.	213.	-223.	-10
0.1519	754.67	2.259	-0.725	4955.6	500.00	1.45	5.51	-557.	213.	-223.	-10
0.1520	755.16	2.260	-0.722	4955.6	500.00	1.45	5.51	-557.	213.	-223.	-10
0.1521	755.65	2.261	-0.719	4955.6	500.00	1.45	5.51	-557.	213.	-223.	-10
0.1522	756.15	2.262	-0.716	4955.6	500.00	1.45	5.51	-557.	213.	-223.	-10
0.1523	756.65	2.263	-0.713	4955.6	500.00	1.45	5.51	-557.	213.	-223.	-10
0.1524	757.14	2.264	-0.710	4955.6	500.00	1.45	5.51	-557.	213.	-223.	-10
0.1525	757.64	2.265	-0.707	4955.6	500.00	1.45	5.51	-557.	213.	-223.	-10
0.1526	758.13	2.266	-0.704	4955.6	500.00	1.45	5.51	-557.	213.	-223.	-10
0.1527	758.63	2.267	-0.701	4955.6	500.00	1.45	5.51	-557.	213.	-223.	-10
0.1528	759.12	2.268	-0.698	4955.6	500.00	1.45	5.51	-557.	213.	-223.	-10
0.1529	759.62	2.269	-0.695	4955.6	500.00	1.45	5.51	-557.	213.	-223.	-10
0.1530	760.12	2.270	-0.692	4955.6	500.00	1.45	5.51	-557.	213.	-223.	-10
0.1531	760.61	2.271	-0.689	4955.6	500.00	1.45	5.51	-557.	213.	-223.	-10
0.1532	761.11	2.272	-0.686	4955.6	500.00	1.45	5.51	-557.	213.	-223.	-10
0.1533	761.60	2.273	-0.683	4955.6	500.00	1.45	5.51	-557.	213.	-223.	-10
0.1534	762.10	2.274	-0.680	4955.6	500.00	1.45	5.51	-557.	213.	-223.	-10
0.1535	762.60	2.275	-0.677	4955.6	500.00	1.45	5.51	-557.	213.	-223.	-10
0.1536	763.10	2.276	-0.674	4955.6	500.00	1.45	5.51	-557.	213.	-223.	-10
0.1537	763.60	2.277	-0.671	4955.6	500.00	1.45	5.51	-557.	213.	-223.	-10
0.1538	764.08	2.278	-0.668	4955.6	500.00	1.45	5.51	-557.	213.	-223.	-10
0.1539	764.58	2.279	-0.665	4955.6	500.00	1.45	5.51	-557.	213.	-223.	-10
0.1540	765.07	2.280	-0.662	4955.6	500.00	1.45	5.51	-557.	213.	-223.	-10
0.1541	765.57	2.281	-0.659	4955.6	500.00	1.45	5.51	-557.	213.	-223.	-10
0.1542	766.07	2.282	-0.656	4955.6	500.00	1.45	5.51	-557.	213.	-223.	-10
0.1543	766.55	2.283	-0.653	4955.6	500.00	1.45	5.51	-557.	213.	-223.	-10
0.1544	767.05	2.284	-0.650	4955.6	500.00	1.45	5.51	-557.	213.	-223.	-10
0.1545	767.55	2.285	-0.647	4955.6	500.00	1.45	5.51	-557.	213.	-223.	-10
0.1546	768.05	2.286	-0.644	4955.6	500.00	1.45	5.51	-557.	213.	-223.	-10
0.1547	768.55	2.287	-0.641	4955.6	500.00	1.45	5.51	-557.	213.	-223.	-10
0.1548	769.05	2.288	-0.638	4955.6	500.00	1.45	5.51	-557.	213.	-223.	-10

ELECHETTE GROUND POINT

PAGE 32

T SEC	X FT	Y FT	Z FT	V FT/SEC	RAD/SEC	ALPHA DEG	BETA DEG	GAMMA DEG	L-P MSEC	M-P MSEC	S-P MSEC	L-T MSEC	M-T MSEC	S-T MSEC
0.1550	770.03	2.319	-0.939	4.6582	549.00	590.30	1.46	6.44	1.33	-1.0	-5.5	2336	-2243	-1
0.1551	770.53	2.329	-0.831	4.6588	549.00	590.30	1.45	6.44	1.25	-1.1	-5.5	2336	-2243	-1
0.1552	771.02	2.332	-0.832	4.6585	549.00	590.30	1.42	6.47	1.13	-1.2	-5.5	2336	-2243	-1
0.1553	771.52	2.325	-0.812	4.6586	549.00	590.30	1.42	6.47	1.12	-1.3	-5.5	2336	-2243	-1
0.1554	772.02	2.327	-0.833	4.6582	549.00	590.30	1.44	6.44	1.05	-1.4	-5.5	2336	-2243	-1
0.1555	772.51	2.329	-0.833	4.6585	549.00	590.30	1.44	6.44	1.05	-1.5	-5.5	2336	-2243	-1
0.1556	773.01	2.331	-0.839	4.6582	549.00	590.30	1.43	6.44	1.02	-1.6	-5.5	2336	-2243	-1
0.1557	773.50	2.313	-0.835	4.6572	549.00	590.30	1.43	6.44	1.02	-1.7	-5.5	2336	-2243	-1
0.1558	774.00	2.336	-0.835	4.6593	549.00	590.30	1.42	6.44	0.98	-1.8	-5.5	2336	-2243	-1
0.1559	774.50	2.336	-0.835	4.6586	549.00	590.30	1.42	6.44	0.98	-1.9	-5.5	2336	-2243	-1
0.1560	774.99	2.340	-0.835	4.6586	549.00	590.30	1.42	6.44	0.98	-2.0	-5.5	2336	-2243	-1
0.1561	775.49	2.332	-0.831	4.6585	549.00	590.30	1.42	6.44	0.95	-2.1	-5.5	2336	-2243	-1
0.1562	775.99	2.334	-0.836	4.6582	549.00	590.30	1.42	6.44	0.95	-2.2	-5.5	2336	-2243	-1
0.1563	776.49	2.367	-0.836	4.6582	549.00	590.30	1.42	6.44	0.92	-2.3	-5.5	2336	-2243	-1
0.1564	776.97	2.336	-0.837	4.6586	549.00	590.30	1.42	6.44	0.92	-2.4	-5.5	2336	-2243	-1
0.1565	777.47	2.331	-0.837	4.6582	549.00	590.30	1.42	6.44	0.92	-2.5	-5.5	2336	-2243	-1
0.1566	777.97	2.353	-0.837	4.6582	549.00	590.30	1.42	6.44	0.92	-2.6	-5.5	2336	-2243	-1
0.1567	778.46	2.335	-0.837	4.6586	549.00	590.30	1.42	6.44	0.92	-2.7	-5.5	2336	-2243	-1
0.1568	778.96	2.354	-0.837	4.6582	549.00	590.30	1.42	6.44	0.92	-2.8	-5.5	2336	-2243	-1
0.1569	779.45	2.336	-0.837	4.6586	549.00	590.30	1.42	6.44	0.92	-2.9	-5.5	2336	-2243	-1
0.1570	779.95	2.331	-0.837	4.6582	549.00	590.30	1.42	6.44	0.92	-3.0	-5.5	2336	-2243	-1
0.1571	780.45	2.336	-0.837	4.6586	549.00	590.30	1.42	6.44	0.92	-3.1	-5.5	2336	-2243	-1
0.1572	780.94	2.326	-0.837	4.6582	549.00	590.30	1.42	6.44	0.92	-3.2	-5.5	2336	-2243	-1
0.1573	781.44	2.334	-0.837	4.6586	549.00	590.30	1.42	6.44	0.92	-3.3	-5.5	2336	-2243	-1
0.1574	781.93	2.357	-0.837	4.6582	549.00	590.30	1.42	6.44	0.92	-3.4	-5.5	2336	-2243	-1
0.1575	782.43	2.336	-0.837	4.6586	549.00	590.30	1.42	6.44	0.92	-3.5	-5.5	2336	-2243	-1
0.1576	782.93	2.371	-0.837	4.6582	549.00	590.30	1.42	6.44	0.92	-3.6	-5.5	2336	-2243	-1
0.1577	783.42	2.373	-0.837	4.6586	549.00	590.30	1.42	6.44	0.92	-3.7	-5.5	2336	-2243	-1
0.1578	783.92	2.375	-0.837	4.6582	549.00	590.30	1.42	6.44	0.92	-3.8	-5.5	2336	-2243	-1
0.1579	784.42	2.375	-0.837	4.6586	549.00	590.30	1.42	6.44	0.92	-3.9	-5.5	2336	-2243	-1
0.1580	784.92	2.376	-0.837	4.6582	549.00	590.30	1.42	6.44	0.92	-4.0	-5.5	2336	-2243	-1
0.1581	785.42	2.376	-0.837	4.6586	549.00	590.30	1.42	6.44	0.92	-4.1	-5.5	2336	-2243	-1
0.1582	785.91	2.375	-0.837	4.6582	549.00	590.30	1.42	6.44	0.92	-4.2	-5.5	2336	-2243	-1
0.1583	786.41	2.376	-0.837	4.6586	549.00	590.30	1.42	6.44	0.92	-4.3	-5.5	2336	-2243	-1
0.1584	786.91	2.376	-0.837	4.6582	549.00	590.30	1.42	6.44	0.92	-4.4	-5.5	2336	-2243	-1
0.1585	787.41	2.376	-0.837	4.6586	549.00	590.30	1.42	6.44	0.92	-4.5	-5.5	2336	-2243	-1
0.1586	787.91	2.376	-0.837	4.6582	549.00	590.30	1.42	6.44	0.92	-4.6	-5.5	2336	-2243	-1
0.1587	788.41	2.376	-0.837	4.6586	549.00	590.30	1.42	6.44	0.92	-4.7	-5.5	2336	-2243	-1
0.1588	788.91	2.376	-0.837	4.6582	549.00	590.30	1.42	6.44	0.92	-4.8	-5.5	2336	-2243	-1
0.1589	789.41	2.376	-0.837	4.6586	549.00	590.30	1.42	6.44	0.92	-4.9	-5.5	2336	-2243	-1
0.1590	790.36	2.376	-0.837	4.6582	549.00	590.30	1.42	6.44	0.92	-5.0	-5.5	2336	-2243	-1
0.1591	790.86	2.376	-0.837	4.6586	549.00	590.30	1.42	6.44	0.92	-5.1	-5.5	2336	-2243	-1
0.1592	791.36	2.376	-0.837	4.6582	549.00	590.30	1.42	6.44	0.92	-5.2	-5.5	2336	-2243	-1
0.1593	791.86	2.376	-0.837	4.6586	549.00	590.30	1.42	6.44	0.92	-5.3	-5.5	2336	-2243	-1
0.1594	792.36	2.376	-0.837	4.6582	549.00	590.30	1.42	6.44	0.92	-5.4	-5.5	2336	-2243	-1
0.1595	792.86	2.376	-0.837	4.6586	549.00	590.30	1.42	6.44	0.92	-5.5	-5.5	2336	-2243	-1
0.1596	793.36	2.376	-0.837	4.6582	549.00	590.30	1.42	6.44	0.92	-5.6	-5.5	2336	-2243	-1
0.1597	793.86	2.376	-0.837	4.6586	549.00	590.30	1.42	6.44	0.92	-5.7	-5.5	2336	-2243	-1
0.1598	794.36	2.376	-0.837	4.6582	549.00	590.30	1.42	6.44	0.92	-5.8	-5.5	2336	-2243	-1
0.1599	794.86	2.376	-0.837	4.6586	549.00	590.30	1.42	6.44	0.92	-5.9	-5.5	2336	-2243	-1

ELLECHETTE GAGNON PATRIT

PAGEL

T	X	Y	Z	V	P			ALPHA MATCH			PHI			KUTA			L-P			L-TAU		
					FT	FT/SEC	FT/SEC	DEG	DEG	DEG	DEG	DEG	DEG	DEG	DEG	DEG	DEG	DEG	DEG	DEG	DEG	DEG
SEC	SEC	SEC	SEC	SEC	0.1650	915.60	2.655	-0.869	4957.7	510.00	1.644	2.44	45.91	1.63	-0.013	-0.95	0.77	2.33	-0.8	-0.	-0.	-0.
0.1650	920.50	2.657	-0.976	4957.7	510.00	1.644	2.44	45.91	1.63	-0.115	-0.53	0.77	2.33	-0.73	-0.1	-0.1	-0.	-0.	-0.	-0.	-0.	
0.1652	820.55	2.459	-0.871	1957.0	510.00	1.644	2.44	45.91	1.62	-0.22	-0.22	0.77	2.33	-0.73	-0.6	-0.	-0.	-0.	-0.	-0.	-0.	
0.1654	821.05	2.460	-0.373	4957.7	510.00	1.644	2.44	45.91	1.61	-0.23	-0.23	0.77	2.33	-0.73	-0.6	-0.	-0.	-0.	-0.	-0.	-0.	
0.1654	821.50	2.462	-0.474	4957.7	510.00	1.644	2.44	45.91	1.60	-0.34	-0.34	0.77	2.33	-0.73	-0.6	-0.	-0.	-0.	-0.	-0.	-0.	
0.1655	822.00	2.461	-0.875	4957.7	510.00	1.644	2.44	45.91	1.59	-0.43	-0.43	0.77	2.33	-0.73	-0.6	-0.	-0.	-0.	-0.	-0.	-0.	
0.1655	822.50	2.464	-0.876	4957.7	510.00	1.644	2.44	45.91	1.58	-0.50	-0.50	0.77	2.33	-0.73	-0.6	-0.	-0.	-0.	-0.	-0.	-0.	
0.1657	823.07	2.467	-0.374	4957.7	510.00	1.644	2.44	45.91	1.57	-0.57	-0.57	0.77	2.33	-0.73	-0.6	-0.	-0.	-0.	-0.	-0.	-0.	
0.1658	823.57	2.469	-0.379	4957.7	510.00	1.644	2.44	45.91	1.56	-0.59	-0.59	0.77	2.33	-0.73	-0.6	-0.	-0.	-0.	-0.	-0.	-0.	
0.1658	824.05	2.471	-0.843	4957.7	510.00	1.644	2.44	45.91	1.55	-0.62	-0.62	0.77	2.33	-0.73	-0.6	-0.	-0.	-0.	-0.	-0.	-0.	
0.1660	824.56	2.473	-0.581	4957.7	510.00	1.644	2.44	45.91	1.54	-0.74	-0.74	0.77	2.33	-0.73	-0.6	-0.	-0.	-0.	-0.	-0.	-0.	
0.1661	825.05	2.475	-0.982	4957.7	510.00	1.644	2.44	45.91	1.53	-0.87	-0.87	0.77	2.33	-0.73	-0.6	-0.	-0.	-0.	-0.	-0.	-0.	
0.1662	825.55	2.477	-0.383	4957.7	510.00	1.644	2.44	45.91	1.52	-0.97	-0.97	0.77	2.33	-0.73	-0.6	-0.	-0.	-0.	-0.	-0.	-0.	
0.1663	826.05	2.479	-0.384	4957.7	510.00	1.644	2.44	45.91	1.51	-1.07	-1.07	0.77	2.33	-0.73	-0.6	-0.	-0.	-0.	-0.	-0.	-0.	
0.1664	826.50	2.480	-0.345	4957.7	510.00	1.644	2.44	45.91	1.50	-1.17	-1.17	0.77	2.33	-0.73	-0.6	-0.	-0.	-0.	-0.	-0.	-0.	
0.1665	827.03	2.482	-0.236	4957.7	510.00	1.644	2.44	45.91	1.49	-1.27	-1.27	0.77	2.33	-0.73	-0.6	-0.	-0.	-0.	-0.	-0.	-0.	
0.1666	827.53	2.485	-0.887	4957.7	510.00	1.644	2.44	45.91	1.48	-1.37	-1.37	0.77	2.33	-0.73	-0.6	-0.	-0.	-0.	-0.	-0.	-0.	
0.1667	828.03	2.487	-0.934	4957.7	510.00	1.644	2.44	45.91	1.47	-1.47	-1.47	0.77	2.33	-0.73	-0.6	-0.	-0.	-0.	-0.	-0.	-0.	
0.1668	828.52	2.489	-0.232	4957.7	510.00	1.644	2.44	45.91	1.46	-1.57	-1.57	0.77	2.33	-0.73	-0.6	-0.	-0.	-0.	-0.	-0.	-0.	
0.1669	829.02	2.491	-0.340	4957.7	510.00	1.644	2.44	45.91	1.45	-1.67	-1.67	0.77	2.33	-0.73	-0.6	-0.	-0.	-0.	-0.	-0.	-0.	
0.1670	829.51	2.493	-0.231	4957.7	510.00	1.644	2.44	45.91	1.44	-1.77	-1.77	0.77	2.33	-0.73	-0.6	-0.	-0.	-0.	-0.	-0.	-0.	
0.1671	830.01	2.495	-0.532	4957.7	510.00	1.644	2.44	45.91	1.43	-1.87	-1.87	0.77	2.33	-0.73	-0.6	-0.	-0.	-0.	-0.	-0.	-0.	
0.1672	830.50	2.497	-0.633	4957.7	510.00	1.644	2.44	45.91	1.42	-1.97	-1.97	0.77	2.33	-0.73	-0.6	-0.	-0.	-0.	-0.	-0.	-0.	
0.1673	831.00	2.499	-0.934	4957.7	510.00	1.644	2.44	45.91	1.41	-2.07	-2.07	0.77	2.33	-0.73	-0.6	-0.	-0.	-0.	-0.	-0.	-0.	
0.1674	831.50	2.501	-0.334	4957.7	510.00	1.644	2.44	45.91	1.40	-2.17	-2.17	0.77	2.33	-0.73	-0.6	-0.	-0.	-0.	-0.	-0.	-0.	
0.1675	831.93	2.504	-0.935	4957.7	510.00	1.644	2.44	45.91	1.39	-2.27	-2.27	0.77	2.33	-0.73	-0.6	-0.	-0.	-0.	-0.	-0.	-0.	
0.1676	832.46	2.505	-0.869	4957.7	510.00	1.644	2.44	45.91	1.38	-2.37	-2.37	0.77	2.33	-0.73	-0.6	-0.	-0.	-0.	-0.	-0.	-0.	
0.1677	832.96	2.507	-0.532	4957.7	510.00	1.644	2.44	45.91	1.37	-2.47	-2.47	0.77	2.33	-0.73	-0.6	-0.	-0.	-0.	-0.	-0.	-0.	
0.1678	833.46	2.510	-1.937	4957.7	510.00	1.644	2.44	45.91	1.36	-2.57	-2.57	0.77	2.33	-0.73	-0.6	-0.	-0.	-0.	-0.	-0.	-0.	
0.1679	833.97	2.512	-0.360	4957.7	510.00	1.644	2.44	45.91	1.35	-2.67	-2.67	0.77	2.33	-0.73	-0.6	-0.	-0.	-0.	-0.	-0.	-0.	
0.1680	834.47	2.515	-0.243	4957.7	510.00	1.644	2.44	45.91	1.34	-2.77	-2.77	0.77	2.33	-0.73	-0.6	-0.	-0.	-0.	-0.	-0.	-0.	
0.1681	834.96	2.517	-0.934	4957.7	510.00	1.644	2.44	45.91	1.33	-2.87	-2.87	0.77	2.33	-0.73	-0.6	-0.	-0.	-0.	-0.	-0.	-0.	
0.1682	835.46	2.518	-0.865	4957.7	510.00	1.644	2.44	45.91	1.32	-2.97	-2.97	0.77	2.33	-0.73	-0.6	-0.	-0.	-0.	-0.	-0.	-0.	
0.1683	835.96	2.521	-0.560	4957.7	510.00	1.644	2.44	45.91	1.31	-3.07	-3.07	0.77	2.33	-0.73	-0.6	-0.	-0.	-0.	-0.	-0.	-0.	
0.1684	836.45	2.523	-0.370	4957.7	510.00	1.644	2.44	45.91	1.30	-3.17	-3.17	0.77	2.33	-0.73	-0.6	-0.	-0.	-0.	-0.	-0.	-0.	
0.1685	836.95	2.526	-0.561	4957.7	510.00	1.644	2.44	45.91	1.29	-3.27	-3.27	0.77	2.33	-0.73	-0.6	-0.	-0.	-0.	-0.	-0.	-0.	
0.1686	837.45	2.528	-0.931	4957.7	510.00	1.644	2.44	45.91	1.28	-3.37	-3.37	0.77	2.33	-0.73	-0.6	-0.	-0.	-0.	-0.	-0.	-0.	
0.1687	837.96	2.530	-0.434	4957.7	510.00	1.644	2.44	45.91	1.27	-3.47	-3.47	0.77	2.33	-0.73	-0.6	-0.	-0.	-0.	-0.	-0.	-0.	
0.1688	840.91	2.532	-0.231	4957.7	510.00	1.644	2.44	45.91	1.26	-3.57	-3.57	0.77	2.33	-0.73	-0.6	-0.	-0.	-0.	-0.	-0.	-0.	
0.1689	841.41	2.534	-0.192	4957.7	510.00	1.644	2.44	45.91	1.25	-3.67	-3.67	0.77	2.33	-0.73	-0.6	-0.	-0.	-0.	-0.	-0.	-0.	
0.1690	841.90	2.537	-0.291	4957.7	510.00	1.644	2.44	45.91	1.24	-3.77	-3.77	0.77	2.33	-0.73	-0.6	-0.	-0.	-0.	-0.	-0.	-0.	
0.1691	842.40	2.540	-0.602	4957.7	510.00	1.644	2.44	45.91	1.23	-3.87	-3.87	0.77	2.33	-0.73	-0.6	-0.	-0.	-0.	-0.	-0.	-0.	
0.1692	842.89	2.541	-0.342	4957.7	510.00	1.644	2.44	45.91	1.22	-3.97	-3.97	0.77	2.33	-0.73	-0.6	-0.	-0.	-0.	-0.	-0.	-0.	
0.1693	843.39	2.545	-0.902	4957.7	510.00	1.644	2.44	45.91	1.21	-4.07	-4.07	0.77	2.33	-0.73	-0.6	-0.	-0.	-0.	-0.	-0.	-0.	
0.1694	843.89	2.546	-0.502	4957.7	510.00	1.644	2.44	45.91	1.20	-4.17	-4.17	0.77	2.33	-0.73	-0.6	-0.	-0.	-0.	-0.	-0.	-0.	
0.1695	844.39	2.548	-0.202	4957.7	510.00	1.644	2.44	45.91	1.19	-4.27	-4.27	0.77	2.33	-0.73	-0.6	-0.	-0.	-0.	-0.	-0.	-0.	
0.1696	844.89	2.551	-0.802	4957.7	510.00	1.644	2.44	45.91	1.18	-4.37	-4.37	0.77	2.33	-0.73	-0.6	-0.	-0.	-0.	-0.	-0.	-0.	
0.1697	845.39	2.555	-0.402	4957.7	510.00	1.644	2.44	45.91	1.17	-4.47	-4.47	0.77	2.33	-0.73	-0.6	-0.	-0.	-0.	-0.	-0.	-0.	
0.1698	846.89	2.556	-0.102	4957.7	510.00	1.644	2.44	45.91	1.16	-4.57	-4.57	0.77	2.33	-0.73	-0.6	-0.	-0.	-0.	-0.	-0.	-0.	

329

**COPY AVAILABLE TO B&W STUDIOS
PERMIT FULLY LEGIBLE PRODUCTION**

FCHETTE ET AL.

331

**COPY AVAILABLE TO LEG LEGS NOT
PERMIT FULLY LEGIBLE PRODUCTION**

FLECHETTE GROUND POINT

PAGE 37

T SEC	X FT	Y FT	Z FT	V FT SEC	P FT SEC	ALPHA DEG	DELTA DEG	LNU SEC	LNU SEC	WNU SEC	WNU SEC	PAI SEC	PAI SEC	DIS FT
0.1756	893.94	2.689	-0.560	4.955.9	500.00	1.63	6.44	23.97	1.37	1.42	-1.37	-57.	2337	-2.34
0.1810	894.00	2.651	-0.561	4.955.9	500.00	1.43	6.44	25.47	0.35	1.38	-1.35	-57.	2337	-2.34
0.1821	894.03	2.653	-0.561	4.955.9	500.00	1.43	6.44	25.47	0.22	1.42	-1.42	-57.	2337	-2.34
0.1822	894.02	2.653	-0.562	4.955.9	500.00	1.43	6.44	25.47	0.21	1.42	-1.42	-57.	2337	-2.34
0.1803	895.92	2.538	-0.983	4.955.9	500.00	1.63	4.44	45.45	2.14	1.42	-1.42	-57.	2337	-2.34
0.1804	895.92	2.769	-0.982	4.955.9	500.00	1.63	4.44	45.45	2.14	1.42	-1.42	-57.	2337	-2.34
0.1805	895.91	2.732	-0.982	4.955.9	500.00	1.63	4.44	45.45	2.17	1.42	-1.42	-57.	2337	-2.34
0.1806	897.41	2.735	-0.982	4.955.9	500.00	1.63	4.44	45.45	2.17	1.42	-1.42	-57.	2337	-2.34
0.1807	897.40	2.737	-0.982	4.955.9	500.00	1.63	4.44	45.45	2.17	1.42	-1.42	-57.	2337	-2.34
0.1808	898.93	2.707	-0.985	4.955.9	500.00	1.63	4.44	45.45	2.15	1.42	-1.42	-57.	2337	-2.34
0.1809	898.93	2.711	-0.985	4.955.9	500.00	1.63	4.44	45.45	2.15	1.42	-1.42	-57.	2337	-2.34
0.1810	899.88	2.713	-0.985	4.955.9	500.00	1.63	4.44	45.45	2.15	1.42	-1.42	-57.	2337	-2.34
0.1811	899.88	2.715	-0.985	4.955.9	500.00	1.63	4.44	45.45	2.15	1.42	-1.42	-57.	2337	-2.34
0.1812	899.88	2.718	-0.986	4.955.9	500.00	1.63	4.44	45.45	2.15	1.42	-1.42	-57.	2337	-2.34
0.1813	899.88	2.720	-0.987	4.955.9	500.00	1.63	4.44	45.45	2.15	1.42	-1.42	-57.	2337	-2.34
0.1814	901.95	2.722	-0.987	4.955.9	500.00	1.63	4.44	45.45	2.15	1.42	-1.42	-57.	2337	-2.34
0.1815	902.36	2.724	-0.987	4.955.9	500.00	1.63	4.44	45.45	2.15	1.42	-1.42	-57.	2337	-2.34
0.1816	902.65	2.726	-0.987	4.955.9	500.00	1.63	4.44	45.45	2.15	1.42	-1.42	-57.	2337	-2.34
0.1817	902.65	2.728	-0.987	4.955.9	500.00	1.63	4.44	45.45	2.15	1.42	-1.42	-57.	2337	-2.34
0.1818	903.35	2.730	-0.987	4.955.9	500.00	1.63	4.44	45.45	2.15	1.42	-1.42	-57.	2337	-2.34
0.1819	903.85	2.732	-0.988	4.955.9	500.00	1.63	4.44	45.45	2.15	1.42	-1.42	-57.	2337	-2.34
0.1820	904.34	2.734	-0.988	4.955.9	500.00	1.63	4.44	45.45	2.15	1.42	-1.42	-57.	2337	-2.34
0.1821	904.84	2.736	-0.988	4.955.9	500.00	1.63	4.44	45.45	2.15	1.42	-1.42	-57.	2337	-2.34
0.1822	905.32	2.738	-0.988	4.955.9	500.00	1.63	4.44	45.45	2.15	1.42	-1.42	-57.	2337	-2.34
0.1823	905.83	2.740	-0.989	4.955.9	500.00	1.63	4.44	45.45	2.15	1.42	-1.42	-57.	2337	-2.34
0.1824	906.32	2.742	-0.989	4.955.9	500.00	1.63	4.44	45.45	2.15	1.42	-1.42	-57.	2337	-2.34
0.1825	906.82	2.744	-0.987	4.955.9	500.00	1.63	4.44	45.45	2.15	1.42	-1.42	-57.	2337	-2.34
0.1826	907.31	2.746	-0.987	4.955.9	500.00	1.63	4.44	45.45	2.15	1.42	-1.42	-57.	2337	-2.34
0.1827	907.21	2.748	-0.987	4.955.9	500.00	1.63	4.44	45.45	2.15	1.42	-1.42	-57.	2337	-2.34
0.1828	907.20	2.750	-0.987	4.955.9	500.00	1.63	4.44	45.45	2.15	1.42	-1.42	-57.	2337	-2.34
0.1829	907.20	2.752	-0.987	4.955.9	500.00	1.63	4.44	45.45	2.15	1.42	-1.42	-57.	2337	-2.34
0.1830	907.20	2.754	-0.987	4.955.9	500.00	1.63	4.44	45.45	2.15	1.42	-1.42	-57.	2337	-2.34
0.1831	907.20	2.756	-0.987	4.955.9	500.00	1.63	4.44	45.45	2.15	1.42	-1.42	-57.	2337	-2.34
0.1832	910.23	2.757	-0.988	4.955.9	500.00	1.63	4.44	45.45	2.15	1.42	-1.42	-57.	2337	-2.34
0.1833	910.78	2.759	-0.988	4.955.9	500.00	1.63	4.44	45.45	2.15	1.42	-1.42	-57.	2337	-2.34
0.1834	911.30	2.761	-0.988	4.955.9	500.00	1.63	4.44	45.45	2.15	1.42	-1.42	-57.	2337	-2.34
0.1835	911.30	2.763	-0.988	4.955.9	500.00	1.63	4.44	45.45	2.15	1.42	-1.42	-57.	2337	-2.34
0.1836	911.27	2.764	-0.987	4.955.9	500.00	1.63	4.44	45.45	2.15	1.42	-1.42	-57.	2337	-2.34
0.1837	912.27	2.765	-0.985	4.955.9	500.00	1.63	4.44	45.45	2.15	1.42	-1.42	-57.	2337	-2.34
0.1838	912.27	2.766	-0.985	4.955.9	500.00	1.63	4.44	45.45	2.15	1.42	-1.42	-57.	2337	-2.34
0.1839	912.75	2.767	-0.985	4.955.9	500.00	1.63	4.44	45.45	2.15	1.42	-1.42	-57.	2337	-2.34
0.1840	912.75	2.769	-0.985	4.955.9	500.00	1.63	4.44	45.45	2.15	1.42	-1.42	-57.	2337	-2.34
0.1841	914.74	2.770	-0.985	4.955.9	500.00	1.63	4.44	45.45	2.15	1.42	-1.42	-57.	2337	-2.34
0.1842	915.24	2.771	-0.985	4.955.9	500.00	1.63	4.44	45.45	2.15	1.42	-1.42	-57.	2337	-2.34
0.1843	915.73	2.773	-0.984	4.955.9	500.00	1.63	4.44	45.45	2.15	1.42	-1.42	-57.	2337	-2.34
0.1844	915.23	2.774	-0.984	4.955.9	500.00	1.63	4.44	45.45	2.15	1.42	-1.42	-57.	2337	-2.34
0.1845	916.72	2.775	-0.984	4.955.9	500.00	1.63	4.44	45.45	2.15	1.42	-1.42	-57.	2337	-2.34
0.1846	917.22	2.776	-0.984	4.955.9	500.00	1.63	4.44	45.45	2.15	1.42	-1.42	-57.	2337	-2.34
0.1847	917.72	2.777	-0.984	4.955.9	500.00	1.63	4.44	45.45	2.15	1.42	-1.42	-57.	2337	-2.34
0.1848	918.21	2.778	-0.984	4.955.9	500.00	1.63	4.44	45.45	2.15	1.42	-1.42	-57.	2337	-2.34

COPY AND USE
BY THE
DEFENSE
PRODUCTION

332

FLECHETTE GROUND POINT

PAGE 32

	T SEC	X FT	Y FT	Z FT	V EY/SEC	R SEC	P EY/SEC	G SEC	PHI DEG	ALPHA DEG	BETA DEG	S DEG	T DEG	M-T DEG
0.1859	916.71	2.772	-0.614	1.63	4.44	4.54	-1.15	0.15	-1.15	-1.15	-1.15	-0.15	-0.15	0.15
0.1860	919.30	2.753	-0.613	4.35	4.44	4.54	-1.11	0.91	-1.11	-1.11	-1.11	-0.91	-0.91	0.91
0.1861	918.70	2.752	-0.613	4.95	4.44	4.54	-1.09	0.95	-1.09	-1.09	-1.09	-0.95	-0.95	0.95
0.1862	920.16	2.79	-0.615	4.35	4.44	4.54	-1.02	1.02	-1.02	-1.02	-1.02	-0.98	-0.98	0.98
0.1863	921.69	2.723	-0.613	4.65	4.44	4.54	-1.02	1.02	-1.02	-1.02	-1.02	-0.98	-0.98	0.98
0.1864	921.18	2.714	-0.614	4.35	4.44	4.54	-1.02	1.02	-1.02	-1.02	-1.02	-0.98	-0.98	0.98
0.1865	921.43	2.735	-0.614	4.95	4.44	4.54	-1.02	1.02	-1.02	-1.02	-1.02	-0.98	-0.98	0.98
0.1866	922.17	2.766	-0.614	4.35	4.44	4.54	-1.02	1.02	-1.02	-1.02	-1.02	-0.98	-0.98	0.98
0.1867	922.67	2.737	-0.614	4.65	4.44	4.54	-1.02	1.02	-1.02	-1.02	-1.02	-0.98	-0.98	0.98
0.1868	923.14	2.782	-0.614	4.35	4.44	4.54	-1.02	1.02	-1.02	-1.02	-1.02	-0.98	-0.98	0.98
0.1869	923.66	2.792	-0.612	4.65	4.44	4.54	-1.02	1.02	-1.02	-1.02	-1.02	-0.98	-0.98	0.98
0.1860	924.16	2.773	-0.614	4.35	4.44	4.54	-1.02	1.02	-1.02	-1.02	-1.02	-0.98	-0.98	0.98
0.1861	924.65	2.792	-0.614	4.95	4.44	4.54	-1.02	1.02	-1.02	-1.02	-1.02	-0.98	-0.98	0.98
0.1862	925.15	2.781	-0.615	4.35	4.44	4.54	-1.02	1.02	-1.02	-1.02	-1.02	-0.98	-0.98	0.98
0.1863	925.64	2.772	-0.613	4.65	4.44	4.54	-1.02	1.02	-1.02	-1.02	-1.02	-0.98	-0.98	0.98
0.1864	926.14	2.763	-0.614	4.95	4.44	4.54	-1.02	1.02	-1.02	-1.02	-1.02	-0.98	-0.98	0.98
0.1865	926.63	2.764	-0.614	4.35	4.44	4.54	-1.02	1.02	-1.02	-1.02	-1.02	-0.98	-0.98	0.98
0.1866	927.13	2.792	-0.614	4.65	4.44	4.54	-1.02	1.02	-1.02	-1.02	-1.02	-0.98	-0.98	0.98
0.1867	927.62	2.775	-0.617	4.95	4.44	4.54	-1.02	1.02	-1.02	-1.02	-1.02	-0.98	-0.98	0.98
0.1868	928.12	2.795	-0.617	4.35	4.44	4.54	-1.02	1.02	-1.02	-1.02	-1.02	-0.98	-0.98	0.98
0.1869	928.61	2.767	-0.614	4.65	4.44	4.54	-1.02	1.02	-1.02	-1.02	-1.02	-0.98	-0.98	0.98
0.1870	929.11	2.757	-0.615	4.35	4.44	4.54	-1.02	1.02	-1.02	-1.02	-1.02	-0.98	-0.98	0.98
0.1871	929.60	2.768	-0.614	4.65	4.44	4.54	-1.02	1.02	-1.02	-1.02	-1.02	-0.98	-0.98	0.98
0.1872	930.10	2.769	-0.610	4.95	4.44	4.54	-1.02	1.02	-1.02	-1.02	-1.02	-0.98	-0.98	0.98
0.1873	930.59	2.760	-0.611	4.35	4.44	4.54	-1.02	1.02	-1.02	-1.02	-1.02	-0.98	-0.98	0.98
0.1874	931.08	2.801	-0.612	4.65	4.44	4.54	-1.02	1.02	-1.02	-1.02	-1.02	-0.98	-0.98	0.98
0.1875	931.59	2.801	-0.612	4.95	4.44	4.54	-1.02	1.02	-1.02	-1.02	-1.02	-0.98	-0.98	0.98
0.1876	932.08	2.812	-0.612	4.35	4.44	4.54	-1.02	1.02	-1.02	-1.02	-1.02	-0.98	-0.98	0.98
0.1877	932.58	2.803	-0.617	4.65	4.44	4.54	-1.02	1.02	-1.02	-1.02	-1.02	-0.98	-0.98	0.98
0.1878	933.07	2.812	-0.617	4.35	4.44	4.54	-1.02	1.02	-1.02	-1.02	-1.02	-0.98	-0.98	0.98
0.1879	933.57	2.805	-0.617	4.65	4.44	4.54	-1.02	1.02	-1.02	-1.02	-1.02	-0.98	-0.98	0.98
0.1880	934.06	2.816	-0.616	4.95	4.44	4.54	-1.02	1.02	-1.02	-1.02	-1.02	-0.98	-0.98	0.98
0.1881	934.52	2.816	-0.617	4.35	4.44	4.54	-1.02	1.02	-1.02	-1.02	-1.02	-0.98	-0.98	0.98
0.1882	935.05	2.807	-0.617	4.65	4.44	4.54	-1.02	1.02	-1.02	-1.02	-1.02	-0.98	-0.98	0.98
0.1883	935.55	2.818	-0.616	4.35	4.44	4.54	-1.02	1.02	-1.02	-1.02	-1.02	-0.98	-0.98	0.98
0.1884	936.04	2.806	-0.617	4.65	4.44	4.54	-1.02	1.02	-1.02	-1.02	-1.02	-0.98	-0.98	0.98
0.1885	936.54	2.816	-0.617	4.95	4.44	4.54	-1.02	1.02	-1.02	-1.02	-1.02	-0.98	-0.98	0.98
0.1886	937.03	2.811	-0.612	4.35	4.44	4.54	-1.02	1.02	-1.02	-1.02	-1.02	-0.98	-0.98	0.98
0.1887	937.53	2.812	-0.612	4.65	4.44	4.54	-1.02	1.02	-1.02	-1.02	-1.02	-0.98	-0.98	0.98
0.1888	938.03	2.815	-0.612	4.35	4.44	4.54	-1.02	1.02	-1.02	-1.02	-1.02	-0.98	-0.98	0.98
0.1889	938.52	2.815	-0.612	4.65	4.44	4.54	-1.02	1.02	-1.02	-1.02	-1.02	-0.98	-0.98	0.98
0.1890	939.02	2.815	-0.617	4.95	4.44	4.54	-1.02	1.02	-1.02	-1.02	-1.02	-0.98	-0.98	0.98
0.1891	939.51	2.811	-0.612	4.35	4.44	4.54	-1.02	1.02	-1.02	-1.02	-1.02	-0.98	-0.98	0.98
0.1892	940.01	2.813	-0.616	4.65	4.44	4.54	-1.02	1.02	-1.02	-1.02	-1.02	-0.98	-0.98	0.98
0.1893	940.50	2.819	-0.617	4.95	4.44	4.54	-1.02	1.02	-1.02	-1.02	-1.02	-0.98	-0.98	0.98
0.1894	941.49	2.822	-0.613	4.35	4.44	4.54	-1.02	1.02	-1.02	-1.02	-1.02	-0.98	-0.98	0.98
0.1895	941.69	2.823	-0.614	4.65	4.44	4.54	-1.02	1.02	-1.02	-1.02	-1.02	-0.98	-0.98	0.98
0.1896	942.48	2.825	-0.615	4.95	4.44	4.54	-1.02	1.02	-1.02	-1.02	-1.02	-0.98	-0.98	0.98
0.1897	942.98	2.826	-0.607	4.35	4.44	4.54	-1.02	1.02	-1.02	-1.02	-1.02	-0.98	-0.98	0.98

333

COPY AVAILABLE TO RDC BEES NOT
PERMIT FULLY LEGIBLE PRODUCTION

ELECHETTE GROUND POINT

PAGE 39

T SEC	X FT	Y FT	Z FT	P SEC	A SEC	R SEC	W SEC	PHI DEG	ALPHA DEG	BETA DEG	L-N SEC	E-N SEC	S SEC	T-N SEC	R-T SEC
3.1839	943.47	2.629	-0.308	4554.8	500.00	1.43	4.44	1.43	1.43	1.43	-0.5	-0.5	0.0	0.0	0.0
0.1930	943.07	2.873	-0.509	4554.8	500.00	1.43	4.44	1.43	1.43	1.43	-0.5	-0.5	0.0	0.0	0.0
0.1901	942.67	2.631	-0.093	4554.7	502.00	1.43	4.44	1.43	1.43	1.43	-0.5	-0.5	0.0	0.0	0.0
0.1902	944.05	2.612	-1.062	4554.7	501.00	1.43	4.44	1.43	1.43	1.43	-0.5	-0.5	0.0	0.0	0.0
0.1903	945.43	2.534	-1.053	4554.7	500.00	1.43	4.44	1.43	1.43	1.43	-0.5	-0.5	0.0	0.0	0.0
0.1904	945.05	2.834	-1.006	4554.7	500.00	1.43	4.44	1.43	1.43	1.43	-0.5	-0.5	0.0	0.0	0.0
0.1915	946.45	2.637	-1.005	4554.7	500.00	1.43	4.44	1.43	1.43	1.43	-0.5	-0.5	0.0	0.0	0.0
1.1901	945.56	2.531	-1.005	4554.7	500.00	1.43	4.44	1.43	1.43	1.43	-0.5	-0.5	0.0	0.0	0.0
0.1907	947.46	2.361	-1.002	4554.7	500.00	1.43	4.44	1.43	1.43	1.43	-0.5	-0.5	0.0	0.0	0.0
0.1908	947.93	2.862	-1.005	4554.7	500.00	1.43	4.44	1.43	1.43	1.43	-0.5	-0.5	0.0	0.0	0.0
0.1909	948.43	2.514	-1.010	4554.7	500.00	1.43	4.44	1.43	1.43	1.43	-0.5	-0.5	0.0	0.0	0.0
0.1910	948.92	2.915	-1.011	4554.6	500.00	1.43	4.44	1.43	1.43	1.43	-0.5	-0.5	0.0	0.0	0.0
0.1911	949.42	2.912	-1.012	4554.6	500.00	1.43	4.44	1.43	1.43	1.43	-0.5	-0.5	0.0	0.0	0.0
0.1912	949.51	2.850	-1.013	4554.6	500.00	1.43	4.44	1.43	1.43	1.43	-0.5	-0.5	0.0	0.0	0.0
0.1913	950.41	2.852	-1.014	4554.6	500.00	1.43	4.44	1.43	1.43	1.43	-0.5	-0.5	0.0	0.0	0.0
0.1914	950.50	2.854	-1.016	4554.6	500.00	1.43	4.44	1.43	1.43	1.43	-0.5	-0.5	0.0	0.0	0.0
0.1915	951.0	2.856	-1.017	4554.5	500.00	1.43	4.44	1.43	1.43	1.43	-0.5	-0.5	0.0	0.0	0.0
0.1916	951.5	2.858	-1.018	4554.5	500.00	1.43	4.44	1.43	1.43	1.43	-0.5	-0.5	0.0	0.0	0.0
0.1917	952.0	2.620	-1.018	4554.6	500.00	1.43	4.44	1.43	1.43	1.43	-0.5	-0.5	0.0	0.0	0.0
0.1918	952.49	2.852	-1.023	4554.5	500.00	1.43	4.44	1.43	1.43	1.43	-0.5	-0.5	0.0	0.0	0.0
0.1919	952.38	2.964	-1.020	4554.5	500.00	1.43	4.44	1.43	1.43	1.43	-0.5	-0.5	0.0	0.0	0.0
0.1920	953.46	2.966	-1.021	4554.5	500.00	1.43	4.44	1.43	1.43	1.43	-0.5	-0.5	0.0	0.0	0.0
0.1921	954.37	2.559	-1.022	4554.5	500.00	1.43	4.44	1.43	1.43	1.43	-0.5	-0.5	0.0	0.0	0.0
0.1922	955.87	2.870	-1.023	4554.5	500.00	1.43	4.44	1.43	1.43	1.43	-0.5	-0.5	0.0	0.0	0.0
0.1923	955.36	2.872	-1.024	4554.5	500.00	1.43	4.44	1.43	1.43	1.43	-0.5	-0.5	0.0	0.0	0.0
0.1924	955.85	2.355	-1.025	4554.5	500.00	1.43	4.44	1.43	1.43	1.43	-0.5	-0.5	0.0	0.0	0.0
0.1925	955.35	2.877	-1.025	4554.5	500.00	1.43	4.44	1.43	1.43	1.43	-0.5	-0.5	0.0	0.0	0.0
0.1926	955.85	2.879	-1.026	4554.5	500.00	1.43	4.44	1.43	1.43	1.43	-0.5	-0.5	0.0	0.0	0.0
0.1927	957.34	2.821	-1.027	4554.4	500.00	1.43	4.44	1.43	1.43	1.43	-0.5	-0.5	0.0	0.0	0.0
0.1928	957.84	2.833	-1.027	4554.4	500.00	1.43	4.44	1.43	1.43	1.43	-0.5	-0.5	0.0	0.0	0.0
0.1929	958.34	2.834	-1.028	4554.4	500.00	1.43	4.44	1.43	1.43	1.43	-0.5	-0.5	0.0	0.0	0.0
0.1930	958.83	2.869	-1.029	4554.4	500.00	1.43	4.44	1.43	1.43	1.43	-0.5	-0.5	0.0	0.0	0.0
0.1931	959.33	2.893	-1.029	4554.4	500.00	1.43	4.44	1.43	1.43	1.43	-0.5	-0.5	0.0	0.0	0.0
0.1932	960.32	2.832	-1.030	4554.3	500.00	1.43	4.44	1.43	1.43	1.43	-0.5	-0.5	0.0	0.0	0.0
0.1933	961.32	2.864	-1.030	4554.3	500.00	1.43	4.44	1.43	1.43	1.43	-0.5	-0.5	0.0	0.0	0.0
0.1934	960.81	2.887	-1.031	4554.3	500.00	1.43	4.44	1.43	1.43	1.43	-0.5	-0.5	0.0	0.0	0.0
0.1935	961.31	2.894	-1.032	4554.3	500.00	1.43	4.44	1.43	1.43	1.43	-0.5	-0.5	0.0	0.0	0.0
0.1936	961.81	2.901	-1.032	4554.3	500.00	1.43	4.44	1.43	1.43	1.43	-0.5	-0.5	0.0	0.0	0.0
0.1937	962.31	2.513	-1.032	4554.3	500.00	1.43	4.44	1.43	1.43	1.43	-0.5	-0.5	0.0	0.0	0.0
0.1938	962.79	2.545	-1.032	4554.3	500.00	1.43	4.44	1.43	1.43	1.43	-0.5	-0.5	0.0	0.0	0.0
0.1939	963.29	2.907	-1.032	4554.3	500.00	1.43	4.44	1.43	1.43	1.43	-0.5	-0.5	0.0	0.0	0.0
0.1940	963.79	2.913	-1.032	4554.3	500.00	1.43	4.44	1.43	1.43	1.43	-0.5	-0.5	0.0	0.0	0.0
0.1941	964.28	2.712	-1.032	4554.3	500.00	1.43	4.44	1.43	1.43	1.43	-0.5	-0.5	0.0	0.0	0.0
0.1942	964.77	2.914	-1.032	4554.3	500.00	1.43	4.44	1.43	1.43	1.43	-0.5	-0.5	0.0	0.0	0.0
0.1943	965.27	2.916	-1.033	4554.2	500.00	1.43	4.44	1.43	1.43	1.43	-0.5	-0.5	0.0	0.0	0.0
0.1944	965.77	2.918	-1.033	4554.2	500.00	1.43	4.44	1.43	1.43	1.43	-0.5	-0.5	0.0	0.0	0.0
0.1945	966.26	2.920	-1.033	4554.2	500.00	1.43	4.44	1.43	1.43	1.43	-0.5	-0.5	0.0	0.0	0.0
0.1946	966.76	2.922	-1.033	4554.2	500.00	1.43	4.44	1.43	1.43	1.43	-0.5	-0.5	0.0	0.0	0.0
0.1947	967.25	2.924	-1.033	4554.2	500.00	1.43	4.44	1.43	1.43	1.43	-0.5	-0.5	0.0	0.0	0.0
0.1948	967.75	2.926	-1.033	4554.2	500.00	1.43	4.44	1.43	1.43	1.43	-0.5	-0.5	0.0	0.0	0.0

FLECHETTE GROUND POINT

PAGE 40

SFC	X	Y	Z	PT	V	ST/SEC	PAT/SEC	PTG	ALPHA	MACH	FAT	SUPH	ASTA	L-N	L-S	W-N	W-S	S-T	E-C
									D-G	V-S/C	G-S								
2.1329	958.24	2.628	-1.033	4654.1	5.07	4.4	5.49	1.16	-0.57	223	-2.935	-	-	0	0	0	0	0	0
0.1550	958.74	2.639	-1.039	4654.2	5.09	4.4	5.49	1.18	-0.57	223	-2.937	-	-	0	0	0	0	0	0
0.1551	959.23	2.632	-1.033	4654.2	5.05	4.4	5.49	1.22	-0.57	233	-2.135	-	-	0	0	0	0	0	0
0.1552	959.23	2.635	-1.032	4654.2	5.06	4.4	5.49	1.25	-0.68	233	-2.135	-	-	0	0	0	0	0	0
0.1553	959.23	2.635	-1.032	4654.2	5.07	4.4	5.49	1.25	-0.68	233	-2.135	-	-	0	0	0	0	0	0
0.1554	959.22	2.635	-1.032	4654.1	5.07	4.4	5.49	1.25	-0.68	233	-2.135	-	-	0	0	0	0	0	0
0.1555	970.72	2.637	-1.032	4654.1	5.09	4.4	5.49	1.25	-0.68	233	-2.135	-	-	0	0	0	0	0	0
0.1556	971.21	2.639	-1.032	4654.1	5.09	4.4	5.49	1.25	-0.68	233	-2.135	-	-	0	0	0	0	0	0
0.1557	971.71	2.641	-1.032	4654.1	5.09	4.4	5.49	1.25	-0.68	233	-2.135	-	-	0	0	0	0	0	0
0.1558	972.21	2.642	-1.032	4654.1	5.09	4.4	5.49	1.25	-0.68	233	-2.135	-	-	0	0	0	0	0	0
0.1559	972.70	2.646	-1.032	4654.1	5.09	4.4	5.49	1.25	-0.68	233	-2.135	-	-	0	0	0	0	0	0
0.1560	973.20	2.648	-1.031	4654.1	5.09	4.4	5.49	1.25	-0.68	233	-2.135	-	-	0	0	0	0	0	0
0.1561	973.69	2.654	-1.031	4654.1	5.09	4.4	5.49	1.25	-0.68	233	-2.135	-	-	0	0	0	0	0	0
0.1562	974.19	2.656	-1.031	4654.0	5.09	4.4	5.49	1.25	-0.68	233	-2.135	-	-	0	0	0	0	0	0
0.1563	974.68	2.656	-1.031	4654.0	5.09	4.4	5.49	1.25	-0.68	233	-2.135	-	-	0	0	0	0	0	0
0.1564	975.18	2.652	-1.031	4654.0	5.09	4.4	5.49	1.25	-0.68	233	-2.135	-	-	0	0	0	0	0	0
0.1565	975.67	2.656	-1.031	4654.0	5.09	4.4	5.49	1.25	-0.68	233	-2.135	-	-	0	0	0	0	0	0
0.1566	976.17	2.656	-1.032	4654.0	5.09	4.4	5.49	1.25	-0.68	233	-2.135	-	-	0	0	0	0	0	0
0.1567	976.66	2.658	-1.031	4654.0	5.09	4.4	5.49	1.25	-0.68	233	-2.135	-	-	0	0	0	0	0	0
0.1568	977.16	2.664	-1.031	4654.0	5.09	4.4	5.49	1.25	-0.68	233	-2.135	-	-	0	0	0	0	0	0
0.1569	977.65	2.664	-1.031	4654.0	5.09	4.4	5.49	1.25	-0.68	233	-2.135	-	-	0	0	0	0	0	0
0.1570	978.15	2.669	-1.032	4654.0	5.09	4.4	5.49	1.25	-0.68	233	-2.135	-	-	0	0	0	0	0	0
0.1571	978.64	2.674	-1.032	4654.0	5.09	4.4	5.49	1.25	-0.68	233	-2.135	-	-	0	0	0	0	0	0
0.1572	979.14	2.676	-1.032	4654.0	5.09	4.4	5.49	1.25	-0.68	233	-2.135	-	-	0	0	0	0	0	0
0.1573	979.64	2.681	-1.032	4654.0	5.09	4.4	5.49	1.25	-0.68	233	-2.135	-	-	0	0	0	0	0	0
0.1574	980.13	2.686	-1.032	4654.0	5.09	4.4	5.49	1.25	-0.68	233	-2.135	-	-	0	0	0	0	0	0
0.1575	980.63	2.691	-1.032	4654.0	5.09	4.4	5.49	1.25	-0.68	233	-2.135	-	-	0	0	0	0	0	0
0.1576	981.12	2.696	-1.032	4654.0	5.09	4.4	5.49	1.25	-0.68	233	-2.135	-	-	0	0	0	0	0	0
0.1577	981.62	2.696	-1.032	4654.0	5.09	4.4	5.49	1.25	-0.68	233	-2.135	-	-	0	0	0	0	0	0
0.1578	982.11	2.696	-1.032	4654.0	5.09	4.4	5.49	1.25	-0.68	233	-2.135	-	-	0	0	0	0	0	0
0.1579	982.61	2.697	-1.032	4654.0	5.09	4.4	5.49	1.25	-0.68	233	-2.135	-	-	0	0	0	0	0	0
0.1580	983.10	2.701	-1.032	4654.0	5.09	4.4	5.49	1.25	-0.68	233	-2.135	-	-	0	0	0	0	0	0
0.1581	983.59	2.706	-1.032	4654.0	5.09	4.4	5.49	1.25	-0.68	233	-2.135	-	-	0	0	0	0	0	0
0.1582	984.09	2.707	-1.032	4654.0	5.09	4.4	5.49	1.25	-0.68	233	-2.135	-	-	0	0	0	0	0	0
0.1583	984.59	2.707	-1.032	4654.0	5.09	4.4	5.49	1.25	-0.68	233	-2.135	-	-	0	0	0	0	0	0
0.1584	985.08	2.707	-1.032	4654.0	5.09	4.4	5.49	1.25	-0.68	233	-2.135	-	-	0	0	0	0	0	0
0.1585	985.57	2.707	-1.032	4654.0	5.09	4.4	5.49	1.25	-0.68	233	-2.135	-	-	0	0	0	0	0	0
0.1586	986.05	2.707	-1.032	4654.0	5.09	4.4	5.49	1.25	-0.68	233	-2.135	-	-	0	0	0	0	0	0
0.1587	986.54	2.707	-1.032	4654.0	5.09	4.4	5.49	1.25	-0.68	233	-2.135	-	-	0	0	0	0	0	0
0.1588	987.03	2.707	-1.032	4654.0	5.09	4.4	5.49	1.25	-0.68	233	-2.135	-	-	0	0	0	0	0	0
0.1589	987.52	2.707	-1.032	4654.0	5.09	4.4	5.49	1.25	-0.68	233	-2.135	-	-	0	0	0	0	0	0
0.1590	988.01	2.707	-1.032	4654.0	5.09	4.4	5.49	1.25	-0.68	233	-2.135	-	-	0	0	0	0	0	0
0.1591	988.50	2.707	-1.032	4654.0	5.09	4.4	5.49	1.25	-0.68	233	-2.135	-	-	0	0	0	0	0	0
0.1592	988.99	2.707	-1.032	4654.0	5.09	4.4	5.49	1.25	-0.68	233	-2.135	-	-	0	0	0	0	0	0
0.1593	989.48	2.707	-1.032	4654.0	5.09	4.4	5.49	1.25	-0.68	233	-2.135	-	-	0	0	0	0	0	0
0.1594	989.97	2.707	-1.032	4654.0	5.09	4.4	5.49	1.25	-0.68	233	-2.135	-	-	0	0	0	0	0	0
0.1595	990.46	2.707	-1.032	4654.0	5.09	4.4	5.49	1.25	-0.68	233	-2.135	-	-	0	0	0	0	0	0
0.1596	990.95	2.707	-1.032	4654.0	5.09	4.4	5.49	1.25	-0.68	233	-2.135	-	-	0	0	0	0	0	0
0.1597	991.03	2.707	-1.032	4654.0	5.09	4.4	5.49	1.25	-0.68	233	-2.135	-	-	0	0	0	0	0	0
0.1598	991.52	2.707	-1.032	4654.0	5.09	4.4	5.49	1.25	-0.68	233	-2.135	-	-	0	0	0	0	0	0
0.1599	992.51	2.707	-1.032	4654.0	5.09	4.4	5.49	1.25	-0.68	233	-2.135	-	-	0	0	0	0	0	0
0.1600	992.51	2.707	-1.032	4654.0	5.09	4.4	5.49	1.25	-0.68	233	-2.135	-	-	0	0	0	0	0	0

335 COPY AVAILABLE TO EBC BEGS NOT
PERMIT FULLY LEGIBLE PRODUCTION

FLECPETTE GROUND POINT

PAGE 41

T	X	Y	Z	P	ALPHA	MACH	PHI	LEO	L-N	L-P	W-O	S-T	E-G
SEC	FT	FT	FT	FT SEC	RA SEC	DEC	DEG	1/SEC	1/SEC	1/SEC	1/SEC	1/SEC	1/SEC
0.1999	993.01	2.987	-1.036	4.952.6	310.00	1.63	4.44	2.546	0.943	1.34	0.55	0.	1.
0.2000	993.50	2.985	-1.036	4.952.6	500.00	1.63	4.44	2.546	0.943	1.35	0.55	0.	1.
0.2001	994.00	2.985	-1.036	4.953.4	500.00	1.63	4.44	2.546	0.943	1.35	0.55	0.	1.
0.2002	994.50	2.985	-1.036	4.953.4	500.00	1.63	4.44	2.546	0.943	1.35	0.55	0.	1.
0.2003	995.00	2.985	-1.036	4.953.4	500.00	1.63	4.44	2.546	0.943	1.35	0.55	0.	1.
0.2004	995.49	2.985	-1.036	4.953.4	500.00	1.63	4.44	2.546	0.943	1.35	0.55	0.	1.
0.2005	995.98	2.985	-1.036	4.953.4	500.00	1.63	4.44	2.546	0.943	1.35	0.55	0.	1.
0.2006	996.49	2.985	-1.036	4.953.4	500.00	1.63	4.44	2.546	0.943	1.35	0.55	0.	1.
0.2007	997.00	2.985	-1.036	4.953.4	500.00	1.63	4.44	2.546	0.943	1.35	0.55	0.	1.
0.2008	997.50	2.985	-1.036	4.953.4	500.00	1.63	4.44	2.546	0.943	1.35	0.55	0.	1.
0.2009	998.00	2.985	-1.036	4.953.4	500.00	1.63	4.44	2.546	0.943	1.35	0.55	0.	1.
0.2010	998.49	2.985	-1.036	4.953.4	500.00	1.63	4.44	2.546	0.943	1.35	0.55	0.	1.
0.2011	998.98	2.985	-1.036	4.953.4	500.00	1.63	4.44	2.546	0.943	1.35	0.55	0.	1.
0.2012	999.49	2.985	-1.036	4.953.4	500.00	1.63	4.44	2.546	0.943	1.35	0.55	0.	1.
0.2013	999.98	2.985	-1.036	4.953.4	500.00	1.63	4.44	2.546	0.943	1.35	0.55	0.	1.
0.2014	1000.49	3.001	-1.036	4.953.4	500.00	1.63	4.44	2.546	0.943	1.35	0.55	0.	1.
0.2015	1000.98	3.002	-1.036	4.953.4	500.00	1.63	4.44	2.546	0.943	1.35	0.55	0.	1.
0.2016	1001.49	3.003	-1.036	4.953.4	500.00	1.63	4.44	2.546	0.943	1.35	0.55	0.	1.
0.2017	1001.98	3.003	-1.036	4.953.4	500.00	1.63	4.44	2.546	0.943	1.35	0.55	0.	1.
0.2018	1002.49	3.003	-1.036	4.953.4	500.00	1.63	4.44	2.546	0.943	1.35	0.55	0.	1.
0.2019	1002.98	3.007	-1.036	4.953.4	500.00	1.63	4.44	2.546	0.943	1.35	0.55	0.	1.
0.2020	1003.49	3.016	-1.036	4.953.4	500.00	1.63	4.44	2.546	0.943	1.35	0.55	0.	1.
0.2021	1003.98	3.016	-1.036	4.953.4	500.00	1.63	4.44	2.546	0.943	1.35	0.55	0.	1.
0.2022	1004.49	3.016	-1.036	4.953.4	500.00	1.63	4.44	2.546	0.943	1.35	0.55	0.	1.
0.2023	1004.98	3.016	-1.036	4.953.4	500.00	1.63	4.44	2.546	0.943	1.35	0.55	0.	1.
0.2024	1005.49	3.016	-1.036	4.953.4	500.00	1.63	4.44	2.546	0.943	1.35	0.55	0.	1.
0.2025	1005.98	3.016	-1.036	4.953.4	500.00	1.63	4.44	2.546	0.943	1.35	0.55	0.	1.
0.2026	1006.49	3.016	-1.036	4.953.4	500.00	1.63	4.44	2.546	0.943	1.35	0.55	0.	1.
0.2027	1006.98	3.016	-1.036	4.953.4	500.00	1.63	4.44	2.546	0.943	1.35	0.55	0.	1.
0.2028	1007.49	3.016	-1.036	4.953.4	500.00	1.63	4.44	2.546	0.943	1.35	0.55	0.	1.
0.2029	1007.98	3.016	-1.036	4.953.4	500.00	1.63	4.44	2.546	0.943	1.35	0.55	0.	1.
0.2030	1008.49	3.016	-1.036	4.953.4	500.00	1.63	4.44	2.546	0.943	1.35	0.55	0.	1.
0.2031	1008.98	3.016	-1.036	4.953.4	500.00	1.63	4.44	2.546	0.943	1.35	0.55	0.	1.
0.2032	1009.49	3.016	-1.036	4.953.4	500.00	1.63	4.44	2.546	0.943	1.35	0.55	0.	1.
0.2033	1009.98	3.016	-1.036	4.953.4	500.00	1.63	4.44	2.546	0.943	1.35	0.55	0.	1.
0.2034	1010.49	3.039	-1.036	4.953.4	500.00	1.63	4.44	2.546	0.943	1.35	0.55	0.	1.
0.2035	1010.98	3.039	-1.036	4.953.4	500.00	1.63	4.44	2.546	0.943	1.35	0.55	0.	1.
0.2036	1011.49	3.039	-1.036	4.953.4	500.00	1.63	4.44	2.546	0.943	1.35	0.55	0.	1.
0.2037	1011.98	3.039	-1.036	4.953.4	500.00	1.63	4.44	2.546	0.943	1.35	0.55	0.	1.
0.2038	1012.49	3.039	-1.036	4.953.4	500.00	1.63	4.44	2.546	0.943	1.35	0.55	0.	1.
0.2039	1012.98	3.039	-1.036	4.953.4	500.00	1.63	4.44	2.546	0.943	1.35	0.55	0.	1.
0.2040	1013.49	3.039	-1.036	4.953.4	500.00	1.63	4.44	2.546	0.943	1.35	0.55	0.	1.
0.2041	1013.98	3.039	-1.036	4.953.4	500.00	1.63	4.44	2.546	0.943	1.35	0.55	0.	1.
0.2042	1014.49	3.039	-1.036	4.953.4	500.00	1.63	4.44	2.546	0.943	1.35	0.55	0.	1.
0.2043	1014.98	3.039	-1.036	4.953.4	500.00	1.63	4.44	2.546	0.943	1.35	0.55	0.	1.
0.2044	1015.49	3.039	-1.036	4.953.4	500.00	1.63	4.44	2.546	0.943	1.35	0.55	0.	1.
0.2045	1015.98	3.039	-1.036	4.953.4	500.00	1.63	4.44	2.546	0.943	1.35	0.55	0.	1.
0.2046	1016.49	3.039	-1.036	4.953.4	500.00	1.63	4.44	2.546	0.943	1.35	0.55	0.	1.
0.2047	1016.98	3.039	-1.036	4.953.4	500.00	1.63	4.44	2.546	0.943	1.35	0.55	0.	1.
0.2048	1017.49	3.039	-1.036	4.953.4	500.00	1.63	4.44	2.546	0.943	1.35	0.55	0.	1.

REFERENCES

1. Fowler, R.M., Gallop, E.G., Lock, C.N.M., and Richmond, N.W., "Aerodynamic of a Spinning Shell" Phil. Trans. Royal Society, London, 1920.
2. Sterne, T.E., "On Jump Due to Bore Clearance," BRL Report No. 491, 28 Sept. 1944.
3. Murphy, C.H., "Comments on Projectile Jump," BRL Report No. 1071, April, 1957.
4. Kent, R.H., "First Memorandum Report on 3.3 inch Design Data Firings in Connection with O.B. Program 2627-3," BRL 14 May 1920.
5. Zaroodny, S.J., "On Jump Due to Muzzle Disturbances," BRL Report No. 703, June, 1949.
6. Murphy, C.H., Bradley, J.W., "Jump Due to Aerodynamic Asymmetry of a Missile with Varying Roll Rate," BRL Report No. 1077, May, 1959.
7. Nicolaides, J.D., "On the Free Flight Motion of Missiles Having Slight Configurational Asymmetries," BRL Report No. 858, June, 1953.
8. Nicolaides, J.D., McAllister, L.D., "A Note on the Contribution of Configurational Asymmetries to the Free Flight Motion of Missiles," Journal of the Aeronautical Sciences, Vol. 19, No. 12, Dec., 1952.
9. Nicolaides, J.D., "Free Flight Dynamics," Text, Aerospace Engineering Department, University of Notre Dame, 1964.
10. Ingram, C.W., "A Computer Program for Integrating the Six-Degree-of-Freedom Equations of Motion of a Symmetrical Missile," Aerospace Engineering Dept., University of Notre Dame, 1970.
11. Ingram, C.W., Daniels, P., "A Spin Scale Theory for Rigid Body Integration Using the Frick Slip Frame," AIAA Journal, Vol. 5, No. 1, Jan. 1967.

REFERENCES (concluded)

12. Ingram, C.W., "Analytical Program for the Evaluation and Reduction of Dispersion and Jump of Fin Bodies," U.S. Army Frankford Arsenal Contract No. DAAA25-71-C0447, August, 1972.
13. Eikenberry, R.S., "Wobble, Analysis of Missile Dynamic Data," Prepared for Sandia Corp., Albuquerque, N.M., 1969.
14. Ingram, C.W., Nicolaides, J.D., Eikenberry, R.S., Lijewski, L.E., "A Computer Program to Fit the Initial Angular Data from Test Firing of Flechettes," Prepared for U.S. Army, Frankford Arsenal, Phila. Pa., 1973.
15. Piddington, M., "The Aerodynamic Characteristics of a Spin Projectile," BRL Memo Rpt. No. 1594, Ballistics Research Laboratory, Aberdeen Proving Ground, Md., Sept., 1964.
16. Garsik, M., "Dynamic Supersonic Wind Tunnel Testing," Masters Thesis, University of Notre Dame, Aerospace Dept., May, 1974.

APPENDIX D

FRANKFORD ARSENAL EXPERIMENTAL BALLISTICS FIRING PROGRAM OF FLECHETTES

During the spring and summer of 1974, eleven flechette firings were carried out in the Frankford Arsenal X-ray Ballistic Range. The data was measured from the x-ray plates by Frankford Arsenal personnel and is given in Figure D-1.

The flechette used in this test is very similar to the flechette used in lot 3 of the previous test data. It is assumed that the C.G. and the axial and transverse moments are the same. The C.G. is 0.94 inches from the nose; the axial moment is 0.0107 grain in² and the transverse moment is 1.78 grain in². It is also assumed that the average spin rate is 2750 rev/sec.

The coordinate axis for the target data is defined as having plot (0,0) coincident with the aim point as established with a laser.

Times of flight were obtained between the first x-ray station and the sixth x-ray station. The baseline for determining the velocity was then a variable where the distance was measured between the flechette C.G. at the first station and at the sixth station.

The data used in the ND analysis is given in Figure D-2. The horizontal and vertical angles for Round 17 are plotted in D-3. In the case of Round 17 and Rounds 35, 23, 21 and 25 the motion was nearly 1d and therefore reductions and analysis could be carried out. The motions, however, on the

other rounds were highly 2 d and therefore computer fits were not possible.

The results for Round 17 are presented herein in order to provide the reader with an example. Figure D-4 contains the original α , β data and the new data as determined by computer fit. The final α , β data is given in Figure D-5 which is used in the basic jump equation.

The trajectory data given in Figure D-1 is fitted on the computer with second degree, third degree and fourth degree polynomials as shown in Figure D-6. The third degree fit was used and a summary of the trajectory data is given in Figure D-7 which is also used in the basic jump equation.

Therefore, the α and β data from Figure D-5 and the trajectory data from Figure D-7 is used with the basic jump equation to provide the results given in Figure D-8.

Figure D-8, therefore, is the final result of the firing program and the jump analysis which shows the agreement between the experimentally determined jump and the jump predicted from the translational ballistics motion parameters as determined in the Frankford Arsenal X-Ray Ballistics Range.

LOT TBP
AUG 26 1976

NOSE TO CG IS .940 INCHES

Figure D-1

ROUND 17 TIME = 2031.4

FILM	X	Y	Z	EPR	VERT ANGLE	HOR ANGLE	ABS ANGLE	DIRECTION
1	-.0770	-.1363	10.9399	.0366	-2.1564	1.0221	-2.3860	156.4353 .0001012
2	.0633	-.1537	33.0985	.048	-5.2285	1.9080	-5.5622	161.8446 C.0001012
3	.2172	-.1991	55.581	.0085	-5.3931	.8609	-5.4606	172.9318 .0001012
4	.3963	-.285	80.6581	-.0066	-1.8322	.2348	-1.8412	-176.6961 .0011012
5	.5537	-.3637	103.8862	-.1123	2.4678	.5549	2.5510	-15.6269 .0011012
6	.7172	-.4031	126.1695	-.2049	6.6616	4.6607	-5.2615	-2022.1012

AVERAGE VELOCITY = 4752. FT/SEC

ROUND 35 TIME = 2029.5

FILM	X	Y	Z	ERR	VERT ANGLE	HOR ANGLE	ABS ANGLE	DIRECTION
1	-.1154	-.1406	10.6052	.0191	.9013	1.2915	-1.5147	126.3521 .0001012
2	.0311	-.1407	32.8970	.0882	-2.3010	.7494	-2.4216	163.9556 .0001012
3	.1841	-.1711	56.1766	-.0889	-.5331	.9839	-1.1190	119.8155 ..0001012
4	.3364	-.2003	79.3832	-.0499	1.6433	.9455	1.8957	30.3541 ..0012812
5	.4957	-.2079	103.6674	-.0635	2.6546	.0061	2.5546	1.1327 ..0012812
6	.6364	-.1778	126.2009	-.1251	2.2742	-1.1278	2.2778	-3.2311 .0021012

AVERAGE VELOCITY = 4746. FT/SEC

ROUND 23 TIME = 2032.7

FILM	X	Y	Z	ERR	VERT ANGLE	HOR ANGLE	ABS ANGLE	DIRECTION
1	-.1640	-.1583	13.9515	.0332	.4711	-.0979	-.4912	-11.8711 .00022112
2	.0311	-.1688	33.6919	-.0046	-.0734	-.990	-.9327	-9.3307 .00022112
3	.1912	-.1619	52.4623	.0253	-.1429	-.7920	-.6336	-152.7508 .0010112
4	.3485	-.1776	80.3243	-.0158	-2.1346	-.0180	-2.1380	-179.9655 .0010112
5	.4910	-.1607	104.2197	-.1972	-.1244	.5873	-.2685	-154.1842 .0010112
6	.6360	-.1618	126.4914	-.1822	.2545	1.4526	1.5144	81.2546 .0021012

AVERAGE VELOCITY = 4656. FT/SEC

ROUND 2 TIME = 2033.6

FILM	X	Y	Z	ERR	VERT ANGLE	HOR ANGLE	ABS ANGLE	DIRECTION
1	-0.696	-1.638	10.5592	.0108	-0.004	.3910	-3911	92.4315 .0001873
2	.0659	.1694	33.3137	.0789	-1156	1.2237	-1.2311	96.4905 .0205723
3	.2686	.1783	55.7173	.0155	-1293	3.0829	-3.0856	93.4655 .00019512
4	.3594	.1917	80.4189	.0415	-1647	2.8075	2.8123	87.6643 .0013853
5	.5340	.1794	104.9778	.0738	-1934	1.6753	1.6864	86.3817 .0018161
6	.1037	.1529	128.0976	.1210	.0988	-2.6213	.6291	-81.8971 .0022160

AVERAGE VELOCITY = 4864. FT/SEC

ROUND 4 TIME = 2031.1

FILM	X	Y	Z	ERR	VERT ANGLE	HOR ANGLE	ABS ANGLE	DIRECTION
1	-0.677	-1.514	11.3160	.0155	-2449	.7507	-7912	109.6656 .0001835
2	.0986	.1451	33.9186	.0229	-6783	.9779	-1.1844	20.530
3	.2521	.1558	56.6122	.0153	-8190	1.3149	-1.5400	12.3238 .3205632
4	.4346	.1599	82.7313	.0041	-2680	1.0164	-1.0511	105.9825 .00141473
5	.6058	.1533	106.0647	.0406	-4102	-0.3112	.4114	-4.3984 .00118123
6	.7760	.1338	129.4768	.0841	.5251	-0.0261	.5258	-2.8748 .0022139

AVERAGE VELOCITY = 4848. FT/SEC

ROUND 2 TIME = 1996.1

FILM	X	Y	Z	ERR	VERT ANGLE	HOR ANGLE	ABS ANGLE	DIRECTION
1	-1.109	-1.466	11.6143	.0261	1.0107	.6916	1.6614	24.8773 .0001960
2	.0324	.152	34.9057	.0164	2.6938	1.9501	3.2240	36.3072 .0001965
3	.1612	.1626	57.3612	.0249	3.2340	2.1342	3.9611	32.9843 .0001964
4	.2396	.1287	81.8297	.0067	1.3399	1.3983	1.9363	46.7552 .0013292
5	.4950	.0898	105.2557	.1631	-2.2221	.2987	-4.478	135.9067 .0017316
6	.6688	.0326	128.1422	.1071	-2.8496	-7241	-2.9205	-167.5708 .00221912

AVERAGE VELOCITY = 4865. FT/SEC

ROUND 5 TIME = 2031.8

FILM	X	Y	Z	ERR	VERT ANGLE	HOR ANGLE	ABS ANGLE	DIRECTION
1	.6504	.1666	11.1459	.0055	2.1431	1.4189	2.5695	33.8883 .0001829
2	.1328	.4874	.0364	.57425	5.1260	6.1186	20.4372 .0001953	

Figure D-1 (continued)

2	.0500	-1.1716	33.4574	-	-0.376	5.7425	-	2.1200	6.1110	20.4414	-
3	.1923	-1.1892	56.1273	-	.0162	2.9876	-	7.1620	7.1220	25.4419	-00.1475
4	.3561	-1.115	61.4707	-	.0165	4.2813	-	2.0130	4.1779	128.5055	00.18225
5	.5199	-0.0263	104.7454	-	.0165	2.7779	-	.3683	-4.6614	-171.8303	.0022552
6	.6586	.0854	127.0886	-	.0529	-4.0700	-	.0014	-4.1477	-	

AVERAGE VELOCITY = 4198. FT/SEC

ROUND 25	TIME = 2030.1
----------	---------------

FILM	X	Y	Z	ERR	VERT ANGLE	HOR ANGLE	ABS ANGLE	DIRECTION
1	-1.253	-.1501	10.9129	.0342	.6746	1.5046	1.7401	63.5253 .00193
2	-.0116	-.1462	32.7991	.0440	1.6006	4.6842	4.9515	12.0126 .0015805
3	.1336	-.1408	56.3469	.0465	1.9755	5.8105	6.1386	72.116 .001473
4	.3220	-.1226	79.1842	-.0445	.9627	4.4618	4.5837	78.7452 .0016012
5	.5126	-.0865	103.3855	-.1231	1.1622	1.1622	1.1827	80.2229 .0016249
6	.6856	-.0297	125.5950	-.2131	-.1632	-2.0623	-2.1987	-111.5728 .0022220

AVERAGE VELOCITY = 4708. FT/SEC

ROUND 22	TIME = 1981.0
----------	---------------

FILM	X	Y	Z	ERR	VERT ANGLE	HOR ANGLE	ABS ANGLE	DIRECTION
1	-.1164	-.1561	12.0050	.0208	-.5206	-.1123	-.5325	-169.7685 .0002124
2	.0097	-.1576	33.7631	.0128	.9450	-.9450	-1.3459	-16.6050 .0002176
3	.1557	-.1883	57.4906	.0158	-.5403	-2.7707	-2.8227	-162.1945 .0010157
4	.2767	-.2887	80.5107	-.0006	-.8122	*2.2402	-2.3826	-111.919 .00101250
5	.4112	-.2176	102.6321	-.2085	-.4978	-.1.0202	-.0886	-113.0768 .001018171
6	.4595	-.2698	123.7467	-.1795	.1003	1.3582	1.3582	86.7690 .0021903

AVERAGE VELOCITY = 4701. FT/SEC

ROUND 26	TIME = 2031.9
----------	---------------

FILM	X	Y	Z	ERR	VERT ANGLE	HOR ANGLE	ABS ANGLE	DIRECTION
1	-.9706	-.1922	10.9858	.0177	.4859	.3060	.5742	32.5670 .0001878
2	.6937	-.1189	33.6055	-.075	.9667	-.4654	1.0746	26.1987 .0001875
3	.2396	-.2136	57.2682	-.0156	1.1981	-2.2085	2.5103	22.2175 .00019792
4	.3870	-.2226	80.7300	-.0192	.8300	-1.9856	2.1554	81.9086 .0013205
5	.5145	-.1923	105.9170	-.0222	-.3738	-.3760	.5302	-136.3904 .0018111
6	.6307	-.1588	129.1873	-.0859	-.1116	1.8329	-2.1782	126.1322 .0022200

AVERAGE VELOCITY = 4848. FT/SEC

Figure V-1 (continued)

Figure D-1 (continued)

	ROUND	8	TIME	=	2030.9			
FILM	X	Y	Z	ERR	VERT ANGLE	HOR ANGLE	ABS ANGLE	DIRECTION
1	-0.0750	-1.1429	11.0242	.0386	-1.3051	.5355	-1.4106	159.5169 .CCCCC7
2	.0712	-1.1516	33.3321	.0516	-2.2016	.3321	-2.2567	161.3413 .00006796
3	.2307	-1.1946	55.9490	.0249	.4507	.3150	.3191	-81.7950 .00026912
4	.4342	-2.2324	61.7539	-.0202	-2.2448	-2.1247	3.0594	-41.9266 .00141452
5	.5190	-2.2384	106.8275	-.0708	3.0946	-.5940	3.1477	-0.0181 .0018135
6	.6706	-2.2111	127.9104	-.0993	2.3495	.3856	2.3813	9.4223 .00222128

AVERAGE VELOCITY = .4796. FT/SEC

Figure D-2

R&D PARAMETERS

$$d = 0.00587 \text{ ft.}$$

$$m = 0.00004573 \text{ slugs}$$

$$I_x = 0.000\ 000\ 000\ 330 \text{ slugs-ft}^2$$

$$I_y = 0.000\ 000\ 054\ 883 \text{ slugs-ft}^2$$

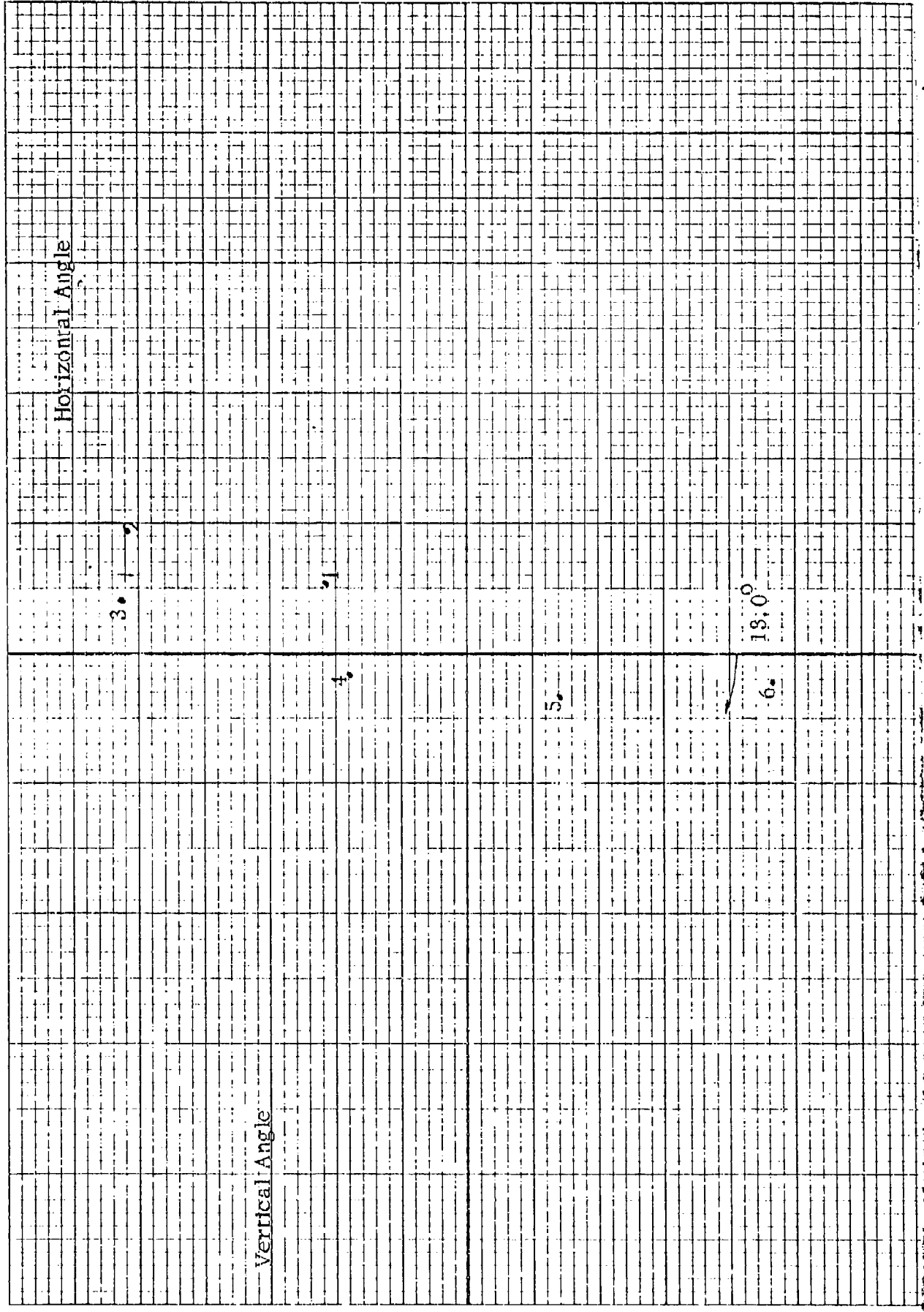
$$p = 17279 \text{ rad/sec}$$

NO. 340-R-1C DIETZGEN GRAPH PAPER
10 X 10 PER INCH

EUGENE DIETZGEN CO.
MADE IN U. S. A.

Round 17

Figure D-3



PNL 22 8/30/88 J08 22 KU 12, 15/4

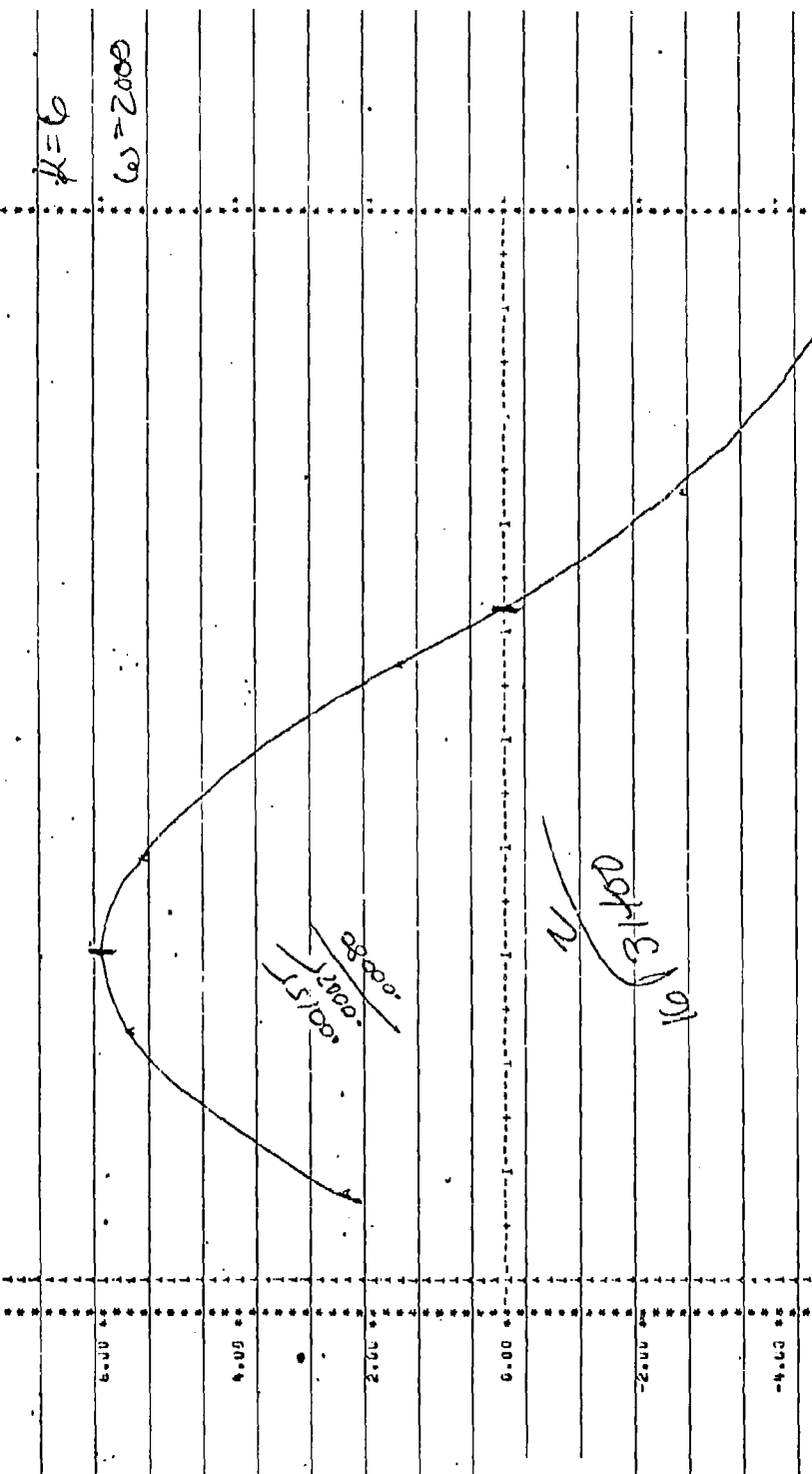
Figure 4 (continued)

TIME	FLIGHT (sec.)
0.3130E+02	0.250017E+01
0.3750E+02	0.350311E+01
0.4727E+02	0.353707E+01
0.5441E+02	0.353707E+01
0.6165E+02	0.353707E+01
0.22163E+02	-0.454914E+01

PAGE 23 0955JUL 22 AUS 121 174

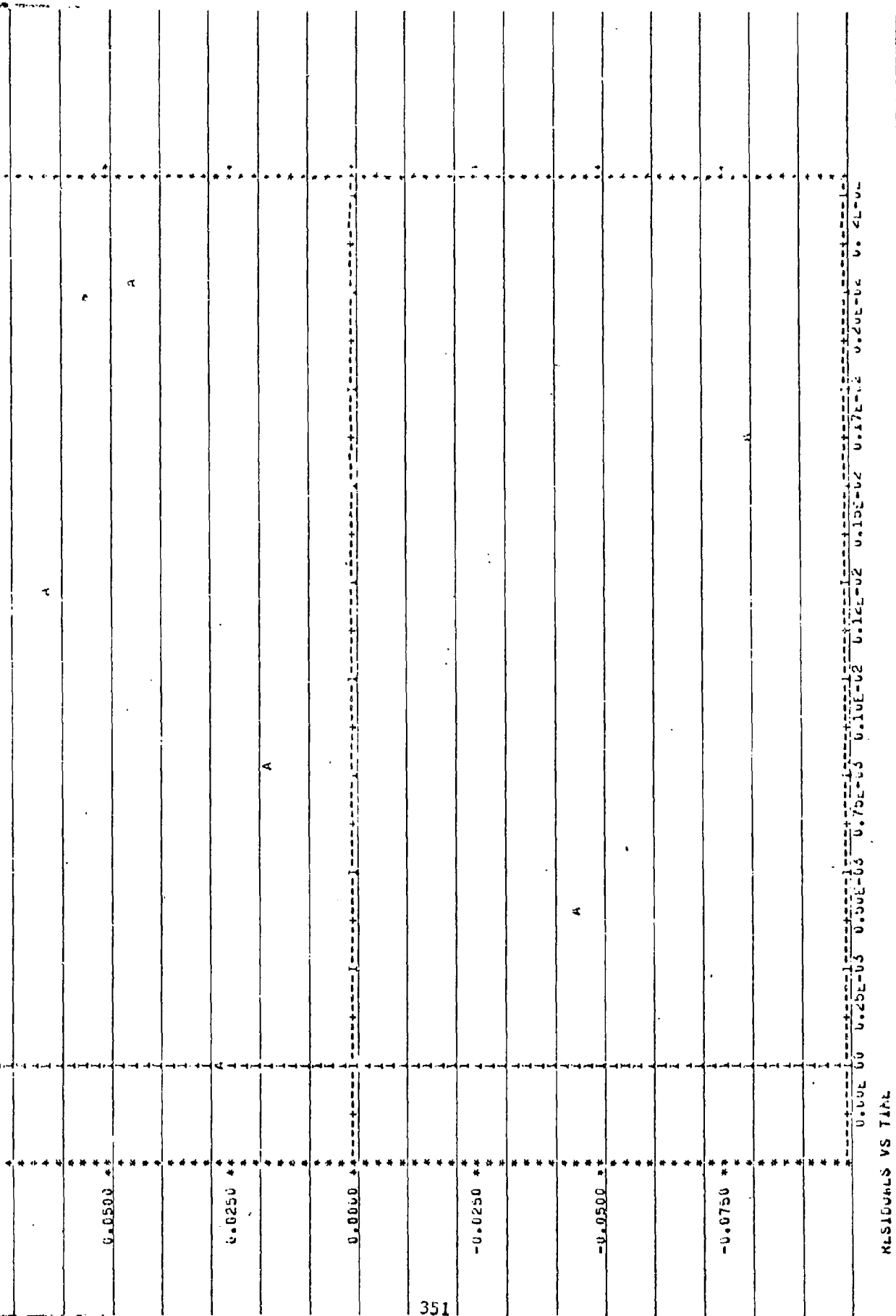
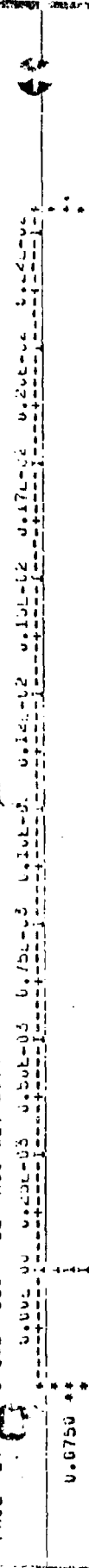
Figure D-4 (continued)

0.00 0.25 0.50 0.75 1.00 1.25 1.50 1.75 2.00 2.25 2.50



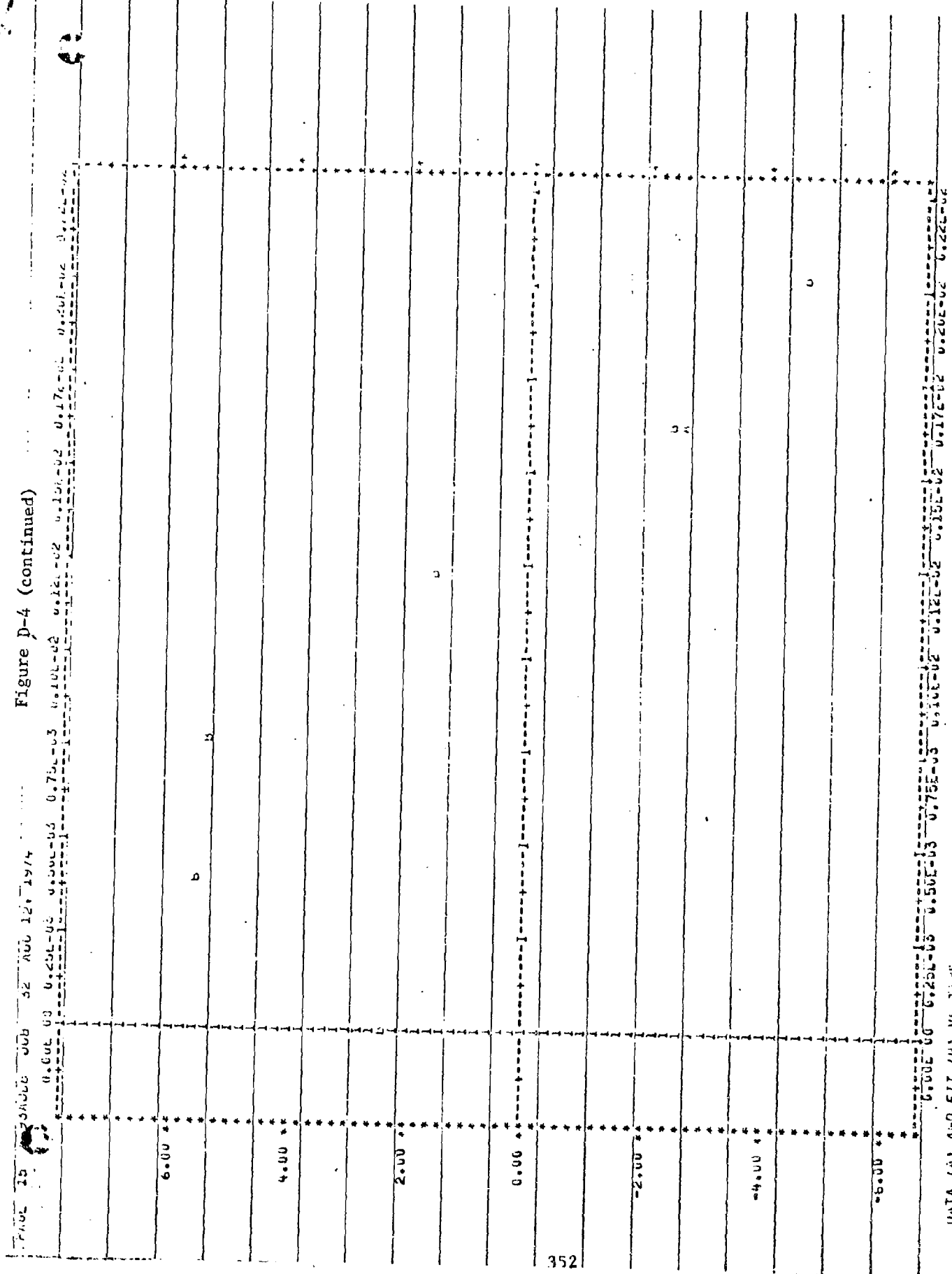
PRICE 14 35000 32 AUG 12, 1974

Figure D-4 (continued)



RESIDUALS VS TIME

Figure D-4 (continued)



ROUND 17

Figure D-5

	T	A	B	ALPHA	CA	OB	DALPHA
	C.001191	-2.2214	0.7352	2.3399	-198.1504	65.5778	208.7700
	0.000291	-3.2863	1.0376	3.4615	-172.3991	57.0554	181.5951
	0.000391	-4.1653	1.3851	4.4086	-140.5085	46.5012	148.0033
	0.000491	-4.8876	1.6175	5.1483	-103.9553	34.4039	105.5004
	0.000591	-5.3778	1.7795	5.6573	-64.3590	21.2996	67.7920
	0.000691	-5.6225	1.968	5.9225	-23.4107	7.7478	24.6594
	0.000791	-5.6398	1.8665	5.9406	-17.1974	-5.6915	-18.1147
	0.000891	-5.4292	1.7968	5.7188	-55.8395	-18.4800	-58.8180
	0.000991	-5.065	1.6569	5.2735	91.0273	-30.1231	-95.8754
	0.001091	-4.3953	1.4546	4.6297	121.4303	-46.1873	-127.9775
	0.001191	-3.6261	1.203	3.6195	145.4939	-48.3166	-153.7814
	0.001291	-2.7349	0.951	2.6808	163.9044	-54.2441	-172.6473
	0.001391	-1.7614	0.5829	1.8554	174.6488	-57.7999	-183.9648
	0.001491	-0.7475	0.2474	0.7874	178.5187	-58.9152	-187.5144
	0.001591	0.2647	-0.2876	-0.2869	174.1094	-57.6214	-183.3966
	0.001691	1.2346	-0.4386	-1.3067	163.3067	-54.0462	-172.0176
	0.001791	2.1243	-0.7630	-2.2376	146.2620	-48.4053	-154.0638
	0.001891	2.9015	-0.9559	-3.5552	123.8577	-40.9906	-130.4645
	0.001991	3.5355	-1.171	-3.7241	97.1649	-32.1567	-102.3478
	0.002091	4.0081	-1.3265	-4.2219	67.3933	-22.3038	-9881
	0.002191	4.3044	-1.4245	-4.5340	35.8394	-11.8619	-37.7511
	0.002291	4.4161	-1.4621	-4.6536	3.8305	-1.2677	-4.0348
	0.002391	4.3503	-1.4396	-4.5820	-27.3295	9.1447	28.7873
353	0.002491	4.1088	-1.3518	-4.3279	-56.4113	18.6693	59.4203
	0.002591	3.7096	-1.2217	-3.9174	-82.3682	27.2399	66.6987
	0.002691	3.1734	-1.052	-3.4227	-104.0767	34.4441	109.6283
	0.002791	2.5262	-0.8363	-2.6609	-120.9689	40.0346	127.4216
	0.002891	1.7974	-0.5949	-1.8933	-132.4570	43.8366	139.5224
	0.002991	1.191	-0.3373	-1.0735	-138.2473	45.7529	145.6216
	0.003091	0.2241	-0.0742	-0.2361	-139.2854	45.7655	145.6618
	0.003191	-0.5555	0.1837	0.5846	-132.7499	43.9335	139.8309

Figure D-6

17X

POLYNOMIAL COEFFICIENTS

$$C_1 = -0.1447$$

$$C_2 = 0.3404$$

$$C_3 = 0.0796$$

THE POLYNOMIAL EQUATION OF FIT IS

POLYNOMIAL COEFFICIENTS

$$C_1 = -0.1447$$

$$C_2 = 0.3404$$

$$C_3 = 0.0796$$

$$C_4 = -0.0252$$

$$X = -0.1447t + 0.3404t^2 + 0.0796t^3 - 0.0252t^4$$

$$\dot{X} = 0.3404 + 0.0796t - 0.0252t^2$$

THE POLYNOMIAL EQUATION OF FIT IS

POLYNOMIAL COEFFICIENTS

$$C_1 = -0.1447$$

$$C_2 = 0.3404$$

$$C_3 = 0.0796$$

$$C_4 = -0.0252$$

$$C_5 = 0.1483$$

Figure D-6 (continued)

一

卷之三

卷之三

ט'ז ב' תרנ"ה - ינואר 1895 - ס' יב

THE JOURNAL

زیارت

卷之三

$$\dot{y} = 0.1359 - 0.50244t + 0.1884t^2$$

$$C_3 = -0.231245$$

355

LEADERSHIP IN THE INFORMATION AGE

卷之三

C149 - 0135 - 71

ארכיאולוגיה

卷之三

卷之三

卷之三

Figure D-7

$X \times 10^{-3}$	X	Y	Z	S	DX	DY	DZ
0.000000	-0.012008	-0.012025	0.017642	0.026367	0.011325	0.030544	
0.100000	-0.009139	-0.011997	0.015081	0.025959	0.017295	0.029912	
0.200000	-0.006218	-0.011455	0.013029	0.029615	0.013580	0.029826	
0.300000	-0.003219	-0.011270	0.011721	0.030176	0.010178	0.011173	
0.400000	-0.000175	-0.011409	0.011411	0.030568	-0.012913	0.013086	
0.500000	-0.002518	-0.011342	0.012196	0.031165	-0.015683	0.016179	
0.600000	0.006056	0.012536	0.013922	0.031606	-0.008143	0.022632	
0.700000	0.005236	0.013460	0.016324	0.031293	-0.010289	0.033607	
0.800000	-0.012454	-0.014583	0.019177	0.032345	-0.012120	0.034542	
0.900000	-0.015714	-0.015873	0.022329	0.032656	-0.013638	0.030389	
1.000000	0.018583	-0.017300	0.025684	0.032925	-0.014842	0.036116	
1.100000	0.022088	-0.018331	0.029178	0.033153	-0.015731	0.036696	
1.200000	0.025612	-0.021336	0.032766	0.033339	-0.016337	0.037113	
1.300000	0.028954	-0.022882	0.036414	0.033433	-0.016569	0.037358	
1.400000	0.032308	-0.023739	0.040092	0.033586	-0.016516	0.037428	
1.500000	0.035670	-0.025375	0.043775	0.033648	-0.016150	0.037223	
1.600000	0.039036	-0.026959	0.047440	0.033668	-0.015470	0.037052	
1.700000	0.042452	-0.026458	0.051067	0.033647	-0.014475	0.036628	
1.800000	0.045764	-0.029843	0.054635	0.033584	-0.013167	0.036413	
1.900000	0.049117	-0.03181	0.058125	0.033479	-0.011545	0.035414	
2.000000	0.052458	-0.032142	0.061522	0.033333	-0.009608	0.034693	
2.100000	0.055783	-0.032493	0.064809	0.033146	-0.007358	0.033953	
2.200000	0.059186	-0.033603	0.067973	0.032917	-0.005479	0.033264	
2.300000	0.062365	-0.033541	0.071032	0.032647	-0.0034915	0.032703	
2.400000	0.065614	-0.033975	0.073889	0.032335	0.001277	0.032350	
2.500000	0.068833	-0.033675	0.076626	0.031981	0.004783	0.032337	
2.600000	0.072059	-0.03308	0.079214	0.031586	0.006804	0.032737	
2.700000	0.075146	-0.031944	0.081654	0.031150	0.012738	0.033654	
2.800000	0.078237	-0.033450	0.083954	0.030672	0.017186	0.035159	
2.900000	0.081279	-0.028496	0.086130	0.030153	0.021949	0.037295	
3.000000	0.084267	-0.02650	0.088201	0.029592	0.027025	0.040075	

CORE USAGE OBJECT_CODE= 1720 BYTES, ARRAY AREA= 866 BYTES, TOTAL AREA AVAILABLE= 86112 BYTES

DIAGNOSTICS NUMBER OF ERRORS= 0, NUMBER OF WARNINGS= 0, NUMBER OF EXTENSIONS= 0

COMPILE TIME= 0.08 SEC, EXECUTION TIME= 0.15 SEC, WAITIV - VERSION 1 LEVEL 3 MARCH 1971 DATE= 74/225

356

Table D-8
DISPERSION ANALYSIS
(127 ft. Target)

R O U N D	Position Downrange (ft)	Initial Conditions			\bar{S}_0 (ft/sec)	$\bar{\alpha}_0$ (deg)	$\bar{\alpha}'_0$ (rad/sec)	Frankford Dispersion mils	6-D Dispersion mils
		u_0 (ft/sec)	p_0 (rad/sec)	\dot{S}_0 (ft/sec)					
1	17279	-0.006208	0.029610+	0.7352-	65.6-			-0.087	0.2657
3	4752	-0.011455i	0.003580i	2.2214i	198.2i			+0.251i	
17	5	0.006056-	0.031600-	1.7775-	21.3-			-0.019	0.1472
7		0.012536i	0.008143i	3.3708i	64.4i			+0.146	
1		0.018983-	0.032925-	1.6569-	-30.1			+0.3739	
1		0.017300i	0.014842i	5.0065i	+91.0i			+0.0921	
3		0.032308-	0.033586-	0.5829-	-57.8				
21	5	0.023739i	0.016516i	1.7614i	+174.6i				
7		-0.009130	0.029123-	1.1027i	73.6i			-0.225i	0.2427
1		-0.012263i	0.004831i	1.1028i	73.6i			-0.698	0.1304
21	3	0.002832-	0.030624-	2.3922i	-34.5i			-0.35	
1		0.013482i	0.001223i	2.3925i	34.5i			-0.0442	
21	5	0.015317-	0.031733-	2.5669i	-19.7			0.0667+	
7		0.013208i	0.002633i	2.5672i	-19.7i			0.0683i	
1		0.028167-	0.032451+	1.5643+	-64.1				
3		0.011342i	0.006737i	1.5644i	-64.1i				
23	5	-0.009095	0.030700+	-0.0187	0.9-			-0.007	0.0099
3		-0.012963i	0.009724i	+0.6239i	29.2i			+0.071	
7		0.003109-	0.030350-	0.0085-	1.4-			0.170+	0.1806
23	5	0.013058i	0.011001i	0.2842i	47.1i			0.061i	
7		0.015208-	0.030175-	0.0403-	1.2-			0.2049	
1		0.013608i	0.001558i	1.3458i	40.6i			0.005+	0.0344
3		0.027273-	0.030176-	0.0574-	-0.2			0.019+	
7		0.014148i	0.000948i	1.9201i	-5.1i			0.0081	
1		0.010197	0.018419+	1.6128+	174.1+			-0.201	0.2163
3		0.012496i	0.000672i	0.5056i	54.6i			-0.080i	
25	5	0.00791	0.028081+	4.8205+	97.0+			-0.137	0.1379
7		0.012241i	0.000818i	1.5112i	30.4i			0.154+	0.1594
1		0.011842-	0.034550+	5.8206i	-11.1			0.041i	
3		-0.009245	0.031137+	0.2731-	10.1-			-0.027	0.0658
35	5	-0.011629i	0.032966i	1.5468i	56.9i			+0.060i	
3		0.003296-	0.031503-	0.3742-	-1.9+			-0.007	0.0076
7		0.011988i	0.004026i	2.1193i	10.6i			+0.003i	
35	5	0.015908-	0.031500-	0.1959-	-12.7			0.043-	0.1089
7		0.028446-	0.031129-	-0.1344	-14.2			0.100i	
		0.016681i	0.004780i	+0.7614i	+80.5i			0.050-	0.1003

DISTRIBUTION

Commander
U.S. Army Armament Command
Attn: AMCRD
5001 Eisenhower Avenue
Alexandria, VA 22333

Commander
U.S. Army Armament Command
Attn: AMSAR-RD
Rock Island, IL 61202

Commander
Ballistics Research Laboratories
Attn: AMXRD-BEL
Aberdeen Proving Ground, MD 21005

Defense Documentation Center (2)
Attn: DDC-TCA
Cameron Station
Alexandria, VA 22314

Frankford Arsenal:

3 Attn: TSP-L/51-2
(1 - Circulation copy
1 - Reference copy
1 - Record copy)

1 Attn: MDS-D/220-2
Mr. Walter Schupp

Printing & Reproduction Division
FRANKFORD ARSENAL
Date Printed: 3 Sept. 1975

DEPARTMENT OF THE ARMY

FRANKFORD ARSENAL

PHILADELPHIA, PA. 19137

OFFICIAL BUSINESS

PENALTY FOR PRIVATE USE \$500

SARFA-TSP-T

POSTAGE AND FEES PAID

DEPARTMENT OF THE ARMY

E0Q-314

